EFFECTS OF NUTRACEUTICAL TREATMENTS BASED ON METABOLIC COFACTORS AND HISTIDINE AMINO ACIDS METABOLISM ON NAFLD AND OBESITY RESOLVING GUT-LIVER-ADIPOSE CROSSTALK

Sergio Quesada Vázquez

UNIVERSITAT ROVIRA i VIRGILI

Effects of nutraceutical treatments based on metabolic cofactors and histidine amino acids metabolism on NAFLD and obesity resolving gut-liver-adipose crosstalk

SERGIO QUESADA VÁZQUEZ

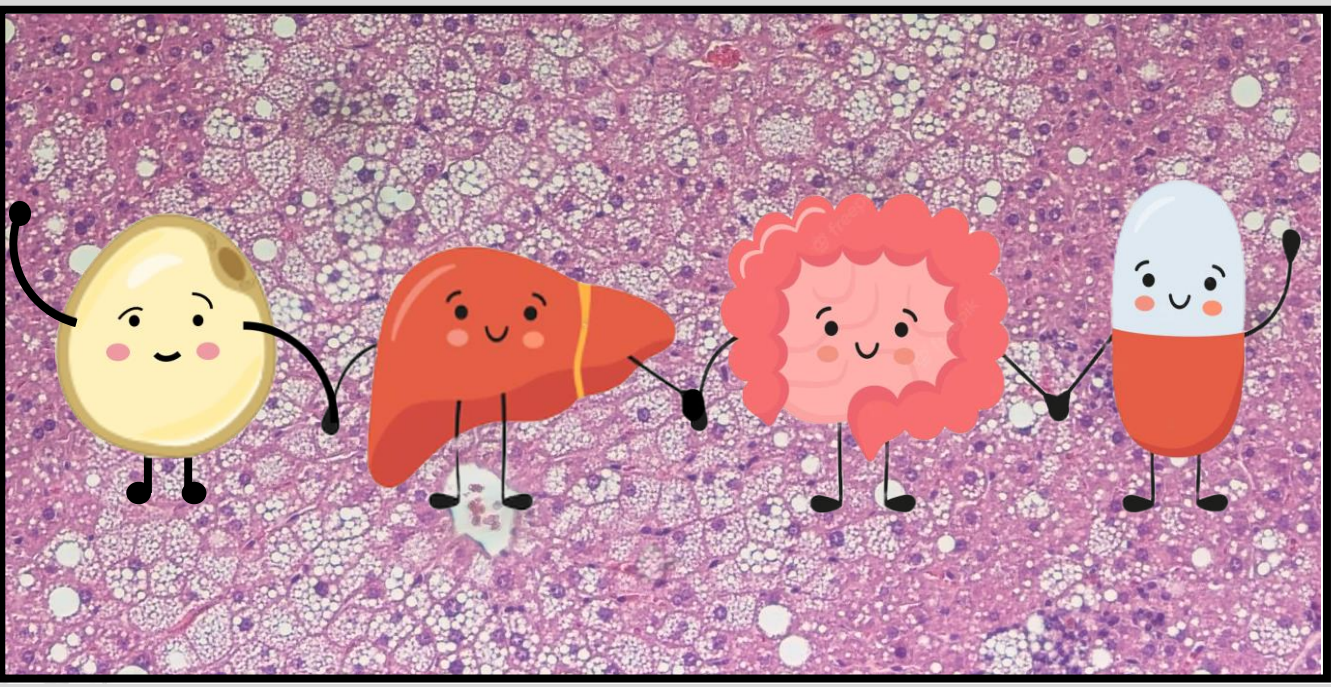

DOCTORAL THESIS
2023

UNIVERSITAT ROVIRA I VIRGILI
EFFECTS OF NUTRACEUTICAL TREATMENTS BASED ON METABOLIC COFACTORS AND HISTIDINE AMINO ACIDS METABOLISM ON NAFLD AND OBESITY RESOLVING GUT-LIVER-ADIPOSE CROSSTALK
Sergio Quesada Vázquez

UNIVERSITAT ROVIRA I VIRGILI
EFFECTS OF NUTRACEUTICAL TREATMENTS BASED ON METABOLIC COFACTORS AND HISTIDINE AMINO ACIDS METABOLISM ON NAFLD AND OBESITY RESOLVING GUT-LIVER-ADIPOSE CROSSTALK
Sergio Quesada Vázquez

SERGIO QUESADA VÁZQUEZ

Effects of nutraceutical treatments based on metabolic cofactors and histidine amino acids metabolism on NAFLD and obesity resolving gut-liver-adipose crosstalk

Doctoral Thesis

Directed by Dr. Xavier Escoté Miró and

Dr. Gerard Aragonès Bargalló

Departament de Bioquímica i Biotecnologia

Unitat Tecnològica de Nutrició i Salut

Reus 2022

UNIVERSITAT ROVIRA I VIRGILI
EFFECTS OF NUTRACEUTICAL TREATMENTS BASED ON METABOLIC COFACTORS AND HISTIDINE AMINO ACIDS METABOLISM ON NAFLD AND OBESITY RESOLVING GUT-LIVER-ADIPOSE CROSSTALK
Sergio Quesada Vázquez

UNIVERSITAT ROVIRA i VIRGILI

Departament of Biochemistry and Biotechnology

Marcel·lí Domingo St, 1

Sescelades Campus

43007, Tarragona

Phone +34 977 55 84 97

Fax +34 977 55 82 32

WE STATE that the present thesis entitled **Effects of nutraceutical treatments based on metabolic cofactors and histidine amino acids metabolism on NAFLD and obesity resolving gut-liver-adipose crosstalk**, presented by Sergio Quesada Vázquez to obtain the award of Doctor, has been carried out under our supervision in the Unitat Tecnològica de Nutrició i Salut at Eurecat and at the Department of Biochesmitry and Biotechnology of this university, and fulfil the demanded requirements to get the European Mention.

FEM CONSTAR que la present tesi, titulada **Effects of nutraceutical treatments based on metabolic cofactors and histidine amino acids metabolism on NAFLD and obesity resolving gut-liver-adipose crosstalk**, presentada per Sergio Quesada Vázquez per a l'obtenció del títol de Doctor, ha estat sota la nostra direcció a la Unitat Tecnològica de Nutrició i Salut a Eurecat i al department de Bioquímica i Biotecnologia d'aquesta universitat, i que acompleix els requeriments per optar a la Menció Europea.

Tarragona, 8th of January of 2022

Doctoral thesis supervisors/ Els directors de la tesi doctoral

Dr. Xavier Escoté Miró

Dr. Gerard Aragonès Bargalló

UNIVERSITAT ROVIRA I VIRGILI
EFFECTS OF NUTRACEUTICAL TREATMENTS BASED ON METABOLIC COFACTORS AND HISTIDINE AMINO ACIDS METABOLISM ON NAFLD AND OBESITY RESOLVING GUT-LIVER-ADIPOSE CROSSTALK
Sergio Quesada Vázquez

ACKNOWLEDGMENTS

Three and a half years have passed, and I have finally been able to deposit my doctoral thesis. Who would have told me before starting it, when all my doubts and fears were running through my mind. I have never considered myself a brilliant person, but I have been constant and hard-working, but at the same time absent-minded. It seems unbelievable to think that the COVID pandemic has helped me to be able to do my doctoral thesis, but it has really been like that. But I am sure that I would not have been able to complete this doctoral thesis without the help of such important people who have encouraged and helped me during this long and hard journey.

First of all, I would like to thank Eurecat, specifically the nutrition and health unit that has given me the opportunity to do such an interesting PhD project. I strongly appreciate the economic support provided by the Vicente Lopez's grant. You have always offered me any kind of help in order to be able to do my doctoral thesis with full guarantee and support. Many thanks to Toni Caimari and Josep Mª del Bas for always leaving me an open door and for being able to return to the center to do my doctoral thesis, grateful for the confidence you showed in me. Also, thanks to the Scientific Direction, especially Cesc, for the support given.

A very special thankyou to my thesis supervisor, Xavier Escoté, to whom it feels almost impossible to express my most sincere gratitude and admiration. You have been the best mentor I could have ever imagined having. You welcomed me as your predoctoral researcher in such an important and great project we have worked on together. You have always believed in me and, thanks to that, I have been able to achieve each of my professional goals little by little. I will thank you for the rest of my life. I really hope we can keep working together because we have created a magnificent team.

A word of gratitude to Gerard Aragonés, who always gave me excellent advice and gave me the peace of mind I needed during the whole process. You have always given me security and a much-needed different vision. Your kindness is a characteristic that I will always keep in mind and will try to follow.

Acknowledgments

I would like to thank all my colleagues from Eurecat: Julia, Julio, Anna A, Cris, Anna M, Jordi, Ignasi for your unconditional support and for all those breaks and shared meals that were a moment of breath. To Juanma and Yaiza, for their patience and predisposition to teach me any protocol I had to face.

I would like to express my appreciation to the members of Quadram Institute in Norwich, UK, form the warm welcome and valuable support. Naiara Beraza, thank you so much for accepting me and supporting me in my journey in British lands. Mar, Sian, Meha, Caitlin, Jack, Ana, Maria, Ari, Ton, Victor and Helen, my family there, who have made me feel so well accompanied and found friendships for life.

I could not finish these words without showing my eternal gratitude to the ones who have really put up with my fears, my insecurities, my doubts, and my uncontrolled behaviors: my family. Mom and Dad, you have been my unconditional support all my life and you have supported me in every decision I have made with all its consequences. You are my pride and my example to follow. Without you I would not have made it. My sisters, Helena and Letty, who have been my role models and who were the people who understood me the most along the journey. Jandro, my twin, my friend, and my confidant, with just one look we know how we are feeling and what we need, thank you for your support. To my nephews, Marc and Laia, you are the joy of our family. To Rodrigo and my uncles in Madrid for cheering me up every time we see each other. I also want to thank my other family, Mercé, Guillem, Enric, Maria, Carme, Manuel and Martí. To Lolo and Rumba, the most special cats I have ever met. And for putting up with me, helping me, encouraging me, pushing me, taking care of me, making me laugh and above all loving me, to Maria.

Finally, I would not like to finish without remembering the best friends I have ever met: El Gremi, La Family, Els Baranerus, you are the joy of my life and a reason to keep enjoying it.

Thank you all for having written a part of my life.

“Non gogoa, han zangoa”

Donde van tus pensamientos, van tus pasos (Basque proverb).

TABLE OF CONTENTS

Table of contents

SUMMARY

Obesity is the most common major disease in adults and young people worldwide. Obesity is related to different risk factors such as abdominal adiposity and insulin resistance, considered the main cause of the development of the metabolic syndrome. Metabolic syndrome is described as a multifactorial disease associated with diet-related metabolic pathologies via the gut- liver-adipose tissue axis, manifesting in different metabolic organs, such as fatty liver disease (NAFLD), and intestinal barrier dysfunction and dysbiosis. In this sense, nutraceuticals are natural bioactive compounds with antilipemic, anti-inflammatory and antioxidant properties that could act on different molecular mechanisms affected during the development of these metabolic diseases.

In this scenario, the present thesis has been designed to clarify the possible role of a specific combination of metabolic cofactors and histidine-related amino acids in ameliorating the pathological features of NAFLD; the pathological features of obesity and maintaining intestinal barrier and intestinal microbial homeostasis in animal models.

To achieve this overall objective, it was examined the impact of supplementation of the specific combination of metabolic cofactors on liver health status during NAFLD, analyzing the improvement of the pathological features of the disease, and subsequently the effect of this supplementation on extrahepatic factors such as adipose tissue dysfunction, which occurs when adipose tissue exceeds the threshold for lipid accumulation and free fatty acids are released and accumulated in other tissues, such as liver and muscle through ectopic lipid deposition, which over time can degenerate into diseases such as lipotoxicity or NAFLD; and the increased intestinal barrier permeability and dysbiosis during NAFLD. Second, it was analyzed the role of histidine during NAFLD progression and obesity in both preclinical and clinical models, taking into account the microbial composition of patients and animals. To better understand the involvement of histidine in these metabolic diseases, the effect of histidine-related amino acid supplementation on the characteristic pathological features of NAFLD and obesity was examined in animal models.

In summary, the present thesis revealed that oral administration of a specific combination of metabolic cofactors and histidine-related amino acids are promising treatments against NAFLD, obesity and intestinal barrier dysfunction.

Summary

RESUMEN

La obesidad es la enfermedad grave más frecuente en adultos y jóvenes de todo el mundo. La obesidad está relacionada con diferentes factores de riesgo como la adiposidad abdominal y la resistencia a la insulina, consideradas causas principales del desarrollo del síndrome metabólico. El síndrome metabólico se describe como una enfermedad multifactorial asociada a patologías metabólicas conectadas con la dieta a través del eje intestino-hígado-tejido adiposo, expresándose en diferentes órganos metabólicos, como la enfermedad del hígado graso (NAFLD), la disfunción y disbiosis intestinal. En este sentido, los nutracéuticos son compuestos bioactivos naturales antilipémicos, antiinflamatorios y antioxidantes que podrían actuar sobre diferentes mecanismos moleculares afectados en el desarrollo de enfermedades metabólicas.

En este escenario, la presente tesis ha sido diseñada para definir el papel de una combinación específica de cofactores metabólicos y aminoácidos relacionados con la histidina en la mejora de las propiedades patológicas de la NAFLD; las de la obesidad y el mantenimiento de la barrera y la homeostasis microbiana intestinal en modelos animales.

Para alcanzar este objetivo, se examinó el impacto del tratamiento con la combinación de cofactores metabólicos sobre el estado del hígado durante la NAFLD, analizando la mejora de las propiedades patológicas de la enfermedad. Posteriormente se analizó el efecto del tratamiento sobre factores extrahepáticos: la disfunción del tejido adiposo, producido cuando el tejido adiposo supera el umbral de acumulación de lípidos y acaban liberados, acumulándose en otros tejidos, como el hígado o músculo, a través de la deposición ectópica de lípidos, pudiendo generar lipotoxicidad o NAFLD en el hígado; y el aumento de la permeabilidad y disbiosis intestinal durante NAFLD. En segundo lugar, se analizó el papel de la histidina durante la progresión de NAFLD y la obesidad en modelos preclínicos y clínicos, teniendo en cuenta la composición microbiana de pacientes y animales. Para comprender la implicación de la histidina en estas enfermedades metabólicas se examinó en modelos animales el efecto de la suplementación con aminoácidos relacionados con la histidina sobre los rasgos patológicos de la NAFLD y la obesidad.

En resumen, la presente tesis reveló que la administración oral de una combinación específica de cofactores metabólicos y aminoácidos relacionados con la histidina son tratamientos prometedores contra la NAFLD, la obesidad y la disfunción de la barrera intestinal.

Resumen

Abbreviations

- ACC1: Acetyl-CoA Carboxylase
- ACOX1: Acyl-CoA Oxidase
- AdipoQ: Adiponectin
- AKT/PKB: Protein kinase B
- ALT: Alanine Aminotransferase
- AMP: Adenosine Monophosphate
- AST: Aspartate Aminotransferase
- ATGL: Adipose Triglyceride Lipase
- ATP: Adenosine Triphosphate
- BAT: Brown Adipose Tissue
- BC: Body composition
- BMI: Body Mass Index
- BW: Body Weight
- CACT: Carnitine-acylcarnitine translocase
- CARNS1: Carnosine Synthase 1
- CCL2: C-C Motif Chemokine Ligand 2
- CGI-58: Comparative Gene Identification-58
- CNDP1: Carnosine Dipeptidase 1
- CPT: Carnitine Palmitoyltranferase
- DAG: Diacylglycerol
- DAMPs: Damage-associated molecular patterns
- DCs: Dendritic cells
- DGAT: Diacylglycerol Acyltransferase
- DIO: Iodothyronine Deiodinase
- F4/80: Adhesion G Protein-Coupled Receptor E1
- FABP: Fatty Acid Binding Protein
- FADS2: Fatty Acid Desaturase 2
- FASN: Fatty Acid Synthase
- FAT: Fatty Acid Translocase
- FATP: Fatty Acid Transport Protein
- FFA: Free Fatty Acid
- FGF21: Fibroblast Growth Factor 21
- FMT: Fecal material transfer/transplantation
- G0S2: G0/G1 switch gene 2
- GLUT: Glucose Transporter
- GTT: Glucose Tolerance Test
- GSH: Glutathione
- HAA: Histidine-related amino acids
- HAL: Histidine ammino-lyase
- HDC: Histidine decarboxylase
- HDL: High-Density Lipoprotein-Cholesterol
- H&E: Hematoxylin and Eosin
- HFD: High Fat Diet
- HMG-CoA: 3-hidroxi-3-metilglutaril-coenzima A
- HNMT: Histamine N-Methyltransferase
- HR: Histamine receptor
- HSC: Hepatic stellate cells
- HSL: Hormone-Sensitive Lipase
- IGF-1: Insulin-like growth factor-1

Abbreviations

- IL: Interleukin
- IRS: Insulin Receptor Substrate
- ITT: Insulin Tolerance Test
- KCs Kupffer cells
- KO: Knock-out
- LC: L-carnitine
- LDL: Low-Density Lipoprotein-Cholesterol
- LEP: Leptin
- LEPR: Leptin receptor
- LPL: Lipoprotein Lipase
- LPS: Lipopolysaccharide
- MCP1: Monocyte chemoattractant protein-1
- MetS: Metabolic Syndrome
- MI/MC: Multi-ingredient
- mWAT: Mesenteric White Adipose Tissue
- NAC: N-acetyl cisteine
- NAFLD: Non-alcoholic fatty liver disease
- NASH: Non-alcoholic steatohepatitis
- NEFA: Non-Esterified Fatty Acid
- NK: Natural killer
- NR: Nicotinamide riboside
- PA: Palmitic acid
- PAMPs: Pathogen-associated molecular patterns
- PI3K: phosphatidylinositol 3-kinase
- PPAR: Peroxisome Proliferator Activated Receptor
- PRDM16: PR/SET Domain 16
- RC: Respiratory Chain
- RT-PCR: Real Time-PCR
- rtWAT: Retroperitoneal White Adipose Tissue
- ROS: Reactive oxygen species
- SCD1: Stearoyl-CoA Desaturase 1
- scWAT: Subcutaneous White Adipose Tissue
- SREBP: sterol regulatory element-binding protein
- TAAR1: Trace Amine-Associated Receptor 1
- TCA: Tricarboxylic Acid Cycle
- T2DM: Type 2 Diabetes *Mellitus*
- TLR: Toll-Like Receptor
- Tmem64: Transmembrane Protein 64
- TNFα: Tumor Necrosis Factor-alpha
- UCP1: Uncoupling Protein 1
- VAT: Visceral White Adipose Tissue
- VLDL: Very Low-Density lipoprotein-Cholesterol
- WAT: White Adipose Tissue
- WHO: World Health Organization
- WHtR: Waist-to-Height Ratio
- WT: Wild Type

LIST OF FIGURES

List of figures

1. INTRODUCTION

1.1 OBESITY

Obesity has been described as a complex, multifactorial, and chronic condition with a harmful impact on human health and healthcare systems [1]. According to the World Health Organization (WHO), overweight and obesity are characterized by abnormal or excessive fat accumulation that triggers several health complications. Obesity is a multifactorial disease where fat accumulation is mainly caused by a chronic positive energy balance between energy intake and energy expenditure, which is directly related to lifestyle increasing the intake of energetic foods and sedentarism [2]. Excess energy is transformed into triglycerides which will be stored in the different adipose tissue depots contributing to increased body fat and causing weight gain [3]. Despite this being the fundamental cause of obesity, additional factors play an important role in the development of this disease, such as genetic, epigenetic, endocrine, environmental, psychological, social economic, and political factors, which together contribute to the development of obesity [4]. Besides, changes in diets and physical activity patterns are often influenced by a westernized society in developed countries increasing obesity prevalence [5]. During the last 50 years, the prevalence of obesity has increased worldwide tripling rates in adults and reaching up to 2 billion of the world population [2,6] (**Figure 1**). In fact, the third part of the world population is considered overweight or obese [3]. The fact that obesity is becoming more and more frequent each year and that up to now approaches to decrease obesity levels have failed [7], underlines the necessity to find efficient solutions to prevent and reduce this disease. The body mass index (BMI) is a widely used measurement to calculate obesity, despite its limitations (**Table 1**). BMI is calculated by dividing weight (kg) by the square of the person's height in meters (BMI = kg/m^2) [8]. Thereby, a healthy subject is someone who has less than 25 kg/m2; a subject between 25.0 and 29.9 kg/m2 is rated as overweight; and a person who reaches 30 kg/m2 or more is considered obese. Obesity is stratified in three degrees of severity: class I (from 30.0 to 34.9 kg/m^2), class II (from 35.0 to 39.9 kg/m^2) and class III (> 40.0 kg/m^2)[1,9] (Table 1). Nevertheless, using this classification obese subjects can present similar BMI with different amounts of body fat. To complement the limitations of the BMI score, a determination of body composition and body fat percentage is included, being considered as obesity above 35% of body fat for women and above 25% of body fat for

men [10]. Different techniques are used to assess body fat percentages, such as skin-fold measurement to magnetic resonance imaging or prediction using tools like Clínica Universidad de Navarra - Body Adiposity Estimator (CUN-BAE) [11]. Subjects with a waist-to-height ratio (WHtR) higher than 0.5 are considered to have increased abdominal adiposity [12], even though it may differ in different populations and individuals with high muscle mass [13,14]. Therefore, the WHtR indicates abdominal adiposity while BMI indicates overall adiposity, which together are indicators of body weight status [15].

Table 1. **WHO classification of obesity according to BMI** [9].

BMI (kg/m^2)	WHO classification
<18.5	Underweight
18.5-24.9	Normal weight
25.0-29.9	Preobesity
30.0-34.9	Obesity class I
35.0-39.9	Obesity class II
>40.0	Obesity class III

Obesity, whose etiology is complex and heterogenic, is the principal risk factor for developing multiple disease conditions and several comorbidities, such as metabolic disorders and cardiovascular diseases that shape metabolic syndrome (MetS), musculoskeletal diseases, neurological diseases, depression, and some types of cancer, all of which have negative effects on the quality of life, work productivity, and healthcare costs for the healthcare systems [3,5]. Moreover, obese and overweight patients are more prone to suffer intensive care unit-acquired infections and complications of common infections than individuals in lower BMI categories as a result of their immune status[16]. This predisposition in obese patients is associated with a chronic inflammatory state, leptin resistance, and increased adiposity, which are characteristic features in obesity that modulate the immune response [17]. One of the main pathophysiological mechanisms in metabolic disorders is fat distribution, and an increase in waist circumference (WC) as part of a more

reliable estimate of metabolic risk is tightly connected with an increased abdominal fat distribution [18]. In this direction, the increase in BMI is usually accompanied by a development of dyslipidemia, with the growth of low-density lipoprotein (LDL)-cholesterol particles that rise the risk of coronary heart diseases [19,20]. On the other hand, most of the subjects who develop type 2 diabetes mellitus (TD2M) present a BMI higher than 23 kg/m^2 [21]. Furthermore, Non-alcoholic fatty liver disease (NAFLD) is the hepatic manifestation of the MetS. Thereby, 91% of obese individuals (BMI > 30 kg/m^2) were found with hepatic steatosis on ultrasound in a large population-based study [22,23].

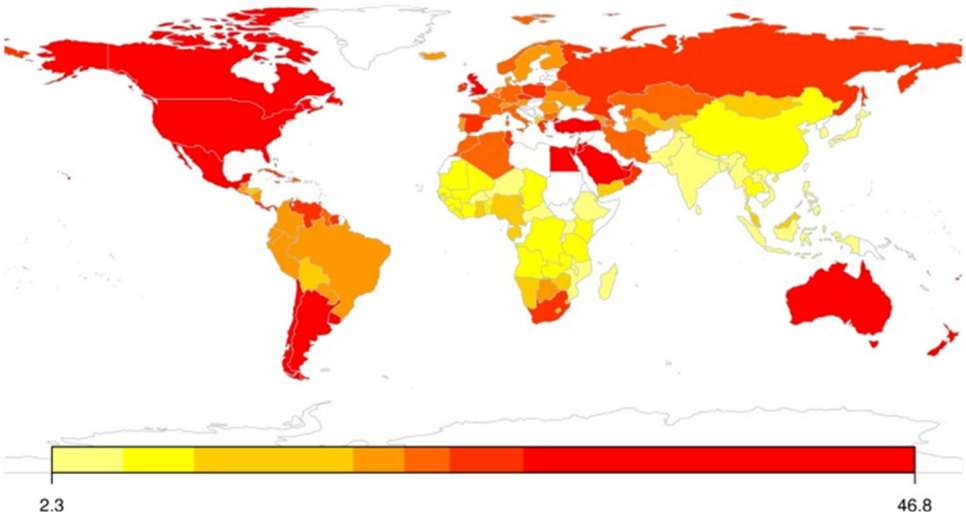

Figure 1. The prevalence of adult obesity in 147 countries is represented in a color scale in percentage. Countries are colored considering their adult obesity prevalence described below the map in a color gradual bar that goes from 2.3 % of obesity prevalence (yellow) to 46.8% (red). Data is missing in countries in white. The most developed countries with westernized lifestyles showed the highest prevalence in comparison with less developed countries. Obtained from Talukdar et al. (2020) [6].

Obesity is one of the characteristic features of MetS development, which is diagnosed under the following criteria: the presence of insulin resistance (IR) or type 2 diabetes mellitus (T2DM) plus two of these characteristics: waist/hip ratio > 0.90 (men), > 0.85 (women) or BMI > 30 kg/m^2; triglycerides > 150 mg/dL or high-density lipoprotein (HDL)-cholesterol < 35 mg/dL (men), < 39 mg/dL (women); or blood pressure >

140/90 mm Hg; or microalbuminuria [23]. Moreover, obesity and MetS not only are associated with these qualifying parameters but also with IR and chronic low-grade inflammation [22]. There are several theories about how obesity affects the immune system and causes inflammation. On the one hand, metabolic disturbances in obesity may disturb immunity by altering lymphoid tissue architecture and integrity and changing leukocyte populations and inflammatory phenotypes [22]. On the other hand, it could probably be related to homeostatic stress caused by a positive energy balance and by a hyper-anabolic state in adipocytes [19,24]. Together, these factors promote the activation of a chronic, pro-inflammatory state first in adipose tissue and after in other tissues implicated in metabolic dysfunctions. Continuous inflammation and stress can trigger inflammatory leukocyte infiltration in the adipocytes, such as M1 macrophages, producing interleukin-1β (IL-1β) and interleukin 6 (IL-6) and increasing secretion of tumor necrosis factor α (TNFα) and C-C Motif Chemokine Ligand 2 (CCL2), also known as monocyte chemoattractant protein-1 (Mcp1) [25,26]. In addition, innate immune T and B cells are also involved in adipocyte inflammation in obesity, while the anti-inflammatory regulatory T cells (Treg) are reduced. Therefore, both innate and adaptative immune cells are partly responsible for obesity-induced inflammation (**Figure 2**) [25]. Thus, the release of cytokines and adipokines with autocrine, paracrine, and endocrine actions that promote this adaptative inflammatory response, also enables adipocyte expansion promoting adipose tissue rremodeling[24]. In brief, the development of obesity is linked to multiple factors accumulating fat in the adipose tissue, which induces an inflammatory state and enhances obesity-related comorbidities [26].

1.2 OBESITY AND THE ADIPOSE TISSUE

As aforementioned, obesity is characterized by an expansion of the adipose tissue. Nonetheless, the adipose tissue not only has an important role in fat storage, but it also is an endocrine organ [27,28]. Although adipocytes are mainly in charge of energy homeostasis control, they are also crucial to modulate endocrine function by secreting heterogeneous bioactive factors such as hormones (known as adipokines) to regulate

distant organs through systemic circulation [28,29]. For example, adipocytes secrete the leptin hormone when a high energy state is reached and there is a need to reduce food intake and increase energy expenditure, regulating appetite signaling [9]. Adipokines are crucial in the balance between appetite and satiety, energy expenditure, glucose tolerance, regulation of body fat stores, insulin release and sensitivity, cell growth, and inflammation as main regulated pathways [29]. Therefore, adipokines are one of the principal actors in the crosstalk between adipose tissue and other distant organs.

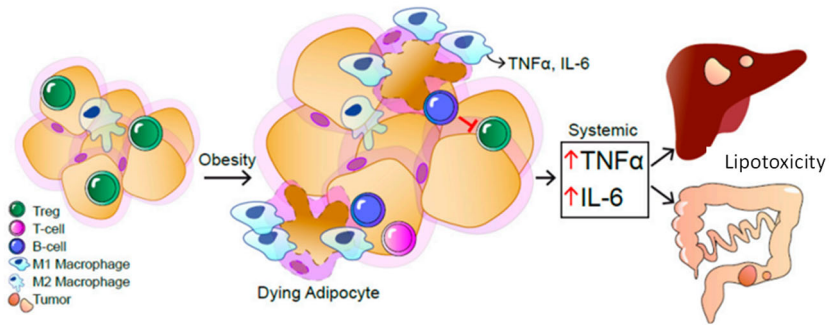

Figure 2. Obesity contributes to the induction of low-grade inflammation in adipose tissue, which triggers lipotoxicity in peripheral tissues. Obesity induces an expansion of the adipose tissue by hyperplasia and hypertrophy, which triggers an infiltration of immune cells, such as T- and B- cells and macrophages, which lead to an increase in proinflammatory factors such as TNFα and IL-6 that affect other tissues developing lipotoxicity. Image adapted from Kern et al. (2019) [25].

Adipose tissue is a complex organ characterized by high cellular heterogeneity. Despite mature adipocytes being considered the main cells present in adipose tissue, other cell types are present in the stroma-vascular fraction [30]. The proportion of these stroma-vascular cells is variable and depends on the physiological situation and location of adipose tissue. The stroma-vascular fraction includes: preadipocytes, macrophages, stem cells, endothelial cells, and even neutrophils and lymphocytes [30], which are responsible for cytokines release, which is implicated in cell signalling and immune regulation. In obesity, adipose tissue is altered in depot size and function characterized by a modified cell composition and leads to dysregulated fat storage and adipocyte endocrine dysfunction [29]. Hence, an imbalanced adipokine production and secretion with a notorious increase in pro-inflammatory cytokines release

play a critical role in adipose tissue dysfunction and the development of IR [31].

Adipose tissue is classified into white adipose tissue (WAT) and brown adipose tissue (BAT), which are characterized by morphological and biological specifications that differ from one another and determine their physiological functions [32] (**Figure 3)**.

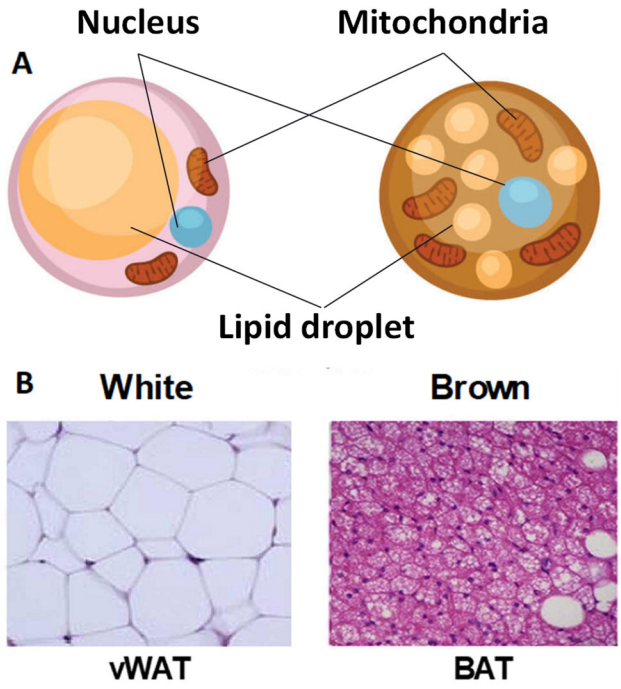

Figure 3. Principal morphological characteristics of adipose tissue. Differences between white and brown adipocytes in number of lipid droplets and mitochondria (A) and representative histological hematoxylin and eosin (H&E) adipose tissues micrographs (B). Adapted from Kwok et al. (2016) [33].

The differences are visibly distinguishable due to tissue color because each tissue has different cell composition and mitochondrial density that confers differences in color and function within energy metabolism [32,34]. Thus, WAT store energy as triglycerides, which can be released as FFAs during physical activity or fasting in normal conditions. WAT mature adipocyte is composed of an unilocular lipid droplet, which fills almost the entire cytoplasm and is primarily involved in fat storage and has a small mitochondrial density. On the other hand, BAT mature

adipocyte is composed of multiple lipid droplets and a high mitochondrial density, which confers them the ability to carry out its main function of energy dissipation in a process known as non-shivering thermogenesis [35]. Non-shivering thermogenesis is highly dependent on the uncoupling protein 1 (UCP1), which is localized into the mitochondria and dissipates energy as heat by uncoupling the electron transport chain instead of producing adenosine triphosphate (ATP) [36]. In rodents, BAT is found throughout life, but in humans is essentially found in the early stages of life to maintain body temperature [37,38]. Apart from thermogenic function, BAT is also described to participate in glucose homeostasis, triglyceride clearance and insulin sensitivity [39]. As opposed to the WAT situation in obesity, characterized by tissue expansion, BAT is inversely associated with BMI and age, reducing thermogenic activity and the amount of functional BAT when BMI and age increase [37,40]. Finally, mainly within subcutaneous WAT (scWAT) depots beige adipocytes can be found and act as brown adipocytes [41] .

1.2.1 White adipose tissue

Adipose tissue divided into WAT and BAT are situated in different parts of the body according to their characteristics and functions (**Figure 4**). Indeed, WAT is localized throughout the whole body and is divided into subcutaneous (scWAT) and visceral adipose tissue (VAT), which includes omental mesenteric, retroperitoneal, gonadal, and pericardial WAT. Whereas scWAT accounts for 80% of total body fat, VAT, which is more metabolically active, occupies the 20% left [42,43]. scWAT is located under the skin, where it carries out a protective function and isolates against heat-loss and acts as a buffer for high-caloric diets storing excess triglycerides. On the other hand, VAT is found surrounding vital organs in the peritoneum and rib cage [33]. Despite both being white adipose tissue, the heterogeneity of the tissues confers different implications on in the metabolic complications caused by obesity, being VAT strongly associated with IR and increased risk of MetS. Whereas scWAT expansion by fat accumulation, especially in the gluteofemoral area, is defined to have beneficial effects against MetS, VAT expansion is described to facilitate the development of obesity-associated metabolic comorbidities [33,44].

Therefore, scWAT expansion is considered healthier than VAT expansion [33].

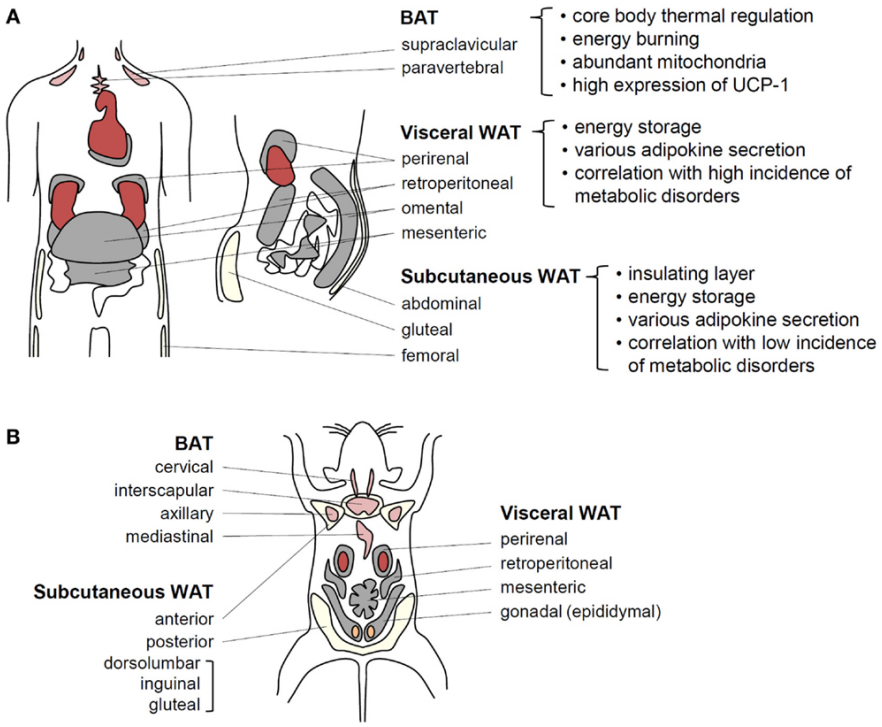

Figure 4. Anatomical adipose tissue distribution of major fat depots and functions in humans and rodents. Adipose tissue depots and functions in humans (A) and adult mice (B). Obtained from Choe et al. (2016) [45].

In regard to cellular differences, scWAT is observed to be composed of smaller adipocytes than VAT, as well as scWAT mature adipocytes are more insulin sensitive and capable of absorbing triglycerides and free fatty acids (FFAs) preventing their deposition in distant organs avoiding ectopic lipotoxicity development [32,46]. scWAT hyperplasia is usually associated with protective functions against obesity-related comorbidities avoiding fat deposition in visceral depots. However, preferential accumulation in VAT triggering hyperplasia and cell hypertrophy are linked to dyslipidemia, IR and T2DM [47], and, consequently, to the development of metabolic and cardiovascular risk [48]. Indeed, the presence of smaller adipocytes and more numerous is associated with a healthy adipose tissue expansion in obesity, as is observed in scWAT [46]. One of the reasons for this opposite effect may lie in the location of each depot being VAT more accessible to the portal

circulation and draining FFAs, triglycerides and cytokines to metabolism-related distant organs [47]. Therefore, VAT expansion by fat accumulation appears to be implicated in the secretion of pro-inflammatory adipokines and cytokines by adipocytes and macrophages, which contribute to the characteristic physiopathological changes in chronic low-grade inflammation and IR development, and consequently, induce obesity-related metabolic disorders [49,50].

1.2.1.1 White adipose tissue remodelling

The adipose tissue is the main fat storage in the body and its activity is responsible for the regulation of energy homeostasis. Thereby, mature adipocytes act according to the current situation. If a situation of an excessive caloric intake is found, mature adipocytes accumulate energy as triglycerides by activating lipogenic pathways [51]. On the contrary, in a situation of caloric restriction, mature adipocytes activate lipolysis signaling, promoting triglycerides release and providing nutrients and energy to other tissues [52]. In obesity, the accumulation of fat due to an excessive caloric intake can be driven either by hypertrophy (increase in size) or hyperplasia (increase in number) of mature adipocytes [53]. Indeed, a prolonged positive energy balance at any age, but importantly during childhood, induces adipogenesis and adipocyte differentiation contributing, together with adipocyte hypertrophy, to an increased fat mass to compensate for the need for increased lipid storage. Hypertrophic mature adipocytes release adipokines and cytokines to favor the recruitment of new preadipocytes and promote their differentiation to mature adipocytes [45]. However, mature adipocytes can come to a point where cell and tissue have expansion limitations. This anabolic pressure can produce stress in adipocytes and induce inflammatory signaling responding to this stress [54]. All these adaptative processes are called “adipose tissue remodeling”, and it can be disrupted by obesity through promoting pathological remodeling of the adipose tissue and being a critical determinant of insulin sensitivity [45,46,54].

Even though obesity impairs adipose tissue remodeling, this disease is heterogeneous, and it can be translated in a subgroup of obese individuals called “healthy obesity”, in which IR and risk of metabolic

comorbidities are not linked to this state. Moreover, in healthy obese patients an adequate accumulation of fat in scWAT is more common than in VAT, which reduces adipose tissue inflammation, lowers ectopic fat presence and is characterized by the formation of new vasculature [55,56]. On the contrary, when obesity promotes a pathological adipose tissue remodeling, the latter is characterized by hypertrophic adipocytes, hypoxia, fibrosis, and accumulation of proinflammatory macrophages [46] that leads to ectopic fat accumulation and increases the risk of suffering obesity-associated metabolic disorders [32]. An unhealthy WAT expansion induces WAT dysfunction (**Figure 5**), which is characterized by reduced secretion of anti-inflammatory adipokines (adiponectin) and by an increased release of leptin, resistin, TNFα, interleukins (IL-6, IL-8, IL-1β) and CCL2 among others, which are pro-inflammatory adipokines promoting the infiltration and activation of pro-inflammatory immune cells [57].

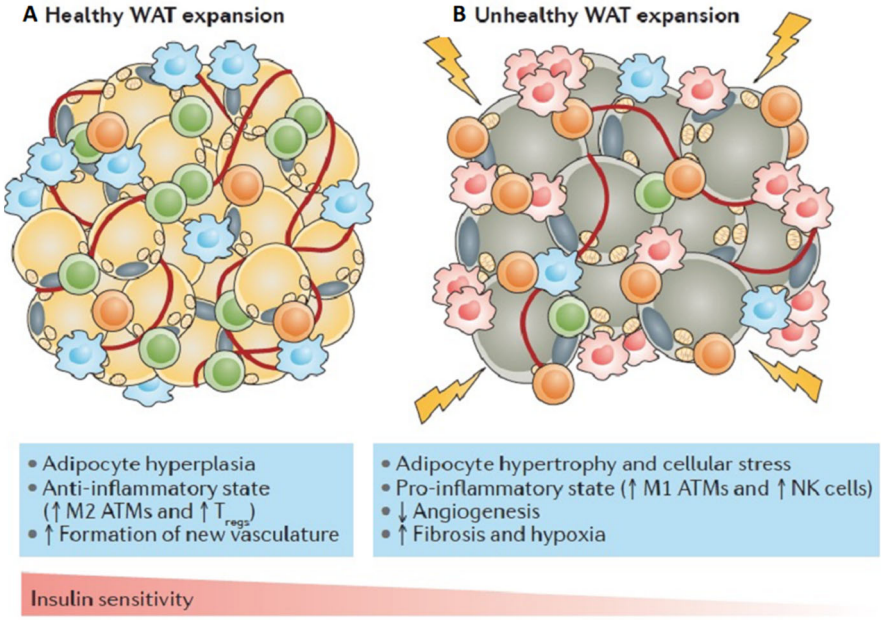

Figure 5. **Representation of healthy and unhealthy WAT expansion.** (A) In healthy expansion, white adipose tissue (WAT) is in an anti-inflammatory state, has enough vasculature and can undergo hyperplasia. Within the tissue, elevated levels of regulatory T cells (T_{reg} cells) (green cells) and M2 adipose tissue macrophages (ATM; blue cells) can be found. It also exhibits high insulin sensitivity. (B) Unhealthy WAT contains hypertrophic adipocytes (gray cells) and presents an enhanced inflammatory state with high infiltration of pro-

inflammatory M1 ATMs (red cells)/anti-inflammatory M2 ATM and natural killer cells (orange cells). This is accompanied by a decrease in T_{reg} cells. Enhanced fibrosis and hypoxia together with reduced formation of new vasculature are also present. These events lead to IR. Image obtained from Kusminski et al. (2016) [27].

Infiltrated macrophages by MCP-1 signal and the increased presence of pro-inflammatory M1 adipose tissue macrophages (ATM) over the anti-inflammatory M2 ATM are a hallmark of obesity-related effects on WAT and contribute to the secretion of pro-inflammatory mediators previously mentioned [45,58]. In obesity, other immune cells can also be infiltrating WAT, contributing to the activation of the inflammasome and promoting systemic, local, and chronic low-grade inflammation. These immune cells are regulatory T cells, $CD8^+$ and $CD4^+$ (Th1 and Th2) T cells, natural killer T cells (NKT), B cells, dendritic cells, eosinophils, neutrophils, and mast cells that are implicated in the pathogenesis of obesity and IR [59]. In addition, the increased size of the adipocytes in WAT can reach their limitation, and together with the activation of inflammatory processes may induce moderate local hypoxia and trigger adipocyte apoptosis and autophagy, which potentiate the chronic low-grade inflammatory response in WAT [45,59].

1.2.1.2 WAT as an energy storage organ

The main characteristic feature of WAT in energy storage is the ability to store the excess of calories in form of triglycerides, which are loaded into lipid droplets that occupy most of the cell. Systemic signals modulate adipocytes' response mobilizing or storing nutrients depending on the organism's needs [53]. However, in obesity, the regulation of lipid metabolism in WAT is impaired favoring dyslipidemia, which is a risk factor in MetS-related comorbidities [60]. The process to store energy in form of triglycerides in the adipocyte is called lipogenesis, and its mobilization and processing are modulated by lipolysis and fatty acid oxidation (also known as β-oxidation) (**Figure 6** and **Figure 7**). Responding to hormonal and energy requirements, adipocytes reduce their lipid storage and release fatty acids to target tissues in need of energy. In contrast, adipocyte lipid uptake, esterification, and storage of energy in form of triglycerides into the lipid droplet is an adaptative response to overnutrition. Accumulation of triglycerides can be a consequence of either a *de novo* synthesis or a

reesterification of dietary fatty acids [61,62]. The fatty acids used for triglycerides biosynthesis in adipocytes are mainly from circulating.

The energy storage process starts assembling dietary fatty acids and transporting them by chylomicrons and very low-density lipoprotein (VLDL)-cholesterol particles through the bloodstream to the adipose tissue, where they end up stored forming lipid droplets within the adipocytes. These lipoproteins-triglycerides must be first hydrolysed into glycerol and non-esterified fatty acids (NEFAs) by the enzyme lipoprotein lipase (LPL), which is localized in the vascular endothelium of the adipocyte and responds to insulin [63]. NEFAs and glycerol molecules are transported into the adipocytes through specific transporters known as fatty acid binding protein (FABP), fatty acid translocase (FAP) and fatty acid transport protein (FATP). FABP, which is the major cytosolic protein found in adipocytes, facilitates the trafficking of NEFAs throughout cellular compartments and participates in lipid storage and lipolysis activities [63,64] (**Figure 6).** Cd36 also participates in FFAs uptake by mediating s long-chain fatty acid uptake into cells to be used for triglycerides synthesis [65]. Once FFAs enter the adipocyte, a reesterification of NEFAs to triglycerides is performed, storing them in the lipid droplet. The transformation process is dependent on the activity of the diglyceride O-acyltransferase (DGAT), which catalyzes its final and critical step in the triglyceride's synthesis pathway. Contrariwise, triglycerides can also be formed from carbon sources like glucose through *de novo* lipogenesis (DNL) fatty acid synthesis from acetyl-coenzyme A (acetyl-CoA). Glucose act as a substrate for *de novo* synthesis by inducing the expression of acetyl-CoA carboxylase (ACC), which is a rate-limiting enzyme of lipogenesis that stimulates pancreatic insulin secretion [62]. ACC transforms acetyl-CoA to malonyl-CoA and is inactivated by AMP-activated protein kinase (AMPK, which is considered a cellular energy sensor that contributes to regulating energy balance) through posttranslational modification (phosphorylation) [66]. Then, malonyl-CoA is converted to saturated fatty acid palmitate by fatty acid synthase (FASN), being the first fatty acid product from DNL. In the presence of NADPH, palmitate is transformed into monounsaturated acid by the action of stearoyl-CoA Desaturase 1 (SCD1) and stored in the lipid droplet [67]. Insulin activates the expression of lipogenic gene sterol regulatory element-binding protein 1 (SREBP1) and carbohydrate response element binding protein (ChREBP), which are transcriptional

factors that promote DNL gene expression controlling cholesterol, fatty acids, triglycerides, and phospholipid synthesis [62].

Opposite to lipogenesis, the catabolic process leading to the breakdown of triglycerides stored in the lipid droplets in adipocytes is called lipolysis, releasing FFAs and glycerol. Lipolysis is principally composed of three consecutive steps that involve three lipases. Adipose triglyceride lipase (ATGL) initiates the lipolytic process cutting the first fatty acid from the triglyceride converting it to diacylgicerol (DAGs). Then, hormone-sensitive lipase (HSL) is responsible for the hydrolysis of DAGs to monoacylglicerols (MGs). Finally, monoacylglycerol lipase (MGL) hydrolyzes MGs resulting in FFAs and glycerol. Lipolysis is regulated at different levels modulating lipases action [68]. ATGL needs the coactivator protein comparative gene identification-58 (CGI-58) for its activation.

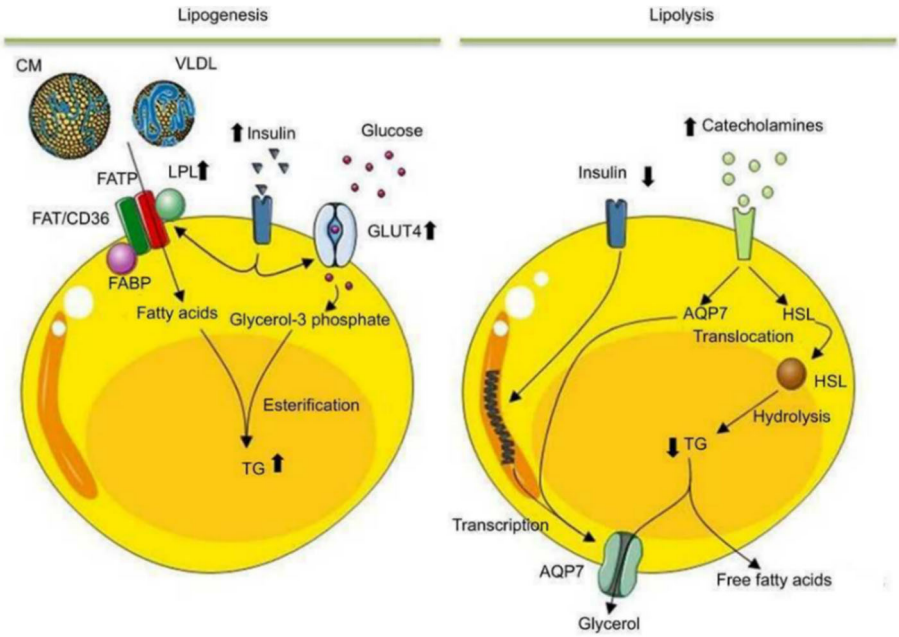

Figure 6. Regulation of lipogenesis and lipolysis processes in mature adipocytes. In lipogenesis, adipocytes, through the action of lipoprotein lipase (LPL), transform triglycerides within chylomicrons (CM) and very-low-density lipoprotein (VLDL) into fatty acids. Fatty acids penetrate in the adipocyte and are esterified with glycerol-3 phosphate and resulting in triglycerides that are stored in the lipid droplet. In the adipocyte, insulin also stimulates uptake and metabolism of glucose to glycerol-3 phosphate. Contrariwise, in lipolysis, the accumulated triglycerides are mobilized to produce free fatty acids and glycerol to obtain energy. When blood glucose decreases, catabolic hormones activate the

synthesis and migration of hormone-sensitive lipase from the cytosol to the surface of the lipid droplet, where it hydrolyzes triglycerides. The fatty acids produced are released to the blood stream, where they are transported by albumin to the target organs to produce energy. Glycerol is exported from the adipocyte by aquaporin-7 (AQP7); FABP, fatty acid-binding protein; FAT/CD36, fatty acid translocase; FATP, fatty acid transport protein; GLUT4, glucose transporter type 4; HSL, hormone-sensitive lipase; TG, triglycerides. Image obtained from Badimon et al. (2015) [69].

However, pirilipin1 (PLIN1), which is a structural protein found in the surface of lipid droplets, interacts with CGI-58 preventing its binding to ATGL and avoiding its activation. Moreover, ATGL can be particularly inhibited by G0/G1 switch gene 2 (G0S2) and activated by CGI-58 [68]. Hormones are also relevant in the regulation of lipolysis, as they can modulate the activity of lipases and other proteins involved in the process [61]. β-adrenergic receptors are stimulated by catecholamines resulting in an increase of adenylate cyclase (AC) activity, which rises levels of the second messenger cyclic adenosine monophosphate (cAMP) activity that modulates lipolytic enzymes via stimulation of the cAMP-dependent kinase [70]. In particular, the activation of the protein kinase A (PKA) is regulated by cAMP increased levels within the cell, phosphorylating PLIN1, which moves out of the lipid droplet making it accessible to lipases and releasing CGI-58 for the activation of ATGL. Moreover, the phosphorylation of the activating amino acids Ser^{563} and Ser^{660} in HSL by PKA are essential for the migration of HSL from the cytosol to the surface of the lipid droplet to interact with phosphorylated PLIN1, which is needed for HSL activation [61,70]. However, if insulin signal is detected by its receptor in the adipocyte, PKA activation is inhibited suppressing lipolysis activation [71]. In addition, adenosine presence inhibits lipolysis by blocking the action of AC [72].

And additional process involved in the metabolism of fatty acids is the fatty acid oxidation (β-oxidation) (**Figure 7**), a catabolic process that takes place in mitochondria and peroxisomes [73]. Energy homeostasis in organs is highly influenced by fatty acid oxidation in mitochondria, being the principal pathway of fatty acid catabolism to generate energy [74]. Acetyl-CoA from circulating glucose is not capable of going through the mitochondrial membrane and must be processed by the carnitine palmitoyltranferase 1 (CPT1), which has three isoforms CPT1A, CPT1B and CPT1C, which are expressed in different organs [74]. CPT1 transforms acyl-

CoA into acylcarnitine, allowing its entrance into the mitochondria where CPT2 converts it back to acyl-CoA. Afterwards, acyl-CoA undergoes a series of reactions called β-oxidation, resulting in the obtention of acetyl-CoA which enters the tricarboxylic acid cycle (TCA) to produce energy in the form of ATP [75]. β-oxidation also takes place within peroxisomes similarly as it occurs in mitochondria, except for the first reaction which is performed by the enzyme acyl-CoA oxidase (ACOX1) [73].

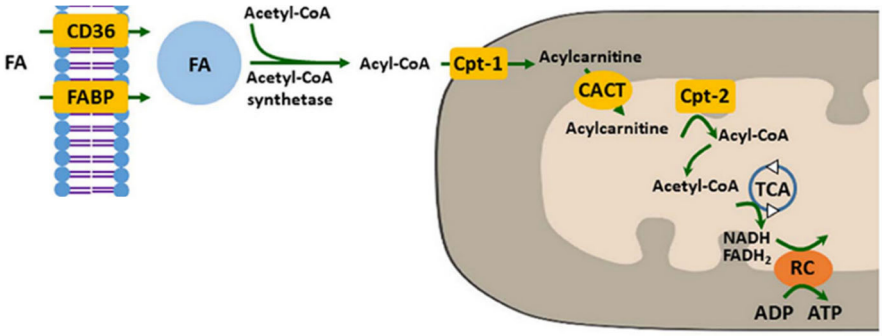

Figure 7. Mitochondrial fatty acid oxidation. Fatty acids enter the cytosol via FABP or CD36 and are transformed from acetyl-CoA to acyl-CoA by acetyl-CoA synthetase and then transported to the mitochondrial matrix by CPT1, carnitine-acylcarnitine translocase (CACT), and CPT2. Acyl-CoA undergoes β-oxidation to produce acetyl-CoA to supply the tricarboxylic acid cycle (TCA). Then, NADH and FADH2 resulted from the TCA act as electron donors for the respiratory chain (RC). FA, fatty acid; FAO, fatty acid β-oxidation; Cpt, carnitine O-palmitoyltransferase. Adapted from Jang et al. (2020) [76].

1.2.1.3 WAT as an endocrine organ

In adipose tissue, not only can adipocytes store fat, but they also can execute their paracrine or endocrine function releasing bioactive molecules [32]. These bioactive molecules include inflammatory cytokines, miRNA, exosomes, peptide hormones and adipokines. Leptin was the first hormone discovered [77], and as it pointed above, leptin is essential for the regulation of the homeostasis of satiety and appetite modulating energy expenditure at a hypothalamic level [78]. Thus, leptin deficiency trigger hyperphagia and obesity in human and mice [79,80]. Even though the regulation of fat storage is the principal role of leptin, it is also implicated

in other physiological processes within WAT, such as browning, inflammation and apoptosis [78]. Indeed, leptin is more produced in scWAT than VAT depots and is higher in woman than man [81]. In obesity, patients show increased circulatory levels of leptin due to the development of leptin resistance, which make the subject insensitive to the exogenous administration of leptin by the inability of its anorexigenic effects [82]. When leptin arrives in several organs, it promotes the generation of inflammatory factors and activates immune cells, polarising them to an inflammatory phenotype, which has been strongly linked to IR development [83,84]. In contrast, another hormone secreted principally by adipocytes is adiponectin (Adipoq), whose circulatory levels are high in healthy subjects and positively correlates with an augment of scWAT/VAT ratio and insulin sensitivity, while in obese patients, adiponectin gets reduced, being negative correlated to weight gain and high BMI [85,86]. It is determined that Adipoq knock-out (KO) mice develop IR and exhibit lipid accumulation in ectopic organs [84]. Thus, adiponectin supresses M1 macrophages activation by downregulating the synthesis of proinflammatory cytokines such as CCL2, IL-6, IL-18 and TNFα, whereas this hormone induces M2 proliferation and activation promoting the expression of anti-inflammatory cytokines, such as IL-10 [87]. Besides, adiponectin has anti-hyperglycaemic and anti-atherogenic effects [32]. Therefore, the loss of protective adiponectin functions is associated with a major pathogenic development of metabolic disorders [88]. It is determined that adiponectin activates AMPK and reduces the expression of gluconeogenic enzymes and enhances ceramidase activity regulating ceramide content and improving insulin sensitivity [62]. Finally, adipose-resident immune cells and endothelial cells are the main sources of other adipokines explained above, such as pro-inflammatory cytokines. Obesity disrupts the production and secretion of adipokines in WAT which may cause adipose tissue dysfunction characterized by inflammation and IR development [62].

1.2.2 Brown adipose tissue

As explained above, BAT performs a different role from WAT by exerting a thermogenic function through energy dissipation mainly dependent on UCP1 activity. UCP1 is located in the inner mitochondrial

membrane where it uncouples the respiratory chain pathway converting the energy into heat instead of ATP [34]. Non-shivering thermogenesis is modulated by β-adrenergic stimulation through the participation of epinephrine and norepinephrine stimulating β3-adrenoreceptors located on BAT [89].

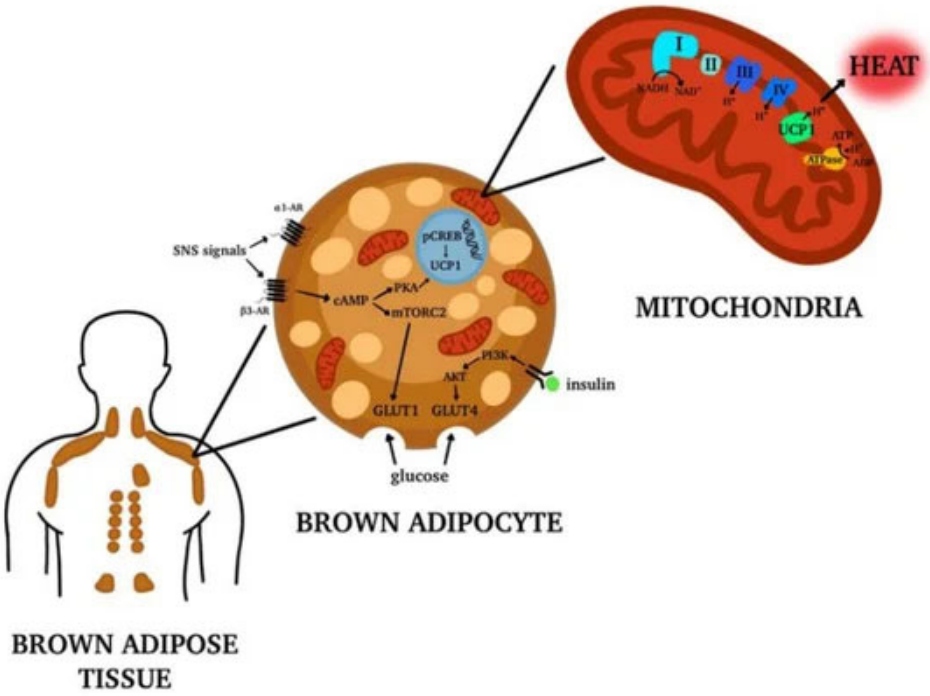

Figure 8. Brown adipose tissue distribution and function in the adult human body. In adult humans, BAT depots are located mainly in the supraclavicular, paravertebral, axillar, cervical, and per-aortic areas. Adrenergic stimulation by SNS signals increases cAMP, which activates PKA and mTORC2. mTORC2 increases the expression and translocation of glucose transporters GLUT1 to the membrane, and insulin increases the expression and translocation of GLUT4 to the membrane via the PI3K-PDK-Akt pathway. cAMP-PKA-pCREB signaling induces UCP1 expression, which promotes non-shivering thermogenesis releasing energy in the form of heat and contributing to systemic clearance of glucose and lipids. SNS, Sympathetic nervous system; cAMP, Cyclic adenosine monophosphate; mTORC2, mTOR Complex 2; PKA, cAMP-dependent protein kinase; pCREB, cAMP response element-binding; UCP1, Uncoupling protein 1. Image adapted from Verduci et al. (2021) [89].

BAT is characterized by a high mitochondrial density and multilocular lipid droplets, and this tissue is specialized on triglycerides hydrolysis and fatty acid oxidation [90], which together with glucose are the main fuel source for thermogenic activity [89]. Thereby, BAT is a key regulator of triglyceride, FFAs, and glucose metabolism [38,91,92]. The activation of BAT boosts energy expenditure, which is tightly related to weight loss and fat mass by consuming glucose, triglycerides, and FFAs. Moreover, BAT activation is negatively associated with obesity, IR, BMI [93,94], and fasting glycemia [95]. BAT is composed of around 30% of mature brown adipocytes and a stromal vascular fraction in which adipose stem cells, preadipocytes, endothelial cells, hematopoietic cells, and neural cells are found [96]. In contrast with WAT, mature and thermochemically activated brown adipocytes secrete different bioactive mediators and hormones denominated batokines, which are composed of fibroblast growth factor 21 (FGF21), retinol-binding protein 4 (RBP4) and IL-6, C-X-C motif chemokine ligand 14 (CXCL14), bone morphogenetic protein 8b (BMP8b), and lipokines (12,13-diHOME), which regulate the function of BAT and other distant metabolic tissues [34,97,98].

There are some differences in the location of BAT in rodents and humans. In rodents, BAT depots can be found mainly in the interscapular area but also, around the spinal cord, the mediastinum, and the axillary and perirenal areas [99]. On the contrary, BAT in humans is present mainly around the cervical-supraclavicular region, with some additional paravertebral, axillar, cervical, and pre-aortic areas (**Figure 8**) [89,99]. Nevertheless, during human life stages BAT suffers changes. In new-borns, BAT is highly present in the supraclavicular area. During childhood and adolescence, BAT remains located in in the supraclavicular region even though BAT activity is reduced. In the last stages of life during the old age, BAT mass and activity is reduced to almost undetectable levels [100]. Actually, the superficial interscapular BAT vanishes in adult humans. Nonetheless, in adolescence and younger adults active BAT is situated in the superficial supraclavicular area and deeper depots [96]. Although BAT activity declines with age, when there is a prolonged episode of cold, the tissue is stimulated and increases in quantity and function [100]. When the presence of BAT was reported in adult humans, its activation has been observed as a therapeutic target to promote a leaner phenotype, lower fasting insulin, improved insulin sensitivity and anti-inflammatory adipokine secretion [101,102]. Some studies observed that different

therapeutics strategies focus on increasing BAT activation ameliorated obesity and associated metabolic disorders [103,104].

Non-shivering thermogenesis is regulated by multiple signaling pathways (**Fig 7**). These pathways are initially modulated by sympathetic nervous system (SNS). SNS induce norepinephrine (NE) and epinephrine release reaching the adrenergic receptors from BAT (mainly β1 and β3 subtypes) and activating them [89,105]. The activation of these adrenergic receptors promotes cAMP levels in the brown adipocyte and leads to activate cAMP-dependent protein kinase (PKA) [105]. PKA induces lipolysis generating FFAs, which are used as thermogenic substrate in BAT. Activation of peroxisome proliferator activated receptor gamma coactivator-1alpha (PGC-1α) via adrenergic signaling and the presence of FFAs induce UCP1 transcription by binding to peroxisome proliferator-activated receptor gamma (PPARγ) and the UCP1 promoter. Indeed, cAMP response element-binding (pCREB) is phosphorylated by PKA and binds with cAMP to directly induce UCP1 and PGC-1α expression [105]. In addition, there are other transcriptional cascades that control the development of BAT and browning in WAT. PR domain zinc finger protein (PRMD16) determines BAT differentiation via regulating PPARγ, CEBPs and PGC-1α expression [106], and is implicated in WAT browning by stimulating mitochondrial biogenesis and uncoupled cellular respiration [105,107]. In addition, type 2 iodothyronine deiodinase (DIO2), which is activated by adrenergic signaling, activates the thyroid hormone receptor by generating its most active ligand triiodothyronine (T3) from thyroxine (T4) in BAT, increasing the thermogenic potential of the tissue by increasing UCP1 content with the synergistic thyroid and adrenergic action [108]. Other important genes implicated in brown adipose tissue mitochondrial biogenesis are mitochondrial transcription factor A (TFAM) and transmembrane protein 26 (TMEM26) used as makers of thermogenic activation [109,110].

Regarding obesity, BAT can suffer morphological changes and dysfunction when this pathological disease is developed. One of the situations that can take place is the transdifferentiation, in which BAT does not receive adrenergic stimulation and it is gradually transformed into WAT-like tissue composed by unilocular cells losing BAT characteristics. Moreover, it is also observed a UCP1 inhibition accompanied with a transformed vascular and nerve supply [111]. Another situation is the increased macrophage infiltration and concentration of pro-inflammatory

cytokines induced by obesity [112]. These pro-inflammatory mediators are partly responsible for the reduction of BAT activity, by inhibiting PPARγ and reducing UCP1 expression via the suppression of SIRT1 expression, which implies an impairment of the thermogenic activity [113]. In addition, the reduction of glucose uptake due to a loss of insulin sensitivity can contribute to the reduction of BAT activity [114]. As explained above, the sympathetic signalling is crucial for the thermogenic function of BAT. However, in obesity, sympathetic signalling is impaired by inflammation through reducing cAMP synthesis caused by chronic activation of nuclear factor kappa-light-chain-enhancer of activated B cells (NF-κB) pathway and increased import and degradation of norepinephrine by macrophages [115]. In obese patients, a more active BAT is associated to a healthier metabolic phenotype by improving body fat distribution, which supports a role of BAT in protection from VAT [116].

1.2.3 Obesity, IR and lipotoxicity

One of the most characteristic features in pathogenic obesity and MetS development is IR, which clearly plays an important role in the physio-pathogenesis of obesity-related metabolic disorders with the loss of insulin sensitivity in adipose tissue and other distant organs [117]. Insulin binds to its specific receptors placed on the cell membrane of insulin-sensitive peripheral tissues, mainly skeletal muscle, liver, and adipose tissue, including mature adipocytes, to carry out its functions [118]. Regarding the mechanisms, insulin stimulus activates phosphatidylinositol (PI)-3 kinase by binding its p85 subunit or indirectly to insulin receptor substrate (IRS)-1. This binding produces PIP3 that leads to the phosphorylation of proteinase kinase B (PKB), also known as AKT [119] (**Figure 9**). This cascade of phosphorylation and dephosphorylation modulates glucose transport 4 (GLUT4) trafficking. When AKT is phosphorylated, GLUT4 in the cytosol containing vesicles is activated and migrate to the plasma membrane of the adipocyte [120]. Opposite to the insulin-mediated glucose uptake, there is a mature adipocyte insulin-independent glucose uptake through glucose transporter 1 (GLUT1) [121]. However, in adipose tissue, glucose transport into the cell is principally enhanced by the insulin-mediated action of GLUT4 because GLUT4 is more

abundant in adipocytes than GLUT1 and the most glucose uptake is mediated by insulin [122].

IR has been associated to endothelial dysfunction, glucose intolerance, dyslipidemia, hypertension, and visceral obesity [123]. During obesity, several amounts of NEFAs, glycerol, hormones, and pro-inflammatory cytokines released by adipose tissue participate in the development of IR [117]. Indeed, chronic inflammation caused by elevated pro-inflammatory stimuli and the generation of reactive oxygen species (ROS) resulting from oxidative stress may impair insulin signaling in insulin target tissues [124]. Overstimulation of inflammatory processes through cytokines secreted by visceral adipocytes predispose VAT to develop IR.

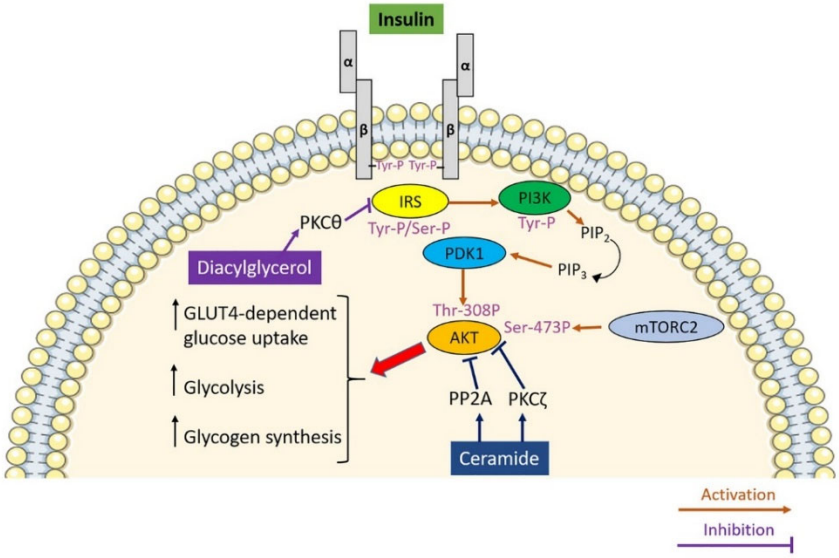

Figure 9. Insulin signaling pathway and IR development. Insulin via binding to its receptor activates a signal transduction pathway concluding in the PDK1 and mTORC2-mediated phosphorylation and activation of AKT, which, by modulating its downstream effectors, promotes glucose uptake, glycolysis, and glycogen synthesis. In obesity, Diacylglycerol inhibits insulin signaling by activating protein kinase C θ (PKCθ), which phosphorylates insulin receptor substrate (IRS) on serine residues, thus inhibiting it. In the case of increased ceramide presence, it impedes insulin signaling via two separate mechanisms involving PKCζ-induced phosphorylation and protein phosphatase 2A (PP2A)-mediated dephosphorylating of AKT. Image adapted from Domenico et al. (2019) [119].

These cytokines and saturated fatty acids contribute to activating a series of intracellular signaling pathways that impair insulin signaling, such as the IKK/NF-κB pathway, c-Jun N-terminal kinases (JNKs) and mitogen activated protein kinases (MAPKs) activation, which are responsible for serine phosphorylation of IRS-1, inhibiting insulin signaling and losing insulin sensitivity [125,126]. Apart from IR induced by inflammation, the abundance of circulatory FFAs promote the formation of lipid moieties that reduce insulin-regulated glucose metabolism [117,127]. Elevated plasma TNFα levels are positively correlated with increased DAG and ceramide content in adipose tissue in rodents and humans [128,129]. The excessive accumulation of diacylglycerol (DAG) leads to the activation of protein kinase C (PKC), which participates in the insulin signalling impairment and inhibiting GLUT4 trafficking [130]. In contrast, ceramides block insulin signalling by the inhibition of the transmission of signals through PI3K and avoiding the activation of AKT/PKB enzyme by impairing Akt2 action. [127,131] (**Figure 9**). Saturated FFAs also activate toll-like receptor 4 (TLR-4) and leads to the induction of inflammatory responses and promoting IR [117]. Indeed, in animals' models, high fat diet (HFD) is described to induce inflammation coupled to TLR-4 activation [127]. On the contrary, the lack of TLR-4 activation protected from ceramide accumulation and IR in a study with mice [132]. When the impairment of fat mobilization within adipocytes occurs, and insulin is not able to restrain lipolysis in obesity, mature adipocytes start to release cholesterol and fatty acids to the circulatory system, ending up in ectopic sites causing lipotoxicity and systemic IR. Lipotoxicity is characterized by an accumulation of fat in different non-adipose tissues with harmful and deleterious consequences [61,125,133]. In fact, increased levels of NEFAs cause IR in liver and muscle and restricts insulin secretion by the β pancreatic cells [134]. Furthermore, a growth of NEFAs circulatory concentration is related to disrupted glucose oxidation and glycogen synthesis and reduced glucose transport and phosphorylation in several tissues [135–137]. Finally, disruption of bioenergetics and redox function in the mitochondria can lead to cell death [138]. Therefore, IR in WAT induces FFA release to the circulatory system and triggers lipotoxicity, which is the ectopic fat deposition that can lead to promote metabolic disorders in insulin-sensitive peripheral tissues, such as NAFLD in the liver with fat deposition into hepatocytes called hepatic steatosis [139].

1.3 Non-alcoholic fatty liver disease (NAFLD)

NAFLD, or currently known as metabolic associated fatty liver disease (MAFLD), is the hepatic manifestation of MetS that has emerged as one of the most common causes of chronic liver diseases in the entire world [140,141], becoming one of the major health problems in the westernized countries with an incidence between 20 and 30% [140]. NAFLD has been associated with westernized diets and sedentary lifestyle, with a higher prevalence in urban regions than rural regions. Dietary patterns and sedentary habits are critical in NAFLD progression. Increased consumption of saturated fats, high carbohydrates and sweetened beverages, and the decreased consumption of vegetables, fruits, proteins, grains, and omega-3 fatty acids are key factors engaged in the pathogenesis of NAFLD [142,143]. Pathologies associated with NAFLD, obesity, dyslipidemia, IR, cardiovascular risk, T2DM and arterial hypertension have been positively correlated with NAFLD development [140,141,144], and may lead to hepatic IR, malfunctioned lipid metabolism, oxidative stress, inflammation, apoptosis, and necrosis [145,146]. The prevalence of NAFLD in diabetic patients raises up to 30-50% and to 80-90% in obese people [147].

NAFLD is a multifactorial hepatic disease that embraces a broad range of hepatic disorders. Classified by severity (**Figure 10**), It goes from a simple lipid accumulation in hepatocytes (hepatic steatosis) known as NAFL to hepatocyte ballooning, lobular inflammation and fibrosis at the most severe level called non-alcoholic steatohepatitis (NASH). These are all reversible diagnoses [148]. A worse prognosis occurs when NASH is prolonged with fibrotic progression and can lead to irreversible stages, such as cirrhosis and hepatocellular carcinoma (HCC) [149,150]. The first stage of NAFLD is characterized by more than 5% of hepatocytes with fat deposition of cytoplasmatic triglycerides in the form of macro and micro-vesicular lipid droplets. Hepatic steatosis is mainly origin from increased peripheral lipolysis resulting from adipose tissue disruption by obesity-associated IR [151]. To develop NAFLD an initial “hit” in the liver is needed, caused by the accumulation of FFAs principally derived from adipose tissue lipolysis and secondly, FFAs originated from hepatic DNL, which together can trigger IR. Thus, this “first hit” is responsible for inducing hepatic steatosis and increases the vulnerability to many factors related to the progression of the disease. These factors constitute the “second

hits", which induce a worse prognosis in the following steps associated with hepatic injury, inflammation, and fibrosis [142,152].

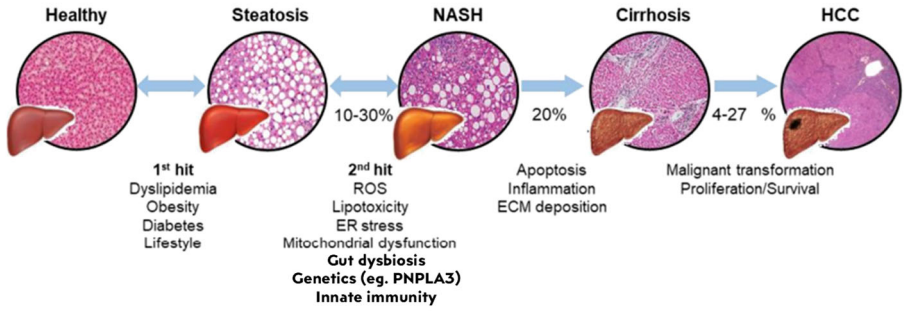

Figure 10. NAFLD progression from NAFL to hepatocellular carcinoma. Schematic representation of all the stages of the NAFLD progression with hematoxilin and eosin (H&E) staining micrographs from each state of the disease, and a description of the "multiple hit hypothesis" and probability to reach the next stage. 1st hit involves dyslipidemia, obesity, diabetes, and westernized lifestyle which can lead to hepatic steatosis development. 2nd hit involves ROS, lipotoxicity, ER stress, mitochondrial dysfunction, gut dysbiosis, genetics and innate immunity, which may trigger NASH. Apoptosis, prolonged inflammation and fibrosis, ECM deposition promote cirrhosis development. Finally, HCC can be developed by malignant transformation and cellular proliferation. ROS, reactive oxygen species; ER, endoplasmic reticulum-, ECM, extracellular matrix; HCC, hepatocellular carcinoma. Image adapted from Simon et al. (2020) [148].

These "second hits" have been described as the activation of endoplasmic reticulum (ER) stress and the increase of oxidative stress by ROS overproduction due to impaired fatty acid oxidation, followed by decreased antioxidant capacity, inflammatory cytokine production and infiltration, and collagen deposition promoting fibrosis, key features in NASH [151,153]. However, this "two-hit hypothesis" has become outdated and has been replaced by the "multiple-hit" hypothesis to explain the several molecular and metabolic changes during NAFLD development both inside and outside the liver, such as lipotoxicity, innate immune activation and the microbiome on a background of genetic and environmental factors [153]. It is evident that there are multiple factors acting and gathering synergistically to NAFLD progression. Thus, this more accurate denomination explains detailly the several concatenated processes in NAFLD development [153]. Primary hits are associated with fat accumulation in hepatocytes, which sensitize the liver to a cascade of inflammation,

while secondary hits contributed to generating free radicals, inflammatory state, and endoplasmic reticulum stress that result in mitochondrial dysfunction [154,155]. In the following sections "multiple hit hypothesis" will be explained in detail, starting with the beginning of the disease development, the mechanisms are implicated and how it progresses to further stages through all the factors required for the development of NAFLD.

1.3.1 Primary multiple hit theory: Alterations in hepatic lipid homeostasis

As aforementioned, the accumulation of fat in hepatocytes called hepatic steatosis and IR are considered as primary hits in NAFL stage. Hepatic fat accumulation is the result of the imbalance between the processes involved in the increased fat synthesis and delivery (FFAs uptake from dietary sources or lipolysis in adipose tissue and DNL) and those implicated in their elimination or export (VLDL export and fatty acid oxidation) in the liver [156]. Hepatic steatosis is produced from the esterification of FFAs and glycerol within the hepatocyte [157]. Moreover, hypercaloric diet, sedentary lifestyle and genetic predisposition are described to participate as risk factors in this "primary hit hypothesis" associated with hepatic lipid accumulation [158–160] (**Figure 11**). It was determined that approximately 60% of liver triglyceride content derived from FFA influx from adipose tissue, 26% from DNL, and 15% from diet in patients with NAFLD, whereas in healthy subjects DNL just contributes <5% in hepatic triglyceride formation [161–163].

1.3.1.1 Increased hepatic free fatty acid uptake

As explained above, an increase in the release of FFAs and triglycerides in the circulatory system due to obesity-associated adipose tissue disruption increases the excess of FFAs supply, which can end up stored in ectopic insulin-sensitive tissues. Hence, when the rate of FFAs uptake from plasma FFAs is greater than the rate of FFAs output in the liver, which depends on liver's capacity for FFA delivery and transport, lipid

fat accumulation can take place [164]. Indeed, it was found that the expression of hepatic lipase and hepatic LPL increased more in obese patients with NAFLD than subjects without NAFLD, suggesting that FFAs originated from the lysis of triglycerides contribute to hepatic steatosis development [165,166]. Moreover, the increase of these hepatic lipases could be also involved in the postprandial incorporation of dietary fatty acids into the liver inducing hepatic steatosis [164]. In addition, it has been shown that the expression of transmembrane proteins participating in FFAs uptake from plasma, such as CD36, are higher in liver and skeletal muscle but reduced in adipose tissue in obese patients with NAFLD compared with obese patients without hepatic steatosis presence [167,168]. Thus, this suggests that the dysregulated hepatic expression of fatty acid transporters may be an important factor in FFAs uptake preferably into the liver than into the adipose tissue [164]. Therefore, the combination of these explained factors can alter the hepatic FFAs uptake increasing the ectopic fat deposition into the liver promoting NAFLD development.

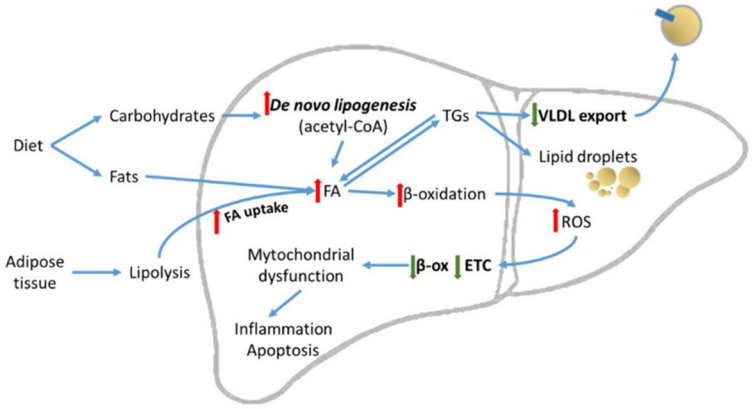

Figure 11. Principal pathways implicated in lipid accumulation during NAFLD. The increased uptake of FFAs from diet and produced by adipose tissue lipolysis, and the increased hepatic *de novo* lipogenesis associated with NAFLD promote hepatic fat accumulation stored as triglycerides (TGs). Moreover, very low-density lipoprotein (VLDL) export is reduced, which induce an increased β-oxidation for the elimination of FFAs. The consequence of this alteration in lipid metabolism is the generation of higher levels of reactive oxygen species (ROS) that leads to oxidative stress inducing a reduction of electron transport chain and β-oxidation, causing mitochondrial dysfunction, and activating inflammation and cell apoptosis. Adapted from Mato et al. 2019 [160].

1.3.1.2 Increased hepatic *de novo* lipogenesis

DNL in the liver is a metabolic mechanism in which a complex cytosolic polymerization converts acetyl-CoA to malonyl-CoA and is mainly regulated by two important enzymes: ACC and FASN [169]. Not only ACC and FASN are implicated in the molecular mechanisms of DNL, but also we find SCD1 and DGAT 1/2 , and several nuclear transcription factors that regulate these enzymes that participate in the metabolic pathway, such as sterol regulatory element-binding protein-1 (SREBPs), carbohydrate response element-binding protein (ChREBP), liver X receptor α [LXRα], farnesoid X receptor [FXR], and peroxisome proliferator-activated receptors [PPARs] [169]. Indeed, SREBP-1C is stimulated by insulin and ChREBP is stimulated by glucose, the latter is more active in tissues with DNL activity including liver and adipose tissue, and both act in synergy for the full induction of glycolytic and lipogenic gene expression in liver [170,171] (**Figure 12**).

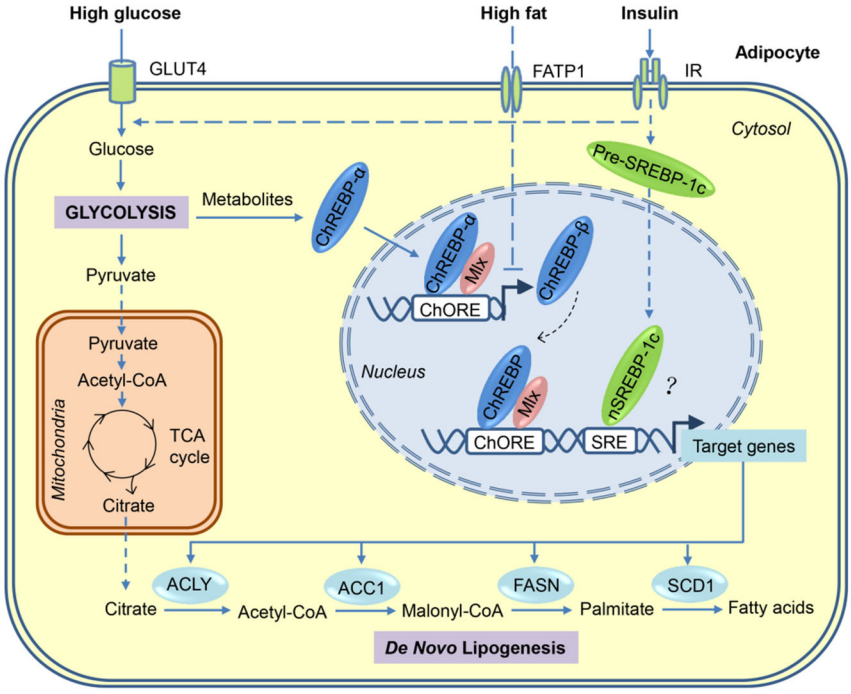

Figure 12. Transcriptional regulation of *de novo* lipogenesis process in the hepatocyte. *De novo* lipogenesis is regulated by SREBP-1c and ChREBP. The presence of high levels of glucose induces ChREBP dephosphorilation, which

facilitates the uptake of ChREBP into the nucleus and it binds with ChORE, promoting the transcription of glycolytic and lipogenic enzymes. At the same time, the secretion of insulin due to high levels of glucose induces both transcription and cleavage of SREBP-1c. Activated SREBP-1c enters nucleus and binds with SRE promoting transcription of glycolytic and lipogenic enzymes Glucose transporter 4, GLUT4; Fatty acid transport protein 1, FATP1; Insulin receptor, IR; ATP Citrate Lyase, ACLY; Acetyl-CoA carboxylase 1, ACC1; Fatty Acid Synthase, FASN; stearoyl-CoA desaturase 1, SCD1; sterol regulatory element-binding protein 1c, SREBP-1c; Carbohydrate-responsive element-binding protein, ChREBP; carbohydrate response elements, ChORE; tricarboxylic acid cycle, TCA. Image obtained from Song et al. (2018) [171].

However, lipogenic transcription factors and ACC can be restricted through phosphorylation by the AMP-dependent protein kinase (AMPK) [172,173]. As aforementioned, in healthy subjects DNL is not a big contributor of hepatic triglycerides being less than 5%, but in NAFLD patients, it increases between 15-23%. Diet is the principal contributor as an important source of both in carbohydrates and FFAs for the intra-hepatic triglycerides' formation [161,163,174]. Hence, SREBP-1C and ChREBP are associated with NAFLD, up-regulating enzymes implicated in lipogenesis, ACC isoforms and FASN [175], and a reduction of each transcriptional factor was observed to be beneficial in reducing hepatic steatosis in a study with mice [176,177]. SREBP-1C was observed increased in a NAFLD patients, whereas its ablation in KO mice was associated with decreased expression of lipogenic enzymes [178–180]. On the other hand, ChREBP has been found more associated with human NASH than patients with less severe NAFLD [181,182].

1.3.1.3 Disrupted hepatic fatty acid oxidation

Most of the intrahepatocellular FFAs are oxidated by β-oxidation, which mainly takes places in the mitochondria but also in peroxisomes [169]. Most of the key enzymes implicated in β-oxidation are regulated by PPARα, which is the most expressed PPAR in the liver [183]. The expression of CPT1 and CPT2, which allows the translocation of FFAs in acyl-CoA form, is needed to transport FFAs into the mitochondria. Finally, the resulting acetyl-CoA derived from β-oxidation will be used in the TCA cycle for total oxidation and energy generation as ATP or will be condensed in ketone

bodies [164]. In addition, NADH and FADH2 are produced during β-oxidation which are crucial for the electron transport chain [184]. CPT1 is positively modulated by PPARα, which promotes malonyl-CoA production, but is negatively regulated by malonyl-CoA produced from acetyl-CoA during DNL, inhibiting the uptake of FFAs into the mitochondria [164]. Finally, AMPK phosphorylation increases β-oxidation because DNL is inhibited and PPARα binding is induced [172].

Despite of the fact that fatty acid oxidation disruption has been associated with NAFLD, its contribution is not well described. Although an increase in β-oxidation is expected as a consequence of hepatic lipid accumulation, there are some studies that show controversies between them, and sometimes β-oxidation is found downregulated, while others upregulated, or it does not show any significant effect [185–188]. Nevertheless, a dysfunctional fatty acid oxidation characteristic in NAFLD produce elevated levels of ROS, which can induce inflammation and oxidative stress that leads to NASH development [189]. In patients with NAFLD, PPARα levels decrease [190], and PPARα KO mice fed with a high fat diet show an increase of the accumulation of hepatic triglycerides and markers of oxidative stress, inflammation, and cell death [191,192].

1.3.1.4 Hepatic Insulin Resistance

IR developed in the liver is strongly related to hepatic steatosis, contributing to human NAFLD progression [193]. Overnutrition is associated with development of IR promoting the accumulation of specific lipid metabolites, such as DAGs and ceramides, which are described to impair insulin signaling [194]. Under insulin resistant conditions, elevated rates of DNL are observed because insulin conserve its ability to promote DNL through SREBP1c while being unable to suppress gluconeogenesis [195]. SREBP1c participates indirectly in the development of IR by contributing to the accumulation of DAGS and ceramides, which are harmful lipid species [175]. Hepatic DAGs accumulation is linked to proximal defect in insulin signaling with decreased tyrosine phosphorylation of IRS-1 and IRS-2 by the insulin receptor due to an activation of a PKCε, which is overactivated in NAFLD [193]. The inhibition of IRS-1 impairs insulin-stimulated glucose transporter 2 (GLUT2) translocation and activation in

hepatocytes, resulting in IR [196]. Know-down rat models of de gene encoding PKCε fed with a high-fat diet showed a reduction of lipid-induced defects in hepatic insulin signaling [197], thereby hepatic DAGs and PKCε activation are relevant predictors of IR in NAFLD [198]. Moreover, it is believed that IR induce excessive ER stress and activate the degradation of apoB-100, which is needed for VLDL formation, thus reducing triglycerides export and aggravating hepatic steatosis [194]. In addition, adiponectin, which is an adipokine that regulates FFAs oxidation and inhibits lipid accumulation in adipocytes and hepatocytes [199], is reduced in the systemic circulation in patients with NAFLD, impairing lipid metabolism and leading to a chronic hepatic inflammation [200,201].

In NAFLD, a first ER stress response is implicated in IR and DNL during steatosis, contributing to lipid accumulation because VLDL secretion is previously impaired. Indeed, hepatic steatosis induces ER stress and, consequently ER stress promotes hepatic steatosis, contributing to NAFLD progression. Insulin sensitivity is disrupted by ER stress via different pathways [202,203].

1.3.2 Secondary multiple hit theory: Drivers of NASH progression

In the previous section, the mechanisms underlying the development of NAFLD have been explained. However, NAFLD can become harmful if it is prolonged in time by different “hits”, called NASH. In this chapter “second multiple hits” will be discussed, which promote the characteristic features of NASH, such as inflammation, fibrosis, and hepatocyte’s ballooning [149]. These drivers of NASH progression are ROS overproduction, ER stress, inflammation, mitochondrial dysfunction.

1.3.2.1 Reactive oxygen species overload

ROS are chemically reactive compounds that cells generate because of oxidative metabolism. ROS have a crucial role in cell signaling and are implicated in several mechanisms associated with free-radical-

induced lipid peroxidation, DNA strand breaks, and oxidized proteins, but also ROS are modulators of different pathways that control normal biological functions, such as signal transduction pathways, defense against invading microorganisms and gene expression to the promotion of growth or death [204]. ROS are divided into non-radical species, such as hydrogen peroxide (H_2O_2) and singlet oxygen ($^1O_2$), and radical species, including superoxide anion (O_2^-), hydroxyl radical (OH^-), alkoxyl radical (RO^-), and peroxyl radical (ROO^-) [205]. ROS levels are regulated by the consumption of antioxidants in diet, endogenous antioxidant production and systems which inactivate an excess of radicals, thereby maintain the balance between ROS and antioxidants. These antioxidants are composed by superoxide dismutase (SOD), catalases and glutathione (GSH), and participate in ROS clearance [206].

In the liver, ROS can be originated in different cell compartments during physiological processes: mitochondria, ER, and peroxisomes, even though the first one is considered the most important source [206]. In mitochondria, fatty acid oxidation and TCA cycle processes are linked to electronic transport chain to produce energy in ATP form by oxidative phosphorylation. During oxidative phosphorylation, electron transport chain transports electrons and protons through the different complexes that participate in the process, each one with higher reduction capacity than the previous one, transforming O_2 in water in the final step. However, an excessive electron flow can lead to increased ROS production caused by electron leakage from complexes I and III in the electron transport chain [184,207], also seen in NAFLD initial stages due to an increased fatty acid oxidation [208]. There are two different mechanisms that explain the ROS overproduction during NAFLD: an increased cytochrome P450 2E1 (CYP2E1) expression, which is a ROS-producing enzyme located within the ER and mitochondria that is closely associated with lipid peroxidation[209], and fatty acid oxidation in peroxisomes, producing H_2O_2. ROS overload due to a decreased detoxification associated with reduced GSH levels in NAFLD induce oxidative stress [184].

Methionine metabolism is tightly connected with impaired VLDL secretion and GSH production. Cano et al. (2011) observed that KO mice of methionine adenosyltransferase 1A gene ($Mat1a^{-/-}$) presented a development of NASH associated with disruption of VLDL export. Hence, it suggests that MAT1A is required for normal VLDL assembly [210]. MAT1A is an enzyme responsible for the metabolism of the essential amino acid

methionine (Met) into S-adenosylmethionine (SAMe), which is the most important biological methyl donor in the cell, using ATP as co-substrate [211]. SAMe is an important molecule involved in transsulfuration pathway, in which it converts the sulfur atom of methionine to cysteine and glutathione (GSH) [212]. Several animal studies demonstrated that methyl-groups deficient diet, such as methionine, choline and folate trigger hepatic steatosis and progression to NASH, fibrosis, and HCC if prolonged in time, and vice versa [213–216]. SAMe, methionine and other participants of the transsulfuration pathway are regulated by a group of enzymes present in the different cycles linked to this pathway (**Figure 13**).

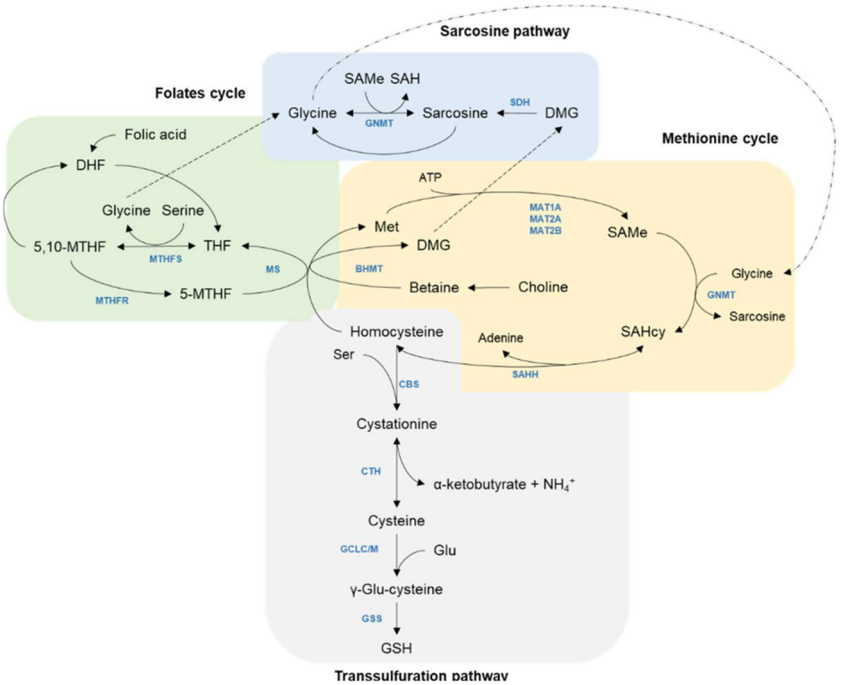

Figure 13. Representation of the transsulfuration pathway linked to the folate and methionine cycle and the sarcosine pathway. (Met, methionine; MAT, methionine S-adenosyltransferase; SAMe, S-adenosylmethionine; GNMT, glycine N-methyltransferase; SAHcy, S-adenosylhomocysteine; SAHH, S-adenosylhomocysteine hydrolase; CBS, cystathionine beta synthase; CTH, cystathionine gamma lyase; GCLC/M, glutamate-cysteine ligase, catalytic/modulator subunit; BHMT, betaine homocysteine methyltransferase; MS, methionine synthase; 5-MTHF, 5-methyltetrahydrofolate; 5,10-MTHF, 5,10-methyltetrahydrofolate; THF, tetrahydrofolate; MTHFS, 5,10-methyltetrahydrofolate synthase; MTHFR, 5,10-methyltetrahydrofolate

reductase ; DHF, dihydrofolate; DMG, dimethylglycine; SDH, sarcosine dehydrogenase). Image adapted from Dahlhoff et al. (2013) [217].

Homocysteine, which is an important substrate in the transsulfuration pathway for liver normal activity, is metabolized by cystathionine-β-synthase (CBS), and then by cystathionine gamma-lyase (CTH) generating cysteine, which is a key amino acid to produce GSH by the action of glutamate cysteine ligase (GCL) and glutathione synthase (GSS) [218]. Alternatively, homocysteine can be used to produce methionine by remethylation; however, betaine is needed as a co-substrate for this reaction. Homocysteine remethylation is regulated by betaine homocysteine methyltransferase (BHMT) and methionine synthase (MS). Regarding transsulfuration pathway in NAFLD, betaine was found reduced in obese mice [217], and deficient expression of CBS and CTH induced hepatic steatosis, inflammation, and fibrosis in animal models [219–221]. Therefore, transsulfuration pathway is essential for many metabolic processes, such as methylation, GSH production, amino acid metabolism, and H_2S production, which are crucial for a healthy liver state protecting against ROS [222].

1.3.2.2 Mitochondrial disfunction in NASH progression

Mitochondria is the main organelle that contributes as an energy source in the hepatocyte and other type of cells, and it is the major participant in the oxidative metabolism. This energy is produced as ATP and is reduced as $NADH+H^+$ and FADH2 in the mitochondria. The three principal convergent pathways needed for the generation of energy are β-oxidation, TCA cycle, and electron transport chain. However, mitochondrial activity is disrupted by lipid accumulation during NAFLD [223]. Although it is not clear whether mitochondrial dysfunction is a cause or a consequence of NAFLD progression to NASH, several studies point out that it is one of the causes that participates in NASH development [184,207]. In addition, hyperglycemia has been suggested to induce hyperpolarization of the mitochondrial membrane, which leads to mitochondrial dysfunction and high risk of the collapse of potential membrane promoting cell apoptosis [224]. If mitochondrial function cannot deal with the increase of lipid flux, oxidative metabolism can collapse with the impairment of lipid

homeostasis, generating lipid-derived toxic metabolites and ROS overload [69,209]. All these affections contribute to inflammation in hepatocytes and worsen mitochondrial damage [225]. Furthermore, various proteins, specially PGC1α, that are implicated in mitochondrial biogenesis and electron transport chain were observed downregulated in NAFLD mice model [226]. Additionally, electron transport chain complexes activity was found altered in human NASH patients and in a NASH mice model [227,228]. Hence, electron transport chain impairment is critical in mitochondrial dysfunction during NASH progression and is associated with the progressive reduction of energy status and ATP levels during NASH. Therefore, the increased oxidation activity in the mitochondria during NAFLD can induces ROS overproduction, which can lead to mitochondrial dysfunction and electron transport chain deficiency. Both affections contribute to the induction of inflammation and fibrosis, hallmarks in NASH progression (**Figure 14**).

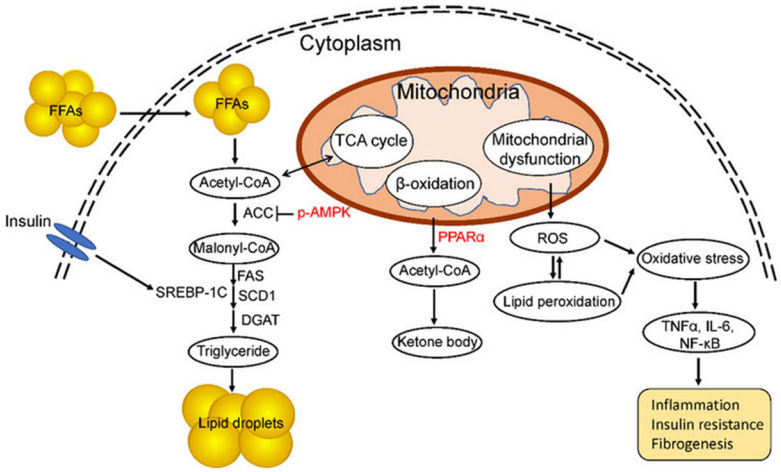

Figure 14. Schematic representation of mitochondrial dysfunction in the progression of NAFLD and NASH. De novo lipogenesis plays a crucial role in the development of NASH. Acetyl-CoA is a substrate for fatty acid synthesis, and circulating insulin induces the expression of SREBP-1c and its target genes encoding lipogenic enzymes. Phosphorylation of AMP -activated protein kinase (AMPK) inhibits acetyl-CoA carboxylase activity (ACC), thereby reducing fat accumulation. Peroxisome proliferator-activated receptor (PPAR) α catalyzes β-fatty acid oxidation in mitochondria. Mitochondrial dysfunction increases the production of ROS and lipid peroxidation, leading to high levels of oxidative stress, chronic inflammation, and fibrosis in the liver. Obtained from Xu et al. (2019) [69].

1.3.2.3 From inflammation to Fibrosis in NASH progression

Lipotoxicity is a combination of alterations in hepatocytes that induce the release of pro-inflammatory cytokines, such as TNFα, IL-1β, and IL-6, downregulating hepatic insulin sensitivity through inhibition of IRS-1 and 2, and it contributes to inflammation and fibrosis among other alterations explained above [229]. When hepatocytes release damage-associated molecular patterns (DAMPs), it triggers activation of inflammatory pathways (**Figure 15**). If this activation is prolonged in time, it results in chronic inflammation with chronic injury. The principal target of DAMPs are Kupffer cells (KCs) and hepatic stellate cells (HSC), which promote inflammation and fibrosis respectively [230]. KCs are the resident macrophages in the liver situated in the hepatic sinusoids, the portal tract and hepatic lymph nodes [231]. In NAFLD progression, KCs activation is a key factor in the induction of inflammation by the recruitment of other immune cells [232]. As explained above, KCs present two phenotypes classified in activated M1 macrophages and alternative M2 phenotype. The macrophages markers F4/80, CD11b, and CD68 are expressed on KCs [233]. There are some activators of the M1 phenotype of KCs. Pathogen-associated molecular pattern molecules (PAMPs) and lipopolysaccharides (LPS), which are bacterial products originated in the gut that arrives in the liver via portal vein, are activators that binds to TLRs in KCs [234]. Other activators are cytokines and chemokines and adipokines, such as TNFα, IL-1β, IL-6 and CCL2, that come from disrupted adipocytes [229] and have a key implication in the local inflammation by triggering DAMPs release. DAMPs activate KCs through TLRs binding, developing a vicious inflammatory process [230]. Lastly, lipid overload can activate KCs by lipid-derived toxic metabolites determining the overexpression of TLRs [235].

In contrast, although M2 macrophages are implicated in anti-inflammatory cytokines secretion, the implication in NAFLD/NASH is still undefined [231]. Furthermore, KCs are responsible in secretion of tumor growth factor-b (TGF-b) and platelet-derived growth factor (PDGF) that are detected by HSCs, which is the major myofibroblastic cell in the liver responsible for collagen production and scar formation, through the mitogenic stimuli of these factors promoting fibrosis [230]. Once HSCs are activated, they migrate across the liver, getting accumulated in damaged

sites and replacing injured or dead hepatocytes while secreting extracellular matrix [236].

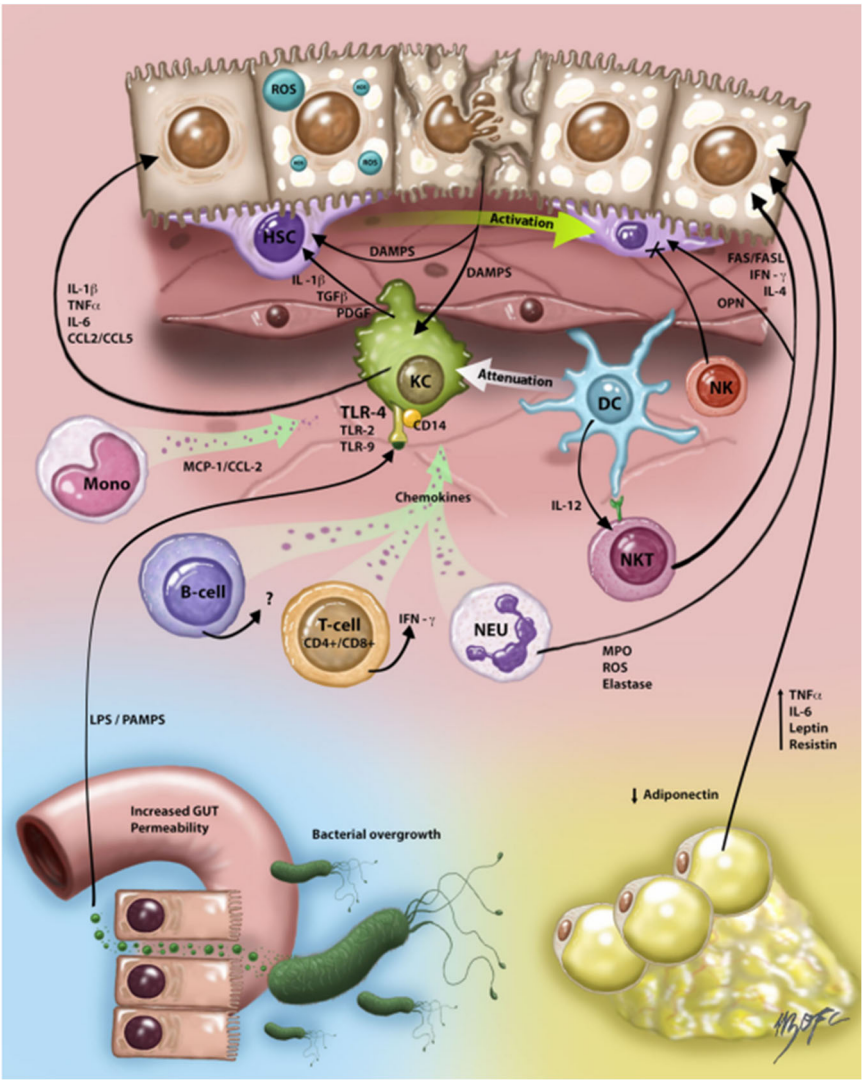

Figure 15. The inflammatory response in NAFLD/NASH through innate and adaptative immune activation. Damage-associated molecular patterns (DAMPs); Kupffer cells (KCs); hepatic stellate cells (HSC); tumor necrosis factor-alpha (TNFα); interleukin-1β (IL-1β); interleukin-6 (IL-6); C–C motif ligand 2 and 5 (CCL2 and CCL5); tumor growth factor-b (TGF-b); platelet-derived growth factor (PDGF); pathogen-associated molecular patterns (PAMPs); lipopolysaccharides (LPS); natural killer (NK) T cells (NKT); interleukin-4 (IL-4); osteopontin (OPN); interferon-gamma (IFN-c); FAS ligand (FASL); neutrophils (NEU); reactive oxygen

species (ROS); Dendritic cells (DCs); monocyte (Mono); toll-like receptor (TLR). Image obtained from Arrese et al. (2016) [230].

Activated and recruited KCs are key participants in the development of NASH by recruiting inflammatory immune cells and secreting chemokines. CCL2 released by KCs attracts bone marrow-derived macrophages into the liver [199]. Indeed, increased levels of CCL2 are observed increased in serum and liver in NASH patients [237]. On the other hand, bone marrow-derived monocytes, which are infiltrated in response to an inflammatory stimulus, act as drivers of steatohepatitits through CCL2-CC2 axis mainly. These proinflammatory monocytes express CC-chemokine receptor 2 (CCR2) that binds with CCL2 in KCs and together induce chemotaxis of KCs and activate HSC in the liver, contributing to inflammation and fibrosis in NASH development [230,238].

In the case of neutrophils, KCs secret CXCR1 and CXCR2 to attract this type of immune cells, which are characterized by released ROS, elastase and proteases promoting hepatic necrosis [239]. On the other hand, natural killer (NK) cells are lymphoid cells that are important in the link between innate and adaptative immune responses in the liver. NK-T cells are recruited together with $CD4^+$ and $CD8^+$ lymphocytes through chemokines secreted by KCs, and these lymphocytes are identified as the main drivers of inflammation [230]. Specifically, NK-T cells regulate a cluster of immune responses and produce Th1 or Th2 cytokines, but in NASH NKT promote an unbalanced production of Th1 cytokines. Moreover, NKT cells secrete osteopontin, interferon-gamma (IFN-γ), IL-4 and of hedgehog ligands promoting collagen mRNA and leading to fibrogenesis [240,241]. Therefore, NKT enhanced together with $CD4^+$ and $CD8^+$ steatosis, NASH development, and transition to HCC.

1.4 Gut-liver axis and the adipose tissue

The gut-liver axis is a concept that defines the physiological cross-talk between the liver and the intestine which are connected through the portal vein. A cluster of signals are evoked with relevant immunological and metabolic effects that affect both gut and liver, in which the gut microbiota also participate [231,232]. Gut microbiota modifications can occur in relation with different factors, such as diets, antibiotics use, and alcohol

abuse [242]. In normal conditions, the liver has an important role in the clearance of gut-derived LPS and other bacterial products which reach the liver via the portal vein [230]. In obesity, LPS levels and other bacterial-derived compounds increase in the portal blood, inducing the activation of hepatic TLRs and leading to local inflammatory and fibrogenic processes. Moreover, obesity is associated with downregulation of intestinal tight-junctions' proteins (*i.e.*, zonula occludens-1 (ZO1) and occludin), which are crucial for the permeability of the intestinal barrier, observed in NAFLD patients [243,244]. When the expression of intestinal tight junctions is disrupted, intestinal barrier is more permeable, thereby facilitating LPS and other bacterial-products filtration to the portal vein, activating TLRs and inducing a local chronic inflammatory state that may cause liver injury [245,246]. As aforementioned, both adipose tissue dysfunction and intestinal dysbiosis are external factors implicated in the "multiple hit" hypothesis of the NAFLD development. On the one hand, as explained in the section 1.2.3, adipose disruption is implicated because insulin-resistant adipose tissue leads to disrupted lipolysis releasing FFAs to the systemic circulation ending up in ectopic fat accumulation in the liver and other insulin-sensitive organs promoting lipotoxicity. On the other hand, the second will be explained in the next section 1.4.2 **Manuscript 1**, focusing on the effect of diet, gut microbiota, and gut dysfunction on the development of NAFLD

1.4.2. MANUSCRIPT 1

Literature review

Diet, Gut Microbiota and Non-Alcoholic Fatty Liver Disease: Three Parts of the Same Axis

Sergio Quesada-Vázquez, Gerard Aragonès, Josep M Del Bas and Xavier Escoté

Published by *Cells* (Impact factor 7.666)

January 2020; Volume 9 (1): pp. 176

JCR category rank: Q1: Biochemistry, Genetics and Molecular Biology (miscellaneous)

cells

MDPI

Review

Diet, Gut Microbiota and Non-Alcoholic Fatty Liver Disease: Three Parts of the Same Axis

Sergio Quesada-Vázquez [1], Gerard Aragonès [2], Josep M Del Bas [1] and Xavier Escoté [1,*]

[1] Unitat de Nutrició i Salut, Centre Tecnològic de Catalunya, Eurecat, 43204 Reus, Spain; sergio.quesada@eurecat.org (S.Q.-V.); josep.delbas@eurecat.org (J.M.D.B.)
[2] Department of Biochemistry and Biotechnology, Universitat Rovira i Virgili, Nutrigenomics Research Group, 43007 Tarragona, Spain; gerard.aragones@urv.cat
* Correspondence: xavier.escote@eurecat.org; Tel.: +34-977-302057 (ext. 4824)

Received: 15 December 2019; Accepted: 7 January 2020; Published: 10 January 2020

Abstract: Non-Alcoholic Fatty Liver Disease (NAFLD) is the most common liver disease in the world. NAFLD is principally characterized by an excessive fat accumulation in the hepatocytes. Diet is considered as one of the main drivers to modulate the composition of gut microbiota, which participate in different processes, affecting human metabolism. A disruption in the homeostasis of gut microbiota may lead to dysbiosis, which is commonly reflected by a reduction of the beneficial species and an increment in pathogenic microbiota. Gut and liver are in close relation due to the anatomical and functional interactions led by the portal vein, thus altered intestinal microbiota might affect liver functions, promoting inflammation, insulin resistance and steatosis, which is translated into NAFLD. This review will highlight the association between diet, gut microbiota and liver, and how this axis may promote the development of NAFLD progression, discussing potential mechanisms and alterations due to the dysbiosis of gut microbiota. Finally, it will revise the variations in gut microbiota composition in NAFLD, and it will focus in specific species, which directly affect NAFLD progression.

Keywords: Non-Alcohol Fatty Liver Disease; gut microbiota; NAFLD; dysbiosis; bacterial translocation

1. Introduction

Non-Alcohol Fatty Liver Disease (NAFLD) is the most common liver disease in the world [1]. An incidence between 20% and 30% is estimated within of the adult population in Western countries. Meanwhile, in Eastern societies, this disease presents a lower prevalence, although some recent studies are pointing at the fact that its incidence is rising due to changes in Eastern nutritional habits, together with a decreasing of physical activity that is typical of a sedentary lifestyle ("Westernized society") [2]. Regarding nutrition, an improper and excessive intake of saturated fats and caloric oversupply, together with a low intake of vegetables, fruits, proteins, grains and ω3-fatty acids, are key causes to develop NAFLD [3].

NAFLD is principally characterized by an excessive fat accumulation in the hepatocytes (hepatic steatosis). Although NALFD shares many characteristic features with alcoholic liver disease (ALD), NALFD is not induced by the consumption of toxic levels of alcohol [4]. The excessive fat accumulation in the liver is strongly associated with multifactorial risk factors such as obesity, leptin and insulin resistance (IR), dyslipidemia and metabolic syndrome. However, these processes and the causality of these factors are not fully understood [5,6].

NAFLD shows two main stages: The most common stage is nonalcoholic fatty liver (NAFL), a non-progressive and less-dangerous state of the liver condition, whereas nonalcoholic steatohepatitis (NASH) is less frequent, but its potential progression to advanced liver damage is worryingly

difficult to revert, and could trigger worst diagnoses such as fibrosis progression, cirrhosis or even hepatocarcinoma (HCC) [2,7]. The principal causes of NASH are steatosis, hepatocyte ballooning and lobular inflammation, and it can only be diagnosed by liver biopsy, which is the only existing reliable diagnosis method nowadays [7]. Several studies have also described age and obesity as risk factors to develop NAFLD, but there are other less known factors that need to be further studied, such as the role of gut microbiota in the NAFLD progression.

Gut microbiota is a complex and dynamic community of different microorganisms which are in symbiotic relationship with the host, exerting a marked influence on several aspects of the host metabolism, maintaining immune health, participating in the metabolic homeostasis and protecting the host against pathogenic infection [8]. Diet is considered as one of the main drivers to modulate the composition of gut microbiota in terms of species richness. Dysbiosis, which is defined as any alteration that affects gut bacterial composition, and is commonly reflected by a reduction of the species number, has been associated with the pathogenesis of several inflammatory diseases and potential infections [9]. These studies foster a better understanding of interindividual species' variations, the heterogeneity of bacterial communities along and across the intestinal tract, functional redundancy and the need to distinguish the cause from the effect in states of dysbiosis. Mainly, six different phyla are present in the gut microbiota: *Firmicutes, Bacteroidetes, Proteobacteria, Verrucomicrobia, Actinobacteria* and *Fusobacteria* [9]. As previously mentioned, these bacteria might participate in different important processes that affect the human metabolism, including the fermentation of diet polysaccharides, the regulation of bile acid production, the contribution to regulate the choline metabolism and the processes of energy harvest, providing protection against pathogens or even stimulating the endogenous ethanol production [10,11]. Thus, microbiota contribute to the whole intestinal homeostasis. Despite the numerous beneficial aspects of the gut microbiota over host homeostasis, sometimes an excessive proliferation of particular species may be translated into an overproduction of some metabolites that may exert a harmful effect for the intestine and even provoke a systemic inflammation in the worst scenario [12].

Gut and liver are in close relation due to anatomical and functional interactions led by the portal vein [13]. Indeed, the portal vein supplies 70% of the total amount of blood in the liver, thereby the liver is exposed to factors that are mostly originated from the gut. These factors are nutrients and metabolites needed for a proper homeostasis. In other cases, the liver can receive other products directly originated by the gut microbiota, such as endotoxins, peptidoglycans and even complete bacteria, which may cause a large deregulation of several metabolic pathways presented in the liver [14]. This constant influx of microbial-derived products from the intestine to the liver generate a response from pathogen-recognition-receptors located at plasmatic membrane of several hepatic cells, such as the Kupffer cells (stellate macrophages), sinusoidal cells, biliary epithelial cells and hepatocytes [14]. Numerous studies have demonstrated that altered intestinal microbiota might affect in some way the liver functions, causing inflammation, insulin resistance (IR), and fat accumulation, which is translated into obesity and NAFLD as well [15]. In the present study, we have reviewed the latest studies to categorize the effects of intestinal dysbiosis, the role of the diet in this disruption, and the identification of specific gut bacteria mainly associated with NAFLD progression.

2. Effects of Dysbiosis in the Gut Microbiota

Gut microbiota is a highly dynamic entity and presents a constant flow in its composition. These variations in the percentages of different bacterial species depend upon several environmental factors with different impacts in the gut microbiota composition. Among others, these environmental factors include the intestinal mucosa state (which directly affects the degree of permeability of the gut barrier), the immune system health of the host (which promotes an increased proliferation of particular and hazardous species in case of immune deficits), drugs presence (because some bacteria are more sensitive to particular medicines which allow proliferation of other species to occupy the empty niche), the type of diet (food rich in fats, fiber or some phytochemicals directly affects the proliferation of

specific bacteria) and even other microbiota members [9]. Therefore, these environmental factors might produce stressful culture conditions that can alter the natural composition of the gut microbiota by decreasing microbial diversity, known as dysbiosis, and they may be the cause of increased risk to develop some diseases [16]. Indeed, dysbiosis is directly related with an increased intestinal permeability as a consequence of some aspects, including the epithelial barrier deterioration, small intestinal bacterial overgrowth, tight junctions' alteration, and even the whole bacterial translocation, causing endotoxemia, which might reach and damage the liver through the portal vein [11,17–19].

2.1. Obesity and HF Diets Lead to Gut Microbiota Dysbiosis

Microbiota plays a role in obesity development, and that was confirmed in different studies [20]. Food oversupply, food shortage or even changes on food composition are facts that may contribute to a dysbiosis state [21]. Indeed, preclinical studies using different mice models have demonstrated that both obesity and a specific diet that drives to obesity (known as a high fat diet (HFD), characterized by a higher percentage of energy in the form of saturated lipids), induce gut microbiota dysbiosis and an overgrowth of some bacteria phyla and a reduction of other phyla, which cause undesired consequences, such as intestinal inflammation or epithelial barrier disruption [22]. Moreover, in some HFD models, it has also been suggested that gastrointestinal microbiome alterations may affect NAFLD pathogenesis by enhancing its development through different pathways, including an increase of energy harvesting, a rise in metabolism harvesting and an increase in the expression levels of some pro-inflammatory cytokines in liver cells [23]. Additionally, some studies have demonstrated differences in the gut bacterial composition between healthy patients and patients with obesity-related NAFLD, which may suggest a connection between gut microbiota dysbiosis and obesity-related NAFLD progression [24].

An archetypal Western diet is generally characterized by high intakes of red and processed meats, pre-packaged foods, butter and fried foods, high-fat dairy products, eggs and high-sugar drinks. Thus, a Western diet is not only associated with a higher susceptibility to develop obesity, but also to several metabolic disarrangements, some of which are regulated through the signaling pathway of the Toll-like receptor (TLR) family, which is activated by lipopolysaccharide (LPS, a component of the outer membrane gram-negative bacteria) [25].

2.2. Role of LPS in Gut Microbiota Dysbiosis

When LPS levels increase in the human systemic circulation, it may indicate a potential dysbiosis of the gut microbiota [26]. NAFLD and obesity are associated with higher gut barrier permeability, causing metabolic endotoxemia and an increase in the blood levels of LPS. Subsequently, it also causes hepatic and systemic inflammation as well as alterations in gene expression, hormone secretion, and energy consumption in distal peripheral tissues, such as the white adipose tissue [27]. This LPS role was corroborated in a preclinical study in which mice injected with LPS showed a similar phenotype than those obtained after a high fat diet (body weight gain, IR and increased NAFLD progression) [15]. Besides, *in vitro* studies have demonstrated that fatty acids can promote LPS absorption, presumably by inducing endoplasmic reticulum stress in epithelial cells and inhibiting the formation of tight junctions between these cells [13].

2.3. Role of Short-Chain Fatty Acids (SCFAs) in Gut Microbiota Dysbiosis

Another metabolic disarrangement, and a consequence of the Western diet, is an altered pattern of the short-chain fatty acid (SCFA) production [25]. SCFAs are mainly derived from intestinal microbial fermentation of indigestible food when dietary fibers are fermented in the colon [28], and afterwards, these SCFAs can be absorbed by the intestine [29]. Acetate, propionate and butyrate are the three most common SCFAs [30], and during lipid digestion, SCFAs are primarily absorbed and reach the liver through the portal vein, where acetate can be used as an energy source [31–33].

Saturated fatty acid (SFA) can also promote a mitochondrial dysfunction because of changes in the endoplasmic reticulum due to oxidative stress, impaired phospholipid metabolism and raised IR.

These affections could induce hepatic steatosis, promoting liver inflammation via an enhancement of LPS-induced inflammasomes in hepatocytes [34,35].

2.4. *Effect of Choline Deficiency in Gut Microbiota Dysbiosis*

In the liver, lipids from the diet, together with apolipoproteins, cholesterol, cholesteryl esters and triglycerides, are assembled to form the nascent very-low-density lipoprotein (VLDL) [32]. VLDL production and the hepatic lipid transfer are modulated by dietary choline, and the choline metabolism is affected by the gut microbiota dysbiosis [33]. In fact, choline-depleted diets are applied in animal models to induce NAFLD, and this liver alteration is reflected into lowered amounts of VLDL and a reduced lipid β-oxidation [33]. Consequently, choline depletion causes cholesterol metabolism disorders, alterations in the c-ytokines pattern, increased hepatocyte oxidative stress and a higher deposition of fatty acids, which triggers inflammation, lipotoxicity and fibrosis [33]. In parallel, choline deficiency is modulated by the conversion of choline to trimethylamine (TMA) [34]. It has been demonstrated that gut bacteria are essential to transform the dietary choline into TMA [31]. TMA can be absorbed and metabolized in the liver into trimethylamine N-oxide (TMAO) [35], which is a metabolite that seems to be involved in the development of metabolic diseases acting as a link between inflammation and obesity [36]. TMAO affects the liver through modulating glucose metabolism, causing inflammation in the adipose tissue and influencing lipid absorption and cholesterol homeostasis [37].

2.5. *Role of Bile Acids in Gut Microbiota Dysbiosis*

Bile acids are amphipathic molecules synthesized in hepatocytes as primary bile acids (cholic acid and chenodeoxycholic acid), both secreted in the lumen of the duodenum, where the bacterial flora transform them into the secondary bile acids (deoxycholic acid and lithocholic acid) [35]. All four of these bile acids can be reabsorbed into the gut and returned to the liver in a process known as enterohepatic circulation [35]. One of the main physiologic functions of bile acids is to emulate fats and bring them near the intestinal brush border membrane, which results in fat absorption in the gut [36]. Besides, HFD modifies the bile acid composition, which might influence the environment in the gut and cause changes in the intestinal conditions, which are more susceptible to induce a dysbiosis state [37]. Moreover, bile acids have other metabolic actions in the body resembling those of hormones, acting through the specific farnesoid X receptor (FXR or bile acid receptor (BAR)), which develops a key role in the control of hepatic de novo lipogenesis, VLDL and plasma triglyceride turnover [38,39]. In fact, a study demonstrated that gut microbiota is able to modify bile acid secretion through FXR stimulation, thereby fostering lipid peroxidation and hepatic steatosis [40]. Finally, bile acids have bacteriostatic and antimicrobial properties that foster a reduction of the microbiota found in the small intestine and biliary tract [41]. Therefore, dysbiosis may induce changes in the bile acids' production and intestine reabsorption, and at the same time, a reduction in the bile acids' secretion allows the proliferation of a particular bacterial species, becoming a vicious circle of microbiota dysbiosis.

2.6. *Effect of Endogenous Alcohol in Gut Microbiota Dysbiosis*

Other processes that can be affected by the gut microbiota dysbiosis is the endogenous ethyl alcohol production through the fermentation of carbohydrates in the intestinal lumen [42]. Endogenous ethyl alcohol reaches the liver by the portal vein, which contributes to induce the liver damage that aggravates the pathology of NAFLD [42]. Indeed, there was ethyl alcohol detected which was exhaled in the breath in obese mice, although these animals were not fed with any alcohol [43]. Besides, clinical studies have demonstrated that NAFLD patients presented higher levels of blood ethanol concentrations (BACs) than healthy patients, suggesting that the worsening liver damage was contributed by endogenous ethanol production [42–44].

Thus, to deeper understand the processes that conducts to intestinal dysbiosis, it is necessary to identify the factors and mechanisms which originate the changes of gut microbiota in order to design accurate strategies aimed to prevent and to treat intestinal dysbiosis.

3. Role of Diet in NAFLD Progression and Gut Microbiota Dysbiosis

As commented in previous sections, NAFLD is strongly related with obesity [41]. As expected, in the NAFLD patients, mRNA expression of fatty acid synthase (FAS, a key enzyme in the hepatic de novo lipogenesis) increased, together with the LPS receptors TLR2 and TLR4. Consequently, the circulating levels of gut microbiota-derived metabolites were analyzed observing that TMAO, glycocholic acid and deoxycholic acid plasma levels were significantly increased in NAFLD patients, suggesting the use of circulating microbiota-derived metabolites as a scoring system for the clinical diagnosis of NAFLD [45]. The up-regulation of lipogenic genes due to a high intake of saturated fatty acids (SFAs) triggers triglyceride (TG) formation [46]. TGs from dietary fats are metabolized to diglycerols, monoacylglycerols and fatty acids in the intestinal lumen and transported by enterocytes to the portal vein, where finally fatty acids are introduced in hepatocytes [47]. These fatty acids might be saturated or unsaturated (monounsaturated fatty acids, MUFAs, or polyunsaturated fatty acids, PUFAs) with a different impact upon hepatic health. Indeed, it is described that the concentration of MUFAs is increased in NAFLD patients compared to healthy controls [48]. In contrast, lower circulating levels of n-3 PUFAs negatively affects β-oxidation, meaning a reduction in liver lipid oxidation, which supports the idea of a link between a low dietary intake of PUFAs and NAFLD progression [48], whereas excess n-6 PUFAs are more related with steatohepatitis by induction of the intracellular oxidative stress, hepatocellular injury inflammation [49].

Besides, gene expression involved in adipose tissue lipid storage can be upregulated by microbiota, as demonstrated in different studies in animals and humans [50,51]. Therefore, the diet is an important exogenous factor, which directly contributes to the health state of the liver and the gut microbiota. Other key energy nutrients are sugars and an excessive energy consumption in the form of carbohydrates, especially fructose, which is a major risk of NAFLD development and severity of the disease [52]. Fructose is highly used in processed foods and beverages, and these products have usually been consumed in higher quantities by NAFLD patients, causing higher lipogenesis by upregulating the activity of the critical transcription factor, the sterol regulatory-element binding protein-1c (SREBP-1c), which promotes mitochondrial dysfunction [53]. Moreover, high amounts of fructose participate in the development of hepatic oxidative stress [54] and may also inhibit β-oxidation, which increases the amount of TG in the liver [55]. In addition, lower fiber, polyphenols, vitamins and mineral nutrients' intake is associated with the development and progression of NAFLD [56,57].

Deficiency in both Vitamin D and copper increase the risk of inducing NAFLD [58,59]. Vitamin D inhibits liver fibrosis through the transforming growth factor beta (TGF-β) pathway and IR by the induction of the hepatic resistin [60]. In addition, deficiency of vitamin D stimulates the oxidative stress and inflammation of the liver via activation of some hepatic TLR receptors members [61]. On the other hand, deficiency in copper also promotes IR and hepatic steatosis, leading to lipid peroxidation [62]. Presence of high amounts of fructose also aggravates this situation, impairing copper absorption into the intestine, which contributes to enlarge liver damage [62]. Finally, polyphenols have been suggested as beneficial bioactive compounds for the prevention and the treatment of NAFLD. Notably, several studies have shown that polyphenols, including quercetin, epigallocatechin gallate, anthocyanins and resveratrol, can prevent the development of NAFLD by exerting lipid-lowering, antioxidant, anti-inflammatory and antifibrotic effects [63].

Taken together, it seems well established that diet may modulate NAFLD progression, and at the same time, diet is able to transform intestinal flora to a healthier or more harmful microbiota profile, making it necessary to deeply explore the straight connections between gut dysbiosis and non-alcoholic fatty liver disease.

4. How Variations in the Taxonomic Composition of the Gut Microbiota Affects NAFLD Progression

Several studies have obtained similar results regarding the differences at taxonomic level between the gut microbiota of healthy subjects and patients affected with NAFLD [29]. Usually theses variations

might be beneficial for a resilience of the gut microbiota, but if a continuous external stimulation is stressful and disruptive, it might trigger unstructured microbiome, and dysbiosis contributes to NAFLD progression [29].

4.1. Changes at the Phylum Level

In the human gut, there are two dominant phyla of bacteria, *Bacteroidetes* and *Firmicutes*, which represent 90% of gut microbiota, and in less proportion, others phyla: Actinobacteria, Proteobacteria, *Fusobacteria*, and *Verrucomicrobia* [9,58]. Studies based on animal models have reported that HFD increases *Firmicutes* and *Proteobacteria* proportion, raising the ratio *Firmicutes:Bacteroidetes* [64]. On the contrary, human studies based in high-fat intake have demonstrated an opposite effect, with a decrease in *Firmicutes* and *Proteobacteria* proportion together with an increase of the *Bacteroidetes* [59]. In the same direction, a study comparing the gut microbiome between lean subjects and NAFLD patients, observed an increase of 20% in *Bacteroidetes* and a decrease of 24% in *Firmicutes*, with a higher gram-negative bacteria concentration, which showed an increase of the presence of pathogenic bacteria that produce LPS in NAFLD patients [20,63]. Reduction in *Firmicutes* is mainly a consequence of a decrease in SCFA-producing bacteria, such as the *Lachnospiraceae, Lactobacillaceae*, and *Ruminococcaceae* families [64]. Differences in the composition of the microbiota phylum between human and animals might be due to the differences in the type of fat that animals and humans consumed and absorbed [59]. Indeed, in animals' models, it is described that an imbalance between the *Bacteroidetes* and *Firmicutes* ratio can alter mucin glycosylation [61]. In another human study, the abundance of *Firmicutes* and *Bacteroidetes* were similar between obese subjects and NASH patients, observing higher levels of *Proteobacteria* in NASH patients [42] and highly represented in fibrosis [62].

In one study it is described that ethanol-producing bacteria, from the phyla *Proteobacteria*, increased in metabolic abnormalities [65] and in NAFLD patients [66], contributing to intensify liver pathogenesis [66]. Moreover, it is reported that these heterolactic bacteria are involved in compromising the intestinal barrier integrity (leading a breakdown of the epithelial barrier), which compromise initiates mucosal inflammation and finally produces additional hepatoxical events [43], [66,67]. In addition, *Lentisphaerae*, a phylum with low representation in the gut microbiota, is observed being decreased in NAFLD patients in comparison with healthy patients [67]. Finally, *Fusobacteria* (a phylum with more bacterial pathogens, together with *Proteobacteria*) increased about 2.76% in NAFLD patients, causing the increase of the microbial gut toxins' level [68].

4.2. Variations at the Family and Genus Level

Although there are many clinical and animal studies about changes at the family and the genus levels associated with NAFLD presence, those results are controversial [23]. In a mice model fed with HFD, whose members develop steatosis and metabolic disorders, gut microbiota was compared to the control-fed group, observing an increase of the *Barnesiella* and *Roseburia* genus and a decrease of the *Allobaculum* genus in the HFD group [23]. A clinical study compared the gut microbiome of 30 NAFLD patients *vs*. 30 healthy subjects and showed higher levels of those of the *Lactobacillaceae* and *Lachnospiraceae* families, but lower levels of the *Ruminococcaceae* family in NAFLD patients [68]. Furthermore, and in the genus level, were over-expressed the genera *Lactobacillus, Dorea, Robinsoniella* and *Roseburia*, but there was also under-represented the *Oscillibacter* in the same NAFLD patients [68].

These results were partially supported by a prospective cross-sectional study with 39 patients, being biopsy-proven of having NAFLD, observing that *Lactobacillaceae* family and *Lactobacillus* genus increased in the patients compared to healthy controls, whereas the *Coprococcus* and *Ruminococcus* genus levels decreased [69]. However, in obese children with NAFLD, there was observed an increase in the *Prevotellaceae* family because of the higher levels of the *Prevotella* genus [70].

Some studies found differences between healthy subjects and NAFLD patients and also between NAFLD early stages and NASH. One study viewed how the *Enterobacteriaceae* family and *Escherichia* genus were more present in NASH microbiota than in obese subjects, presenting a significantly elevated

ethanol level in blood that probably contributed to the liver physiopathology [42]. A big difference found in a clinical study between NAFLD and NASH was the increased abundance of *Bacteroides* genus associated with the NASH presence [71]. *Bacteroides* caused an increase in the deoxycholic bile acid levels, which is related with the induction of apoptosis in hepatocytes [71]. These increases of the abundance of *Bacteroides* in NASH was inversely related to a decrease in *Prevotella* levels, contrary to the results obtained with NAFLD patients, in which this *Prevotella* level increased [71]. It might be a consistent finding due to the fact that *Bacteroides* and *Prevotella* are niche competitors, and the diet is a key contributor to influence in the levels of these genera in the gut: A Western diet is favorable for *Bacteroides*, whereas diets based on vegetables, fruits, plants polysaccharides and food rich in fiber are favorable for *Prevotella* [72]. Moreover, in the advanced stages of fibrosis, the genus increased was *Ruminococcus* [71], and in this genus there are species producers of alcohol, which could drive additional harmful actions on intestinal permeability and hepatic inflammation [72].

4.3. Variations of Specific Bacteria Associated with NAFLD

Several studies have enumerated the contribution in the NAFLD progression of specific gut microbiota bacteria affecting different processes: SCFAs homeostasis, de novo lipogenesis; VLDL metabolism; bile acid homeostasis; endogenous ethanol formation and increased levels of LPS, which is related to an inflammatory response in hepatocytes (Table 1) [73]. In this section, we will review recent studies that explain the contribution of some bacteria from the gut microbiota in the NAFLD physiopathology.

Table 1. Summary of bacteria that are directly related to the progression of Non-Alcoholic Fatty Liver Disease (NAFLD).

Bacteria Species	Characteristics	Main Effects	Experimental Models	Refs.
Faecalibacterium prausnitzii	*Firmicutes* phylum. Butyrate-producing bacteria. >5% of the total gut microbiota in healthy humans.	↓ [*F. prausnitzii*] → >5% fat hepatic content and ↑ adipose tissue inflammation in humans. ↑ [*F. prausnitzii*] → Lower lipid content, ↓ ALT and ↓ AST, ↑ *CDKN1A* (inversely correlated with NAFLD), ↓ hepatic fibrosis.	Clinical study with 31 participants with high hepatic fat content. HFD mice fed with *F. prausnitzii* vs. control mice and HFD mice not fed.	[74,75]
Bilophila wadsworthia	Gram-negativeBacteria. *Proteobacteria* phylum. Associated with diets rich in fat.	↑ [*Bilophila wadsworthia*] → ↑ Serum liver enzymes, hepatic steatosis and ↑ cholesterol levels. ↑ Hepatic lipid content and ↑ hepatic TG, ↓ butyrate metabolism pathway activation and ↑ SAA and IL-6. ↑ [*Bilophila wadsworthia*] → Stimulate systemic inflammation, intestinal barrier defect, bile acid dysmetabolism and interrupting tight junction integrity.	*B. wadsworthia* infection on specific pathogen-free mice. HFD mice fed with *B. wadsworthia.*	[76,77]
Helicobacter pylori	Gram-negative Bacteria. *Proteobacteria* phylum. Common infection in humans.	↑ [*H. pylori*] → -↑ Chronic inflammation and IR → ↑ TNF-α, IL-1β, IL-6 and IL-8. ↑ [*H. pylori*] → ↓adiponectin and leptin, ↑ fetuin-A → cytokines release ↑ [*H. pylori*] → ↑ Flora dysbiosis and mucosal permeability → ↑endotoxemia.	Clinical studies of NAFLD patients with *H. pylori* in a meta-analysis study.	[78–80]
Klebsiella pneumoniae	Gram-negative Bacteria. *Proteobacteria* phylum Endogenous alcohol-producing bacteria.	↑ [K. *pneumoniae*] → ↑ Endogenous OH → ↑ ROS, ↑ hepatic steatosis, ↑ TG, AST and AST. ↑ Immune cells and inflammation in liver ↑ Biosynthesis FAs and Fat storage	Clinical study with NAFLD and controls individuals colonized by *K. pneumoniae.* NAFLD mice induced by *K. pneumoniae.*	[81]
Akkermansia muciniphila	Gram-negative Bacteria *Verrucomicrobia* phylum 3–5% of the Gut microbiota Mucin-degrading activity.	↓ [*A. muciniphila*] → ↑ obesity, metabolic disorders, ↑ fat mass gain, ↑ body weight, ↑ inflammation, ↑ insulin resistance and ↑ glucose tolerance ↑ [*A. muciniphila*] → ↓ metabolic disorders, ↓ obesity, ↓ insulin sensitivity, ↓ fat mass and liver steatosis, ↓ [cholesterol] Regulation of mucus layer thickness → ↓ permeability → ↓ Endotoxemia	*A. muciniphila* in HFD-induced obese mice *A. muciniphila* supplementation in specific pathogen-free-grade mice.	[82,83]

4.3.1. *Faecalbacterium prausnitzii*

Faecalbacterium prausnitzii is a butyrate-producing bacterium, from the *Firmicutes* phylum (Figure 1) [84]. This bacterium is the dominant member of the *Clostridium leptum* subgroup, representing >5% of the total gut microbiota in healthy humans [84]. *F. prausnitzii* modulates the intestinal immune system, the oxidative stress and the metabolism of the colon epithelial cells (colonocytes) [85], and produces a microbial anti-inflammatory (MAM) protein [86]. In humans, it was observed that the low abundance of *F. prausnitzii* was associated with >5% fat hepatic content and with an increased adipose tissue inflammation, which may contribute to aggravate the NAFLD state [75]. These findings were corroborated in mice fed with HFD, observing that those animals that were treated with *F. prausnitzii* as a probiotic presented a lower hepatic lipid and lower plasma levels of liver transaminases (AST and ALT), suggesting a healthier liver than the one of the HFD counterpart mice (Table 1) [74]. Moreover, the presence of *F. prausnitzii* increases the expression levels of an inhibitor cell cycle progression, *CDKN1A*, which encodes for the p21 protein, whose levels are inversely associated with NAFLD progression and fibrosis [87].

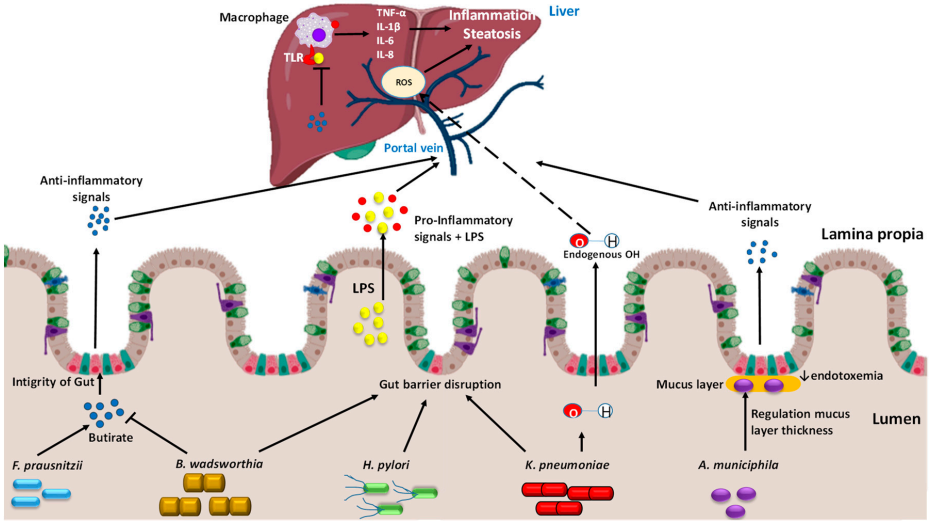

Figure 1. Pathways in the gut-liver axis of some bacteria which act differently in the gut and through the portal vein connected with the liver, contributing positively or negatively to NAFLD. In a healthy gut, *Faecalbacterium prausnitzii* contributes with the integrity of the gut, participating in the butyrate production, which interacts with the cells from the barrier modulating mucin and the tight junction's formation, and the production of anti-inflammatory molecules. In dysbiosis, the microbiota concentration changes, and damaging bacteria grow above healthy bacteria. *Bilophila wadsworthia* reduces the production of secondary bile acids in the gut, while first bile acids are linked with the farnesoid X receptor (FXR) that provokes a decreased production of first bile acid in the liver, contributing to disrupted microbiota, and the increase of lipopolysaccharide (LPS) release. Moreover, it decreases the activation of butyrate production. *Helicobacter pylori* also participates in the gut barrier disruption, boosting the bacterial endotoxins' passage to the liver, modulating pro-inflammatory cytokines and downregulating leptin and adiponectin. In dysbiosis, *Klebsiella pneumoniae* produces high quantities of endogenous alcohol, which arrives to the liver and increases the source of reactive oxygen species (ROS), related with NAFLD progression. *Akkermansia muciniphila* is found in the mucus layer of the gut barrier, which is reinforced due to the presence of *A. muciniphila* activity, modulating tight-junction proteins, regulation of mucus layer thickness and the promotion of antimicrobial peptides and immunity.

4.3.2. *Bilophila wadsworthia*

B. wadsworthia is a gram-negative *Proteobacterium* associated with fat rich diets [76]. This *B. wadsworthia* metabolizes sulfated compounds and produces hydrogen sulfide that promotes direct inflammation and impairs the gut barrier [76], and consequently an increased abundance of *B. wadsworthia* implies a negative effect in intestinal inflammation (Figure 1) [59]. In addition, a recent study demonstrated that hepatic lipid and triglyceride content increased in mice that had been fed with HFD and *B. wadsworthia* in comparison to HFD mice counterparts, which weakens liver function and potentiates metabolic syndrome [77]. As other gram-negative bacteria, *B. wadsworthia* may release LPS as endotoxin which stimulates a systemic inflammatory response, raising the circulating levels of key cytokines such as serum amyloid A (SAA) and interleukin-6 (IL-6) [76]. Besides, *B. wadsworthia* decreased butyrate metabolism, which interrupts the tight junction integrity of the gut barrier, allowing the circulation of LPS from the gut lumen into the portal vein arriving to the liver, where it acts upon hepatic macrophages, increasing a pro-inflammatory cytokine release (Table 1) [77]. Finally, *B. wadsworthia* promotes a reduction of the primary bile acids' production, contributing to a disrupted microbiota, and the increase of LPSs release [82,83].

4.3.3. *Helicobacter pylori*

Helicobacter pylori is a gram-negative *Proteobacterium* and represents, in humans, a key factor in the etiology of various gastrointestinal infections [88]. Several studies have observed a significantly increased risk of NAFLD in patients affected by an *H. pylori* infection, and this bacterium also plays an important role in IR, which is described as a factor of NAFLD's development due its chronic inflammation state [85,89]. When the infection is eradicated, the risk of NAFLD development is reduced. Besides, *H. pylori* infection modulates the release of several inflammatory cytokines (tumor necrosis factor α (TNF-α) and some interleukins, IL-1β, IL-6 and IL-8) which drive an important role in hepatocellular injury associated with NAFLD (Figure 1) [80]. In addition, leptin release from white adipose tissue is induced by *H. pylori* infection [80]. Leptin is a key adipokine which contributes to IR by its role in the regulation of glucose, energy homeostasis and lipid metabolism. Increased leptin levels activate the liver stearoyl CoA desaturase, thus accelerating VLDL formation and fat deposition in the liver [80]. Finally, *H. pylori* infection has the greatest impact on the homeostasis of upper digestive tract, which affects the gut–liver axis. This bacterium might increase the mucosal permeability of the gut and cause flora dysbiosis, thereby boosting the bacterial endotoxins passage to the liver through the portal vein circulation [80]. These endotoxins trigger pro-inflammatory cytokines release such as TNF-α and interleukin-8 (IL-8) via TLR, which triggers the hepatic migration of neutrophils and monocytes [89], increasing IR and lipid accumulation in the liver (Table 1). However, more clinical studies are necessary to understand the complete role of *H. pylori* in the NAFLD progression.

4.3.4. *Klebsiella pneumoniae*

In a healthy state, microbiota is constantly producing ethylic alcohol in the gut, which is normally metabolized in the liver by alcohol-dehydrogenase (ADH) and other hepatic enzymes [90]. When the gut microbiota is enriched in alcohol-producing bacteria, the production of alcohol is more constant than in healthy microbiota, exceeding the liver detoxification capacity and therefore producing a constant source of reactive oxygen species (ROS) towards the liver, which induce hepatic inflammation, often ending in steatohepatitis [90,91]. In fact, more bacterial species with stronger alcohol-production ability have been shown in patients with NAFLD than in control patients [81,92]. In a very recent study, two strains of a same bacterium were identified, which are related with endogenous alcohol production and is more abundant in NAFLD patients, *K. pneumonia*, a gram-negative *Proteobacterium* [81], a phylum significantly elevated in NASH [92].

Moreover, both in aerobic and anaerobic conditions, *K. pneumoniae* induced a higher blood alcohol concentration (BAC) in NAFLD patients than in control patients due to its higher alcohol-producing

ability [81]. In addition, after inducing a reduction in the *K. pneumoniae* abundance, a double effect was observed: A body weight loss and a decreased endogenous alcohol production by the fecal flora, suggesting an association between *K. pneumoniae* presence and NAFLD progression (Figure 1) [81]. In mice, the transplant of *K. pneumoniae* is sufficient to induce hepatic NAFLD, increasing triglycerides, ALT and AST concentration in the serum [81]. Different pathways were also affected, with increased expression of genes related to progressive fat storage, enrichment of the biosynthesis of unsaturated fatty acid and other metabolisms related with the development of hepatic steatosis and inflammation [81]. In fact, in NAFLD mice induced by *K. pneumoniae;* higher alcohol concentrations are reported in the portal vein than in the peripheral veins, demonstrating the alcohol production by the microbiome [81]. Moreover, these evidences were corroborated in NAFLD patients, because endogenous alcohol production is enlarged, possibly due to the actions of *K. pneumoniae* (Table 1) [81]. To sum up, *K. pneumoniae* contributes to the NAFLD physiopathology with an etiological behavior similar to alcoholic fatty liver disease.

4.3.5. *Akkermansia muciniphila*

Akkermansia muciniphila, a gram-negative bacterium from the *Verrucomicrobia* phylum, is one of the most abundant microorganisms in the human intestinal microbiota, representing between 3–5% of the whole bacteria community [82]. It is described as a beneficial microbe, which could be considered as a potential probiotic treatment [93]. This bacterium is found in the mucus layer of the intestine, with a mucin-degrading activity [94], and it is established in the intestine during the first month of life [83]. In a mice model, *A. muciniphila* is less abundant in obese and NAFLD animals than in their counterparts [93]. This decrease is also inversely correlated with fat mass gain, body weight, inflammation, IR and glucose tolerance [93]. Besides, a thinner intestinal mucus layer was observed in obese animals, causing greater gut permeability and allowing the entrance of bacterial compounds into the circulatory system [94]. Accordingly, a higher presence of *A. muciniphila* induce an improvement in metabolic disorders, lowering the cholesterol levels and liver steatosis (Table 1) [93]. It has been shown that metformin, widely used as a first-line antidiabetic treatment, improved glucose homeostasis correlated with an *A. muciniphila* increased population [93]. Reinforcement of gut barrier and the reversed fat gain has been related to the increase of the circulating levels of endocannabinoids and gut peptides, due to the presence of *A. muciniphila* activity, modulating tight-junction proteins, regulation of mucus layer thickness and the promotion of antimicrobial peptides and immunity [93].

A. muciniphila is capable of obtain carbon, energy and nitrogen source from mucin and then releases free sulfate from mucin fermentation [94]. Amuc_100 is described as a protein synthetized by the *A. muciniphila* layer that plays an important immunomodulatory role [94]. A study from S. Zhao et al. in preclinical models of specific pathogen-free (SPF)-grade mice described the improvements in metabolic profiles due to daily supplementation by gavage of *A. muciniphila* [83]. The findings resulted in an improvement of glucose tolerance and insulin sensitivity in the liver by a significant reduction in the expression levels of genes involved in the glucose metabolism (phosphoenolpyruvate carboxykinase (PEPCK) and glucose-6-phosphatase (G6PC)) [83]. Besides, a significant reduction in the expression levels of liver genes involved in fatty acid synthesis (SREBP1c) and transport (fatty acid translocase (CD36)) were observed due to *A. muciniphila* supplementation, which drives to a lower fat deposition and ER stress induced by *A. muciniphila* in this essential organ [83]. In addition, the plasma lipopolysaccharide binding protein (LBP) binds LPS, helping LPS to be recognized by the TLR4 receptor, initiating downstream signaling that results in inflammation [83]. LBP levels were reduced in systemic circulation by the increased presence of *A. muciniphila*, reducing metabolic endotoxemia and downstream signaling [83]. Taken together, these metabolic benefits induced by *A. muciniphila* could provide possibilities to prevent or ameliorate health disturbances in the general population.

5. Future Perspectives

Apart from the extended studies focused on bacterial gut microbiota, intestinal flora are also composed by nonbacterial members that may develop an important role in the processes affecting health and disease. Eukaryotes contribute to less than 0.03% of the total fecal microbes and are primarily composed of 200–300 fungal species [95]. Fungi have been found altered in the gut microbiome by some diseases that affect gut permeability, such as inflammatory bowel disease (IBD) [96]. In fact, obese mice fed with kefir, which contains yeast as *Saccharomides spp* and *Candida spp*, ameliorate NAFLD, with improvements in hepatic lesions and lower levels of steatosis [97]. These results point at yeast as an important contributor in the improvement of NAFLD progression and its necessity to have yeasts in mind in order to design effective strategies against the development of NAFLD. Other nonbacterial members of the gut microbiota are virus and a meta-analysis of gut virome, which have displayed that bacteriophages compromise the 90% approximately of the gut virome and have an important participation in bacterial dynamics and mechanisms in gut microbiota [98]. Despite the important role of virus over the gut homeostasis, the potential effects of gut virus in the NAFLD development has not been explored yet, making it necessary to consider this virus as an additional tool to fight against this important disease in a holistic manner.

In addition, both the gut microbiome and NAFLD are closely connected with the circadian clock. Microbiota rhythms are regulated by diet and time of feeding which can alter both microbial community structure and metabolic activity that can significantly impact metabolic function [99]. Indeed, an increasing number of circadian rhythm studies have provided important insights correlating the expression of the circadian clock gene with metabolism in NAFLD [100]. However, the exact mechanisms of circadian metabolism remain obscure and unresolved at this time, and clearly require additional experimentation to further increase our comprehension of lipid metabolism in the liver. Therefore, new studies that target key circadian clock genes with the aim of treating or preventing NAFLD may provide more effective strategies of intervention in the future.

6. Conclusions

To sum up, gut microbiota plays a significant role in the pathogenesis of obesity and NAFLD progression [47]. Gut dysbiosis and bacterial translocation in combination with a Western diet and lifestyle with inflammasome dysfunction lead to NAFLD progression [62]. This dysbiosis produces an increase in harmful bacteria and/or a decrease in beneficial bacteria, affecting the health of both the intestine and the liver. The mechanisms modulated by these bacteria should be further investigated to know where and how they affect the principal pathways, which involve the homeostasis of the intestine and the liver health. Moreover, the mechanisms that clarify the link between ingredients and metabolites from the gut microbiome with NAFLD have been analyzed in some studies, but it is necessary to devote more efforts in this field to obtain a complete picture. This review summarizes the assessed and characterized bacteria related with the NAFLD progression in depth. However, considering the high number of different species that are present in the gut microbiota, it is logical to think that other bacteria and non-bacteria species may play an important unknown role in the development of this disease.

Author Contributions: S.Q.-V. wrote the manuscript; G.A. and J.M.D.B. participated in the discussion and X.E. revised the manuscript. All authors have read and agreed to the published version of the manuscript.

Funding: The work was supported by ACC1Ó (TECCT11-1-0012) and by the European Union's Horizon 2020 Research and Innovation Programme under grant agreement: Preventomics project-No 818318.

Acknowledgments: S.Q.-V. is supported by a fellowship from the Vicente Lopez Program (Eurecat). G.A. is a Serra Húnter fellow.

Conflicts of Interest: The authors declare no conflict of interest.

References

1. Bell, J. NASH Drug Pipeline Headed toward Uncertain Market. Available online: https://www.biopharmadive.com/news/nash-drug-pipeline-market-liver-disease/523492/ (accessed on 21 May 2018).
2. Dibba, P.; Li, A.; Perumpail, B.; John, N.; Sallam, S.; Shah, N.; Kwong, W.; Cholankeril, G.; Kim, D.; Ahmed, A. Emerging Therapeutic Targets and Experimental Drugs for the Treatment of NAFLD. *Diseases* **2018**, *6*, 83. [CrossRef] [PubMed]
3. Argo, C.K.; Northup, P.G.; Al-Osaimi, A.M.S.; Caldwell, S.H. Systematic review of risk factors for fibrosis progression in non-alcoholic steatohepatitis. *J. Hepatol.* **2018**, *51*, 371–379. [CrossRef] [PubMed]
4. Ludwig, J.; Viggiano, T.R.; McGill, D.B.; Oh, B.J. Nonalcoholic steatohepatitis: Mayo Clinic experiences with a hitherto unnamed disease. *Mayo Clin. Proc.* **1980**, *55*, 434–438. [PubMed]
5. Jegatheesan, P.; Beutheu, S.; Ventura, G.; Sarfati, G.; Nubret, E.; Kapel, N.; Waligora-Dupriet, A.; Bergheim, I.; Cynober, L.; De-Bandt, J. Effect of specific amino acids on hepatic lipid metabolism in fructose-induced non-alcoholic fatty liver disease. *Clin. Nutr.* **2016**, *35*, 175–182. [CrossRef]
6. Zelber-Sagi, S.; Nitzan-Kaluski, D.; Halpern, Z.; Oren, R. Prevalence of primary non-alcoholic fatty liver disease in a population-based study and its association with biochemical and anthropometric measures. *Liver Int.* **2006**, *26*, 856–863. [CrossRef]
7. Bugianesi, E. EASL–EASD–EASO Clinical Practice Guidelines for the management of non-alcoholic fatty liver disease: Disease mongering or call to action? *Diabetologia* **2016**, *59*, 1145–1147. [CrossRef]
8. Shreiner, A.B.; Kao, J.Y.; Young, V.B. The gut microbiome in health and in disease. *Curr. Opin. Gastroenterol.* **2016**, *31*, 69–75. [CrossRef]
9. Donaldson, G.P.; Lee, S.M.; Mazmanian, S.K. Gut biogeography of the bacterial microbiota. *Nat. Rev. Microbiol.* **2015**, *14*, 20–32. [CrossRef]
10. Guohong, L.; Qingxi, Z.; Hongyun, W. Characteristics of intestinal bacteria with fatty liver diseases and cirrhosis. *Ann. Hepatol.* **2019**, *10*, 796–803. [CrossRef]
11. He, J.; Yang, X.F. Gut microbiota and nonalcoholic fatty liver disease. *World Chin. J. Dig.* **2017**, *25*, 2480–2485. [CrossRef]
12. Wood, N.J. Microbiota: Dysbiosis driven by inflammasome deficiency exacerbates hepatic steatosis and governs rate of NAFLD progression. *Nat. Rev. Gastroenterol. Hepatol.* **2012**, *9*, 123. [CrossRef] [PubMed]
13. Brandl, K.; Kumar, V.; Eckmann, L. Gut-liver axis at the frontier of host-microbial interactions. *Am. J. Physiol. Gastrointest. Liver Physiol.* **2017**, *312*, G413–G419. [CrossRef] [PubMed]
14. Adams, D.H.; Eksteen, B.; Curbishley, S.M. Immunology of the gut and liver: A love/hate relationship. *Gut* **2008**, *57*, 838–848. [CrossRef] [PubMed]
15. Cani, P.; Amar, J.; Iglesias, M.; Poggi, M.; Knauf, C.; Bastelica, D.; Neyrinck, A.; Fava, F.; Tuohy, K.; Chabo, C.; et al. Metabolic Endotoxemia Initiates Obesity and Insulin Resistance. *Diabetes* **2007**, *56*, 1761–1772. [CrossRef] [PubMed]
16. Weiss, G.A.; Hennet, T. Mechanisms and consequences of intestinal dysbiosis. *Cell. Mol. Life Sci.* **2017**, *74*, 2959–2977. [CrossRef] [PubMed]
17. Sabaté, J.; Jouët, P.; Harnois, F.; Mechler, C.; Msika, S.; Grossin, M.; Coffin, B. High prevalence of small intestinal bacterial overgrowth in patients with morbid obesity: A contributor to severe hepatic steatosis. *Obes. Surg.* **2008**, *18*, 371–377. [CrossRef]
18. Shanab, A.; Scully, P.; Crosbie, O.; Buckley, M.; O'Mahony, L.; Shanahan, F.; Gazareen, S.; Murphy, E.; Quigley, E. Small intestinal bacterial overgrowth in nonalcoholic steatohepatitis: Association with toll-like receptor 4 expression and plasma levels of interleukin 8. *Dig. Dis. Sci.* **2011**, *56*, 1524–1534. [CrossRef]
19. Gottardi, A.D.; McCoy, K.D. Evaluation of the gut barrier to intestinal bacteria in non-alcoholic fatty liver disease. *J. Hepatol.* **2011**, *55*, 1181–1183. [CrossRef]
20. Aron-Wisnewsky, J.; Gaborit, B.; Dutour, A.; Clement, K. Gut microbiota and non-alcoholic fatty liver disease: New insights. *Clin. Microbiol. Infect.* **2013**, *19*, 338–348. [CrossRef]
21. Demehri, F.R.; Barrett, M.; Teitelbaum, D.H. Changes to the intestinal microbiome with parenteral nutrition: Review of a murine model and potential clinical implications. *Nutr. Clin. Pr.* **2015**, *30*, 798–806. [CrossRef]
22. Febbraio, M.; Reibe, S.; Shalapour, S.; Ooi, G.; Watt, M.; Karin, M. Preclinical Models for Studying NASH-Driven HCC: How Useful Are They? *Cell Metab.* **2019**, *29*, 18–26. [CrossRef] [PubMed]

23. Le Roy, T.; Llopis, M.; Lepage, P.; Bruneau, A.; Rabot, S.; Bevilacqua, C.; Martin, P.; Philippe, C.; Walker, F.; Bado, A.; et al. Intestinal microbiota determines development of non-alcoholic fatty liver disease in mice. *Gut* **2013**, *62*, 1787–1794. [CrossRef] [PubMed]
24. Miele, L.; Valenza, V.; La Torre, G.; Montalto, M.; Cammarota, G.; Ricci, R.; Mascianà, R.; Forgione, A.; Gabrieli, M.; Perotti, G.; et al. Increased intestinal permeability and tight junction alterations in nonalcoholic fatty liver disease. *Hepatology* **2009**, *49*, 1877–1887. [CrossRef] [PubMed]
25. Parekh, P.J.; Balart, L.A.; Johnson, D.A. The influence of the gut microbiome on obesity, metabolic syndrome and gastrointestinal disease. *Clin. Transl. Gastroenterol.* **2015**, *6*, e91. [CrossRef]
26. Boulangé, C.L.; Neves, A.L.; Chilloux, J.; Nicholson, J.K.; Dumas, M.E. Impact of the gut microbiota on inflammation, obesity, and metabolic disease. *Genome Med.* **2016**, *8*, 1–12. [CrossRef]
27. Bohan, R.; Tianyu, X.; Tiantian, Z.; Ruonan, F.; Hongtao, H.; Qiong, W.; Chao, S. Gut microbiota: A potential manipulator for host adipose tissue and energy metabolism. *J. Nutr. Biochem.* **2019**, *64*, 206–217. [CrossRef]
28. Bidlack, W.R. Nutritional Biochemistry, 2nd ed.; Tom Brody. San Diego, 1999. *J. Am. Coll. Nutr.* **2000**, *19*, 419–420. [CrossRef]
29. Rinninella, E.; Raoul, P.; Cintoni, M.; Franceschi, F.; Miggiano, G.; Gasbarrini, A.; Mele, M. What is the Healthy Gut Microbiota Composition? A Changing Ecosystem across Age, Environment, Diet, and Diseases. *Microorganisms* **2019**, *7*, 14. [CrossRef]
30. Abed-Meraim, F.; Combescure, A. New prismatic solid-shell element: Assumed strain formulation and hourglass mode analysis. *Struct. Eng. Mech.* **2011**, *37*, 253–256.
31. Kuksis, A. Biochemistry of Glycerolipids and Formation of Chylomicrons. In *Fat Digestion and Absorption*; AOCS Press: Urbana, IL, USA, 2000; p. 164.
32. Roy, C.C.; Kien, C.L.; Bouthillier, L.; Levy, E. Short-chain fatty acids: Ready for prime time? *Nutr. Clin. Pr.* **2006**, *21*, 351–366. [CrossRef]
33. Zeisel, S.H.; Warrier, M. Trimethylamine N-Oxide, the Microbiome, and Heart and Kidney Disease. *Annu. Rev. Nutr.* **2017**, *37*, 157–181. [CrossRef] [PubMed]
34. Sui, Y.H.; Luo, W.J.; Xu, Q.Y.; Hua, J. Dietary saturated fatty acid and polyunsaturated fatty acid oppositely affect hepatic NOD-like receptor protein 3 inflammasome through regulating nuclear factor-kappa B activation. *World J. Gastroenterol.* **2016**, *22*, 2533–2544. [CrossRef] [PubMed]
35. Chiang, J.Y.L. Regulation of bile acid synthesis: Pathways, nuclear receptors, and mechanisms. *J. Hepatol.* **2004**, *40*, 539–551. [CrossRef] [PubMed]
36. AF, H. THe continuing importance of bile acids in liver and intestinal disease. *Arch. Intern. Med.* **1999**, *159*, 2647–2658.
37. Turnbaugh, P.J. Microbiology: Fat, bile and gut microbes. *Nature* **2012**, *486*, 47–48. [CrossRef]
38. Fuchs, M. Non-Alcoholic Fatty Liver Disease: The Bile Acid-Activated Farnesoid X Receptor as an Emerging Treatment Target. *J. Lipids* **2012**, *2012*, 934396. [CrossRef]
39. Trauner, M.; Claudel, T.; Fickert, P.; Moustafa, T.; Wagner, M. Bile acids as regulators of hepatic lipid and glucose metabolism. *Dig. Dis.* **2010**, *28*, 220–224. [CrossRef]
40. Swann, J.; Want, E.; Geier, F.; Spagou, K.; Wilson, I.; Sidaway, J.; Nicholson, J.; Holmes, E. Systemic gut microbial modulation of bile acid metabolism in host tissue compartments. *Proc. Natl. Acad. Sci. USA* **2011**, *108*, 4523–4530. [CrossRef]
41. Machado, M.V.; Cortez-Pinto, H. Diet, microbiota, obesity, and NAFLD: A dangerous quartet. *Int. J. Mol. Sci.* **2016**, *17*, 481. [CrossRef]
42. Zhu, L.; Baker, S.; Gill, C.; Liu, W.; Alkhouri, R.; Baker, R.; Gill, S. Characterization of gut microbiomes in nonalcoholic steatohepatitis (NASH) patients: A connection between endogenous alcohol and NASH. *Hepatology* **2013**, *57*, 601–609. [CrossRef]
43. Cope, K.; Risby, T.; Diehl, A.M. Increased gastrointestinal ethanol production in obese mice: Implications for fatty liver disease pathogenesis. *Gastroenterology* **2000**, *119*, 1340–1347. [CrossRef] [PubMed]
44. Safari, Z.; Gérard, P. The links between the gut microbiome and non-alcoholic fatty liver disease (NAFLD). *Cell. Mol. Life Sci.* **2019**, *76*, 1541–1558. [CrossRef]
45. Aragonès, G.; Colom-Pellicer, M.; Aguilar, C.; Guiu-Jurado, E.; Martínez, S.; Sabench, F.; Antonio Porras, J.; Riesco, D.; Del Castillo, D.; Richart, C.; et al. Circulating microbiota-derived metabolites: A "liquid biopsy? *Int. J. Obes.* **2019**. [CrossRef] [PubMed]

46. Hodson, L.; Fielding, B.A. Stearoyl-CoA desaturase: Rogue or innocent bystander? *Prog. Lipid Res.* **2013**, *52*, 15–42. [CrossRef] [PubMed]
47. Matikainen, N.; Adiels, M.; Söderlund, S.; Stennabb, S.; Ahola, T.; Hakkarainen, A.; Borén, J.; Taskinen, M. Hepatic lipogenesis and a marker of hepatic lipid oxidation, predict postprandial responses of triglyceride-rich lipoproteins. *Obesity* **2014**, *22*, 1854–1859. [CrossRef] [PubMed]
48. Panera, N.; Barbaro, B.; Della Corte, C.; Mosca, A.; Nobili, V.; Alisi, A. A review of the pathogenic and therapeutic role of nutrition in pediatric nonalcoholic fatty liver disease. *Nutr. Res.* **2018**, *58*, 1–16. [CrossRef] [PubMed]
49. Santoro, N.; Savoye, M.; Kim, G.; Marotto, K.; Shaw, M.; Pierpont, B.; Caprio, S. Hepatic fat accumulation is modulated by the interaction between the rs738409 variant in the PNPLA3 gene and the dietary Omega6/Omega3 PUFA intake. *PLoS ONE* **2012**, *7*, 6–11. [CrossRef]
50. Sonnenburg, J.; Xu, J.; Leip, D.; Chen, C.; Westover, B.; Weatherford, J.; Buhler, J.; Gordon, J. Glycan foraging in vivo by an intestine-adapted bacterial symbiont. *Science* **2005**, *307*, 1955–1959. [CrossRef]
51. Gill, S.; Pop, M.; DeBoy, R.; Eckburg, P.; Turnbaugh, P.; Samuel, B.; Gordon, J.; Relman, D.; Fraser-Liggett, C.; Nelson, K. Metagenomic Analysis of the Human Distal Gut Microbiome. *Science* **2006**, *312*, 1355–1359. [CrossRef]
52. Ouyang, X.; Cirillo, P.; Sautin, Y.; McCall, S.; Bruchette, J.; Diehl, A.; Johnson, R.; Abdelmalek, M. Fructose consumption as a risk factor for non-alcoholic fatty liver disease. *J. Hepatol.* **2008**, *48*, 993–999. [CrossRef]
53. Chen, Q.; Wang, T.; Li, J.; Wang, S.; Qiu, F.; Yu, H.; Zhang, Y.; Wang, T. Effects of natural products on fructose-induced nonalcoholic fatty liver disease (NAFLD). *Nutrients* **2017**, *9*, 2. [CrossRef] [PubMed]
54. Handy, D.; Castro, R.; Loscalzo, J. Epigenetic modifications: Basic mechanisms and role in cardiovascular disease. *Circulation* **2011**, *19*, 2145–2156. [CrossRef] [PubMed]
55. Kohli, R.; Kirby, M.; Xanthakos, S.; Softic, S.; Feldstein, A.; Saxena, V.; Tang, P.; Miles, L.; Miles, M.; Balistreri, W.; et al. High-fructose, medium chain trans fat diet induces liver fibrosis and elevates plasma coenzyme Q9 in a novel murine model of obesity and nonalcoholic steatohepatitis. *Hepatology* **2010**, *52*, 934–944. [CrossRef] [PubMed]
56. Van Herck, M.A.; Vonghia, L.; Francque, S.M. Animal models of nonalcoholic fatty liver disease—A starter's guide. *Nutrients* **2017**, *9*, 72. [CrossRef]
57. Wehmeyer, M.; Zyriax, B.; Jagemann, B.; Roth, E.; Windler, E.; Wiesch, J.; Lohse, A.; Kluwe, J. Nonalcoholic fatty liver disease is associated with excessive calorie intake rather than a distinctive dietary pattern. *Medicine* **2016**, *95*, e3887. [CrossRef]
58. Suárez, M.; Boqué, N.; del Bas, J.; Mayneris-Perxachs, J.; Arola, L.; Caimari, A. Mediterranean diet and multi-ingredient-based interventions for the management of non-alcoholic fatty liver disease. *Nutrients* **2017**, *9*, 1052. [CrossRef]
59. Ley, R.; Bäckhed, F.; Turnbaugh, P.; Lozupone, C.; Knight, R.; Gordon, J. Human gut microbes associated with obesity. *Nature* **2006**, *444*, 1021–1022. [CrossRef]
60. Devkota, S.; Wang, Y.; Musch, M.; Leone, V.; Fehlner-Peach, H.; Nadimpalli, A.; Antonopoulos, D.; Jabri, B.; Chang, E. Dietary fat-induced taurocholic acid production promotes pathobiont and colitis in IL-10 −/− mice HHS Public Access. *Nature* **2012**, *487*, 104–108. [CrossRef]
61. Wang, B.; Jiang, X.; Cao, M.; Ge, J.; Bao, Q.; Tang, L.; Chen, Y.; Li, L. Altered fecal microbiota correlates with liver biochemistry in nonobese patients with non-alcoholic fatty liver disease. *Sci. Rep.* **2016**, *6*, 1–11. [CrossRef]
62. Consolandi, C.; Turroni, S.; Emmi, G.; Severgnini, M.; Fiori, J.; Peano, C.; Biagi, E.; Grassi, A.; Rampelli, S.; Silvestri, E.; et al. Behçet's syndrome patients exhibit specific microbiome signature. *Autoimmun. Rev.* **2015**, *14*, 269–276. [CrossRef]
63. Wrzosek, L.; Miquel, S.; Noordine, M.; Bouet, S.; Chevalier-Curt, M.; Robert, V.; Philippe, C.; Bridonneau, C.; Cherbuy, C.; Robbe-Masselot, C.; et al. Bacteroides thetaiotaomicron and Faecalibacterium prausnitzii influence the production of mucus glycans and the development of goblet cells in the colonic epithelium of a gnotobiotic model rodent. *BMC Biol.* **2013**, *11*, 61. [CrossRef] [PubMed]
64. Loomba, R.; Seguritan, V.; Li, W.; Long, T.; Klitgord, N.; Bhatt, A.; Dulai, P.; Caussy, C.; Bettencourt, R.; Highlander, S.; et al. Gut Microbiome-Based Metagenomic Signature for Non-invasive Detection of Advanced Fibrosis in Human Nonalcoholic Fatty Liver Disease. *Cell Metab.* **2017**, *25*, e5. [CrossRef] [PubMed]

65. Le Chatelier, E.; Nielsen, T.; Qin, J.; Prifti, E.; Hildebrand, F.; Falony, G.; Almeida, M.; Arumugam, M.; Batto, J.; Kennedy, S.; et al. Richness of human gut microbiome correlates with metabolic markers. *Nature* **2013**, *500*, 541–546. [CrossRef] [PubMed]
66. Baker, S.S.; Baker, R.D.; Liu, W.; Nowak, N.J.; Zhu, L. Role of alcohol metabolism in non-alcoholic steatohepatitis. *PLoS ONE* **2010**, *5*, e9570. [CrossRef]
67. Jiang, W.; Wu, N.; Wang, X.; Chi, Y.; Zhang, Y.; Qiu, X.; Hu, Y.; Li, J.; Liu, Y. Dysbiosis gut microbiota associated with inflammation and impaired mucosal immune function in intestine of humans with non-alcoholic fatty liver disease. *Sci. Rep.* **2015**, *5*, 1–7. [CrossRef]
68. Raman, M.; Ahmed, I.; Gillevet, P.; Probert, C.; Ratcliffe, N.; Smith, S.; Greenwood, R.; Sikaroodi, M.; Lam, V.; Crotty, P.; et al. Fecal microbiome and volatile organic compound metabolome in obese humans with nonalcoholic fatty liver disease. *Clin. Gastroenterol. Hepatol.* **2013**, *11*, 868–875. [CrossRef]
69. Da Silva, H.; Teterina, A.; Comelli, E.; Taibi, A.; Arendt, B.; Fischer, S.; Lou, W.; Allard, J. Nonalcoholic fatty liver disease is associated with dysbiosis independent of body mass index and insulin resistance. *Sci. Rep.* **2018**, *8*, 1–12. [CrossRef]
70. Michail, S.; Lin, M.; Frey, M.; Fanter, R.; Paliy, O.; Hilbush, B.; Reo, N. Altered gut microbial energy and metabolism in children with non-alcoholic fatty liver disease. *Fems Microbiol. Ecol.* **2015**, *91*, 1–9. [CrossRef]
71. Aranha, M.; Cortez-Pinto, H.; Costa, A.; Da Silva, I.; Camilo, M.; De Moura, M.; Rodrigues, C. Bile acid levels are increased in the liver of patients with steatohepatitis. *Eur. J. Gastroenterol. Hepatol.* **2008**, *20*, 519–525. [CrossRef]
72. Boursier, J.; Mueller, O.; Barret, M.; Machado, M.; Fizanne, L.; Araujo-Perez, F.; Guy, C.; Seed, P.; Rawls, J.; Lawrence, A. In the Metabolic Function of the Gut Microbiota. *Hepatology* **2017**, *63*, 764–775. [CrossRef]
73. Jasirwan, C.; Lesmana, C.; Hasan, I.; Sulaiman, A.; Gani, R. The role of gut microbiota in non-alcoholic fatty liver disease: Pathways of mechanisms. *Biosci. Microbiota Food Heal.* **2019**, *38*, 81–88. [CrossRef] [PubMed]
74. Munukka, E.; Rintala, A.; Toivonen, R.; Nylund, M.; Yang, B.; Takanen, A.; Hänninen, A.; Vuopio, J.; Huovinen, P.; Jalkanen, S.; et al. Faecalibacterium prausnitzii treatment improves hepatic health and reduces adipose tissue inflammation in high-fat fed mice. *ISME J.* **2017**, *11*, 1667–1679. [CrossRef] [PubMed]
75. Munukka, E.; Pekkala, S.; Wiklund, P.; Rasool, O.; Borra, R.; Kong, L.; Ojanen, X.; Cheng, S.; Roos, C.; Tuomela, S.; et al. Gut-adipose tissue axis in hepatic fat accumulation in humans. *J. Hepatol.* **2014**, *61*, 132–138. [CrossRef] [PubMed]
76. Feng, Z.; Long, W.; Hao, B.; Ding, D.; Ma, X.; Zhao, L.; Pang, X. A human stool-derived Bilophila wadsworthia strain caused systemic inflammation in specific-pathogen-free mice. *Gut Pathog.* **2017**, *9*, 1–10. [CrossRef] [PubMed]
77. Natividad, J.; Lamas, B.; Pham, H.; Michel, M.; Rainteau, D.; Bridonneau, C.; Da Costa, G.; Van Hylckama, V.J.; Sovran, B.; Chamignon, C.; et al. Bilophila wadsworthia aggravates high fat diet induced metabolic dysfunctions in mice. *Nat. Commun.* **2018**, *9*, 1–15. [CrossRef] [PubMed]
78. Popescu, D.; Andronescu, D.; Babeş, P.A. Association between Helicobacter Pylori infection and insulin resistance: A systematic review. *Rom. J. Diabetes Nutr. Metab. Dis.* **2017**, *24*, 149–154. [CrossRef]
79. Wijarnpreecha, K.; Thongprayoon, C.; Panjawatanan, P.; Manatsathit, W.; Jaruvongvanich, V.; Ungprasert, P. Helicobacter pylori and Risk of Nonalcoholic Fatty Liver Disease. *J. Clin. Gastroenterol.* **2018**, *52*, 386–391. [CrossRef]
80. Ning, L.; Liu, R.; Lou, X.; Du, H.; Chen, W.; Zhang, F.; Li, S.; Chen, X.; Xu, G. Association between Helicobacter pylori infection and nonalcoholic fatty liver disease: A systemic review and meta-analysis. *Eur. J. Gastroenterol. Hepatol.* **2019**, *31*, 735–742. [CrossRef]
81. Yuan, J.; Chen, C.; Cui, J.; Lu, J.; Yan, C.; Wei, X.; Zhao, X.; Li, N.; Li, S.; Xue, G.; et al. Fatty Liver Disease Caused by High-Alcohol-Producing Klebsiella pneumoniae. *Cell Metab.* **2019**, *30*, 675–688. [CrossRef]
82. Everard, A.; Belzer, C.; Geurts, L.; Ouwerkerk, J.; Druart, C.; Bindels, L.; Guiot, Y.; Derrien, M.; Muccioli, G.; Delzenne, N.; et al. Cross-talk between Akkermansia muciniphila and intestinal epithelium controls diet-induced obesity. *Proc. Natl. Acad. Sci. USA* **2013**, *110*, 9066–9071. [CrossRef]
83. Zhao, S.; Liu, W.; Wang, J.; Shi, J.; Sun, Y.; Wang, W.; Ning, G.; Liu, R.; Hong, J. Akkermansia muciniphila improves metabolic profiles by reducing inflammation in chow diet-fed mice. *J. Mol. Endocrinol.* **2017**, *58*, 1–14. [CrossRef] [PubMed]
84. Brahe, L.K.; Astrup, A.; Larsen, L.H. Is butyrate the link between diet, intestinal microbiota and obesity-related metabolic diseases? *Obes. Rev.* **2013**, *14*, 950–959. [CrossRef] [PubMed]

85. Hamer, H.; Jonkers, D.; Venema, K.; Vanhoutvin, S.; Troost, F.; Brummer, R. The role of butyrate on colonic function. *Aliment. Pharm.* **2008**, *27*, 104–119. [CrossRef] [PubMed]
86. Quévrain, E.; Maubert, M.; Michon, C.; Chain, F.; Marquant, R.; Miquel, S.; Carlier, L.; Pigneur, B.; Kharrat, P.; Thomas, G.; et al. Identification of an anti-inflammatory protein from Faecalibacterium prausnitzii, a commensal bacterium deficient in Crohn's disease. *Gut* **2016**, *65*, 415–425. [CrossRef]
87. De Azevedo Silva, J.; Addobbati, C.; Sandrin-Garcia, P.; Crovella, S. Systemic Lupus Erythematosus: Old and New Susceptibility Genes versus Clinical Manifestations. *Curr. Genom.* **2014**, *15*, 52–65. [CrossRef]
88. Kusters, J.G.; Van Vliet, A.H.M.; Kuipers, E.J. Pathogenesis of Helicobacter pylori infection. *Clin. Microbiol. Rev.* **2006**, *19*, 449–490. [CrossRef]
89. Singh, R.; Bullard, J.; Kalra, M.; Assefa, S.; Kaul, A.; Vonfeldt, K.; Strom, S.; Conrad, R.; Sharp, H.; Kaul, R. Status of bacterial colonization, Toll-like receptor expression and nuclear factor-kappa B activation in normal and diseased human livers. *Clin. Immunol.* **2011**, *138*, 41–49. [CrossRef]
90. Teschke, R. Alcoholic liver disease: Alcohol metabolism, cascade of molecular mechanisms, cellular targets, and clinical aspects. *Biomedicines* **2018**, *6*, 106. [CrossRef]
91. Boursier, J.; Diehl, A.M. Nonalcoholic Fatty Liver Disease and the Gut Microbiome. *Clin. Liver Dis.* **2016**, *20*, 263–275. [CrossRef]
92. Lau, E.; Carvalho, D.; Freitas, P. Gut microbiota: Association with NAFLD and metabolic disturbances. *Biomed. Res. Int.* **2015**, *2015*, 979515. [CrossRef]
93. Cani, P. Human gut microbiome: Hopes, threats and promises. *Gut* **2018**, *67*, 1716–1725. [CrossRef] [PubMed]
94. Miura, K.; Ohnishi, H. Role of gut microbiota and Toll-like receptors in nonalcoholic fatty liver disease. *World J. Gastroenterol.* **2014**, *20*, 7381–7391. [CrossRef] [PubMed]
95. Hillman, E.T.; Lu, H.; Yao, T.; Nakatsu, C.H. Microbial ecology along the gastrointestinal tract. *Microbes Environ.* **2017**, *32*, 300–313. [CrossRef] [PubMed]
96. Sokol, H.; Leducq, V.; Aschard, H.; Pham, H.; Jegou, S.; Landman, C.; Cohen, D.; Liguori, G.; Bourrier, A.; Nion-Larmurier, I.; et al. Fungal microbiota dysbiosis in IBD. *Gut* **2017**, *66*, 1039–1048. [CrossRef] [PubMed]
97. Kim, D.; Kim, H.; Jeong, D.; Kang, I.; Chon, J.; Kim, H.; Song, K.; Seo, K. Kefir alleviates obesity and hepatic steatosis in high-fat diet-fed mice by modulation of gut microbiota and mycobiota: Targeted and untargeted community analysis with correlation of biomarkers. *J. Nutr. Biochem.* **2017**, *44*, 35–43. [CrossRef] [PubMed]
98. Reyes, A.; Semenkovich, N.P.; Whiteson, K.; Rohwer, F.; Gordon, J.I. Going viral: Next-generation sequencing applied to phage populations in the human gut. *Nat. Rev. Microbiol.* **2012**, *10*, 607–617. [CrossRef] [PubMed]
99. Voigt, R.M.; Forsyth, C.B.; Green, S.J.; Engen, P.A.; Keshavarzian, A. Circadian Rhythm and the Gut Microbiome. *Int. Rev. Neurobiol.* **2016**, *131*, 192–205.
100. Shi, D.; Chen, J.; Wang, J.; Yao, J.; Huang, Y.; Zhang, G.; Bao, Z. Circadian clock genes in the metabolism of non-alcoholic fatty liver disease. *Front. Physiol.* **2019**, *10*, 423. [CrossRef]

1.5 Nutraceutical therapies for metabolic disorders

NAFLD, as aforementioned, is the liver manifestation of MetS and the pathogenesis of this liver disease is influenced by the "multiple hit hypothesis", which is composed of hepatic and non-hepatic participants that lead to hepatic lipid accumulation and inflammatory and fibrogenic responses [247]. Hence, these affections have been studied as potential therapeutic targets to ameliorate NAFLD progression. Currently, the most prescribed treatments for the amelioration of NAFLD relies on lifestyle modifications, following healthier diets avoiding overnutrition of fats and carbohydrates, and changing sedentarism by physical activity. In this lifestyle intervention, diets rich in vitamin C, E and K, folate, omega-3 PUFAs, whole grains, prebiotic fiber, vegetable protein, MUFAs and nuts and seeds consumption were negatively associated with NAFLD [248]. These recommended macronutrients for the amelioration of NAFLD are adhered to Mediterranean diets [249]. On the contrary, simple sugars (fructose, sucrose), saturated and trans fats, and animal protein (red and processed meat) are strongly associated with NAFLD development [248]. The available drugs interventions proposed are principally based on association of several compounds to reverse comorbidities of NAFLD. However, up to date there is no drug therapy approved for NAFLD treatment, and robust results have not been obtained [250]. In addition, the difficulty associated with drug development also contributes to pursuing new strategies for NAFLD treatment. This situation boosts a need to find alternative therapeutic solution to ameliorate this liver disease.

A promising alternative to ameliorate metabolic disorders are the nutraceuticals or functional food, which are mainly natural and safe. Firstly, nutraceuticals are natural compounds isolated or purified from foods that provides medical or health benefits, including the prevention and/or treatment of a disease, protecting the human body against harmful metabolic changes [251,252]. On the other hand, functional food is usual food consumed as a part of a diet that have a physiological benefit to human health and reduce the risk of suffering from chronic diseases [253]. Both alternatives are further studied to become an attractive approach to overcome the reticence toward lifestyle changes that patients find sometimes so difficult to change, or to become a supplement to use together with lifestyle interventions. Moreover, several bioactive

compounds have been observed to induce beneficial effects in the cellular mechanisms and biochemical pathways that are disrupted or affected from the onset of the diseases until their progression [254–256]. In NAFLD these mechanisms are associated with fat accumulation, IR, inflammation, oxidative stress, mitochondrial dysfunction, ER stress, bacterial overgrowth, and genetic predisposition [254]. Hence, this evidence supports the use of bioactive compounds as a promising strategy to tackle the progression of NAFLD. Nowadays, nutraceuticals are thought as de futural primary intervention in metabolic disorders due to the results obtained in preclinical models. However, the translation of this data to clinical studies needs better results which has been unsatisfactory due to the variations in the effective dosage, bioavailability, duration of the treatment, differences in the purity of the compound, and lack of standardization [253,257]. Therefore, with the aim to design successful nutraceutical treatments against NAFLD, it is essential to understand the pathophysiology of the different metabolic alterations found in this liver disease to clarify the underlying mechanisms in the progression of NAFLD. Thus, there are studies that used the integration and analysis of multi-layer omics data using biological networks, to elucidate the molecular mechanisms implicated in NAFLD pathogenesis [258–261]. Thereafter, a personalized genome-scale metabolic modeling was employed to integrate clinical studies with stable isotopes, in-depth multi-omics profiling, and liver-specific networks with the aim to select promising therapeutic targets to develop nutraceutical strategies for the prevention and treatment of NAFLD [262].

A clear example of nutraceuticals that can activate or recover altered metabolic pathways are the supplementation of metabolic cofactors or activators, and amino acids. Both could be used as a new therapeutic approach against NAFLD pathogenesis by improving metabolic parameters in the disease and stopping NAFLD progression to severe stages of this disease including NASH, cirrhosis, and HCC [263,264]. Therefore, the combination of different nutraceuticals and functional food resurface as clear strategies to tackle the different hits that are implicated in the NAFLD pathogenesis.

1.5.1 Metabolic cofactors

Considering the potential techniques found in omics technologies to design multi-ingredients combination to tackle NAFLD development through the discovery of molecular mechanisms underlying the pathogenesis of the disease, it was possible to uncover therapeutic targets and uncover biomarkers and predict successful combination of ingredients that can act as metabolic activators in NAFLD prevention or treatment [262]. The integrated analysis of omics techniques, such as liver transcriptomics and plasma metabolomics data, demonstrate that there is an elevated requirement for Nicotinamide adenine dinucleotide $(NAD)^+$ and reduced GSH in patients with NAFLD. On the one hand, an amount of NAD^+ is essential for a correct fatty acid oxidation by activating mitochondria. On the other hand, GSH is the most important endogenous antioxidant that reduces ROS, which is produced from the impaired oxidation causing oxidative stress [265]. As Mardinoglu et al. (2017) showed, the lower levels of glycine that NAFLD patients presented is correlated with a reduction of *de novo* synthesis of GSH [262].

In previous studies, supplementation of a combination of L-carnitine (LC), nicotinamide riboside (NR), serine, and N-acetyl cysteine (NAC) was used as a strategy to treat NAFLD both in humans and animals. These studies were performed as a proof of concept to study the kinetics of these metabolites and finally adjust the doses for future human clinical trials and preclinical studies [262,266]. Moreover, this combination of metabolic cofactors composed of NR, LC, serine, and NAC was used in mice fed with western diet to increase fatty acid uptake and oxidation in the mitochondria and to increase GSH availability [263]. However, betaine, which is degraded to sarcosine and glycine, was proposed to substitute serine as a glycine and serine precursor, and its participation in the metabolism of choline was also therapeutically promising due to the raise of SAM levels that play a role in decreasing hepatic steatosis [267]. The strategy proposed by previous analysis to treat or prevent NAFLD is based on (*1*) increasing mitochondrial fatty acid uptake; (*2*) increasing mitochondrial fatty acid oxidation; and (*3*) increasing the availability of GSH, which can be applied to decrease the amount of hepatic steatosis in NAFLD patients (**Figure 16**).

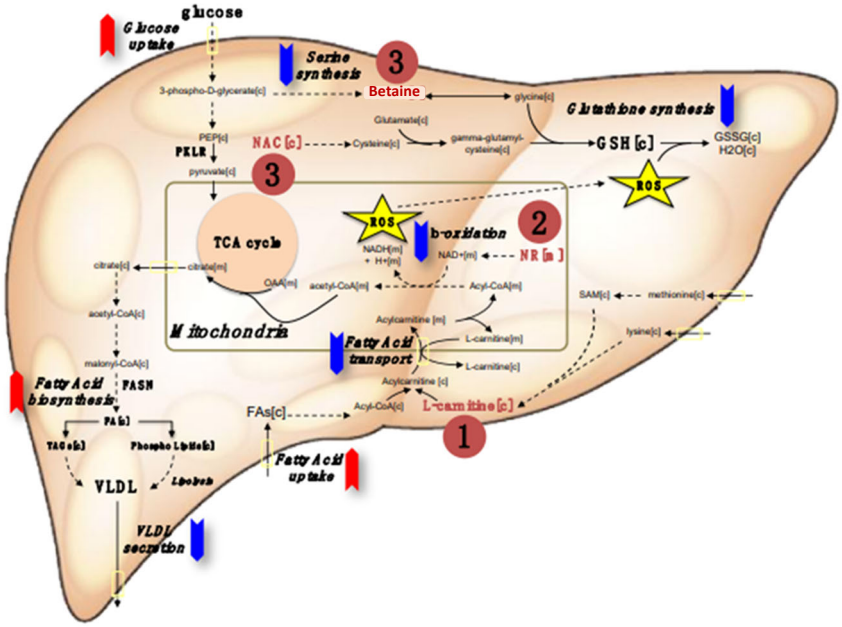

Figure 16. Metabolic pathways altered in NAFLD and the three-step strategy to ameliorate NAFLD progression. Through the supplementation of the combination of the metabolic cofactors l-carnitine, nicotinamide riboside (NR), N-acetyl cysteine (NAC) and betaine, the altered metabolic pathways observed in NAFLD are reverted following the three-step strategy: L-carnitine to enhance the uptake of fatty acids from the cytosol to the mitochondrial across the mitochondrial membrane, (2) the NAD^+ precursor NR to enhance the β-oxidation of fatty acids in mitochondria, and the (3) glutathione (GSH) precursors including betaine and N-acetyl-L-cysteine (NAC) to produce GSH, which is required to protect the liver against the increased levels of ROS triggered by the increased β-oxidation of fatty acids in the mitochondria. Red arrows: upregulation of metabolic pathways. Blue arrows: downregulation of metabolic pathways. TCA: The citric acid cycle, VLDL: Very-low-density lipoprotein, ROS: Reactive oxygen species. PKLR: pyruvate kinase L/R. Image adapted from Mardinoglu et al. (2019) [263].

1.5.1.1 Betaine

Betaine (trimethyl-glycine), which is a natural element found in microorganisms, plants, and animals, and a significant component of many foods with low cost, high tolerability, high solubility [268]. Extended

explanation of betaine characteristics is detailed in the introduction of **Chapter 1**.

Betaine supplementation has been observed to enhanced insulin sensitivity in adipose tissue by improving extracellular signal regulating kinases 1/2 and AKT/PKB activations. Betaine improved adipokine production, such as adiponectin, which is related to an improved plasma insulin and glucose levels. Therefore, betaine can improve insulin signaling recovering kinases AKT and ERK activations by insulin binding to its receptors, and adipose tissue function [269]. In addition, betaine supplementation reduced fatty acid oxidation and restored mitochondrial function in WAT of high-fat-fed mice [270]. Furthermore, a study with high-fat-fed mice showed betaine supplementation promote conversion of existing WAT to BAT by stimulating mitochondrial biogenesis [271]. Betaine also prevents hepatic cysteine and GSH depletion and suppresses proinflammatory factors, ameliorating oxidative stress and inflammation in the liver. Betaine act as an osmolyte in KCs preventing suppression of TNFα release and induction of prostaglandin formation and CCL2 expression [270]. In a study with high-fat diet fed rats, betaine supplementation upregulated key enzymes of one-carbon metabolism in the liver [272], and betaine also decreased hepatic lipid accumulation reducing lipogenesis by enhancing expression of PPARα, and elevated expression of fatty acid oxidation-related genes in a $ApoE^{-/-}$mice model [273]. In agreement, betaine supplementation alleviated hepatic steatosis, inflammation, apoptosis, and oxidative stress, normalized mitochondrial size and respiratory chain function and stimulated β-oxidation of fatty acids in a NAFLD mice model [274].

In addition, betaine supplementation maintains intestinal epithelial barrier integrity by upregulating the expression of zonula occludens-1, claudin-1, and occluding-tight junction proteins as well as enriching gut microbiota composition in NAFLD [270,275]. Therefore, betaine is proposed as a functional ingredient for a promising nutraceutical combination to tackle metabolic disorders.

1.5.1.2 N-acetyl Cysteine

NAC is an antioxidant that is derived from the amino acid cysteine, which is stable in gastric and intestinal fluids and rapidly absorbed. NAC effect on

GSH and proinflammatory cytokines enhancing an antioxidant and anti-inflammatory effect is detailed in the introduction of **Chapter 1** and **3**. In rats fed with high-fat diet, NAC supplementation reduced circulating triglycerides [276,277], and in a study with high-fat diet fed mice, NAC reduced hepatic lipid accumulation showing lower levels of triglyceride and cholesterol in the liver [277], indicating that NAC has a role in the regulation of hepatic lipid metabolism. NAC presented the capacity to revert NASH in preclinical models by reducing lipid accumulation through the regulation of FFAs signaling molecules and transcriptional factors [278,279].

Furthermore, NAC also produce beneficial effects on WAT, increasing the gene expression of adiponectin, which is connected with an amelioration of hyperglycemia and hyperinsulinemia by improving insulin sensitivity, and reducing macrophage infiltration, related to inflammatory processes. In addition, NAC upregulates the expression of thermogenic genes in BAT, such as Dio2 and Pgc-1α, thereby activating BAT activity and inhibiting BAT whitening by reducing lipid accumulation [277].

Lastly, NAC supplementation improved intestinal barrier function and reduced systemic endotoxemia in a bile duct ligand rat model [280]. Overall, NAC is suggested to be a functional ingredient for a promising nutraceutical combination to tackle metabolic disorders.

1.5.1.3 L-carnitine

Unlike the metabolic cofactors mentioned above, which are GSH precursors, l-carnitine (LC) supplementation has been linked to an increase in fatty acid uptake to mitochondria boosting fatty acid oxidation, and LC neutralizes the incomplete products formed during fatty acid oxidation [262]. LC is mainly found in meat and can be synthetized endogenously from lysine and methionine. LC is required in mammalian energy metabolism because facilitates the uptake of long-chain fatty acids, which were previously transformed into acetyl-carnitine necessary for fatty acid oxidation and energy production, in the mitochondria through the inner mitochondrial membrane [281]. The enzymes CPT1, CPT2 and carnitine-acylcarnitine translocase (CACT) are indispensable for fatty acid uptake (**Figure 7)**. CPT1 participates in the binding between acyl-CoA and LC to form acyl-carnitine. CACT transports the acyl-carnitine across the inner mitochondrial membrane in exchange for free LC. Once acyl-CoA is

in the mitochondria, then it is used for fatty acid oxidation producing acetyl-CoA [282]. The effect of LC on lipid accumulation on hepatocytes is described in the introduction of **Chapter 1**. When intramitochondrial LC is reduced, it can induce oxidative stress destabilizing the cell membrane [283,284]. In NAFLD, LC supplementation can be used as a therapeutic option due to its capacity to boost fatty acid oxidation in the liver and reduce lipid accumulation within hepatocytes. Moreover, LC has anti-inflammatory properties by upregulating PPARγ in the liver [285]. In addition, the accumulation of fat can lead to a dysfunctional LC biosynthesis and consequently an impaired fatty acid oxidation [281]. Thus, LC supplementation cause an upregulation of CPT1, elevation of HDL and reduction of fat accumulation in patients with NAFLD [286].

Moreover, insulin sensitivity and glucose uptake are modulated by LC supplementation that can regulate glycolytic and gluconeogenic enzymes and stimulate insulin-like growth factor-1 (IGF-1) signaling cascades [287–290]. In their clinical study, Askapour et al. (2020) observed that LC has significant effects on obesity, in which LC reduced weight, fat mass and BMI [291]. Extended explanation of LC effect on lipid metabolism in adipose tissue is detailed in the introduction of **Chapter 2**.

1.5.1.4 Nicotinamide Riboside

NR is one of the three vitamins' precursors of NAD^+, which is an endogenous substance involved in vital cell functions linked to signal transduction, DNA repair and post-translational protein modifications [263]. Extended explanation of NR effects as a NAD^+ precursor on the hepatocytes is detailed in the introduction of **Chapter 1**. As is explained in the introduction of **Chapter 2**, NR maintains redox reactions and play an important role in lipid and energy metabolism which is crucial for oxidative metabolism and metabolic homeostasis in adipose tissue. Indeed, NR supplementation promotes the activation of SIRT1 and SIRT3 boosting the deacetylation of SREBP1, which results in downregulation of lipogenic genes, such as FASN and ACC, and enhancing oxidative metabolism and protecting against metabolic disorders. In addition, insulin sensitivity is recovered after NR supplementation [292]. In murine white adipose tissue, NR supplementation promotes upregulation of *Pparγ* and antioxidant genes improving WAT function and reducing obesity [293].

Furthermore, in a study with HFD-diet fed mice, fecal material transfer (FMT) was performed to elucidate the effect of NR in gut microbiota and obesity. FMT from NR-treated donors to mice fed a HFD reduced weight gain and increased energy expenditure by improving gut microbiota signature through the enrichment of butyrate-producing *Firmicutes* [294]. Meanwhile, in other study with a liver damage mice model, NR supplementation improved gut dysbiosis by changing the gut microbiota composition at the phylum, family, and genus levels, which was like the composition in the control group [295].

Therefore, the use of these metabolic cofactors as a part of a nutraceutical supplementation can be a therapeutic strategy to tackle the pathogenesis of metabolic disorders and recover histidine levels.

1.5.2 Histidine metabolism-related Amino Acids

The liver is an important organ for the synthesis and degradation of proteins, as well as for the metabolism of amino acids (AAs). AAs are the basic unit of proteins and intermediates of other biomolecules; and some of them are found in abundant quantities in the liver, such as histidine, serine, or alanine. Recent studies indicate the possible role of certain AAs as agents with therapeutic functions in liver metabolism [264]. AAs metabolisms are essential for redox balance, energetic regulation, biosynthetic support, and homeostatic maintenance [296]. Patients with NAFLD have shown reduced levels of some essential AAs, which were negatively correlated with hepatic IR, such as histidine and glycine [297]. In fact, our group has published a study in a model of NAFLD in hamsters, in which it is observed that histidine metabolism is profoundly altered in these animals [298]. In humans, the role of histidine is corroborated by preliminary results obtained by Dr. Fernández-Real's group, which indicates a clear decrease in circulating histidine levels in NAFLD patients [299]. Therefore, it is very evocative to think of a therapeutic and/or nutritional strategy to combat NAFLD in which is tried to recover the circulating levels of histidine in these patients through the supplementation of amino acids that participates in the histidine catabolism pathways (**Figure 17**).

Obesity risk is inversely associated with different AAs: histidine, cysteine, and serine. Thus, MetS parameters, appetite regulation and body

composition can be therapeutic targets to consider when combination with AAs are used as treatments against obesity [300]. Moreover, AAs are necessary for the maintenance of mucosal integrity and barrier function in the intestinal tract because AAs are used as important precursors for metabolically active proteins, GSH, and other molecules used by small intestinal mucosal cells [301]. Additionally, there are bacteria that can use AAs to synthetize bacterial proteins and metabolites [302].

1.5.2.1 L-Histidine

Histidine is an essential amino acid for mammals and other species that cannot be *de novo* synthetized in the body and is obtained through the diet [303]. Besides, it modulates gene expression and biological activity of proteins through methylation [264]. Histidine has been described to be an effective ROS scavenger and reduce the levels of oxidative stress in obesity [304,305]. When histidine levels are increased then an anti-inflammatory, antioxidant, glucoregulatory activity is observed and body weight is maintained [306,307]. Histidine supplementation in obese rats upregulated *Pparγ* and *Adiponectin* in adipose tissue, which triggers an amelioration of inflammation and oxidative stress by inhibiting NF-kB and downregulating *Il-6, Tnfα* and C-reactive protein [308]. Moreover, histidine supplementation improved insulin sensitivity in obese patients [309]. In the case of BAT, Yasuda et al. (2004) supplemented rats with histidine, which regulated sympathetic nerve activity in this tissue through the transformation of histidine into histamine, and thereby participating in the regulation of energy expenditure [310]. Histidine role in hepatic lipid accumulation, IR and antioxidant activity is extensively detailed in the introduction of **Chapter 5**.

Histidine is obtained from the diet, so gut microbiota has an important role in the regulation of histidine levels [311]. It has been shown that histidine degradation pathway from gut microbiota is clustered in obese patients demonstrating that the reduction of histidine bioavailability by obesity-induced gut dysbiosis plays a crucial role in the pathogenesis of metabolic disorders [312].

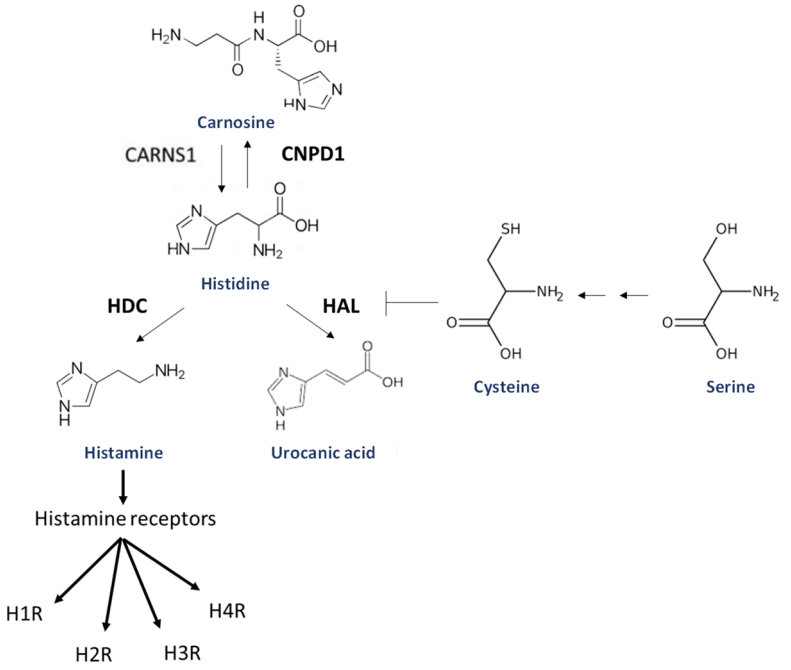

Figure 17. Histidine catabolism pathways. On the first hand, histidine can be catabolized into histamine by the enzyme HDC. Then, histamine can be binded by histamine receptors present in different tissues. On the other hand, histidine can be catabolized into urocanic acid by HAL. HAL activity can be regulated by cysteine, which is a natural inhibitor of HAL. Serine act as a precursor of cysteine. Finally, histidine can be transformed into carnosine by the action of CNDP1, and carnosine can be degraded into histidine by CARNS1 activity. CARNS1, Carnosine synthase 1; CNDP1, Carnosine dipeptidase 1; HDC, Histidine decarboxylase; HAL, Histidine ammonialyase; H1R, Histamine receptor 1. Adapted from Moro et al. (2020) [303].

1.5.2.2 L-Serine

On the contrary, serine is a non-essential amino acid which can be obtained from diet and *de novo* synthesis [264]. Serine is the precursor of glycine and cysteine and is key in in the central metabolism, as it is involved in protein, nucleic acids, and lipid production [313]. Serine deficiency has been detected in NAFLD and NASH patients [314,315]. However, serine administration provides important beneficial effects on hepatic state in injured-liver mice models, such as reduced hepatic triglycerides levels and lipid accumulation, and increased levels of GSH and SAMe [314,315].

Moreover, serine administration decreased ROS levels and activated AMPK subunit α in primary hepatocytes treated with palmitic acid (PA) [314]. Serine supplementation also showed beneficial effects on obesogenic and diabetic pathological features, reducing body weight accompanied by reduced homeostatic model assessment-insulin resistance (HOMA-IR), blood glucose levels and improved glucose tolerance and insulin sensitivity [314,316]. As aforementioned, serine regulates cysteine levels, which are implicated in the hepatic detoxification and histidine levels regulation by histidine ammino lyase (HAL) inhibition [317].

1.5.2.3 L-Cysteine

Cysteine is an essential amino acid that is an important precursor of GSH, hydrogen sulfide (H_2S) and taurine, which is implicated in appetite. Thus, Mcgavigan et al. (2015) used cysteine as a supplementation to reduce appetite in rodents and humans, which produced a reduction of food intake in both cases [318]. Regarding cysteine-containing compounds, their use as supplementation caused a decrease in triglycerides and cholesterol accumulation in mice liver by downregulating the expression of lipogenic enzymes, and a protection against high saturated fat-associated oxidative stress by GSH metabolism, such as NAC administration [319]. Moreover, supplementation of cysteine can boost the formation of circulatory vitamin D, and thereby increase GSH levels preventing oxidative stress and ROS formation associated to T2DM [320]. In addition, previously mentioned, the promising property of cysteine as a natural inhibitor of HAL could imply an increase of histidine levels through the inhibition of the catabolic activity [317].

1.5.2.4 L-Carnosine

Carnosine is obtained from diet and is synthetized through ATP hydrolysis of histidine and β-alanine [321]. Carnosine is synthetized by carnosine synthase 1 (CARNS1) and degraded by carnosine dipeptidase 1 (CNDP1). Carnosine supplementation has been considered a promising treatment against obesity, IR and T2DM [322]. In fact, carnosine supplementation can normalize serum adipokine levels, such as leptin, implicated in glucose metabolism [323], and reduce insulin and glucose levels

in obese patients [324]. Mon et al. (2011) used carnosine as a supplementation in a high-fat diet mice model, and it demonstrated an antilipogenic effect of carnosine on the liver reducing hepatic steatosis by downregulating and reducing the activity of lipogenic genes. Thus, a reduction of body weight, hepatic triglycerides and cholesterol was observed after l-carnosine supplementation [325]. Moreover, carnosine succeeded in alleviating hepatic oxidative stress in liver injury mice models by reducing ROS and increasing GSH and reducing proinflammatory cytokines such as TNFα and CCL2 [326,327]. Therefore, the use of these amino acids as a part of a nutraceutical supplementation can be a therapeutic strategy to tackle the pathogenesis of metabolic disorders and recover histidine levels.

2. HYPOTHESIS & OBJECTIVES

2.1 Hypothesis

The sedentary lifestyle and the increased consumption of processed food are spreading comorbidities such as obesity, hypertension, or insulin resistance. Obesity is a worldwide problem affecting millions of adults. It is characterized by excessive fat accumulation, increasing the risk of suffering several metabolic diseases such as MetS, NAFLD and gut dysfunction. Diet-induced obesity and gut dysbiosis may eventually promote NAFLD development by the dysfunction of adipose tissue releasing FFAs into the circulatory system and gut endotoxemia due to the increased gut permeability that, thereby, ends up inducing fat ectopic deposition and the emergence of pro-inflammatory processes. Currently, there is no effective treatment for these metabolic disorders, and the main tools available to physicians are limited to behavioral changes focused on weight loss through the combination of exercise and a healthy diet. However, the complexity of the pathologies and the multifactorial nature associated with obesity and NAFLD make it difficult to manage and treat them.

Nowadays, nutraceuticals, such as metabolic cofactors or organic molecules, have been considered a promising alter the ability to induce beneficial effects in the cellular mechanisms and biochemical pathways disrupted or affected by native treatment against metabolic disorders due to their capacity to induce beneficial effects in the cellular mechanisms and biochemical pathways that are disrupted or affected from the onset of the diseases until their progression.

Thus, taken into consideration previously exposed, this work hypothesizes that the combination of different functional metabolic cofactors and specific amino acids can be used as treatments to revert obesity and NAFLD progression through the amelioration of adipose tissue dysfunction and hepatic steatosis, activating anti-inflammatory processes within the hepatic, adipose and intestinal tissue and promoting the gut microbiota homeostasis.

2.2 Objectives

The **general objective** of the present study was to determine if a combination of metabolic cofactors or histidine-related amino acids are effective promising treatments against metabolic disorders, such as obesity and NAFLD by modulating the characteristic mechanisms that are disrupted during the development and progression of these diseases and resolving intestinal-liver crosstalk.

Consequently, the **specific objectives** were:

1. To study the impact of the **supplementation with a specific combination of metabolic cofactors on a NAFLD mice model** focusing on the changes in hepatic steatosis and inflammation, and the modulation of insulin sensitivity in the liver.
2. To investigate the effects of the **administration of a specific combination of metabolic cofactors on obesity in a diet-induced mice model** focusing on the changes in the main pathological characteristics in the adipose tissue and circulatory system.
3. To demonstrate that the **supplementation of a specific combination of metabolic cofactors** in a preclinical model of NAFLD not only could reverse NAFLD pathogenesis in the liver, but also may **ameliorate gut morphological changes, gut barrier permeability, and reduce intestinal inflammation** by improving intestinal microbiota composition directly related to NAFLD development.
4. To assess the relationship between **histidine metabolism and NAFLD** by identifying plasma metabolomics, hepatic transcriptomics and fecal metagenomics signatures linked to the liver disease, and to study the effects of histidine-related amino acid (HAA) supplementation in *in vitro* and *in vivo* models as a novel strategy for the treatment of NAFLD.
5. To perform integrative systems medicine approach in large well-characterized obese cohorts using plasma metabolomics, and adipose tissue transcriptomics **to discern the relationship between histidine levels and obesity**, and to evaluate the impact of HAA supplementation in an obese mice model.

3. Methods

3.1 Experimental models and subject details

The experimental models and clinical designs used for each chapter are described in this section. All experimental protocols performed in animal experiments at Eurecat facilities were approved by the Animal Ethics Committee of the Technological Unit of Nutrition and Health of Eurecat (Reus, Spain) and the Generalitat de Catalunya (10281). The experimental protocols followed the "Principles of Laboratory Care" guidelines and were carried out in accordance with the European Communities Council Directive (2010/63/EEC). All experimental procedures of the second mouse model developed in **Chapter 4** were approved by the local ethical committee (approval number 31-278) of Rangueil University Hospital (Toulouse, France).

3.1.1 Mouse models and experimental design for Chapter 1

The study of **Chapter 1** was carried out in male C57BL/6J mice obtained from Envigo (Barcelona, Spain). Forty-eight 7-week-old mice were kept under controlled conditions of temperature (21 ± 2 ºC), light/dark cycles (12 h/12 h) and humidity (50 ± 10%) (**Fig. 18**). After 7 days of acclimation, mice were split into the following groups: a control group made up of mice fed with a standard-chow diet (*n* = 16), and an experimental group made up of NAFLD mice fed with a high-fat high-fructose (HFHFr) diet (*n* = 32). The standard diet D12328 provided 11% fat, 16% proteins and 73% carbohydrates (Research Diets, New Brunswick, IN, USA), and the HFHFr diet was composed of D12331 58% fat, 23% protein and 28 kcal% carbohydrates (Research Diets, New Brunswick, IN, USA) supplemented with Fructose/Sucrose (23.1 g/L; 18.9 g/L) in drinking water. Control mice (*n* = 16) and NAFLD mice (*n* = 32) were fed *ad libitum* for 16 weeks. Once the NAFLD model was obtained, the groups were re-organized for the purpose of the study into the following: CT-vehicle mice (*n* = 16), NAFLD-vehicle mice (*n* = 16), and NAFLD-MI mice (*n* = 16). MI is a mix of the following compounds: 400 mg/kg of LC tartrate (Cambridge Commodities, Ely, UK), 400 mg/kg NAC (Cambridge Commodities), 800 mg/kg Betaine (Cambridge Commodities) and 400 mg/kg NR (ChromaDex, Los Angeles, CA, USA). LC was administrated through LC tartrate (LCT), containing 68.2% LC, providing 560 mg/kg to reach the 400 mg LC/kg dose.

Betaine, LCT, NAC and NR were diluted with drinking water with fructose and sucrose (vehicle). These specific doses were determined based on previous studies and a calculation of dose translation from human to animal dosage through the conversion of drug doses from animal studies to human studies described by Reagan-Shaw et al.[328] . Fresh solutions were prepared three times per week, prepared from stock powders, and protected from light. Before being euthanized, 10 animals per group were randomly selected to perform an insulin challenge. They were intraperitoneally injected with 1 mU/g of insulin (*n* = 5 per group) or saline (*n* = 5 per group) and after 15 min, they were sacrificed. After overnight fasting, mice were sacrificed at the endpoint of the experimental design, plasma was extracted, and serum was obtained by centrifugation and stored at −80 ◦C for further analysis. Livers were rapidly collected, weighed, and divided into two sections—the lobus hepatis sinister medialis was kept in formalin for histological analysis, and the remaining tissue was frozen in liquid nitrogen and stored at −80 ◦C until further analysis (mRNA expression analysis, protein quantification or biochemical analysis, among others).

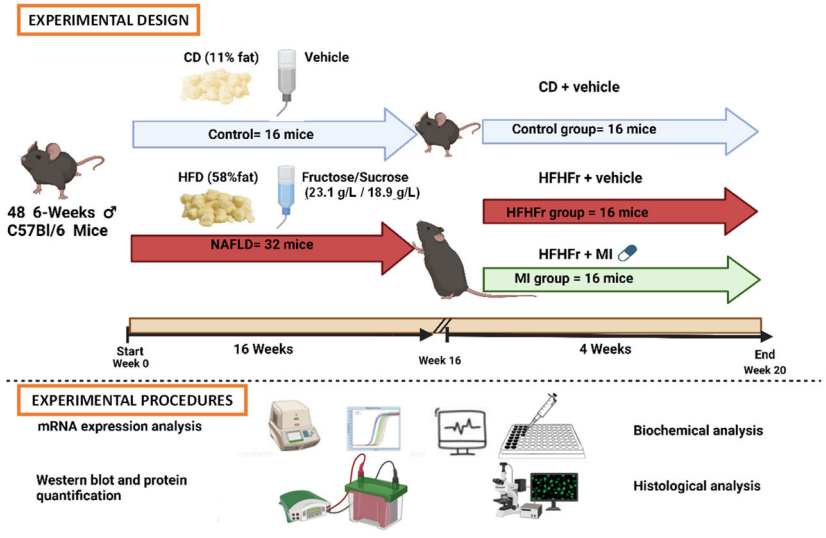

Figure 18. **Experimental design of the animal study and laboratory procedures for Chapter 1**. 48 male mice were divided into control (16) and NAFLD (32) groups, and were subjected to a standard control diet (CD) (Control group) or to a high-fat and high fructose and sucrose in drinking water (HFHFr diet) respectively for 16 weeks. 16 Control mice were fed with a vehicle, 16 mice from the NAFLD group were fed with a vehicle (HFHFr group), and 16 mice with multi-ingredient

supplementation (MI group) for 4 weeks. All mice were sacrificed after 4 weeks of treatment. Experimental procedures performed: mRNA expression analysis, biochemical analysis, Western blot and protein quantification; and histological analysis.

3.1.2 Mouse models and experimental design for Chapter 2

In **Chapter 2**, sixteen six-week-old C57BL/6J male mice (Envigo) were housed in groups under controlled conditions of temperature, humidity and light/dark cycle as explained in the mouse experimental design for **Chapter 1**. After acclimatization, animals were fed with a high-fat diet, high fructose, and high sucrose in the drinking water, as exposed in the experimental design for **Chapter 1**. Mice took these diets for twenty weeks in *ad libitum* conditions. From week six to week twenty, obese mice were randomly distributed into two groups: 8 mice were kept under the same feed conditions described before (Obese + vehicle group), and 8 mice were supplemented with a metabolic cofactors' combination (Obese + MC group). All the concentrations of the metabolic cofactors used in mix are detailed in the mouse experimental design for **Chapter 1**. Solutions were freshly prepared three times per week prepared from stock powders and protected from light. Body weight and food intake data were collected once a week during the entire study. In week nineteen, insulin and glucose tolerance tests (ITT and GTT, respectively) were performed for insulin sensitivity estimation. Metabolic phenotyping (indirect calorimetry and food intake) was also carried out in animals. After week twenty, animals were sacrificed, being deprived of food for eight hours before being euthanized. Blood was collected and serum was obtained by centrifugation and stored at -80 ºC for further biochemical analysis. Brown adipose tissue (BAT) and white adipose tissue (WAT), depots (inguinal (IWAT), epididymal (EWAT), retroperitoneal (RWAT) and mesenteric (MWAT)) were immediately collected, weighed and snap-frozen in liquid nitrogen to finally be kept at -80 ºC for further determinations, such as mRNA expression analysis, or fixed in formalin to perform histological analyses.

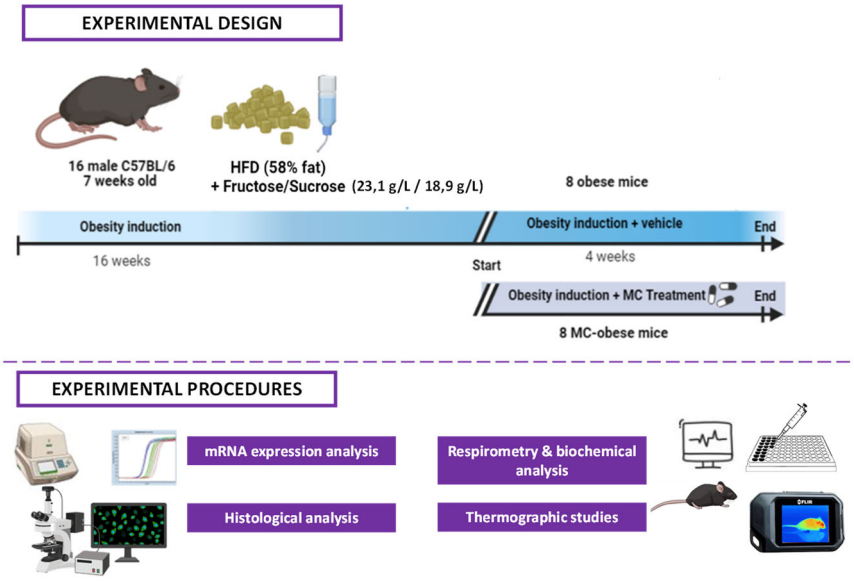

Figure 19. **Experimental design of the animal study and laboratory procedures for Chapter 2**. 16 male mice were subjected to a high-fat diet and fructose and sucrose in drinking water (HFHFr diet) to induce obesity for 16 weeks. 8 obese mice were fed with a vehicle (Obese + vehicle group), and 8 mice with a specific combination of metabolic cofactors (Obese + MC group) for 4 weeks. All mice were sacrificed after 4 weeks of treatment. Experimental procedures performed: mRNA expression analysis, biochemical analysis, histological analysis, and thermographic camera assessment.

3.1.3 Mouse models and experimental design for Chapter 3

Chapter 3 was carried out with twenty-four C57BL/6J; six-week-old male mice (Envigo) were housed in groups under controlled conditions of temperature, humidity, and on a 12-h light/dark cycle with free access to food and water. After acclimatization, animals were randomly divided into different experimental groups: Control mice (n = 8) kept on a standard diet (Research Diets) and NAFLD group (n = 16) fed with a high-fat diet (HFHC: D12331, Research Diets) supplemented with 23.1 g/L fructose and 18.9 g/L sucrose in the drinking water. Mice took each diet respectively for a period of twenty weeks in *ad libitum* conditions. For the last four weeks of the study (from week sixteen to week twenty), NAFLD mice were randomly distributed into two groups: 8 mice were kept under the same fed conditions described above (NAFLD group), and 8 mice were exposed to multi-ingredient (MI) treatment (NAFLD-MI).

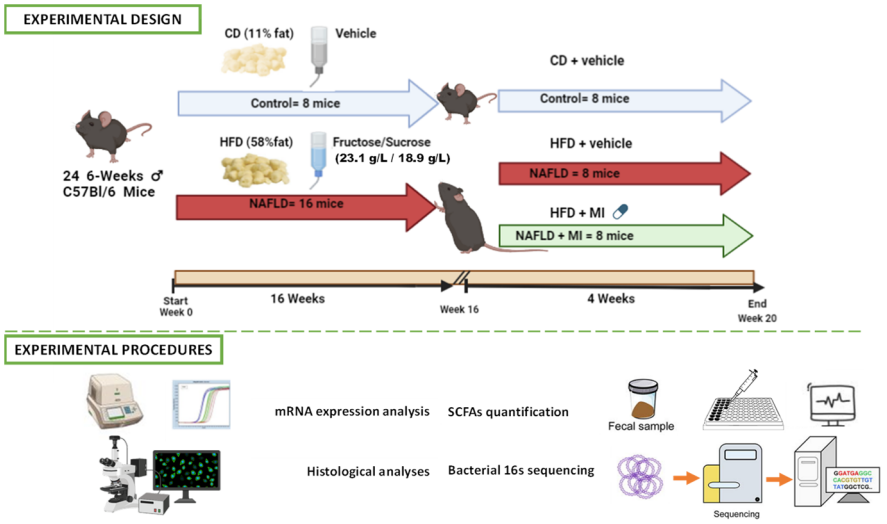

Figure 20. **Experimental design of the animal study and laboratory procedures for Chapter 3**. 24 male mice were subjected to a control diet (CD) (Control group n = 8) or to a high-fat diet and fructose and sucrose in drinking water (HFHFr diet) (NAFLD mice n = 16) for 16 weeks. Then, control mice were fed with a vehicle, 8 mice from the NAFLD group were fed with a vehicle (NAFLD group), and 8 mice with multi-ingredient supplementation (NAFLD+MI group) for 4 weeks. All mice were sacrificed after 4 weeks of treatment. Experimental procedures performed: mRNA expression analysis, histological analyses, SCFAs quantification, and bacterial 16S sequencing analysis.

MI composition was analogous as exposed in the experimental animal model for **Chapter 1** and was diluted with drinking water. Solutions were freshly prepared three times per week from stock powders and protected from light. Fresh fecal pellets were rapidly collected two days before sacrifice and frozen at -80 ◦C. Bacterial DNA was extracted and 16S sequencing was performed in these DNA samples in other to obtain the relative abundances of the different bacteria present in the feces. Moreover, short-chain fatty acids (SCFAs) quantification was realized in feces. After week twenty, animals were sacrificed, being deprived of food for eight hours before being euthanized. Small intestines were rapidly collected, measured, weighed, and divided into two sections (the first section was fixed in formalin and the other section was frozen in liquid nitrogen and stored at −80 ◦C until further analysis, such as histological and mRNA expression analysis.

3.1.4 Mouse models and experimental design for Chapter 4

The animal study of **Chapter 4** was carried out with twenty-four C57BL/6J; six-week-old male mice (Envigo) were housed in groups under controlled conditions of temperature, humidity, and light/dark cycle as explained in the experimental design for **Chapter 1**. After acclimatization, animals were randomly divided into different experimental groups: Lean mice (*n* = 8) fed with a standard diet and Obese group (*n* = 16) fed with a high-fat diet supplemented with fructose and sucrose in the drinking water as detailed in animal model for **Chapter 1**. Mice took these diets for a period of twenty weeks in *ad libitum* conditions. For the last four weeks of the study (from week sixteen to week twenty), obese mice were randomly distributed into two groups: eight mice were kept under the same fed conditions described above (Obese + vehicle group), and eight mice were exposed to histidine-related amino acids treatment (Obese + HAA group). Histidine amino acids combination is a mix of the following compounds: 210 mg/kg of histidine monohydrochloride monohydrate (Merck, GmbH Germany), 490 mg/kg cysteine hydrochloride (Merck, GmbH Germany), 210 mg/kg serine (Merck) and 210 mg/kg carnosine 98% (Acros Organics, Geel, Belgium). Histidine, cysteine, serine, and carnosine were diluted with drinking water (vehicle). Fresh solutions were prepared from stock powders three times per week and protected from light. Body weight and food intake data were collected once a week during the entire study. In week nineteen, ITT and GTT were performed for insulin sensitivity estimation. Metabolic analysis techniques (indirect calorimetry and food intake) were also carried out in animals. After week twenty, animals were sacrificed, being deprived of food for eight hours before being euthanized. Blood was collected and serum was obtained by centrifugation and stored at -80 ºC for further biochemical analysis. BAT and white depots (IWAT; EWAT, RWAT and MWAT) were immediately collected, weighed and snap-frozen in liquid nitrogen to finally be kept at -80 ºC for further determinations, such as mRNA expression analysis and protein quantification, or fixed in formalin to perform histological analyses.

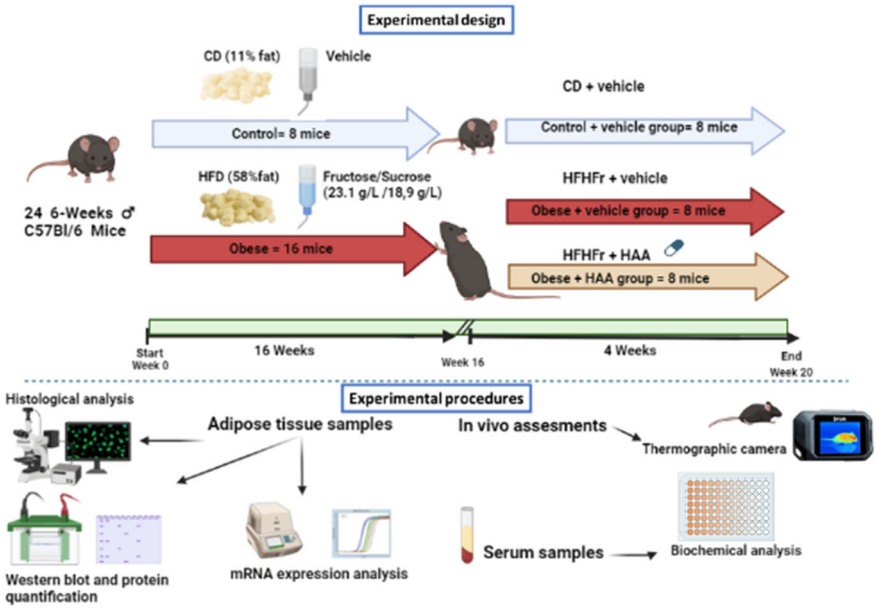

Figure 21. **Experimental design of the animal study with a NAFLD mice model and laboratory procedures for Chapter 4**. 24 male mice were subjected to a control diet (CD) (control group n = 8) or to a high-fat diet and fructose and sucrose in drinking water (obese mice n = 16) for 16 weeks. Then, control mice were fed with a vehicle, 8 mice from the obese group were fed with a vehicle (Obese + vehicle group), and 8 mice with histidine-related amino acids supplementation (Obese + HAA group) for 4 weeks. All mice were sacrificed after 4 weeks of treatment. Experimental procedures performed: In vivo assessments and thermographic camera analyses; in adipose tissue samples, mRNA expression analysis, histological analyses, protein quantification; in serum samples, biochemical analysis.

3.1.5 Human study design for Chapter 4

The clinical study in **Chapter 4** was carried out through a cohort from FLORINASH study assessed by body mass index (BMI) that included 74 obese patients aged twenty-two to sixty-three years old at the Endocrinology Service of the Hospital Universitari de Girona Dr Josep Trueta (FLORINASH; Girona, Spain). The associations were further validated in an independent cohort recruited in the Imageomics2 study that comprised 961 obese patients aged < 50 years old. Obesity status was subdivided into categories: a) normal weight (18.5-24.9), b) overweight (25-29.9), c) Grade 1 obesity (30-34.9), d) grade 2 obesity (35-39.9), and e)

grade 3 obesity (>40). Circulant histidine levels were analyzed in all the participants. The sample size was not determined by statistical methods and is comparable to other studies in the field [329–331]. Moreover, participants from the OUTBRAT cohort (*n* = 251) underwent a subcutaneous adipose tissue (scWAT) biopsy to carry out RNA-sequencing assessment and study genes involved in histidine catabolism in relation to obesity status. Transcriptome and metabolome analysis was carried out from scWAT samples obtained in FLORINASH cohort (*n* = 74) and in an independent cohort from IRONMET study (*n* = 17) in order to find genes and pathways signatures in scWAT associated with plasma histidine levels.

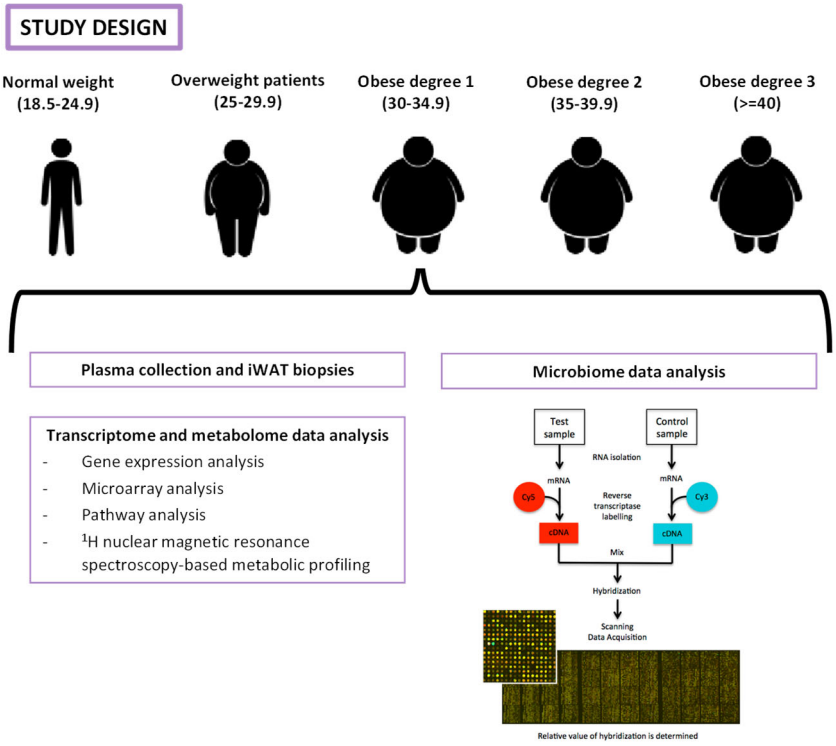

Figure 22. **Experimental design of the clinical study with obese patient cohorts and laboratory procedures for Chapter 4**. Obese men and women were divided into four groups according to their obesity condition (BMI) (lean, overweight, obese degree 1 and obese degree 2) in the four cohorts. Plasma collection and iWAT biopsies were performed to carry out biochemical, transcriptomic, metabolomic, and microbiome analyses. Cy3 and Cy5 are fluorescent dyes used in transcriptomic analysis.

All the subjects gave written informed consent, validated, and approved by the ethical committee of the Hospital Universitari Dr. Josep Trueta (Comitè d'Ètica d'Investigació Clínica, approval number 2009 046). Inclusion criteria included Caucasian origin, stable body weight three months before the study, free of any infection 1 month before the study, and absence of systemic disease. Exclusion criteria were the following: the presence of liver disease (specifically tumoral disease and hepatitis C virus infection) and thyroid dysfunction (based on biochemical work-up), alcohol consumption (> 20 g/day), hepatitis B (anti-HD virus antibodies), drug-induced liver injury (using a drug questionnaire).

3.1.6 Mouse models and experimental design for Chapter 5

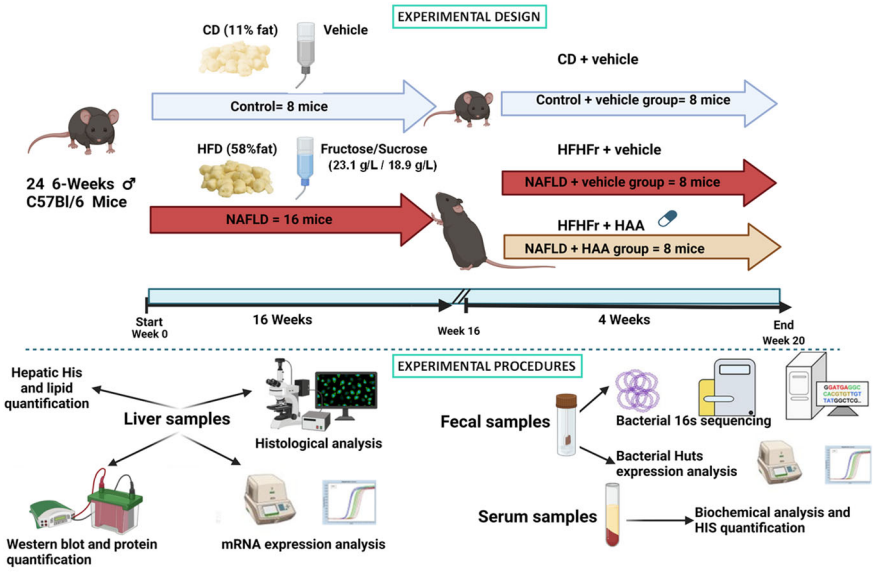

Figure 23. **Experimental design of the animal study with a NAFLD mice model and laboratory procedures in Chapter 5**. 24 C57BL6 male mice were subjected to a control diet (CD) (control group n = 8) or to a high-fat diet and fructose and sucrose in drinking water (HFHFr diet) (NAFLD mice n = 16) for 16 weeks. Control mice were fed with a vehicle, 8 mice from the NAFLD group were fed with a vehicle (NAFLD + vehicle group), and 8 mice with histidine-related amino acids supplementation (NAFLD+HAA group) for 4 weeks. All mice were sacrificed after 4 weeks of treatment. Experimental procedures performed: in liver samples, mRNA expression analysis, histological analysis, protein quantification, and hepatic histidine (His) and lipid quantification; in fecal samples, bacterial 16S

sequencing and bacterial Huts expression analysis; in serum samples, biochemical analysis and circulatory His quantification.

One of the studies with mice in **Chapter 5** was carried out with forty-eight C57BL/6J (Envigo); six-week-old male mice at the beginning of the experiment were used. Animals housing conditions and distribution of groups and diets are explained in **Chapter 5**. Mice took these diets for a period of twenty weeks in *ad libitum* conditions. These specific doses were determined based on previous studies and a calculation of dose translation from human to animal dosage. For the last four weeks of the experiment (from the 16^{th} to 20^{th} week), NAFLD mice were randomly distributed into two groups: sixteen mice were kept under the same fed conditions described before (NAFLD group), and sixteen mice were exposed to histidine-related amino acids treatment (Histidine amino acids group; HAA). Histidine-related amino acids supplementation's composition and preparation is explained in the animal model for **Chapter 5**. Fresh fecal pellets were rapidly collected two days before sacrifice and frozen at -80 ◦C. Bacterial DNA was extracted from fecal samples and 16S sequencing was performed in these DNA samples in other to obtain the relative abundances of the different bacteria present in the feces, and qPCR analyses for the bacterial HutH and HutG genes were performed from the same bacterial DNA samples. Before being euthanized, 10 animals per group were randomly selected to perform an insulin challenge. They were intraperitoneally injected with 1 mU/g of insulin (n = 5 per group) or saline (n = 5 per group) and after 15 min they were sacrificed. Serum was obtained by centrifugation and stored at −80 °C for further analysis. Serum alanine aminotransferase (ALT) and aspartate aminotransferase (AST) were quantified by enzymatic colorimetric assays (QCA, Barcelona, Spain). Fasting insulinemia and glycemia were measured in serum with the Mouse Insulin ELISA Kit (Mercodia, Uppsala, Sweden) and the Glucose Liquid Kit (QCA, Barcelona, Spain), respectively. Circulatory histidine quantification in murine samples was performed by LC-MS. Livers were rapidly collected, weighed, and divided into two sections—the lobus hepatis sinister medialis was kept in formalin for histological analysis, and the remaining tissue was frozen in liquid nitrogen and stored at −80 °C until further analysis, such as mRNA analysis, hepatic fat quantification, histidine quantification by LC-MS, protein quantification.

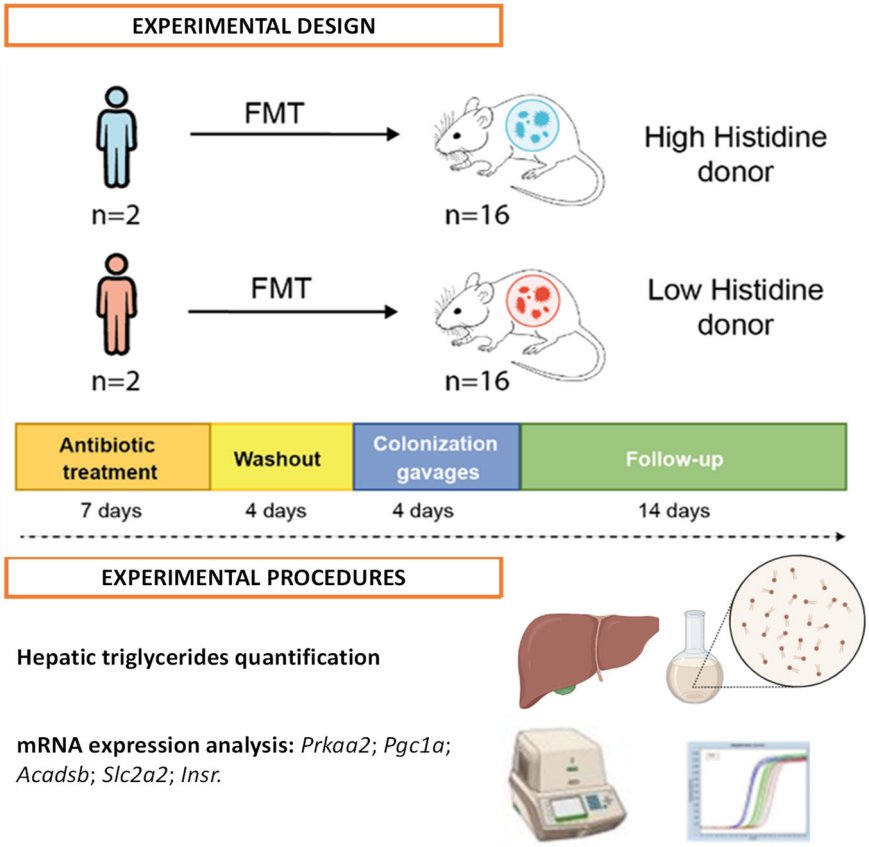

Figure 24. Experimental design of the animal study of fecal microbiota transplantation from human donors and laboratory procedures in Chapter 5. 32 C57BL6 male mice were subjected to antibiotic treatment for 7 days, and after a 4-day washout, mice were administered 20 mg/day of fecal matter from low and high histidine donors for 4 consecutive days. After the treatment, 14 days of follow-up were conducted. All mice were sacrificed, and hepatic triglycerides quantification and mRNA expression analysis was performed in liver samples.

The second mouse model developed in **Chapter 4** was a fecal microbiota xenotransplantation (FMT) study. Fecal samples from low- (n = 2) and high- (n = 2) histidine donors (according to the media) and matched for age and BMI were suspended in sterile reduced PBS. Eight mice (eight-week-old C57BL6 male, Charles River) per donor were treated with an antibiotic mixture (Ampicillin, Neomycin, Metronidazol 0.1 g /100 mL of each in water, in free access) for seven days. After four days of a wash-out period, C57BL/6 germ-free male mice were administered 20 mg/day of fecal matter for four consecutive days. Two weeks later, mice were

sacrificed, and liver and plasma were collected and frozen. Liver from both low and high donor mice groups were used to perform analysis of hepatic triglycerides quantification and mRNA expression of several genes coding for key enzymes involved in regulating *de novo* biosynthesis of fatty acid and cholesterol, glucose and insulin metabolism.

3.1.7 Human study design for Chapter 5

The clinical study in **Chapter 5** was carried out through a discovery cohort assessed by liver biopsy that included 102 obese patients aged twenty-four to sixty-three years old at the Endocrinology Service of the Hospital Universitari de Girona Dr Josep Trueta (FLORINASH; Girona, Spain) and through a discovery cohort assessed by echography included 96 obese patients aged twenty-four to sixty-three years old at the same center (Echography; Girona, Spain). The associations were further validated in an independent cohort that comprised 596 obese patients aged twenty to sixty-seven years old. The validation cohort 1 comprised aged twenty-five to sixty-six years old at the Center for Atherosclerosis of Policlinico Tor Vergata University of Rome (Rome, Italy) and the validation cohort 2 comprised 283 obese patients aged twenty-five to sixty-six years old at the Endocrinology Service of the Hospital Universitari de Girona Dr. Josep Trueta. The sample size was comparable to other studies in the field [329–331]. All the subjects gave written informed consent, validated, and approved by the ethical committee of the Hospital Universitari Dr. Josep Trueta (Comitè d'Ètica d'Investigació Clínica, approval number 2009 046) and Policlinico Tor Vergata University of Rome (Comitato Etico Indipendente, approval number 28-05-2009). Inclusion criteria included Caucasian origin, a stable body weight three months before the study, free of any infection one month before the study, and absence of systemic disease. Exclusion criteria were the following: the presence of liver disease (specifically tumoral disease and hepatitis C virus infection) and thyroid dysfunction (based on biochemical work-up), alcohol consumption (> 20 g/day), hepatitis B (anti-HD virus antibodies), drug-induced liver injury (using a drug questionnaire).

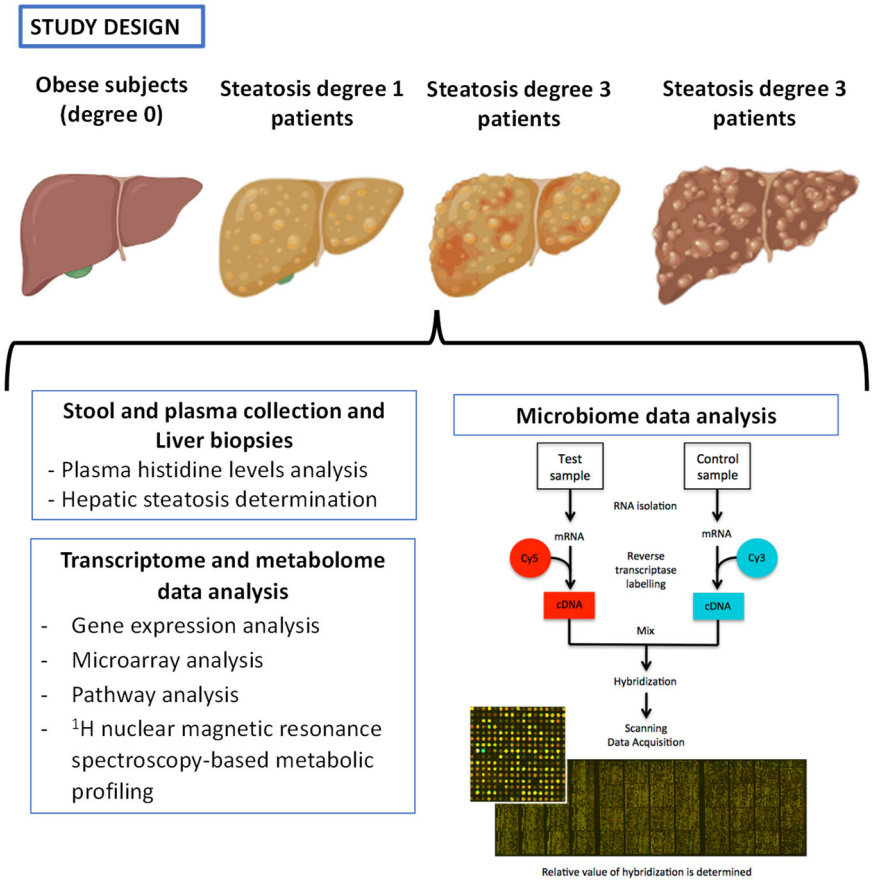

Figure 25. **Experimental design of the clinical study with patient cohorts with NAFLD and laboratory procedures for Chapter 5**. Obese men and women from the cohorts were divided into four groups according to their steatosis degree (0, 1, 2 or 3). Stool, plasma collection, and liver biopsies were performed to carry out biochemical, transcriptomic, metabolomic, and microbiome analyses. Cy3 and Cy5 are fluorescent dyes used in the transcriptomic analysis.

3.1.8 *Primary hepatocytes and experimental design for Chapter 5*

Cryopreserved primary human hepatocytes were commercially sourced (Innoprot, Bizkaia, Spain) and cultured with hepatocytes medium (Innoprot) supplemented with 5% fetal bovine serum, 1% hepatocytes growth supplement (mixture of growth factors, hormones, and protein necessary for the culture of primary hepatocytes) and 100 U/ml penicillin and streptomycin. Primary human hepatocytes were grown on poly-L-lysine pre-coated cell dishes at 37 °C and 5% CO_2 atmosphere following

the manufacturer's recommendations. For histidine supplementation experiments in steatosis, histidine was dissolved in 0.5 M HCl and was used at 500 nM to treat HHs. After forty-eight hours of histidine treatment, cells were treated with PA for twenty-four hours. PA was prepared as follows: 27.84 mg of PA (Sigma, San Luis, MO) was dissolved in 1 mL sterile water to obtain a 100 mM stock solution. BSA was used in all treatments as the vehicle. All experimental conditions were performed in four biological replicates. After treatment, cells were washed with PBS and collected with Qiazol for RNA purification.

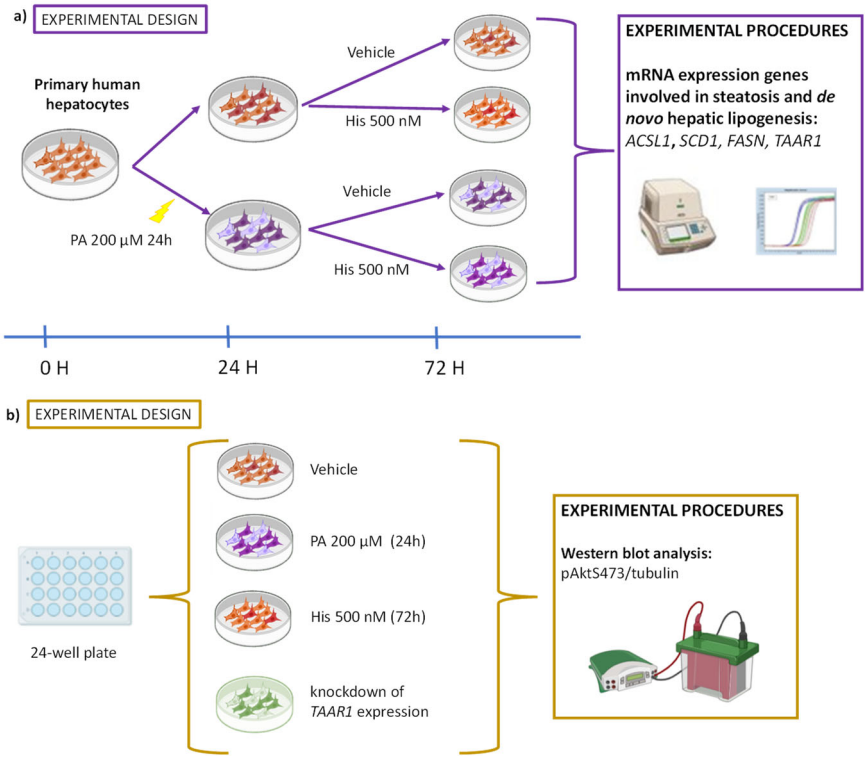

Figure 26. **Experimental designs of the *in vitro* studies with primary human hepatocytes and laboratory procedures for Chapter 5**. a) First, primary hepatocytes cultured with hepatocytes medium were divided into not treated cells and treated cells with 200 µm palmitate (PA) for 24h. Second, both groups were divided into 2 new treatments for 48h: vehicle and His 500nM. After that, cells were washed with PBS and collected with Qiazol for RNA purification. Gene expression analysis was performed by RT- and qPCR. b) 24-weell plate was seed 24h with primary hepatocytes with hepatocytes medium. Then, they were divided into control cells, cells treated with PA 200µM for 24h, cells treated with 500 nM His for 72h, or knock-down of TAAR1 expression. Then, western blotting and

densitometry analysis of phosphorylated AktS473 and tubulin ratio in primary hepatocytes treated with PA or histidine (500 nM), or knock-down of TAAR1 expression. Histidine, His; phosphorylated AKT, pAKT.

For TAAR1 silencing experiments, the siRNA (Sigma-Aldrich, St. Louis, MO, USA) against TAAR1 and Lipofectamine RNAiMAX (LifeTechnologies, Darmstadt, Germany) were diluted separately with Opti-MEM I Reduced Serum Medium (Life Technologies, Darmstadt, Germany) and mixed by pipetting afterwards. The siRNA-RNAiMAX complexes were left to incubate for twenty minutes at room temperature and subsequently added on the top of the adherent cells drop-wise. The final concentrations of Lipofectamine RNAiMAX and siRNAs were 1.6 mL/cm^2 and 75 nM, respectively, in 24-well cell culture plates, and the final amount of medium per well was 1 mL. Twenty-four hours after seeding, HHS were transfected with siRNA against TAAR1 or treated with histidine for seventy-two hours alone, or in combination with palmitic acid (PA) for twenty-four hours following the siTAAR1/histidine treatment. Transfection efficiency was assessed by real-time PCR. After treatment, cell lysates were collected by scraping on ice with cell lysis buffer. For proteins extracts were obtained for western blotting.

3.2 Experimental procedures and assays

Specific materials and methods for each Chapter are detailed in the correspondence chapter.

4.RESULTS

Chapter 1

Supplementation with a specific combination of metabolic cofactors ameliorates non-alcoholic fatty liver disease and, hepatic fibrosis, and insulin resistance in mice

S. Quesada-Vázquez [1], M. Colom-Pellicer [2], E. Navarro-Masip [2], G. Aragonès [2], J. M. Del Bas [1], A. Caimari [3], X. Escoté, [1*]

1. Eurecat, Technology Centre of Catalunya, Nutrition and Health Unit, 43204 Reus, Spain; sergio.quesada@eurecat.org (S.Q.-V.); josep.delbas@eurecat.org (J.M.D.B); xavier.escote@eurecat.org (X.E.)
2. Department of Biochemistry and Biotechnology, Universitat Rovira i Virgili, Nutrigenomics Research Group, 43007 Tarragona, Spain; marina.colom@urv.cat (M.C.-P.); elia.navarro@urv.cat (E.N.-M.); gerard.aragones@urv.cat (G.A.)
3. Eurecat, Centre Tecnològic de Catalunya, Biotechnology Area, Reus, Spain; antoni.caimari@eurecat.org (A.C.)

* Correspondence: xavier.escote@eurecat.org (X.E.); Tel.: +34-977-302057 (ext. 4824)

Published in: Nutrients. 2021 Oct; 13, 3532

Impact Factor (2022): 6.706

JCR category rank: Q1: Nutrition & Dietetics

nutrients

MDPI

Article

Supplementation with a Specific Combination of Metabolic Cofactors Ameliorates Non-Alcoholic Fatty Liver Disease, Hepatic Fibrosis, and Insulin Resistance in Mice

Sergio Quesada-Vázquez [1], Marina Colom-Pellicer [2], Èlia Navarro-Masip [2], Gerard Aragonès [2], Josep M. Del Bas [1], Antoni Caimari [3] and Xavier Escoté [1,*]

[1] Eurecat, Technology Centre of Catalunya, Nutrition and Health Unit, 43204 Reus, Spain; sergio.quesada@eurecat.org (S.Q.-V.); josep.delbas@eurecat.org (J.M.D.B.)
[2] Nutrigenomics Research Group, Department of Biochemistry and Biotechnology, Universitat Rovira i Virgili, 43007 Tarragona, Spain; marina.colom@urv.cat (M.C.-P.); elia.navarro@urv.cat (È.N.-M.); gerard.aragones@urv.cat (G.A.)
[3] Eurecat, Centre Tecnològic de Catalunya, Biotechnology Area, 43204 Reus, Spain; antoni.caimari@eurecat.org
* Correspondence: xavier.escote@eurecat.org; Tel.: +34-977-302057 (ext. 4824)

Abstract: Non-alcoholic fatty liver disease (NAFLD) and non-alcoholic steatohepatitis (NASH) have emerged as the leading causes of chronic liver disease in the world. Obesity, insulin resistance, and dyslipidemia are multifactorial risk factors strongly associated with NAFLD/NASH. Here, a specific combination of metabolic cofactors (a multi-ingredient; MI) containing precursors of glutathione (GSH) and nicotinamide adenine dinucleotide (NAD^+) (betaine, N-acetyl-cysteine, L-carnitine and nicotinamide riboside) was evaluated as effective treatment for the NAFLD/NASH pathophysiology. Six-week-old male mice were randomly divided into control diet animals and animals exposed to a high fat and high fructose/sucrose diet to induce NAFLD. After 16 weeks, diet-induced NAFLD mice were distributed into two groups, treated with the vehicle (HFHFr group) or with a combination of metabolic cofactors (MI group) for 4 additional weeks, and blood and liver were obtained from all animals for biochemical, histological, and molecular analysis. The MI treatment reduced liver steatosis, decreasing liver weight and hepatic lipid content, and liver injury, as evidenced by a pronounced decrease in serum levels of liver transaminases. Moreover, animals supplemented with the MI cocktail showed a reduction in the gene expression of some proinflammatory cytokines when compared with their HFHFr counterparts. In addition, MI supplementation was effective in decreasing hepatic fibrosis and improving insulin sensitivity, as observed by histological analysis, as well as a reduction in fibrotic gene expression (*Col1α1*) and improved Akt activation, respectively. Taken together, supplementation with this specific combination of metabolic cofactors ameliorates several features of NAFLD, highlighting this treatment as a potential efficient therapy against this disease in humans.

Keywords: NAFLD; liver disease; steatosis; hepatic inflammation; hepatic insulin resistance

Citation: Quesada-Vázquez, S.; Colom-Pellicer, M.; Navarro-Masip, È.; Aragonès, G.; Del Bas, J.M.; Caimari, A.; Escoté, X. Supplementation with a Specific Combination of Metabolic Cofactors Ameliorates Non-Alcoholic Fatty Liver Disease, Hepatic Fibrosis, and Insulin Resistance in Mice. *Nutrients* **2021**, *13*, 3532. https://doi.org/10.3390/nu13103532

Academic Editor: Henricus A. M. Mutsaers

Received: 30 July 2021
Accepted: 30 September 2021
Published: 9 October 2021

1. Introduction

Non-alcoholic fatty liver disease (NAFLD) and non-alcoholic steatohepatitis (NASH) have emerged as the leading causes of chronic liver ailments worldwide, with a prevalence rising in most developed countries [1]. NAFLD is a multifactorial disease that affects the liver and other peripheral organs and regulatory pathways and is characterized by excessive fat liver accumulations in the absence of alcohol consumption [2]. In Western countries, an incidence of NAFLD of around 20–30% of the adult population is estimated. The prevalence is lower in Eastern countries, but a rising tendency has been recently observed due to the changes in dietary habits, together with the sedentary lifestyle associated with Westernized societies [1]. These Western dietary habits are characterized by a

predominant and excessive intake of saturated fats and caloric oversupply that, together with an impoverishment of lifestyle, are the key causes of developing NAFLD/NASH [3]. Moreover, lower consumption of vegetables, fruits, whole grains, ω3-fatty acids, and proteins facilitates NAFLD progression [3].

These chronic liver diseases are characterized by several pathologic features, including hepatic steatosis (HS), hepatocyte hypertrophy, and ballooning in NAFLD, together with fibrosis and inflammation in NASH [4,5]. Regarding the affected metabolic pathways associated with NAFLD progression, a mitochondrial dysfunctionality has been described. This alteration is caused by the imbalance between prooxidant and antioxidant mechanisms, which results in an increased production of reactive oxygen species (ROS), impairing the functionality of the electron transport chains and leading to an abnormal fatty acid oxidation [6,7]. Another key contributor to the pathogenesis of NAFLD is an increased visceral adipose tissue dysfunction, which is related to adipose hypertrophy, increased proinflammatory cytokine production and progressive fibrosis [8]. The adipose tissue dysfunction results in insulin resistance, limiting the amount of fat storage, and implicating a decreased de novo lipogenesis and increased lipolysis in the adipose tissue (due to inefficiency of insulin to block lipolysis) with consequent increased flux of fatty acids from adipose tissue to the liver [8,9]. This elevates free fatty acid (FFA) fluxes from adipose depots to the liver, which results in an increased hepatic de novo lipogenesis and an impaired inhibition of adipose tissue lipolysis [9]. These FFAs are accumulated in liver as triacyclglycerol (TG) and diacylglycerol (DAG). Increased production of DAGs promotes the synthesis of intermediates such as ceramides, which are associated with the development of high resistance in the hepatic insulin-signaling pathway through decreasing Akt activation. These metabolic alterations promote hepatic inflammation and the risk of progressive fibrosis. The synthesis of hepatic non-esterified fatty acids also induces endoplasmic reticulum stress, contributing to hepatic production of inflammatory cytokines as tumor necrosis factor-α (TNFα) [2].

Fatty liver is a primary stage of liver disease that is considered reversible and benign, whereas NASH is an advanced and more-dangerous phase that could progress to worse diagnoses such as cirrhosis and liver cancer [5,10]. Currently, there is no effective treatment for NAFLD and the main tools available to physicians are limited to behavioral changes focused on weight loss through the combination of exercise and a healthy diet [11,12]. Thus, novel medical or nutritional approaches are needed to fight against these diseases.

Previous studies have shown that a multifactorial dietary intervention with bioactive cofactors that modulate the activity of the deregulated metabolic pathways can effectively revert hepatic steatosis in NAFLD patients [5]. This intervention intends to reduce liver fat content by increasing both mitochondrial fatty acid uptake and oxidation and glutathione (GSH) availability [5,13]. An integrated analysis performed by Mardinoglu et al., which combined personalized genome-scale metabolic models and in-depth multiomics profiling based on human data, indicated augmented requirements for nicotinamide adenine dinucleotide $(NAD)^+$ and reduced GSH in patients with NAFLD, which could be related to this mitochondrial dysfunction [5,14,15]. Thus, the limited availability of serine and glycine in NAFLD patients reduced de novo GSH synthesis, protecting against ROS [7].

A clinical study in healthy subjects supplemented with a promising combination of metabolic cofactors to target fat liver accumulations and revert altered metabolic processes showed an improvement in blood inflammatory parameters, pointing out that this combination is a promising treatment for NAFLD [5,7,14]. These cofactors were present in a multi-ingredient mixture (MI) composed of L-carnitine (LC, an enhancer of fatty acid uptake across the mitochondrial membrane), n-acetyl cysteine (NAC) and serine (glutathione precursors protecting against ROS), and nicotinamide riboside (NR) as an NAD^+ precursor [5,7,14]. Xia et al. described LC protective effects by accelerating FFAs transport into mitochondria in hepatocytes [16]. NR can increase NAD^+ levels and accelerate oxidative metabolism and protection against obesity ameliorating metabolic disorders induced by impaired mitochondrial function [17]. NAC has a protective effect, reducing

oxidative stress by increasing GSH availability, and can increase fatty acid re-uptake and fatty acid oxidation [13]. In other studies, serine was replaced by betaine, which is a methyl donor involved in methionine metabolism and may regulate cysteine levels, being a GSH precursor, because betaine can be converted to glycine and sarcosine [13,18]. These studies elucidated that supplementation with NAD^+ and GSH precursors might be useful as a treatment of NAFLD, promoting fat oxidation in liver mitochondria, reducing liver fat content, increasing de novo GSH synthesis and improving liver function parameters [7].

To validate this hypothesis, a preclinical study in a well-established dietary mice model of NAFLD induced by high fat and high sugar consumption was performed [19]. This model had previously shown an aggravating effect of fructose on glucose and lipid metabolism, resulting in hepatic triglyceride accumulation, insulin resistance and a characteristic microvesicular, macrovesicular and steatosis effect similar to those described in humans [20,21]. In the present study, the impact of supplementation with this specific combination of metabolic cofactors was evaluated for the first time, focusing on the main features of NAFLD/NASH, liver steatosis, hepatic inflammation and hepatic insulin resistance.

2. Materials and Methods

2.1. Animal Model and Diets

Forty-eight C57BL/6J male mice (Envigo, Sant Feliu de Codines, Barcelona, Spain), 6 weeks old at the beginning of the experiment, were used (Figure S1). Animals were housed in groups (4 mice per cage) under controlled conditions of temperature (22 ± 2 °C) and humidity (55 ± 10%), and on a 12-h light/dark cycle with free access to food and water. Mice were left undisturbed to acclimate to the animal facility for one week. After the acclimatation period, animals were randomly divided into two experimental groups with different diets. Sixteen control mice were kept on a standard diet (D12328, Research Diets, New Brunswick, NJ, USA) and 32 animals (NAFLD group) were fed with HFHFr diet (HFHC: D12331, Research Diets) supplemented with 23.1 g/L fructose and 18.9 g/L sucrose in the drinking water. Mice were kept on these diets for a period of 20 weeks in ad libitum conditions. These specific doses were determined based on previous studies and a calculation of dose translation from human to animal dosage [22]. All experimental protocols were approved by the Animal Ethics Committee of the Technological Unit of Nutrition and Health of Eurecat (Reus, Spain) and the Generalitat de Catalunya approved all the procedures (10281). The experimental protocol followed the "Principles of Laboratory Care" guidelines and was carried out in accordance with the European Communities Council Directive (2010/63/EEC).

For the last 4 weeks of the experiment (from the 16th to 20th week), NAFLD mice were randomly distributed into two groups: 16 mice were kept under the same fed conditions described before (HFHFr group), and 16 mice were exposed to multi-ingredient treatment (MI group). MI is a mix of the following compounds: 400 mg/kg of LC tartrate (Cambridge Commodities, Ely, UK), 400 mg/kg NAC (Cambridge Commodities), 800 mg/kg Betaine (Cambridge Commodities) and 400 mg/kg NR (ChromaDex, Los Angeles, CA, USA). LC was administrated through LC tartrate (LCT), containing 68.2% LC, providing 560 mg/kg to reach the dose of 400 mg LC/kg. Betaine, LCT, NAC and NR were diluted with drinking water with 23.1 g/L fructose and 18.9 g/L sucrose (vehicle). Fresh solutions were freshly prepared three times per week and prepared from stock powders and protected from light. Before being euthanized, 10 animals per group were randomly selected to perform an insulin challenge. They were intraperitoneally injected with 1 mU/g of insulin (n = 5 per group) or saline (n = 5 per group) and after 15 min, they were sacrificed.

Serum was obtained by centrifugation and stored at −80 °C for further analysis. Serum alanine amino-transferase (ALT) and aspartate amino-transferase (AST) were quantified by enzymatic colorimetric assays (QCA, Barcelona, Spain). Fasting insulinemia and glycemia were measured with the Mouse Insulin ELISA Kit (Mercodia, Uppsala, Sweden) and the Glucose Liquid Kit (QCA, Barcelona, Spain), respectively. Livers were rapidly collected,

weighed and divided into two sections—the lobus hepatis sinister medialis was kept in formalin, and the remaining tissue was frozen in liquid nitrogen and stored at −80 °C until further analysis.

2.2. Hepatic Fat Quantification

Hepatic lipids were extracted and quantified following a method previously described [23]. Briefly, total lipids were extracted from 80–100 mg liver sections by adding 1 mL of hexane/isopropanol (3:2, *v/v*) and degassing with gas nitrogen. Then, they were left overnight under orbital agitation, at room temperature, protected from light. After extracting with 0.3 mL of Na_2SO_4 (0.47 M), the organic layer was separated and dried with gas nitrogen. Total lipids were quantified gravimetrically before emulsifying, as described previously [24]. Triglycerides, total cholesterol, and phospholipids were measured using commercial enzymatic kits (QCA).

2.3. Histological Evaluation

Liver portions fixed in buffered formalin (4% formaldehyde, 4 gr/L NaH2PO4, 6.5 gr/L Na_2HPO_4; pH 6.8) were cut at a thickness of 3.5 µm and stained with hematoxylin & eosin (H&E) and trichrome stain. Liver images (magnification 40X) were taken with a microscope (ECLIPSE Ti; Nikon, Tokyo, Japan) coupled to a digital sight camera (DS-Ri1, Nikon) and analyzed using ImageJ NDPI software (National Institutes of Health, Bethesda, MD, USA; https://imagej.nih.gov/ij, version 1.52a). To avoid any bias in the analysis, the study had a double-blind design, preventing the reviewers from knowing any data from the mice during the histopathological analysis. A General NAFLD Scoring System was established to diagnose mice with NAFLD/NASH. The key features of NAFLD and NASH were categorized as follows: steatosis was assessed by analyzing macrovesicular (0–3) and microvesicular steatosis (0–3) separately, followed by hepatocellular hypertrophy (0–3), which evaluates abnormal cellular enlargement, and finally giving a total score of 9 points of steatosis state. Inflammation was scored by counting cell aggregates (inflammatory foci). The score 0 to 3 depends on the grade of the feature. It is categorized as 0 (<5%), 1 (5–33%), 2 (34–66%) and 3 (>66%), and this scoring is used in each feature of steatosis and then added to the total steatosis score [25]. Ballooning was not included in the scoring system, because only quantitative measures were considered for the rodent NAFLD score. It is important to highlight that hypertrophy is not a sign of cellular injury and slightly refers to an anomalous enlargement of the cells without recognizing the source of this enlargement [25]. Knowing that chronic inflammatory state might trigger fibrogenesis [26], liver fibrosis was analyzed by Masson's trichrome-stained sections considering the collagen proportional area, as previously described [27,28].

2.4. RNA Extraction and Quantitative Polymerase Chain Reaction

Homogenates from 6 livers per groups were used for total RNA extractions using TriPure reagent (Roche Diagnostic, Sant Cugat del Vallès, Barcelona, Spain) according to the manufacturer's instructions. RNA concentration and purity were determined using a nanophotometer (Implen GmbH, München, Germany). RNA was converted to cDNA using the High-Capacity RNA-to-cDNA Kit (Applied Biosystems, Wilmington, DE, USA). The cDNAs were diluted 1:10 before incubation with commercial LightCycler 480 Sybr green I master on a Lightcycler® 480 II (Roche Diagnostics GmbH, Manheim, Germany). Table 1 shows a list of used primers that were previously described in other studies and verified with Primer-Blast software (National Center for Biotechnology Information, Bethesda, MD, USA). As previously described, 36b4 was used as a housekeeping gene [29–31].

2.5. Protein Extraction and Western Blot Analysis

Approximately 20 mg of liver was homogenized with Tyssuelyser LT (Qiagen, Hilden, Germany) for 50 s in 300 µL lysis buffer (8 mmol/L NaH_2PO_4, 42 mmol/L Na_2HPO_4, 1% SDS, 0.1 mol/L NaCl, 0.1% NP40, 1 mmol/L NaF, 10 mmol/L sodium orthovanadate,

2 mmol/L PMSF, and 1% protease inhibitor cocktail 1 (Millipore Sigma, Darmstadt, Germany)). The protein extracts were quantified by the standardized BCA method (Bio-Rad Protein Assay; BioRad, Hercules, CA, USA). Protein extracts (20–25 µg) were electrophoretically separated on 10% SDS-PAGE and electroblotted to nitrocellulose membranes (Li-cor biosciences, NE, USA) [32]. Efficient protein transfer was monitored by Ponceau-S stain. Next, membranes were blocked (5% BSA) at room temperature and probed with specific primary antibodies (diluted 1:1000) overnight at 4° C in 1% BSA: total Akt (4685) (CST, Danvers, MA, USA), phospho-Akt (Ser473) (4060) (CST) and β-Actin (Santa Cruz Biotechnology, Inc.; Dallas, TX, USA). Thereafter, infrared fluorescent secondary antibodies anti-rabbit 680, anti-rabbit 800 and anti-mouse 680 (LI-COR Biosciences, Lincoln, NE, USA; 926-32211, 926-68071 and 926-68070, respectively) were used for detection and quantified using ImageJ [33].

Table 1. Sequences of the used RT-PCR oligonucleotides.

Primers	Forward	Reverse	Reference
Ppara	5′-CCCTGTTTGTGGCTGCTATAATTT-3′	5′-GGGAAGAGGAAGGTGTCATCTG-3′	[34]
Fasn	5′-GCTGCGGAAACTTCAGGAAAT-3′	5′-AGAGACGTGTCACTCCTGGACTT-3′	[35]
Col1a1	5′-TAGGCCATTGTGTATGCAGC-3′	5′-ACATGTTCAGCTTTGTGGACC-3′	[36]
Tnfa	5′-AGGGTCTGGGCCATAGAACT-3′	5′-CCACCACGCTCTTCTGTCTAC-3′	[36]
Il6	5′-AGTTGCCTTCTTGGGACTGA-3′	5′-TCCACGATTTCCCAGAGAAC-3′	[37]
Il1a	5′-CCAGAAGAAAATGAGGTCGG-3′	5′-AGCGCTCAAGGAGAAGACC-3′	[38]
F4/80	5′-CATAAGCTGGGCAAGTGGTA-3′	5′-GGATGTACAGATGGGGGATG-3′	[39]
Scd1	5′-AGATCTCCAGTTCTTACACGACCAC-3′	5′-GACGGATGTCTTCTTCCAGGTG-3′	[40]
Acc1	5′-GATGAACCATCTCCGTTGGC-3′	5′-CCCAATTATGAATCGGGAGTGC-3′	[40]
Cd36	5′-GAACCACTGCTTTCAAAAACTGG-3′	5′-TGCTGTTCTTTGCCACGTCA-3′	[40]
Fabp4	5′-TGAAAGAAGTGGGAGTGGGC-3′	5′-CGAATTCCACGCCCAGTTTG-3′	[41]
Cpt1a	5′-CTCAGTGGGAGCGACTCTTCA-3′	5′-GGCCTCTGTGGTACACGACAA-3′	[42]
Cbs	5′-GCAGCGCTGTGTGGTCATC-3′	5′-CATCCATTTGTCACTCAGGAACTT-3′	[43]
Fgf21	5′-CCTCTAGGTTTCTTTGCCAACAG-3′	5′-AAGCTGCAGGCCTCAGGAT-3′	[44]
Ucp2	5′-GGTCGGAGATACCAGAGCAC-3′	5′-ATGAGGTTGGCTTTCAGGAG-3′	This study
Glut2	5′-ACCCTGTTCCTAACCGGG-3′	5′-TGAACCAAGGGATTGGACC-3′	[45]
G6pd	5′-GTGGGATCCTGAGGGAAGAGT-3′	5′-GATGGTGGGATAGATCTTCTTCTTG-3′	[34]
Srebp1c	5′-TGACCCGGCTATTCCGTGA-3′	5′-CTGGGCTGAGCAATACAGTTC-3′	[46]
Ucp1	5′-ACTGCCACACCTCCAGTCATT-3′	5′-CTTTGCCTCACTCAGGATTGG-3′	[47]
36bB4	5′-AGTCCCTGCCCTTTGTACACA-3′	5′-CGATCCGAGGGCCTCACTA-3′	[48]

2.6. Statistical Analysis

Statistical analyses were performed using GraphPad Prism 9 software (Graph-Pad Soft-ware, La Jolla, CA, USA). Data are presented as mean ± SEM. Data distribution was analyzed by the Shapiro–Wilk normality test. Differences between two groups were determined using an unpaired *t*-test (two-tailed, 95% confidence interval). One-way analysis of variance (ANOVA) was conducted to examine differences between three groups. A *p*-value below 0.05 was considered statistically significant.

3. Results

3.1. MI Supplementation Reduced Liver Injury and Macroscopic Liver Features of NAFLD

After 4 weeks of treatment, MI supplementation (treatment composed of betaine, NR, NAC and L-carnitine) promoted a reduction in body weight (Figure S2a) and a tendency to reduce adiposity (Figure S2b). These reductions were not a consequence of food intake decrease, because no differences were observed between MI and HFHFr groups (Figure S2c,d). Liver injury was evaluated by measuring ALT and AST serum levels. Both transaminases were clearly increased in serum of HFHFr mice (Figure 1a,b). In contrast, MI mice presented a decreased level of both transaminases (Figure 1a,b), almost to control mice levels, lowering these liver injury markers at similar levels than non-NAFLD animals (HFHFr group). The AST/ALT ratio was significantly decreased in the HFHFr mice group

compared to control mice. However, the AST/ALT ratio was significantly recovered in MI supplemented mice close to control group results (Figure 1c). In addition, macroscopic assessment showed fatty liver appearance in HFHFr animals compared to the control group, whereas MI intervention partially recovered a healthy liver appearance in comparison with HFHFr animals (Figure 1d). In fact, MI supplementation significantly attenuated the liver weight increase observed in HFHFr group (Figure 1e). This phenomenon was also observed in liver weight relative to body weight (Figure 1f).

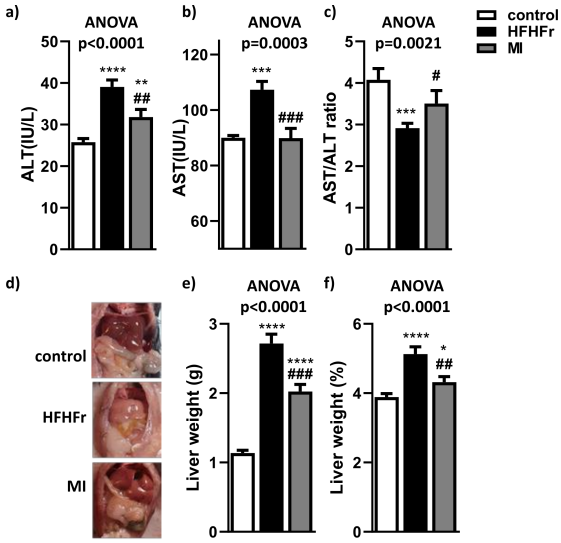

Figure 1. Effects of treatments on (**a**) serum ALT (alanine amino-transferase); (**b**) serum AST (aspartate amino-transferase); (**c**) serum AST/ALT ratio; (**d**) representative macroscopic appearance of livers; (**e**) liver weight; and (**f**) liver weight/body weight (%). Data are mean ± SEM; n = 16 animals/group. * $p < 0.05$, ** $p < 0.01$, *** $p < 0.001$, **** $p < 0.0001$ vs. control mice; # $p < 0.05$, ## $p < 0.01$, ### $p < 0.001$ vs. HFHFr mice.

3.2. MI Supplementation Decreased Hepatic Lipid Content and Liver Steatosis

To determine if MI intervention reduced liver lipid accumulation, hepatic lipid content was evaluated. As expected, hepatic lipid content was increased in the HFHFr group compared to the control group (Figure 2a), and MI treatment significantly reduced this effect observed in HFHFr mice. A similar pattern was observed in hepatic triglyceride content (Figure 2b), in hepatic cholesterol content (Figure 2c), and in phospholipid content (Figure 2d), observing that the HFHFr diet significantly increased these lipid species compared to the control group counterparts. In contrast, MI supplementation significantly reduced hepatic triglyceride and cholesterol content and showed a tendency to reduce phospholipid levels.

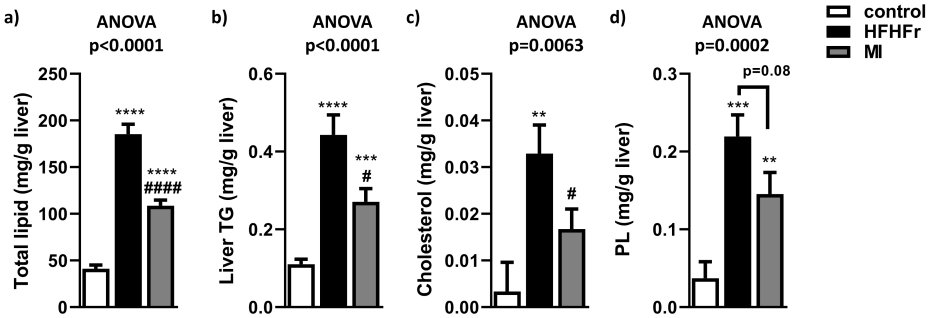

Figure 2. Effects of treatments on (**a**) total liver lipid content; (**b**) total hepatic triglyceride (TG) content; (**c**) total hepatic cholesterol content; and (**d**) total hepatic phospholipid (PL) content. Data are mean ± SEM; $n = 16$ animals/group. ** $p < 0.01$, *** $p < 0.001$, **** $p < 0.0001$ vs. control mice; # $p < 0.05$; #### $p < 0.0001$ vs. HFHFr mice.

Consistent with biochemical analysis, liver histology analysis showed that the HFHFr group developed pronounced liver steatosis by the presence of micro- and macrovesicular steatosis with nuclear displacement due to hypertrophy (Figure 3a–c). Interestingly, treatment with MI ameliorated liver steatosis, as microvesicular steatosis was almost absent, macrovesicular steatosis was markedly reduced, there was a pronounced reduction in the amount of lipid droplets (Figure 3a–c) and hypertrophy and disturbance of nucleus were diminished. These results, corroborated by the general NAFLD Scoring System, demonstrate a noticeable amelioration of different parameters analyzed in animals treated with MI supplementation compared with the HFHFr group (Figure 3d).

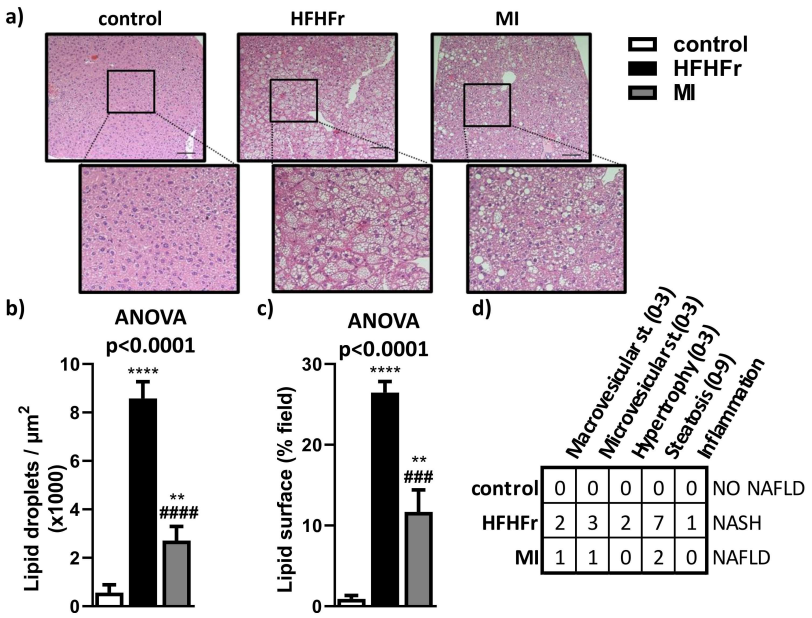

Figure 3. Liver histopathology and image analysis were determined by (**a**) H&E (hematoxylin-eosin staining) and an amplification of the selected area showing a magnified area in the lower panel; (**b**) lipid droplets count; (**c**) lipid droplet surface field; and (**d**) NAFLD/NASH scoring table. st., steatosis. Bar = 100 µm. Data are mean ± SEM; $n = 6$ animals/group. ** $p < 0.01$, **** $p < 0.0001$ vs. control mice; ### $p < 0.001$; #### $p < 0.0001$ vs. HFHFr mice.

3.3. Beneficial Effects of MI Supplementation Did Not Involve Lipogenesis, Lipid Transport or Fatty Acid Oxidation Pathways

To discern which metabolic pathways could be involved in NAFLD improvement after MI supplementation, analysis of gene expression related to hepatic lipogenesis, lipid transport and fatty acid oxidation were carried out. The HFHFr group showed a significant increase in lipid transport-related genes Cd36 (Figure 4a) and Fabp4 (Figure 4b). Interestingly, a tendency to decrease expression of Cd36 and Fapb4 was observed in MI-supplemented mice compared to the HFHFr group (Figure 4a,b). No significant changes were observed in mRNA levels of the genes involved in de novo hepatic lipogenesis, Acc1 (Figure 4c) and Fasn (Figure 4d). Although expression of Scd1 was induced in the HFHFr and MI groups compared with the control group, there was no difference between both groups (Figure 4e). Regarding fatty acid oxidation, increased expression of Cpt1a (Figure 4f) and Pparα (Figure 4g) was observed in the HFHFr group compared with the control group, but no significant differences were observed in the supplemented MI group compared with the HFHFr group. In contrast, hepatic expression levels of the main uncoupling proteins (Ucp1 and Ucp2) were increased in the HFHFr group, in comparison with the control group (Figure 4h,i). However, after MI supplementation, hepatic expression of Ucp1 and Ucp2 reverted to similar levels as in control mice. In addition, hepatic Cbs expression levels (a key enzyme in GSH levels to defense against oxidative stress) were downregulated in the HFHFr animals (Figure 4j). In contrast, animals treated with the MI supplementation reversed this downregulation, with hepatic Cbs expression levels similar to control animals (Figure 4j).

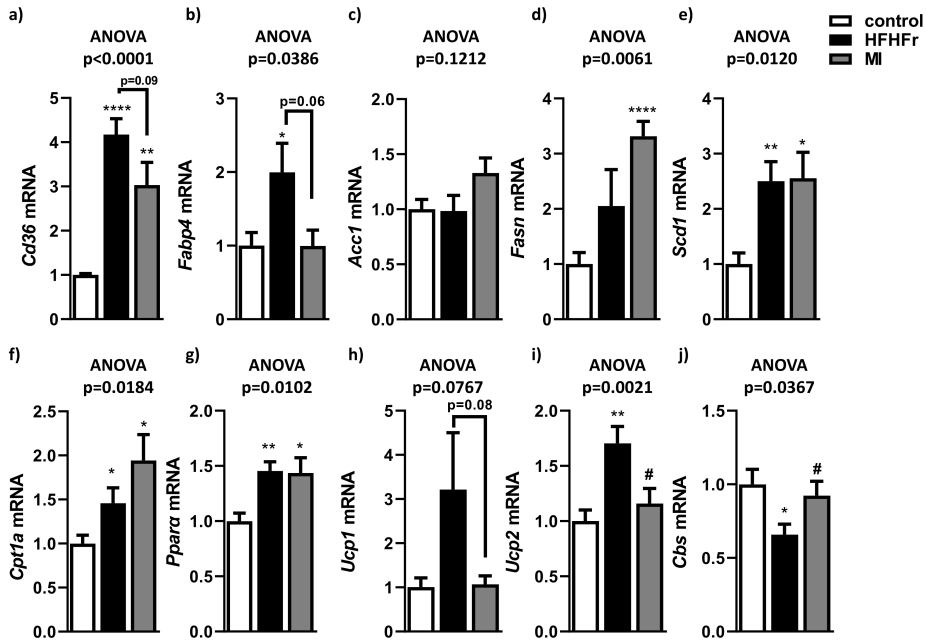

Figure 4. Hepatic mRNA expression of genes related to lipid transport, (**a**) Cd36 and (**b**) Fabp4, de novo hepatic lipogenesis (**c**) Acc1, (**d**) Fasn and (**e**) Scd1 and fatty acid oxidation (**f**) Cpt1a and (**g**) Pparα; antioxidative defense (**h**) Ucp1, (**i**) Ucp2 and (**j**) Cbs. Data are mean ± SEM. $n = 6$ animals/group. * $p < 0.05$, ** $p < 0.01$, **** $p < 0.0001$ vs. control mice; # $p < 0.05$ vs. HFHFr mice.

3.4. MI Supplementation Reduced Hepatic Inflammation Associated to NAFLD

To evaluate whether supplementation with MI modulated the levels of proinflammatory markers, the expression levels of some representative inflammatory genes were assessed. As expected, F4/80 mRNA levels, a marker of macrophage infiltration, were significantly upregulated in the HFHFr group compared to control mice (Figure 5a). In contrast, MI treatment significantly corrected this upregulation of F4/80 expression. Similar results were observed in the expression of Il1α (Figure 5b) and Tnfα (Figure 5c), which was upregulated in HFHFr animals but supplementation with MI reversed it to levels analogous to the control group. However, in the case of Il1α, it was just a statistical tendency. Moreover, the expression of Il6 did not show any differences between groups (Figure 5d).

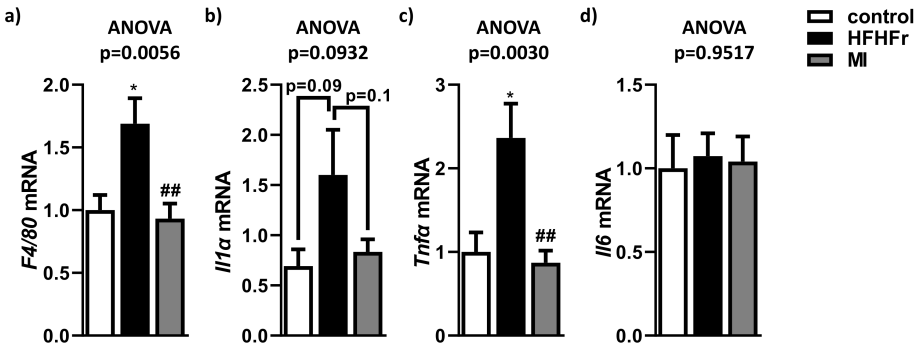

Figure 5. Effects of treatments on (**a**) expression of F4/80, (**b**) Il1α, (**c**) Tnfα, (**d**) Il6. Data are mean ± SEM. $n = 6$ animals/group. * $p < 0.05$ vs. control mice; ## $p < 0.01$ vs. HFHFr mice.

3.5. MI Supplementation Reduced Fibrosis Markers Associated to NAFLD

Liver fibrosis was analyzed by Masson's trichome staining and quantified through the number of collagen fibers stained afterwards. These liver sections showed an increase in the fibrotic state in the HFHFr group compared to control group due to an increase in stained collagen fibers (Figure 6a,b), although the MI-supplemented group showed a better % of area occupied by collagen in comparison with the HFHFr group. Indeed, hepatic expression of the pro-fibrotic gene Col1α1 was significantly increased in the HFHFr group in comparison with the control group (Figure 6c). In contrast, supplementation with MI significantly reduced Col1α1 and Fgf21 hepatic levels compared to the HFHFr group [49,50] (Figure 6c,d).

3.6. MI Supplementation Reduced Hepatic Insulin Resistance Associated to NAFLD

Considering that impaired hepatic insulin signaling plays an important role in NAFLD development, in order to evaluate insulin resistance, animals were challenged with an intraperitoneal insulin bolus determining Akt activation (phosphorylation on Serine 473) or saline. As expected, control group showed a significant Akt phosphorylation ($pAkt^{S473}$) in insulin challenged mice compared to vehicle injected mice (Figure 7a,b). This fact was not observed in the HFHFr group, indicating hepatic insulin resistance in these animals. In contrast, the MI-supplemented group showed a tendency to improve insulin signaling (Figure 7a,b). In addition, systemic fasting glycaemia and fasting insulinemia were improved after the MI supplementation (Figure S3a,b). To validate the amelioration of hepatic insulin signalling, we evaluated the liver expression of a key transcription factor involved in the insulin response, Srebpc1 (Figure 7c); the main hepatic glucose transporter, Glut2 (Figure 7d); and an important regulator of the lipid and carbohydrate metabolism, G6pd (Figure 7e). As expected, Srebp1c expression was increased in the HFHFr group compared with the control group (Figure 7c). Similar results were observed in the MI-supplemented animals. In contrast, Glut2 expression was increased in the

MI-supplemented group (Figure 7d). Finally, G6pd expression tended to be higher in the HFHFr group compared with the control animals, whereas this effect was almost completely abolished in the MI-supplemented group (Figure 7e).

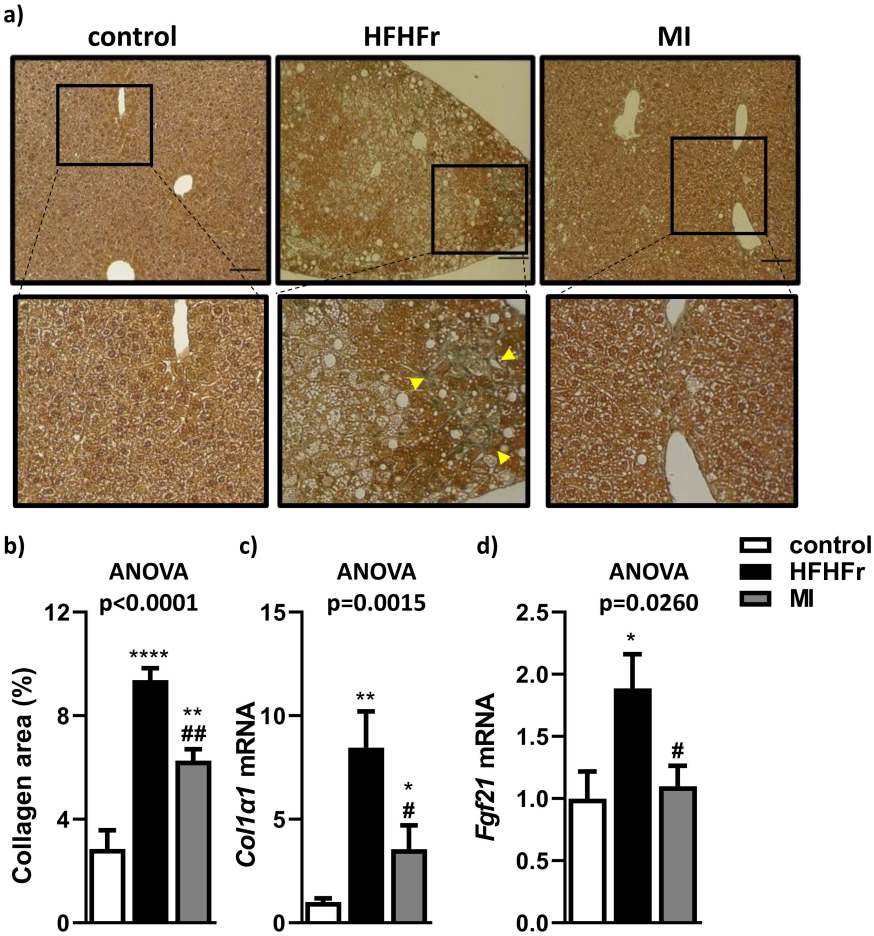

Figure 6. Effects of treatments on hepatic fibrosis. (**a**) Representative images of Masson's trichrome staining showing a magnified area in the lower panel; (**b**) quantification of collagen fiber area; (**c**) hepatic mRNA expression of Col1α1 and (**d**) Fgf21. Bar = 100 µm. Data are mean ± SEM. $n = 6$ animals/group. * $p < 0.05$, ** $p < 0.01$, **** $p < 0.0001$ vs. control mice; # $p < 0.05$, ## $p < 0.01$ vs. HFHFr mice. Yellow arrowheads show the fibrotic structures.

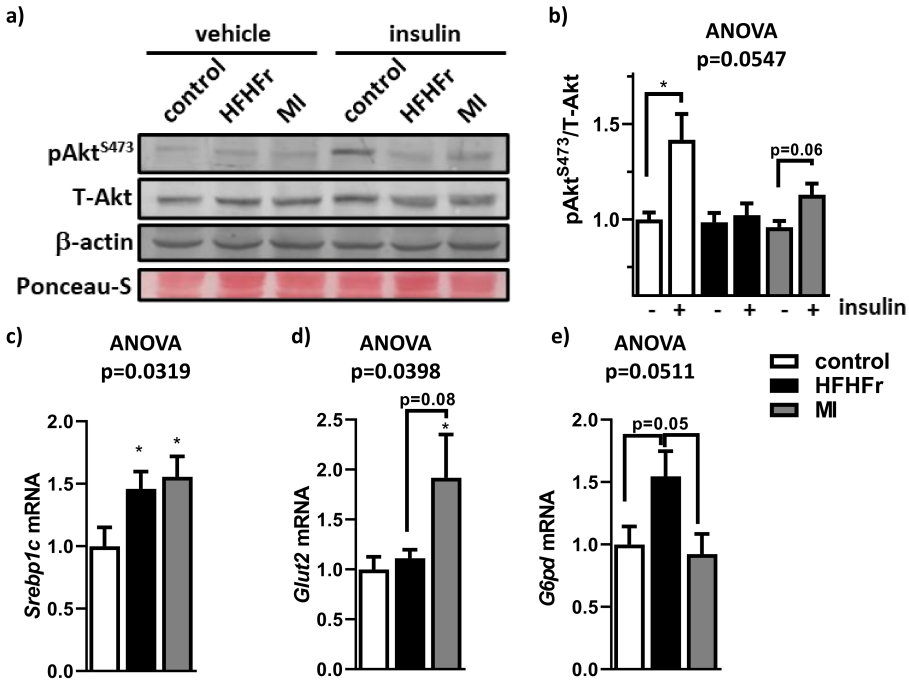

Figure 7. Effects of treatments on liver insulin resistance. (**a**) A representative Western blot analysis with Akt activation (pAkt^{S473}), total Akt protein levels (T-Akt), housekeeping β-actin levels and protein loading with Ponceau-S membrane staining; (**b**) densitometry analysis of phosphorylated and total Akt ratio. Hepatic mRNA expression of: (**c**) Srebp1, (**d**) Glut2 and (**e**) G6pd. Data are mean ± SEM. n = 5–6 animals/group. * $p < 0.05$ vs. control mice.

4. Discussion

NAFLD is a multifactorial disease, which is related to obesity, dyslipidemia and insulin resistance, all risk factors that can favor the development of this disease [51]. Novel medical or nutritional approaches to modulate the different alterations associated with NAFLD are needed. In this study, the effect of a multi-ingredient supplementation was evaluated as a treatment for this pathology. MI consisted of a mix of NAC, NR, LC and betaine. In this study, betaine was used instead of serine because of its efficiency to promote mitochondrial fatty acid absorption and GSH biosynthesis through the folate cycle, which can be converted to sarcosine and glycine, leading to a decrease in liver fat content [5,7,13]. In this line, a study with glycine n-methyltransferase-deficient mice (glycine n-methyltransferase participates in the catabolism of betaine to glycine) showed that these deficient mice developed hyperlipidemia and steatohepatitis [52]. Furthermore, in a clinical study NAC, LC and betaine plasma levels were negatively correlated with hepatic steatosis [53], and the administration of GSH and NAD^+ precursors significantly decreased hepatic steatosis in a preventive treatment study in mice [53]. Supplementation with MI is supported by previous studies describing an increase in fat oxidative metabolism in the liver after the administration of this combination in patients suffering from NAFLD [14].

In the present study, after NAFLD was established [54], the effects of MI supplementation for 4 weeks were evaluated. The MI-supplemented group showed significant reductions in systemic AST and ALT levels compared to their HFHFr counterparts, improving liver injury associated to NAFLD. These results correlate with previous clinical studies with NAC and LC, which showed a reduction in circulatory levels of transaminases [55,56]. However, there are some inconsistencies in the literature about the alterations in the AST/ALT ratio associated with NAFLD. In the present study, HFHFr mice exhib-

ited a decreased AST/ALT ratio compared to the control group, which was consistent with other studies in obese and NAFLD mouse models fed with a high-fat, high-fructose diet [57–61]. However, there are some discrepancies between our results and other studies with an increased AST/ALT ratio due to NAFLD and different circulating transaminases levels that must be considered [62]. Therefore, more efforts are needed to discern AST/ALT relationships in the context of NAFLD. Although liver weight was increased in this model of NAFLD [19], 4 weeks with MI supplementation decreased liver weight. As expected, the HFHFr group showed a significant increase in the severity of HS compared to control mice, with higher hypertrophy, presence of inflammatory foci and disturbance of nucleus [54]. Interestingly, these findings were accompanied by a significant improvement in all markers of hepatic steatosis evaluated in the MI-supplemented group. These findings are in agreement with recent investigations where HS was lowered by either serine treatment in a clinical study, as well as by a combination of NR, NAC and serine in a preclinical study [14].

Furthermore, a glycine-based treatment in animal models with liver damage has been observed to protect against oxidative stress mediated by free radicals, which could reduce cellular damage and the presence of inflammatory and fibrotic foci [63,64]. Interestingly, NAD+, which was found increased by the presence of its precursor NR, protected against steatosis in mice [17,65], and triggered inflammation [66]. These NAD+ and GSH-based studies suggested that MI supplementation would be a promising strategy to reduce fatty liver. In NAFLD, hepatic overload of FFAs and fatty acid oxidation impairment are central to its pathogenesis. When FFA are delivered to the liver, or hepatic de novo lipogenesis exceeds triglycerides export or oxidation, NAFLD might progress [67]. In agreement with other preclinical studies, the HFHFr group presented a significant increase in total hepatic lipids, triglycerides and cholesterol compared to the control group [23,68]. On the contrary, MI-supplemented mice showed a significant reduction in these lipid parameters. These results agree with a preclinical study, in which obese mice were supplemented with a similar nutritional cocktail composed of NR, NAC and serine, decreasing hepatic lipid parameters [14]. The first two components would stimulate FFA transfer from cytosol to the mitochondria and raise NAD^+ levels, thereby increasing mitochondrial FFAs oxidation. The last two components would help increase GSH levels, protecting against ROS [19].

Fatty acid transport into the liver occurs via fatty acid transporters such as fatty acid translocases (Cd36) and fatty acid binding proteins (Fabp4) [69]. The expression of these genes was positively related to liver fat content, developing hepatosteatosis and hepatic insulin resistance [70]. Interestingly, the tendency to decrease hepatic expression of Cd36 and Fabp4 found in response to MI supplementation suggests that this multi-ingredient treatment would tackle NAFLD by reducing FFA uptake into the liver. Different previous studies contribute to reinforce this hypothesis. Thereby, a preclinical study showed that FABP expression tended to increase in obesogenic studies, but a methyl donor supplementation may revert this rise [71], such as betaine, which is a methyl donor in the MI treatment. Cd36 was shown as a possible target of NAC, since NAC treatment in male rats with NASH displayed a reduction in Cd36 expression [72]. NR supplementation also showed a lowering effect on Cd36 mRNA expression in an experimental NAFLD mice model related to amelioration of the disease [65]. Therefore, the tendency to reduce expression of fatty acid transport-related genes is correlated with a reduction in fatty liver.

Regarding hepatic lipogenesis (Fasn, Acc1 and Scd1) and fatty acid oxidation (Cpt1a and Pparα), there were no significant differences between MI-supplemented mice and their HFHFr mice counterparts. However, previous studies showed opposite results for these determinations. For example, *Fasn* mRNA expression, a key enzyme involved in liver de novo lipogenesis, did not show significant differences in a previous mice study treated with an NR, NAC and L-serine cocktail [14]. In contrast, administration of NR in a fatty liver mice model showed a significant reduction in Fasn, Acc1 and Scd1 expression [65]. Pparα gene expression (a regulator of mitochondrial biogenesis and contributor to better NR function by enhancing β-oxidation and mitochondrial biogenesis) was increased in

the MI group, but also in the HFHFr group compared to the control group. According to another preclinical study, in which NAFLD mice were treated with a combination of cofactors (including NR), no changes in Pparα expression were observed in the NAFLD group and treated group [65]. Therefore, the main effects observed by supplementation with MI do not appear to be related neither to liver lipogenesis nor to fatty acid oxidation.

Liver inflammation is a key feature of NAFLD, especially in the NASH stage. There are several altered processes that activate the inflammatory pathways triggering the progression to steatohepatitis [73], which include intrahepatic accumulation of several lipid species: increased lipid peroxidation, Kupffer cells activation by ROS accumulation and hepatic infiltration of macrophages [74]. Moreover, macrophage and Kupffer cell infiltration contribute to the progression of NAFLD and insulin resistance secreting pro-inflammatory cytokines such as TNF-α, IL-6 and IL-1β. Therefore, macrophage infiltration and inflammatory cytokines release increase hepatic lipid accumulation, which leads to dysregulation of lipid metabolism and exacerbates insulin by degradation of insulin receptor substrate 1 (IRS1) [75,76]. Hence, F4/80 expression, which is a macrophage marker, is increased in HFHFr group compared to control group. In this sense, supplementation with MI significantly attenuated the expression of the macrophage infiltration marker F4/80 observed in HFHFr group. These results are consistent with the previously reported reduced macrophage infiltration as a response to a glycine-based treatment, which was assessed by histological studies in livers of NASH mice [64]. Similar results, regarding decreased F4/80 presence in liver sections of NAFLD mice, were observed in a study using NR-based treatment [77]. In concordance with lower macrophage infiltration, supplementation with MI promotes a downregulation of some pro-inflammatory cytokines. Thus, Tnfα expression was also attenuated in the MI-supplemented group, suggesting that this cocktail was helpful in preventing inflammation of NAFLD in mice. This effect was also observed in other clinical and preclinical NASH studies, presenting a significant regression of Tnfα mRNA expression after L-carnitine supplementation [56], after glycine treatment [64] or in NR-treated mouse livers [65,77,78], supporting the hypothesis that NR treatment improves hepatic inflammation by modulating pyrin domain containing 3 (NLRP3) inflammasome. In addition, Il1α was also described to be up-regulated in patients with NAFLD [79] and, in the present study, Il1α tended to be elevated in HFHFr mice, but in the MI-supplemented group, this cytokine tended to be down-regulated, suggesting an anti-inflammatory effect. Unexpectedly, no significant effects were observed in Il6 mRNA expression in mice between the three groups. Indeed, data on the hepatic expression of *Il6* are contradictory. There are cases where treatments decrease this cytokine's levels: with NR [65,78] or with betaine [80] and others, treated with LC and NR, no significant impact on the hepatic expression of Il6 was observed [81].

Several reports have strongly suggested that NAFLD could activate fibrotic pathways in advanced stages such as NASH [1,26]. In the present study, the anti-fibrotic effect of MI supplementation was evaluated in the context of NAFLD. Results showed that Col1α1 expression (the most abundant type of collagen found in scar tissue [82]), which was importantly increased in HFHFr group, was significantly reduced in MI-supplemented group. These findings were corroborated by the histological Masson's trichome staining analysis, showing a significant reduction in collagen fibers due to MI treatment. These antifibrotic effects are in consonance with other NAFLD/NASH studies where NR treatment prevented the abnormal expression of hepatic Col1α1 and reduced Masson's trichome staining in liver sections [65,83]. In addition, a recent study showed that glycine-based supplementation attenuated hepatic Col1α1 expression in NASH mice [64]. Taken together, supplementation with MI could be efficient as a treatment even in advanced stages of NAFLD/NASH. Betaine increase folate and methionine metabolism, which are closely related to an increased GSH production [7]. To check betaine's effect in the MI supplementation, the hepatic expression of Cbs expression, which is translated as a key enzyme in GSH production [84], was analyzed in each group. HFHFr mice showed a significant decrease in Cbs expression compared to the control group. A deficient expression of Cbs

was related to hepatic steatosis, inflammation, and fibrosis [84]. In contrast, the MI group significantly recovered Cbs expression in comparison with the HFHFr group, reaching similar levels to control animals. These results could be related to an increased antioxidant response due to betaine supplementation, concordant with another preclinical study [85]. Fgf21 and Ucp2 mRNA expression were assessed in order to evaluate the protective role of these molecules against inflammation and fibrosis. Fgf21 was overexpressed as a protective response against inflammation by obesogenic diets [49,86]. Moreover, ER stress, oxidative stress and lipotoxicity stimulate Fgf21 expression in NAFLD [87,88]. Concordant with previous studies, Fgf21 mRNA expression was upregulated in the HFHFr group, elucidating the protective response of hepatocytes against hepatic inflammation and fibrosis, which may end up in hepatocellular carcinoma [49]. The increased Fgf21 expression could be linked to Pparα upregulation and may suggest a need for increased hepatic FGF signaling as a protective response to NAFLD [86,89]. In the MI group, Fgf21 upregulation was mitigated compared to the HFHFr group and it could be related to a reduction in oxidative stress, increasing glutathione biosynthesis and antioxidant responses by betaine supplementation, which reduced the ratio of oxidized/reduced glutathione [90]. Therefore, this decrease in Fgf21 levels could be related with the amelioration of NAFLD progression by MI supplementation. In the case of Ucp2, it plays a role in proton leak through the mitochondrial membranes and prevents ROS production. Hepatic accumulation of FFAs facilitates the development and progression of NAFLD by impairing mitochondrial function, exceeding NADH in the mitochondrial matrix that needs to be re-oxidized [91]. The wastage of this mitochondrial membrane potential is a hallmark of mitochondrial dysfunction in NAFLD [92]. Hepatocytes up-regulate Ucp2 as an adaptation to obesity, but cells become vulnerable to ATP depletion and these cells are vulnerable to necrosis [93]. The HFHFr group showed a significant increase in this gene expression compared to the control group. These results are concordant with another preclinical study [94]. On the other hand, MI-supplemented mice showed a significant decrease in Ucp2 expression compared to the HFHFr group, in accordance with a preclinical study where NR caused a significant decrease in Ucp2 mRNA levels in obese mice, which was related to improved oxidative metabolism and protection against high-fat diet-induced metabolic abnormalities [17]. An assessment of plasma acylcarnitine would have been of interest to determine the effects related to fatty acid processing and β-oxidation due to LC and NR from MI treatment. Salic et al. [81] demonstrated, in an experimental NAFLD mice model, elevated acylcarnitine plasma levels and loss of fat were correlated, mimicking some processes that are also activated during exercise, leading to lipid oxidation. Indeed, the researchers assessed expression levels of some representative inflammatory genes and evaluated hepatic steatosis and fibrosis, which are related to oxidative stress and the accumulation of ROS, as Ali et al. explained [95]. However, considering that Laurent et al. [96] demonstrated how NAC treatment reduces oxidative stress and increases intracellular GSH levels in an experimental NAFLD mice model, and that Khodayar et al. [18] showed how betaine reduces mitochondrial ROS, regenerates mitochondrial GSH levels and increases antioxidant defense capacity, our results point the antioxidant activity of NAC and betaine.

Insulin resistance is critical for the progression of NAFLD. The first hit is when increased dietary intake leads the body to produce excess fatty acids induced by lipogenesis and FFA synthesis, and they circulate in peripheral tissues, including the liver. The second hit occurs when hepatic FFAs accumulation is combined with oxidative stress, lipid peroxidation and mitochondrial dysfunction, contributing to insulin resistance [75,76]. Previous studies in humans and animals demonstrated that LC administration improved insulin sensitivity related to reduction in steatosis [56,73]. Insulin regulates glucose and lipid metabolism, where the PI3K/Akt pathway is their main effector. Thus, the PI3K/Akt pathway malfunction leads to insulin resistance, which is indeed linked to obesity and type 2 diabetes [97]. In the present study, a pronounced hepatic insulin resistance was observed in the HFHFr group. Nevertheless, the MI-supplemented group showed a tendency to improve insulin signaling. These results are in accordance with an in vitro study using

insulin-resistant HepG2 cells, where betaine addition restored Akt activation [98]. This suggests that the mix of bioactive cofactors used in this study was helpful to recover hepatic insulin sensitivity and, therefore, the progression to NAFLD. Insulin resistance could be caused by inhibition of insulin receptor substrate-1 (IRS-1), and it could impair glucose transporter 2 (GLUT2) translocation in hepatocytes [99]. No significant differences were found in Glut2 mRNA expression between the HFHFr group and the control group, despite steatosis in HFHFr mice. However, circulating glucose and insulin are increased in HFHFr mice compared to control group, increasing insulin resistance. The reduced phosphorylation of Akt resulted in reduced activation of insulin signaling, which is related to impaired Glut2 expression. In contrast, the MI group showed tendency to increase Glut2 expression compared to HFHFr mice, accompanied by a reduction in circulating glucose and insulin levels and correlated with the tendency to improve Akt phosphorylation. These effects reduced the circulating glucose and insulin levels and improved insulin signaling [81], which could mean that MI supplementation induces Glut2 expression as an insulin sensitizing action. These results suggest that the mix of bioactive cofactors used in this study was helpful to recover hepatic insulin sensitivity and attenuate the progression to NAFLD. Srebp1c expression (which is closely related to Akt activation, lipogenesis in hepatocytes and is regulated by insulin signaling) was analyzed in each group [100–102]. SREBP1c plays an intermediary role in lipid homeostasis by orchestrating the gene transcription of enzymes involved in lipogenesis and lipolysis [100]. The HFHFr group showed an increased *Srebp1c* expression compared to the control group, agreeing with previous studies with obese animal models [103]. Srebp1c overexpression in mice with fatty livers was related to significant increases in lipid biosynthesis gene expression after *Srebp1c* activation, such as G6pd [104–106]. G6pd is a lipogenic gene linked to *Srebp1c*, which acts as a key transcriptional factor [107]. A decreased *Srebp1c* expression in the MI group compared to the HFHFr group was expected in a study with mice models with liver injuries treated with NR, and another study with an experimental NAFLD rat model treated with betaine [80,108]. However, the MI group did not show a significant difference in *Srebp1c* expression compared to the HFHFr group, probably because a longer treatment time was necessary to see the effects on the regulation of this gene. Despite this, a significant difference in G6pd expression being downregulated in MI supplementation was observed, which could indicate an amelioration in lipid homeostasis by decreasing lipogenesis. Indeed, increased expression of G6pd promotes hepatic steatosis and insulin resistance [109], but in the MI group, G6dp expression is decreased, which could be ameliorating this effect. G6pd expression tended to be higher in the HFHFr group compared to the control group (Figure 7). Contrarily, the expression of G6pd in MI-supplemented animals tended to be lower than the HFHFr group, achieving similar levels to the control group, which could point to an amelioration in lipid homeostasis by decreasing lipogenesis.

There are some limitations of this observational study. First, the lack of use of single-housing and paired-feeding techniques to control food intake individually in mice. However, social housing is essential for rodents, so housing them in individual cages is discouraged [110]. Second, conclusions derived from the present study are sustained in young male mice. Although this situation occurs commonly in other studies [14,81,111], it is necessary to validate the effect of supplementation with MI in other models, both in older mice and in females. Third, the present study lacks an MI-treated group without NAFLD, but the study design was similar to other studies [14,81,112] and no deleterious effect was expected for this treatment. Fourth, more studies with NASH models are needed to obtain more accurate information on the impact of MI supplementation on liver fibrosis.

5. Conclusions

To summarize, this study is the first to use a combination of cofactors composed of NAC, NR, betaine, and LC as a possible dietary strategy to treat NAFLD development in an animal model due to its implication in different metabolic pathways that are pathologically affected in this disease. Data from the present study suggest that 4-week supplementation

with this specific combination of bioactive cofactors, at intended human clinical doses, ameliorates NAFLD features in mice. These improvements involved a reduction in liver weight, hepatic steatosis, inflammation, fibrosis and partially improved insulin sensitivity. Hepatic lipid metabolism is modulated through a reduction in lipid transport-related genes, and MI markedly reduces inflammatory markers, suggesting that it could prevent the progression from NAFLD to NASH. Furthermore, MI reduced fibrotic markers, proposing that it could also be considered as a treatment for advanced stages of NAFLD. Finally, this study also unraveled that the combination of these cofactors might have some additional beneficial effects on the amelioration of insulin resistance, and, therefore, in the development of NAFLD associated to HFHFr diets. To conclude, all these results suggest that supplementation with MI can be useful to improve obesity and an effective tool to treat NAFL and improve insulin resistance.

Supplementary Materials: The following are available online at https://www.mdpi.com/article/10.3390/nu13103532/s1, Figure S1: Schematic diagram of the animal study; Figure S2a: Body weight before and after 4 weeks of MI supplementation; Figure S2b: Adiposity at the end of the supplementation calculated as the sum of as the white adipose depots (epididymal, retroperitoneal, inguinal and mesenteric); Figure S2c,d: Data of the solid and liquid food intake per week; Figure S3a: Fasting glycaemia; Figure S3b: Fasting insulinemia after MI supplementation.

Author Contributions: S.Q.-V., G.A., J.M.D.B., A.C. and X.E. contributed to the study conception and design. S.Q.-V., M.C.-P., È.N.-M. and X.E. conducted the study. S.Q.-V., M.C.-P., È.N.-M. and X.E. carried out the data acquisition. S.Q.-V. and X.E. performed the data analysis. S.Q.-V., È.N.-M. and X.E. drafted the manuscript. S.Q.-V. and X.E. interpreted the data. All authors have read and agreed to the published version of the manuscript.

Funding: This work was financially supported by the Catalan Government through the funding grant ACCIÓ-Eurecat, by the Centre for the Development of Industrial Technology (CDTI) of the Spanish Ministry of Science and Innovation (under grant agreement TECNOMIFOOD, project CER-20191010).

Institutional Review Board Statement: All experimental protocols were approved by the Animal Ethics Committee of the Technological Unit of Nutrition and Health of Eurecat (Reus, Spain) and the Generalitat de Catalunya approved all the procedures (10281). The experimental protocol followed the "Principles of Laboratory Care" guidelines and was carried out in accordance with the European Communities Council Directive (2010/63/EEC).

Informed Consent Statement: Not applicable.

Data Availability Statement: Not applicable.

Acknowledgments: This work was financially supported by the Agency for Business Competitiveness of the Government of Catalonia (ACCIÓ) (TECCT11-1-0012); by the Centre for the Development of Industrial Technology (CDTI) of the Spanish Ministry of Science and Innovation (under grant agreement TECNOMIFOOD, project CER-20191010). We thank J.M. Alcaide, Y. Tobajas, A. Antolin, G. Chomiciute, C. Egea and I. Triguero for their valuable technical support. We thank Cambridge Commodities and ChromaDex for providing the ingredients of the multi-ingredient. S.Q.-V. is supported by a fellowship from the Vicente Lopez Program (Eurecat), M.C.-P. is supported by fellowship 2021 FI_B2 00150 and È.N.-M. is supported by a fellowship from the Martí i Franquès Program PIPF (2019PMF-PIPF-73).

Conflicts of Interest: The authors declare no conflict of interest.

References

1. Quesada-Vázquez, S.; Aragonès, G.; del Bas, J.M.; Escoté, X. Diet, Gut Microbiota and Non-Alcoholic Fatty Liver Disease: Three Parts of the Same Axis. *Cells* **2020**, *9*, 176. [CrossRef]
2. Byrne, C.D.; Targher, G. NAFLD: A Multisystem Disease. *J. Hepatol.* **2015**, *62*, S47–S64. [CrossRef]
3. Argo, C.K.; Northup, P.G.; Al-Osaimi, A.M.S.; Caldwell, S.H. Systematic Review of Risk Factors for Fibrosis Progression in Non-Alcoholic Steatohepatitis. *J. Hepatol.* **2009**, *51*, 371–379. [CrossRef]
4. Pai, R.K. NAFLD Histology: A Critical Review and Comparison of Scoring Systems. *Curr. Hepatol. Rep.* **2019**, *18*, 473–481. [CrossRef]

5. Mardinoglu, A.; Ural, D.; Zeybel, M.; Yuksel, H.H.; Uhlén, M.; Borén, J. The Potential Use of Metabolic Cofactors in Treatment of NAFLD. *Nutrients* **2019**, *11*, 1578. [CrossRef] [PubMed]
6. Masarone, M.; Rosato, V.; Dallio, M.; Gravina, A.G.; Aglitti, A.; Loguercio, C.; Federico, A.; Persico, M. Review Article Role of Oxidative Stress in Pathophysiology of Nonalcoholic Fatty Liver Disease. *Oxidative Med. Cell. Longev.* **2018**, *11*, 9547613. [CrossRef]
7. Zhang, C.; Bjornson, E.; Arif, M.; Tebani, A.; Lovric, A.; Benfeitas, R.; Ozcan, M.; Juszczak, K.; Kim, W.; Kim, J.T.; et al. The Acute Effect of Metabolic Cofactor Supplementation: A Potential Therapeutic Strategy against Non-alcoholic Fatty Liver Disease. *Mol. Syst. Biol.* **2020**, *16*, 1–16. [CrossRef]
8. Cimini, F.A.; Barchetta, I.; Carotti, S.; Bertoccini, L.; Baroni, M.G.; Vespasiani-Gentilucci, U.; Cavallo, M.G.; Morini, S. Relationship between Adipose Tissue Dysfunction, Vitamin D Deficiency and the Pathogenesis of Non-Alcoholic Fatty Liver Disease. *World J. Gastroenterol.* **2017**, *23*, 3407–3417. [CrossRef] [PubMed]
9. Buzzetti, E.; Pinzani, M.; Tsochatzis, E.A. The Multiple-Hit Pathogenesis of Non-Alcoholic Fatty Liver Disease (NAFLD). *Metab. Clin. Exp.* **2016**, *65*, 1038–1048. [CrossRef]
10. Marin, V.; Gazzin, S.; Gambaro, S.E.; Ben, M.D.; Calligaris, S.; Anese, M.; Raseni, A.; Avellini, C.; Giraudi, P.J.; Tiribelli, C.; et al. Effects of Oral Administration of Silymarin in a Juvenile Murine Model of Non-Alcoholic Steatohepatitis. *Nutrients* **2017**, *9*, 1006. [CrossRef]
11. Beaton, M.D. Current Treatment Options for Nonalcoholic Fatty Liver Disease and Nonalcoholic Steatohepatitis. *Can. J. Gastroenterol.* **2012**, *26*, 353–357. [CrossRef]
12. Abeysekera, K.W.M.; Fernandes, G.S.; Hammerton, G.; Portal, A.J.; Gordon, F.H.; Heron, J.; Hickman, M. Prevalence of Steatosis and Fibrosis in Young Adults in the UK: A Population-Based Study. *Lancet Gastroenterol. Hepatol.* **2020**, *5*, 295–305. [CrossRef]
13. Suárez, M.; Boqué, N.; Del Bas, J.M.; Mayneris-Perxachs, J.; Arola, L.; Caimari, A. Mediterranean Diet and Multi-Ingredient-Based Interventions for the Management of Non-Alcoholic Fatty Liver Disease. *Nutrients* **2017**, *9*, 1052. [CrossRef] [PubMed]
14. Mardinoglu, A.; Bjornson, E.; Zhang, C.; Klevstig, M.; Söderlund, S.; Ståhlman, M.; Adiels, M.; Hakkarainen, A.; Lundbom, N.; Kilicarslan, M.; et al. Personal Model-assisted Identification of NAD^+ and Glutathione Metabolism as Intervention Target in NAFLD. *Mol. Syst. Biol.* **2017**, *13*, 916. [CrossRef] [PubMed]
15. Mardinoglu, A.; Agren, R.; Kampf, C.; Asplund, A.; Uhlen, M.; Nielsen, J. Genome-Scale Metabolic Modelling of Hepatocytes Reveals Serine Deficiency in Patients with Non-Alcoholic Fatty Liver Disease. *Nat. Commun.* **2014**, *5*, 3083. [CrossRef] [PubMed]
16. Xia, Y.; Li, Q.; Zhong, W.; Dong, J.; Wang, Z.; Wang, C. L-Carnitine Ameliorated Fatty Liver in High-Calorie Diet/STZ-Induced Type 2 Diabetic Mice by Improving Mitochondrial Function. *Diabetol. Metab. Syndr.* **2011**, *3*, 31. [CrossRef] [PubMed]
17. Cantó, C.; Houtkooper, R.H.; Pirinen, E.; Youn, D.Y.; Oosterveer, M.H.; Cen, Y.; Fernandez-Marcos, P.J.; Yamamoto, H.; Andreux, P.A.; Cettour-Rose, P.; et al. The NAD^+ Precursor Nicotinamide Riboside Enhances Oxidative Metabolism and Protects against High-Fat Diet-Induced Obesity. *Cell Metab.* **2012**, *15*, 838–847. [CrossRef]
18. Khodayar, M.J.; Kalantari, H.; Khorsandi, L.; Rashno, M.; Zeidooni, L. Betaine Protects Mice against Acetaminophen Hepatotoxicity Possibly via Mitochondrial Complex II and Glutathione Availability. *Biomed. Pharmacother.* **2018**, *103*, 1436–1445. [CrossRef]
19. Marin, V.; Rosso, N.; Dal Ben, M.; Raseni, A.; Boschelle, M.; Degrassi, C.; Nemeckova, I.; Nachtigal, P.; Avellini, C.; Tiribelli, C.; et al. An Animal Model for the Juvenile Non-Alcoholic Fatty Liver Disease and Non-Alcoholic Steatohepatitis. *PLoS ONE* **2016**, *11*, e0158817. [CrossRef]
20. Sanches, S.C.L.; Ramalho, L.N.Z.; Augusto, M.J.; Da Silva, D.M.; Ramalho, F.S. Nonalcoholic Steatohepatitis: A Search for Factual Animal Models. *BioMed Res. Int.* **2015**, *2015*, 574832. [CrossRef]
21. Nassir, F.; Rector, R.S.; Hammoud, G.M.; Ibdah, J.A. Pathogenesis and Prevention of Hepatic Steatosis. *Gastroenterol. Hepatol.* **2015**, *11*, 167–175.
22. Reagan-Shaw, S.; Nihal, M.; Ahmad, N. Dose Translation from Animal to Human Studies Revisited. *FASEB J.* **2008**, *22*, 659–661. [CrossRef] [PubMed]
23. Caimari, A.; Bas, J.M.; Crescenti, A.; Arola, L. Low Doses of Grape Seed Procyanidins Reduce Adiposity and Improve the Plasma Lipid Profile in Hamsters. *Int. J. Obes.* **2013**, *37*, 576–583. [CrossRef] [PubMed]
24. Rodríguez-sureda, V.; Peinado-onsurbe, J. A Procedure for Measuring Triacylglyceride and Cholesterol Content Using a Small Amount of Tissue. *Anal. Biochem.* **2005**, *343*, 277–282. [CrossRef] [PubMed]
25. Liang, W.; Menke, A.L.; Driessen, A.; Koek, G.H.; Lindeman, J.H. Establishment of a General NAFLD Scoring System for Rodent Models and Comparison to Human Liver Pathology. *PLoS ONE* **2014**, *9*, e0115922. [CrossRef] [PubMed]
26. Lee, U.E.; Friedman, S.L. Mechanisms of Hepatic Fibrogenesis. *Best Pr. Res. Clin. Gastroenterol.* **2011**, *25*, 195–206. [CrossRef]
27. Huang, Y.; de Boer, W.B.; Adams, L.A.; Macquillan, G.; Rossi, E.; Rigby, P.; Raftopoulos, S.C.; Bulsara, M.; Jeffrey, G.P. Image Analysis of Liver Collagen Using Sirius Red Is More Accurate and Correlates Better with Serum Fibrosis Markers than Trichrome. *Liver Int.* **2013**, *33*, 1249–1256. [CrossRef]
28. Flint, M.H.; Lyons, M.F.; Meaney, M.F.; Williams, D.E. The Masson Staining of Collagen—An Explanation of an Apparent Paradox. *Histochem. J.* **1975**, *7*, 529–546. [CrossRef]
29. Yang, J.; Neira, S.; Elisa, F.; Gil-iturbe, E.; Castilla-madrigal, R.; Fern, M.; Mart, J.A.; Moreno-aliaga, M.J. Effects of Long-Term DHA Supplementation and Physical Aged Female Mice. *Nutrients* **2021**, *13*, 501. [CrossRef]

30. Ballak, D.B.; Van Diepen, J.A.; Moschen, A.R.; Jansen, H.J.; Hijmans, A.; Groenhof, G.J.; Leenders, F.; Bufler, P.; Boekschoten, M.V.; Müller, M.; et al. IL-37 Protects against Obesity-Induced Inflammation and Insulin Resistance. *Nat. Commun.* **2014**, *5*, 4711. [CrossRef]
31. Antraco, V.J.; Hirata, B.K.S.; de Jesus Simão, J.; Cruz, M.M.; da Silva, V.S.; de Sá, R.D.C.; Abdala, F.M.; Armelin-Correa, L.; Alonso-Vale, M.I.C. Omega-3 Polyunsaturated Fatty Acids Prevent Nonalcoholic Steatohepatitis (Nash) and Stimulate Adipogenesis. *Nutrients* **2021**, *13*, 622. [CrossRef] [PubMed]
32. López-Yoldi, M.; Fernández-Galilea, M.; Laiglesia, L.M.; Larequi, E.; Prieto, J.; Martínez, J.A.; Bustos, M.; Moreno-Aliaga, M.J. Cardiotrophin-1 Stimulates Lipolysis through the Regulation of Main Adipose Tissue Lipases. *J. Lipid Res.* **2014**, *55*, 2634–2643. [CrossRef] [PubMed]
33. Miranda, M.; Escote, X.; Ceperuelo-Mallafre, V.; Megia, A.; Caubet, E.; Naf, S.; Gomez, J.M.; Gonzalez-Clemente, J.M.; Vicente, V.; Vendrell, J. Relation between Human LPIN1, Hypoxia and Endoplasmic Reticulum Stress Genes in Subcutaneous and Visceral Adipose Tissue. *Int. J. Obes.* **2010**, *34*, 679–686. [CrossRef] [PubMed]
34. Montagner, A.; Polizzi, A.; Fouché, E.; Ducheix, S.; Lippi, Y.; Lasserre, F.; Barquissau, V.; Régnier, M.; Lukowicz, C.; Benhamed, F.; et al. Liver PPARα Is Crucial for Whole-Body Fatty Acid Homeostasis and Is Protective against NAFLD. *Gut* **2016**, *65*, 1202–1214. [CrossRef]
35. Zhou, J.; Febbraio, M.; Wada, T.; Zhai, Y.; Kuruba, R.; He, J.; Lee, J.H.; Khadem, S.; Ren, S.; Li, S.; et al. Hepatic Fatty Acid Transporter Cd36 Is a Common Target of LXR, PXR, and PPARγ in Promoting Steatosis. *Gastroenterology* **2008**, *134*, 556–567. [CrossRef]
36. Zhao, X.; Li, R.; Liu, Y.; Zhang, X.; Zhang, M.; Zeng, Z.; Wu, L.; Gao, X.; Lan, T.; Wang, Y. Polydatin Protects against Carbon Tetrachloride-Induced Liver Fibrosis in Mice. *Arch. Biochem. Biophys.* **2017**, *629*, 1–7. [CrossRef]
37. Mazzolini, G.; Atorrasagasti, C.; Onorato, A.; Peixoto, E.; Schlattjan, M.; Sowa, J.P.; Sydor, S.; Gerken, G.; Canbay, A. SPARC Expression Is Associated with Hepatic Injury in Rodents and Humans with Non-Alcoholic Fatty Liver Disease. *Sci. Rep.* **2018**, *8*, 725. [CrossRef]
38. Zhang, Y.; Pu, W.; Bousquenaud, M.; Cattin, S.; Zaric, J.; Sun, L.K.; Rüegg, C. Emodin Inhibits Inflammation, Carcinogenesis, and Cancer Progression in the AOM/DSS Model of Colitis-Associated Intestinal Tumorigenesis. *Front. Oncol.* **2021**, *10*, 564674. [CrossRef]
39. Grabner, G.F.; Fawzy, N.; Schreiber, R.; Pusch, L.M.; Bulfon, D.; Koefeler, H.; Eichmann, T.O.; Lass, A.; Schweiger, M.; Marsche, G.; et al. Metabolic Regulation of the Lysosomal Cofactor Bis(Monoacylglycero)Phosphate in Mice. *J. Lipid Res.* **2020**, *61*, 995–1003. [CrossRef]
40. Zhang, M.; Sun, W.; Qian, J.; Tang, Y. Fasting Exacerbates Hepatic Growth Differentiation Factor 15 to Promote Fatty Acid β-Oxidation and Ketogenesis via Activating XBP1 Signaling in Liver. *Redox Biol.* **2018**, *16*, 87–96. [CrossRef]
41. Liu, J.; Huang, R.; Li, X.; Guo, F.; Li, L.; Zeng, X.; Ma, L.; Fu, P. Genetic Inhibition of FABP4 Attenuated Endoplasmic Reticulum Stress and Mitochondrial Dysfunction in Rhabdomyolysis-Induced Acute Kidney Injury. *Life Sci.* **2021**, *268*, 119023. [CrossRef]
42. Kimura, R.; Takahashi, N.; Lin, S.; Goto, T.; Murota, K.; Nakata, R.; Inoue, H.; Kawada, T. DHA Attenuates Postprandial Hyperlipidemia via Activating PPARα in Intestinal Epithelial Cells. *J. Lipid Res.* **2013**, *54*, 3258–3268. [CrossRef]
43. Markó, L.; Szijártó, I.A.; Filipovic, M.R.; Kaßmann, M.; Balogh, A.; Park, J.-K.; Przybyl, L.; N'diaye, G.; Krämer, S.; Anders, J.; et al. Role of Cystathionine Gamma-Lyase in Immediate Renal Impairment and Inflammatory Response in Acute Ischemic Kidney Injury. *Sci. Rep.* **2016**, *6*, 27517. [CrossRef]
44. Markan, K.R.; Naber, M.C.; Small, S.M.; Peltekian, L.; Kessler, R.L.; Potthoff, M.J. FGF21 Resistance Is Not Mediated by Downregulation of Beta-Klotho Expression in White Adipose Tissue. *Mol. Metab.* **2017**, *6*, 602–610. [CrossRef]
45. Stolarczyk, E.; Le Gall, M.; Even, P.; Houllier, A.; Serradas, P.; Brot-laroche, E.; Leturque, A. Loss of Sugar Detection by GLUT2 Affects Glucose Homeostasis in Mice. *PLoS ONE* **2007**, *2*, e1288. [CrossRef]
46. Ahn, H.Y.; Kim, H.H.; Hwang, J.-Y.; Park, C.; Cho, B.Y.; Park, Y.J. Effects of Pioglitazone on Nonalcoholic Fatty Liver Disease in the Absence of Constitutive Androstane Receptor Expression. *PPAR Res.* **2018**, *2018*, 9568269. [CrossRef] [PubMed]
47. Cao, Y.; Liu, X.; Zhao, J.; Du, M. AMPKα1 Regulates Idh2 Transcription through H2B O-GlcNAcylation during Brown Adipogenesis. *Acta Biochim. Biophys. Sin.* **2021**, *53*, 112–118. [CrossRef] [PubMed]
48. Dunoyer-Geindre, S.; Kruithof, E.K.O. Epigenetic Control of Tissue-Type Plasminogen Activator Synthesis in Human Endothelial Cells. *Cardiovasc. Res.* **2011**, *90*, 457–463. [CrossRef] [PubMed]
49. Singhal, G.; Kumar, G.; Chan, S.; Fisher, F.M.; Ma, Y.; Vardeh, H.G.; Nasser, I.A.; Flier, J.S.; Maratos-Flier, E. Deficiency of Fibroblast Growth Factor 21 (FGF21) Promotes Hepatocellular Carcinoma (HCC) in Mice on a Long Term Obesogenic Diet. *Mol. Metab.* **2018**, *13*, 56–66. [CrossRef] [PubMed]
50. Baffy, G. Uncoupling protein-2 and non-alcoholic fatty liver disease. *Front. Biosci.* **2005**, *10*, 2082–2096. [CrossRef] [PubMed]
51. Di Costanzo, A.; Belardinilli, F.; Bailetti, D.; Sponziello, M.; D'Erasmo, L.; Polimeni, L.; Baratta, F.; Pastori, D.; Ceci, F.; Montali, A.; et al. Evaluation of Polygenic Determinants of Non-Alcoholic Fatty Liver Disease (NAFLD) By a Candidate Genes Resequencing Strategy. *Sci. Rep.* **2018**, *8*, 3702. [CrossRef]
52. Liao, Y.J.; Chen, T.L.; Lee, T.S.; Wang, H.A.; Wang, C.K.; Liao, L.Y.; Liu, R.S.; Huang, S.F.; Chen, Y.M.A. Glycine N-Methyltransferase Deficiency Affects Niemann-Pick Type C2 Protein Stability and Regulates Hepatic Cholesterol Homeostasis. *Mol. Med.* **2012**, *18*, 412–422. [CrossRef]

53. Mardinoglu, A.; Wu, H.; Bjornson, E.; Zhang, C.; Hakkarainen, A.; Söderlund, S.; Matikainen, N.; Ståhlman, M.; Bergh, P.; Adiels, M.; et al. An Integrated Understanding of the Rapid Metabolic Benefits of a Carbohydrate-Restricted Diet on Hepatic Steatosis in Humans. *Cell Metab.* **2018**, *27*, 559–571. [CrossRef]
54. Clapper, J.R.; Hendricks, M.D.; Gu, G.; Wittmer, C.; Dolman, C.S.; Herich, J.; Athanacio, J.; Villescaz, C.; Ghosh, S.S.; Heilig, J.S.; et al. Diet-Induced Mouse Model of Fatty Liver Disease and Nonalcoholic Steatohepatitis Reflecting Clinical Disease Progression and Methods of Assessment. *Am. J. Physiol. Gastrointest. Liver Physiol.* **2013**, *305*, 483–495. [CrossRef] [PubMed]
55. Khoshbaten, M.; Aliasgarzadeh, A.; Masnadi, K.; Tarzamani, M.K.; Farhang, S.; Babaei, H.; Kiani, J.; Zaare, M.; Najafipoor, F. N-Acetylcysteine Improves Liver Function in Patients with Non-Alcoholic Fatty Liver Disease. *Hepat. Mon.* **2010**, *10*, 12–16. [PubMed]
56. Malaguarnera, M.; Gargante, M.P.; Russo, C.; Antic, T.; Vacante, M.; Malaguarnera, M.; Avitabile, T.; Li Volti, G.; Galvano, F. L-Carnitine Supplementation to Diet: A New Tool in Treatment of Nonalcoholic Steatohepatitis—A Randomized and Controlled Clinical Trial. *Am. J. Gastroenterol.* **2010**, *105*, 1338–1345. [CrossRef] [PubMed]
57. Huang, X.; Chen, W.; Yan, C.; Yang, R.; Chen, Q.; Xu, H.; Huang, Y. Gypenosides Improve the Intestinal Microbiota of Non-Alcoholic Fatty Liver in Mice and Alleviate Its Progression. *Biomed. Pharmacother.* **2019**, *118*, 109258. [CrossRef]
58. Liu, Z.; Qiao, Q.; Sun, Y.; Chen, Y.; Ren, B.; Liu, X. Sesamol Ameliorates Diet-Induced Obesity in C57BL/6J Mice and Suppresses Adipogenesis in 3T3-L1 Cells via Regulating Mitochondria-Lipid Metabolism. *Mol. Nutr. Food Res.* **2017**, *61*, 1–43. [CrossRef] [PubMed]
59. Toita, R.; Kang, J.H. Long-Term Profile of Serological Biomarkers, Hepatic Inflammation, and Fibrosis in a Mouse Model of Non-Alcoholic Fatty Liver Disease. *Toxicol. Lett.* **2020**, *332*, 1–6. [CrossRef]
60. Peris-Sampedro, F.; Cabré, M.; Basaure, P.; Reverte, I.; Domingo, J.L.; Teresa Colomina, M. Adulthood Dietary Exposure to a Common Pesticide Leads to an Obese-like Phenotype and a Diabetic Profile in ApoE3 Mice. *Environ. Res.* **2015**, *142*, 169–176. [CrossRef]
61. El-Boghdady, N.A.; Abdeltawab, N.F.; Nooh, M.M. Resveratrol and Montelukast Alleviate Paraquat-Induced Hepatic Injury in Mice: Modulation of Oxidative Stress, Inflammation, and Apoptosis. *Oxidative Med. Cell. Longev.* **2017**, *2017*, 9396425. [CrossRef]
62. Choi, S.Y.; Park, J.S.; Shon, C.H.; Lee, C.Y.; Ryu, J.M.; Son, D.J.; Hwang, B.Y.; Yoo, H.S.; Cho, Y.C.; Lee, J.; et al. Fermented Korean Red Ginseng Extract Enriched in Rd and Rg3 Protects against Non-Alcoholic Fatty Liver Disease through Regulation of MTORC1. *Nutrients* **2019**, *11*, 2963. [CrossRef]
63. Senthilkumar, R.; Sengottuvelan, M.; Nalini, N. Protective Effect of Glycine Supplementation on the Levels of Lipid Peroxidation and Antioxidant Enzymes in the Erythrocyte of Rats with Alcohol-Induced Liver Injury. *Cell Biochem. Funct.* **2004**, *22*, 123–128. [CrossRef] [PubMed]
64. Rom, O.; Liu, Y.; Liu, Z.; Zhao, Y.; Wu, J.; Ghrayeb, A.; Villacorta, L.; Fan, Y.; Chang, L.; Wang, L.; et al. Glycine-Based Treatment Ameliorates NAFLD by Modulating Fatty Acid Oxidation, Glutathione Synthesis, and the Gut Microbiome. *Sci. Transl. Med.* **2020**, *12*, 1–16. [CrossRef] [PubMed]
65. Gariani, K.; Menzies, K.J.; Ryu, D.; Wegner, C.J.; Wang, X.; Ropelle, E.R.; Moullan, N.; Zhang, H.; Perino, A.; Lemos, V.; et al. Eliciting the Mitochondrial Unfolded Protein Response by Nicotinamide Adenine Dinucleotide Repletion Reverses Fatty Liver Disease in Mice. *Hepatology* **2016**, *63*, 1190–1204. [CrossRef] [PubMed]
66. Zhou, C.C.; Yang, X.; Hua, X.; Liu, J.; Fan, M.B.; Li, G.Q.; Song, J.; Xu, T.Y.; Li, Z.Y.; Guan, Y.F.; et al. Hepatic NAD+ deficiency as a Therapeutic Target for Non-Alcoholic Fatty Liver Disease in Ageing. *Br. J. Pharmacol.* **2016**, 2352–2368. [CrossRef] [PubMed]
67. Friedman, S.L.; Neuschwander-Tetri, B.A.; Rinella, M.; Sanyal, A.J. Mechanisms of NAFLD Development and Therapeutic Strategies. *Nat. Med.* **2018**, *24*, 908–922. [CrossRef] [PubMed]
68. Hernandez-Baixauli, J.; Puigbò, P.; Torrell, H.; Palacios-Jordan, H.; Ripoll, V.J.R.; Caimari, A.; Bas, J.M.D.; Baselga-Escudero, L.; Mulero, M. A Pilot Study for Metabolic Profiling of Obesity-Associated Microbial Gut Dysbiosis in Male Wistar Rats. *Biomolecules* **2021**, *11*, 303. [CrossRef]
69. Greco, D.; Kotronen, A.; Westerbacka, J.; Puig, O.; Arkkila, P.; Kiviluoto, T.; Laitinen, S.; Kolak, M.; Fisher, R.M.; Hamsten, A.; et al. Gene Expression in Human NAFLD. *Am. J. Physiol. Gastrointest. Liver Physiol.* **2008**, *294*, 1281–1287. [CrossRef]
70. Steneberg, P.; Sykaras, A.G.; Backlund, F.; Straseviciene, J.; Söderström, I.; Edlund, H. Hyperinsulinemia Enhances Hepatic Expression of the Fatty Acid Transporter Cd36 and Provokes Hepatosteatosis and Hepatic Insulin Resistance. *J. Biol. Chem.* **2015**, *290*, 19034–19043. [CrossRef]
71. Cordero, P.; Gomez-Uriz, A.M.; Campion, J.; Milagro, F.I.; Martinez, J.A. Dietary Supplementation with Methyl Donors Reduces Fatty Liver and Modifies the Fatty Acid Synthase DNA Methylation Profile in Rats Fed an Obesogenic Diet. *Genes Nutr.* **2013**, *8*, 105–113. [CrossRef]
72. Lai, I.K.; Dhakal, K.; Gadupudi, G.S.; Li, M.; Ludewig, G.; Robertson, L.W.; Olivier, A.K. N-Acetylcysteine (NAC) Diminishes the Severity of PCB 126-Induced Fatty Liver in Male Rodents. *Toxicology* **2012**, *302*, 25–33. [CrossRef] [PubMed]
73. Savic, D.; Hodson, L.; Neubauer, S.; Pavlides, M. The Importance of the Fatty Acid Transporter L-Carnitine in Non-Alcoholic Fatty Liver Disease (Nafld). *Nutrients* **2020**, *12*, 2178. [CrossRef] [PubMed]
74. Miura, K.; Yang, L.; van Rooijen, N.; Ohnishi, H.; Seki, E. Hepatic Recruitment of Macrophages Promotes Nonalcoholic Steatohepatitis through CCR2. *Am. J. Physiol. Gastrointest. Liver Physiol.* **2012**, *302*, G1310–G1321. [CrossRef] [PubMed]
75. Kitade, H.; Chen, G.; Ni, Y.; Ota, T. Nonalcoholic Fatty Liver Disease and Insulin Resistance: New Insights and Potential New Treatments. *Nutrients* **2017**, *9*, 387. [CrossRef] [PubMed]

76. Alam, S.; Mustafa, G.; Alam, M.; Ahmad, N. Insulin Resistance in Development and Progression of Nonalcoholic Fatty Liver Disease. *World J. Gastrointest. Pathophysiol.* **2016**, *7*, 211. [CrossRef]
77. Han, X.; Bao, X.; Lou, Q.; Xie, X.; Zhang, M.; Zhou, S.; Guo, H.; Jiang, G.; Shi, Q. Nicotinamide Riboside Exerts Protective Effect against Aging-Induced NAFLD-like Hepatic Dysfunction in Mice. *PeerJ* **2019**, *2019*, 1–14. [CrossRef]
78. Lee, H.J.; Hong, Y.S.; Jun, W.; Yang, S.J. Nicotinamide Riboside Ameliorates Hepatic Metaflammation by Modulating NLRP3 Inflammasome in a Rodent Model of Type 2 Diabetes. *J. Med. Food* **2015**, *18*, 1207–1213. [CrossRef]
79. Poniachik, J.; Csendes, A.; Díaz, J.C.; Rojas, J.; Burdiles, P.; Maluenda, F.; Smok, G.; Rodrigo, R.; Videla, L.A. Increased Production of IL-1α and TNF-α in Lipopolysaccharide-Stimulated Blood from Obese Patients with Non-Alcoholic Fatty Liver Disease. *Cytokine* **2006**, *33*, 252–257. [CrossRef]
80. Ge, C.X.; Yu, R.; Xu, M.X.; Li, P.Q.; Fan, C.Y.; Li, J.M.; Kong, L.D. Betaine Prevented Fructose-Induced NAFLD by Regulating LXRα/PPARα Pathway and Alleviating ER Stress in Rats. *Eur. J. Pharmacol.* **2016**, *770*, 154–164. [CrossRef]
81. Salic, K.; Gart, E.; Seidel, F.; Verschuren, L.; Caspers, M.; van Duyvenvoorde, W.; Wong, K.E.; Keijer, J.; Bobeldijk-Pastorova, I.; Wielinga, P.Y.; et al. Combined Treatment with L-Carnitine and Nicotinamide Riboside Improves Hepatic Metabolism and Attenuates Obesity and Liver Steatosis. *Int. J. Mol. Sci.* **2019**, *20*, 4359. [CrossRef] [PubMed]
82. Wang, M.E.; Chen, Y.C.; Chen, I.S.; Hsieh, S.C.; Chen, S.S.; Chiu, C.H. Curcumin Protects against Thioacetamide-Induced Hepatic Fibrosis by Attenuating the Inflammatory Response and Inducing Apoptosis of Damaged Hepatocytes. *J. Nutr. Biochem.* **2012**, *23*, 1352–1366. [CrossRef]
83. Varela-Rey, M.; Martínez-López, N.; Fernández-Ramos, D.; Embade, N.; Calvisi, D.F.; Woodhoo, A.; Rodríguez, J.; Fraga, M.F.; Julve, J.; Rodríguez-Millán, E.; et al. Fatty Liver and Fibrosis in Glycine N-Methyltransferase Knockout Mice Is Prevented by Nicotinamide. *Hepatology* **2010**, *52*, 105–114. [CrossRef]
84. Werge, M.P.; McCann, A.; Galsgaard, E.D.; Holst, D.; Bugge, A.; Albrechtsen, N.J.W.; Gluud, L.L. The Role of the Transsulfuration Pathway in Non-Alcoholic Fatty Liver Disease. *J. Clin. Med.* **2021**, *10*, 1081. [CrossRef]
85. Deminice, R.; Da Silva, R.P.; Lamarre, S.G.; Kelly, K.B.; Jacobs, R.L.; Brosnan, M.E.; Brosnan, J.T. Betaine Supplementation Prevents Fatty Liver Induced by a High-Fat Diet: Effects on One-Carbon Metabolism. *Amino Acids* **2015**, *47*, 839–846. [CrossRef]
86. Keinicke, H.; Sun, G.; Mentzel, C.M.J.; Fredholm, M.; John, L.M.; Andersen, B.; Raun, K.; Kjaergaard, M. Fgf21 Regulates Hepatic Metabolic Pathways to Improve Steatosis and Inflammation. *Endocr. Connect.* **2020**, *9*, 755–768. [CrossRef] [PubMed]
87. Inagaki, T. Research Perspectives on the Regulation and Physiological Functions of FGF21 and Its Association with NAFLD. *Front. Endocrinol.* **2015**, *6*, 147. [CrossRef]
88. Rusli, F.; Deelen, J.; Andriyani, E.; Boekschoten, M.V.; Lute, C.; Van Den Akker, E.B.; Müller, M.; Beekman, M.; Steegenga, W.T. Fibroblast Growth Factor 21 Reflects Liver Fat Accumulation and Dysregulation of Signalling Pathways in the Liver of C57BL/6J Mice. *Sci. Rep.* **2016**, *6*, 30484. [CrossRef] [PubMed]
89. Vernia, S.; Cavanagh-Kyros, J.; Garcia-Haro, L.; Sabio, G.; Barrett, T.; Jung, D.Y.; Kim, J.K.; Xu, J.; Shulha, H.P.; Garber, M.; et al. The PPARα-FGF21 Hormone Axis Contributes to Metabolic Regulation by the Hepatic JNK Signaling Pathway. *Cell Metab.* **2014**, *20*, 512–525. [CrossRef] [PubMed]
90. Ejaz, A.; Martinez-Guino, L.; Goldfine, A.B.; Ribas-Aulinas, F.; De Nigris, V.; Ribó, S.; Gonzalez-Franquesa, A.; Garcia-Roves, P.M.; Li, E.; Dreyfuss, J.M.; et al. Dietary Betaine Supplementation Increases Fgf21 Levels to Improve Glucose Homeostasis and Reduce Hepatic Lipid Accumulation in Mice. *Diabetes* **2016**, *65*, 902–912. [CrossRef] [PubMed]
91. Li, L.; Chen, J.; Ni, Y.; Feng, X.; Zhao, Z.; Wang, P.; Sun, J.; Yu, H.; Yan, Z.; Liu, D.; et al. TRPV1 Activation Prevents Nonalcoholic Fatty Liver through UCP2 Upregulation in Mice. *Pflug. Arch. Eur. J. Physiol.* **2012**, *463*, 727–732. [CrossRef] [PubMed]
92. Serviddio, G.; Bellanti, F.; Tamborra, R.; Rollo, T.; Capitanio, N.; Romano, A.D.; Sastre, J.; Vendemiale, G.; Altomare, E. Uncoupling Protein-2 (UCP2) Induces Mitochondrial Proton Leak and Increases Susceptibility of Non-Alcoholic Steatohepatitis (NASH) Liver to Ischaemia-Reperfusion Injury. *Gut* **2008**, *57*, 957–965. [CrossRef] [PubMed]
93. Chavin, K.D.; Yang, S.Q.; Lin, H.Z.; Chatham, J.; Chacko, V.P.; Hock, J.B.; Walajtys-Rode, E.; Rashid, A.; Chen, C.H.; Huang, C.C.; et al. Obesity Induces Expression of Uncoupling Protein-2 in Hepatocytes and Promotes Liver ATP Depletion. *J. Biol. Chem.* **1999**, *274*, 5692–5700. [CrossRef] [PubMed]
94. Bellanti, F.; Villani, R.; Tamborra, R.; Blonda, M.; Iannelli, G.; di Bello, G.; Facciorusso, A.; Poli, G.; Iuliano, L.; Avolio, C.; et al. Synergistic Interaction of Fatty Acids and Oxysterols Impairs Mitochondrial Function and Limits Liver Adaptation during Nafld Progression. *Redox Biol.* **2018**, *15*, 86–96. [CrossRef] [PubMed]
95. Ali, M.H.H.; Messiha, B.A.S.; Abdel-Latif, H.A.T. Protective Effect of Ursodeoxycholic Acid, Resveratrol, and N-Acetylcysteine on Nonalcoholic Fatty Liver Disease in Rats. *Pharm. Biol.* **2016**, *54*, 1198–1208. [CrossRef] [PubMed]
96. Laurent, A.; Nicco, C.; Van Nhieu, J.T.; Borderie, D.; Chéreau, C.; Conti, F.; Jaffray, P.; Soubrane, O.; Calmus, Y.; Weill, B.; et al. Pivotal Role of Superoxide Anion and Beneficial Effect of Antioxidant Molecules in Murine Steatohepatitis. *Hepatology* **2004**, *39*, 1277–1285. [CrossRef]
97. Huang, X.; Liu, G.; Guo, J.; Su, Z. The PI3K/AKT Pathway in Obesity and Type 2 Diabetes. *Int. J. Biol. Sci.* **2018**, *14*, 1483–1496. [CrossRef]
98. Kathirvel, E.; Morgan, K.; Nandgiri, G.; Sandoval, B.C.; Caudill, M.A.; Bottiglieri, T.; French, S.W.; Morgan, T.R. Betaine Improves Nonalcoholic Fatty Liver and Associated Hepatic Insulin Resistance: A Potential Mechanism for Hepatoprotection by Betaine. *Am. J. Physiol. Gastrointest. Liver Physiol.* **2010**, *299*, G1068–G1077. [CrossRef]

99. Jwa, H.; Choi, Y.; Park, U.H.; Um, S.J.; Yoon, S.K.; Park, T. Piperine, an LXRα Antagonist, Protects against Hepatic Steatosis and Improves Insulin Signaling in Mice Fed a High-Fat Diet. *Biochem. Pharmacol.* **2012**, *84*, 1501–1510. [CrossRef]
100. Hagiwara, A.; Cornu, M.; Cybulski, N.; Polak, P.; Betz, C.; Trapani, F.; Terracciano, L.; Heim, M.H.; Rüegg, M.A.; Hall, M.N. Hepatic MTORC2 Activates Glycolysis and Lipogenesis through Akt, Glucokinase, and SREBP1c. *Cell Metab.* **2012**, *15*, 725–738. [CrossRef]
101. Iizuka, K.; Horikawa, Y. ChREBP: A Glucose-Activated Transcription Factor Involved in the Development of Metabolic Syndrome. *Endocr. J.* **2008**, *55*, 617–624. [CrossRef]
102. Liu, X.; Cui, J.; Li, Z.; Xu, J.; Wang, J.; Xue, C.; Wang, Y. Comparative Study of DHA-Enriched Phospholipids and EPA-Enriched Phospholipids on Metabolic Disorders in Diet-Induced-Obese C57BL/6J Mice. *Eur. J. Lipid Sci. Technol.* **2014**, *116*, 255–265. [CrossRef]
103. Li, W.; Li, Y.; Wang, Q.; Yang, Y. Crude Extracts from Lycium Barbarum Suppress SREBP-1c Expression and Prevent Diet-Induced Fatty Liver through AMPK Activation. *BioMed Res. Int.* **2014**, *2014*, 196198. [CrossRef]
104. Ono, H.; Shimano, H.; Katagiri, H.; Yahagi, N.; Sakoda, H.; Onishi, Y.; Anai, M.; Ogihara, T.; Fujishiro, M.; Viana, A.Y.I.; et al. Hepatic Akt Activation Induces Marked Hypoglycemia, Hepatomegaly, and Hypertriglyceridemia with Sterol Regulatory Element Binding Protein Involvement. *Diabetes* **2003**, *52*, 2905–2913. [CrossRef]
105. Hu, X.Q.; Wang, Y.M.; Wang, J.F.; Xue, Y.; Li, Z.J.; Nagao, K.; Yanagita, T.; Xue, C.H. Dietary Saponins of Sea Cucumber Alleviate Orotic Acid-Induced Fatty Liver in Rats via PPAR and SREBP-1c Signaling. *Lipids Health Dis.* **2010**, *9*, 1–9. [CrossRef] [PubMed]
106. Shimomura, I.; Bashmakov, Y.; Horton, J.D. Increased Levels of Nuclear SREBP-1c Associated with Fatty Livers in Two Mouse Models of Diabetes Mellitus *. *J. Biol. Chem.* **1999**, *274*, 30028–30032. [CrossRef] [PubMed]
107. Pan, Y.X.; Zhuo, M.Q.; Li, D.D.; Xu, Y.H.; Wu, K.; Luo, Z. SREBP-1 and LXRA Pathways Mediated Cu-Induced Hepatic Lipid Metabolism in Zebrafish Danio Rerio. *Chemosphere* **2019**, *215*, 370–379. [CrossRef] [PubMed]
108. Wang, S.; Wan, T.; Ye, M.; Qiu, Y.; Pei, L.; Jiang, R.; Pang, N.; Huang, Y.; Liang, B.; Ling, W.; et al. Nicotinamide Riboside Attenuates Alcohol Induced Liver Injuries via Activation of SirT1/PGC-1α/Mitochondrial Biosynthesis Pathway. *Redox Biol.* **2018**, *17*, 89–98. [CrossRef] [PubMed]
109. Ge, T.; Yang, J.; Zhou, S.; Wang, Y.; Li, Y.; Tong, X. The Role of the Pentose Phosphate Pathway in Diabetes and Cancer. *Front Endocrinol.* **2020**, *11*, 365. [CrossRef]
110. Van Loo, P.L.P.; Kuin, N.; Sommer, R.; Avsaroglu, H.; Pham, T.; Baumans, V. Impact of "living Apart Together" on Postoperative Recovery of Mice Compared with Social and Individual Housing. *Lab. Anim.* **2007**, *41*, 441–455. [CrossRef]
111. Liu, Y.; Li, Q.; Wang, H.; Zhao, X.; Li, N.; Zhang, H.; Chen, G.; Liu, Z. Fish Oil Alleviates Circadian Bile Composition Dysregulation in Male Mice with NAFLD. *J. Nutr. Biochem.* **2019**, *69*, 53–62. [CrossRef] [PubMed]
112. Martínez-Fernández, L.; González-Muniesa, P.; Sáinz, N.; Laiglesia, L.M.; Escoté, X.; Martínez, J.A.; Moreno-Aliaga, M.J. Maresin 1 Regulates Hepatic FGF21 in Diet-Induced Obese Mice and in Cultured Hepatocytes. *Mol. Nutr. Food Res.* **2019**, *63*, e1900358. [CrossRef] [PubMed]

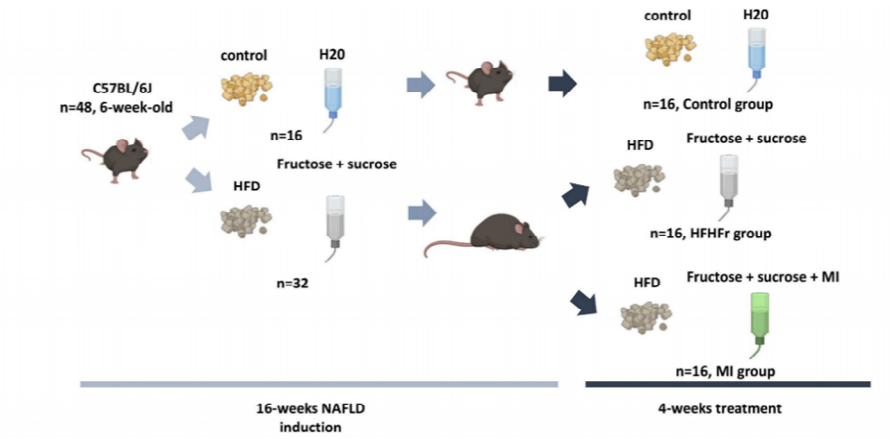

Figure S1. Schematic diagram of the animal study

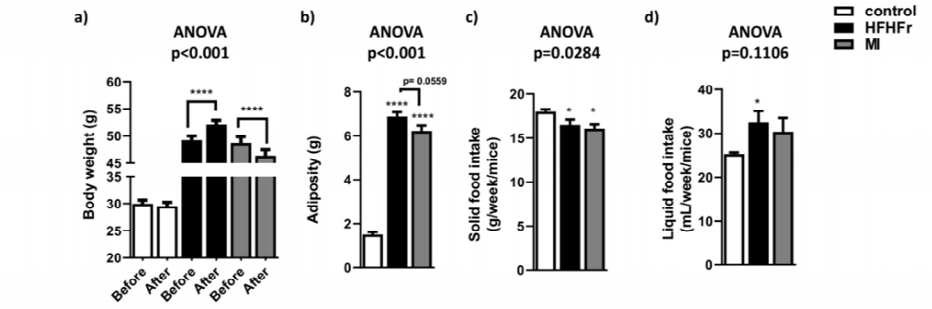

Figure S2. a) Body weight before and after 4 weeks of MI supplementation; b) Adiposity at the end of the supplementation calculated as the sum of as the white adipose depots (epididymal, retroperitoneal, inguinal and mesenteric); c,d) Data of the solid and liquid food intake per week

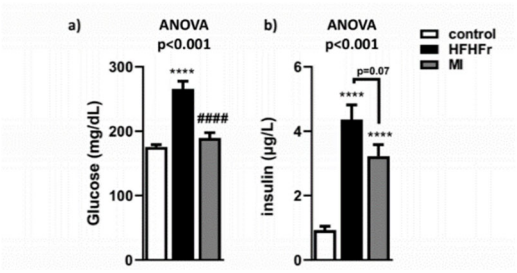

Figure S3. a) Fasting glycaemia; b) Fasting insulinemia after MI supplementation.

Chapter 2

Reduction of Obesity and Insulin Resistance through Dual Targeting of VAT and BAT by a Novel Combination of Metabolic Cofactors

Sergio Quesada-Vázquez [1], Anna Antolín [1], Marina Colom-Pellicer [2], Gerard Aragonès [2], Laura Herrero [3,4], Josep Maria Del Bas [5], Antoni Caimari [5] and Xavier Escoté [1,*]

1. Eurecat, Centre Tecnològic de Catalunya, Unitat de Nutrició i Salut, 43204 Reus, Spain; sergio.quesada@eurecat.org (S.Q.-V.); anna.antolin@eurecat.org (A.A.)
2. Nutrigenomics Research Group, Department of Biochemistry and Biotechnology, Universitat Rovira i Virgili, 43007 Tarragona, Spain; marina.colom@urv.cat (M.C.-P.); gerard.aragones@urv.cat (G.A.)
3. Department of Biochemistry and Physiology, School of Pharmacy and Food Sciences, Institut de Biomedicina de la Universitat de Barcelona (IBUB), Universitat de Barcelona, 08028 Barcelona, Spain; lherrero@ub.edu
4. Centro de Investigación Biomédica en Red de Fisiopatología de la Obesidad y la Nutrición (CIBEROBN), Instituto de Salud Carlos III, 28029 Madrid, Spain
5. Eurecat, Centre Tecnològic de Catalunya, Àrea de Biotecnologia, 43204 Reus, Spain; josep.delbas@eurecat.org (J.M.D.B.); antoni.caimari@eurecat.org (A.C.)

* Correspondence: xavier.escote@eurecat.org; Tel.: +34-977-302057 (ext. 4824)

Published in: International Journal of Molecular Sciences (IJMS). 2022 Nov; 23, 14923

Impact Factor (2022): 6.208

JCR category rank: Q1: Biochemistry & Molecular Biology

International Journal of
Molecular Sciences

MDPI

Article

Reduction of Obesity and Insulin Resistance through Dual Targeting of VAT and BAT by a Novel Combination of Metabolic Cofactors

Sergio Quesada-Vázquez [1], Anna Antolín [1], Marina Colom-Pellicer [2], Gerard Aragonès [2], Laura Herrero [3,4], Josep Maria Del Bas [5], Antoni Caimari [5] and Xavier Escoté [1,*]

[1] Eurecat, Centre Tecnològic de Catalunya, Unitat de Nutrició i Salut, 43204 Reus, Spain
[2] Nutrigenomics Research Group, Department of Biochemistry and Biotechnology, Universitat Rovira i Virgili, 43007 Tarragona, Spain
[3] Department of Biochemistry and Physiology, School of Pharmacy and Food Sciences, Institut de Biomedicina de la Universitat de Barcelona (IBUB), Universitat de Barcelona, 08028 Barcelona, Spain
[4] Centro de Investigación Biomédica en Red de Fisiopatología de la Obesidad y la Nutrición (CIBEROBN), Instituto de Salud Carlos III, 28029 Madrid, Spain
[5] Eurecat, Centre Tecnològic de Catalunya, Àrea de Biotecnologia, 43204 Reus, Spain
* Correspondence: xavier.escote@eurecat.org; Tel.: +34-977-302057 (ext. 4824)

Abstract: Obesity is an epidemic disease worldwide, characterized by excessive fat accumulation associated with several metabolic perturbations, such as metabolic syndrome, insulin resistance, hypertension, and dyslipidemia. To improve this situation, a specific combination of metabolic cofactors (MC) (betaine, N-acetylcysteine, L-carnitine, and nicotinamide riboside) was assessed as a promising treatment in a high-fat diet (HFD) mouse model. Obese animals were distributed into two groups, orally treated with the vehicle (obese + vehicle) or with the combination of metabolic cofactors (obese + MC) for 4 weeks. Body and adipose depots weights; insulin and glucose tolerance tests; indirect calorimetry; and thermography assays were performed at the end of the intervention. Histological analysis of epididymal white adipose tissue (EWAT) and brown adipose tissue (BAT) was carried out, and the expression of key genes involved in both fat depots was characterized by qPCR. We demonstrated that MC supplementation conferred a moderate reduction of obesity and adiposity, an improvement in serum glucose and lipid metabolic parameters, an important improvement in lipid oxidation, and a decrease in adipocyte hypertrophy. Moreover, MC-treated animals presented increased adipose gene expression in EWAT related to lipolysis and fatty acid oxidation. Furthermore, MC supplementation reduced glucose intolerance and insulin resistance, with an increased expression of the glucose transporter *Glut4*; and decreased fat accumulation in BAT, raising non-shivering thermogenesis. This treatment based on a specific combination of metabolic cofactors mitigates important pathophysiological characteristics of obesity, representing a promising clinical approach to this metabolic disease.

Keywords: obesity; adipose tissue; insulin resistance; thermogenesis; metabolic cofactors

Citation: Quesada-Vázquez, S.; Antolín, A.; Colom-Pellicer, M.; Aragonès, G.; Herrero, L.; Del Bas, J.M.; Caimari, A.; Escoté, X. Reduction of Obesity and Insulin Resistance through Dual Targeting of VAT and BAT by a Novel Combination of Metabolic Cofactors. *Int. J. Mol. Sci.* **2022**, *23*, 14923. https://doi.org/10.3390/ijms232314923

Academic Editor: Andrea Frontini

Received: 21 September 2022
Accepted: 26 November 2022
Published: 29 November 2022

1. Introduction

The World Health Organization (WHO) defines obesity as an epidemic disease caused by an imbalance in energy consumption and storage, characterized by an expansion of adipose tissue, which negatively affects health and healthcare systems worldwide [1]. Obesity is a complex disease associated with several comorbidities including metabolic syndrome, insulin resistance (IR), hypertension, and dyslipidemia [2]. It is imperative to find new strategies to fight against this disease. Current therapies focus on increasing physical activity and reducing excess calorie intake that causes energy imbalance, but with low adherence by the general population, or include invasive approaches such as bariatric surgery [3]. Adipose tissue is especially important due to its capacity to secrete

several substances that regulate metabolic pathways, such as hormones, cytokines, and adipokines [4]. When adipocytes reach their maximal fat storage capacity and insulin fails to promote the appropriate storage of more fatty acids due to IR, lipolysis is activated in adipocytes, and lipids are released as free fatty acids (FFA) into the circulatory system [5] and are deposited in other peripheral tissues where they may produce lipotoxicity [6,7].

Mardinoglu et al. [8] performed personal model-assisted identification of NAD+ and glutathione (GSH) metabolism to elucidate mechanisms underlying NAFLD, a disease strongly related to obesity, and to discover which substances could be used as treatments due to their participation in the affected metabolic pathways. Prior studies have described how different bioactive co-factors separately related to GSH and NAD^+ metabolism can modulate metabolic pathways and improve white adipose tissue dysfunction in preclinical models [9–15]. N-acetylcysteine (NAC) and betaine were selected because both ingredients are GSH precursors [16,17], and nicotinamide riboside (NR), which is a precursor of NAD^+, and L-carnitine were employed to boost fatty acid oxidation promoting the uptake of FFA to mitochondria, thus accelerating FFA oxidation and protecting against impaired mitochondrial function [18–20]. NAC improved glucose and insulin tolerance by reducing insulin levels in HFD-fed mice [10]. After betaine administration, IR was ameliorated [12] and the dysfunctional lipolysis in adipose tissue was restored [20]. L-carnitine demonstrated its boosting function in FFA transport to the mitochondrial matrix [21], whereas L-carnitine deficiency reduces FFA oxidation and increases lipolysis in adipose tissue [14]. Finally, NR is an NAD^+ donor essential for maintaining a cellular redox state and producing energy for oxidative metabolism [11]. NR in combination with L-carnitine reduced mice's visceral and subcutaneous WAT depots [21]. Thus, this work evaluated for the first time the beneficial effects on adipose tissue of this novel combination of metabolic cofactors. Taking into consideration the importance of adipose dysfunction in metabolic disorders and in light of previous studies we hypothesized that these metabolic cofactors in combination could activate fatty acid oxidation and FFA uptake in adipocytes by improving IR in an obese animal model. To validate this hypothesis, we analyzed the administration of a combination of MC that included NAC, NR, L-carnitine, and betaine, for 1 month in a diet-induced obese mouse model [22,23], focusing on the main pathological characteristics of adipose tissues.

2. Results

2.1. MC Supplementation Alleviates Obese Diet-Induced Obesity

Bodyweight gain in the obese + MC group was reduced in comparison with the obese + vehicle group from two and a half weeks of the supplementation (Figure 1A). Similar results were observed in the percentage of body weight gain (Figure S1A). These differences were not the consequences of a reduction in food intake (Figure S1B). Regarding this effect on body weight, indirect calorimetry was performed to analyze lipid oxidation through the analysis of the respiratory quotient (RQ) (Figure 1B,C). As a result, the obese + MC animals showed significantly decreased RQ in comparison with the obese + vehicle, directly related to an increase in fat oxidation. In contrast, no differences were observed regarding energy expenditure (EE) (Figure S2A), oxygen consumption (VO_2) (Figure S2B), or carbon dioxide production (VCO_2) (Figure S2C). Due to the increased lipid oxidation observed with MC supplementation, adipose tissue depots were analyzed. However, supplementation of MC did not cause any effect on IWAT (Figures 1D and S1B) although it significantly reduced the visceral WAT depots' weights (EWAT, RWAT, and MWAT) (Figure 1E–G) and the sum of visceral depots (VAT, Figure 1H) compared with the obese + vehicle group, suggesting that MC could induce a reduction of lipid content in the VAT of obese mice through different processes such as inhibition of adipogenesis or lipogenesis, or an increase of lipolysis or lipid oxidation [24]. Similar results were observed in the percentage of each adipose depot in relation to the total body weight (Figure S1D–G). In addition, biochemical analyses showed no significant differences in serum triglyceride levels (Figure 1I) or HDL levels (Figure 1L). However, significant decreases in circulating total cholesterol (Figure 1J) and LDL-cholesterol levels (Figure 1K) and in the LDL/HDL

ratio (Figure 1M) were found in the MC group compared to the obese + vehicle group, suggesting an improvement in the lipid profile of these supplemented mice.

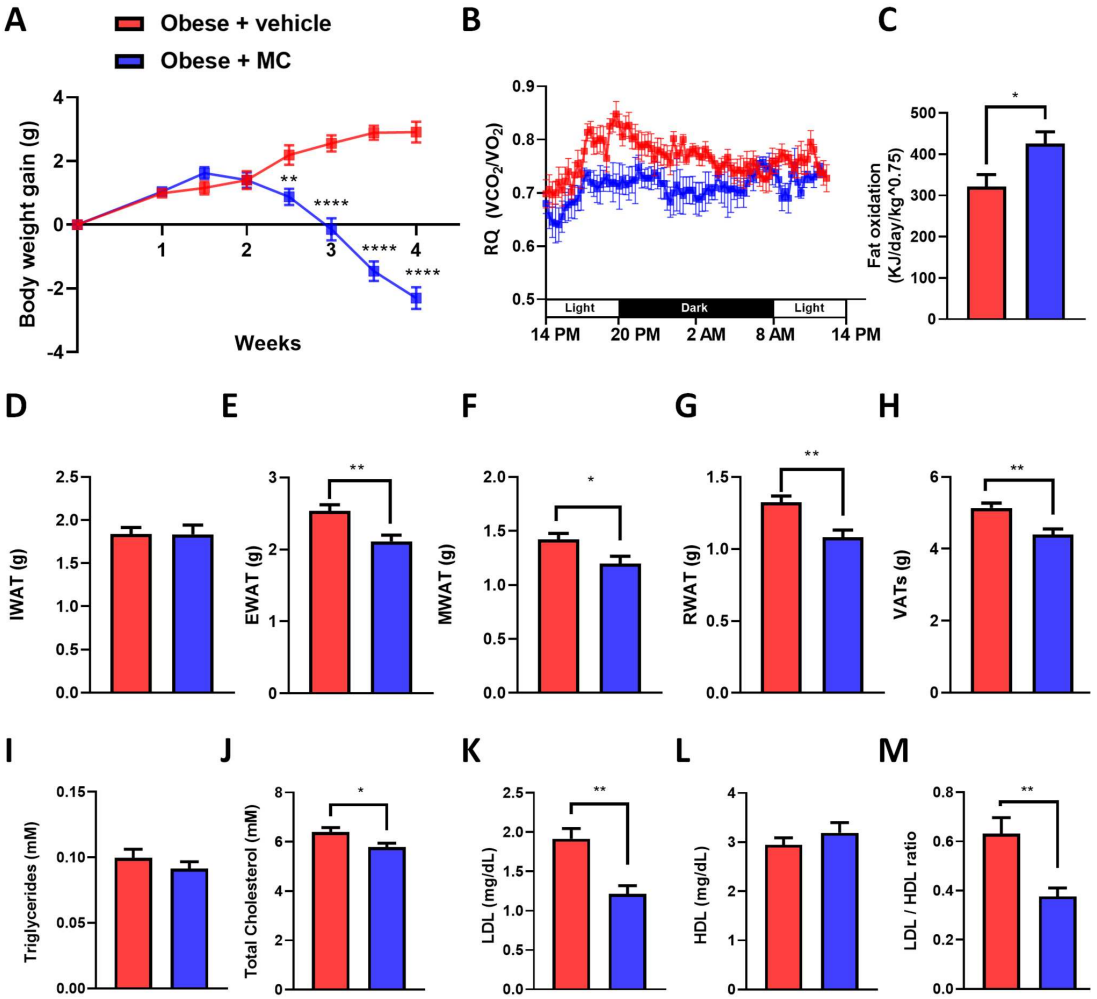

Figure 1. Obese mice supplemented with MC had reduced body weight and smaller visceral WAT depots with an improved biochemical profile. Effects of MC treatment on: (**A**) body weight gain; (**B**) RQ for 24 h; (**C**) fat oxidation. Weights of different adipose tissue depots: (**D**) inguinal (IWAT); (**E**) epididymal (EWAT); (**F**) mesenchymal (MWAT); (**G**) retroperitoneal (RWAT). (**H**) weight of VATs (EWAT + MWAT + RWAT). Serum biochemical parameters of: (**I**) triglycerides; (**J**) total cholesterol; (**K**) LDL-cholesterol; (**L**) HDL-cholesterol; and (**M**) LDL/HDL ratio. Data are mean ± SEM. * $p < 0.05$, ** $p < 0.01$, **** $p < 0.0001$.

2.2. MC Supplementation Improves Adiposity by Decreasing Adipocyte Hypertrophy in Epididymal Adipose Tissue, with Beneficial Effects on Lipolysis and Fatty Acid Oxidation

Representative histological images revealed notorious larger adipocytes in the obese + vehicle animals compared with obese + MC animals (Figure 2A). To evaluate these changes, a quantitative analysis of the adipose area was performed (Figure 2B). A reduction in the average adipocyte area was observed in the obese + MC group compared to the obese + vehicle group. the adipocyte size distribution showed a reduction in

the percentage of larger adipocytes and a tendency for smaller adipocytes to increase in MC-supplemented mice (Figure 2C).

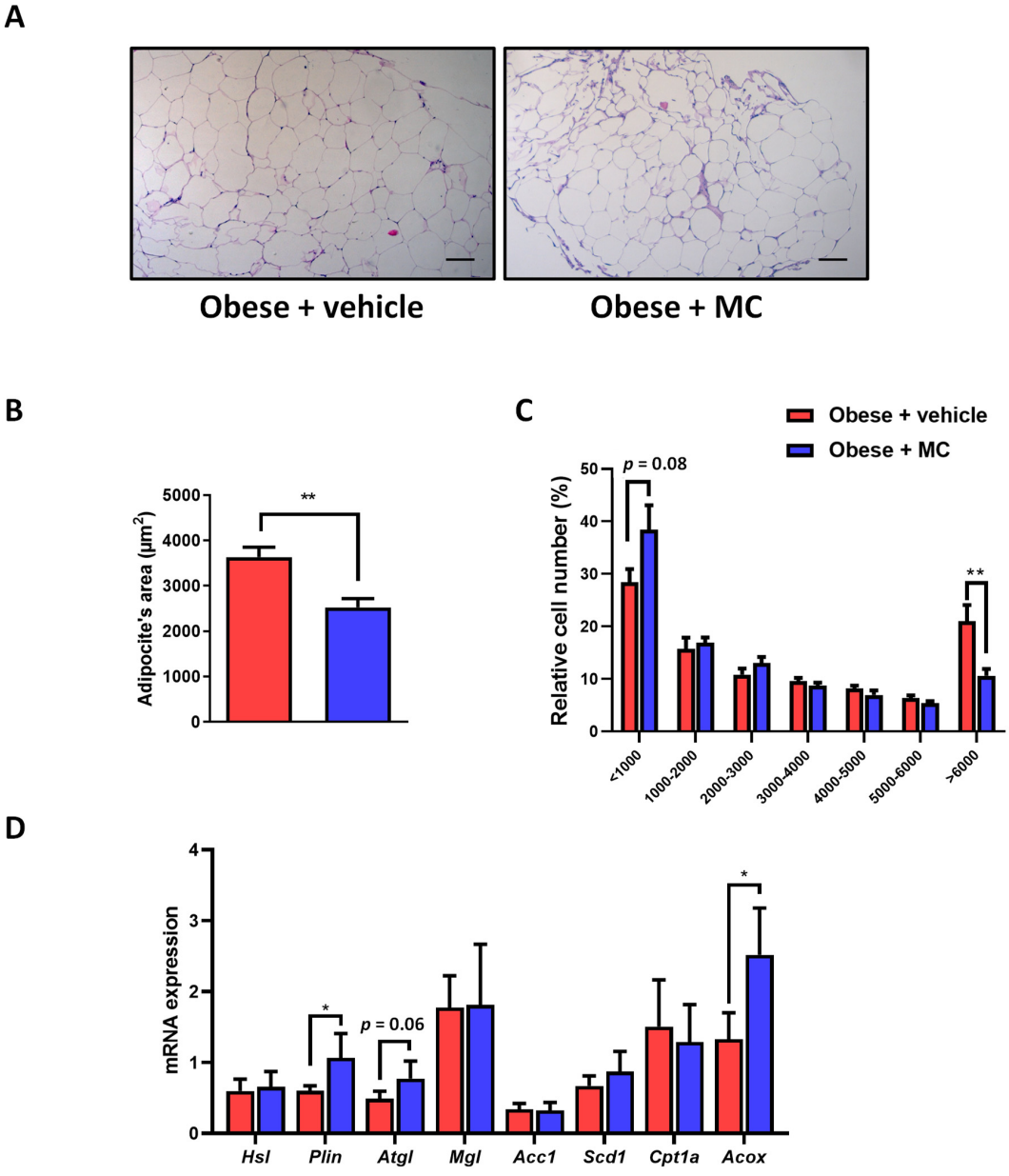

Figure 2. MC supplementation promotes a reduction in the adipocyte size, increasing lipolysis and fatty acid oxidation. Effects of treatments on adipocyte hypertrophy (**A**) Representative micrographs of hematoxylin–eosin stained EWAT sections from obese + vehicle and obese + MC groups (bar = 100 μm); (**B**) adipocyte area; (**C**) adipocyte size distribution; and (**D**) EWAT mRNA expression of genes related to lipolysis (*Hsl*, *Plin*, *Atgl* and *Mgl*), de novo lipogenesis (*Acc1* and *Scd1*), and fatty acid oxidation (*Cpt1a* and *Acox1*). Data are mean ± SEM. * $p < 0.05$, ** $p < 0.01$.

To determine which metabolic pathways could be involved in improving adipose tissue metabolism after MC supplementation, gene expression was evaluated for genes related to adipose lipolysis, de novo lipogenesis, and fatty acid oxidation (Figure 2D). MC-supplemented mice showed an up-regulation in *Plin1* expression compared to obese + vehicle mice, pointing to a possible effect on lipolytic activity. No significant effects on *Mgl* and *Hsl* expression were observed. In contrast, *Atgl* expression showed a tendency to increase in MC-supplemented animals. On the other hand, MC supplementation did not modify de novo lipogenesis gene expression (*Acc1* and *Scd1*). Interestingly, *Acox1* showed a significant increase in its expression in lipid oxidation after MC supplementation, but no changes were observed in *Cpt1a* expression.

2.3. MC Supplementation Reduced Insulin Resistance Associated with Obesity

Fasting glucose (Figure 3A), fasting insulin (Figure 3B), and HOMA-IR (Figure 3C) were determined. The MC group reverted significantly to the increase in circulatory glucose levels observed in the obese + vehicle group, and showed a significant tendency towards reduced circulatory insulin levels. Reductions in glucose and insulin levels were accompanied by a reduction in HOMA-IR [25]. GTT (Figure 3D) and ITT (Figure 3E) were performed to analyze glucose and insulin sensitivity. In both tests, significant differences were observed from basal time until the end of the tests, with an important amelioration in glucose tolerance and IR in the animals supplemented with MC. To validate the amelioration of IR, the EWAT expression was evaluated for key genes in glucose uptake, *Glut1* and *Glut4* (Figure 3F). No significant effects between groups were observed in *Glut1* expression. However, the MC group showed an increased expression of *Glut4* in the EWAT, which could be related to an improvement in IR.

2.4. MC Supplementation Reduces Fat Accumulation in Brown Adipose Tissue by Activation of Lipolysis, Lipid Oxidation and Thermogenesis

BAT activation provides a protective mechanism against excessive body weight and accumulation of fat mass by non-shivering thermogenesis, with important roles in triglyceride clearance, glucose homeostasis, and insulin sensitivity [26]. To better understand the molecular mechanisms associated with the improvement of lipid metabolism, the impact of MC supplementation on BAT was analyzed. BAT weight showed a significant decrease in MC-supplemented mice compared with their counterparts (Figure 4A). Similar results were observed in the percentage of BAT in relation to total body weight (Figure S1H). In addition, histological studies revealed increased fat accumulation in BAT in the obese + vehicle animals compared with obese + MC animals (Figure 4B–D), with a reduction in the number of lipid droplets (Figure 4C) and the lipid surface area (Figure 4D) in the obese + MC animals.

To determine which metabolic pathways could be involved in the reduction of fat accumulation in BAT after MC supplementation, mRNA expression analysis was carried out for genes related to main BAT functions (Figure 4E). MC-supplemented mice showed an up-regulation in *Ucp1*, *Fgf21*, *Pgc1a* and *Dio2* expression compared with obese + vehicle mice, and a tendency towards increased *Prmd16* levels, pointing to a possible increase in thermogenic capacity. In contrast, no significant effects were observed in the expression of de novo lipogenesis-related genes, *Fasn* and *Ppara*. Meanwhile, genes related to lipolysis (*Atgl*, *Hsl*, and *Mgl*) and fatty acid oxidation (*Acox1*) showed a significant increase in their levels in MC-supplemented animals compared with obese + vehicle animals. No changes were observed in *Cpt1b* levels or the glucose transporter *Glut1*, whereas a strong tendency towards a reduced expression of *Glut4* was observed in the obese + MC mice.

To corroborate whether MC supplementation increases non-shivering thermogenesis, infrared thermography was applied to analyze the temperature of the animal's back surface covering the interscapular BAT (Figure 4F,G), indicating an increased temperature after MC supplementation compared with the obese + vehicle group.

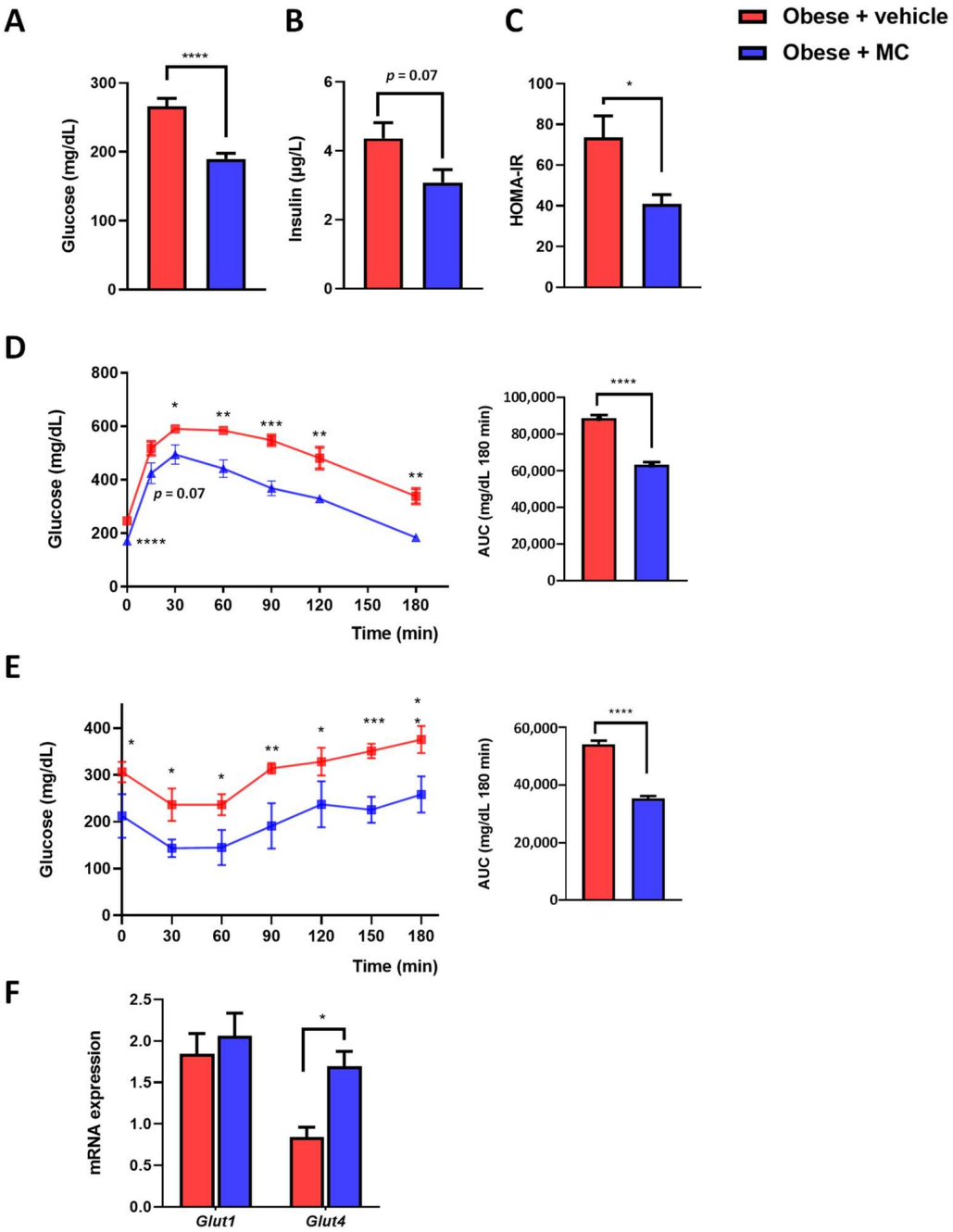

Figure 3. MC supplementation promotes improved glucose and insulin resistance by increasing the expression of *Glut4* in EWAT. (**A**) Fasting glucose; (**B**) fasting insulin; (**C**) HOMA-IR; (**D**) glucose tolerance test (GTT) and area under the curve (AUC); (**E**) insulin tolerance test (ITT) and AUC; (**F**) EWAT mRNA expression of *Glut1* and *Glut4*. Data are mean ± SEM. * $p < 0.05$, ** $p < 0.01$, *** $p < 0.001$, **** $p < 0.0001$.

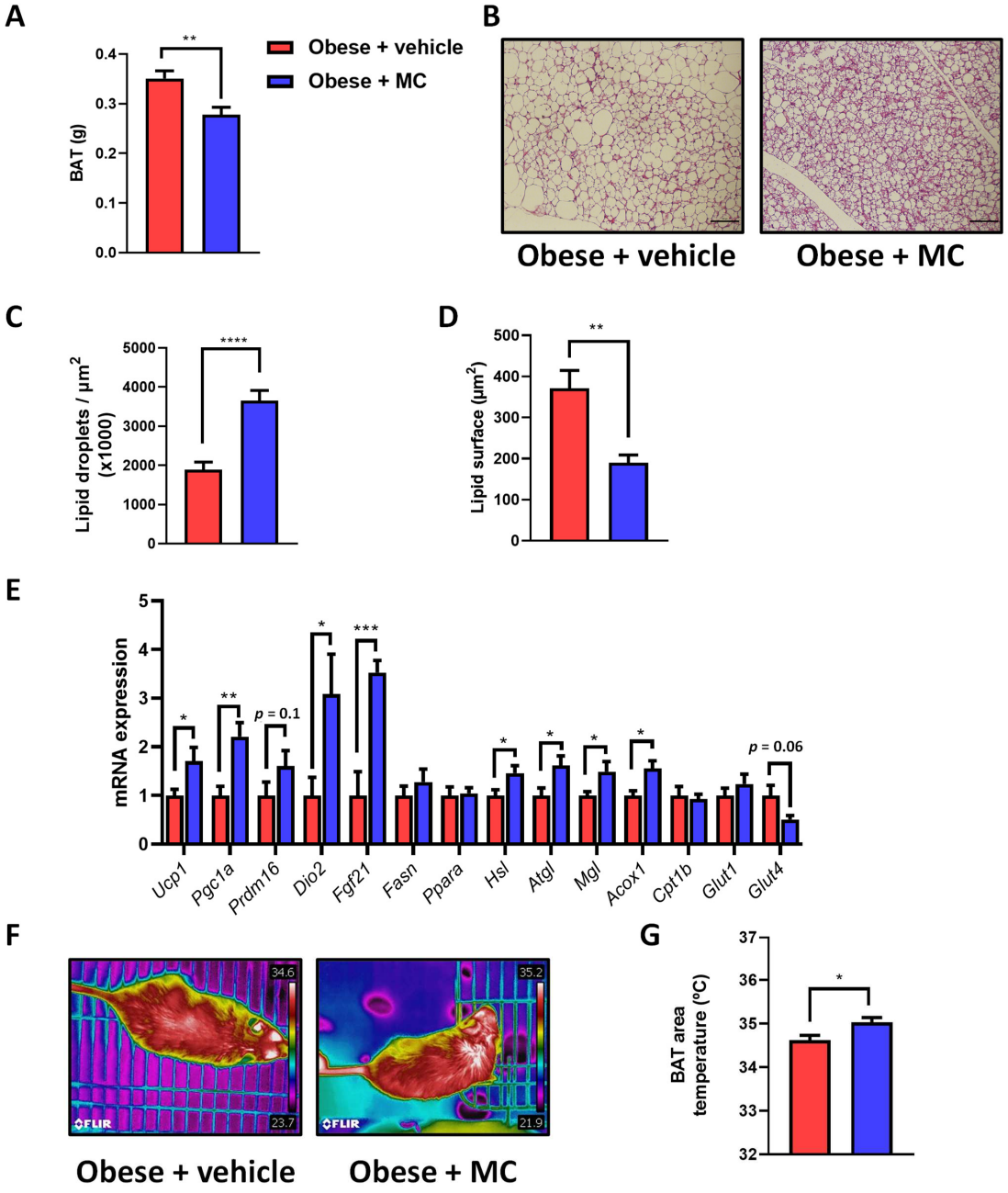

Figure 4. MC supplementation increases BAT thermogenesis. Effects of treatments on: (**A**) brown adipose tissue (BAT) weight; (**B**) representative micrographs of hematoxylin–eosin-stained BAT sections (Bar = 100 µm); (**C**) lipid droplets, and (**D**) and quantification of the lipid droplet surface. (**E**) BAT mRNA expression of genes related to BAT function (*Ucp1*, *Pgc1a*, *Prdm16*, *Dio2*, and *Fgf21*); de novo lipogenesis (*Fasn* and *Ppara*); lipolysis (*Hsl*, *Atgl* and *Mgl*); fatty acid oxidation (*Acox* and *Cpt1b*); and glucose uptake (*Glut1* and *Glut4*). (**F**,**G**) Representative thermographic images of the BAT skin area and quantification. Data are mean ± SEM. * $p < 0.05$, ** $p < 0.01$, *** $p < 0.001$, **** $p < 0.0001$.

3. Discussion

The prevalence of obesity has increased due to westernized diets and sedentary lifestyles, and it is strongly related to other metabolic disorders [27]. It is well-established that an improvement of adipose tissue function could be a therapeutic target to trigger an amelioration in the development of these diseases [3,7,28,29]. However, there is a lack of therapeutic solutions to combat obesity. Recently, we described the combination of NAC, NR, LC, and betaine as a nutraceutical treatment that ameliorates NAFLD development [30]. However, the effect of this specific combination on other diseases has not been described. It has been shown how these individual metabolic cofactors could have an important effect on adipose tissue in obesity. Betaine has been reported to activate Akt, enhancing insulin sensitivity in adipose tissue [12]. Moreover, betaine can increase lipid oxidation and mitochondrial function in adipose tissue [15]. L-carnitine is essential to the correct transport of FFAs into the mitochondria for β-oxidation [14]. N-acetylcysteine has been linked to increased expression of thermogenic genes and improved glucose and insulin tolerance [10], and NR to improved insulin sensitivity through the regulation of sirtuin activity [11]. The present study investigated how the combination of these four metabolic cofactors could help to improve adipose tissue dysfunction, glucose tolerance, and insulin sensitivity in a diet-induced obese mouse model. It was found that MC-supplemented mice showed a reduction in body weight gain compared to the obese group. This result agrees with other studies in which betaine or L-carnitine supplementation decreased body weight [15,31,32]. A supplementation combining L-carnitine and NR also reduced body weight [21], and NAC also reduced body weight in different studies using mice with diet-induced obesity [33,34]. Interestingly, total and LDL cholesterol levels were reduced in MC-supplemented mice, confirming the effect of MC on lipid metabolism. These results of cholesterol levels correlate with the results found in different preclinical studies involving the ingredients used in the MC treatment [31,34].

The reduction of body weight due to MC supplementation was linked to amelioration in visceral adiposity, mimicking previous results in other preclinical studies [22,35,36]. Increased VAT can secrete adipokines and cytokines, leading to a pro-inflammatory state and causing IR and metabolic syndrome. Hence, a reduction of VAT can provide a significant benefit for the metabolism [37]. Indeed, indirect calorimetry confirmed that MC supplementation can increase oxidative metabolism and fat oxidation. These results correlate with the increased oxidative capacity observed in an obese model after betaine or NR supplementation [19,38]. Moreover, L-carnitine increased lipid oxidation in a clinical trial [39]. Thus, MC influences energy homeostasis and accounts for the reduction of adiposity in VAT depots. In contrast, the measurement of energy expenditure did not show the differences observed in RQ. These results are in concordance with other similar studies [40–42], which may indicate that the observed increase in fat oxidation after MC supplementation is probably more related to peroxisomal β-oxidation than to mitochondrial oxidation [43–45].

MC supplementation reduces the increase of visceral fat pads in obese mice by diminishing adipocyte size, with a decrease in the largest adipocytes and a tendency for the smallest adipocytes to increase, which correlates with the effect observed with L-carnitine supplementation in obese mice [46]. These results suggested an amelioration in adiposity, attributable to an increase in lipid oxidation. Similar results in terms of VAT were also reported using these ingredients separately in preclinical obese models [31,33,34]. In the case of NR, an NR precursor showed a reducing effect on adipocyte area in EWAT [47].

To look deeper into the molecular mechanisms regulated by MC supplementation in adipose tissue amelioration, genes related to main adipose functions were analyzed [5]. Adipose lipolysis occurs after hydrolysis of triglycerides to FFA and glycerol by the consecutive action of Atgl, Hsl, and Mgl; with the contribution of Plin1 in the Atgl activation [48]. Thus, MC supplementation showed a boosting effect on *Atgl* and *Plin1* expression, which may indicate an amelioration of adipose tissue function. Accordingly, individual betaine or L-carnitine treatments up-regulated *Atgl* expression in adipose tissue [49]. In addition, this increase in lipolysis could be related to the increment of fatty oxidation due to MC sup-

plementation, as observed in the *Acox1* expression results that correlate with those results obtained in the indirect calorimetry and for the reduction of fat mass. Moreover, similar effects were also observed in a diet-induced obese study with betaine supplementation [50].

Moreover, the reduction of BAT weight observed with MC supplementation was consistent with other studies in which the ingredients of MC were used separately [10,51,52]. In addition, BAT weight reduction through MC supplementation was linked to a reduction in the number and size of lipid droplets in BAT after MC supplementation. This reduction of large lipid droplets correlates with preceding studies of NAC or L-carnitine supplementation [10,51]. Moreover, mRNA expression analysis showed that genes related to lipolysis and fatty acid oxidation were also increased by MC supplementation, which can explain the increased oxidation of lipids in BAT and is coherent with previous studies using the ingredients of MC supplementation that managed to increase the expression of these genes in the adipose tissue, as described above [48–50]. Furthermore, increased thermogenesis by MC supplementation was verified through the significantly raised expression of certain thermogenic BAT genes, consistent with the capabilities of NR, L-carnitine, and NAC [34,51,52]. These results can be linked with increased BAT thermogenesis in MC-supplemented mice, which was previously reported in previous studies using one of the ingredients in the MC [10,51,52], and they confirm the improvement of BAT activity through MC supplementation.

IR is an important risk factor in the development of adipose tissue in obesity [53]. Fasting levels of glucose and insulin, HOMA-IR, GTT and ITT showed significant amelioration after MC supplementation. These results correlate with preclinical studies using HFD mice models treated separately with betaine, NAC, and NR, in which glucose and insulin tolerance were improved [10,50,54]. To understand the increased insulin sensitivity, gene expression analysis was performed for the main adipose glucose transporters [55,56]. *Glut1* expression levels did not show any significant difference between groups in EWAT or BAT. In contrast, *Glut4,* which is regulated by insulin, was up-regulated in the EWAT of the MC-supplemented group, but not in the BAT, which could indicate an increase in glucose uptake into visceral adipose tissue. That correlates with a previous study of L-carnitine supplementation in rats with a metabolic syndrome, where *Glut4* was up-regulated, and insulin sensitivity was improved [55]. Moreover, betaine was found to improve *Glut4* expression through increasing AMPK activation [57], and a precursor of NR improved adipose gene expression of *Glut4* through the same mechanism [58].

There were some limitations in this study. One of them was its design as a 4-week MC treatment on obese mice, as a corrective evaluation against obesity. However, a long-term study would have been of value to elucidate where obesity and lipid expression patterns can be reversed or modified more effectively. In addition, the possibility of shorter times or other doses should be evaluated to determine whether the effect is immediate or needs more time to be effective. However, we chose this study design because using this 4-week "corrective" evaluation we have seen good results in both mice and hamster studies [30,59,60]. Given the promising results obtained, it would be very interesting to carry out further studies to assess the potential of this combination of metabolic cofactors as a preventive treatment for obesity. Another potential limitation of the present study is that MC supplementation was applied only to obese animals. Therefore, further studies are needed to discern the effects of MC treatment on other metabolic disturbances, as well as to compare the impact of MC supplementation on obesity in lean animals.

To sum up, MC supplementation promotes the amelioration of adipose tissue dysfunction observed in the diet-induced obese mouse model. This study demonstrated the implication of the metabolic cofactors in the different pathways affected in the adipose tissue during metabolic dysfunction, involving a reduction of body weight and visceral adiposity, decreasing fat depots, improved BAT activity, and improved circulatory biomarkers of obesity, such as total cholesterol and LDL-cholesterol. Furthermore, the MC promoted lipid oxidation through the upregulation of genes related to lipolysis and fatty acid oxidation, in addition to the increased thermogenic gene expression in BAT. Finally, MC

supplementation displayed beneficial effects on insulin sensitivity, improving blood insulin and glucose levels and up-regulating *Glut4*. Altogether, this study suggests that MC supplementation ameliorates adipose tissue dysfunction acting in different pathways affected by obesity, and can be an effective treatment for reducing the incidence of obesity-related metabolic disorders.

4. Materials and Methods

4.1. Animal Model

Groups of 6-week-old male C57BL/6J mice (Envigo, Sant Feliu de Codines, Spain) were housed under controlled conditions of temperature (22 ± 2 °C) and humidity (55 ± 10%) and a 12-h light/dark cycle, with free access to food and water. Animals were fed with a high-fat diet (D12331, Research Diets, New Brunswick, NJ, USA) supplemented with 23.1 g/L fructose and 18.9 g/L sucrose in the drinking water. Mice were kept on these diets for 20 weeks in ad libitum conditions. All experimental protocols were approved by the Animal Ethics Committee of the Technological Unit of Nutrition and Health of Eurecat (Reus, Spain), and the Generalitat de Catalunya approved all the procedures (10281). The experimental protocol followed the "Principles of Laboratory Care" guidelines and was carried out following the European Communities Council Directive (2010/63/EEC). From the 16th to 20th week, obese mice were randomly distributed into two groups: 8 mice were kept under the same feed conditions described before (obese + vehicle group), and 8 mice were supplemented with a combination of metabolic cofactors (obese + MC group). The MC comprised a mix of the following compounds: 400 mg/kg of LC tartrate (Cambridge Commodities, Ely, UK), 400 mg/kg NAC (Cambridge Commodities, Ely, UK), 800 mg/kg betaine (Cambridge Commodities, Ely, UK), and 400 mg/kg NR (ChromaDex, Los Angeles, CA, USA). LC was administrated through LC tartrate (LCT) containing 68.2% LC, providing 560 mg/kg to reach the dose of 400 mg LC/kg. Betaine, LCT, NAC, and NR were diluted with drinking water. These specific doses were determined based on previous studies and a calculation of dose translation from human to animal [61]. Solutions were freshly prepared three times per week from stock powders and protected from light. Bodyweight and food intake data were recorded once a week during the entire study. In week 19, insulin and glucose tolerance tests (ITT and GTT respectively) were performed (see below). In the 20th week, animals were sacrificed, being deprived of food for 8 h before being euthanized. Blood was collected and serum was obtained by centrifugation and stored at −80 °C for further analysis. Brown adipose tissue (BAT) and white adipose tissue (WAT) depots (inguinal (IWAT), epididymal (EWAT), retroperitoneal (RWAT), and mesenteric (MWAT)) were immediately collected, weighed, and snap-frozen in liquid nitrogen to be kept at −80 °C for further determinations or fixed to perform histological analyses.

4.2. Serum and Blood Analysis

Serum fasting glucose, total cholesterol, and triglycerides (QCA, Barcelona, Spain) were analyzed by enzymatic colorimetric assays after sacrifice. Serum fasting insulinemia was analyzed using an insulin ELISA kit (Mercodia, Uppsala, Sweden), and serum HDL and LDL levels were analyzed using an EnzyChrom ™ AF HDL and LDL/VLDL assay kit (BioAssay System, Hayward, CA, USA). Lastly, LDL/HDL ratio was calculated. HOMA-IR (homeostatic model assessment for insulin resistance), which is an assessment that estimates insulin resistance in terms of beta-cell function and insulin sensitivity, was calculated from circulating levels of fasting glucose and insulin (glucose (mmol/L) × insulin (UI/L) × 22.5) [25].

For the GTT, during the third week of supplementation, mice fasted overnight and after fasted blood glucose levels, were measured, mice were injected i.p. with 1.5 g glucose/kg body weight (Merck KGaA, Darmstadt, Germany), and blood glucose levels were measured every 30, 60, 90, 120, 150, and 180 min, collecting blood from the mice's tails. For the ITT, during the fourth week of treatment, mice fasted for 6 h and baseline levels of blood glucose were measured using a standard glucometer (LifeScan, Milpitas, CA, USA). Animals were then injected (i.p. 0.375 mU/g of body weight) with human rapid insulin

(Actrapid® Innolet®, Novo Nordisk A/S, Bagsvaerd, Denmark), and blood glucose levels were measured as explained in the GTT test process above.

4.3. Indirect Calorimetry

Indirect calorimetry analyses were performed 2 weeks before all mice were sacrificed. An OxyletProTM system (PANLAB, Cornellà, Spain) was employed to perform calorimetry. Mice were left in acrylic boxes with free access to their diet and vehicle or treatment. After an acclimation period of 3 h, oxygen consumption (VO_2) and carbon dioxide production (VCO_2) were measured every 9 min by an O_2 and CO_2 analyzer at a constant flow rate of 600 mL/min. The respiratory quotient (RQ) as the VCO_2/VO_2 ratio was calculated by Metabolism 2.1.02 software (PANLAB, Cornellà, Spain). The fat rate was calculated using the VCO_2 and the VO_2 measures and applying the Frayn stoichiometric equations, which define fat oxidation rates as $1.67 \times VO_2 - 1.67 \times VCO_2 - 1.92$ n (g/min) [62]. A nitrogen excretion rate (n) of 135 μg kg^{-1} min^{-1} was assumed. Finally, fat oxidation level was obtained using the Atwater general conversion factor. The fat rate was multiplied by 37 [63]. Total energy expenditure (EE), oxygen consumption (VO_2), and carbon dioxide production (VCO_2) were also calculated using the Metabolism 2.1.02 software (PANLAB, Cornellà, Spain).

4.4. Histological Analysis

EWAT and BAT portions fixed in buffered formalin (4% formaldehyde, 4 gr/L NaH_2PO_4, 6.5 gr/L Na_2HPO_4; pH 6.8) were cut at a thickness of 5 μm and stained with hematoxylin & eosin (H & E). BAT and EWAT images (magnification 40×) were taken with a microscope (ECLIPSE Ti; Nikon, Tokyo, Japan) coupled to a digital sight camera (DS-Ri1, Nikon), and analyzed using ImageJ NDPI software (National Institutes of Health, Bethesda, MD, USA; https://imagej.nih.gov/ij, accessed on 25 July 2022, version 1.52a). To avoid any bias in the analysis, the study had a double-blind design, preventing the reviewers from viewing any data from the mice during the histopathological analysis. Area quantification of adipocytes was analyzed using the Adiposoft plugin to assess the state of EWAT between groups. Lipid droplet quantification in BAT was analyzed using the Droplet Finder plugin.

4.5. mRNA Extraction and Quantitative Polymerase Chain Reaction

According to the manufacturer's instructions, homogenates from EWATs and BATs were used for total mRNA extractions with TriPure reagent (Roche Diagnostic, Sant Cugat del Vallès, Barcelona, Spain). mRNA concentration and purity were determined using a nanophotometer (Implen GmbH, München, Germany). RNA was converted to cDNA using the high-capacity RNA-to-cDNA Kit (Applied Biosystems, Wilmington, DE, USA). The cDNAs were diluted 1:10 before incubation with commercial LightCycler 480 Sybr green I master on a Lightcycler® 480 II (Roche Diagnostics GmbH, Manheim, Germany). The relative gene expression levels were calculated using the $2^{-\Delta\Delta Ct}$ method [64]. Table 1 shows a list of primers used that were previously described in other studies and verified with Primer-Blast software (National Center for Biotechnology Information, Bethesda, MD, USA). *36b4* was used as a housekeeping gene [30].

Table 1. Sequences of the oligonucleotides used in the RT-PCR.

Primers	Forward	Reverse	Reference
Acc1	GATGAACCATCTCCGTTGGC	CCCAATTATGAATCGGGAGTGC	[65]
Acox1	CTATGGGATCAGCCAGAAAG	AGTCAAAGGCATCCACCAAAG	[66]
Atgl	CAACGCCACTCACATCTACGG	GGACACCTCAATAATGTTGGCAC	[67]
Cpt1α	CTCAGTGGGAGCGACTCTTCA	GGCCTCTGTGGTACACGACAA	[68]
Cpt1b	CGAGGATTCTCTGGAACTGC	GGCCTCTGTGGTACACGACAA	[69]
Dio2	AGAGTGGAGGCGCATGCT	GGCATCTAGGAGGAAGCTGTTC	[70]
Fasn	GCTGCGGAAACTTCAGGAAAT	AGAGACGTGTCACTCCTGGACTT	[71]
Glut1	TCAACACGGCCTTCACTG	CACGATGCTCAGATAGGACATC	[72]
Glut4	AAAAGTGCCTGAAACCAGAG	TCACCTCCTGCTCTAAAAGG	[73]
Hsl	TCCTGGAACTAAGTGGACGCAAG	CAGACACACTCCTGCGCATAGAC	[74]
Mgl	CGGAACAAGTCGGAGGTTGA	TGTCCTGACTCCGGGATGAT	[67]
Pgc1a	AGCCGTGACCACTGACAACGAG	GCTGCATGGTTCTGAGTGCTAAG	[75]
Plin1	GTCAATGAACAAGGGCCCAAC	CACAGGCAGCTGCAGAACTCTC	[74]
Pparα	CCCTGTTTGTGGCTGCTATAATTT	GGGAAGAGGAAGGTGTCATCTG	[76]
Prdm16	CAGCACGGTGAAGCCATTC	GCGTGCATCCGCTTGTG	[77]
Scd1	AGATCTCCAGTTCTTACACGACCAC	GACGGATGTCTTCTTCCAGGTG	[65]
Ucp1	ACTGCCACACCTCCAGTCATT	CTTTGCCTCACTCAGGATTGG	[78]
36b4	AGTCCCTGCCCTTTGTACACA	CGATCCGAGGGCCTCACTA	[30]

4.6. BAT Temperature Measurements

The temperature surrounding the BAT was visualized using a high-resolution infrared camera (FLIR Systems) and analyzed with a dedicated software package (FLIR-Tools-Software, FLIR; Kent, UK), as previously described [79]. For each image, the area surrounding the BAT was delimited and the average temperature of the skin area was calculated as the average of 3 pictures for each animal.

4.7. Statistical Analysis

Statistical analyses were performed using GraphPad Prism 9 software (Graph-Pad Software, La Jolla, CA, USA). Data are presented as mean ± SEM. Data distribution was analyzed by the Shapiro–Wilk normality test. Differences between the two groups were determined using an unpaired *t*-test (two-tailed, 95% confidence interval). A *p*-value below 0.05 was considered statistically significant.

Supplementary Materials: The following supporting information can be downloaded at: https://www.mdpi.com/article/10.3390/ijms232314923/s1.

Author Contributions: S.Q.-V., G.A., L.H., J.M.D.B., A.C. and X.E. contributed to the study conception and design. S.Q.-V., M.C.-P., A.A. and X.E. conducted the study. S.Q.-V., A.A. and X.E. acquired and analyzed the data. All authors have read and agreed to the published version of the manuscript.

Funding: This work was financially supported by the Catalan Government through the funding grant ACCIÓ-Eurecat (Project PRIV2020-EURHEPAD to X.E.), by the Centre for the Development of Industrial Technology (CDTI) of the Spanish Ministry of Science and Innovation under a grant agreement: TECNOMIFOOD project CER-20191010 (to A.C.). S.Q.-V. is supported by a fellowship from the Vicente Lopez Program (Eurecat) and M.C.-P. is supported by a fellowship 2021 FI_B2 00150.

Institutional Review Board Statement: All experimental protocols were approved by the Animal Ethics Committee of the Technological Unit of Nutrition and Health of Eurecat (Reus, Spain), and the Generalitat de Catalunya approved all the procedures (10281). The experimental protocol followed the "Principles of Laboratory Care" guidelines and was carried out in accordance with the European Communities Council Directive (2010/63/EEC).

Informed Consent Statement: Not applicable.

Acknowledgments: We thank J.M. Alcaide; Y. Tobajas; I. Triguero; G. Chomiciute; J. Romero and C. Egea for their valuable technical support. We thank Cambridge Commodities and ChromaDex for providing the ingredients of the multi-ingredient.

Conflicts of Interest: The authors declare no conflict of interest.

References

1. WHO. New WHO Report: Deaths from Noncommunicable Diseases on the Rise, with Developing World Hit Hardest. *Cent. Eur. J. Public Health* **2011**, *19*, 114–120.
2. Duval, C.; Thissen, U.; Keshtkar, S.; Accart, B.; Stienstra, R.; Boekschoten, M.V.; Roskams, T.; Kersten, S.; Müller, M. Adipose Tissue Dysfunction Signals Progression of Hepatic Steatosis towards Nonalcoholic Steatohepatitis in C57Bl/6 Mice. *Diabetes* **2010**, *59*, 3181–3191. [CrossRef] [PubMed]
3. Mohamed, S. Functional Foods against Metabolic Syndrome (Obesity, Diabetes, Hypertension and Dyslipidemia) and Cardiovascular Disease. *Trends Food Sci. Technol.* **2014**, *35*, 114–128. [CrossRef]
4. Petta, S.; Amato, M.C.; di Marco, V.; Cammà, C.; Pizzolanti, G.; Barcellona, M.R.; Cabibi, D.; Galluzzo, A.; Sinagra, D.; Giordano, C.; et al. Visceral Adiposity Index Is Associated with Significant Fibrosis in Patients with Non-Alcoholic Fatty Liver Disease. *Aliment. Pharmacol. Ther.* **2012**, *35*, 238–247. [CrossRef]
5. Azzu, V.; Vacca, M.; Virtue, S.; Allison, M.; Vidal-Puig, A. Adipose Tissue-Liver Cross Talk in the Control of Whole-Body Metabolism: Implications in Nonalcoholic Fatty Liver Disease. *Gastroenterology* **2020**, *158*, 1899–1912. [CrossRef]
6. Rinella, M.E. Nonalcoholic Fatty Liver Disease a Systematic Review. *JAMA J. Am. Med. Assoc.* **2015**, *313*, 2263–2273. [CrossRef]
7. Basak Engin, A.; Atilla, E. (Eds.) *Obesity and Lipotoxicity*; Springer: Cham, Switzerland, 2017; Volume 960.
8. Mardinoglu, A.; Bjornson, E.; Zhang, C.; Klevstig, M.; Söderlund, S.; Ståhlman, M.; Adiels, M.; Hakkarainen, A.; Lundbom, N.; Kilicarslan, M.; et al. Personal Model-Assisted Identification of NAD + and Glutathione Metabolism as Intervention Target in NAFLD. *Mol. Syst. Biol.* **2017**, *13*, 916. [CrossRef]
9. Shi, W.; Hegeman, M.A.; Doncheva, A.; Bekkenkamp-Grovenstein, M.; de Boer, V.C.J.; Keijer, J. High Dose of Dietary Nicotinamide Riboside Induces Glucose Intolerance and White Adipose Tissue Dysfunction in Mice Fed a Mildly Obesogenic Diet. *Nutrients* **2019**, *11*, 2439. [CrossRef]
10. Charron, M.J.; Williams, L.; Seki, Y.; Du, X.Q.; Chaurasia, B.; Saghatelian, A.; Summers, S.A.; Katz, E.B.; Vuguin, P.M.; Reznik, S.E. Antioxidant Effects of N-Acetylcysteine Prevent Programmed Metabolic Disease in Mice. *Diabetes* **2020**, *69*, 1650–1661. [CrossRef]
11. Shi, W.; Hegeman, M.A.; van Dartel, D.A.M.; Tang, J.; Suarez, M.; Swarts, H.; van der Hee, B.; Arola, L.; Keijer, J. Effects of a Wide Range of Dietary Nicotinamide Riboside (NR) Concentrations on Metabolic Flexibility and White Adipose Tissue (WAT) of Mice Fed a Mildly Obesogenic Diet. *Mol. Nutr. Food Res.* **2017**, *61*, 1600878. [CrossRef]
12. Wang, Z.; Yao, T.; Pini, M.; Zhou, Z.; Fantuzzi, G.; Song, Z.; Betaine, S.Z. Betaine Improved Adipose Tissue Function in Mice Fed a High-Fat Diet: A Mechanism for Hepatoprotective Effect of Betaine in Nonalcoholic Fatty Liver Disease. *Am. J. Physiol. Gastrointest. Liver Physiol.* **2010**, *298*, 634–642. [CrossRef] [PubMed]
13. Ranjbar Kohan, N.; Tabandeh, M.R.; Nazifi, S.; Soleimani, Z. L-Carnitine Improves Metabolic Disorders and Regulates Apelin and Apelin Receptor Genes Expression in Adipose Tissue in Diabetic Rats. *Physiol. Rep.* **2020**, *8*, e14641. [CrossRef] [PubMed]
14. Malaguarnera, M.; Gargante, M.P.; Russo, C.; Antic, T.; Vacante, M.; Malaguarnera, M.; Avitabile, T.; Li Volti, G.; Galvano, F. L-Carnitine Supplementation to Diet: A New Tool in Treatment of Nonalcoholic Steatohepatitisa Randomized and Controlled Clinical Trial. *Am. J. Gastroenterol.* **2010**, *105*, 1338–1345. [CrossRef] [PubMed]
15. Zhou, X.; Chen, J.; Chen, J.; Wu, W.; Wang, X.; Wang, Y. The Beneficial Effects of Betaine on Dysfunctional Adipose Tissue and N6-Methyladenosine MRNA Methylation Requires the AMP-Activated Protein Kinase A1 Subunit. *J. Nutr. Biochem.* **2015**, *26*, 1678–1684. [CrossRef] [PubMed]
16. Suárez, M.; Boqué, N.; del Bas, J.M.; Mayneris-Perxachs, J.; Arola, L.; Caimari, A. Mediterranean Diet and Multi-Ingredient-Based Interventions for the Management of Non-Alcoholic Fatty Liver Disease. *Nutrients* **2017**, *9*, 1052. [CrossRef] [PubMed]
17. Khodayar, M.J.; Kalantari, H.; Khorsandi, L.; Rashno, M.; Zeidooni, L. Betaine Protects Mice against Acetaminophen Hepatotoxicity Possibly via Mitochondrial Complex II and Glutathione Availability. *Biomed. Pharmacother.* **2018**, *103*, 1436–1445. [CrossRef]
18. Xia, Y.; Li, Q.; Zhong, W.; Dong, J.; Wang, Z.; Wang, C. L-Carnitine Ameliorated Fatty Liver in High-Calorie Diet/STZ-Induced Type 2 Diabetic Mice by Improving Mitochondrial Function. *Diabetol. Metab. Syndr.* **2011**, *3*, 31. [CrossRef]
19. Cantó, C.; Houtkooper, R.H.; Pirinen, E.; Youn, D.Y.; Oosterveer, M.H.; Cen, Y.; Fernandez-Marcos, P.J.; Yamamoto, H.; Andreux, P.A.; Cettour-Rose, P.; et al. The NAD+ Precursor Nicotinamide Riboside Enhances Oxidative Metabolism and Protects against High-Fat Diet-Induced Obesity. *Cell Metab.* **2012**, *15*, 838–847. [CrossRef]
20. Dou, X.; Xia, Y.; Chen, J.; Qian, Y.; Li, S.; Zhang, X.; Song, Z. Rectification of Impaired Adipose Tissue Methylation Status and Lipolytic Response Contributes to Hepatoprotective Effect of Betaine in a Mouse Model of Alcoholic Liver Disease. *Br. J. Pharmacol.* **2014**, *171*, 4073–4086. [CrossRef]
21. Salic, K.; Gart, E.; Seidel, F.; Verschuren, L.; Caspers, M.; van Duyvenvoorde, W.; Wong, K.E.; Keijer, J.; Bobeldijk-Pastorova, I.; Wielinga, P.Y.; et al. Combined Treatment with L-Carnitine and Nicotinamide Riboside Improves Hepatic Metabolism and Attenuates Obesity and Liver Steatosis. *Int. J. Mol. Sci.* **2019**, *20*, 84359. [CrossRef]

22. Marin, V.; Rosso, N.; Dal Ben, M.; Raseni, A.; Boschelle, M.; Degrassi, C.; Nemeckova, I.; Nachtigal, P.; Avellini, C.; Tiribelli, C.; et al. An Animal Model for the Juvenile Non-Alcoholic Fatty Liver Disease and Non-Alcoholic Steatohepatitis. *PLoS ONE* **2016**, *11*, e0158817. [CrossRef] [PubMed]
23. Sanches, S.C.L.; Ramalho, L.N.Z.; Augusto, M.J.; da Silva, D.M.; Ramalho, F.S. Nonalcoholic Steatohepatitis: A Search for Factual Animal Models. *BioMed Res. Int.* **2015**, *2015*, 574832. [CrossRef] [PubMed]
24. Moreno-Indias, I.; Tinahones, F.J. Impaired Adipose Tissue Expandability and Lipogenic Capacities as Ones of the Main Causes of Metabolic Disorders. *J. Diabetes Res.* **2015**, *2015*, 970375. [CrossRef] [PubMed]
25. Houjeghani, S.; Kheirouri, S.; Faraji, E.; Jafarabadi, M.A. L-Carnosine Supplementation Attenuated Fasting Glucose, Triglycerides, Advanced Glycation End Products, and Tumor Necrosis Factor–α Levels in Patients with Type 2 Diabetes: A Double-Blind Placebo-Controlled Randomized Clinical Trial. *Nutr. Res.* **2018**, *49*, 96–106. [CrossRef] [PubMed]
26. Townsend, K.L.; Tseng, Y.H. Brown Fat Fuel Utilization and Thermogenesis. *Trends Endocrinol. Metab.* **2014**, *25*, 168–177. [CrossRef]
27. Yu, J.; Shen, J.; Sun, T.T.; Zhang, X.; Wong, N. Obesity, Insulin Resistance, NASH and Hepatocellular Carcinoma. *Semin. Cancer Biol.* **2013**, *23*, 483–491. [CrossRef]
28. Friedman, S.L.; Neuschwander-Tetri, B.A.; Rinella, M.; Sanyal, A.J. Mechanisms of NAFLD Development and Therapeutic Strategies. *Nat. Med.* **2018**, *24*, 908–922. [CrossRef]
29. Huang, X.; Liu, G.; Guo, J.; Su, Z. The PI3K/AKT Pathway in Obesity and Type 2 Diabetes. *Int. J. Biol. Sci.* **2018**, *14*, 1483–1496. [CrossRef]
30. Quesada-Vázquez, S.; Colom-Pellicer, M.; Navarro-Masip, È.; Aragonès, G.; del Bas, J.M.; Caimari, A.; Escoté, X. Supplementation with a Specific Combination of Metabolic Cofactors Ameliorates Non-Alcoholic Fatty Liver Disease and, Hepatic Fibrosis, and Insulin Resistance in Mice. *Nutrients* **2021**, *13*, 3532. [CrossRef]
31. Jang, A.; Kim, D.; Sung, K.S.; Jung, S.; Kim, H.J.; Jo, C. The Effect of Dietary α-Lipoic Acid, Betaine, l-Carnitine, and Swimming on the Obesity of Mice Induced by a High-Fat Diet. *Food Funct.* **2014**, *5*, 1966–1974. [CrossRef]
32. Mun, E.G.; Soh, J.R.; Cha, Y.S. L-Carnitine Reduces Obesity Caused by High-Fat Diet in C57BL_6J Mice. *Food Sci. Biotechnol.* **2007**, *16*, 228–233.
33. Shen, F.C.; Weng, S.W.; Tsao, C.F.; Lin, H.Y.; Chang, C.S.; Lin, C.Y.; Lian, W.S.; Chuang, J.H.; Lin, T.K.; Liou, C.W.; et al. Early Intervention of N-Acetylcysteine Better Improves Insulin Resistance in Diet-Induced Obesity Mice. *Free Radic. Res.* **2018**, *52*, 1296–1310. [CrossRef] [PubMed]
34. Ma, Y.; Gao, M.; Liu, D. N-Acetylcysteine Protects Mice from High Fat Diet-Induced Metabolic Disorders. *Pharm. Res.* **2016**, *33*, 2033–2042. [CrossRef] [PubMed]
35. Zhuhua, Z.; Zhiquan, W.; Zhen, Y.; Yixin, N.; Weiwei, Z.; Xiaoyong, L.; Yueming, L.; Hongmei, Z.; Li, Q.; Qing, S. A Novel Mice Model of Metabolic Syndrome: The High-Fat-High-Fructose Diet-Fed ICR Mice. *Exp. Anim.* **2015**, *64*, 435–442. [CrossRef]
36. Luo, Y. The Role of Sugar-Sweetened Water in the Progression of Nonalcoholic Fatty Liver Disease. Ph.D. Thesis, Auburn University, Auburn, AL, USA, 2016.
37. Donohoe, C.L.; Doyle, S.L.; Reynolds, J.V. Visceral Adiposity, Insulin Resistance and Cancer Risk. *Diabetol. Metab. Syndr.* **2011**, *3*, 12. [CrossRef] [PubMed]
38. Ejaz, A.; Martinez-Guino, L.; Goldfine, A.B.; Ribas-Aulinas, F.; de Nigris, V.; Ribó, S.; Gonzalez-Franquesa, A.; Garcia-Roves, P.M.; Li, E.; Dreyfuss, J.M.; et al. Dietary Betaine Supplementation Increases Fgf21 Levels to Improve Glucose Homeostasis and Reduce Hepatic Lipid Accumulation in Mice. *Diabetes* **2016**, *65*, 902–912. [CrossRef]
39. Bruls, Y.M.; de Ligt, M.; Lindeboom, L.; Phielix, E.; Havekes, B.; Schaart, G.; Kornips, E.; Wildberger, J.E.; Hesselink, M.K.; Muoio, D.; et al. Carnitine Supplementation Improves Metabolic Flexibility and Skeletal Muscle Acetylcarnitine Formation in Volunteers with Impaired Glucose Tolerance: A Randomised Controlled Trial. *EBioMedicine* **2019**, *49*, 318–330. [CrossRef]
40. Klaus, S.; Pültz, S.; Thöne-Reineke, C.; Wolfram, S. Epigallocatechin Gallate Attenuates Diet-Induced Obesity in Mice by Decreasing Energy Absorption and Increasing Fat Oxidation. *Int. J. Obes.* **2005**, *29*, 615–623. [CrossRef]
41. Singh, A.; Zapata, R.C.; Pezeshki, A.; Chelikani, P.K. Dietary Lactalbumin and Lactoferrin Interact with Inulin to Modulate Energy Balance in Obese Rats. *Obesity* **2017**, *25*, 1050–1060. [CrossRef]
42. Crescenti, A.; del Bas, J.M.; Arola-Arnal, A.; Oms-Oliu, G.; Arola, L.; Caimari, A. Grape Seed Procyanidins Administered at Physiological Doses to Rats during Pregnancy and Lactation Promote Lipid Oxidation and Up-Regulate AMPK in the Muscle of Male Offspring in Adulthood. *J. Nutr. Biochem.* **2015**, *26*, 912–920. [CrossRef]
43. Wanders, R.J.A.; Vreken, P.; Ferdinandusse, S.; Jansen, G.A.; Waterham, H.R.; van Roermund, C.W.T.; van Grunsven, E.G. Peroxisomal Fatty Acid α- and β-Oxidation in Humans: Enzymology, Peroxisomal Metabolite Transporters and Peroxisomal Diseases. *Biochem. Soc. Trans.* **2001**, *29*, 250. [CrossRef] [PubMed]
44. Fiamoncini, J.; Turner, N.; Hirabara, S.M.; Salgado, T.M.L.; Marçal, A.C.; Leslie, S.; da Silva, S.M.A.; Deschamps, F.C.; Luz, J.; Cooney, G.J.; et al. Enhanced Peroxisomal β-Oxidation Is Associated with Prevention of Obesity and Glucose Intolerance by Fish Oil-Enriched Diets. *Obesity* **2013**, *21*, 1200–1207. [CrossRef] [PubMed]
45. Wanders, R.J.A.; Waterham, H.R. Biochemistry of Mammalian Peroxisomes Revisited. *Annu. Rev. Biochem.* **2006**, *75*, 295–332. [CrossRef] [PubMed]

46. Zhu, K.; Tan, F.; Mu, J.; Yi, R.; Zhou, X.; Zhao, X. Anti-Obesity Effects of Lactobacillus Fermentum CQPC05 Isolated from Sichuan Pickle in High-Fat Diet-Induced Obese Mice through PPAR-α Signaling Pathway. *Microorganisms* **2019**, *7*, 194. [CrossRef] [PubMed]
47. Méndez-Lara, K.A.; Rodríguez-Millán, E.; Sebastián, D.; Blanco-Soto, R.; Camacho, M.; Nan, M.N.; Diarte-Añazco, E.M.G.; Mato, E.; Lope-Piedrafita, S.; Roglans, N.; et al. Nicotinamide Protects Against Diet-Induced Body Weight Gain, Increases Energy Expenditure, and Induces White Adipose Tissue Beiging. *Mol. Nutr. Food Res.* **2021**, *65*, 2100111. [CrossRef] [PubMed]
48. Morigny, P.; Houssier, M.; Mouisel, E.; Langin, D. Adipocyte Lipolysis and Insulin Resistance. *Biochimie* **2016**, *125*, 259–266. [CrossRef]
49. Gao, X.; Sun, G.; Randell, E.; Tian, Y.; Zhou, H. Systematic Investigation of the Relationships between Trimethylamine N-Oxide and L-Carnitine with Obesity in Both and Rodents. *Food Funct.* **2020**, *11*, 7707–7716. [CrossRef]
50. Du, J.; Shen, L.; Tan, Z.; Zhang, P.; Zhao, X.; Xu, Y.; Gan, M.; Yang, Q.; Ma, J.; Jiang, A.; et al. Betaine Supplementation Enhances Lipid Metabolism and Improves Insulin Resistance in Mice Fed a High-Fat Diet. *Nutrients* **2018**, *10*, 131. [CrossRef]
51. Ozaki, K.; Sano, T.; Tsuji, N.; Matsuura, T.; Narama, I. Carnitine Is Necessary to Maintain the Phenotype and Function of Brown Adipose Tissue. *Lab. Investig.* **2011**, *91*, 704–710. [CrossRef]
52. Crisol, B.M.; Veiga, C.B.; Lenhare, L.; Braga, R.R.; Silva, V.R.R.; da Silva, A.S.R.; Cintra, D.E.; Moura, L.P.; Pauli, J.R.; Ropelle, E.R. Nicotinamide Riboside Induces a Thermogenic Response in Lean Mice. *Life Sci.* **2018**, *211*, 1–7. [CrossRef]
53. Huang, B.-W.; Chiang, M.-T.; Yao, H.-T.; Chiang, W. The Effect of High-Fat and High-Fructose Diets on Glucose Tolerance and Plasma Lipid and Leptin Levels in Rats. *Diabetes Obes. Metab.* **2004**, *6*, 120–126. [CrossRef] [PubMed]
54. Williams, A.S.; Koves, T.R.; Pettway, Y.D.; Draper, J.A.; Slentz, D.H.; Grimsrud, P.A.; Ilkayeva, O.R.; Muoio, D.M. Nicotinamide Riboside Supplementation Confers Marginal Metabolic Benefits in Obese Mice without Remodeling the Muscle Acetyl-Proteome. *iScience* **2022**, *25*, 103635. [CrossRef] [PubMed]
55. Zayed, E.A.; AinShoka, A.A.; el Shazly, K.A.; Abd El Latif, H.A. Improvement of Insulin Resistance via Increase of GLUT4 and PPARγ in Metabolic Syndrome-Induced Rats Treated with Omega-3 Fatty Acid or l-Carnitine. *J. Biochem. Mol. Toxicol.* **2018**, *32*, e22218. [CrossRef] [PubMed]
56. Koivisto, U.M.; Martinez-Valdez, H.; Bilan, P.J.; Burdett, E.; Ramlal, T.; Klip, A. GLUT-1 and GLUT-4 in Muscle Cells. *J. Biol. Chem.* **1991**, *266*, 2615–2621. [CrossRef]
57. Zhao, G.; He, F.; Wu, C.; Li, P.; Li, N.; Deng, J.; Zhu, G.; Ren, W.; Peng, Y. Betaine in Inflammation: Mechanistic Aspects and Applications. *Front. Immunol.* **2018**, *9*, 1070. [CrossRef]
58. Nejabati, H.R.; Samadi, N.; Shahnazi, V.; Mihanfar, A.; Fattahi, A.; Latifi, Z.; Bahrami-asl, Z.; Roshangar, L.; Nouri, M. Nicotinamide and Its Metabolite N1-Methylnicotinamide Alleviate Endocrine and Metabolic Abnormalities in Adipose and Ovarian Tissues in Rat Model of Polycystic Ovary Syndrome. *Chem. Biol. Interact.* **2020**, *324*, 109093. [CrossRef]
59. Quesada-Vázquez, S.; Bone, C.; Saha, S.; Triguero, I.; Colom-Pellicer, M.; Aragonès, G.; Hildebrand, F.; del Bas, J.M.; Caimari, A.; Beraza, N.; et al. Microbiota Dysbiosis and Gut Barrier Dysfunction Associated with Non-Alcoholic Fatty Liver Disease Are Modulated by a Specific Metabolic Cofactors' Combination. *Int. J. Mol. Sci.* **2022**, *23*, 13675. [CrossRef]
60. Yang, H.; Mayneris-Perxachs, J.; Boqué, N.; del Bas, J.M.; Arola, L.; Yuan, M.; Türkez, H.; Uhlén, M.; Borén, J.; Zhang, C.; et al. Combined Metabolic Activators Decrease Liver Steatosis by Activating Mitochondrial Metabolism in Hamsters Fed with a High-Fat Diet. *Biomedicines* **2021**, *9*, 1440. [CrossRef]
61. Reagan-Shaw, S.; Nihal, M.; Ahmad, N. Dose Translation from Animal to Human Studies Revisited. *FASEB J.* **2008**, *22*, 659–661. [CrossRef]
62. Carraro, F.; Stuart, C.A.; Hartl, W.H.; Rosenblatt, J.; Wolfe, R.R.; Robert Wolfee, A.R. Effect of Exercise and Recovery on Muscle Protein Synthesis in Human Subjects. *Am. J. Physiol.-Endocrinol. Metab.* **1990**, *259*, E470–E476. [CrossRef]
63. Bircher, S.; Knechtle, B. Relationship between Fat Oxidation and Lactate Threshold in Athletes and Obese Women and Men. *J. Sports Sci. Med.* **2004**, *3*, 174–181. [PubMed]
64. Livak, K.J.; Schmittgen, T.D. Analysis of Relative Gene Expression Data Using Real-Time Quantitative PCR and the 2−ΔΔCT Method. *Methods* **2001**, *25*, 402–408. [CrossRef] [PubMed]
65. Zhang, M.; Sun, W.; Qian, J.; Tang, Y. Fasting Exacerbates Hepatic Growth Differentiation Factor 15 to Promote Fatty Acid β-Oxidation and Ketogenesis via Activating XBP1 Signaling in Liver. *Redox Biol.* **2018**, *16*, 87–96. [CrossRef] [PubMed]
66. Geurts, L.; Everard, A.; van Hul, M.; Essaghir, A.; Duparc, T.; Matamoros, S.; Plovier, H.; Castel, J.; Denis, R.G.P.; Bergiers, M.; et al. Adipose Tissue NAPE-PLD Controls Fat Mass Development by Altering the Browning Process and Gut Microbiota. *Nat. Commun.* **2015**, *6*, 6495. [CrossRef] [PubMed]
67. Wang, X.; Xu, M.; Peng, Y.; Naren, Q.; Xu, Y.; Wang, X.; Yang, G.; Shi, X.; Li, X. Triptolide Enhances Lipolysis of Adipocytes by Enhancing ATGL Transcription via Upregulation of P53. *Phytother. Res.* **2020**, *34*, 3298–3310. [CrossRef]
68. Kimura, R.; Takahashi, N.; Lin, S.; Goto, T.; Murota, K.; Nakata, R.; Inoue, H.; Kawada, T. DHA Attenuates Postprandial Hyperlipidemia via Activating PPARα in Intestinal Epithelial Cells. *J. Lipid Res.* **2013**, *54*, 3258–3268. [CrossRef]
69. Ma, Y.; Gao, M.; Sun, H.; Liu, D. Interleukin-6 Gene Transfer Reverses Body Weight Gain and Fatty Liver in Obese Mice. *Biochim. Biophys. Acta Mol. Basis Dis.* **2015**, *1852*, 1001–1011. [CrossRef]
70. Li, Y.; Wong, K.; Giles, A.; Jiang, J.; Lee, J.W.; Adams, A.C.; Kharitonenkov, A.; Yang, Q.; Gao, B.; Guarente, L.; et al. Hepatic SIRT1 Attenuates Hepatic Steatosis and Controls Energy Balance in Mice by Inducing Fibroblast Growth Factor 21. *Gastroenterology* **2014**, *146*, 539–549.e7. [CrossRef]

71. Zhou, J.; Febbraio, M.; Wada, T.; Zhai, Y.; Kuruba, R.; He, J.; Lee, J.H.; Khadem, S.; Ren, S.; Li, S.; et al. Hepatic Fatty Acid Transporter Cd36 Is a Common Target of LXR, PXR, and PPARγ in Promoting Steatosis. *Gastroenterology* **2008**, *134*, 556–567. [CrossRef]
72. Vinaik, R.; Barayan, D.; Auger, C.; Abdullahi, A.; Jeschke, M.G. Regulation of Glycolysis and the Warburg Effect in Wound Healing. *JCI Insight* **2020**, *5*, e138949. [CrossRef]
73. Atkinson, B.J.; Griesel, B.A.; King, C.D.; Josey, M.A.; Olson, A.L. Moderate Glut4 Overexpression Improves Insulin Sensitivity and Fasting Triglyceridemia in High-Fat Diet-Fed Transgenic Mice. *Diabetes* **2013**, *62*, 2249–2258. [CrossRef] [PubMed]
74. Liu, H.; Liu, M.; Jin, Z.; Yaqoob, S.; Zheng, M.; Cai, D.; Liu, J.; Guo, S. Ginsenoside Rg2 Inhibits Adipogenesis in 3T3-L1 Preadipocytes and Suppresses Obesity in High-Fat-Diet-Induced Obese Mice through the AMPK Pathway. *Food Funct.* **2019**, *10*, 3603–3614. [CrossRef] [PubMed]
75. Whitehead, N.; Gill, J.F.; Brink, M.; Handschin, C. Moderate Modulation of Cardiac PGC-1α Expression Partially Affects Age-Associated Transcriptional Remodeling of the Heart. *Front. Physiol.* **2018**, *9*, 242. [CrossRef] [PubMed]
76. Montagner, A.; Polizzi, A.; Fouché, E.; Ducheix, S.; Lippi, Y.; Lasserre, F.; Barquissau, V.; Régnier, M.; Lukowicz, C.; Benhamed, F.; et al. Liver PPARα Is Crucial for Whole-Body Fatty Acid Homeostasis and Is Protective against NAFLD. *Gut* **2016**, *65*, 1202–1214. [CrossRef]
77. Shen, Y.; Zhou, H.; Jin, W.; Lee, H.J. Acute Exercise Regulates Adipogenic Gene Expression in White Adipose Tissue. *Biol. Sport* **2016**, *33*, 381–391. [CrossRef]
78. Choi, H.; Kim, C.S.; Yu, R. Quercetin Upregulates Uncoupling Protein 1 in White/Brown Adipose Tissues through Sympathetic Stimulation. *J. Obes. Metab. Syndr.* **2018**, *27*, 102–109. [CrossRef]
79. Martínez-Sánchez, N.; Seoane-Collazo, P.; Contreras, C.; Varela, L.; Villarroya, J.; Rial-Pensado, E.; Buqué, X.; Aurrekoetxea, I.; Delgado, T.C.; Vázquez-Martínez, R.; et al. Hypothalamic AMPK-ER Stress-JNK1 Axis Mediates the Central Actions of Thyroid Hormones on Energy Balance. *Cell Metab.* **2017**, *26*, 212–229.e12. [CrossRef]

Supp Figure S1

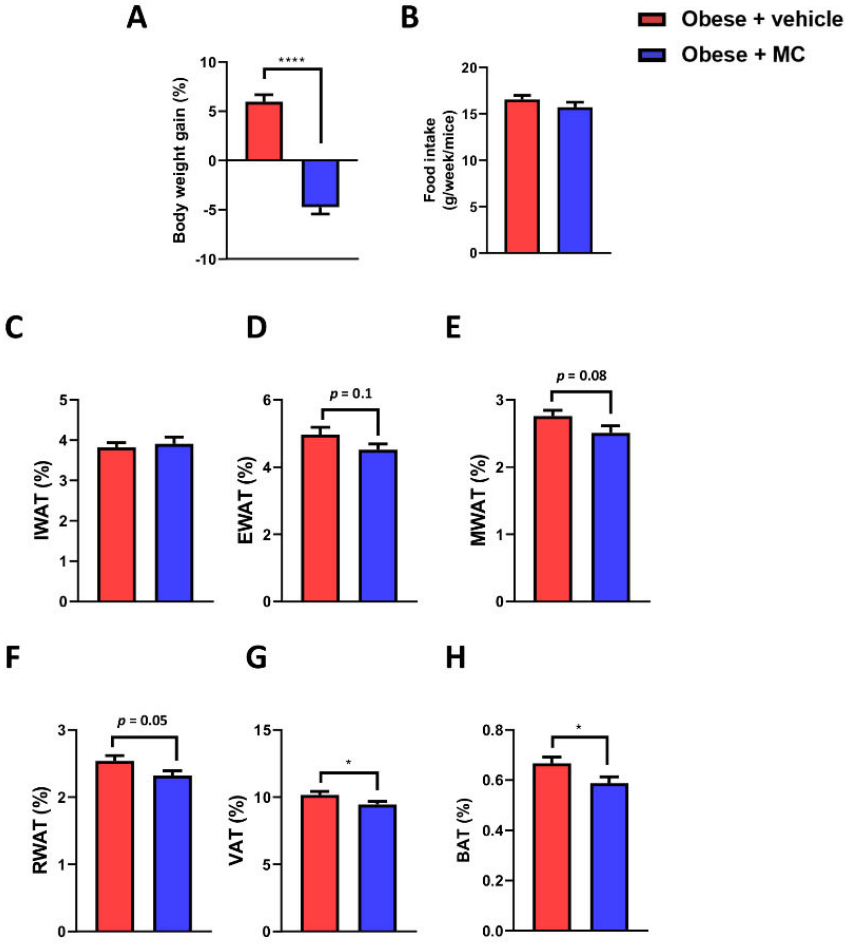

Figure S1. Obese mice supplemented with MC reduce body weight gain and presented smaller visceral WAT depots. Effects of MC treatment on: (A) percentage of body weight gain; (B) food intake, percentage from the total body weight of (C) IWAT (D) EWAT, (E) MWAT, (F) RWAT, (G) VAT and (H) BAT. Data are mean ± SEM. * $p < 0.05$, **** $p < 0.0001$.

Supp Figure S2

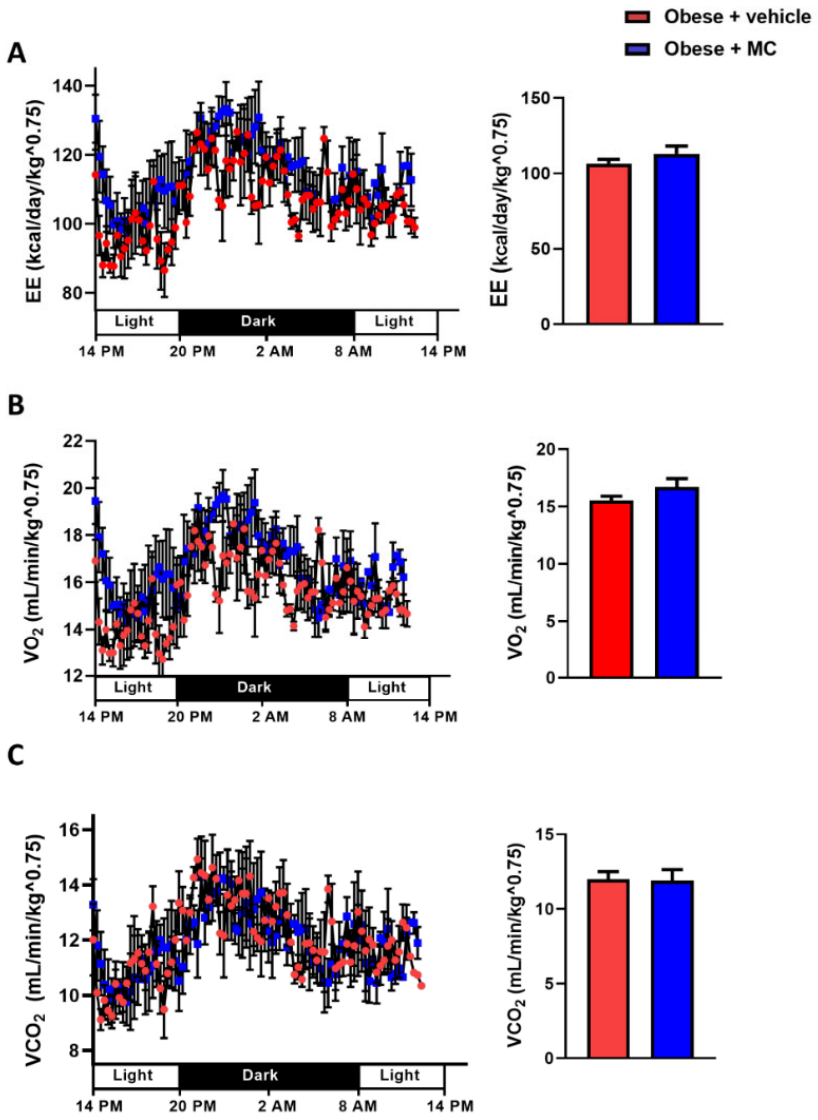

Figure S2. Effect of MC treatment on (A) energy expenditure (EE), (B) VO_2, and (C) VCO_2 during 24 h (left panels) and the mean of these measurement (right panels). Data are mean ± SEM.

Chapter 3

Microbiota Dysbiosis and Gut Barrier Dysfunction Associated with Non-Alcoholic Fatty Liver Disease Are Modulated by a Specific Metabolic Cofactors' Combination

Sergio Quesada-Vázquez [1], Caitlin Bone [2], Shikha Saha [3], Iris Triguero [1], Marina Colom-Pellicer [4], Gerard Aragonès [4], Falk Hildebrand [2,5], Josep M. del Bas [6], Antoni Caimari [6], Naiara Beraza [2,3,†] and Xavier Escoté [1,*,†]

1. Eurecat, Technology Centre of Catalunya, Nutrition and Health Unit, 43204 Reus, Spain
2. Gut Microbes and Health Institute Strategic Programme, Quadram Institute Bioscience, Norwich Research Park, Norwich NR4 7UQ, Norfolk, UK
3. Food Innovation and Health Institute Strategic Programme, Quadram Institute Bioscience, Norwich Research Park, Norwich NR4 7UQ, Norfolk, UK
4. Nutrigenomics Research Group, Department of Biochemistry and Biotechnology, Universitat Rovira i Virgili, 43007 Tarragona, Spain
5. Digital Biology, Earlham Institute, Norwich Research Park, Norwich NR4 7UZ, Norfolk, UK
6. Eurecat, Centre Tecnològic de Catalunya, Biotechnology Area, 43204 Reus, Spain

* Correspondence: xavier.escote@eurecat.org; Tel.: +34-977-302057 (ext. 4824)

† These authors share senior authorship.

Published in: International Journal of Molecular Sciences (IJMS). 2022 Nov; 23, 13675

Impact Factor (2022): 6.208

JCR category rank: Q1: Biochemistry & Molecular Biology

International Journal of
Molecular Sciences

MDPI

Article

Microbiota Dysbiosis and Gut Barrier Dysfunction Associated with Non-Alcoholic Fatty Liver Disease Are Modulated by a Specific Metabolic Cofactors' Combination

Sergio Quesada-Vázquez [1], Caitlin Bone [2], Shikha Saha [3], Iris Triguero [1], Marina Colom-Pellicer [4], Gerard Aragonès [4], Falk Hildebrand [2,5], Josep M. del Bas [6], Antoni Caimari [6], Naiara Beraza [2,3,†] and Xavier Escoté [1,*,†]

[1] Eurecat, Technology Centre of Catalunya, Nutrition and Health Unit, 43204 Reus, Spain
[2] Gut Microbes and Health Institute Strategic Programme, Quadram Institute Bioscience, Norwich Research Park, Norwich NR4 7UQ, Norfolk, UK
[3] Food Innovation and Health Institute Strategic Programme, Quadram Institute Bioscience, Norwich Research Park, Norwich NR4 7UQ, Norfolk, UK
[4] Nutrigenomics Research Group, Department of Biochemistry and Biotechnology, Universitat Rovira i Virgili, 43007 Tarragona, Spain
[5] Digital Biology, Earlham Institute, Norwich Research Park, Norwich NR4 7UZ, Norfolk, UK
[6] Eurecat, Centre Tecnològic de Catalunya, Biotechnology Area, 43204 Reus, Spain
* Correspondence: xavier.escote@eurecat.org; Tel.: +34-977-302057 (ext. 4824)
† These authors share senior authorship.

Citation: Quesada-Vázquez, S.; Bone, C.; Saha, S.; Triguero, I.; Colom-Pellicer, M.; Aragonès, G.; Hildebrand, F.; del Bas, J.M.; Caimari, A.; Beraza, N.; et al. Microbiota Dysbiosis and Gut Barrier Dysfunction Associated with Non-Alcoholic Fatty Liver Disease Are Modulated by a Specific Metabolic Cofactors' Combination. *Int. J. Mol. Sci.* **2022**, *23*, 13675. https://doi.org/10.3390/ijms232213675

Academic Editor: Takemi Akahane

Received: 30 September 2022
Accepted: 4 November 2022
Published: 8 November 2022

Abstract: The gut is a selective barrier that not only allows the translocation of nutrients from food, but also microbe-derived metabolites to the systemic circulation that flows through the liver. Microbiota dysbiosis occurs when energy imbalances appear due to an unhealthy diet and a sedentary lifestyle. Dysbiosis has a critical impact on increasing intestinal permeability and epithelial barrier deterioration, contributing to bacterial and antigen translocation to the liver, triggering non-alcoholic fatty liver disease (NAFLD) progression. In this study, the potential therapeutic/beneficial effects of a combination of metabolic cofactors (a multi-ingredient; MI) (betaine, N-acetylcysteine, L-carnitine, and nicotinamide riboside) against NAFLD were evaluated. In addition, we investigated the effects of this metabolic cofactors' combination as a modulator of other players of the gut-liver axis during the disease, including gut barrier dysfunction and microbiota dysbiosis. Diet-induced NAFLD mice were distributed into two groups, treated with the vehicle (NAFLD group) or with a combination of metabolic cofactors (NAFLD-MI group), and small intestines were harvested from all animals for histological, molecular, and omics analysis. The MI treatment ameliorated gut morphological changes, decreased gut barrier permeability, and reduced gene expression of some proinflammatory cytokines. Moreover, epithelial cell proliferation and the number of goblet cells were increased after MI supplementation. In addition, supplementation with the MI combination promoted changes in the intestinal microbiota composition and diversity, as well as modulating short-chain fatty acids (SCFAs) concentrations in feces. Taken together, this specific combination of metabolic cofactors can reverse gut barrier disruption and microbiota dysbiosis contributing to the amelioration of NAFLD progression by modulating key players of the gut-liver axis.

Keywords: intestinal permeability; gut-liver axis; gut microbiota; metabolic disease; SCFAs

1. Introduction

The gut-liver axis is described as the compilation of events that take place among the liver, the gut, and gut microbiomes, which influence each other. This close connection underlines the critical regulatory effect of the gut microbiota on liver and gut health [1,2]. The liver is supplied with blood from the gut through the portal vein, which supports the close anatomical and functional interaction between gut microbiomes, the gut, and

the liver [1]. This blood supply contains nutrients and (bacterial) metabolites needed for correct homeostasis [3,4]. When metabolic homeostasis is disrupted due to lifestyle deterioration in a westernized society, characterized by an unhealthy diet and reduced physical activity, this triggers multifactorial risk factors such as obesity, dyslipidemia, and metabolic syndrome [3], which could promote the hepatic manifestation known as non-alcoholic fatty liver disease (NAFLD). NAFLD is described as the most common liver disease, with a prevalence of around one-third of the world's population and is still rising [1]. NAFLD is characterized by the accumulation of free fatty acids in the liver, called hepatic steatosis, which can progress to steatohepatitis and fibrosis in further stages.

The gut is a selective barrier that allows the translocation of nutrients and microbe-derived metabolites to the systemic circulation passing through the portal vein to the liver [3,4]. However, this barrier also effectively protects against the translocation of pathogenic bacteria and harmful microbe-derived products, such as bowel luminal antigens and inflammatory factors, through its selective permeability [1,4]. The intestinal epithelium has a self-renewing capacity during homeostasis and regenerates in response to injury via the proliferation of intestinal stem-cell-derived epithelial cells [5]. This intestinal barrier is controlled by tight-junctions (TJ) proteins and its expression and integrity are regulated by the immune system, which is molded by the microbiome composition [4], and by Occludin, Cadherin, and ZO-1 protein interactions [6].

Gut microbiota is composed of trillions of microorganisms that create a symbiotic relationship with the host or reside as commensals and can execute various functions influencing human physiology and pathology, such as the fermentation of indigestible fibers into short-chain fatty acids (SCFAs) that are crucial in some physiological processes [7–10]. When diets are imbalanced and contain excessive energetic and fatty intakes, intestinal microbiota diversity is disturbed, known as dysbiosis [1,3]. Dysbiosis has a critical impact on altering SCFA production, and on altered intestinal permeability, which is induced by TJ alteration that leads to epithelial barrier deterioration, and consequently bacterial products and antigen translocation to the liver associated with an elevated level of proinflammatory cytokines, which may lead to NAFLD development [11,12]. Intestinal microbiota dysbiosis has been connected to hepatic fat accumulation [13]. Thereby, the "leaky" gut hypothesis proposes the increment of energy harvest and altered choline metabolism by overnutrition increase intestinal permeability, which raise the production of proinflammatory mediators, and together with the alteration in SCFAs production due to gut microbiota dysbiosis, contributes to NAFLD pathogenesis [9,12,14].

Our recent studies have demonstrated [15,16] that the specific combination of metabolic cofactors composed of L-carnitine (LC; an enhancer of fatty acid uptake across the mitochondrial membrane), nicotinamide riboside (NR; NAD+ precursor), n-acetyl cysteine (NAC), and betaine (glutathione precursors and betaine a methyl donor) [17–19] is a promising treatment against NAFLD. This multi-ingredient (LC, NAC, Betaine, NR; hereinafter MI) supplementation improved pathological NAFLD features in the liver, reducing inflammation, steatosis, and insulin resistance [15]. Specifically, LC showed a boost effect on FFAs transport into the mitochondria in hepatocytes inducing lipid oxidation [20]; NAC was described to have a protective role in blocking hepatic steatosis and reducing proinflammatory mediators [21]; Khodayar et al. determined betaine is involved in methionine metabolism and may increase glutathione levels as an antioxidant action [22]; and NR can increase NAD^+ levels and accelerate FFAs oxidation by SIRT1 activation and protecting against HFD-induced metabolic disorders [23]. However, the potential of this supplementation strategy in modulating the gut-microbiota-liver axis has not been explored. Thus, considering the strong connection between the liver, the gut, and the gut microbiota plays an important role in hepatic homeostasis and in the pathogenesis of different hepatic diseases [4,11], in the present study we demonstrate that the supplementation of a specific combination of metabolic cofactors in a preclinical model of NAFLD not only reverse NAFLD pathogenesis in the liver, but also ameliorates gut morphological changes, gut barrier permeability, and

reduces intestinal inflammation by improving intestinal microbiota composition directly related to NAFLD development.

2. Results

2.1. Multi-Ingredient Treatment Modified Epithelium Morphology in the Small Intestine in a NAFLD

The lengths of the small intestine shortened significantly in NAFLD mice compared to control mice, but no significant effect was found after one month of MI treatment (Figure 1a). However, further histopathological analysis of different areas of the small intestine showed more evident differences when MI was supplemented by recovering intestinal morphology altered by NAFLD. As expected, control and NAFLD mice showed microscopic differences at the jejunum, with wider and shorter villus in NAFLD mice (Figure 1b). Villus length and width were increased in the NAFLD group compared to their counterparts (Figure 1c,d). In contrast, MI-supplemented mice significantly reduced both villus length and width compared to NAFLD mice (Figure 1c,d). Total intestinal wall thickness was increased in the NAFLD mice compared to the control group, while MI treatment significantly reduced the NAFLD effect on mice (Figure 1e). This effect was also translated both in the mucosa layer length (Figure 1f) and in the muscular layer length (Figure 1g), significantly ameliorating in the MI group compared to NAFLD mice. On the other hand, crypt depth was considerably reduced in NAFLD mice compared to the control group, and MI treatment could significantly increase the crypt depth (Figure 1h).

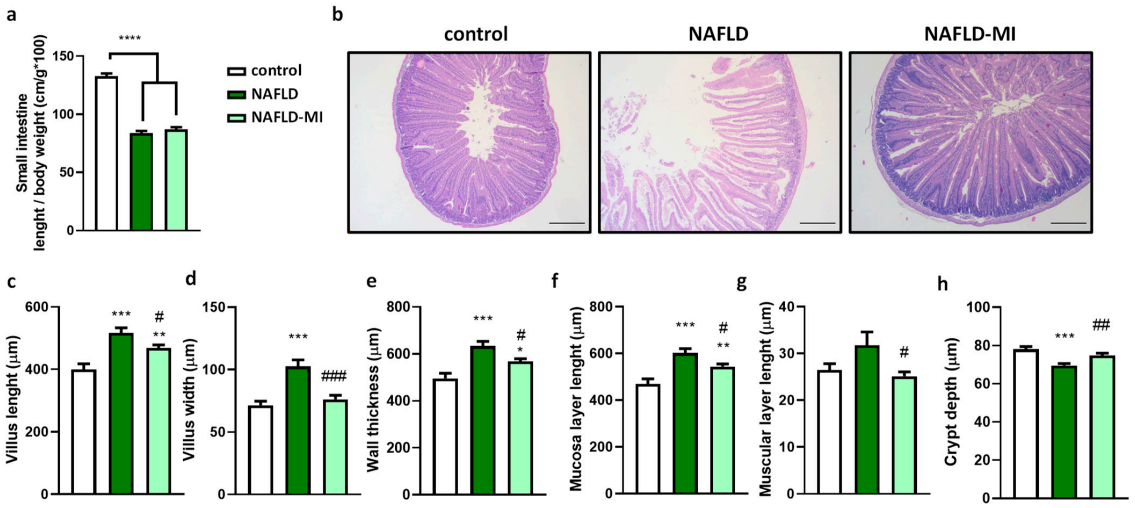

Figure 1. (**a**) Relative length of the small intestine of control, NAFLD, and NAFLD-MI groups. (**b**) Hematoxylin and eosin (H&E) staining of jejunums. Bar = 200 μm. Morphometric intestinal variables associated with NAFLD: (**c**) villus length, (**d**) villus width, (**e**) wall thickness, (**f**) mucosa layer length, (**g**) muscular layer length, and (**h**) crypt depth. Data are mean ± SEM. * $p < 0.05$ vs. control mice; ** $p < 0.01$ vs. control mice; *** $p < 0.001$; **** $p < 0.0001$ vs. control mice. # $p < 0.05$ vs. NAFLD mice; ## $p < 0.01$ vs. NAFLD mice; ### $p < 0.001$ vs. NAFLD mice.

2.2. MI Supplementation Ameliorates Intestinal Permeability and Inflammation

Small intestine permeability was assessed in the jejunum by immunolocalization of Occludin, showing a significant reduction in apical staining in NAFLD mice compared to control mice, while Occludin apical expression was restored in the MI-supplemented group (Figure 2a,b). In accordance with the Occludin distribution, *Ocln* expression was downregulated in NAFLD mice compared to control mice. However, *Ocln* and *Cdh-1* mRNA expressions were up-regulated in the MI-supplemented group in comparison with

the NAFLD mice group, and *Zo-1* tended to be up-regulated in the MI-supplemented group (Figure 2c).

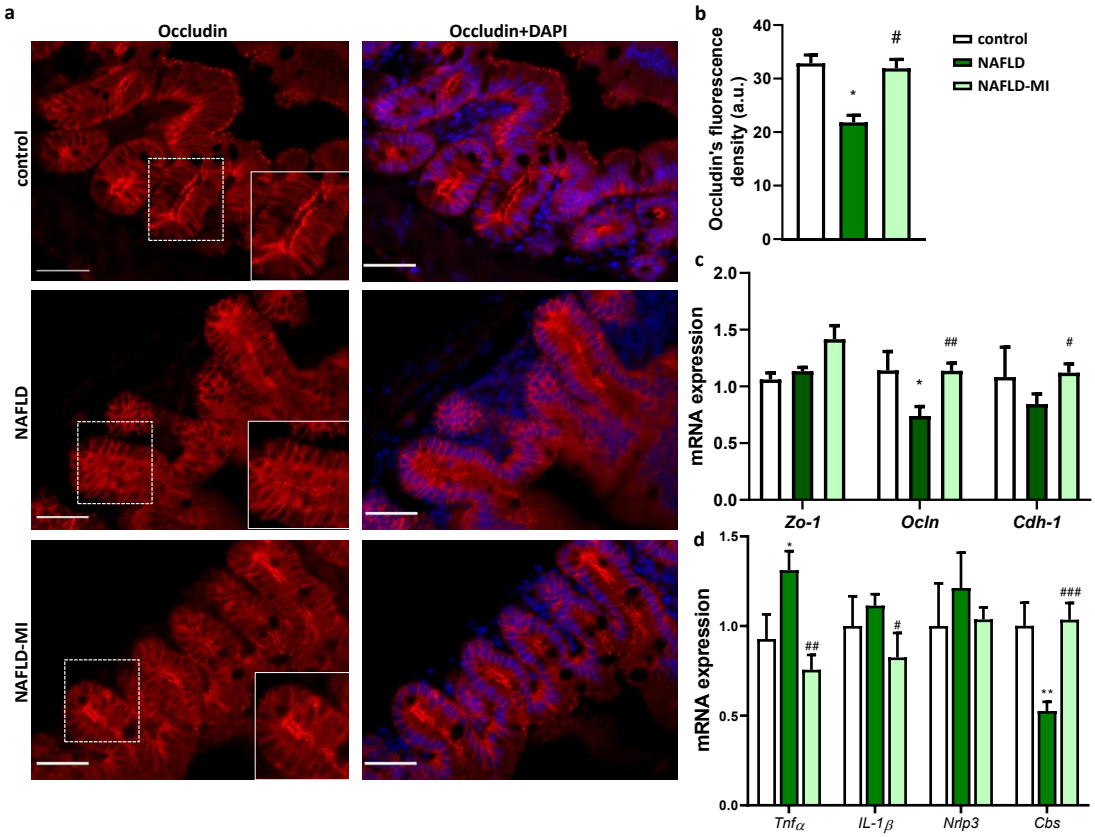

Figure 2. Effects of the MI treatment on intestinal permeability and inflammation. (**a**) Jejunum immunofluorescence of Occludin and DAPI. Bar = 50 µm. (**b**) Occludin's fluorescence intensity. Effects of treatments on (**c**) mRNA expression of intestinal permeability-related genes: *Zo-1* (Zonula Oclnudens-1), *Ocln* (Occludin), and *Cdh-1* (Cadherin-1), on (**d**) mRNA expression of inflammatory and antioxidant related-genes: *Tnfα* (Tumor Necrosis Factor α), *Il-1β* (interleukin 1β), *Nlrp3* (NLR family pyrin domain containing 3), and *Cbs* (cystathionine-β-synthase). Data are mean ± SEM. * $p < 0.05$, ** $p < 0.01$ vs. control mice, # $p < 0.05$; ## $p < 0.01$; ### $p < 0.001$ vs. NAFLD mice.

In addition, NAFLD supplemented with the MI displayed a significant down-regulation in inflammation-related genes *Tnfα* and *Il-1β* expression levels when compared to their NAFLD counterparts, suggesting MI treatment influences the regulatory crosstalk between the immune system and the intestinal barrier function preserving intestinal permeability. In contrast, *Nlrp3* did not show changes in mRNA expression difference between groups (Figure 2d). In addition, intestinal *Cbs* expression levels (a key enzyme in GSH production to defend against oxidative stress) were downregulated in NAFLD animals (Figure 2d). However, animals treated with the MI supplementation reversed this downregulation by increasing intestinal *Cbs* expression levels similar to control animals (Figure 2d). Overall, our results support that MI treatment influences the regulatory crosstalk between the immune system and the intestinal barrier function preserving intestinal permeability.

2.3. MI Supplementation Recovers Proliferative Cells Localization in the Small Intestine

In NAFLD mice, the proliferative cell count and migration revealed a considerable reduction compared to the control groups (Figure 3a–c). Nevertheless, MI treatment increased the number of Ki-67-stained nuclei, both in the villus and crypts, which could mean that MI supplementation improves intestinal cell renewal in response to HF diets (Figure 3a–c).

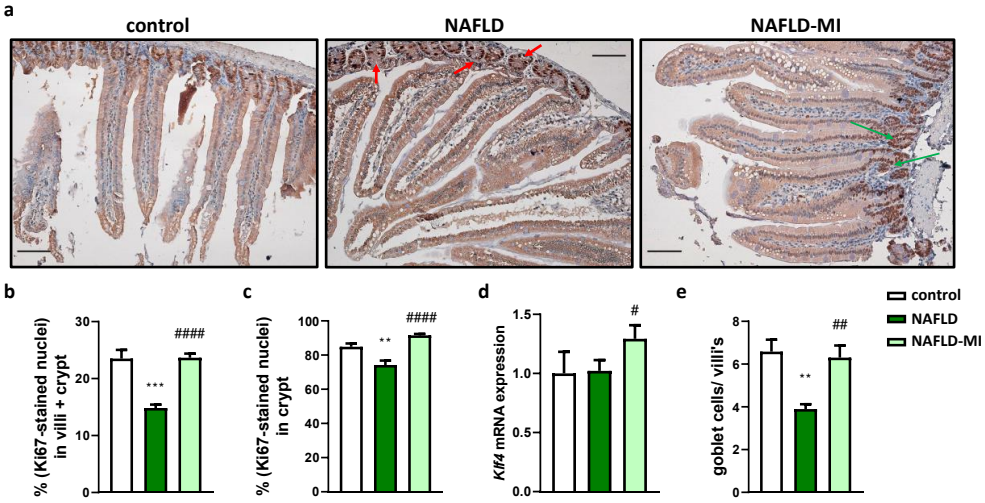

Figure 3. NAFLD mice showed an ectopic localization of proliferative cells which is recovered after MI supplementation. (**a**) Immunohistochemical analysis of small intestine sections of proliferating cells with Ki-67. Red arrows show the reduction of proliferative cells in crypts in NAFLD compared to the control group. Green arrows show the recovery of proliferation cells' localization after MI supplementation. Moreover, in MI-supplemented mice and control mice, proliferative cells were detected in the villus. Bar = 200 μm. (**b**) Percentage of ki-67-stained nuclei in villus and crypts compared to other types of cells, and (**c**) the percentage of ki-67-stained nuclei just in crypts. Improvement of mucosa function was evaluated by intestinal mRNA expression of *Klf4* (Kruppel-like factor 4) (**d**,**e**) goblet cells count. Data are mean ± SEM. ** $p < 0.01$, *** $p < 0.001$ vs. control mice; # $p < 0.05$, ## $p < 0.01$, #### $p < 0.0001$ vs. NAFLD mice.

Next, to assess intestinal mucosa function, it was determined *Klf4* mRNA expression, observing that it was increased in the MI supplementation group compared to NAFLD mice (Figure 3d). In addition, goblet cell count was significantly reduced in NAFLD mice compared to the control group (Figure 3e), while, in accordance with *Klf4* expression results, MI treatment significantly restored the number of goblet cells.

2.4. Microbiota Dysbiosis Present in NAFLD Is Attenuated after MI Supplementation

As expected, in the analysis of the bacterial diversity, NAFLD mice showed a tendency to decrease their diversity compared to control mice, but MI supplementation significantly increased bacterial diversity in comparison with NAFLD mice, suggesting that these metabolic cofactors increased gut microbiota diversity (Figure 4a). Further taxonomic analysis at the genus level showed substantial and significant differences between the study groups were observed (Figure 4b) [23]. NAFLD mice were characterized by a higher presence of *Anaerotruncus*, *Eubacterium nodatum*, *Lachnoclostridium*, *Lachnospiraceae UCG-001*, and *Escherichia/Shigella* in comparison to the control (Table 1). MI supplementation reduced the concentration of these bacteria (Table 1). Moreover, *Faecalibaculum*, *Christensenella*, *Faecalibacterium*, *Eggerthellaceae*, and *Enterococcus* were also increased in NAFLD mice in comparison with control mice, but MI treatment achieved a reduction in these genera similar to control

levels. Interestingly, *Peptococcus*, *Butyricicoccus*, and *Ruminiclostridium* were only significantly increased in MI-treated mice compared to NAFLD and control mice (Table 1).

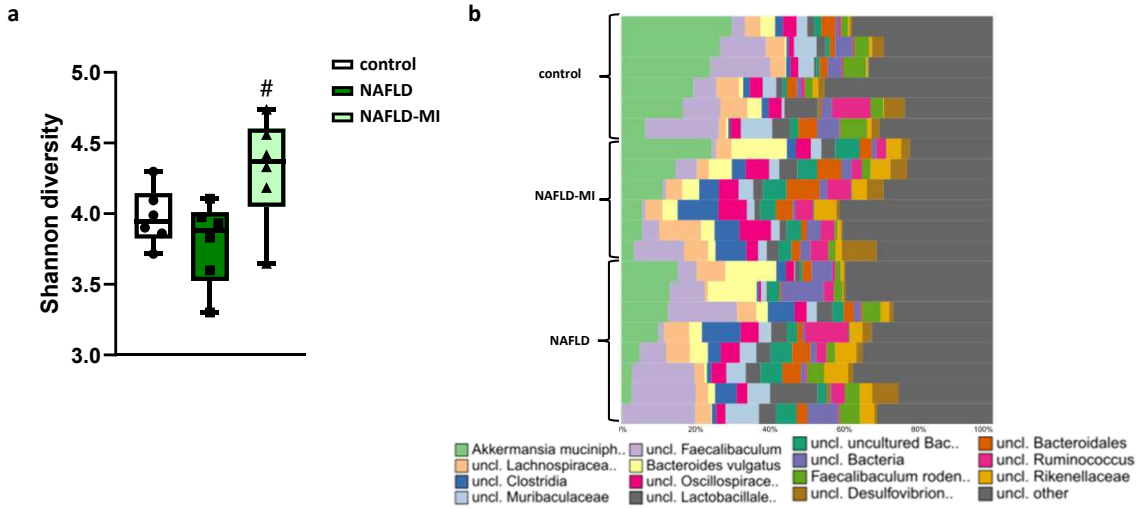

Figure 4. (**a**) Estimation of bacterial diversity as assessed by the Shannon index. (**b**) Overview of microbial composition at genus level in the control, NAFLD, and NAFLD-MI groups. # $p < 0.05$ vs. NAFLD mice.

Table 1. Differences in genus abundance between the different animal groups.

Testing against Control, NAFLD, and MI; Requested Test(s): Wilcox; Used Matrix Type: Normed; Used Test Statistic Is: Kruskal-Wallis Test. Only Genera Are Listed When the *p*-Value < 0.05.Genus	Phylum	Direction	*p*-Value	q-Value
Anaerotruncus	*Firmicutes*	NAFLD > MI >> control	0.0008	0.0291
Butyricicoccus	*Firmicutes*	*MI > control = NAFLD*	*0.0036*	*0.0515*
Christensenella	*Firmicutes*	*NAFLD > MI = control*	*0.0350*	*0.0920*
Eggerthellaceae	*Actinobacteria*	*NAFLD > MI = control*	*0.0139*	*0.0679*
Enterococcus	*Firmicutes*	*NAFLD > control = MI*	*0.0065*	*0.0557*
Eubacterium nodatum	*Firmicutes*	NAFLD > MI > control	0.0011	0.0317
Escherichia/Shigella	*Proteobacteria*	NAFLD > MI > control	0.0015	0.0374
Faecalibaculum	*Firmicutes*	NAFLD > MI = control	0.0270	0.0920
Faecalibacterium	*Firmicutes*	NAFLD > MI = control	0.0167	0.0753
Lachnoclostridium	*Firmicutes*	NAFLD > MI > control	0.0040	0.05
Lachnospiraceae UCG-001	*Firmicutes*	NAFLD > MI > control	0.0065	0.05
Peptococcus	*Firmicutes*	MI > control = NAFLD	0.0349	0.0920
Ruminiclostridium	*Firmicutes*	MI > control = NAFLD	0.021	0.088

2.5. MI Supplementation Modulates the SCFAs Fecal Concentrations

In the analysis of SCFAs concentrations in feces, propionate was significantly increased in NAFLD mice compared to the control group, an effect that tended to be similar in the total fecal SCFAs (Figure 5). Interestingly, MI supplementation caused a significant reduction in propionate levels in feces from NAFLD mice. No important changes were found in other SCFAs detected (Figure 5).

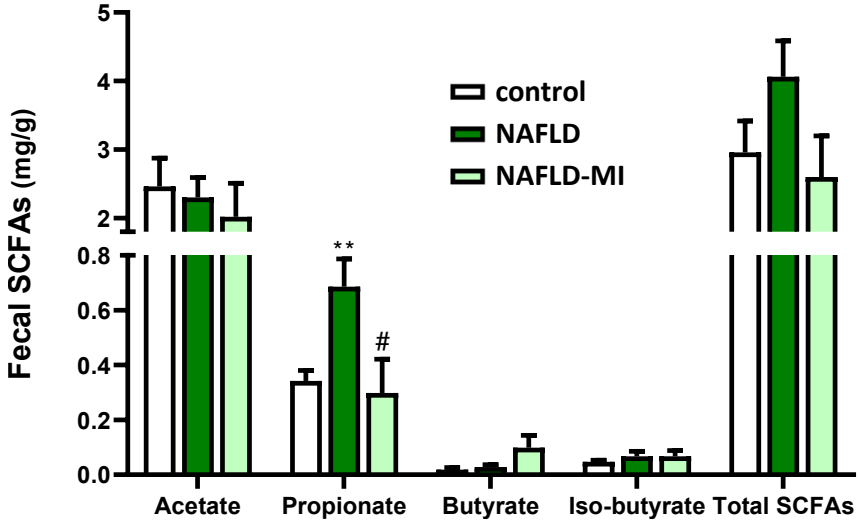

Figure 5. SCFAs quantification in fecal samples. Fecal amounts of the different short-chain fatty acids were analyzed in control, NAFLD, and NAFLD-MI mice. Data are mean ± SEM. ** $p < 0.01$ vs. control mice; # $p < 0.05$ vs. NAFLD mice.

2.6. Fecal SCFAs Levels Are Correlated with Changes in Specific Fecal Genera Bacteria

In the correlation analyses, changes in fecal propionate levels were positively correlated with the *Citrobacter* genus (Figure 6). However, after dividing the animals according to the treatments, only NAFLD mice reproduced this positive correlation of propionate levels with *Citrobacter*. *Eubacterium nodatum*, *Bacteroides*, *Anaerotruncus*, and *Faecalibacterium* showed a positive correlation with propionate, and *Bifidobacterium*, *Odoribacter*, *Lactobacillus*, *Lachnoclostridium*, *Lachnospiraceae UCG-001*, and *Faecalibaculum* were negatively correlated (Table 2). The control group found fecal propionate positively correlated with *Caproiciproducens* and *Ruminiclostridium* levels, and negatively with *Lactobacillus*, *Faecalibacterium*, and *Escherichia/Shigella* (Table 2). In contrast to NAFLD mice, MI supplementation promoted a negative correlation of fecal propionate with *Enterococcus*.

In addition, fecal acetate levels were negatively correlated with *Odoribacter*, *Enterococcus*, and *Lachnoclostridium* (Figure 6). In the control group, *Lactobacillus* and *Lachnoclostridium* were negatively correlated with acetate (Table 2). In NAFLD mice, *Bifidobacterium*, *Odoribacter Lactobacillus*, *Lachnoclostridum*, *Lachnospiraceae UCG-001*, and *Faecalibaculum* were negatively correlated with acetate. On the other hand, in NAFLD-MI mice, fecal acetate was not significantly correlated with any genera (Table 2).

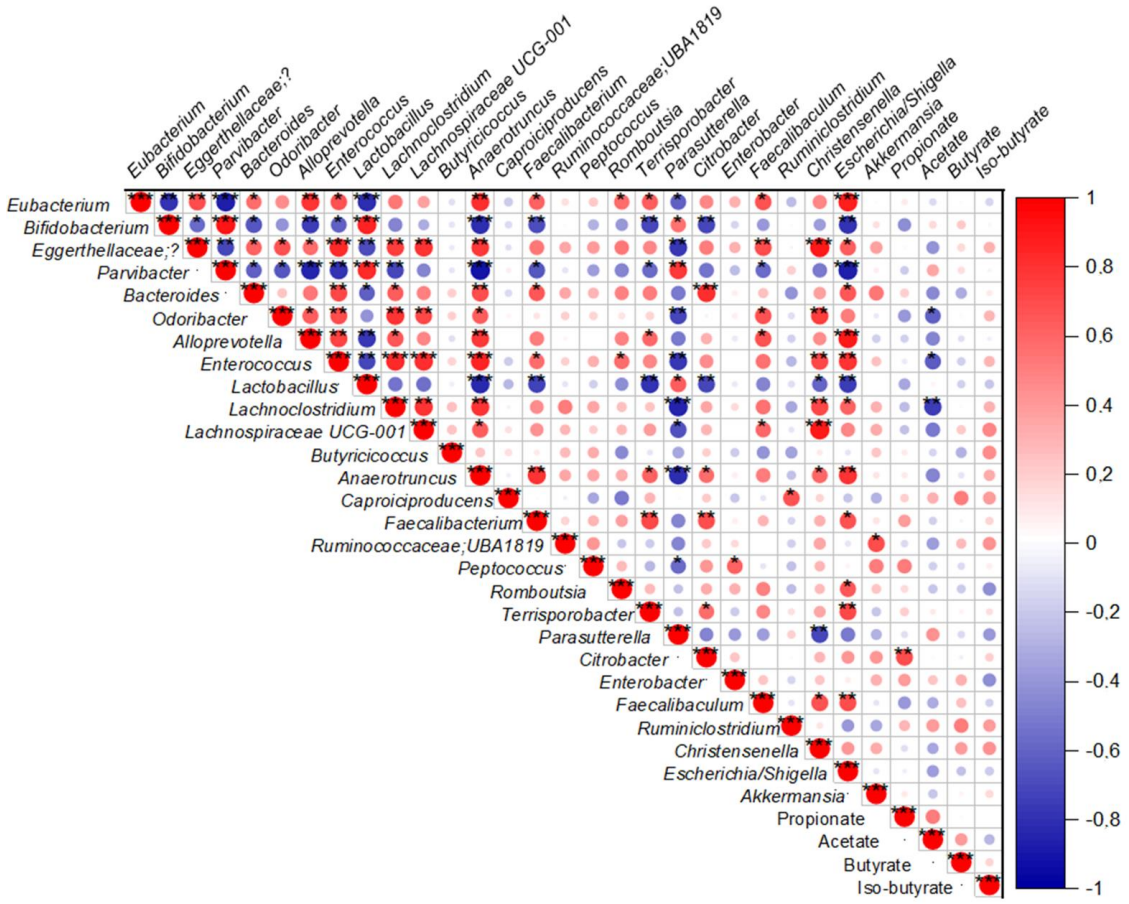

Figure 6. Spearman correlation analysis of fecal SCFAs and selected fecal genus from all mice. Dots in red mean positive correlation, whereas dots in blue mean negative correlation. * $p < 0.05$, ** $p < 0.01$, *** $p < 0.001$.

Variations in fecal butyrate levels were not correlated with any genera (Figure 6). Nevertheless, when groups were arranged by treatment, some differences were found. In control mice, *Odoribacter* and *Lactobacillus* were negatively correlated with fecal butyrate levels, and *Caproiciproducens* was positively correlated. In NAFLD mice, *Eggerthellaceae*, *Ruminococcaceae UBA1819*, and *Christensenella* were positively correlated with butyrate, but *Romboutsia*, *Parasutterella*, and *Escherichia/Shigella* were negatively correlated.

Finally, iso-butyrate did not show any correlation with any bacterial genera (Figure 6). However, when groups were arranged by treatment, in the control group, only *Faecalibacterium* was negatively correlated with iso-butyrate. On the other hand, no correlations were found between iso-butyrate and any genera in NAFLD mice and MI-treated mice (Table 2).

Table 2. Spearman correlation analysis of selected fecal genus bacteria and SCFAs in all animals, control, NAFLD, and NAFLD-MI groups. Boxes in red mean positive correlation and boxes in blue mean negative correlation. * $p < 0.05$, ** $p < 0.01$, *** $p < 0.001$.

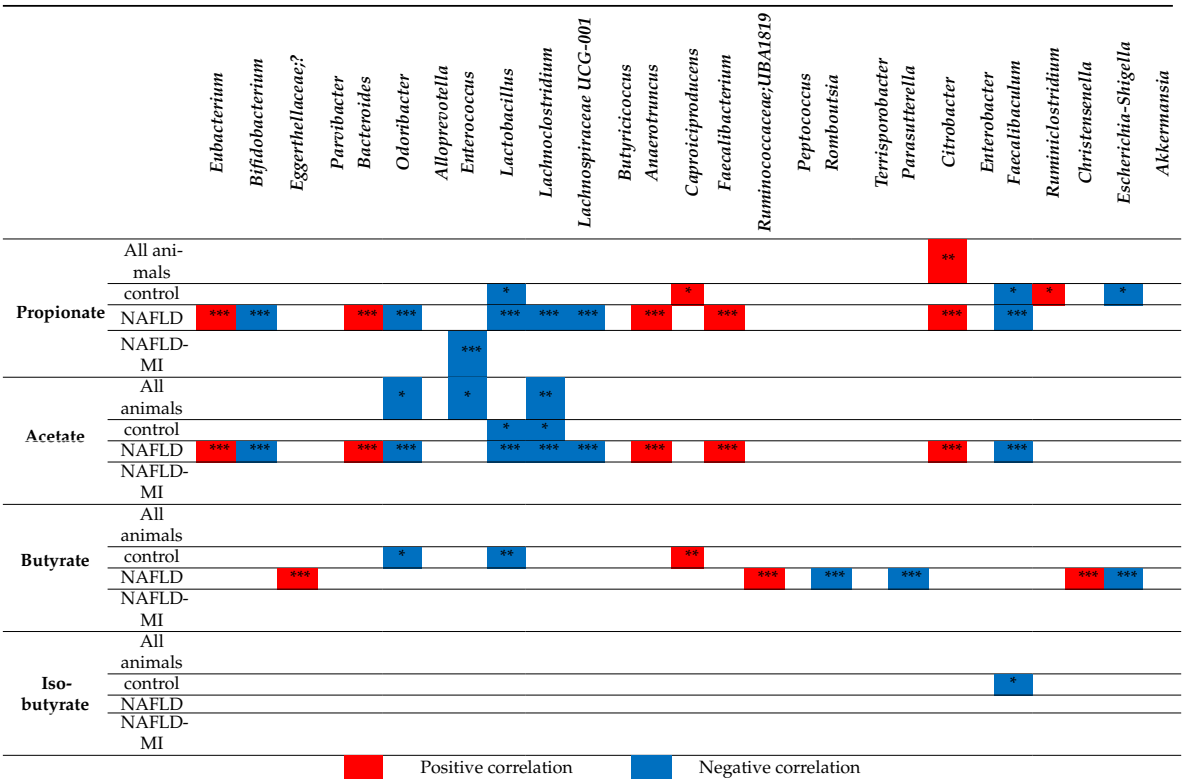

3. Discussion

NAFLD is a multifactorial disease that involves different physio-pathological factors, including environmental, nutritional, genetics, epigenetics, and hormones. Furthermore, some of these factors also affect gut health, promoting intestinal barrier dysfunction and microbiota dysbiosis [1,9]. In turn, this gut impairment increases the development of NAFLD, disrupting the gut-liver axis [1,9]. Previous studies showed intestinal permeability, inflammation, dysbiosis, and gut morphology alterations in this hepatic disease [24–27]. Considering that NAFLD is a multifactorial pathology and that different studies have shown that better responses are obtained when treatments are performed under a multi-faceted approach [17,28], the treatment of NAFLD using different bioactive compounds that act against complementary targets, such as the use of the aforementioned specific combination of metabolic cofactors, could be considered as a potential strategy to ameliorate NAFLD [15,16]. Here, we demonstrate that the MI treatment contributes to revert changes in the gastrointestinal tract linked to NAFLD development associated with ameliorating gut dysfunction and microbiota dysbiosis.

Gut morphology alterations are strongly related to high-caloric diets. Following prior studies, chronic ingestion of a high-fat diet elicits an increased length and width of villi in the jejunum, a decrease in crypt depth, and an increase in the total wall thickness and muscular and mucosa layers [29,30]. Here, it is observed that MI (LC, betaine, NAC, and NR) treatment relieved all these morphologic changes caused by diet-induced NAFLD, improving intestinal morphology to healthy levels. These features may be possible because NR increases intracellular NAD^+ levels and may activate SIRT1, which has been related to

an improvement in colony formation efficiency in crypts and intestinal stem cells [31]. Thus, villi elongation was reduced by NR supplementation linked to an inefficient cell renewal in an aging mice model that correlates with our results [31]. Another metabolic cofactor like betaine also had a protective effect on villus and crypts in a rat model, probably due to both the methyl group donor nature and the osmotic nature of betaine [32] and NAC, with protective effects because of its ability as a scavenger of oxygen free radicals; overall ameliorating histological injuries in the small intestine of rats [33].

A breach of the intestinal barrier caused by westernized diets allows the translocation of harmful bacteria and antigens, increasing liver damage and inflammation [3,34] which, if unresolved, can lead to the progression of NAFLD to advanced hepatic disease [3,35,36]. In this study, mice with NAFLD presented negative effects on key proteins in TJ integrity by reducing Occludin concentration and expression, and increased *Tnf-α* expression inducing inflammation, in accordance with a study with obese mice [37,38], while an improvement of the abnormal distribution of Occludin and *Zo-1* and *Cdh-1* expression and a reduced expression of inflammatory-related genes was induced by MI treatment in NAFLD mice. These results were correlated with a study that used LC supplementation, which reduced inflammatory biomarkers in the colon by modifying oxidative stress activity in a colitis animal model [39]. Interestingly, the increased expression of *Zo-1* and *Ocln* were recovered, and inflammatory biomarkers were decreased by betaine supplementation in acute liver failure mice [40]. In addition, the participation of NAC in modulating permeability and intestinal inflammation has also been described during in vitro and in vivo LPS-induced dysfunction by reducing oxidative stress and increasing *Zo-1*, *Cdh-1*, and *Ocln* gene expression [41]. Therefore, the capacity of the combination of these metabolic cofactors to reduce oxidative stress could diminish intestinal inflammation by ameliorating cytokine-mediated disruption of the intestinal TJ barrier, improving the expression and signaling of multiple integral proteins such as Occluding and Zo-1 [42]. Furthermore, to check the antioxidant effect of betaine and NAC as GSH precursors, *Cbs* expression, which is implicated in GSH and H_2S biosynthesis [43], was analyzed. Intestinal *Cbs* expression was observed to be downregulated in NAFLD mice. The downregulation of *Cbs* expression could decrease H_2S biosynthesis, which has anti-inflammatory and cytoprotective characteristics and could increase homocysteine levels, triggering inflammation in the small intestine [44,45], which connects with the upregulation of *Tnf-α* in this study. In contrast, MI supplementation recovered *Cbs* expression levels that could be related to an increased antioxidant response due to betaine and NAC supplementation, concordant with what has been observed in other tissues affected by NAFLD [15].

Regarding the importance of enterocyte-renewal mechanisms, cell proliferation has been described to be negatively influenced by HFDs [46]. Intracellular oxidative stress is induced by HFDs, predisposing the intestine to chronic diseases by disrupting cell proliferation [47]. In addition, proliferation was also affected by methyl donor deficiency, decreasing in the proximal small intestine mucosa [48]. In this study, disrupted cell proliferation was observed in NAFLD mice, closely related to the loss of intestinal permeability [49]. Further detrimental effects on intestinal cell function have been observed after HFDs, including reducing goblet cell differentiation and TJ alteration, which are critical for the correct mucus layer production and barrier permeability [41,46,50,51]. In addition, proliferative cells and goblet cell numbers in the intestinal epithelium were increased in MI-treated mice compared to NAFLD mice. This improvement may be due to the antioxidant properties of NAC and betaine. NAC offers protection against oxidative stress [41], and betaine is positively correlated with goblet cell differentiation [48] and can boost GSH levels and enhance the activity of antioxidant enzymes [52], as shown above.

The role of the microbiota during the pathogenesis of NAFLD has been widely studied. Differences in the gut bacterial composition may contribute to NAFLD development via different pathways, such as an increase in the expression levels of some pro-inflammatory cytokines in the liver [53]. As has been observed, decreased microbial diversity is associated with increased intestinal permeability and systemic low-grade inflammation [54], and

consequently, linked to hepatic steatosis [9]. Importantly, the success in increasing intestinal bacterial diversity was caused by MI treatment, which may be linked to the beneficial effects found in the intestinal barrier and function. In addition, an increase in the *Firmicutes* levels at the phylum level was shown in NAFLD mice, followed by an increase in *Proteobacteria*, which was consistent with previous studies that demonstrated an increase in *Firmicutes* and *Proteobacteria* during NAFLD [26,55]. These changes in microbiota composition were reverted by MI supplementation, reducing the concentration of these phyla. These results were in accordance with previous studies that used betaine or NAC in HFD animal models to show reduced *Firmicutes* levels [40] and *Proteobacteria* levels [56], respectively. These observations were confirmed in a clinical study combining three of them (NR, NAC, and LC) [57], supporting the potential role of these compounds in modifying the gut bacterial community.

A deeper analysis of microbiota composition at the genus level showed that *Lachnospiraceae* increased in the NAFLD group, resembling the observations from a clinical study with NAFLD patients that found the levels of this genus significantly increased [58]. Moreover, *Anaerotruncus* and *Lachnoclostridium*, which are described as mucin-degrading bacteria that can impact both glycan composition and mucus thickness participating in the degradation of mucin [59], were increased in NAFLD mice in this study, which correlated with other preclinical studies [60,61], supporting the association of impaired intestinal barrier function with NAFLD. Here, we also found the elevated presence of *Eubacterium nodatum* in NAFLD mice, which is closely related to periodontal lesions and influences the pathology of NAFLD [62]. However, the levels of *Eubacterium nodatum* were significantly reduced by MI treatment. Furthermore, Yin et al. found an increased level of *Escherichia/Shigella* in rats with NAFLD, which are gram-negative bacteria containing LPS that may impair the gut barrier and trigger a low-grade chronic inflammation state [63], similarly to in NAFLD mice. Nevertheless, MI treatment succeeded in reducing *Escherichia/Shigella* levels. Furthermore, an elevation of the *Enterococcus* genus was presented in NAFLD mice in this study, a genus of potentially pathogenic bacteria with virulence factors and antibiotic resistance genes [64], which positively correlated with chronic liver diseases [65] and NAFLD [6]. Importantly, all these pathogenic bacteria related to mucin degradation, LPS-producers, or harmful bacteria were reduced after MI treatment. These changes in gut microbiota are associated with improved homeostasis and diversity of gut microbiota, connected with the actions of these metabolic cofactors in metabolic disorders shown separately in prior studies [40,56]. Finally, *Butyricicoccus*, which is a butyrate producer genus that reduces intestinal inflammation, was increased after MI supplementation. This fact is concordant with a previous study with NAFLD patients treated with metabolic cofactors [57]. In addition, the levels of *Peptococcus* were increased after MI supplementation, a similar situation was observed in HFD mice after naringin treatment [66], which correlates high *Peptococcus* abundance with an improvement in NAFLD progression.

A recent study emphasized that high fecal SCFAs content impact NAFLD progression by maintaining intestinal low-grade inflammation [67]. NAFLD and obese patients were characterized by high fecal propionate [67,68], corresponding with increased propionate levels [67,68], similar to the increase observed in NAFLD mice. Propionate is a key precursor for gluconeogenesis and lipogenesis, and inhibits lipolysis favoring lipid accumulation [68]. Importantly, propionate levels were reduced in NAFLD mice by MI supplementation, supporting the beneficial impact of this treatment in restoring gut-microbiota homeostasis. Furthermore, *Christensenella* levels, which were positively correlated with propionate levels [69] and increased in NAFLD [6], were elevated in NAFLD mice and reduced after MI supplementation. While previous studies showed that *Ruminiclostridium* negatively correlated with propionate [70], we here found elevated levels in MI mice, supporting the beneficial effects of this treatment. Considering that excessive propionate levels inevitably result in L-carnitine deficiency, the supplementation of L-carnitine may modulate propionate levels converting it into beneficial propionyl-carnitine and improving β-oxidation pathways [71]. Moreover, NAC also had a neuroprotective role against oxidative stress that

is caused by propionate preserving GSH levels [71], which could be translated also into the gut after MI treatment. In addition, *Citrobacter* was positively correlated with propionate levels; Lee et al. found *Citrobacter* levels elevated according to fibrosis severity in NAFLD patients [72]. However, this positive correlation was exclusively found in NAFLD mice, but not in the control and MI groups. Therefore, the correlation of elevated levels of propionate with *Citrobacter* could be linked to NAFLD development.

There are some limitations of this observational study. First, the lack of use of single housing and paired-feeding techniques to control food intake individually in mice. However, social housing is essential for rodents, so housing them in individual cages is discouraged [73]. Second, conclusions derived from the present study were sustained in young male mice. Although this situation has commonly occurred in other studies [19,74,75], it is necessary to validate the effect of supplementation with MI in other models, both in older mice and in females. Third, the present study lacks an MI-treated group without NAFLD, but the study design was similar to other studies [19,75,76], and no deleterious effect was expected for this treatment.

In summary, this study successfully demonstrated that the specific combination of metabolic cofactors (NAC, NR, betaine, and LC) is a promising NAFLD nutraceutical, targeting gut-liver crosstalk disease and modulating gut dysfunction and dysbiosis. MI supplementation showed the capacity to recover beneficial bacteria levels and prevent harmful bacterial growth that, together with the restoration of the TJ barrier integrity, protects mice against proinflammatory bacterial product leakage and contributes to diminishing NAFLD development. In addition, MI supplementation induces the reduction of gut microbiota-derived propionate levels linked to decreased levels of Firmicutes contributing to the prevention of propionate-induced lipid accumulation in the liver. Therefore, this is the first study using MI supplementation as a potential treatment to treat gut dysfunction and microbiota dysbiosis associated with NAFLD in an animal model and could be a novel therapeutic strategy to ameliorate gut-liver crosstalk in NAFLD in clinical studies.

4. Materials and Methods

4.1. MI Treatment Composition

MI is a mix of the following compounds: 400 mg/kg of LC tartrate (Cambridge Commodities, Ely, UK), 400 mg/kg NAC (Cambridge Commodities), 800 mg/kg Betaine (Cambridge Commodities), and 400 mg/kg NR (ChromaDex, Los Angeles, CA, USA). LC was administrated through LC tartrate (LCT), containing 68.2% LC, and providing 560 mg/kg to reach the 400 mg LC/kg dose.

4.2. Animal Model and Experimental Design

Twenty-four C57BL/6J; 24 6-week-old male mice (Envigo, Barcelona, Spain) were housed in groups under controlled conditions of temperature (22 ± 2 °C) and humidity (55 ± 10%), and on a 12-h light/dark cycle with free access to food and water (Figure 7). After acclimatization, animals were randomly divided into experimental groups: Control mice (n = 8), kept on a standard diet (D12328, Research Diets, New Brunswick, NJ, USA), and a NAFLD group (n = 16), fed with a high-fat diet (HFHC: D12331, Research Diets) supplemented with 23.1 g/L fructose and 18.9 g/L sucrose in the drinking water. Mice were kept on these diets for a period of 20 weeks in ad libitum conditions [15]. For the last 4 weeks of the study (from the 16th to 20th week), NAFLD mice were randomly distributed into two groups: 8 mice were kept under the same fed conditions described above (NAFLD group), and 8 mice were exposed to multi-ingredient (MI) treatment (NAFLD-MI). Betaine, LCT, NAC, and NR were diluted with drinking water. Solutions were freshly prepared three times per week from stock powders and protected from light [15]. Fresh fecal pellets were rapidly collected 2 days before sacrifice and frozen at −80 °C. After 4 weeks of treatment, mice were sacrificed and small intestines were rapidly collected, measured, weighed, and divided into two sections (the first section was kept in formalin, and the other section was frozen in liquid nitrogen and stored at t −80 °C until further analysis)

(Figure 7). All experimental protocols were approved by the Animal Ethics Committee of the Technological Unit of Nutrition and Health of Eurecat (Reus, Spain), and the Generalitat de Catalunya approved all the procedures (10281). The experimental protocol followed the "Principles of Laboratory Care" guidelines and was carried out in accordance with the European Communities Council Directive (2010/63/EEC).

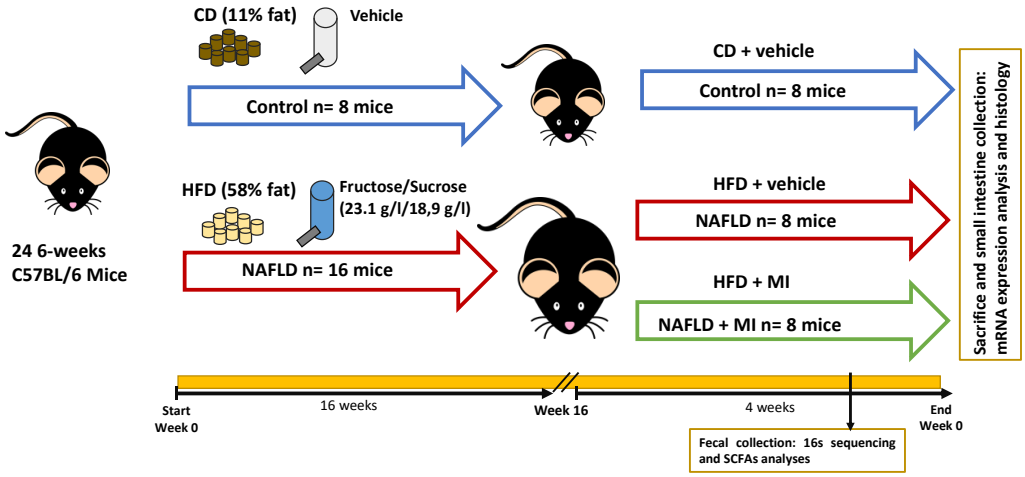

Figure 7. Schematic representation of the study design for the induction of NAFLD in mice (n = 24 animals; n = 8 control mice and n = 16 NAFLD mice), and the following treatment with MI supplementation in NAFLD mice for 4 weeks (n = 8 control mice, n = 8 NAFLD mice, and n = 8 NAFLD-MI mice). The variables analyzed in all study groups are represented. Abbreviations: CD, control-chow diet; HFD, high-fat diet; NAFLD, non-alcoholic fatty liver disease; SCFAS, short chain fatty acids.

4.3. Histological Staining Analysis of Intestinal Sections

To evaluate whether the MI treatment ameliorates intestinal dysfunction associated with NAFLD, physio-pathological features of the jejunum were analyzed. Small intestinal lengths were measured with a ruler. Jejunum sections were fixed in a 4% formaldehyde solution for 24 h and transferred to a 70% ethanol solution until paraffin inclusion. Tissue sections 4 µm thick were cut from paraffin blocks and placed on glass slides. Hematoxylin and eosin (H&E) staining was performed using standard procedures [77]. Small intestine images were taken with a microscope (ECLIPSE Ti; Nikon, Tokyo, Japan) coupled with a digital sight camera (DS-Ri1, Nikon) (10× magnification). To avoid any bias in the analysis, the study had a double-blind design, preventing the reviewers from knowing any data from the mice during the histopathological analysis. The morphometric analysis of the intestinal wall of the jejunum was conducted from these H&E sections. To evaluate villus height (distance from the villus-crypt junction to the top of the villus) and width (measured at the villus, distance between the villus-crypt junctions), crypt depth (depth of the invagination between adjacent villi), muscular layer, and mucosal layer (from the villus apex to the mesothelium of the tunica serosa), three measurements per every section of every animal were randomly made and analyzed using ImageJ NDPI software (National Institutes of Health, Bethesda, MD, USA; available at http://imagej.nih.gov/ij).

4.4. Immunofluorescence Analysis of Intestinal Sections

For intestinal permeability status, immunofluorescence using an anti-Occludin antibody (Abcam, Cambridge, UK) was used in paraffin cut sections of jejunum. A Cy3-labeled secondary antibody was used and slides were mounted in a DAPI-containing solution (Vector Laboratories, Burlingame, CA, USA). Three images per section were taken using a confocal immunofluorescent microscope, Zeiss LSM 800 Axio Observer (Zeiss, Thornwood,

NY, USA) (magnification 40×), and fluorescence intensity was analyzed with Image J software. Fluorescence measured at the lumen of the colonic tissue was used as background fluorescence to subtract from the epithelial fluorescence values. Therefore, fluorescence density values represented the total protein in the epithelial cells [78].

4.5. Immunohistochemistry Analysis of Intestinal Sections

To evaluate epithelial cell proliferation in the small intestine after MI supplementation, Ki-67 immunohistochemistry (IHC) was performed on jejunum sections. Sample sections on slides were deparaffinized and hydrated through a descending scale of alcohol. Antigen retrieval was performed by boiling sections for 10 min in 5 mM sodium citrate buffer (pH 6, Sigma, Darmstadt, Germany) in a microwave oven. Endogenous peroxidase was blocked by incubation with 3% H_2O_2 (Sigma-Aldrich, St. Louis, MO, USA), 50% methanol solution (Sigma, Darmstadt, Germany) in PBS 13 (Lonza, Walkersville, MD, USA) for 20 min at room temperature (RT). The sections were then washed with PBS 1X and incubated for 30 min with rat anti-mouse Ki-67 (Dako, Glostrup, Denmark) diluted 1:50 in PBS, washed and incubated for 30 min RT with biotinylated secondary antibody rabbit anti-rat (Abcam, Cambridge, UK) diluted 1:100 in PBS. Sections were incubated with ABC-kit (Vector Laboratories, Burlingame, CA, USA) and 3,3-diaminobenzidine (DAB, Biocare Medical, Concord, CA, USA), counterstained with hematoxylin, dehydrated through an ascending scale of alcohols and xylene, and mounted with coverslips. All samples were observed and photographed (20× magnification) with a microscope, Olympus BX53, with a digital camera (Olympus Italia s.r.l., Segrate, Italy) and three fields for jejunum sections per mouse were analyzed to quantify proliferative cells by Image J software. Quantification of the number of goblet cells from one side of the villus was performed in these Ki-67-stained images.

4.6. Quantification of Short Chain Fatty Acids in Fecal Samples

Fresh fecal pellets were rapidly collected 2 days before sacrifice and frozen at −80 °C. SCFAs were extracted in 0.5% orthophosphoric acid, as outlined by Zhao et al. and García-Villalba et al. [79,80]. Samples were thawed on ice, centrifuged, and 10 µL of the supernatant was mixed with 90 µL 0.5% orthophosphoric acid containing all isotopically labeled internal standards (5 mM for acetate, 0.25 mM for lactate, and 0.5 mM for the other five). Samples were further centrifuged at 15,000 rpm for 10 min and the supernatant was transferred to the chromatography vials for analysis using LC-MS. For tissue samples, tissues were pulverized using a pestle and mortar under dry ice and mixed into a homogenous powder. An amount of 30 mg of each tissue was mixed with 200 µL of 0.5% orthophosphoric acid in water and homogenized using the Precellys 24 lysis homogenizer at 6000 rpm for two cycles for 30 s (Bertin Technologies, Montigny-le-Bretonneux, France). After centrifugation for 10 min at 4 °C, 45 µL of the supernatant was mixed with 5 µL of 0.5% orthophosphoric acid containing all isotopically labeled internal standards (0.5 mM for all except lactate which was 0.25 mM). Other sample extraction methods, including 100% methanol in 0.5% orthophosphoric acid (85% orthophosphoric acid diluted in methanol) and 50% methanol in 0.5% orthophosphoric acid, were also trialed, but these gave a cloudy mixture that did not completely separate even after centrifugation at 15,000 rpm for 15 min. Quantification of SCFAs by LC-MS/MS analysis was performed following the protocol previously described [81].

4.7. mRNA Extraction for Quantitative Polymerase Chain Reaction

Jejunums were homogenized for total mRNA extractions using TriPure reagent (Roche Diagnostic, Barcelona, Spain) according to the manufacturer's instructions. mRNA concentration and purity were determined using a nanophotometer (Implen GmbH, München, Germany). mRNA was converted to cDNA using a High-Capacity RNA-to-cDNA Kit (Applied Biosystems, Wilmington, DE, USA). The cDNAs were diluted 1:10 before incubation with commercial LightCycler 480 Sybr green I master on a LightCycler® 480 II

(Roche Diagnostics GmbH, Manheim, Germany). Table 3 shows a list of used primers of those genes related to inflammation and intestinal mechanisms to be quantified with qPCR that were previously described in other studies and verified with Primer-Blast software (National Center for Biotechnology Information, Bethesda, MD, USA), using *36b4* as a housekeeping gene [82].

Table 3. Sequences of the oligonucleotides used in the RT-PCR.

Primers	Forward	Reverse	Reference
Cdh-1	5′-CATCCCAGAACCTCGAAACA-3′	5′-TGGGTTAGCTCAGCAGTAA-3′	This study
Cbs	5′-GCAGCGCTGTGTGGTCATC-3′	5′-CATCCATTTGTCACTCAGGAACTT-3′	[15]
Il-1β	5′-GGACCCCAAAAGATGAAGGGCTGC-3′	5′-GCTCTTGTTGATGTGCTGCTGCG-3′	[83]
Klf4	5′-AGCCACCCACACTTGTGACTATG-3′	5′-CAGTGGTAAGGTTTCTCGCCTGTG-3′	[50]
Nlrp3	5′-GCCCAAGGAGGAAGAAGAAG-3′	5′-AGAAGAGACCACGGCAGAAG-3′	[84]
Ocln	5′-ACCCGAAGAAAGATGGATCG-3′	5′-CATAGTCAGATGGGGGTGGA-3′	[85]
Ostα	5′-CACTGGCTCAGTTGCCATTT-3′	5′-GCATACGGCATAAAACGAGGT-3′	[86]
Tnfα	5′-AGGGTCTGGGCCATAGAACT-3′	5′-CCACCACGCTCTTCTGTCTAC-3′	[87]
Zo-1	5′-TGGGAACAGCACACAGTGAC-3′	5′-GCTGGCCCTCCTTTTAACAC-3′	[85]
36b4	5′-AGTCCCTGCCCTTTGTACACA-3′	5′-CGATCCGAGGGCCTCACTA-3′	[82]

4.8. Bacterial Genomic DNA Isolation and 16s rRNA Sequencing

Bacterial genomic DNA was isolated from fecal pellets using an MBP DNA Soil extraction kit. Genomic DNA was normalized to 5 ng/µL with EB (10 mM Tris-HCl), and libraries were performed. Briefly, following a first PCR and clean-up using KAPA Pure Beads (Roche Catalogue No. 07983298001), a second PCR master mix was made up using P7 and P5 of Nextera XT Index Kit v2 index primers (Illumina Catalogue No. FC-131-2001 to 2004). Following the PCR reaction, the libraries were quantified using the Quant-iT dsDNA assay high-sensitivity kit (Catalogue No. 10164582) and run on a FLUOstar Optima plate reader. Libraries were pooled and run on a High Sensitivity D1000 ScreenTape (Agilent Catalogue No. 5067-5579) using the Agilent Tapestation 4200 to calculate the final library pool molarity. The pool was run on an Illumina MiSeq instrument using MiSeq® Reagent Kit v3 (600 cycle) (Illumina Catalogue FC-102-3003) following the Illumina recommended denaturation and loading recommendations, which included a 20% PhiX spike in (PhiX Control v3 Illumina Catalogue FC-110-3001). The raw data was analyzed locally on the MiSeq using MiSeq reporter.

For the 16S sequence analysis, LotuS2 2.19 was used [88] in short read mode, using default quality filtering. Raw 16S rRNA gene amplicon reads were quality filtered to ensure: a minimum length of 170 bp; no more than eight homonucleotides; no ambiguous bases; average quality ≥ 27; and an accumulated read error < 0.5. Filtered reads were clustered using DADA2 [89] into Amplicon sequence variants (ASVs).

Postprocessing included de novo and reference-based chimera removal [90], back mapping dereplicated and mid-quality reads and off-target removal [91], resulting in 1005 ASVs and 4.2Mil out of 5.7Mil read pairs being used in the final analysis. The taxonomy to ASVs was assigned by calculating each ASVs least common ancestor using the LCA of LotuS2 and a mapping against SILVA 138.1 [92]. Abundance matrices were normalized using RTK [93].

4.9. Statistical Analysis

Statistical analyses were performed using GraphPad Prism 9 software (Graph-Pad Software, La Jolla, CA, USA). Data were presented as mean ± SEM. Data distribution was analyzed by the Shapiro–Wilk normality test. Differences between the two groups were determined using an unpaired t-test (two-tailed, 95% confidence interval). One-way analysis of variance (ANOVA) was conducted to examine the differences between the three groups.

Alpha diversity was analyzed using Shannon's diversity index for the bacterial community regarding operational taxonomic units (OTUs) [24].

In addition, 16s rRNA sequencing data analysis was conducted with R statistical language Version 3.00 (The R Foundation; available at https://www.r-project.org/) as described in Hildebrand et al. [94], employing the RTK software [93] or all data normalizations. Statistical differences between multiple samples at Phylum and Genera levels were estimated by Kruskal-Wallis or Mann–Whitney U-test, or Negative Binomial distribution [95] by adjusting for multiple testing according to the method of Benjamini and Hochberg (q-value) [96]. A summary of differences in genus abundance between the different animal groups is listed in Table 1, when the p-value < 0.05.

To investigate further into potential interactions between the SCFAs levels and microbiota diversity, correlation analyses were performed. Origin 8.1 Pro software (OriginLab, Northampton, MA, USA) was used for the Spearman correlation analysis. The genera plotted were those significant in the 16s rRNA sequencing analysis between groups, and those with significant correlations with SCFAs. A p-value below 0.05 was considered statistically significant.

Author Contributions: S.Q.-V., G.A., J.M.d.B., A.C., N.B. and X.E., contributed to the study conception and design. S.Q.-V., C.B., M.C.-P., I.T. and X.E., conducted the study. S.Q.-V., S.S., M.C.-P., F.H. and X.E., did the data acquisition and the data analysis. All authors reviewed the article and were involved in the final version of the manuscript. All authors have read and agreed to the published version of the manuscript.

Funding: The authors gratefully acknowledge the support of the Catalan Government through the funding grant ACCIÓ-Eurecat (PRIV2020-EURHEPAD to X.E.), by the Centre for the Development of Industrial Technology (CDTI) of the Spanish Ministry of Science and Innovation under grant agreement: TECNOMIFOOD project CER-20191010 (to A.C.), by the Biotechnology and Biological Sciences Research Council (BBSRC) Gut Microbes and Health BBS/E/F/00044509 (to N.B and F.H.), the BBSRC Institute Strategic Programme Gut Microbes and Health BB/R012490/1 and its constituent project BBS/E/F/000PR10355, and the BBSRC Core Capability Grant BB/CCG1860/1 as well as the BBSRC Institute Strategic Programme Food Innovation and Health BB/R012512/1 and its constituent project BBS/E/F/000PR10347. F.H. is supported by the European Research Council H2020 StG (erc-stg-948219.EPYC). S.Q.-V. is supported by a fellowship from the Vicente Lopez Program (Eurecat) and M.C.-P. is supported by a fellowship 2021 FI_B2 00150.

Institutional Review Board Statement: All experimental protocols were approved by the Animal Ethics Committee of the Technological Unit of Nutrition and Health of Eurecat (Reus, Spain) and the Generalitat de Catalunya approved all the procedures (10281). The experimental protocol followed the "Principles of Laboratory Care" guidelines and was carried out in accordance with the European Communities Council Directive (2010/63/EEC).

Informed Consent Statement: Not applicable.

Data Availability Statement: The data that support the findings of this study are available from the corresponding author upon reasonable request.

Acknowledgments: We thank J.M. Alcaide; Y. Tobajas; G. Chomiciute; J. Romero and C. Egea for their valuable technical support. We thank Cambridge Commodities and ChromaDex for providing the ingredients of the multi-ingredient.

Conflicts of Interest: The authors declare no conflict of interest.

References

1. Ji, Y.; Yin, Y.; Sun, L.; Zhang, W. The Molecular and Mechanistic Insights Based on Gut–Liver Axis: Nutritional Target for Non-Alcoholic Fatty Liver Disease (NAFLD) Improvement. *Int. J. Mol. Sci.* **2020**, *21*, 3066. [CrossRef] [PubMed]
2. Yao, N.; Yang, Y.; Li, X.; Wang, Y.; Guo, R.; Wang, X.; Li, J.; Xie, Z.; Li, B.; Cui, W. Effects of Dietary Nutrients on Fatty Liver Disease Associated With Metabolic Dysfunction (MAFLD): Based on the Intestinal-Hepatic Axis. *Front. Nutr.* **2022**, *9*, 906511. [CrossRef] [PubMed]
3. Quesada-Vázquez, S.; Aragonès, G.; del Bas, J.M.; Escoté, X. Diet, Gut Microbiota and Non-Alcoholic Fatty Liver Disease: Three Parts of the Same Axis. *Cells* **2020**, *9*, 176. [CrossRef]

4. Isaacs-Ten, A.; Echeandia, M.; Moreno-Gonzalez, M.; Brion, A.; Goldson, A.; Philo, M.; Patterson, A.M.; Parker, A.; Galduroz, M.; Baker, D.; et al. Intestinal Microbiome-Macrophage Crosstalk Contributes to Cholestatic Liver Disease by Promoting Intestinal Permeability in Mice. *Hepatology* **2020**, *72*, 2090–2108. [CrossRef]
5. Liu, Y.; Chen, Y.G. Intestinal Epithelial Plasticity and Regeneration via Cell Dedifferentiation. *Cell Regen.* **2020**, *9*, 14. [CrossRef]
6. Portincasa, P.; Bonfrate, L.; Khalil, M.; de Angelis, M.; Calabrese, F.M.; D'amato, M.; Wang, D.Q.H.; di Ciaula, A. Intestinal Barrier and Permeability in Health, Obesity and NAFLD. *Biomedicines* **2022**, *10*, 83. [CrossRef]
7. Festi, D.; Schiumerini, R.; Birtolo, C.; Marzi, L.; Montrone, L.; Scaioli, E.; di Biase, A.R.; Colecchia, A. Gut Microbiota and Its Pathophysiology in Disease Paradigms. *Dig. Dis.* **2011**, *29*, 518–524. [CrossRef]
8. Jandhyala, S.M.; Talukdar, R.; Subramanyam, C.; Vuyyuru, H.; Sasikala, M.; Reddy, D.N. Role of the Normal Gut Microbiota. *World J. Gastroenterol.* **2015**, *21*, 8836–8847. [CrossRef]
9. Fianchi, F.; Liguori, A.; Gasbarrini, A.; Grieco, A.; Miele, L. Nonalcoholic Fatty Liver Disease (Nafld) as Model of Gut–Liver Axis Interaction: From Pathophysiology to Potential Target of Treatment for Personalized Therapy. *Int. J. Mol. Sci.* **2021**, *22*, 6485. [CrossRef]
10. Tan, J.; McKenzie, C.; Potamitis, M.; Thorburn, A.N.; Mackay, C.R.; Macia, L. The Role of Short-Chain Fatty Acids in Health and Disease. *Adv. Immunol.* **2014**, *121*, 91–119. [CrossRef]
11. Jiang, W.; Wu, N.; Wang, X.; Chi, Y.; Zhang, Y.; Qiu, X.; Hu, Y.; Li, J.; Liu, Y. Dysbiosis Gut Microbiota Associated with Inflammation and Impaired Mucosal Immune Function in Intestine of Humans with Non-Alcoholic Fatty Liver Disease. *Sci. Rep.* **2015**, *5*, 8096. [CrossRef] [PubMed]
12. Lanthier, N.; Delzenne, N. Targeting the Gut Microbiome to Treat Metabolic Dysfunction-Associated Fatty Liver Disease: Ready for Prime Time? *Cells* **2022**, *11*, 2718. [CrossRef] [PubMed]
13. Houghton, D.; Stewart, C.J.; Day, C.P.; Trenell, M. Gut Microbiota and Lifestyle Interventions in NAFLD. *Int. J. Mol. Sci.* **2016**, *17*, 447. [CrossRef] [PubMed]
14. Bauer, K.C.; Littlejohn, P.T.; Ayala, V.; Creus-Cuadros, A.; Finlay, B.B. Nonalcoholic Fatty Liver Disease and the Gut-Liver Axis: Exploring an Undernutrition Perspective. *Gastroenterology* **2022**, *162*, 1858–1875.e2. [CrossRef]
15. Quesada-Vázquez, S.; Colom-Pellicer, M.; Navarro-Masip, È.; Aragonès, G.; del Bas, J.M.; Caimari, A.; Escoté, X. Supplementation with a Specific Combination of Metabolic Cofactors Ameliorates Non-Alcoholic Fatty Liver Disease and, Hepatic Fibrosis, and Insulin Resistance in Mice. *Nutrients* **2021**, *13*, 3532. [CrossRef]
16. Yang, H.; Mayneris-Perxachs, J.; Boqué, N.; del Bas, J.M.; Arola, L.; Yuan, M.; Türkez, H.; Uhlén, M.; Borén, J.; Zhang, C.; et al. Combined Metabolic Activators Decrease Liver Steatosis by Activating Mitochondrial Metabolism in Hamsters Fed with a High-Fat Diet. *Biomedicines* **2021**, *9*, 1440. [CrossRef]
17. Mardinoglu, A.; Ural, D.; Zeybel, M.; Yuksel, H.H.; Uhlén, M.; Borén, J. The Potential Use of Metabolic Cofactors in Treatment of NAFLD. *Nutrients* **2019**, *11*, 1578. [CrossRef]
18. Zhang, C.; Bjornson, E.; Arif, M.; Tebani, A.; Lovric, A.; Benfeitas, R.; Ozcan, M.; Juszczak, K.; Kim, W.; Kim, J.T.; et al. The Acute Effect of Metabolic Cofactor Supplementation: A Potential Therapeutic Strategy against Non-alcoholic Fatty Liver Disease. *Mol. Syst. Biol.* **2020**, *16*, e9495. [CrossRef]
19. Mardinoglu, A.; Bjornson, E.; Zhang, C.; Klevstig, M.; Söderlund, S.; Ståhlman, M.; Adiels, M.; Hakkarainen, A.; Lundbom, N.; Kilicarslan, M.; et al. Personal Model-assisted Identification of NAD + and Glutathione Metabolism as Intervention Target in NAFLD. *Mol. Syst. Biol.* **2017**, *13*, 916. [CrossRef]
20. Xia, Y.; Li, Q.; Zhong, W.; Dong, J.; Wang, Z.; Wang, C. L-Carnitine Ameliorated Fatty Liver in High-Calorie Diet/STZ-Induced Type 2 Diabetic Mice by Improving Mitochondrial Function. *Diabetol. Metab. Syndr.* **2011**, *3*, 31. [CrossRef]
21. Dludla, P.V.; Nkambule, B.B.; Mazibuko-Mbeje, S.E.; Nyambuya, T.M.; Marcheggiani, F.; Cirilli, I.; Ziqubu, K.; Shabalala, S.C.; Johnson, R.; Louw, J.; et al. N-Acetyl Cysteine Targets Hepatic Lipid Accumulation to Curb Oxidative Stress and Inflammation in Nafld: A Comprehensive Analysis of the Literature. *Antioxidants* **2020**, *9*, 1283. [CrossRef] [PubMed]
22. Khodayar, M.J.; Kalantari, H.; Khorsandi, L.; Rashno, M.; Zeidooni, L. Betaine Protects Mice against Acetaminophen Hepatotoxicity Possibly via Mitochondrial Complex II and Glutathione Availability. *Biomed. Pharmacother.* **2018**, *103*, 1436–1445. [CrossRef] [PubMed]
23. Cantó, C.; Houtkooper, R.H.; Pirinen, E.; Youn, D.Y.; Oosterveer, M.H.; Cen, Y.; Fernandez-Marcos, P.J.; Yamamoto, H.; Andreux, P.A.; Cettour-Rose, P.; et al. The NAD+ Precursor Nicotinamide Riboside Enhances Oxidative Metabolism and Protects against High-Fat Diet-Induced Obesity. *Cell Metab.* **2012**, *15*, 838–847. [CrossRef] [PubMed]
24. Zhang, Y.; Tang, K.; Deng, Y.; Chen, R.; Liang, S.; Xie, H.; He, Y.; Chen, Y.; Yang, Q. Effects of Shenling Baizhu Powder Herbal Formula on Intestinal Microbiota in High-Fat Diet-Induced NAFLD Rats. *Biomed. Pharmacother.* **2018**, *102*, 1025–1036. [CrossRef]
25. Zhao, Z.; Chen, L.; Zhao, Y.; Wang, C.; Duan, C.; Yang, G.; Niu, C.; Li, S. Lactobacillus Plantarum NA136 Ameliorates Nonalcoholic Fatty Liver Disease by Modulating Gut Microbiota, Improving Intestinal Barrier Integrity, and Attenuating Inflammation. *Appl. Microbiol. Biotechnol.* **2020**, *104*, 5273–5282. [CrossRef]
26. Wu, S.; Hu, R.; Nakano, H.; Chen, K.; Liu, M.; He, X.; Zhang, H.; He, J.; Hou, D.X. Modulation of Gut Microbiota by Lonicera Caerulea l. Berry Polyphenols in a Mouse Model of Fatty Liver Induced by High Fat Diet. *Molecules* **2018**, *23*, 3213. [CrossRef]
27. Jung, Y.; Kim, I.; Mannaa, M.; Kim, J.; Wang, S.; Park, I.; Kim, J.; Seo, Y.S. Effect of Kombucha on Gut-Microbiota in Mouse Having Non-Alcoholic Fatty Liver Disease. *Food Sci. Biotechnol.* **2019**, *28*, 261–267. [CrossRef]

28. Suárez, M.; Boqué, N.; del Bas, J.M.; Mayneris-Perxachs, J.; Arola, L.; Caimari, A. Mediterranean Diet and Multi-Ingredient-Based Interventions for the Management of Non-Alcoholic Fatty Liver Disease. *Nutrients* **2017**, *9*, 1052. [CrossRef]
29. Taylor, S.R.; Ramsamooj, S.; Liang, R.J.; Katti, A.; Pozovskiy, R.; Vasan, N.; Hwang, S.K.; Nahiyaan, N.; Francoeur, N.J.; Schatoff, E.M.; et al. Dietary Fructose Improves Intestinal Cell Survival and Nutrient Absorption. *Nature* **2021**, *597*, 263–267. [CrossRef]
30. Soares, A.; Beraldi, E.J.; Ferreira, P.E.B.; Bazotte, R.B.; Buttow, N.C. Intestinal and Neuronal Myenteric Adaptations in the Small Intestine Induced by a High-Fat Diet in Mice. *BMC Gastroenterol.* **2015**, *15*, 3. [CrossRef]
31. Igarashi, M.; Miura, M.; Williams, E.; Jaksch, F.; Kadowaki, T.; Yamauchi, T.; Guarente, L. NAD+ Supplementation Rejuvenates Aged Gut Adult Stem Cells. *Aging Cell* **2019**, *18*, e12935. [CrossRef] [PubMed]
32. Wang, H.; Li, S.; Fang, S.; Yang, X.; Feng, J. Betaine Improves Intestinal Functions by Enhancing Digestive Enzymes, Ameliorating Intestinal Morphology, and Enriching Intestinal Microbiota in High-Salt Stressed Rats. *Nutrients* **2018**, *10*, 907. [CrossRef] [PubMed]
33. Lauz Medeiros, S.H.; de Oliveira Menezes, A.; Zogbi, L.; Frasson de Souza Montero, E. N-Acetylcysteine Use in Hepatic Ischemia/Reperfusion in Rats Minimizing Bowel Injury. *Transplant. Proc.* **2016**, *48*, 2371–2374. [CrossRef] [PubMed]
34. Febbraio, M.A.; Reibe, S.; Shalapour, S.; Ooi, G.J.; Watt, M.J.; Karin, M. Preclinical Models for Studying NASH-Driven HCC: How Useful Are They? *Cell Metab.* **2019**, *29*, 18–26. [CrossRef] [PubMed]
35. Strowig, T.; Henao-Mejia, J.; Elinav, E.; Flavell, R. Inflammasomes in Health and Disease. *Nature* **2012**, *481*, 278–286. [CrossRef]
36. Schuppan, D.; Afdhal, N.H. Liver Cirrhosis. *Lancet* **2008**, *371*, 838–851. [CrossRef]
37. Guo, X.; Li, J.; Tang, R.; Zhang, G.; Zeng, H.; Wood, R.J.; Liu, Z. High Fat Diet Alters Gut Microbiota and the Expression of Paneth Cell-Antimicrobial Peptides Preceding Changes of Circulating Inflammatory Cytokines. *Mediat. Inflamm.* **2017**, *2017*, 9474896. [CrossRef]
38. Zhao, W.; Xiao, M.; Yang, J.; Zhang, L.; Ba, Y.; Xu, R.; Liu, Z.; Zou, H.; Yu, P.; Wu, X.; et al. The Combination of Ilexhainanoside D and Ilexsaponin A1 Reduces Liver Inflammation and Improves Intestinal Barrier Function in Mice with High-Fat Diet-Induced Non-Alcoholic Fatty Liver Disease. *Phytomedicine* **2019**, *63*, 153039. [CrossRef]
39. Moeinian, M.; Ghasemi-Niri, S.F.; Mozaffari, S.; Abdolghaffari, A.H.; Baeeri, M.; Navaea-Nigjeh, M.; Abdollahi, M. Beneficial Effect of Butyrate, Lactobacillus Casei and L-Carnitine Combination in Preference to Each in Experimental Colitis. *World J. Gastroenterol.* **2014**, *20*, 10876–10885. [CrossRef]
40. Chen, Q.; Wang, Y.; Jiao, F.; Shi, C.; Pei, M.; Wang, L.; Gong, Z. Betaine Inhibits Toll-like Receptor 4 Responses and Restores Intestinal Microbiota in Acute Liver Failure Mice. *Sci. Rep.* **2020**, *10*, 21850. [CrossRef]
41. Lee, S.I.; Kang, K.S. N-Acetylcysteine Modulates Lipopolysaccharide-Induced Intestinal Dysfunction. *Sci. Rep.* **2019**, *9*, 1004. [CrossRef]
42. Lee, S.H. Intestinal Permeability Regulation by Tight Junction: Implication on Inflammatory Bowel Diseases. *Intest. Res.* **2015**, *13*, 11. [CrossRef] [PubMed]
43. Werge, M.P.; McCann, A.; Galsgaard, E.D.; Holst, D.; Bugge, A.; Albrechtsen, N.J.W.; Gluud, L.L. The Role of the Transsulfuration Pathway in Non-Alcoholic Fatty Liver Disease. *J. Clin. Med.* **2021**, *10*, 1081. [CrossRef] [PubMed]
44. Wu, C.; Xu, Z.; Huang, K. Effects of Dietary Selenium on Inflammation and Hydrogen Sulfide in the Gastrointestinal Tract in Chickens. *Biol. Trace Elem. Res.* **2016**, *174*, 428–435. [CrossRef] [PubMed]
45. Maclean, K.N.; Sikora, J.; Kožich, V.; Jiang, H.; Greiner, L.S.; Kraus, E.; Krijt, J.; Crnic, L.S.; Allen, R.H.; Stabler, S.P.; et al. Cystathionine Beta-Synthase Null Homocystinuric Mice Fail to Exhibit Altered Hemostasis or Lowering of Plasma Homocysteine in Response to Betaine Treatment. *Mol. Genet. Metab.* **2010**, *101*, 163–171. [CrossRef]
46. Rohr, M.W.; Narasimhulu, C.A.; Rudeski-Rohr, T.A.; Parthasarathy, S. Negative Effects of a High-Fat Diet on Intestinal Permeability: A Review. *Adv. Nutr.* **2020**, *11*, 77–91. [CrossRef] [PubMed]
47. Wang, T.; Gotoh, Y.; Jennings, M.H.; Ann Rhoads, C.; Yee, T.A. Lipid Hydroperoxide-Induced Apoptosis in Human Colonic CaCo-2 Cells Is Associated with an Early Loss of Cellular Redox Balance. *FASEB J.* **2000**, *14*, 1567–1576. [CrossRef] [PubMed]
48. Bressenot, A.; Pooya, S.; Bossenmeyer-Pourie, C.; Gauchotte, G.; Germain, A.; Chevaux, J.B.; Coste, F.; Vignaud, J.M.; Guéant, J.L.; Peyrin-Biroulet, L. Methyl Donor Deficiency Affects Small-Intestinal Differentiation and Barrier Function in Rats. *Br. J. Nutr.* **2013**, *109*, 667–677. [CrossRef]
49. Kruidenier, L.; Verspaget, H.W. Oxidative Stress as a Pathogenic Factor in Inflammatory Bowel Disease. *Aliment. Pharmacol. Ther.* **2002**, *16*, 1997–2015. [CrossRef]
50. Gulhane, M.; Murray, L.; Lourie, R.; Tong, H.; Sheng, Y.H.; Wang, R.; Kang, A.; Schreiber, V.; Wong, K.Y.; Magor, G.; et al. High Fat Diets Induce Colonic Epithelial Cell Stress and Inflammation That Is Reversed by IL-22. *Sci. Rep.* **2016**, *6*, 28990. [CrossRef]
51. Katano, T.; Bialkowska, A.B.; Yang, V.W. KLF4 Regulates Goblet Cell Differentiation in BMI1+ Reserve Intestinal Stem Cell Lineage during Homeostasis. *Int. J. Stem Cells* **2020**, *13*, 424–431. [CrossRef] [PubMed]
52. Ommati, M.M.; Farshad, O.; Mousavi, K.; Jamshidzadeh, A.; Azmoon, M.; Heidari, S.; Azarpira, N.; Niknahad, H.; Heidari, R. Betaine Supplementation Mitigates Intestinal Damage and Decreases Serum Bacterial Endotoxin in Cirrhotic Rats. *PharmaNutrition* **2020**, *12*, 100179. [CrossRef]
53. le Roy, T.; Llopis, M.; Lepage, P.; Bruneau, A.; Rabot, S.; Bevilacqua, C.; Martin, P.; Philippe, C.; Walker, F.; Bado, A.; et al. Intestinal Microbiota Determines Development of Non-Alcoholic Fatty Liver Disease in Mice. *Gut* **2013**, *62*, 1787–1794. [CrossRef] [PubMed]

54. Thevaranjan, N.; Puchta, A.; Schulz, C.; Naidoo, A.; Szamosi, J.C.; Verschoor, C.P.; Loukov, D.; Schenck, L.P.; Jury, J.; Foley, K.P.; et al. Age-Associated Microbial Dysbiosis Promotes Intestinal Permeability, Systemic Inflammation, and Macrophage Dysfunction. *Cell Host Microbe* **2017**, *21*, 455–466.e4. [CrossRef] [PubMed]
55. Koliada, A.; Syzenko, G.; Moseiko, V.; Budovska, L.; Puchkov, K.; Perederiy, V.; Gavalko, Y.; Dorofeyev, A.; Romanenko, M.; Tkach, S.; et al. Association between Body Mass Index and Firmicutes/Bacteroidetes Ratio in an Adult Ukrainian Population. *BMC Microbiol.* **2017**, *17*, 120. [CrossRef] [PubMed]
56. Zheng, J.; Yuan, X.; Zhang, C.; Jia, P.; Jiao, S.; Zhao, X.; Yin, H.; Du, Y.; Liu, H. N-Acetylcysteine Alleviates Gut Dysbiosis and Glucose Metabolic Disorder in High-Fat Diet-Fed Mice. *J. Diabetes* **2019**, *11*, 32–45. [CrossRef]
57. Zeybel, M.; Altay, O.; Arif, M.; Li, X.; Yang, H.; Fredolini, C.; Akyildiz, M.; Saglam, B.; Gonenli, M.G.; Ural, D.; et al. Combined Metabolic Activators Therapy Ameliorates Liver Fat in Nonalcoholic Fatty Liver Disease Patients. *Mol. Syst. Biol.* **2021**, *17*, e10459. [CrossRef]
58. Raman, M.; Ahmed, I.; Gillevet, P.M.; Probert, C.S.; Ratcliffe, N.M.; Smith, S.; Greenwood, R.; Sikaroodi, M.; Lam, V.; Crotty, P.; et al. Fecal Microbiome and Volatile Organic Compound Metabolome in Obese Humans with Nonalcoholic Fatty Liver Disease. *Clin. Gastroenterol. Hepatol.* **2013**, *11*, 868–875.e3. [CrossRef]
59. Raimondi, S.; Musmeci, E.; Candeliere, F.; Amaretti, A.; Rossi, M. Identification of Mucin Degraders of the Human Gut Microbiota. *Sci. Rep.* **2021**, *11*, 11094. [CrossRef]
60. Cui, H.; Li, Y.; Wang, Y.; Jin, L.; Yang, L.; Wang, L.; Liao, J.; Wang, H.; Peng, Y.; Zhang, Z.; et al. Da-Chai-Hu Decoction Ameliorates High Fat Diet-Induced Nonalcoholic Fatty Liver Disease Through Remodeling the Gut Microbiota and Modulating the Serum Metabolism. *Front Pharmacol.* **2020**, *11*, 584090. [CrossRef]
61. Zhang, X.; Coker, O.O.; Chu, E.S.H.; Fu, K.; Lau, H.C.H.; Wang, Y.X.; Chan, A.W.H.; Wei, H.; Yang, X.; Sung, J.J.Y.; et al. Dietary Cholesterol Drives Fatty Liver-Associated Liver Cancer by Modulating Gut Microbiota and Metabolites. *Gut* **2021**, *70*, 761–774. [CrossRef] [PubMed]
62. Kudo, C.; Kessoku, T.; Kamata, Y.; Hidaka, K.; Kurihashi, T.; Iwasaki, T.; Takashiba, S.; Kodama, T.; Tamura, T.; Nakajima, A.; et al. Relationship between Non-Alcoholic Fatty Liver Disease and Periodontal Disease: A Review and Study Protocol on the Effect of Periodontal Treatment on Non-Alcoholic Fatty Liver Disease. *J. Transl. Sci.* **2016**, *2*, 340–345. [CrossRef]
63. Yin, X.; Peng, J.; Zhao, L.; Yu, Y.; Zhang, X.; Liu, P.; Feng, Q.; Hu, Y.; Pang, X. Structural Changes of Gut Microbiota in a Rat Non-Alcoholic Fatty Liver Disease Model Treated with a Chinese Herbal Formula. *Syst. Appl. Microbiol.* **2013**, *36*, 188–196. [CrossRef]
64. John, U.V.; Carvalho, J. Enterococcus: Review of Its Physiology, Pathogenesis, Diseases and the Challenges It Poses for Clinical Microbiology. *Front. Biol. (Beijing)* **2011**, *6*, 357–366. [CrossRef]
65. Fukui, H. Role of Gut Dysbiosis in Liver Diseases: What Have We Learned So Far? *Diseases* **2019**, *7*, 58. [CrossRef] [PubMed]
66. Mu, H.; Zhou, Q.; Yang, R.; Zeng, J.; Li, X.; Zhang, R.; Tang, W.; Li, H.; Wang, S.; Shen, T.; et al. Naringin Attenuates High Fat Diet Induced Non-Alcoholic Fatty Liver Disease and Gut Bacterial Dysbiosis in Mice. *Front. Microbiol.* **2020**, *11*, 585066. [CrossRef]
67. Rau, M.; Rehman, A.; Dittrich, M.; Groen, A.K.; Hermanns, H.M.; Seyfried, F.; Beyersdorf, N.; Dandekar, T.; Rosenstiel, P.; Geier, A. Fecal SCFAs and SCFA-Producing Bacteria in Gut Microbiome of Human NAFLD as a Putative Link to Systemic T-Cell Activation and Advanced Disease. *United Eur. Gastroenterol. J.* **2018**, *6*, 1496–1507. [CrossRef]
68. Schwiertz, A.; Taras, D.; Schäfer, K.; Beijer, S.; Bos, N.A.; Donus, C.; Hardt, P.D. Microbiota and SCFA in Lean and Overweight Healthy Subjects. *Obesity* **2010**, *18*, 190–195. [CrossRef]
69. Upadhyaya, B.; McCormack, L.; Fardin-Kia, A.R.; Juenemann, R.; Nichenametla, S.; Clapper, J.; Specker, B.; Dey, M. Impact of Dietary Resistant Starch Type 4 on Human Gut Microbiota and Immunometabolic Functions. *Sci. Rep.* **2016**, *6*, 28797. [CrossRef]
70. Feng, Y.; Huang, Y.; Wang, Y.; Wang, P.; Wang, F. Severe Burn Injury Alters Intestinal Microbiota Composition and Impairs Intestinal Barrier in Mice. *Burns Trauma* **2019**, *7*, s41038-019-0156-1. [CrossRef]
71. Killingsworth, J.; Sawmiller, D.; Shytle, R.D. Propionate and Alzheimer's Disease. *Front. Aging Neurosci.* **2021**, *12*, 580001. [CrossRef] [PubMed]
72. Lee, G.; You, H.J.; Bajaj, J.S.; Joo, S.K.; Yu, J.; Park, S.; Kang, H.; Park, J.H.; Kim, J.H.; Lee, D.H.; et al. Distinct Signatures of Gut Microbiome and Metabolites Associated with Significant Fibrosis in Non-Obese NAFLD. *Nat. Commun.* **2020**, *11*, 4982. [CrossRef] [PubMed]
73. Van Loo, P.L.P.; Kuin, N.; Sommer, R.; Avsaroglu, H.; Pham, T.; Baumans, V. Impact of "living Apart Together" on Postoperative Recovery of Mice Compared with Social and Individual Housing. *Lab. Anim.* **2007**, *41*, 441–455. [CrossRef] [PubMed]
74. Liu, Y.; Li, Q.; Wang, H.; Zhao, X.; Li, N.; Zhang, H.; Chen, G.; Liu, Z. Fish Oil Alleviates Circadian Bile Composition Dysregulation in Male Mice with NAFLD. *J. Nutr. Biochem.* **2019**, *69*, 53–62. [CrossRef] [PubMed]
75. Salic, K.; Gart, E.; Seidel, F.; Verschuren, L.; Caspers, M.; van Duyvenvoorde, W.; Wong, K.E.; Keijer, J.; Bobeldijk-Pastorova, I.; Wielinga, P.Y.; et al. Combined Treatment with L-Carnitine and Nicotinamide Riboside Improves Hepatic Metabolism and Attenuates Obesity and Liver Steatosis. *Int. J. Mol. Sci.* **2019**, *20*, 4359. [CrossRef]
76. Martínez-Fernández, L.; González-Muniesa, P.; Sáinz, N.; Laiglesia, L.M.; Escoté, X.; Martínez, J.A.; Moreno-Aliaga, M.J. Maresin 1 Regulates Hepatic FGF21 in Diet-Induced Obese Mice and in Cultured Hepatocytes. *Mol. Nutr. Food Res.* **2019**, *63*, e1900358. [CrossRef]
77. Cardiff, R.D.; Miller, C.H.; Munn, R.J. Manual Hematoxylin and Eosin Staining of Mouse Tissue Sections. *Cold Spring Harb. Protoc.* **2014**, *2014*, 655–658. [CrossRef]

78. Mir, H.; Meena, A.S.; Chaudhry, K.K.; Shukla, P.K.; Gangwar, R.; Manda, B.; Padala, M.K.; Shen, L.; Turner, J.R.; Dietrich, P.; et al. Occludin Deficiency Promotes Ethanol-Induced Disruption of Colonic Epithelial Junctions, Gut Barrier Dysfunction and Liver Damage in Mice. *Biochim. Biophys. Acta Gen. Subj.* **2016**, *1860*, 765–774. [CrossRef]
79. García-Villalba, R.; Giménez-Bastida, J.A.; García-Conesa, M.T.; Tomás-Barberán, F.A.; Carlos Espín, J.; Larrosa, M. Alternative Method for Gas Chromatography-Mass Spectrometry Analysis of Short-Chain Fatty Acids in Faecal Samples. *J. Sep. Sci.* **2012**, *35*, 1906–1913. [CrossRef]
80. Zhao, G.; Nyman, M.; Jönsson, J.Å. Rapid Determination of Short-Chain Fatty Acids in Colonic Contents and Faeces of Humans and Rats by Acidified Water-Extraction and Direct-Injection Gas Chromatography. *Biomed. Chromatogr.* **2006**, *20*, 674–682. [CrossRef]
81. Saha, S.; Day-Walsh, P.; Shehata, E.; Kroon, P.A. Development and Validation of a Lc-Ms/Ms Technique for the Analysis of Short Chain Fatty Acids in Tissues and Biological Fluids without Derivatisation Using Isotope Labelled Internal Standards. *Molecules* **2021**, *26*, 6444. [CrossRef] [PubMed]
82. Dunoyer-Geindre, S.; Kruithof, E.K.O. Epigenetic Control of Tissue-Type Plasminogen Activator Synthesis in Human Endothelial Cells. *Cardiovasc. Res.* **2011**, *90*, 457–463. [CrossRef] [PubMed]
83. Shynlova, O.; Dorogin, A.; Li, Y.; Lye, S. Inhibition of Infection-Mediated Preterm Birth by Administration of Broad Spectrum Chemokine Inhibitor in Mice. *J. Cell Mol. Med.* **2014**, *18*, 1816–1829. [CrossRef] [PubMed]
84. Beaumont, M.; Neyrinck, A.M.; Olivares, M.; Rodriguez, J.; de Rocca Serra, A.; Roumain, M.; Bindels, L.B.; Cani, P.D.; Evenepoel, P.; Muccioli, G.G.; et al. The Gut Microbiota Metabolite Indole Alleviates Liver Inflammation in Mice. *FASEB J.* **2018**, *32*, 6681–6693. [CrossRef] [PubMed]
85. Zhao, H.; Zhao, C.; Dong, Y.; Zhang, M.; Wang, Y.; Li, F.; Li, X.; McClain, C.; Yang, S.; Feng, W. Inhibition of MiR122a by Lactobacillus Rhamnosus GG Culture Supernatant Increases Intestinal Occludin Expression and Protects Mice from Alcoholic Liver Disease. *Toxicol. Lett.* **2015**, *234*, 194–200. [CrossRef] [PubMed]
86. Moscovitz, J.E.; Kong, B.; Buckley, K.; Buckley, B.; Guo, G.L.; Aleksunes, L.M. Restoration of Enterohepatic Bile Acid Pathways in Pregnant Mice Following Short Term Activation of Fxr by GW4064. *Toxicol. Appl. Pharmacol.* **2016**, *310*, 60–67. [CrossRef] [PubMed]
87. Zhao, X.; Li, R.; Liu, Y.; Zhang, X.; Zhang, M.; Zeng, Z.; Wu, L.; Gao, X.; Lan, T.; Wang, Y. Polydatin Protects against Carbon Tetrachloride-Induced Liver Fibrosis in Mice. *Arch. Biochem. Biophys.* **2017**, *629*, 1–7. [CrossRef]
88. Özkurt, E.; Fritscher, J.; Soranzo, N.; Ng, D.Y.K.; Davey, R.P.; Bahram, M.; Hildebrand, F. LotuS2: An Ultrafast and Highly Accurate Tool for Amplicon Sequencing Analysis. *bioRxiv* **2021**, *12*, 474111. [CrossRef]
89. Callahan, B.J.; McMurdie, P.J.; Rosen, M.J.; Han, A.W.; Johnson, A.J.A.; Holmes, S.P. DADA2: High-Resolution Sample Inference from Illumina Amplicon Data. *Nat. Methods* **2016**, *13*, 581–583. [CrossRef]
90. Edgar, R.C. UNOISE2: Improved Error-Correction for Illumina 16S and ITS Amplicon Sequencing. *bioRxiv* **2016**, 081257. [CrossRef]
91. Bedarf, J.R.; Beraza, N.; Khazneh, H.; Özkurt, E.; Baker, D.; Borger, V.; Wüllner, U.; Hildebrand, F. Much Ado about Nothing? Off-Target Amplification Can Lead to False-Positive Bacterial Brain Microbiome Detection in Healthy and Parkinson's Disease Individuals. *Microbiome* **2021**, *9*, 75. [CrossRef] [PubMed]
92. Quast, C.; Pruesse, E.; Yilmaz, P.; Gerken, J.; Schweer, T.; Yarza, P.; Peplies, J.; Glöckner, F.O. The SILVA Ribosomal RNA Gene Database Project: Improved Data Processing and Web-Based Tools. *Nucleic Acids Res.* **2013**, *41*, D590–D596. [CrossRef] [PubMed]
93. Saary, P.; Forslund, K.; Bork, P.; Hildebrand, F. RTK: Efficient Rarefaction Analysis of Large Datasets. *Bioinformatics* **2017**, *33*, 2594–2595. [CrossRef] [PubMed]
94. Hildebrand, F.; Moitinho-Silva, L.; Blasche, S.; Jahn, M.T.; Gossmann, T.I.; Huerta-Cepas, J.; Hercog, R.; Luetge, M.; Bahram, M.; Pryszlak, A.; et al. Antibiotics-Induced Monodominance of a Novel Gut Bacterial Order. *Gut* **2019**, *68*, 1781–1790. [CrossRef]
95. Love, M.I.; Huber, W.; Anders, S. Moderated Estimation of Fold Change and Dispersion for RNA-Seq Data with DESeq2. *Genome Biol.* **2014**, *15*, 550. [CrossRef]
96. Benjamini, Y. Controlling the False Discovery Rate-A Practical And Powerful Approach To Multiple Testing. *J. R. Stat. Soc. B Stat. Methodol.* **1995**, *57*, 289–300. [CrossRef]

Chapter 4

Histidine metabolism is a key player in the regulation of obesity and adipose tissue

Sergio Quesada-Vázquez [1], Jèssica Latorre [2], Juan María Alcaide-Hidalgo [1], Rémy Burcelin[3,4], Marc-Emmanuel Dumas[5,6,7,8], Massimo Federici[9], Lesley Hoyles[10], Laura Herrero [11], Josep Maria Del Bas [12], Xavier Escoté [1]*, José-Manuel Fernández-Real [2]*, Jordi Mayneris-Perxachs[2]

[1] Eurecat, Centre Tecnològic de Catalunya, Unitat de Nutrició i Salut, Reus, Spain.
[2] Department of Endocrinology, Diabetes and Nutrition, Hospital of Girona "Dr Josep Trueta", University of Girona and CIBERobn Pathophysiology of Obesity and Nutrition, Instituto de Salud Carlos III, Madrid, Spain.
[3] Institut National de la Santé et de la Recherche Médicale (INSERM), Toulouse, France. 8 Université Paul Sabatier (UPS), Unité Mixte de Recherche (UMR) 104.
[4] Institut des Maladies Métaboliques et Cardiovasculaires (I2MC), Team 2: 'Intestinal Risk Factors, Diabetes, Dyslipidemia, and Heart Failure', 31432 Toulouse Cedex 4, France.
[5] Section of Biomolecular Medicine, Division of Systems Medicine, Department of Metabolism, Digestion and Reproduction, Imperial College London, Exhibition Road, London SW7 2AZ, UK.
[6] Section of Genomic and Environmental Medicine, National Heart & Lung Institute, Imperial College London, Dovehouse Street, London SW3 6LY, UK.
[7] European Genomic Institute for Diabetes, CNRS UMR 8199, INSERM UMR 1283, Institut Pasteur de Lille, Lille University Hospital, University of Lille, 59045 Lille, France.
[8] McGill University and Genome Quebec Innovation Centre, 740 Doctor Penfield Avenue, Montréal, QC H3A 0G1, Canada.
[10] Department of Systems Medicine, University of Rome Tor Vergata, Via Montpellier 1, 00133 Rome, Italy.
[11] Department of Biosciences, School of Science and Technology, Nottingham Trent University, Nottingham NG11 8NS, UK.
[11] Department of Biochemistry and Physiology, School of Pharmacy and Food Sciences, Institut de Biomedicina de la Universitat de Barcelona (IBUB), Universitat de Barcelona, E-08028 Barcelona, Spain; Centro de Investigación Biomédica en Red de Fisiopatología de la Obesidad y la Nutrición (CIBEROBN), Instituto de Salud Carlos III, Madrid, Spain.
[12] Eurecat, Centre Tecnològic de Catalunya, Àrea Biotecnologia, Reus, Spain.

* Correspondence: xavier.escote@eurecat.org and jmfreal@idibgi.org

Manuscript in preparation

Abstract

Obesity is one of the most prevalent diseases in the world defined as an abnormal or excessive fat accumulation in adipose tissue depots and is strongly connected to the development of different risk factors, such as metabolic syndrome, insulin resistance (IR), and dyslipidemia, which are linked to adipose tissue disruption. Histidine is an essential amino acid that is obtained through the diet and participates in different metabolic pathways with unique roles. Therefore, we performed a systems medicine analysis in three human cohorts (FLORINASH *n* = 74; IMAGEOMICS2: *n* = 916; OUTBRAT: *n* =251) to assess circulating histidine levels and histamine-related genes expression in obese patients, and histidine-related amino acids (HAA) treatment composed of l-histidine, l-cysteine, l-serine, and l-carnosine was proven as a promising treatment in an obese mouse model. Plasma histidine was negatively associated, and histamine-related genes were positively correlated with obesity. P53 regulation, proteasome degradation, and NOTCH signaling pathways were strongly associated with histidine. HAA treatment ameliorated obesity by improving adiposity and lipid metabolism both in white (WAT) and brown adipose tissue (BAT). In line, insulin resistance was decreased in obese mice, whose insulin sensitizer effect was also observed both in WAT and BAT after HAA supplementation. We have unraveled a significant interplay between HAA supplementation and histamine receptors' activity in the modulation of lipid metabolism in adipose tissue and obesity progression.

Keywords: Obesity, histidine, insulin resistance, adipose tissue, thermogenesis, amino acids

1. Introduction

Obesity is described by the World Health Organization (WHO) as one of the most prevalent diseases in the world defined as an abnormal or excessive fat accumulation in adipose tissue depots increasing body fat and causing weight gain that increases the risk of developing multiple disease conditions and impairs human health [1]. Obesity is strongly connected to the development of different risk factors, such as metabolic syndrome, insulin resistance (IR), and dyslipidemia, which are linked to adipose tissue disruption [2]. Adipose tissue is classified as white adipose tissue (WAT) and brown adipose tissue (BAT) [3]. WAT is determined by its fat storage capacity and endocrine function, and BAT protects the individual against hypothermia by dissipating energy as heat called non-shivering thermogenesis [3]. Adipose tissue remodeling depends on adipose tissue location, classified as subcutaneous adipose tissue (scWAT) or visceral adipose tissue (VAT) in WAT. The exhaustion of the lipid storing capacity in VAT is critical in the induction of ectopic storage and is more susceptible to developing a chronic low-grade inflammatory state due to infiltration of macrophages and immune cells being a key determinant of the relative risk for metabolic disorders [3,4]. On the other hand, BAT mass and activity are decreased in NAFLD and diabetic patients [5,6], and higher levels of inflammation were observed in NAFLD and hyperglycemic mice [7]. Hence, the amelioration of BAT disruption could be a new therapeutic target to reduce obesity.

Amino acids are the basic unit of proteins and intermediates of other biomolecules that are crucial for different metabolic pathways. Thus, amino acid levels have been observed to decrease in some metabolic diseases, such as NAFLD or diabetes [8,9]. Histidine is an essential amino acid that is obtained through the diet and participates in different metabolic pathways with unique roles, such as in proton buffering, metal ion chelation, scavenging of reactive oxygen and nitrogen species, the histaminergic system, and a role of several proteins and peptides [10,11], and a possible role of this amino acid in metabolic disorders is suggested [12]. Nevertheless, low plasma concentrations of histidine have been described in metabolic comorbidities correlated with insulin resistance [13]. In this line, histidine supplementation has been proposed as a potential treatment for different diseases, including insulin resistance in metabolic syndrome [14–16]. These results from several studies have shown that supplementation with histidine and histidine-related amino acids may improve obesity, and

T1DM and T2DM and glycemic control, but further studies are needed to elucidate the effect on mechanisms in adipose tissue during these metabolic disorders [11,17–20]. In addition, it was previously suggested that histamine receptors participate in lipid metabolism, thermogenic activity, and browning processes that are implicated in obesity development [21–24]. Therefore, it is very suggestive to think of a therapeutic and/or nutritional strategy to combat obesity that tries to recover the circulating levels of histidine in obesity.

Overall, in the present study integrative systems medicine approach in large well-characterized NAFLD cohorts has been performed using plasma metabolomics, and adipose tissue transcriptomics; to confirm the relationship between histidine levels and obesity. Parallelly, the impact of histidine-related amino acids (HAA) was evaluated for the first time in a NAFLD mice model, focusing on the adipose tissue, the main pathologic features of obesity and histamine metabolism.

2. Results

2.1. Circulating histidine levels are consistently decreased according to obesity degree in different cohorts

The obesity degree of the patients was by the body mass index (BMI, kg/m^2). Subsequently, obesity status was subdivided into categories: *a*) Normal weight (18.5-24.9), *b*) Overweight (25-29.9), *c*) Grade 1 obesity (30-34.9), *d*) Grade 2 obesity (35-39.9), and *e*) Grade 3 obesity (>40). In subjects recruited as part of the FLORINASH consortium (*n* = 74), plasma histidine levels were decreased according to the obesity degree (**Figure 1a**). Consistently, in participants from the general population aged < 50 years recruited in the PECT Study (IMAGEOMICS2, *n* = 961), the circulating histidine levels decreased according to the obesity status (**Figure 1b**). We next performed and RNA-sequencing of the subcutaneous adipose tissue (scWAT) of participants from the OUTBRAT cohort (*n* = 251) and studied those genes involved in histamine catabolism in relation to the obesity status. Histidine is enzymatically decarboxylated by histidine decarboxylase (HDC) to yield histamine. We found that the scWAT expression of *HDC* was increased in subjects with obesity (**Figure 1c**). In addition, the expression of Histamine *N*-methyltransferase (*HNMT*), which catalyzes the methylation of histamine to *N*-methylhistamine was also increased in subjects' grade 3 obesity (**Figure 1d**). Finally, the expression

of histamine receptors (*HRH1, HRH2, HRH4*) was also increased in patients with obesity (**Figure 1e-g**).

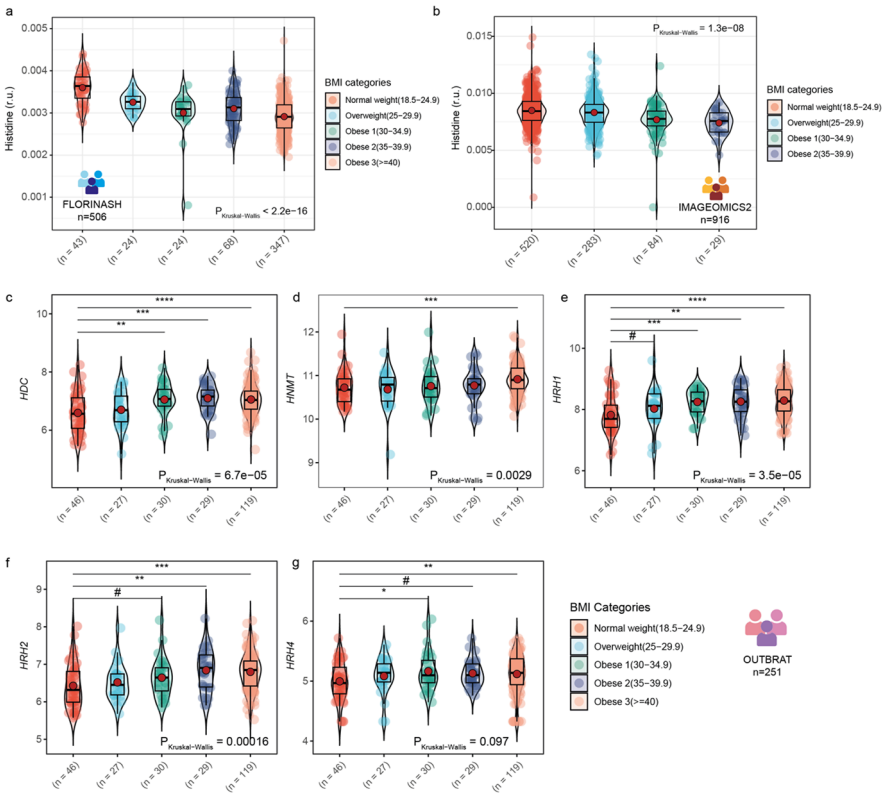

Figure 1. Circulant histidine levels are negatively correlated with BMI in obese patients. a) Violin plot showing the plasma histidine levels according to the degree of obesity assessed by body mass index (BMI) (FLORINASH, *n*=74) **b)** Violin plot showing the plasma histidine levels according to the degree of obesity assessed by BMI (IMAGEOMICS2, *n*=961). **c-g)** Violin plots showing gene expression of HDC, HNMT, HRH1, H2H2 and HRH4 according to the degree of obesity assessed by BMI from RNA-sequencing of the subcutaneous adipose tissue (scWAT) in the OUTBRAT cohort (*n*=251). r.u., relative units. Data are mean ± SEM. * p < 0.05, ** p < 0.01, *** p < 0.001, **** p < 0.0001.

2.2. Circulating histidine levels are associated with subcutaneous adipose tissue genes participating in P53 regulation, proteasome degradation, and NOTCH signaling

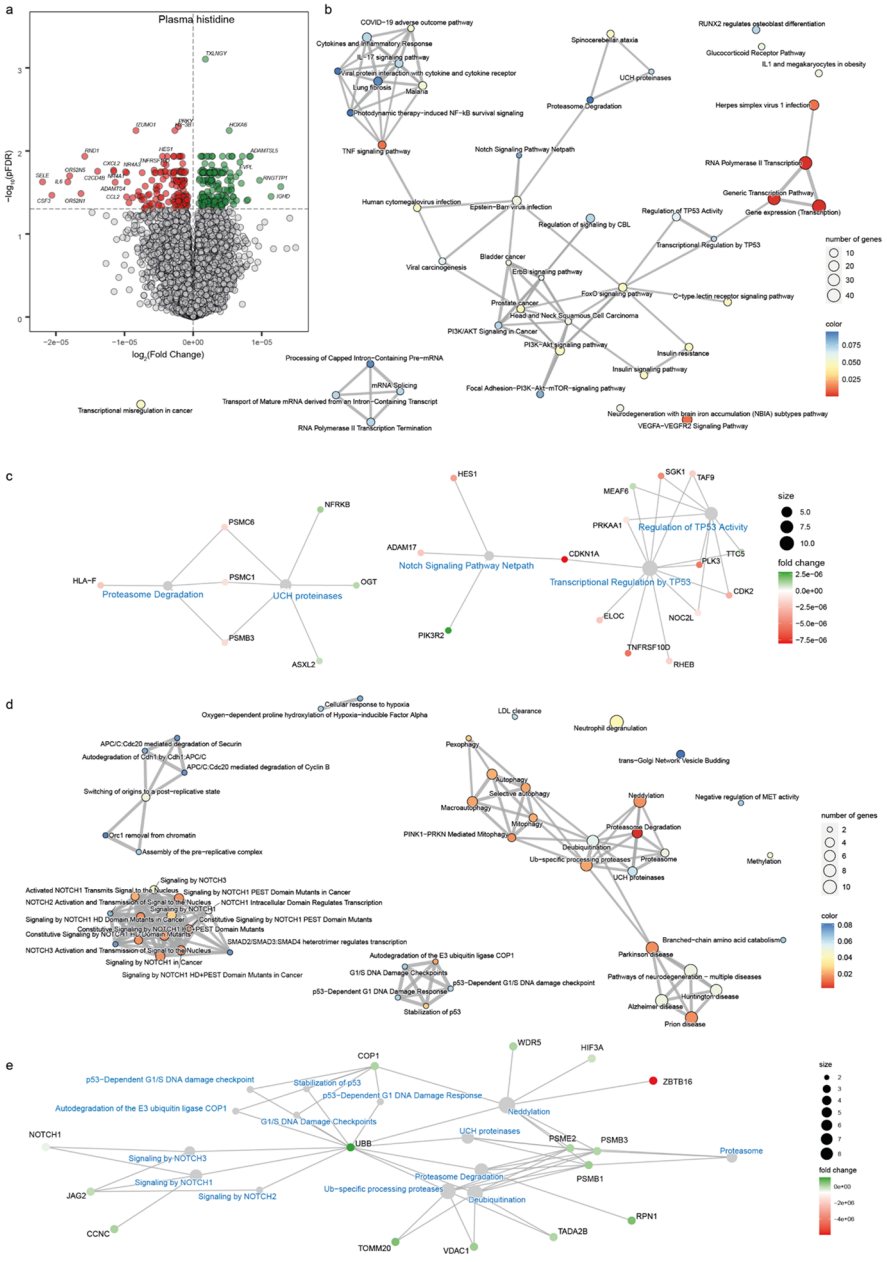

Figure 2. Associations of the subcutaneous adipose tissue transcriptome gene expression with the circulating histidine levels. a) Volcano plot of differentially expressed gene transcripts associated with the plasma histidine levels in FLORINASH cohort (*n*=74) identified using robust linear regression controlling for age, BMI, sex, and country. The $\log_2$(Fold Change) associated with a unit change in the plasma histidine levels and the -$\log_{10}$(p-values) adjusted for multiple testing are plotted for each transcript. **b**) Enrichment map inter-related significant

identified using an active subnetwork-oriented approach. Each color displays a cluster of related pathways using a threshold for kappa statistics = 0.35. The size of the nodes corresponds to its -$\log_{10}$ (pFDR). The thickness of the edges between nodes corresponds to the kappa statistic between the two nodes. **c**) Gene-concept network depicting significant genes involved in enriched pathways from selected clusters. The dot size of the pathways represents the -$\log_{10}$ (pFDR). Pathways with the same color correspond to the same cluster. To replicate the previous results, **d**) Enrichment map inter-related significant pathways and **e**) gene-concept network was replicated in an independent cohort of obese patients recruited for the IRONMET study (*n* = 17).

We next identified sWAT transcriptomic signatures linked to the circulating histidine levels in a subset of patients from the FLORINASH cohort (*n* = 74). We fitted robust regression models (controlling for age, BMI, and sex) with an empirical Bayes moderation of the standard errors using the limma-voom pipeline. We identified 335 genes in the scWAT associated with plasma histidine levels (**Figure 2a**). To facilitate the analysis and interpretation of these associations, we next performed pathway over-representation analyses based on KEGG, Reactome, and Wikipathways databases, followed by clustering of redundant pathways. These analyses highlighted an enrichment of pathways involved in the proteasome degradation, the regulation of TP53 activity, or the NOTCH signaling, among others (**Figure 2b**). The genes significantly associated with the circulating histidine levels participating in these pathways are shown in **Figure 2c.** Next, we tried to replicate these results in an independent cohort of obese patients recruited for the IRONMET study (*n* = 17). Notably, and enrichment analyses of those genes associated with the circulating histidine levels further highlighted an over-representation of pathways involved in the regulation of P53, the proteasome and the signaling by NOTCH (**Figure 2d,e**).

2.3. HAA supplementation alleviates high-fat high-fructose diet-induced obesity by ameliorating the adiposity in eWAT and iWAT and upregulating genes related to lipolysis, FFAs oxidation and insulin sensitivity.

To elucidate the role and underlying mechanisms of histidine in obesity, we supplemented a combination of histidine and histidine-related amino acids (HAA: histidine, serine, carnosine, and cysteine) to diet induced obese mice. It was observed an important reduction in body weight gain in the supplemented obese mice compared with Obese +

vehicle group (**Figure 3a**). To evaluate whether the alleviation of obesity was associated with an amelioration of the adipose tissue state, different adipose tissue depots were analyzed observing that the supplementation of HAA promoted a reduction in the visceral and subcutaneous WAT depots' weights (EWAT, RWAT, MWAT and IWAT) and in the brown adipose tissue (BAT) (**Figure 3b-f**).

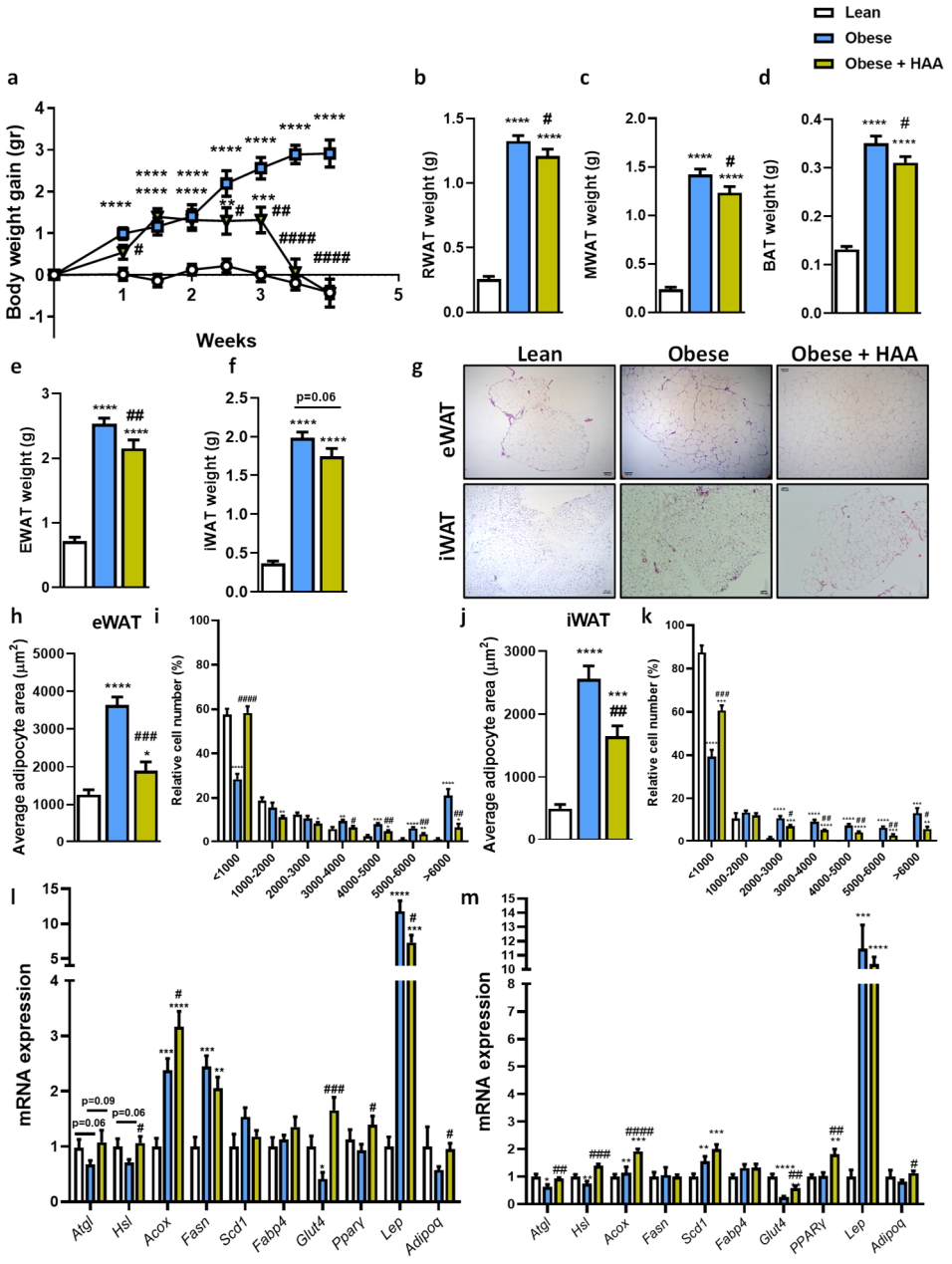

Figure 3. HAA supplementation reduced obesity by ameliorating WAT adiposity and improving the expression of genes related to lipid metabolism. Effects of HAA treatment on (**a**) body weight gain; weights of different white adipose tissue depots: (**b**) retroperitoneal (RWAT); (**c**) mesenchymal (MWAT); (**d**) brown adipose tissue (BAT); (**e**) epididymal (EWAT); (**f**) inguinal (IWAT); (**g**) representative micrographs of hematoxylin-eosin stained eWAT and iWAT sections from Control, Obese + vehicle and Obese + HAA groups (Bar = 100 µm, 4X magnification); (**h**) average adipocyte's area and (**i**) adipocyte size distribution in eWAT; (**j**) average adipocyte's area and (**k**) adipocyte size distribution in iWAT; (**l-m**) eWAT and iWAT mRNA expression of genes related to lipolysis (*Hsl* and *Atgl*), fatty acid oxidation (*Acox1*), *de novo* lipogenesis (*Fasn, Fabp4* and *Scd1*), glucose transporter (*Glut4*), the transcription factor *Pparγ*, leptin (*Lep*) and adiponectin (AdipoQ). Data are mean ± SEM. * $p < 0.05$, ** $p < 0.01$, *** $p < 0.001$, **** $p < 0.0001$ *vs*. control; $^{\#}$ $p < 0.05$, $^{\#\#}$ $p < 0.01$, $^{\#\#\#}$ $p < 0.001$, $^{\#\#\#\#}$ $p < 0.0001$ *vs*. Obese + vehicle.

Histological images of eWAT (as a visceral adipose depot) and iWAT (a subcutaneous depot), revealed notorious smaller adipocytes in the HAA supplemented Obese animals compared with Obese vehicle mice (**Figure 3g**). Accordingly, it was observed a reduction in adipocyte area and in the larger adipocytes size distribution in the Obese + HAA animals in both adipose depots (**Figure 3h-k**). To determine which metabolic pathways could be involved in the improvement of adipose tissue metabolism after HAA supplementation, mRNA expression analysis of genes related to adipose lipogenesis, lipolysis, *de novo* lipogenesis, fatty acid oxidation, insulin-dependent-glucose transporter, and adipokines were carried out both in eWAT and iWAT (**Figure 3l** and **3m**). It was observed an up-regulation in lipolysis related genes (*Atgl* and *Hsl*) after HAA supplementation compared to those mice treated with vehicle. Regarding fatty acid oxidation, *Acox1* was up regulated in Obese + HAA mice compared to the Obese + vehicle group, both in eWAT and in iWAT. In contrast, there was not differences in the expression of lipogenic genes *Fasn* and *Scd1* after the HAA supplementation. Interestingly it was observed an up-regulation of *Glut4* expression in eWAT and iWAT in the Obese + HAA mice compared to Obese + vehicle mice, which may impact in the insulin sensitivity. Besides, the supplementation of HAA upregulated the transcription factor *Pparγ* expression compared to Obese + vehicle mice both in eWAT and iWAT. In the case of adipokines, HAA supplementation downregulated *Lep* in comparison with Obese + vehicle mice in eWAT; and increased *Adipoq* expression in both adipose depots.

2.4. HAA supplementation ameliorates obesity-related insulin resistance

To analyze glucose and insulin sensitivity, fasting serum parameters, GTT and ITT tests were performed, observing a reduction in the insulin fasting levels as well in the LDL cholesterol after the HAA supplementation (**Table S1**). In contrast, HDL cholesterol levels presented a rise in the Obese + HAA mice compared with the Obese + vehicle mice. In addition, GTT showed a tendency to improve in Obese + HAA mice in comparison with the Obese + vehicle group (**Figure S1a**). As expected, the ITT test showed insulin resistance in Obese + vehicle, whereas HAA supplementation produced an important amelioration of insulin sensitivity in these animals (**Figure S1b**). Amelioration in glucose and insulin tolerance were accompanied by a reduction in HOMA-IR and HOMA-β (**Table S1**).

2.5. HAA supplementation reduces fat accumulation in brown adipose tissue by activation of lipolysis, lipid oxidation and thermogenesis

As pointed above, HAA supplementation promoted a reduction BAT weight (**Figure 1d**). BAT activation of non-shivering thermogenesis provides a protective mechanism against excessive body weight and fat mass, with significant roles in triglyceride and glucose homeostasis and insulin sensitivity [25]. To delve into the molecular mechanisms associated with the improvement of lipid metabolism and thermogenesis in BAT, the impact of HAA supplementation on BAT was assessed. Histological analysis revealed that lipid droplet size was reduced in Obese + HAA mice compared to Obese mice counterparts, and consequently, the number of lipid droplets in the area analyzed was increased (**Figure 4a-c**). In addition, thermography analysis was used to determine the skin temperature of the interscapular BAT area, observing an increased BAT temperature in Obese + HAA mice compared to Obese + vehicle mice, suggesting an enhanced BAT activation in these animals (**Figure 4d-e**).

To deepen which metabolic pathways could be involved in the BAT effects after HAA supplementation, mRNA expression of genes related to thermogenic activity and lipid metabolism was carried out (**Figure 4f**). Obese + HAA mice showed upregulated expression of genes related to the thermogenic activity (*Ucp1*, *Pgc1a*, *Prdm16*, *Dio2*, *Dio3, Tmem26* and *Fgf21)* compared to Obese + vehicle mice. In addition, HAA supplementation promoted an increased expression of *Adipoq* and *LepR*.

Interestingly, glucose transporters *Glut1* and *Glut4,* were upregulated after HAA supplementation, which may contribute to the global insulin resistance amelioration. Finally, the administration of HAA promoted an upregulation of *Cpt1b and Pparγ* expression in comparison with Obese + vehicle mice. Consistent with the *Ucp1* mRNA expression, Ucp1 protein was increased in Obese + HAA mice compared to Obese + vehicle mice (**Figure 4g-h**).

2.6 HAA supplementation modulates histamine receptor expression in an adipose tissue depot-dependent manner

To determine whether HAA treatment modulates in mice the differential gene expression detected in the human cohorts, P53 regulation pathway and histamine metabolism mRNA expression was analyzed. Proteosomal gene expression were strongly related with histidine levels in the human cohorts. However, no differences were observed in the expression of *Psmb1* and *Psmb3* in between animal groups (data not shown). Regarding P53 regulation-related genes, *P21* was upregulated in obesity both in eWAT and iWAT (**Figure S2a**). However, in iWAT HAA supplementation downregulated *P21* expression compared with Obese + vehicle animals (**Figure S2a**). No differences were observed in BAT regarding the *P21* expression. Concerning *P53* expression slight differences were observed between groups in the different adipose depots (**Figure S2b**). Interestingly, HAA supplementation downregulated *P53* in iWAT compared with Obese + vehicle animals. A slight tendency to upregulate *P53* expression was observed after HAA supplementation (**Figure S2b**). Regarding the histamine metabolism, Obese + HAA mice showed an upregulation of the histamine receptors (*H1r* to *H4r*) in comparison with Obese + vehicle mice in eWAT (**Figure 5a)**. In contrast, obesity promoted the expression of the catabolic enzymes (*Hnmt* and *Hdc*), but no differences were observed regarding the HAA supplementation. In iWAT, obesity induced the *H1r* expression, whereas repressed the *H2r*, *H3r* and *H4r* expression (**Figure 5b**). Surprisingly, supplementation of HAA partially restored the *H4r* expression to the lean mice. As observed in eWAT, regarding the HAA supplementation, no differences were observed in the expression of *Hnmt* and *Hdc* (**Figure 5b**). In BAT, obese mice supplemented with HAA showed an uprising of H1r, *H2r* and *H4r* expressions whereas *H3r* was downregulated in comparison with obese + vehicle mice (**Figure 5c**). *Hdc* expression was not detected in

BAT, whereas *Hnmt* expression showed an important increase in the HAA supplemented mice (**Figure 5c**).

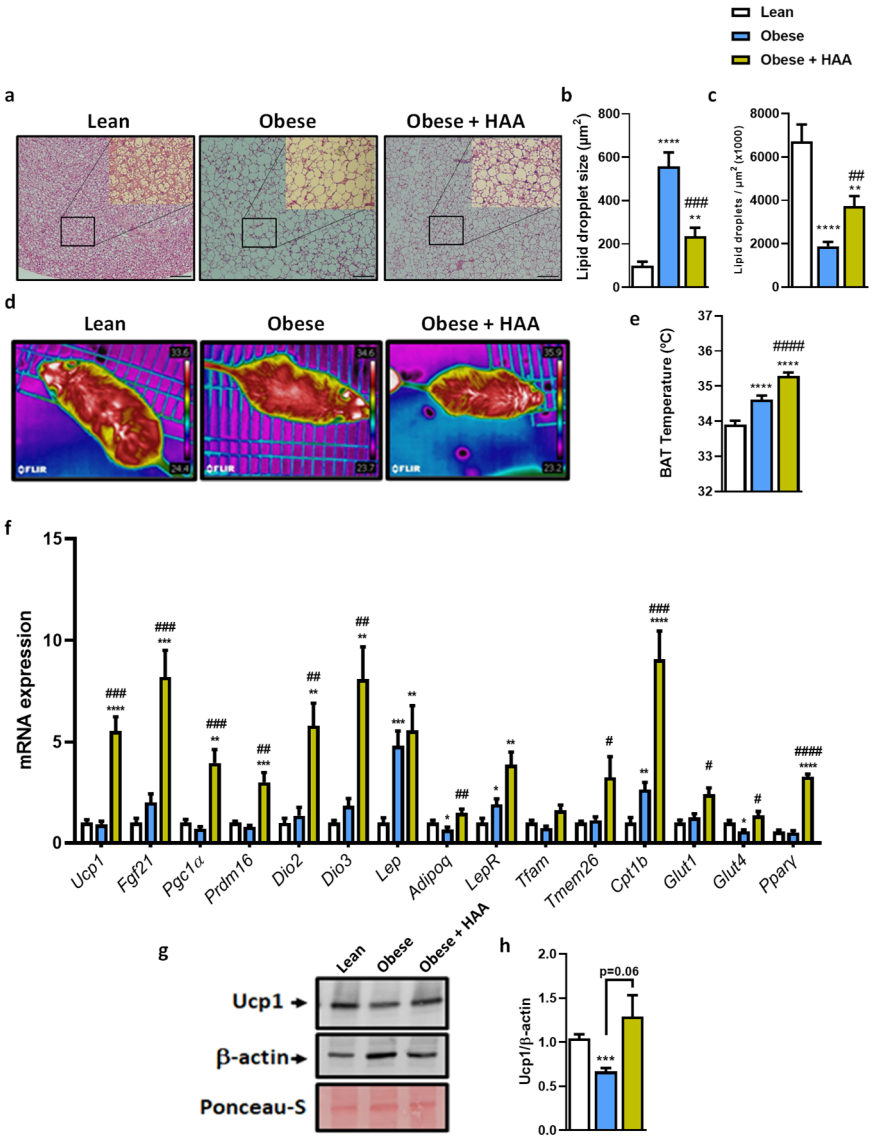

Figure 4. HAA supplementation increases thermogenesis and ameliorates adiposity in BAT. Effects of treatments on: (**a**) representative micrographs of hematoxylin-eosin-stained BAT sections (Bar = 100 µm; 10x magnification); (**b**) lipid droplets size and (**c**) and number of lipid droplets; (**d**) Representative thermographic images of the BAT skin area (**e**) and BAT temperature quantification, (**f**) BAT mRNA expression of genes related to BAT function (*Ucp1*, *Pgc1a*, *Prdm16*, *Dio2*, *Dio3, Tfam, Tmem25* and *Fgf21*); adipokines (*Lep*, *LepR* and

Adipoq); fatty acid oxidation (*Cpt1b*); glucose uptake (*Glut1* and *Glut4*); and the transcription factor *Pparγ*. **g**) A representative Western blot of Ucp1 and β-actin, together with the protein loading with Ponceau-S staining was shown. **h**) Densitometry analysis of Ucp1 and β-actin ratio. Data are mean ± SEM. * $p < 0.05$, ** $p < 0.01$, *** $p < 0.001$, **** $p < 0.0001$ *vs*. control; $^{\#}p < 0.05$, $^{\#\#}p < 0.01$, $^{\#\#\#}p < 0.001$, $^{\#\#\#\#}p < 0.0001$ *vs.* Obese + vehicle.

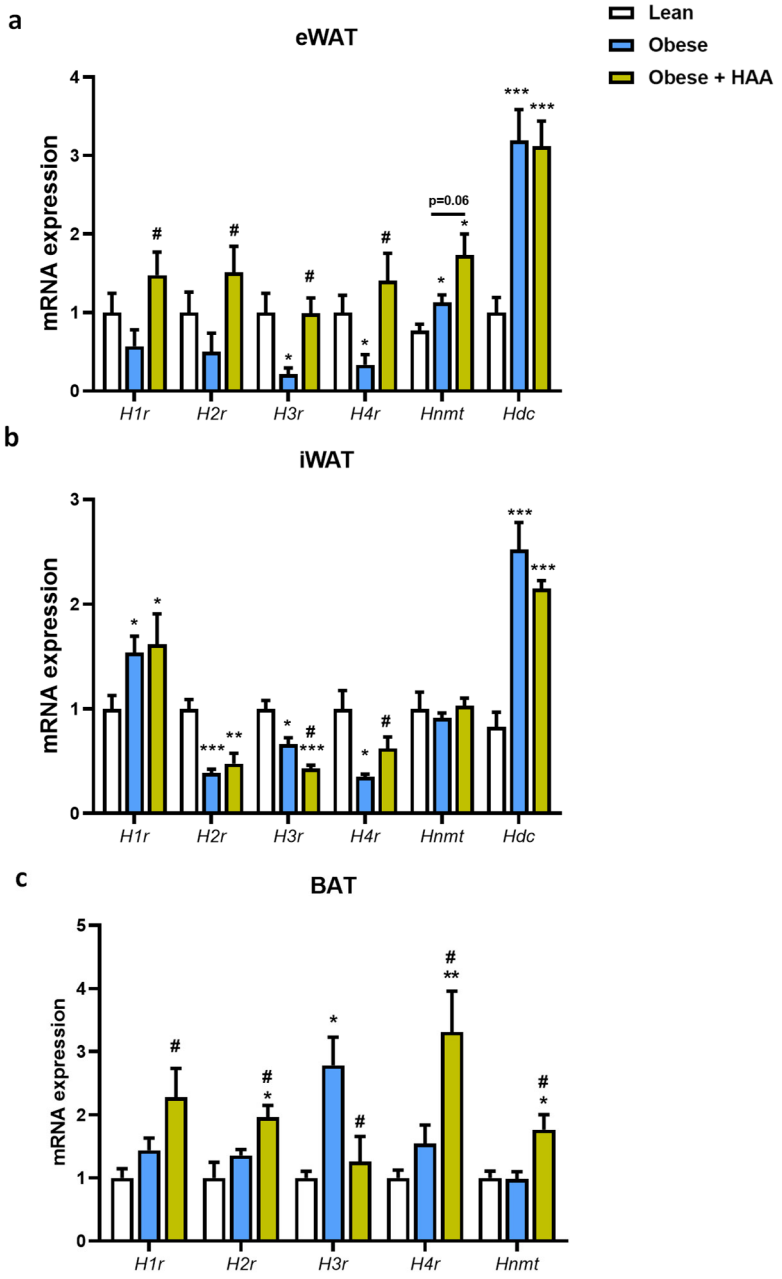

Figure 5. HAA supplementation modulates the expression levels of histamine receptors in eWAT, iWAT and BAT. Histamine receptors (*H1r, H2r, H3r* and *H4r),* histidine decarboxylase (*Hdc*), and histamine N-methyltransferase (*Hnmt*) mRNA expression in: (**a**) eWAT, (**b**) iWAT and (**c**) BAT. Data are mean ± SEM. * $p < 0.05$, ** $p < 0.01$, *** $p < 0.001$ *vs*. control; # $p < 0.05$ *vs*. Obese + vehicle.

3. Discussion

Low histidine has been associated with metabolic disorders in several studies, affecting insulin sensitivity [15,26–29]. However, little is known about the effects of histidine and histidine-related amino acids on obesity and adipose tissue. In this study, we elucidated the negative correlation between obesity and histidine levels by metabolomics and transcriptomics, and afterward, we administered a supplementation of a combination of histidine-related amino acids in an HFHFr-diet-induced obese mice model to analyze the ameliorative effect on obesity and the adipose tissue dysfunction, which is characteristic in this metabolic disorder, after the treatment. Indeed, the systemic lipid profile and white and brown adipose tissue state were analyzed to demonstrate the improvement of obesity after this nutraceutical treatment.

Metabolomics analysis in the clinical study with human cohorts showed the negative association between histidine levels and obesity, and how the more advanced grades of obesity, the lower levels of histidine concentration are found. Moreover, histamine receptors and histamine metabolism-related enzymes were positively correlated with obesity. This negative correlation between plasma histidine levels and obesity is corroborated in a previous study both in preclinical and clinical studies [15,30]. Furthermore, a previous study with HDC knock-out obese mice showed that the lack of HDC activity develops earlier obesity, thereby, the increase in HDC activity may be induced as a compensatory mechanism to prevent excess weight gain and the development of leptin resistance because their development is dependent on the histaminergic system [31]. After transcriptome analysis, the most significant clusters negatively correlated with histidine levels were P53 regulation, proteasome degradation, and NOTCH signaling. This first cluster is related to cell senescence, which can be induced by telomere dysfunction and oxidative stress. This senescent response is regulated by P53, a tumor suppressor protein. Indeed, P53 has been associated with the loss of insulin sensitivity in adipose tissue, promoting the characteristic insulin resistance in

metabolic disorders [32]. Moreover, NOTCH signaling has been related to increased adipose tissue depots size, PPARγ inhibition and BAT whitening by suppressing mitochondrial biogenesis. However, genetic and pharmacological NOTCH inhibition promoted resistance to HFD-induced obesity, elevated energy expenditure, better glucose and insulin profile, and decreased adiposity [33,34]. Therefore, reduced histidine levels in obese patients may be associated with increased activation of the NOTCH signaling and P53 regulation pathways, which can explain the negative correlation between circulant histidine levels and the expression of the NOTCH signaling pathway-related gene *HES1*, and P53 regulation related genes *P53* and *P21* observed in this study.

The obese animal model supplemented with HAA corroborated the beneficial role of histidine treatment in obesity. The supplementation of HAA in obese mice promoted a decrease in body weight gain associated with a reduction of adipose tissue depots' weights. Previous studies with histidine supplementation corroborated the effects seen in this study with the HAA combination on the improvement of body weight and reduced adipose tissue depots in obese patients and animals [15,35,36]. Besides, to assess the reduction of adipose tissue depots at the tissue level, histopathological analysis of the visceral adipose tissue (eWAT) and the subcutaneous adipose tissue (iWAT) was performed. As expected, both eWAT and iWAT increased their adiposity in HFHFr-fed mice by increasing the largest adipocytes and reducing the smallest adipocytes. However, when HAA was supplemented in obese mice, a reduction of adiposity was observed in both adipose tissue depots, which was associated with the upregulation of lipolysis and FFAs oxidation genes. These results agree with a study in rats, in which the increase of lipolysis was positively correlated with histidine administration by activating the sympathetic nerve in WAT [37]. Therefore, the combination of histidine-related amino acids may promote the release of FFAs by lipolysis, which are probably taken into the mitochondria to be oxidated, and subsequently reduce adiposity in WAT. Besides, insulin resistance observed in obese mice was improved after HAA supplementation by ameliorating both insulin and glucose tolerance tests, which suggested an increase in insulin sensitivity after the treatment. In this line, the improvement of IR was also observed in the adipose tissue depots by the increase in *Glut4* expression (which is the main glucose transporter regulated by insulin signaling) in HAA-supplemented obese mice. These results are in tune with the reduction of

insulin resistance in a study in which a NAFLD mice model supplemented with histidine or carnosine [36], and with a clinical study in which dietary histidine levels were inversely correlated with insulin resistance in obese subjects [28]. Moreover, the supplementation of cysteine increased GLUT4 levels in high glucose-treated 3T3-L1 adipocytes [38]. Therefore, this combination of histidine-related amino acids could increase insulin sensitivity in white adipose tissue. In the case of adipokines, Adiponectin is an adipokine with anti-inflammatory properties downregulated in obesity [39], but, in the present study, *Adipoq* expression was upregulated in both WAT depots after HAA supplementation in obese mice, which was strongly associated with the increase in *PPARγ* expression, as it was described previously [40]. Consistent with our findings, in a previous study with obese rats, histidine supplementation upregulated *Adipoq* expression and increased PPARγ levels [15]. Consequently, *Lep* expression was downregulated in iWAT after HAA supplementation associated with the increase in *Adipoq* expression. Moreover, increased leptin is associated with obesity because of leptin resistance [41]. Hence, a reduction in *Lep* expression due to HAA supplementation is associated with an improvement in obesity.

BAT activation is associated with the prevention of excessive body weight and lipid accumulation by non-shivering thermogenesis, which expends a lot of energy. Hence, this activity requires glucose and FFAs as fuel that are obtained from cellular uptake, de novo lipogenesis, and multilocular lipid droplets [25]. Therefore, the activation of BAT is described as a promising target against obesity. Interestingly, in the present study, HAA demonstrated an ameliorative effect on BAT activity by upregulating thermogenesis-related genes and the increase in UCP1 levels, and consequently, an increase in temperature in the skin area surrounding BAT. Thermogenesis was directly associated with a decrease in adiposity in BAT, preventing BAT whitening in obesity [42], corroborating the results observed in this study after HAA supplementation. As explained before, glucose and FFAs are the fuel of thermogenesis, thus Glut4 and Glut1, which are responsible for glucose uptake into the adipocyte, and *Cpt1,* which is responsible for FFAs uptake into the mitochondria [25], were probably upregulated after HAA supplementation to provide sufficient supply for thermogenesis activation. These results are consistent with previous studies with histidine and serine supplementation that activated

BAT thermogenesis in diet-induced obese mice by increasing UCP1 levels [43], and directly linked to an increased glucose uptake in BAT [44].

When histamine pathway-related gene expression was assessed, most of the histamine receptors were upregulated by HAA-supplementation in eWAT, iWAT, and BAT, except *H3r* in iWAT and BAT which was downregulated. In the case of *H1r,* its expression was upregulated after HAA administration in the visceral adipose tissue and BAT. The activation of H1R has been associated with the increase of cAMP and stimulation of lipolysis in adipocytes [45]. Moreover, H1r KO models described this receptor as a key player in appetite suppression and leptin resistance amelioration in obesity [46], and enhanced insulin resistance, hyperleptinemia and visceral adiposity [24]. Therefore, the downregulation of *H1r* in WAT of obese mice and the upregulation after HAA administration is concordant with previous studies and confirms the anti-obesogenic properties of HAA supplementation in WAT by *H1r* stimulation. Moreover, H1r was determined to be involved in Ucp1 expression and activation in BAT [47] and correlates with the upregulation of H1r and Ucp1 in HAA-supplemented obese mice in this study. While, H2R has been correlated with adipokines secretion. Thus, H2r KO mice showed decreased adiponectin levels associated with visceral adiposity, insulin resistance and glucose intolerance, which is critical in the development of lipotoxicity in peripheral tissues [48]. These results correlated with what we 50observed in obese mice that downregulated *H2r* in iWAT and showed a reduction of insulin sensitivity determined by ITT and GTT. Moreover, *Adipoq* expression tended to reduce. However, after HAA supplementation, *H2r* expression was upregulated in eWAT, which may suggest that HAA administration can ameliorate insulin resistance and adiponectin levels in this depot. Moreover, previous study showed H2R activation indirectly participated in the thermogenic response in BAT [49], and in the present study HAA supplementation upregulated *H2r* expression in BAT, which may correlate with the observed activation of BAT thermogenesis. Besides, when H3R is inhibited, it also displayed an obese phenotype with leptin resistance, insulin resistance and reduced energy expenditure, although the mechanisms of action need to be further studied [50,51]. However, H3R is a modulator of histamine synthesis and release in the central nervous system, and the use of compounds that enhance histamine release from nerve terminals, such as H3 receptor antagonists, influenced favorably body weight and glucose tolerance by

increasing synthesis and disinhibition of histamine release and increasing the lipolytic response in WAT, which are mediated by sympathetic nerves that innervate white adipose tissue [50,52]. This is controversial with other studies due to inconsistent results [50]. In this study, *H3r* was downregulated in eWAT and upregulated in BAT in obese mice. However, HAA supplementation reverted the situation and upregulated *H3r* in eWAT and downregulated this histamine receptor in iWAT and BAT, which suggested that *H3r* expression is associated with thermogenic activity in BAT and browning expression in iWAT, improving lipid metabolism in these adipose tissue depots, and is inhibited in eWAT. Finally, H4r is known to be the histidine receptor more expressed in adipocytes and participates in could-induced browning and lipolysis in WAT of mice and cell models [53]. Moreover, silencing H4r caused the impairment of cold-induced browning in WAT by down-regulation of thermogenic genes, including *Ucp1* and *Pgc-1α* [53]. Therefore, these studies suggested that H4R participates as a regulator of cold-induced thermogenesis in WAT, but it might also play a role in UCP1-related thermogenesis in BAT. Hence, after HAA supplementation *H4r* was upregulated in BAT and WAT of obese mice associated with the increased thermogenesis in BAT and lipolysis in WAT.

In conclusion, our results exhibit an important association between circulatory histidine levels and obesity. We have revealed novel histidine-linked transcriptomic and metagenomics signatures and uncovered the potential role of histamine metabolism in the development of obesity. In addition, the supplementation of histidine-related amino acids improved adiposity, lipid metabolism, and insulin resistance in adipose tissue, promoting thermogenic activity in BAT. Moreover, HAA supplementation modulated key participants in histamine metabolism associated with adipose tissue differentiation and function. Overall, these results point to HAA supplementation as a new candidate in the treatment of obesity and adipose tissue dysfunction by regulating histamine metabolism as a therapeutic target.

4. Materials and Methods

4.1. Clinical cohorts

Discovery cohort (FLORINASH). The discovery cohort included *n* = 74 obese patients aged 24 to 66 years old recruited at the Endocrinology Service of

the Hospital Universitari de Girona Dr Josep Trueta (Girona, Spain) for the FLORINASH study. Inclusion criteria included caucasian origin, stable body weight 3 months before the study, free of any infection 1 month preceding the study and absence of any systemic disease. Exclusion criteria included known history of diabetes or use of hypoglycemic agents, presence of liver disease (specifically hepatitis C virus infection and tumoral disease), thyroid dysfunction, > 20g/day of alcohol consumption, hepatitis B, or drug-induced liver injury. All subjects gave written informed consent, validated, and approved by the ethical committee of the Hospital Universitari Dr Josep Trueta (Comitè d'Ètica d'Investigació Clínica, approval number 2009 046).

Validation cohort (IRONMET). From January 2016 to October 2017, a cross-sectional case-control study was undertaken in the Endocrinology Department of Josep Trueta University Hospital (Girona, Spain). In 17 morbidly obese patients (BMI > 35 mg/kg^2) aged 28-60 years old, adipose tissue stranded RNA-seq was analysed. Inclusion criteria: All subjects were of Caucasian origin and reported a body weight stable for at least three months before the study. Subjects were studied in the post-absorptive state. Exclusion criteria were: previous type 2 diabetes mellitus, chronic inflammatory systemic diseases, acute or chronic infections in the previous month; severe disorders of eating behaviour or major psychiatric antecedents; neurological diseases, history of trauma or injured brain, language disorders; and excessive alcohol intake (≥ 40 g OH/day in women or 80 g OH/day in men). Body fat composition was estimated using Bio-electrical impedance analysis (BC-418, Tanita Corporation of America, Illinois, USA). The study protocol was revised, validated, and approved by the Ethics committee of the Hospital Dr Josep Trueta.

Validation cohort Imageomics2 (PECT study): The PECT Study is a multicentric observational study also including participants residing in the province of Girona (Northeast Catalonia, Spain). It includes a representative population of the province of Girona aged ≥16 and ≤ 52 years old recruited in public primary care centers. Exclusion criteria included: age ≥ 52 years, not dwelling in the community (i.e. institutionalized), terminal disease, intellectual disability, diagnosis of dementia, difficulties to understand Catalan or Spanish. The PECT protocol was approved by the ethics committee of the Dr. Josep Trueta University Hospital.

Validation cohort OUTBRAT (FATBANK study): All samples and data from participants included in this study were provided by the FATBANK platform promoted by the Centro de Investigación Biomédica en Red Fisiopatología de la Obesidad y Nutrición (CIBEROBN) and coordinated by the IDIBGI Biobank (B.0000872), integrated in the Spanish National Biobanks Network and they were processed following standard operating procedures with the appropriate approval of the Ethics, External Scientific and FATBANK Internal Scientific

Committees. Two hundred and fifty-one participants from Girona with several degrees of obesity were recruited. Subjects were studied in the post-absorptive state. BMI was calculated as weight (in kg) divided by height (in m) squared. Liver diseases and thyroid dysfunction were specifically excluded by biochemical work-up. Inclusion criteria included caucasian origin, aged ≥18 and ≤ 65 years old and have a surgical procedure scheduled that allows the removal of adipose tissue. Exclusion criteria included failure to meet any of the inclusion criteria, having infections and/or acute inflammation, being diagnosed with infectious diseases, being undergoing oncological treatment, pregnant or breastfeeding women, being diagnosed with systemic diseases (lupus, rheumatoid arthritis, etc.).

Declarations Ethics approval and consent to participate in Human studies: all subjects gave written informed consent, validated, and approved by the ethical committee of the Hospital Universitari Dr Josep Trueta (Comitè d'Ètica d'Investigació Clínica, approval number 2009 046).

4.2 Plasma histidine (metabolomics)

Plasma samples from all subjects were obtained during the week before elective gastric by-pass surgery. The plasma histidine levels were determined using ^{1}H-Nuclear Magnetic Spectroscopy (NMR). The analyses of the discovery and validation cohort 1 were performed on a Bruker DRX600 spectrometer equipped with either a 5-mm TXI probe operating at 600.13 MHz or a 5-mm BBI probe operating at 600.44 MHz. The 90º pulse length was determined prior to each run and field frequency was locked using D_2O as solvent. Plasma samples were thawed at room temperature and 350 µL aliquots were carefully placed in 5-mm NMR tubes. Then, 150 µL of saline solution (0.9% NaCl prepared with 80:20 H_2O/D_2O and sodium azide) was added and the mixture was gently vortexed. Spectra were acquired using water suppressed Carr-Purcell-Meiboom-Gill (CPMG) using the Bruker program cpmgpr (recycle delay (RD) -90º-t1-180º-tm-acquire). An RD of 2 s was employed for net magnetization relaxation, during which noise irradiation was applied to suppress the large water proton signal. Several loops *n* = 100 and a spin-echo delay t = 400 µs were used to allow spectral editing through T2 relaxation and therefore attenuation of broad signals. For each sample, 128 scans were recorded in 32K data points with a spectral of 20 ppm.

The analysis of the cohorts was performed on a Bruker AVANCE II 600 spectrometer fitted with an automatic sample changer and a multinuclear triple resonance (TBI) probe (Bruker Biospin, Germany) at 14.1 T (600.3 MHz). Plasma samples were thawed at room temperature and 400 µL aliquots were combined with 200 µL of saline buffer (9% w/V NaCl, 100% D_2O, 10mM TSP). Samples were mixed by vortex and spun for 10 min at 13,000 rpm prior to transferring 550 to a 5 mm NMR tube. Spectra were acquired using water suppressed Carr-Purcell-Meiboom-Gill (CPMG) using the Bruker program cpmgpr (RD-90ºt1-180º-tm -

acquire free induction decay). The water signal was suppressed by irradiating the RD of 2s with a mixing time (tm) of 10 µs. The acquisition was set to 1.36s and the 90º pulse length of 10.43 µs. Several loops *n* = 40 and a spin-echo delay t = 400 µs were used to allow spectral editing through T2 relaxation and therefore attenuation of broad signals. For each sample, 256 scans were recorded in 32K data points with a spectral of 20 ppm.

Spectra were manually phased, corrected for baseline distortions, and referenced to the center of the α-glucose anomeric doublet (δ 5.23). All spectra were imported to MATLAB and digitized into consecutive integrated spectral regions of equal width. The regions between δ 4.7–4.9 containing the residual water resonance were removed from all spectra in to minimize the effect of baseline effects caused by imperfect water suppression. Each spectrum was then normalized using a probabilistic quotient normalization algorithm.

4.3 Adipose tissue collection and handling.

Adipose tissue samples were obtained from subcutaneous (scWAT) adipose tissue during elective surgical procedures (cholecystectomy, surgery of abdominal hernia and gastric bypass surgery) in patients from the discovery (FLORINASH) and validation (IRONMET) cohorts. scWAT samples were collected from the abdomen, following standard procedures. Samples of adipose tissue were immediately transported to the laboratory (5-10 min). The handling of tissue was carried out under strictly aseptic conditions. Adipose tissue samples were washed in PBS, cut off with forceps and scalpel into small pieces (100 mg), and immediately flash-frozen in liquid nitrogen before stored at -80ºC.

4.4 scWAT stranded RNA sequencing.

scWAT RNA purification was performed using RNeasy-Tissue Mini-Kit (QIAgen). Total RNA was quantified by Qubit® RNA BR Assay kit (Thermo Fisher Scientific) and the integrity was checked by using the RNA Kit (15NT) on 5300 Fragment Analyzer System (Agilent).

The RNA-seq libraries were prepared with Illumina® TruSeq® Stranded Total RNA Sample Preparation kit following the manufacturer´s recommendations with some modifications. Briefly, in function of availability 100-500 ng of total RNA was ribosomal RNA (rRNA) depleted using the RiboZero Magnetic Gold Kit and fragmented by divalent cations. The strand specificity was achieved during the second strand synthesis performed in the presence of dUTP. The cDNA was adenylated and ligated to Illumina platform compatible IDT adaptors with unique dual indexes with unique molecular identifiers (Integrated DNA Technologies), for paired end sequencing. The ligation products were enriched with 15 PCR cycles and the final library was validated on an Agilent 2100 Bioanalyzer with the DNA 7500 assay (Agilent). The libraries were sequenced on NovaSeq 6000 (Illumina) in

a fraction of sequencing flow cell with a read length of 2x101 bp following the manufacturer's protocol for dual indexing. Image analysis, base calling and quality scoring of the run were processed using the manufacturer's software Real Time Analysis (RTA v3.4.4) and followed by generation of FASTQ sequence files.

RNA-seq reads were mapped against human reference genome (GRCh38) using STAR software version 2.5.3a [55] with ENCODE parameters. Genes were quantified using RSEM version 1.3.0 [56] with default parameters and using the annotation file from GENCODE version 29. Only protein-coding genes that were expressed >1 cpm in at least 10 samples were considered for the association of gene expression with clinical variables.

4.5. Animal model

Briefly, 24 twenty-four C57BL/6J; 6-week-old male mice (Envigo, Barcelona, Spain), were housed in groups under controlled conditions of temperature (22 ± 2 ◦C) and humidity (55 ± 10%), and on a 12-h light/dark cycle with free access to food and water. After acclimatization, animals were randomly divided into experimental groups: Control mice (*n* =8) kept on a standard diet (D12328, Research Diets, New Brunswick, NJ, USA) and Obese group (*n* =16) fed with a high-fat diet (HFHC: D12331, Research Diets) supplemented with 23.1 g/L fructose and 18.9 g/L sucrose in the drinking water. Mice were kept on these diets for a period of 20 weeks in ad libitum conditions [57]. These specific doses were determined based on previous studies and a calculation of dose translation from human to animal dosage [58]. For the last 4 weeks of the experiment (from the 16th to 20th week), Obese mice were randomly distributed into two groups: 8 mice were kept under the same fed conditions described before (Obese group), and 8 mice were exposed to HAA group. HAA group is a mix of the following compounds: 210 mg/kg of L-histidine monohydrochloride monohydrate (Merck, GmbH Germany), 490 mg/kg L-cysteine hydrochloride (Merck, GmbH Germany), 210 mg/kg L-serine (Merck, GmbH Germany) and 210 mg/kg L-carnosine 98% (Acros Organics, Geel, Belgium). Histidine, cysteine, serine, and carnosine were diluted with drinking water with 23.1 g/L fructose and 18.9 g/L sucrose (vehicle). Fresh solutions were freshly prepared three times per week and prepared from stock powders and protected from light. Before being euthanized, 10 animals per group were randomly selected to perform an insulin challenge. They were intraperitoneally injected with 1 mU/g of insulin (*n* = 5 per group) or saline (*n* = 5 per group) and after 15 min, they were sacrificed.

Blood was collected and serum was obtained by centrifugation and stored at -80 ºC for further analysis. Brown adipose tissue (BAT) and white adipose tissue (WAT) depots (inguinal (IWAT), epididymal (EWAT), retroperitoneal (RWAT) and mesenteric (MWAT)) were immediately collected, weighed and snap-frozen in liquid nitrogen to finally be kept at -80 ºC for further determinations or fixed to perform histological analyses.

4.6. Serum and blood analysis

Serum fasting glucose, total cholesterol, and triglycerides (QCA, Barcelona, Spain) were analyzed by enzymatic colorimetric assays. Serum fasting insulinemia was analyzed using an insulin ELISA kit (Mercodia, Uppsala, Sweden), and serum HDL and LDL levels were analyzed using EnzyChrom ™ AF HDL and LDL/VLDL Assay Kit (BioAssay System, Hayward, CA, USA). Lately, LDL/HDL ratio was calculated. HOMA-IR (homeostatic model assessment for insulin resistance) and HOMA-β, which are assessments that estimates insulin resistance regarding the state of beta-cell function and insulin sensitivity, are calculated from circulating levels of fasting glucose and insulin (HOMA-IR = glucose (mmol/l) * insulin (UI/L) * 22.5 and HOMA-β (20 * insulin (UI/L)) / (glucose (mmol/l) - 3.5) [20].

For the ITT, mice fasted for 6 h and baseline blood glucose levels were measured with a standard glucometer (LifeScan, Milpitas, California, USA). Animals were then injected (*i.p*. 0.375 mU / g of body weight) with human rapid insulin (Actrapid® Innolet®, Novo Nordisk A/S, Bagsvaerd, Denmark) and blood glucose levels were measured every 30-, 60-, 90-, 120-, 150-, and 180-minutes collecting blood from the mice's tail and measuring glucose. For the GTT, mice fasted overnight and after measuring fasted blood glucose levels, mice were injected *i.p*. with 1.5 g glucose/kg of body weight (Merck KGaA, Darmstadt, Germany), and blood glucose levels were measured as explained in the ITT test.

4.7. Histological analysis

EWAT, IWAT and BAT portions fixed in buffered formalin (4% formaldehyde, 4 gr/L NaH_2PO_4, 6.5 gr/L Na_2HPO_4; pH 6.8) were cut at a thickness of 5 µm and stained with hematoxylin & eosin (H&E). BAT, IWAT and EWAT images (magnification 10X) were taken with a microscope (ECLIPSE Ti; Nikon, Tokyo, Japan) coupled to a digital sight camera (DS-Ri1, Nikon) and analyzed using ImageJ NDPI software (National Institutes of Health, Bethesda, MD, USA; https://imagej.nih.gov/ij, version 1.52a). To avoid any bias in the analysis, the study had a double-blind design, preventing the reviewers from knowing any data from the mice during the histopathological analysis. Area quantification of adipocytes was analyzed by the Adiposoft plugin to assess EWAT and IWAT's state between groups. Lipid droplets quantification in BAT was analyzed by the Droplet Finder plugin.

4.8. RNA extraction and quantitative polymerase chain reaction

According to the manufacturer's instructions, homogenates from EWATs, IWATs and BATs were used for total RNA extractions using the TriPure reagent (Roche Diagnostic, Sant Cugat del Vallès, Barcelona, Spain). RNA concentration and purity were determined using a nanophotometer (Implen GmbH, München,

Germany). RNA was converted to cDNA using the High-Capacity RNA-to-cDNA Kit (Applied Biosystems, Wilmington, DE, USA). The cDNAs were diluted 1:10 before incubation with commercial LightCycler 480 Sybr green I master on a Lightcycler® 480 II (Roche Diagnostics GmbH, Manheim, Germany). **Table 1** shows a list of used primers that were previously described in other studies and verified with Primer-Blast software (National Center for Biotechnology Information, Bethesda, MD, USA). 36b4 was used as a housekeeping gene [57].

4.9. BAT temperature measurements

The temperature surrounding BAT was visualized using a high-resolution infrared camera (FLIR Systems) and analyzed with a specific software package (FLIR-Tools-Software, FLIR; Kent, UK), as previously described [59]. For each image, the area surrounding BAT was delimited and the average temperature of the skin area was calculated as the average of 3 pictures/animal.

Table 1. Sequences of the oligonucleotides used in the RT-PCR

Primers	Forward	Reverse	Reference
Acox1	CTATGGGATCAGCCAGAAAG	AGTCAAAGGCATCCACCAAAG	59
Adipoq	AAGGGAGAGAAAGGAGATGC	TACACATAAGCGGCTTCTCC	60
Atgl	CAACGCCACTCACATCTACGG	GGACACCTCAATAATGTTGGCAC	59
Ccl2	ATTGGGATCATCTTGCTGGT	CCTGCTGTTCACAGTTGCC	61
Cpt1b	CGAGGATTCTCTGGAACTGC	GGCCTCTGTGGTACACGACAA	59
Dio2	AGAGTGGAGGCGCATGCT	GGCATCTAGGAGGAAGCTGTTC	59
Dio3	CTACGTCATCCAGAGTGGCA	CTGTTCATCATAGCGCTCCA	62
F4/80	CATAAGCTGGGCAAGTGGTA	GGATGTACAGATGGGGGATG	59
Fabp4	TGAAAGAAGTGGGAGTGGGC	CGAATTCCACGCCCAGTTTG	59
Fasn	GCTGCGGAAACTTCAGGAAAT	AGAGACGTGTCACTCCTGGACTT	59
Fgf21	CCTCTAGGTTTCTTTGCCAACAG	AAGCTGCAGGCCTCAGGAT	57
Glut4	AAAAGTGCCTGAAACCAGAG	TCACCTCCTGCTCTAAAAGG	59
Hdc	CTGGATTCTGGGTCAAGGACAA	AGAGTTGGCATGTCGGAGGTA	63
Hnmt	CATGGTCTCTTAGCTGCCAGTG	CAGGTCATCCAGTATCTGCGCA	64
Hsl	TCCTGGAACTAAGTGGACGCAAG	CAGACACACTCCTGCGCATAGAC	59

H1r	GCCGGCGGATCAGTGAGACAT	GCCCTGGCTCTATGCTGGTGTC	[65]
H2r	TGCACGGTACAGTGTTGGAG	CTGCCCTTTGTGTCTGGGAT	This study
H3r	CAAGACGGGCTGTTCGGAA	CGGACAGGTACTCCCAACTCA	[66]
H4r	TGCTGTGTCTTATAGGGCTCA	GGCCATTTACCAAGAAAGCCA	[66]
Lep	CTCCATCTGCTGGCCTTCTC	CATCCAGGCTCTCTGGCTTCT	[67]
LepR	TCCAGGAGAGATGCTCACACTTT	TGCGTGGAACAGGTTTGAAA	[68]
P53	CACGTACTCTCCTCCCCTCAAT	AACTGCACAGGGCACGTCTT	[69]
P21	CTGTCTTGCACTCTGGTGTCTGA	CCAATCTGCGCTTGGAGTGA	[69]
Pgc1a	AGCCGTGACCACTGACAACGAG	GCTGCATGGTTCTGAGTGCTAAG	[59]
Pparα	CCCTGTTTGTGGCTGCTATAATTT	GGGAAGAGGAAGGTGTCATCTG	[59]
Pparγ	CACAATGCCATCAGGTTTGG	GCTGGTCGATATCACTGGAGATC	[70]
Prdm16	CAGCACGGTGAAGCCATTC	GCGTGCATCCGCTTGTG	[59]
Scd1	AGATCTCCAGTTCTTACACGACCAC	GACGGATGTCTTCTTCCAGGTG	[59]
Tfam	CACCCAGATGCAAAACTTTCAG	CTGCTCTTTATACTTGCTCACAG	[71]
Tmem26	ACCCTGTCATCCCACAGAG	TGTTTGGTGGAGTCCTAAGGTC	[72]
Tnfα	AGGGTCTGGGCCATAGAACT	CCACCACGCTCTTCTGTCTAC	[59]
Ucp1	ACTGCCACACCTCCAGTCATT	CTTTGCCTCACTCAGGATTGG	[59]
36b4	AGTCCCTGCCCTTTGTACACA	CGATCCGAGGGCCTCACTA	[57]

4.10. Protein Extraction and Western Blot Analysis

Approximately 50 mg of BAT was homogenized with Tyssuelyser LT (Qiagen, Hilden, Germany) for 50 s in 300 µL lysis buffer [59]. The protein extracts were quantified by the standardized BCA method (Bio-Rad Protein Assay; BioRad, Hercules, CA, USA). Protein extracts (20–25 µg) were electrophoretically separated on 10% SDS-PAGE and electroblotted to nitrocellulose membranes (Li-cor biosciences, NE, USA) [73]. Efficient protein transfer was monitored by Ponceau-S stain. Next, membranes were blocked (5% BSA) at room temperature and probed with specific primary antibodies (diluted 1:1000) overnight at 4º C in 1% BSA: Ucp1 (ab10983) (Abcam, Cambridge, UK) and β-Actin (Santa Cruz Biotechnology, Inc.; Dallas, TX, USA). Thereafter, infrared fluorescent secondary antibodies anti-rabbit 800 and anti-mouse 680 (LI-COR Biosciences, Lincoln, NE,

USA; 926-32211, 926-68071 and 926-68070, respectively) were used for detection and quantified using ImageJ [74].

4.11. Quantification and statistical analysis

Statistical analyses for Animal models were performed using GraphPad Prism 9 software (Graph-Pad Software, La Jolla, CA, USA). Data are presented as mean ± SEM. Data distribution was analyzed by the Shapiro–Wilk normality test. Differences between the two groups were determined using an unpaired t-test (two-tailed, 95% confidence interval). A p-value below 0.05 was considered statistically significant.

Transcriptomic and metabolome analysis

For transcriptomic and metabolomic data, we used a combination of multivariate O-PLS modeling and partial Spearman's correlation (pSC) using in-house MATLAB scripts. First, an O-PLS model was built. Here, the omics profiles were used as the descriptor matrix (X) to predict serum histidine as the response variable (Y). Then, the variable selection was achieved by combining the variable importance for projection (O-PLS-VIP) [75] and the O-PLS regression loadings adjusted for multiple testing using the Benjamini-Hochberg procedure (pFDR). A pFDR < 0.05 was used as the reference feature selection criterium. However, a less restrictive threshold (pFDR < 0.1 unless otherwise indicated) was used to include variables with high VIP (> 1). Finally, each individual variable identified from multivariate models was further validated by pSC adjusting for age, BMI, sex, and country.

Differential expression gene analyses were performed on gene counts using the "limma" R package [76]. First, low expressed genes were filtered, so that only genes with more than 10 reads in at least 2 samples were selected. RNA-seq data were then normalized for RNA composition using the trimmed mean of M-value (TMM) as implemented in edgeR package [77]. Normalized counts were then converted to $\log_2$ count per million ($\log_{CPM}$) with associated precision weights to account for variations in precision between different observations using the "voom" function with donor's age, BMI, and sex as covariates. A robust linear regression model adjusted for the previous covariates was then fitted to the data using the "lmFit" function with the option method = "robust", to limit the influence of outlying samples. Finally, an empirical Bayes method was applied to borrow information between genes with the "eBayes" function. P-values were adjusted for multiple comparisons using the Benjamini-Hochberg procedure for False Discovery Rate (pFDR). A cut-off for the pFDR < 0.05 was used a threshold for statistical significance. The functional roles of differentially expressed genes were characterized using over-representation analyses based on the KEGG, Reactome, and Wikipathways databases using ConsensusPathDB [78]. Pathway

significance was assessed using a hypergeometric test and a Storey procedure (qvalue) was applied for multiple testing correction. Statistical significance was set at q value < 0.1.

Acknowledgements

We are in debt with the subjects involved in this project. This work was supported by EU-FP7 FLORINASH (Health-F2-2009-241913) to R.B., M.F., and J.M.F.R., and by the Catalan Government through the funding grant ACCIÓ-Eurecat (PRIV2020-EURHEPAD) to X.E. Infrastructure support was provided by the National Institute for Health Research (NIHR) Imperial Biomedical Research Centre (BRC). L.H. was in receipt of an MRC Intermediate Research Fellowship in Data Science (grant number MR/L01632X/1, UK Med-Bio). This work was also partly supported by funding to M.-E.D. (EU METACARDIS under agreement HEALTH-F4-2012-305312, Neuron II under agreement 291840 and the MRC MR/M501797/1) and by grants from the French National Research Agency (ANR-10-LABX-46 [European Genomics Institute for Diabetes]), from the National Center for Precision Diabetic Medicine – PreciDIAB, which is jointly supported by the French National Agency for Research (ANR-18-IBHU-0001), by the European Union (FEDER), by the Hauts-de-France Regional Council (Agreement 20001891/NP0025517) and by the European Metropolis of Lille (MEL, Agreement 2019_ESR_11) and by Isite ULNE (R-002-20-TALENT-DUMAS), also jointly funded by ANR (ANR-16-IDEX-0004-ULNE) the Hauts-de-France Regional Council (Agreement 20002045) and by the European Metropolis of Lille (MEL). S.Q.-V. is supported by a fellowship from the Vicente Lopez Program (Eurecat). J.M.-P. is funded by the Miguel Servet Program from the Instituto de Salud Carlos III (ISCIII CP18/00009), co-funded by the European Social Fund 'Investing in your future'.

References

1. World Health Organization. Obesity and overweight. (2021).

2. Duval, C. et al. Adipose tissue dysfunction signals progression of hepatic steatosis towards nonalcoholic steatohepatitis in C57Bl/6 mice. Diabetes 59, 3181–3191 (2010).

3. Koenen, M., Hill, M. A., Cohen, P. & Sowers, J. R. Obesity, Adipose Tissue and Vascular Dysfunction. Circ Res 951–968 (2021) doi:10.1161/CIRCRESAHA.121.318093.

4. Choe, S. S., Huh, J. Y., Hwang, I. J., Kim, J. I. & Kim, J. B. Adipose tissue remodeling: Its role in energy metabolism and metabolic disorders. Frontiers in Endocrinology vol. 7 Preprint at https://doi.org/10.3389/fendo.2016.00030 (2016).

5. Saito, M. et al. High incidence of metabolically active brown adipose tissue in healthy adult humans: Effects of cold exposure and adiposity. Diabetes 58, 1526–1531 (2009).

6. Yin, X. et al. The evolving view of thermogenic fat and its implications in cancer and metabolic diseases. Signal Transduction and Targeted Therapy vol. 7 Preprint at https://doi.org/10.1038/s41392-022-01178-6 (2022).

7. Alcalá, M. et al. Increased inflammation, oxidative stress and mitochondrial respiration in brown adipose tissue from obese mice. Sci Rep 7, (2017).

8. Kimura, K. et al. Histidine augments the suppression of hepatic glucose production by central insulin action. Diabetes 62, 2266–2277 (2013).

9. Kennedy, L. et al. Knockout of l-Histidine Decarboxylase Prevents Cholangiocyte Damage and Hepatic Fibrosis in Mice Subjected to High-Fat Diet Feeding via Disrupted Histamine/Leptin Signaling. American Journal of Pathology 188, 600–615 (2018).

10. Moro, J., Tomé, D., Schmidely, P., Demersay, T. C. & Azzout-Marniche, D. Histidine: A systematic review on metabolism and physiological effects in human and different animal species. Nutrients vol. 12 Preprint at https://doi.org/10.3390/nu12051414 (2020).

11. Holeček, M. Histidine in health and disease: Metabolism, physiological importance, and use as a supplement. Nutrients vol. 12 Preprint at https://doi.org/10.3390/nu12030848 (2020).

12. Lee, D.-Y. & Kim, E.-H. Therapeutic Effects of Amino Acids in Liver Diseases: Current Studies and Future Perspectives. J Cancer Prev 24, 72–78 (2019).

13. Mihalik, S. J. et al. Metabolomic profiling of fatty acid and amino acid metabolism in youth with obesity and type 2 diabetes: Evidence for enhanced mitochondrial oxidation. Diabetes Care 35, 605–611 (2012).

14. Feng, R. N. et al. Histidine supplementation improves insulin resistance through suppressed inflammation in obese women with the metabolic syndrome: A randomised controlled trial. Diabetologia 56, 985–994 (2013).

15. Sun, X. et al. Histidine supplementation alleviates inflammation in the adipose tissue of high-fat diet-induced obese rats via the NF-κB-and PPARγ-involved pathways. British Journal of Nutrition 112, 477–485 (2014).

16. Kasaoka, S. et al. Histidine supplementation suppresses food intake and fat accumulation in rats. Nutrition 20, 991–996 (2004).

17. Holm, L. J. & Buschard, K. L-serine: a neglected amino acid with a potential therapeutic role in diabetes. APMIS vol. 127 655–659 Preprint at https://doi.org/10.1111/apm.12987 (2019).

18. Mcgavigan, A. K. et al. L-cysteine suppresses ghrelin and reduces appetite in rodents and humans. Int J Obes 39, 447–455 (2015).

19. Baye, E. et al. Carnosine supplementation improves serum resistin concentrations in overweight or obese otherwise healthy adults: A pilot randomized trial. Nutrients 10, (2018).

20. Houjeghani, S., Kheirouri, S., Faraji, E. & Jafarabadi, M. A. L-Carnosine supplementation attenuated fasting glucose, triglycerides, advanced glycation end products, and tumor necrosis factor–α levels in patients with type 2 diabetes: a double-blind placebo-controlled randomized clinical trial. Nutrition Research 49, 96–106 (2018).

21. Karlstedt, K., Åhman, M. J., Anichtchik, O. v., Soinila, S. & Panula, P. Expression of the H3 receptor in the developing CNS and brown fat suggests novel roles for histamine. Molecular and Cellular Neuroscience 24, 614–622 (2003).

22. Finlin, B. S. et al. Adipose Tissue Mast Cells Promote Human Adipose Beiging in Response to Cold. Sci Rep 9, 8658 (2019).

23. Zhao, Y. et al. Stimulation of histamine H4 receptor participates in cold-induced browning of subcutaneous white adipose tissue. American Journal of Physiology-Endocrinology and Metabolism 317, E1158–E1171 (2019).

24. Wang, K. Y. et al. Histamine regulation in glucose and lipid metabolism via histamine receptors: Model for nonalcoholic steatohepatitis in mice. American Journal of Pathology 177, 713–723 (2010).

25. Townsend, K. L. & Tseng, Y. H. Brown fat fuel utilization and thermogenesis. Trends in Endocrinology and Metabolism vol. 25 168–177 Preprint at https://doi.org/10.1016/j.tem.2013.12.004 (2014).

26. Thalacker-Mercer, A. E. & Gheller, M. E. Benefits and Adverse Effects of Histidine Supplementation. J Nutr 150, 2588S-2592S (2020).

27. Du, S. et al. Effects of Histidine Supplementation on Global Serum and Urine 1H NMR-based Metabolomics and Serum Amino Acid Profiles in Obese Women from a Randomized Controlled Study. J Proteome Res 16, 2221–2230 (2017).

28. Li, Y. C. et al. Relationships of dietary histidine and obesity in northern chinese adults, an internet-based cross-sectional study. Nutrients 8, 1–15 (2016).

29. Feng, R. N. et al. Histidine supplementation improves insulin resistance through suppressed inflammation in obese women with the metabolic syndrome: a randomised controlled trial. Diabetologia 56, 985–994 (2013).

30. Niu, Y. C. et al. Histidine and arginine are associated with inflammation and oxidative stress in obese women. British Journal of Nutrition 108, 57–61 (2012).

31. Jørgensen, E. A. et al. Increased susceptibility to diet-induced obesity in histamine-deficient mice. Neuroendocrinology 83, 289–294 (2006).

32. Minamino, T. et al. A crucial role for adipose tissue p53 in the regulation of insulin resistance. Nat Med 15, 1082–1087 (2009).

33. Bi, P. & Kuang, S. Notch signaling as a novel regulator of metabolism. Trends in Endocrinology and Metabolism vol. 26 248–255 Preprint at https://doi.org/10.1016/j.tem.2015.02.006 (2015).

34. Bi, P. et al. Inhibition of Notch signaling promotes browning of white adipose tissue and ameliorates obesity. Nat Med 20, 911–918 (2014).

35. Feng, R. N. et al. Histidine supplementation improves insulin resistance through suppressed inflammation in obese women with the metabolic syndrome: A randomised controlled trial. Diabetologia 56, 985–994 (2013).

36. Mong, M. C., Chao, C. Y. & Yin, M. C. Histidine and carnosine alleviated hepatic steatosis in mice consumed high saturated fat diet. Eur J Pharmacol 653, 82–88 (2011).

37. Yoshimatsu, H. et al. Histidine induces lipolysis through sympathetic nerve in white adipose tissue. European Journal of Clinical Investigation vol. 32 (2002).

38. Achari, A. E. & Jain, S. K. L-cysteine supplementation increases insulin sensitivity mediated by upregulation of GSH and adiponectin in high glucose treated 3T3-L1 adipocytes. Arch Biochem Biophys 630, 54–65 (2017).

39. Ouchi, N. & Walsh, K. Adiponectin as an anti-inflammatory factor. Clinica Chimica Acta 380, 24–30 (2007).

40. Maeda, N. et al. PPAR Ligands Increase Expression and Plasma Concentrations of Adiponectin, an Adipose-Derived Protein. Diabetes 50, 2094–2099 (2001).

41. Peng, J., Yin, L. & Wang, X. Central and peripheral leptin resistance in obesity and improvements of exercise. Hormones and Behavior vol. 133 Preprint at https://doi.org/10.1016/j.yhbeh.2021.105006 (2021).

42. Kotzbeck, P. et al. Brown adipose tissue whitening leads to brown adipocyte death and adipose tissue inflammation. J Lipid Res 59, 784–794 (2018).

43. López-Gonzales, E. et al. L-Serine Supplementation Blunts Fasting-Induced Weight Regain by Increasing Brown Fat Thermogenesis. Nutrients 14, (2022).

44. Flores, V. et al. Regulation of metabolic health by dietary histidine in mice. J Physiol 1–25 (2022) doi:10.1113/JP283261#support-information-section.

45. Finlin, B. S. et al. Mast cells promote seasonal white adipose beiging in humans. Diabetes 66, 1237–1246 (2017).

46. Masaki, T., Yoshimatsu, H., Chiba, S., Watanabe, T. & Sakata, T. Targeted Disruption of Histamine H 1-Receptor Attenuates Regulatory Effects of Leptin on Feeding, Adiposity, and UCP Family in Mice. DIABETES vol. 50 http://diabetesjournals.org/diabetes/article-pdf/50/2/385/646632/0500385.pdf (2001).

47. Masaki, T., Yoshimatsu, H., Chiba, S., Watanabe, T. & Sakata, T. Central Infusion of Histamine Reduces Fat Accumulation and Upregulates UCP Family in Leptin-Resistant Obese Mice. DIABETES vol. 50 http://diabetesjournals.org/diabetes/article-pdf/50/2/376/646639/0500376.pdf (2001).

48. Wang, K. Y. et al. Histamine regulation in glucose and lipid metabolism via histamine receptors: Model for nonalcoholic steatohepatitis in mice. American Journal of Pathology 177, 713–723 (2010).

49. Desautels, M. et al. Role of mast cell histamine in brown adipose tissue thermogenic response to VMH stimulation. www.physiology.org/journal/ajpregu (1994).

50. Passani, M. B., Blandina, P. & Torrealba, F. The histamine H3 receptor and eating behavior. Journal of Pharmacology and Experimental Therapeutics 336, 24–29 (2011).

51. Zeng, H. et al. Histamine induces the expression of uncoupling protein 2 (UCP2) and acid-binding protein (aP2) in white adipocytes. Clin Chem Lab Med 45, 1199–1206 (2007).

52. Kotańska, M. et al. KSK19 – Novel histamine H3 receptor ligand reduces body weight in diet induced obese mice. Biochem Pharmacol 168, 193–203 (2019).

53. Salazar-Tortosa, D. F., Enard, D., Itan, Y. & Ruiz, J. R. Novel brown adipose tissue candidate genes predicted by the human gene connectome. Sci Rep 12, (2022).

54. Puig, J. et al. The Aging Imageomics Study: rationale, design and baseline characteristics of the study population. Mech Ageing Dev 189, (2020).

55. Dobin, A. et al. STAR: Ultrafast universal RNA-seq aligner. Bioinformatics 29, 15–21 (2013).

56. Li, B. & Dewey, C. N. RSEM: Accurate transcript quantification from RNA-Seq data with or without a reference genome. BMC Bioinformatics 12, (2011).

57. Quesada-Vázquez, S. et al. Supplementation with a Specific Combination of Metabolic Cofactors Ameliorates Non-Alcoholic Fatty Liver Disease and, Hepatic Fibrosis, and Insulin Resistance in Mice. Nutrients 13, 3532 (2021).

58. Reagan-Shaw, S., Nihal, M. & Ahmad, N. Dose translation from animal to human studies revisited. The FASEB Journal 22, 659–661 (2008).

59. Quesada-Vázquez, S. et al. Reduction of obesity and insulin resistance through dual tar-2 geting of VAT and BAT by a novel combination of metabolic 3 cofactors 4. Int. J. Mol. Sci 2022, (2022).

60. Rull, A. et al. Rosiglitazone and fenofibrate exacerbate liver steatosis in a mouse model of obesity and hyperlipidemia. A transcriptomic and metabolomic study. J Proteome Res 13, 1731–1743 (2014).

61. Dalvi, P. S. et al. Long-term metabolic effects of malnutrition: Liver steatosis and insulin resistance following early-life protein restriction. PLoS One 13, (2018).

62. Boelen, A., Kwakkel, J., Wiersinga, W. M. & Fliers, E. Chronic local inflammation in mice results in decreased TRH and type 3 deiodinase mRNA expression in the hypothalamic paraventricular nucleus independently of diminished food intake. Journal of Endocrinology 191, 707–714 (2006).

63. Everaert, I., de Naeyer, H., Taes, Y. & Derave, W. Gene expression of carnosine-related enzymes and transporters in skeletal muscle. Eur J Appl Physiol 113, 1169–1179 (2013).

64. Karer, M. et al. Diamine oxidase knockout mice are not hypersensitive to orally or subcutaneously administered histamine. Inflammation Research 71, 497–511 (2022).

65. Deshetty, U. M. et al. Ameliorative Effect of Hesperidin Against Motion Sickness by Modulating Histamine and Histamine H1 Receptor Expression. Neurochem Res 45, 371–384 (2020).

66. Zhao, Y.-X. et al. Stimulation of histamine H4 receptor participates in cold-induced browning of subcutaneous white adipose tissue. Am J Physiol Endocrinol Metab 317, 1158–1171 (2019).

67. Colón-Mesa, I. et al. Regulation of p27 and cdk2 expression in different adipose tissue depots in aging and obesity. Int J Mol Sci 22, (2021).

68. Cortés, V. A. et al. Leptin ameliorates insulin resistance and hepatic steatosis in Agpat2-/-lipodystrophic mice independent of hepatocyte leptin receptors. J Lipid Res 55, 276–288 (2014).

69. Amelio, I., Cutruzzolá, F., Antonov, A., Agostini, M. & Melino, G. Serine and glycine metabolism in cancer. Trends in Biochemical Sciences vol. 39 191–198 Preprint at https://doi.org/10.1016/j.tibs.2014.02.004 (2014).

70. Cartland, S. P., Erlich, J. H. & Kavurma, M. M. TRAIL deficiency contributes to diabetic nephropathy in fat-fed ApoE -/- mice. PLoS One 9, (2014).

71. Santos, S. S. et al. The mitochondrial antioxidant sirtuin3 cooperates with lipid metabolism to safeguard neurogenesis in aging and depression. Cells 11, (2022).

72. Shen, Y., Zhou, H., Jin, W. & Lee, H. J. Acute exercise regulates adipogenic gene expression in white adipose tissue. Biol Sport 33, 381–391 (2016).

73. López-Yoldi, M. et al. Cardiotrophin-1 stimulates lipolysis through the regulation of main adipose tissue lipases. J Lipid Res 55, 2634–2643 (2014).

74. Miranda, M. et al. Relation between human LPIN1, hypoxia and endoplasmic reticulum stress genes in subcutaneous and visceral adipose tissue. Int J Obes (Lond) 34, 679–686 (2010).

75. Galindo-Prieto, B., Eriksson, L. & Trygg, J. Variable influence on projection (VIP) for orthogonal projections to latent structures (OPLS). J Chemom 28, 623–632 (2014).

76. Ritchie, M. E. et al. Limma powers differential expression analyses for RNA-sequencing and microarray studies. Nucleic Acids Res 43, e47 (2015).

77. Robinson, M. D., McCarthy, D. J. & Smyth, G. K. edgeR: A Bioconductor package for differential expression analysis of digital gene expression data. Bioinformatics 26, 139–140 (2010).

78. Kamburov, A., Stelzl, U., Lehrach, H. & Herwig, R. The ConsensusPathDB interaction database: 2013 Update. Nucleic Acids Res 41, D793–D800 (2013).

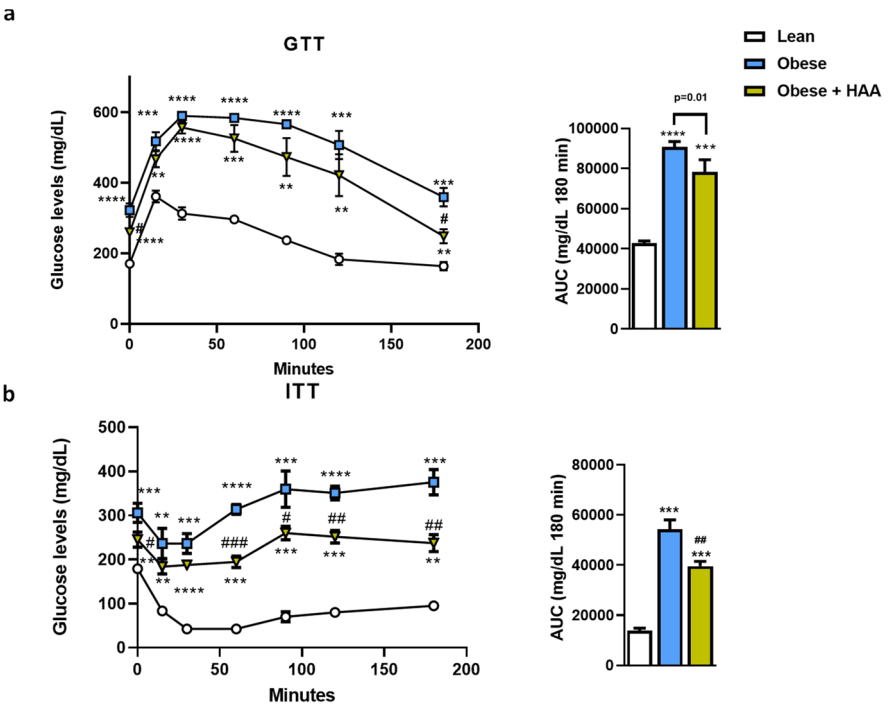

Figure s1. HAA supplementation promotes improved glucose tolerance and insulin resistance. (A) glucose tolerance test (GTT) and AUC; (B) insulin tolerance test (ITT) and AUC. Data are mean ± SEM. Data are mean ± SEM. ** $p < 0.01$, *** $p < 0.001$, **** $p < 0.0001$ *vs*. control; $^{\#}p < 0.05$, $^{\#\#}p < 0.01$, $^{\#\#\#}p < 0.001$ *vs*. Obese + vehicle.

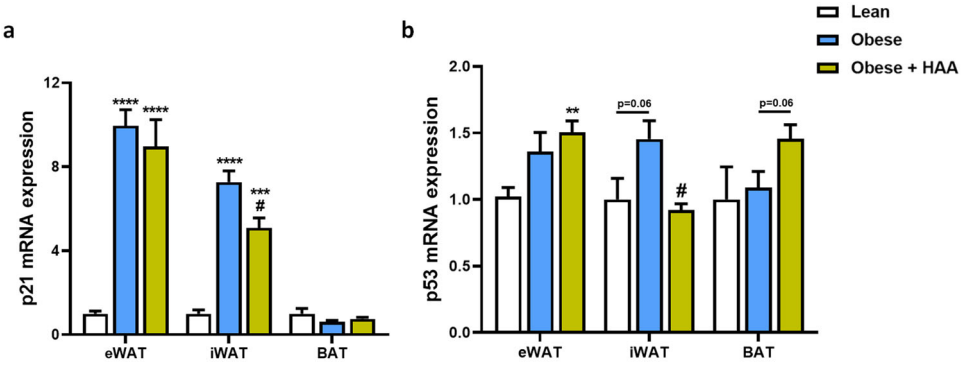

Figure S2. HAA supplementation modulates the expression levels of histamine receptors in eWAT, iWAT and BAT. mRNA expression of genes related to senescence (**a**) *P21* and (**b**) *P53* in eWAT, iWAT and BAT. Data are mean ± SEM. *

** p < 0.01, *** p < 0.001, **** p < 0.0001 *vs*. control; # p < 0.05 *vs*. Obese + vehicle.

Suppl. Table 1. Serum parameters in lean, obese mice and obese mice supplemented with HAA.

	Lean	Obese	Obese + HAA
Glucose (mmol/L)	6.42 ± 0.80	11.64 ± 0.87****	11.35 ± 0.69***
Insulin (µg/L)	0.85 ± 0.09	4.60 ± 0.47****	**3.22 ± 0.40******,#
Triglycerides (mmol/L)	0.59 ± 0.04	0.98 ± 0.06****	0.92 ± 0.04****
Total cholesterol(mmol/L)	2.06 ± 0.15	6.39 ± 0.19****	6.28 ± 0.12****
LDL (mmol/L)	0.48 ± 0.05	1.81 ± 0.15****	**1.22 ± 0.17***,##
HDL (mmol/L)	1.64 ± 0.15	2.94 ± 0.14****	**3.27 ± 0.13****,#
LDL/HDL ratio	0.30 ± 0.04	0.63 ± 0.07***	**0.38 ± 0.07**#
HOMA-IR	7.80 ± 0.79	73.63 ± 9.31****	**44.07 ± 7.28****,#
HOMA-β	91.25 ± 11.89	262.56 ± 19.56****	**207.18 ± 27.25****,#

Data are mean ± SEM. *** p < 0.001, **** p < 0.0001 *vs*. control; # p < 0.05, ## p < 0.01, *vs*. Obese + vehicle.

Chapter 5

Potential therapeutic implications of Histidine catabolism by the gut microbiota in NAFLD

Sergio Quesada-Vázquez[1], Jèssica Latorre[2], Núria Oliveras-Cañellas[2], Noemi Tejera[3], Yaiza Tobajas[1], Falk Hildebrand[3,4], Naiara Beraza[3], Rémy Burcelin[5,6], Marc-Emmanuel Dumas[7,8,9,10], Massimo Federici[11], Lesley Hoyles[12], Josep M. del Bas[13], Xavier Escoté[1]*, José-Manuel Fernández-Real[2]*, Jordi Mayneris-Perxachs[2]*

1. Eurecat, Centre Tecnològic de Catalunya, Unitat de Nutrició i Salut, Reus, Spain.
2. Nutrition, Eumetabolism and Health Group, Girona Biomedical Research Institute (IDIBGI), Girona; and CIBER Fisiopatología de la Obesidad y Nutrición (CIBERobn), Instituto de Salud Carlos III, Madrid, Spain.
3. Microbes in the Food Chain, Institute Strategic Programme; Microbes and Gut Health, Institute Strategic Programme- Quadram Institute Bioscience, Norwich Research Park, Norwich,UK.
4. Digital Biology, Earlham Institute, Norwich Research Park, Norwich, Norfolk NR4 7UZ, UK.
5. Institut National de la Santé et de la Recherche Médicale (INSERM), Toulouse, France. 8 Université Paul Sabatier (UPS), Unité Mixte de Recherche (UMR) 104.
6. Institut des Maladies Métaboliques et Cardiovasculaires (I2MC), Team 2: 'Intestinal Risk Factors, Diabetes, Dyslipidemia, and Heart Failure', 31432 Toulouse Cedex 4, France.
7. Section of Biomolecular Medicine, Division of Systems Medicine, Department of Metabolism, Digestion and Reproduction, Imperial College London, Exhibition Road, London SW7 2AZ, UK.
8. Section of Genomic and Environmental Medicine, National Heart & Lung Institute, Imperial College London, Dovehouse Street, London SW3 6LY, UK.
9. European Genomic Institute for Diabetes, CNRS UMR 8199, INSERM UMR 1283, Institut Pasteur de Lille, Lille University Hospital, University of Lille, 59045 Lille, France.
10. McGill University and Genome Quebec Innovation Centre, 740 Doctor Penfield Avenue, Montréal, QC H3A 0G1, Canada.
11. Department of Systems Medicine, University of Rome Tor Vergata, Via Montpellier 1, 00133 Rome, Italy.
12. Department of Biosciences, School of Science and Technology, Nottingham Trent University, Nottingham NG11 8NS, UK.
13. Eurecat, Centre Tecnològic de Catalunya, Àrea de Biotecnologia, Reus, Spain.

* Correspondence: xavier.escote@eurecat.org, jmfreal@idibgi.org and jmayneris@idibgi.org.

Submitted in: Cell Reports Medicine. 2022 Dec.

Impact Factor (2022): 16.988

JCR category rank: Q1: Biochemistry, Genetics and Molecular Biology (miscellaneous)

Summary

The gut microbiome plays a critical role in the pathophysiology of non-alcoholic fatty liver disease (NAFLD). Histidine is an important energy source for the microbiota, but its synthesis is energetically expensive, and the microbiota may scavenge it from the host. However, the role of the microbiota and histidine in NAFLD is unknown. We performed a systems medicine analysis in three human cohorts (discovery: *n* = 49; validation 1: *n* = 313; validation 2: *n* =283) coupled with human primary hepatocytes experiments, diet-induced NAFLD mice models, and fecal microbiota transplantation (FMT). Plasma histidine was negatively associated with steatosis degree in all cohorts and linked to a hepatic transcriptomic signature involved in insulin signaling activation and inflammatory regulation. The trace-amine-associated receptor-1 (*TAAR1*) expression was strongly associated with histidine. Histidine supplementation in primary hepatocytes decreased the expression of lipogenic genes and activated AKT, which decreased after *TAAR1* silencing. Supplementation of histidine-related amino acids (HAA) improved NAFLD and decreased liver inflammation in mice. Circulating histidine was negatively associated with Proteobacteria, but positively with health-promoting bacteria and bacteria lacking the histidine utilization (Hut) system. In line, patients with higher steatosis degree had increased levels of microbial Hut genes, which decreased after HAA supplementation. FMT from high-histidine patients decreased hepatic triglycerides and the expression of glucose, insulin, and lipid metabolism genes in recipient mice. We have unraveled a significant interplay among gut microbiome, histidine catabolism and liver steatosis that may open a new window for the therapeutic targets against NAFLD.

Keywords: Amino acids, hut operon, *Proteobacteria*, hepatic disease, omics, dysbiosis

Introduction

Non-alcoholic fatty liver disease (NAFLD) affects almost one-third of the world's population, standing out as one of the most prevalent metabolic diseases [1]. NAFLD is characterized by an excessive accumulation of fat in the liver accompanied by low-grade inflammation and insulin resistance and can lead to fibrosis and eventually progress to irreversible stages such as cirrhosis or hepatocarcinoma [2]. Given the paucity of targeted agents to treat/prevent NAFLD, new therapeutic avenues are urgently required.

The liver is a central organ orchestrating amino acid metabolism [3], with these metabolites linked to type 2 diabetes and NAFLD [4–6]. Different medical conditions such as obesity, chronic kidney disease, and heart failure, are associated with decreased histidine levels [7–9]. Histidine has a wide range of beneficial effects, including antioxidant, anti-inflammatory, anti-glycating, and chelating properties [10]. Histidine supplementation had a beneficial effect on ethanol- and acetaminophen-induced mouse models of liver injury through its anti-oxidative and anti-inflammatory effects [11,12]. Results from randomized controlled trials have shown that supplementation with histidine and histidine-containing dipeptides may improve obesity and glycemic control, but the effects on liver function are unclear [13]. In fact, the only clinical study assessing the effects of histidine supplementation in obese women with metabolic syndrome reported an improvement in insulin resistance through suppressed inflammation but no changes in serum liver enzymes after 12-weeks-supplementation [14]. Therefore, little is known about the associations and underlying mechanisms of histidine in NAFLD. Importantly, the gut microbiota plays a key role in regulating dietary histidine bioavailability [15] is involved in hepatic alterations leading to NAFLD [16]. Nevertheless, it is currently unknown whether a connection exists among gut microbiota, histidine metabolism and NAFLD.

Thus, we used an integrative systems medicine approach in large well-characterized NAFLD cohorts, combining plasma metabolomics, fecal metagenomics, hepatic transcriptomics, and fecal microbiota transplantation, to assess the relationship between histidine metabolism and NAFLD. Further in vitro human primary hepatocytes and mice models were used to assess the effects of histidine-related amino acid (HAA) supplementation as a novel strategy for the treatment of NAFLD.

Results

Circulating histidine levels in different cohorts depending on the degree of steatosis

We identified several circulating metabolites significantly correlated with the degree of hepatic steatosis among 102 morbidly obese women from Italy and Spain by applying a ^{1}H-NMR-based metabolome-wide association study. Plasma histidine was one of the metabolites most significantly negatively associated with liver steatosis assessed by liver biopsy (**Figure 1a**) and echography (**Figure 1b**). These associations were further validated in an independent cohort of obese patients (BMI> 30 kg/m^2) from Italy and Spain (*n* = 313) (**Figure 1c**) and another validation cohort including patients only from Spain (*n* = 283) (**Figure 1d**).

Microarray analysis of human liver genes associated with circulatory levels of histidine

We next aimed to identify hepatic transcriptomic signatures associated with plasma histidine levels. We fitted robust linear regression models (controlling for age, BMI, sex, and country) with empirical Bayes moderation of the standard errors in a subset of patients (*n* = 88) from the discovery cohort with hepatic transcriptomes. We identified 82 and 11 gene transcripts that were significantly positively and negatively associated with the circulating histidine levels, respectively (**Figure 2a**). The trace amine-associated receptor 1 (*TAAR1*) was one of the hepatic gene transcripts most significantly associated with plasma histidine levels. To identify potential mechanisms underlying the effects of histidine on liver steatosis, we integrated gene-gene interaction networks with pathway over-representation analyses on the 93 histidine-associated gene transcripts. First, we mapped significant genes to a STRING interaction network. Then, we performed over-representation analyses based on the Reactome and KEGG databases on active subnetworks of interconnected genes identified in the interaction network. Finally, significantly enriched pathways were clustered using agglomerative hierarchical clustering. On the Reactome database, the most significant cluster included the G alpha (s) and the olfactory signaling pathways (**Figure 2b, c**). Other significant clusters involved the regulation of insulin-like growth factors (IGF), the activation of fibroblast growth factor receptors (FGFR), inflammatory regulation pathways, and insulin signaling pathways such as the activation of the PI3K-AKT pathway, and fatty acyl-CoA biosynthesis (**Figure 2b, c**).

The gene transcripts associated with the plasma histidine levels involved in participating in these pathways are shown in **Figure 2d**. KEGG-based analysis also identified the fatty acid biosynthesis, the PI3K-AKT signaling pathway, the inflammatory and immune regulation, and the olfactory transduction as relevant pathways linked to circulating histidine levels (**Figure S1**).

Histidine supplementation modulates NAFLD in human primary hepatocytes

To elucidate the role and underlying mechanisms of histidine in NAFLD, we treated human primary hepatocytes with histidine. Primary hepatocytes were also treated with palmitic acid, a free fatty acid known to trigger hepatic steatosis in human primary hepatocytes [17], with or without histidine. We assessed the expression of genes involved in steatosis and *de novo* hepatic lipogenesis. PA induced the expression of lipid metabolism genes (*ACSL1*, *SCD1*, *FASN*; **Figure 3a**-**c**), whereas co-treatment with PA and histidine led to lower expression of both *SCD1* and *FASN* compared to PA treatment alone, indicating a reduction in the *de novo* hepatic lipogenesis (**Figure 3b**,**c**). As *TAAR1* was one of the genes most strongly associated with circulating histidine levels in patients with NAFLD, we also assessed the effect of histidine supplementation on the expression of *TAAR1* in human primary hepatocytes. Consistent with the results from the human liver microarray, the expression levels of *TAAR1* were strongly induced after co-treatment with PA and histidine (**Figure 3d**). Our pathway enrichment analyses identified the PI3K-AKT signaling as one of the pathways most associated with plasma histidine levels. Thus, we next investigated insulin signaling by monitoring Akt^{S473} phosphorylation (**Figure 3e**). Treatment with PA significantly lowered Akt^{S473} phosphorylation, suggesting that PA reduces the response to insulin, whereas histidine treatment increased phosphorylation (**Figure 3e**). Remarkably, knock-down of *TAAR1* expression with specific siRNA induced a decrease in Akt^{S473} phosphorylation similar to that observed after PA treatment (**Figure 3e**).

Histidine-related amino acids supplementation reduces the main features of NAFLD in mice

To further elucidate the role of histidine in the development of NAFLD, we supplemented a combination of histidine and histidine-related amino

acids (HAA: histidine, serine, carnosine, and cysteine) to mice fed high fructose and high-fat diet (**Figure 3f, g**). We have previously shown that this model induces NAFLD [887]. Although this diet-induced model of NAFLD did not reduce serum histidine levels compared to vehicle supplementation (**Figure 3h**), hepatic histidine levels increased after HAA treatment (**Figure 3i**). HAA supplementation had no effect on alanine transaminase (ALT) levels (**Figure 3j**) but ameliorated several NAFLD-related features such as aspartate aminotransferase (AST) levels (**Figure 3k**), liver weight (**Figure 3l**), and hepatic triglycerides (**Figure 3m**). Total hepatic lipid levels also decreased (**Figure 3n**) in parallel to macroscopical (**Figure 3o**) and microscopical improvements (**Figure 3p**). We also observed an amelioration in the histopathological analysis (**Figure 3q**) and in the lipid droplet quantification (**Figure 3r**). We next analyzed the liver expression of some genes involved in *de novo* lipogenesis, lipid transport, and inflammation (**Figure 3s**). We did not find significant changes in lipid transport, but HAA supplementation increased the expression levels of some genes involved in *de novo* lipid biosynthesis (*Acc1*) and decreased the expression levels of several inflammatory markers (*F4/80*, *Tnfα, Il1α*) (**Figure 3s**). In line with the human findings, HAA increased the hepatic expression of *Taar1* compared to the vehicle group (**Figure 3t**). To evaluate the impact of the HAA supplementation on insulin signaling we performed an intraperitoneal insulin bolus. We observed that NAFLD+HAA mice had higher $pAkt^{S473}$ phosphorylation after the insulin bolus compared to the NAFLD + vehicle mice, thereby indicating better insulin sensitivity in the former group (**Figure 3u**).

Circulating histidine levels are negatively associated with proteobacteria

We next assessed the potential role of the gut microbiota in modulating plasma histidine levels by performing a shotgun metagenomics analysis of 73 fecal samples of patients from the discovery cohort. We applied the analysis of the composition of the microbiome with bias correction (ANCOM-BC) to consider the compositional nature of the metagenomic datasets and identify differential abundant taxa associated with the circulating histidine levels controlling for age, BMI, sex, and country. Both at the family (**Figure 4a**) and genus (**Figure 4b**) levels, we identified a strong negative association between histidine levels and members of the phylum *Proteobacteria*. As we previously described [16], families (**Figure 4c**) and genera (**Figure 4d**) from the phylum *Proteobacteria* were also strongly associated with the degree of hepatic steatosis. Circulating histidine levels

were also strongly positively associated with *Cyanobacteria* and orders *Corynebacteriales* (phylum *Actinobacteria*) and *Marinilabiliales* (phylum *Bacteroidetes*) (**Figure 4a**). At the species level, circulating histidine was positively associated with bacterial indicators of a healthy gut known to produce anti-inflammatory metabolites such as species from the genera *Faecalibacteirum, Bifidobacterium* and *Odoribacter*.

Histidine is an important carbon and nitrogen source in proteobacteria [18] through its conversion to glutamate. The histidine utilization (hut) operon involves four enzyme-encoding genes: *hutH, hutU, hutI, hutG* (**Figure 4e**) [19]. Therefore, we next evaluated the associations of these four microbial functions with degree of the steatosis. Remarkably, compared to patients with a steatosis degree <33 %, those with a >33 % of liver steatosis had higher clr-transformed abundances of microbial genes involved in the first three histidine degradation steps, which appear to be universal and involve the conversion of histidine to urocanate, hydration of urocanate to imidazole propionate and cleavage of the imidazole ring to give formiminoglutamate (**Figure 4f-i**) [19].

Histidine supplementation ameliorates the gut dysbiosis characteristic of NAFLD

To confirm the direct role of histidine in shaping the composition of the microbiota in NAFLD, we used 16S rRNA gene amplicon sequencing to profile the gut microbiota in the diet-induced NAFLD mice groups. Consistent with our findings in humans, histidine supplementation resulted in a strong increase in *Cyanobacteria* (order *Gastranaerophilales*) and higher levels of *Actinobacteria* and *Marinifilaceae* compared to the vehicle-supplemented group (**Figure 5a**). Histidine supplementation also resulted in increased levels of health-promoting bacteria such as families *Lactobacillaceae* and *Christensenellaceae* (**Figure 5a**). Compared to the vehicle, HAA supplementation in the NAFLD mice model tended to reduce the levels of the genus *Roseburia* (**Figure 5b**) and increased the levels of the genus *Akkermansia* (**Figure 5c**), which were decreased with hepatic steatosis in humans (**Figure 4c**). Remarkably, the expression of bacterial histidine utilisation genes (*hutH* and *hutG*), which we found increased in patients with NAFLD, decreased after HAA supplementation in NAFLD-induced mice compared to their vehicle counterparts (**Figure 5d**). Collectively, these results confirm the gut microbiota dysbiosis present in NAFLD and the effects on histidine catabolism.

Gut microbiota from low-histidine donors promotes hepatic triglyceride accumulation

To deepen our insights into the potential role of the microbiota in the progression of NAFLD through alterations in histidine metabolism, we performed a fecal microbiota transplantation (FMT) experiment. We transferred fecal microbiota from donors with histidine levels above the median (high histidine group, *n*=2) and donors with histidine levels below the median (low histidine group, *n*=2) to antibiotic-treated recipient mice (*n* = 8 mice per donor) (**Figure 5e**). Microbiota transfer from the high histidine donors resulted in lower hepatic triglycerides in recipient mice compared to those receiving microbiota from the low histidine donors (**Figure 5f**). We also identified a dose-response effect in the hepatic expression of several genes coding for key enzymes involved in regulating *de novo* biosynthesis of fatty acid and cholesterol (*Prkaa2, Pgc1a, Acadsb*), and glucose (*Slc2a2*) and insulin (*Insr*) metabolism (**Figure 5g-k**).

Discussion

Histidine and microbial-derived histidine metabolites have been shown to modulate insulin signaling and diabetes [14,20,21]. However, little is known about the effects of histidine on NAFLD. Current results open new insight into the role of histidine catabolism in the pathogenesis of NAFLD. We have identified a consistent decrease in circulating histidine levels with an increased degree of hepatic steatosis in humans. To validate this negative association, we assessed whether HAA supplementation ameliorated the features of NAFLD in a mouse model of diet-induced NAFLD. Previous animal models supplementing histidine have only shown a partial improvement in NAFLD features [22,23]. Hence, we used a combination of amino acids involved in histidine regulation aiming at increasing histidine levels. Specifically, we used carnosine, a precursor of histidine; cysteine, which inactivates histidine ammonia-lyase responsible for the catabolism of histidine to urocanate; and serine, as the precursor of cysteine. After HAA treatment, hepatic histidine levels were increased in parallel to a significant reduction in NAFLD features.

Both the diet-induced NAFLD mouse model supplemented with HAA and studies with human primary hepatocytes highlighted the beneficial role of histidine treatment in NAFLD. We observed a reduced expression of de novo lipogenesis-related genes (*FASN, SCD1*), suggesting that histidine

would facilitate the transportation of free fatty acids into the mitochondria to be oxidized, thereby decreasing lipid deposition. Consistent with our findings in human primary hepatocytes, HAA supplementation significantly decreased the hepatic triglyceride levels in parallel to a reduction in the hepatic inflammatory status (decreased gene expression of *F4/80* and *Tnfα*). These results agree with results from a study using a histidine decarboxylase (HDC) KO NAFLD mice model, where the lack of HDC activity reduced *F4/80* expression in the liver [5]. A reduced expression of *Tnfα* is consistent with a clinical study in obese women supplemented with histidine that led to decreased circulating Tnfα levels [14]; and with a preclinical study where histidine reduced hepatic *Tnfα* expression [12]. We also observed an increased response to insulin after HAA supplementation, which agrees with results from a previous study in obese women where histidine supplementation improved peripheral insulin resistance [14].

TAAR1 has recently been proposed as a novel target for the treatment of type 2 diabetes and obesity [24,25]. Notably, TAAR1 activation with a TAAR1 agonist in diet-induced obese mice reduced both postprandial plasma and hepatic triglycerides compared to vehicle-treated animals [24]. Recently, TAAR1 has been shown to be coupled to $G\alpha_s$ signaling pathways in pancreatic β-cell lines to improve insulin secretion, β-cell function, and proliferation [25]. Here, we provide the first evidence that TAAR1 in the liver and its modulation by histidine may also play a key role in NAFLD. In humans, we found that circulating histidine levels were strongly positively associated with liver expression levels of TAAR1 and supplementation of human primary hepatocytes with histidine led to a strong increase in the expression of *TAAR1*. Remarkably, silencing of *TAAR1* in human primary hepatocytes decreased AKT phosphorylation, suggesting a direct role in reducing the response to insulin, whereas histidine supplementation increased AKT phosphorylation.

Microbiota-host interactions potentially contribute to the development of metabolic diseases, and we have recently unraveled molecular networks linking the gut microbiome to hepatic steatosis [16]. Here, we also show that plasma histidine levels are negatively associated with several bacterial families that are also increased in NAFLD. The phylum *Proteobacteria* had the strongest negative association with plasma histidine levels and the strongest positive association with hepatic steatosis. At the family level, we identified several families from the phylum *Proteobacteria* increased

with the degree of hepatic steatosis, including *Xanthomonadaceae*, *Rickettsiaceae*, and *Alteromonadales*, which is consistent with findings from previous studies in NASH [26–28]. At the genus level, *Bilophila* and *Campylobacter* have also been described to be increased in NAFLD [29,30] and we found that both genera were associated with the low histidine levels found in NAFLD patients. In addition, both circulating histidine levels in humans and HAA supplementation in mice were associated with increased levels of well-known health promoting bacteria such as *Actinobacteria*, *Faecalibacterium*, *Lactobacillaceae*, or *Christensenellaceae*. In fact, a decrease in the abundance of *Faecalibacteriu*m has been found in association with irritable and inflammatory bowel diseases, diabetes, or NAFLD [31]. Similarly, the *Christensenellaceae* family has emerged as an important player in human health. Hence, decreased abundance of *Christensenellaceae* has been associated with obesity, IBD, visceral adipose tissue, and an unhealthier metabolic profile [32,33]. HAA supplementation also decreased the levels of *Roseburia*, which have been associated with NAFLD development in obese individuals [34] increased the levels of *Akkermansia* (phylum *Verrucomicrobia*). Notably, we found decreased levels of *Verrucomicrobia* with an increase in the degrees of steatosis and *Akkermansiaceae* administration has shown to improve several metabolic parameters in a NAFLD animal model [35]. Notably, both high circulating histidine levels in humans and HAA-supplemented mice were associated with higher levels of *Marinifilaceae*, which have recently been found depleted in patients with liver fibrosis [36].

Histidine can be used by many bacteria and is an important carbon, nitrogen, and/or energy source for *Proteobacteria*. The histidine utilization (Hut) pathway involves the elimination of ammonia from histidine to produce urocanate, imidazole propionate and formiminoglutamate [19]. Two recent studies have identified an increased abundance of imidazole propionate, a microbial-derived histidine catabolite, and *hutH*, the gene encoding for histidine ammonia-lyase that converts histidine to urocanate, in patients with type 2 diabetes [20,21]. Therefore, to elucidate the potential role of the gut microbiota in lowering the circulating histidine levels in NAFLD, we analyzed four microbial genes involved in histidine catabolism: *hutH, hutU, hutI, hutG* [37]. Notably, we found that patients with a higher degree of liver steatosis had higher clr-transformed levels of *hutH, hutU* and *hutI*, suggesting a higher catabolism of histidine by the gut microbiota which could explain the lower plasma histidine levels found in these

patients. Consistent with these findings, we found that fecal microbiota transplantation from donors with low histidine levels resulted in a higher accumulation of hepatic triglycerides in recipient mice compared to those receiving microbiota from donors with high histidine levels. The reduction in the hepatic triglyceride levels was accompanied by a consistent decrease in the expression levels of genes involved in the regulation (*Pgc1a*) of lipid oxidation (*Acadsb*) and biosynthesis *(Prkaa2*), and glucose transport (*Slc2a2*) and insulin signaling (*Insr*). Importantly, HAA supplementation reduced histidine catabolism observed in NAFLD. Thus, NAFLD mice treated with HAA had decreased levels of *hutH* and *hutG* compared to NAFLD mice counterparts. It is worth noting that although the histidine catabolism pathway is highly conserved among bacteria, it is not universal. Thus, the Hut pathway seems to be absent in *Cyanobacteria*, *Mycoplasmas*, and *Spirochaetes* [19]. In line with these results, we found that plasma histidine levels were strongly positively associated with *Cyanobacteria* in humans, whereas *Spirochaetes* had the strongest negative association with the degrees of steatosis.

In conclusion, our results show an important crosstalk among histidine, hepatic steatosis, and gut microbiota. We have disclosed novel histidine-linked transcriptomic and metagenomics signatures and uncovered the potential role of the microbiota as a regulator of histidine levels by increased abundances of histidine-degradation bacterial species. In addition, the supplementation of histidine ameliorated hepatic steatosis, inflammation, and insulin resistance, pointing to a new candidate in the treatment of NAFLD.

Patient and Public Involvement: Patient and Public were not involved in the research.

Conflict of Interest: The authors declare no competing interests.

Acknowledgements: We are in debt with the subjects involved in this project. This work was supported by EU-FP7 FLORINASH (Health-F2-2009-241913) to R.B., M.F., and J.M.F.R., and by the Catalan Government through the funding grant ACCIÓ-Eurecat (PRIV2020-EURHEPAD) to X.E. This work was also supported Instituto de Salud Carlos III (ISCIII, Madrid, Spain) through the project PI20/01090 (co-funded by the European Union under the European Regional Development Fund (FEDER). “A way to make Europe”) to J.M.-P. Infrastructure support was provided by the National Institute for Health Research (NIHR) Imperial Biomedical Research Centre (BRC). L.H. was in receipt of an MRC Intermediate Research Fellowship in Data Science (grant number MR/L01632X/1, UK Med-Bio). NT was

supported by the Quadram Institute Bioscience BBSRC-funded Strategic Program, Microbes in the Food Chain (BB/R012504/1) and its constituent project, Microbial Survival in the Food Chain BBS/E/F/000PR10349. FH was supported by European Research Council H2020 StG (erc-stg-948219, EPYC), the Biotechnology and Biological Sciences Research Council (BBSRC) Institute Strategic Programme Gut Microbes and Health BB/r012490/1 and its constituent project BBS/e/F/000Pr10355. NB and FH received support from the Biotechnology and Biological Sciences Research Council (BBSRC); this research was funded by the BBSRC Gut Microbes and Health BBS/E/F/00044509 (to N.B.), the BBSRC Institute Strategic Programme Gut Microbes and Health BB/R012490/1 and its constituent project BBS/E/F/000PR10355, and the BBSRC Core Capability Grant BB/CCG1860/1. This work was also partly supported by funding to M.-E.D. (EU METACARDIS under agreement HEALTH-F4-2012-305312, Neuron II under agreement 291840 and the MRC MR/M501797/1) and by grants from the French National Research Agency (ANR-10-LABX-46 [European Genomics Institute for Diabetes]), from the National Center for Precision Diabetic Medicine – PreciDIAB, which is jointly supported by the French National Agency for Research (ANR-18-IBHU-0001), by the European Union (FEDER), by the Hauts-de-France Regional Council (Agreement 20001891/NP0025517) and by the European Metropolis of Lille (MEL, Agreement 2019_ESR_11) and by Isite ULNE (R-002-20-TALENT-DUMAS), also jointly funded by ANR (ANR-16-IDEX-0004-ULNE) the Hauts-de-France Regional Council (Agreement 20002045) and by the European Metropolis of Lille (MEL). S.Q.-V. is supported by a fellowship from the Vicente Lopez Program (Eurecat). J.M.-P. is funded by the Miguel Servet Program from the Instituto de Salud Carlos III (ISCIII CP18/00009), co-funded by the European Social Fund 'Investing in your future'.

Author contributions: S.Q-V. researched the data, performed part of statistical analysis, and wrote the manuscript. J.L and N.O-C. performed the experiments with human primary hepatocytes. N.T., Y.T. performed the histidine supplementation mice experiments. F.H, and N.B. performed the 16S analyses and histidine quantification in serum and mice livers. R.B, M.E-D., M.F., L.H, J.M-B, contributed to the discussion and reviewed the manuscript. X.E., J.M.F-R., and J.M-P. carried out the conception and coordination of the study, performed statistical analysis and wrote the manuscript. All authors approved the final version to be published.

Figures

Fig. 1

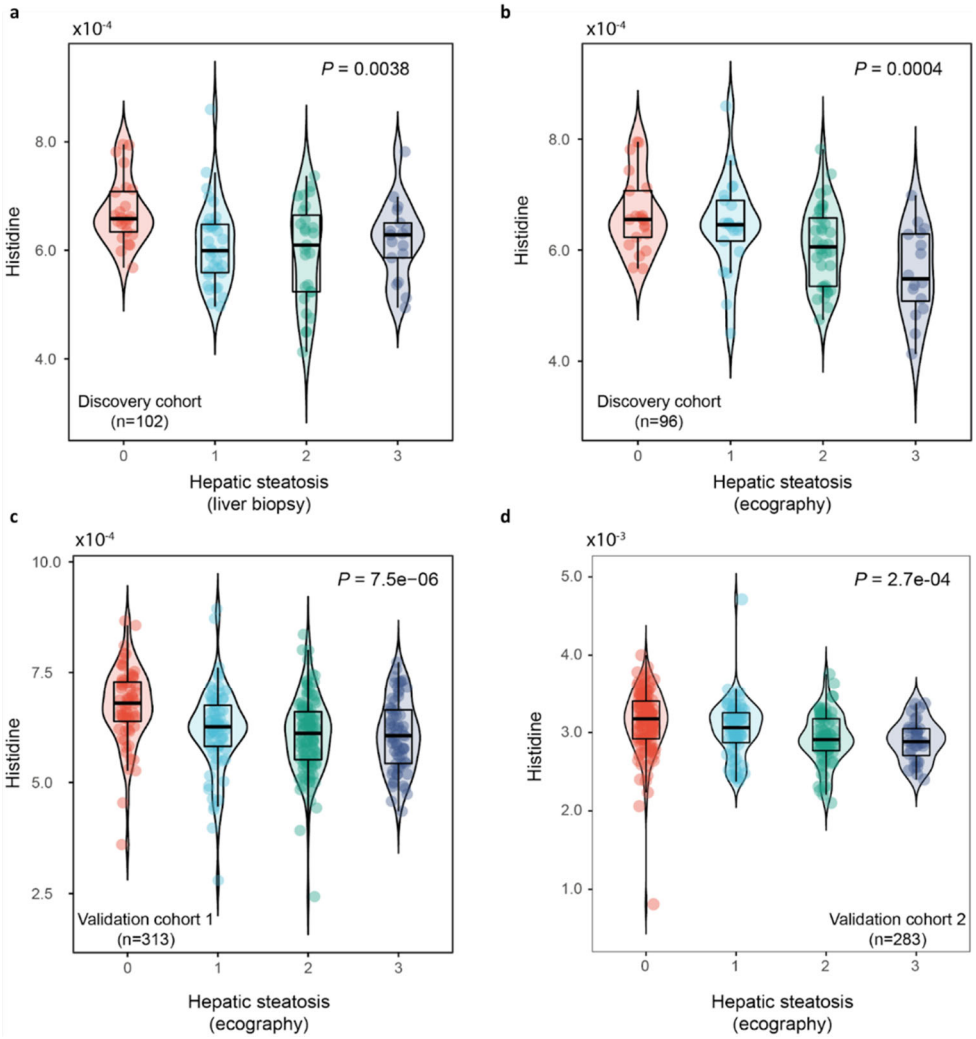

Figure 1. Associations of plasma histidine with the steatosis degree. a) Violin plots showing the plasma histidine levels according to the degree of steatosis assessed by liver biopsy (FLORINASH, *n* = 102) and **b)** echography in the discovery cohort (*n* = 96). **c)** Violin plots showing the plasma histidine levels according to the degree of steatosis assessed by echography in the validation cohort 1 (*n* = 313) and **d)** the validation cohort 2 (*n* = 283). r.u., relative units.

Fig. 2

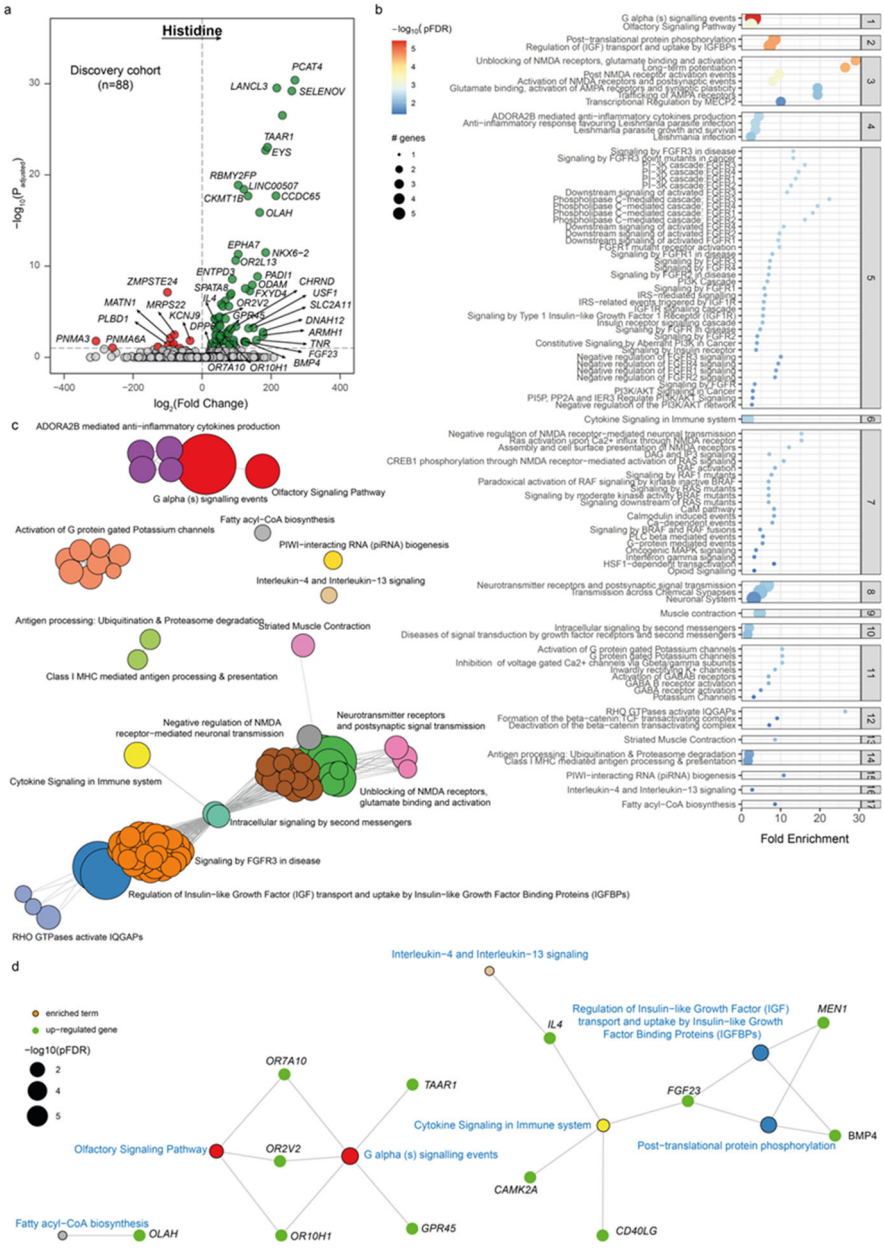

Figure 2. Associations of the liver transcriptome gene expression with the circulating histidine levels. a) Volcano plot of differentially expressed gene transcripts associated with the plasma histidine levels in the discovery cohort (*n* = 88) identified using robust linear regression controlling for age, BMI, sex, and country. The $\log_2$(Fold Change) associated with a unit change in the plasma histidine levels and the -$\log_{10}$(p-values) adjusted for multiple testing are plotted for each transcript. **b)** Dot plot of Reactome-based over-representation

analysis results performed on active subnetworks grouped by hierarchical clustering. The *x*- axis represents the fold enrichment defined as the ratio of the frequency of input genes annotated in a pathway to the frequency of all genes annotated to that pathway. The dot size indicates the number of differentially expressed genes in a given pathway. Dots are colored by the $-\log_{10}$(pFDR), with red indicating higher significance. **c)** Enrichment map inter-related significant pathways identified using an active subnetwork-oriented approach. Each colour displays a cluster of related pathways using a threshold for kappa statistics = 0.35. The size of the nodes corresponds to its $-\log_{10}$(pFDR). The thickness of the edges between nodes corresponds to the kappa statistic between the two nodes. **d)** Gene-concept network depicting significant genes involved in enriched pathways from selected clusters. The dot size of the pathways represents the $-\log_{10}$(pFDR). Pathways with the same colour correspond to the same cluster.

Fig. 3

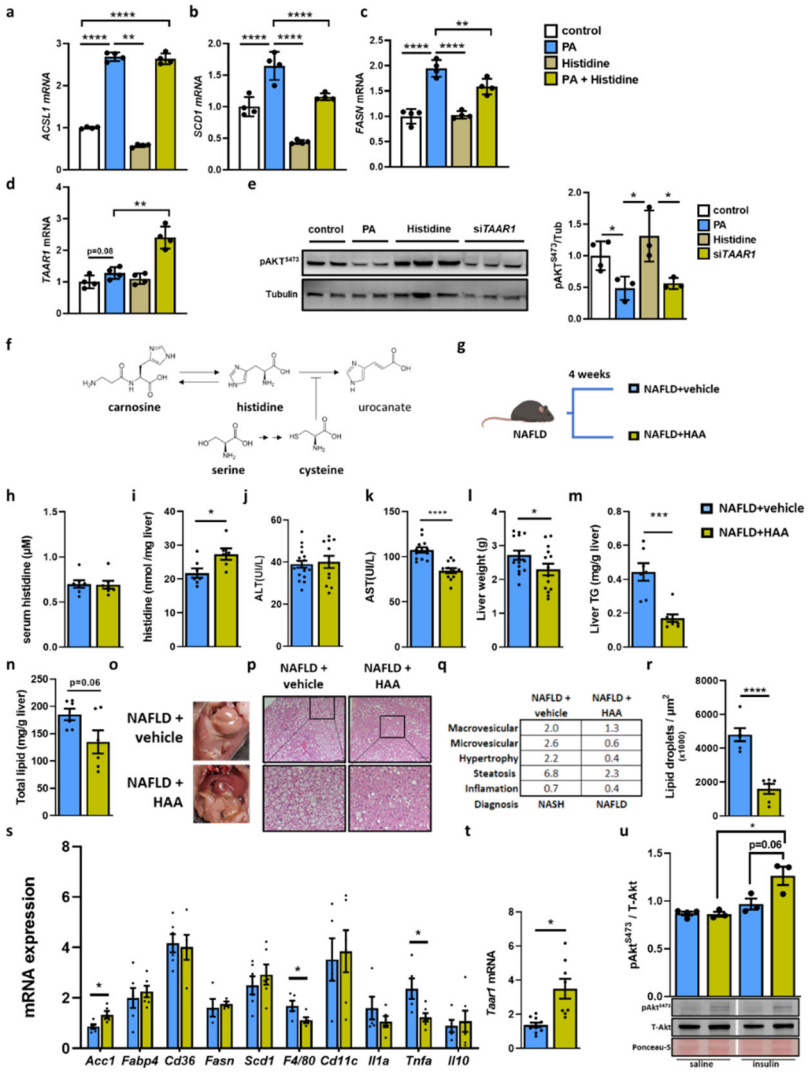

Figure 3. Histidine supplementation modulates NAFLD in human primary hepatocytes and mice. mRNA expression of genes involved in steatosis and de novo hepatic lipogenesis **a)** *ACSL1*, **b)** *SCD1,* **c)** *FASN,* **d)** *TAAR1* in primary human hepatocytes treated with or without histidine (500 nM) and palmitic acid; **e)** A representative Western blot analysis with Akt activation (pAktS473), tubulin levels as housekeeping and densitometry analysis of phosphorylated Akt^{S473} and tubulin ratio in primary hepatocytes treated with PA or histidine (500 nM), or knock-down of *TAAR1* expression; **f)** Schematic illustration of the histidine metabolism pathway, and **g)** Schematic illustration of the Animal model 1: after induction of NAFLD, animals were treated for 4- weeks with a combination of histidine-related metabolism amino acids combination (histidine, serine, carnosine and cysteine; HAA).Effects of histidine amino acids treatments on animal model: **h)** serum histidine

levels; **i)** hepatic histidine levels; **j)** serum ALT; **k)** serum AST; **l)** liver weight; **m)** total TG hepatic content; **n)** total lipid hepatic content; **o)** representative macroscopic appearance of livers; **p**) hepatic histopathology stained with H&E and a magnified area in the lower panel (Bar = 100 µm); **q)** NAFLD/NASH scoring table. st., steatosis; **r)** lipid droplets count; **s)** hepatic mRNA expression of genes related to *de novo* lipogenesis (*Acc1*, *Fasn* and *Scd1*), to lipid transport (*Cd36* and *Fabp4*) and to inflammation (*F4/80*, *Cd11c*, *Il1a*, *Tnfa* and *Il10*); **t**) hepatic mRNA expression of *Taar1.* **u)** Upper panel, representative analysis of Akt activation ($pAkt^{S473}$), total Akt protein levels (T-Akt), and protein loading with Ponceau-S membrane staining. Lower panel, densitometry of $pAkt^{S473}$and total Akt ratio. Data are mean ± SEM. * $p < 0.05$, ** $p < 0.01$, *** $p < 0.001$, **** $p < 0.0001$.

Fig.4

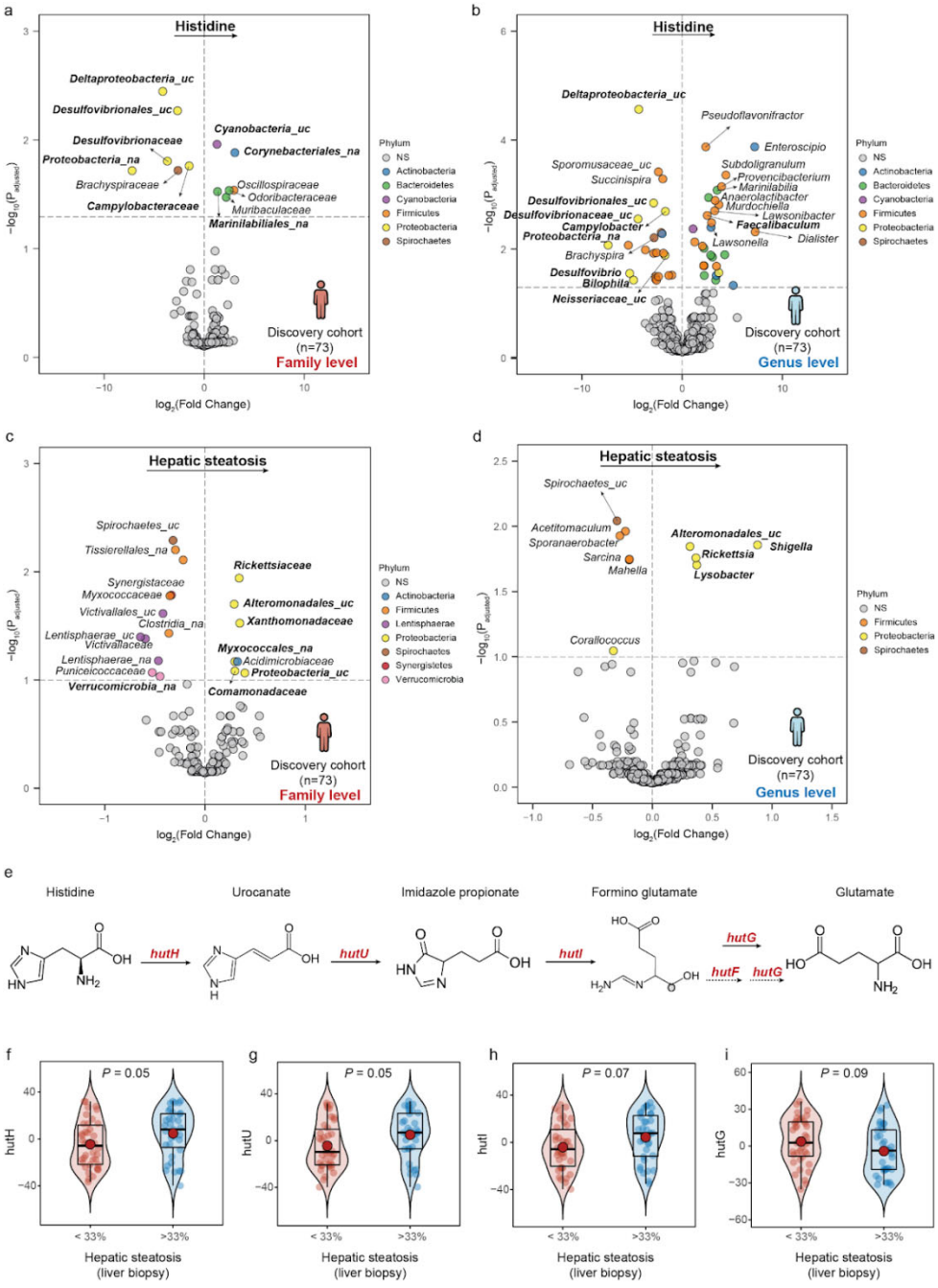

Figure 4. Associations of plasma histidine and steatosis degree with the gut microbiota es and Hut genes in humans. a) Volcano plot of differential bacteria families and **b)** genera associated with the circulating histidine levels in the discovery cohort (*n*=73) identified

using the Analysis of Microbiomes with Bias Correction (ANCOM-BC) controlling for age, BMI, sex, and country. **c)** Volcano plot of differential bacteria families and **d)** genera associated with the hepatic steatosis degree (liver biopsy) in the discovery cohort (*n*=73) identified using the Analysis of Microbiomes with Bias Correction (ANCOM-BC) controlling for age, BMI, sex, and country. The $\log_2$ (Fold Change) associated with a unit change in the plasma histidine levels and the $-\log_{10}$ (p-values) adjusted for multiple testing are plotted for each taxon. Significantly different taxa are colored according to phylum. **e)** Histidine utilisation pathways. The first three pathways appear to be universal. There are two different degradation pathways for formiminoglutamate depending on the genera: hydrolyzation to formamide and glutamate or hydrolyzation to formylglutamate and subsequent hydrolyzation to formate and glutamate. **f-i)** Violin plots of the centered log ratio-transformed microbial genes involved in histidine utilisation *hutH, hutU, hutI* and *hutG*, respectively, in subjects with steatosis degree lower or higher than 33 %.

Fig.5

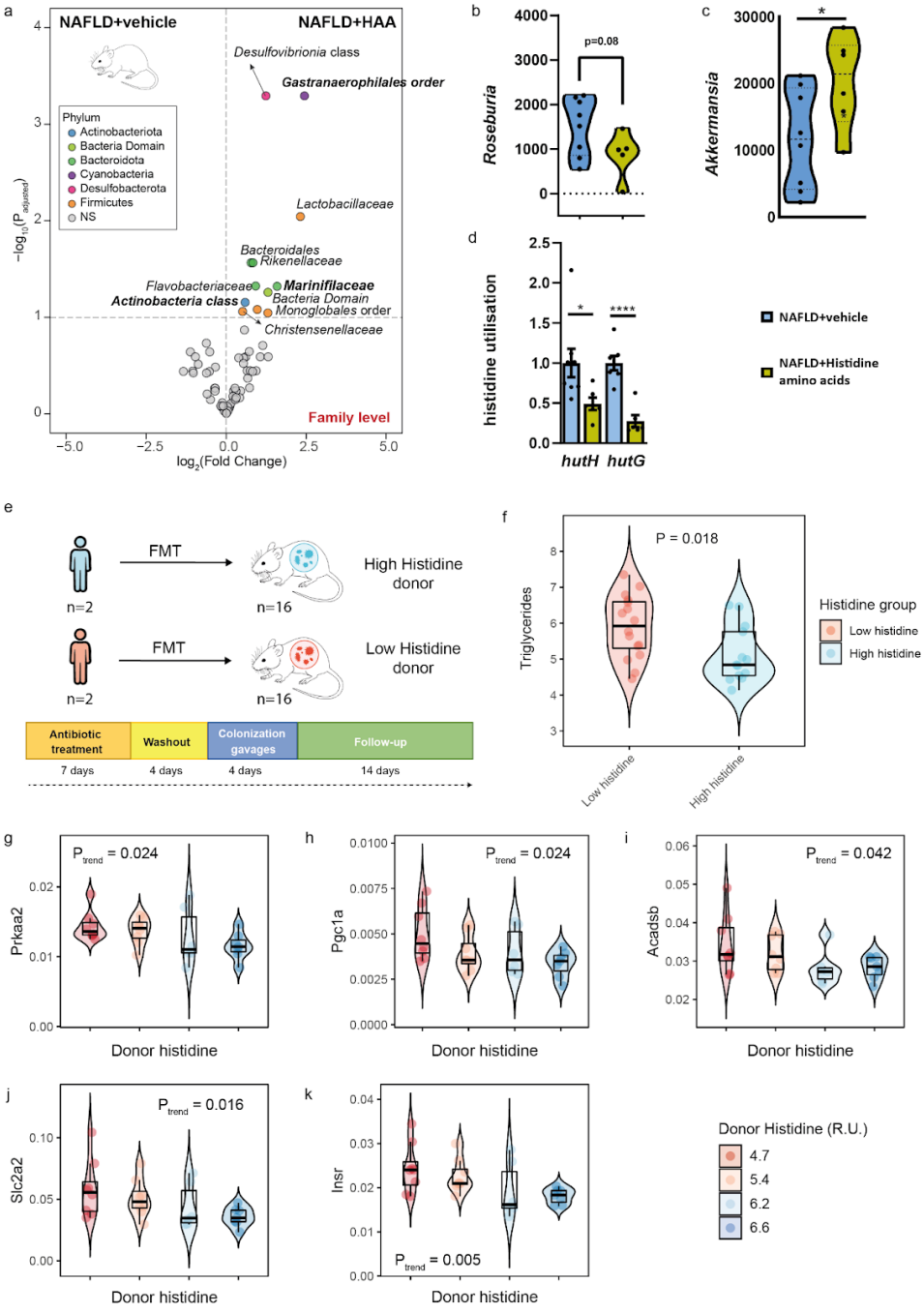

Figure 5. Effects of HAA supplementation on the gut microbiota and FMT in mice. a) Volcano plots of differential bacteria families associated with the hepatic steatosis degree

(liver biopsy) in the animal supplementation study for the comparisons NAFLD + vehicle *vs*. NAFLD + HAA, identified using the Analysis of Microbiomes with Bias Correction (ANCOM-BC) compared. The $\log_2$ (Fold Change) and the $-\log_{10}$ (p-values) adjusted for multiple testing are plotted for each taxon. Significantly different taxa are colored according to phylum. Genera levels of: **b)** *Roseburia,* **c)** *Akkermansia*, and **d)** qPCR of microbial genes expression involved in histidine utilization (*hutH* and *hutG*). **e)** Schematic diagram of the fecal microbiota transplantation study from patients with high and low plasma histidine levels to mice (2 human donors per group; 8 mice per human donor); and the effect on **f)** triglyceride (TG) hepatic content and hepatic mRNA expression of **g)** *Prkaa2*; **h)** *Pgc1a*; **i)** *Acadsb*; **j)** *Slc2a2*; **k)** *Insr.* Data are mean ± SEM. * $p < 0.05$, ** $p < 0.01$, *** $p < 0.001$, **** $p < 0.0001$ *vs*. NAFLD mice.

Fig. S1

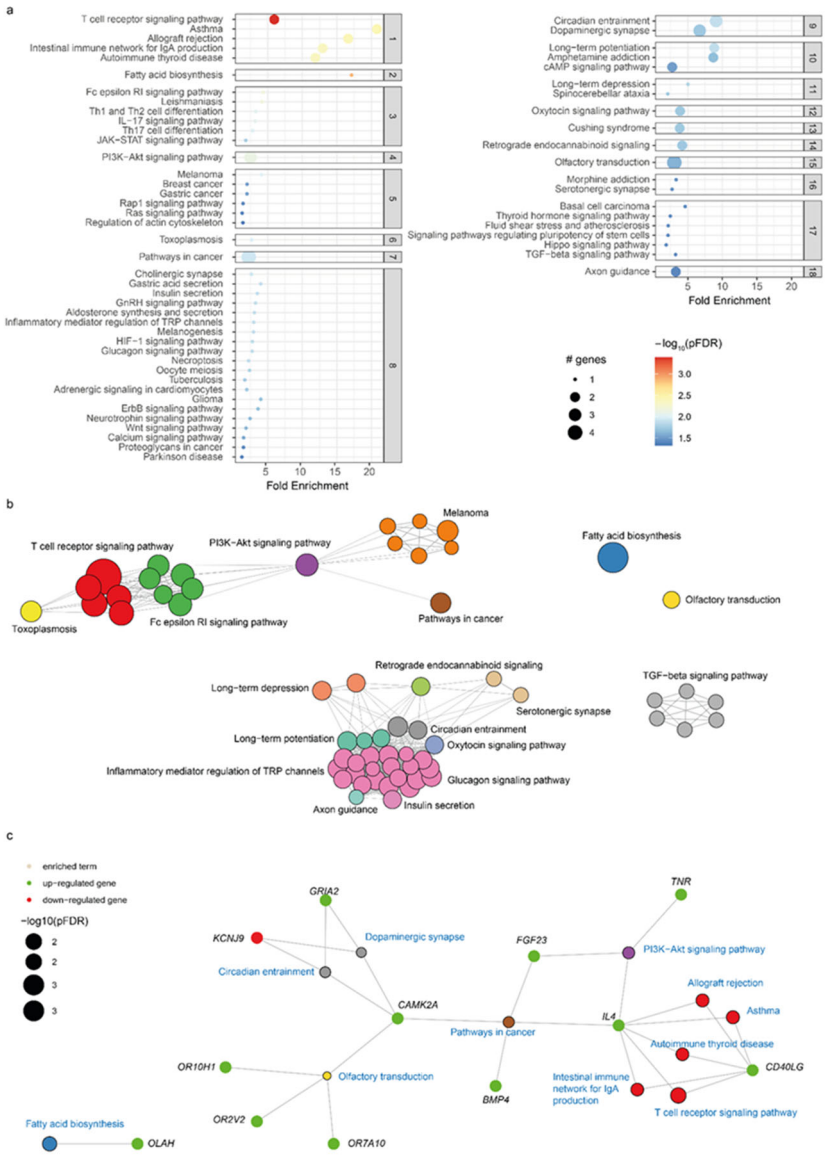

Figure S1. Associations of the liver transcriptome gene expression with the circulating histidine levels. a) Dot plot of KEGG-based over-representation analysis results performed on active subnetworks grouped by hierarchical clustering. The *x*- axis represents the fold enrichment defined as the ratio of the frequency of input genes annotated in a pathway to the frequency of all genes annotated to that pathway. The dot size indicates the number of differentially expressed genes in a given pathway. Dots are colored by the -$\log_{10}$(pFDR),

with red indicating higher significance. **b)** Enrichment map inter-related significant pathways identified using an active subnetwork- oriented approach. Each color displays a cluster of related pathways using a threshold for kappa statistics = 0.35. The size of the nodes corresponds to its -$\log_{10}$(pFDR). The thickness of the edges between nodes corresponds to the kappa statistic between the two nodes. **c)** Gene-concept network depicting significant genes involved in enriched pathways from selected clusters. The dot size of the pathways represents the -$\log_{10}$(pFDR). Pathways with the same colour correspond to the same cluster.

REFERENCES:

1. Mayneris-Perxachs, J. *et al.* Iron status influences non-alcoholic fatty liver disease in obesity through the gut microbiome. *Microbiome* **9**, (2021).

2. Quesada-Vázquez, S. *et al.* Supplementation with a Specific Combination of Metabolic Cofactors Ameliorates Non-Alcoholic Fatty Liver Disease and, Hepatic Fibrosis, and Insulin Resistance in Mice. *Nutrients* **13**, 3532 (2021).

3. Lee, D.-Y. & Kim, E.-H. Therapeutic Effects of Amino Acids in Liver Diseases: Current Studies and Future Perspectives. *J Cancer Prev* **24**, 72–78 (2019).

4. Kasaoka, S. *et al.* Histidine supplementation suppresses food intake and fat accumulation in rats. *Nutrition* **20**, 991–996 (2004).

5. Kennedy, L. *et al.* Knockout of l-Histidine Decarboxylase Prevents Cholangiocyte Damage and Hepatic Fibrosis in Mice Subjected to High-Fat Diet Feeding via Disrupted Histamine/Leptin Signaling. *American Journal of Pathology* **188**, 600–615 (2018).

6. Kimura, K. *et al.* Histidine augments the suppression of hepatic glucose production by central insulin action. *Diabetes* **62**, 2266–2277 (2013).

7. Hayashi, T. *et al.* Uncovering the Role of Gut Microbiota in Amino Acid Metabolic Disturbances in Heart Failure Through Metagenomic Analysis. *Front Cardiovasc Med* **8**, (2021).

8. Niu, Y. C. *et al.* Histidine and arginine are associated with inflammation and oxidative stress in obese women. *British Journal of Nutrition* **108**, 57–61 (2012).

9. Watanabe, M. *et al. Consequences of low plasma histidine in chronic kidney disease patients: associations with inflammation, oxidative stress, and mortality 1-3*. *Am J Clin Nutr* vol. 87 https://academic.oup.com/ajcn/article/87/6/1860/4633369 (2008).

10. Thalacker-Mercer, A. E. & Gheller, M. E. Benefits and Adverse Effects of Histidine Supplementation. *J Nutr* **150**, 2588S-2592S (2020).

11. Liu, W. hu, Liu, T. chung & Yin, M. chin. Beneficial effects of histidine and carnosine on ethanol-induced chronic liver injury. *Food and Chemical Toxicology* **46**, 1503–1509 (2008).

12. Yan, S. L., Wu, S. T., Yin, M. C., Chen, H. T. & Chen, H. C. Protective effects from carnosine and histidine on acetaminophen-induced liver injury. *J Food Sci* **74**, (2009).

13. Menon, K., Marquina, C., Liew, D., Mousa, A. & Courten, B. Histidine-containing dipeptides reduce central obesity and improve glycaemic outcomes: A systematic review and meta-analysis of randomized controlled trials. *Obesity Reviews* **21**, (2020).

14. Feng, R. N. *et al.* Histidine supplementation improves insulin resistance through suppressed inflammation in obese women with the metabolic syndrome: A randomised controlled trial. *Diabetologia* **56**, 985–994 (2013).

15. Portune, K. J. *et al.* Gut microbiota role in dietary protein metabolism and health-related outcomes: The two sides of the coin. *Trends Food Sci Technol* **57**, 213–232 (2016).

16. Hoyles, L. *et al.* Molecular phenomics and metagenomics of hepatic steatosis in non-diabetic obese women. *Nat Med* **24**, 1070–1080 (2018).

17. Latorre, J. *et al.* Decreased lipid metabolism but increased FA biosynthesis are coupled with changes in liver microRNAs in obese subjects with NAFLD. *Int J Obes* **41**, 620–630 (2017).

18. Wirtz, L., Eder, M., Brand, A. K. & Jung, H. HutT functions as the major L-histidine transporter in Pseudomonas putida KT2440. *FEBS Lett* **595**, 2113–2126 (2021).

19. Bender, R. A. Regulation of the Histidine Utilization (Hut) System in Bacteria. *Microbiology and Molecular Biology Reviews* **76**, 565–584 (2012).

20. Koh, A. *et al.* Microbially Produced Imidazole Propionate Impairs Insulin Signaling through mTORC1. *Cell* **175**, 947-961.e17 (2018).

21. Molinaro, A. *et al.* Imidazole propionate is increased in diabetes and associated with dietary patterns and altered microbial ecology. *Nat Commun* **11**, (2020).

22. Lee, Y. T., Hsu, C. C., Lin, M. H., Liu, K. sen & Yin, M. C. Histidine and carnosine delay diabetic deterioration in mice and protect human low density lipoprotein against oxidation and glycation. *Eur J Pharmacol* **513**, 145–150 (2005).

23. Mong, M. C., Chao, C. Y. & Yin, M. C. Histidine and carnosine alleviated hepatic steatosis in mice consumed high saturated fat diet. *Eur J Pharmacol* **653**, 82–88 (2011).

24. Raab, S. *et al.* Incretin-like effects of small molecule trace amine-associated receptor 1 agonists. *Mol Metab* **5**, 47–56 (2016).

25. Michael, E. S., Covic, L. & Kuliopulos, A. Trace amine–associated receptor 1 (TAAR1) promotes anti-diabetic signaling in insulin-secreting cells. *Journal of Biological Chemistry* **294**, 4401–4411 (2019).

26. Quesada-Vázquez, S., Aragonès, G., del Bas, J. M. & Escoté, X. Diet, Gut Microbiota and Non-Alcoholic Fatty Liver Disease: Three Parts of the Same Axis. *Cells* **9**, 1–17 (2020).

27. Sookoian, S. *et al.* Intrahepatic bacterial metataxonomic signature in non-alcoholic fatty liver disease. *Gut* **69**, 1483–1491 (2020).

28. Vallianou, N. *et al.* Understanding the Role of the Gut Microbiome and Microbial Metabolites in Non-Alcoholic Fatty Liver Disease: Current Evidence and Perspectives. *Biomolecules* **12**, 56 (2021).

29. Mu, H. N. *et al.* Caffeic acid prevents non-alcoholic fatty liver disease induced by a high-fat diet through gut microbiota modulation in mice. *Food Research International* **143**, (2021).

30. Jian, C., Luukkonen, P., Sädevirta, S., Yki-Järvinen, H. & Salonen, A. Impact of short-term overfeeding of saturated or unsaturated fat or sugars on the gut microbiota in relation to liver fat in obese and overweight adults. *Clinical Nutrition* **40**, 207–216 (2021).

31. de Filippis, F., Pasolli, E. & Ercolini, D. Newly Explored Faecalibacterium Diversity Is Connected to Age, Lifestyle, Geography, and Disease. *Current Biology* **30**, 4932-4943.e4 (2020).

32. Waters, J. L. & Ley, R. E. The human gut bacteria Christensenellaceae are widespread, heritable, and associated with health. *BMC Biol* **17**, 83 (2019).

33. Tavella, T. *et al.* Elevated gut microbiome abundance of *Christensenellaceae, Porphyromonadaceae and Rikenellaceae* is associated with reduced visceral adipose tissue and healthier metabolic profile in Italian elderly. *Gut Microbes* **13**, (2021).

34. Mokhtari, Z., Gibson, D. L. & Hekmatdoost, A. Nonalcoholic fatty liver disease, the gut microbiome, and diet. *Advances in Nutrition* vol. 8 240–252 Preprint at https://doi.org/10.3945/an.116.013151 (2017).

35. Juárez-Fernández, M. *et al.* The Synbiotic Combination of Akkermansia muciniphila and Quercetin Ameliorates Early Obesity and NAFLD through Gut Microbiota Reshaping and Bile Acid Metabolism Modulation. *Antioxidants* **10**, 2001 (2021).

36. Kwan, S. Y. *et al.* Gut microbiome features associated with liver fibrosis in Hispanics, a population at high risk for fatty liver disease. *Hepatology* **75**, 955–967 (2022).

37. Leyn, S. A. *et al.* Comparative genomics and evolution of transcriptional regulons in Proteobacteria. *Microb Genom* **2**, (2016).

38. Quesada-Vázquez, S. *et al.* Microbiota Dysbiosis and Gut Barrier Dysfunction Associated with Non-Alcoholic Fatty Liver Disease Are Modulated by a Specific Metabolic Cofactors' Combination. *Int J Mol Sci* **23**, 13675 (2022).

39. Marin, V. *et al.* An animal model for the juvenile non-alcoholic fatty liver disease and non-alcoholic steatohepatitis. *PLoS One* **11**, 1–15 (2016).

40. Weber, K. & Rétey, J. *On the Nature of the Irreversible Inhibition of Histidine Ammonia Lyase by Cysteine and Dioxygen*. *Bioorganic & Medicinal Chemistry* vol. 4 (1996).

41. Reagan-Shaw, S., Nihal, M. & Ahmad, N. Dose translation from animal to human studies revisited. *The FASEB Journal* **22**, 659–661 (2008).

42. Kleiner, D. E. *et al.* Design and validation of a histological scoring system for nonalcoholic fatty liver disease. *Hepatology* **41**, 1313–1321 (2005).

43. Strauss, S., Gavish, E., Gottlieb, P. & Katsnelson, L. Interobserver and intraobserver variability in the sonographic assessment of fatty liver. *American Journal of Roentgenology* **189**, 1449 (2007).

44. Fleige, S. & Pfaffl, M. W. RNA integrity and the effect on the real-time qRT-PCR performance. *Molecular Aspects of Medicine* vol. 27 126–139 Preprint at https://doi.org/10.1016/j.mam.2005.12.003 (2006).

45. Smyth, G. K. limma: Linear Models for Microarray Data. in *Bioinformatics and Computational Biology Solutions Using R and Bioconductor* 397–420 (2005). doi:10.1007/0-387-29362-0_23.

46. Schmieder, R. & Edwards, R. Quality control and preprocessing of metagenomic datasets. *Bioinformatics* **27**, 863–864 (2011).

47. Magoč, T. & Salzberg, S. L. FLASH: Fast length adjustment of short reads to improve genome assemblies. *Bioinformatics* **27**, 2957–2963 (2011).

48. Langmead, B. & Salzberg, S. L. Fast gapped-read alignment with Bowtie 2. *Nat Methods* **9**, 357–359 (2012).

49. Li, D. *et al.* MEGAHIT v1.0: A fast and scalable metagenome assembler driven by advanced methodologies and community practices. *Methods* **102**, 3–11 (2016).

50. Hyatt, D. *et al.* Prodigal: prokaryotic gene recognition and translation initiation site identification. *BMC Bioinformatics* **11**, 119 (2010).

51. Durbin, R., Eddy, S. R., Krogh, A. & Mitchison, G. *Biological Sequence Analysis*. (Cambridge University Press, 1998). doi:10.1017/CBO9780511790492.

52. Kanehisa, M. KEGG: Kyoto Encyclopedia of Genes and Genomes. *Nucleic Acids Res* **28**, 27–30 (2000).

53. Arnoriaga-Rodríguez, M. *et al.* Obesity Impairs Short-Term and Working Memory through Gut Microbial Metabolism of Aromatic Amino Acids. *Cell Metab* **32**, 548-560.e7 (2020).

54. Menzel, P., Ng, K. L. & Krogh, A. Fast and sensitive taxonomic classification for metagenomics with Kaiju. *Nat Commun* **7**, 11257 (2016).

55. R Development Core Team. R: A Language and Environment for Statistical Computing. Vienna, Austria. Preprint at (2013).

56. Caimari, A., del Bas, J. M., Crescenti, A. & Arola, L. Low doses of grape seed procyanidins reduce adiposity and improve the plasma lipid profile in hamsters. *Int J Obes* **37**, 576–583 (2013).

57. Rodríguez-sureda, V. & Peinado-onsurbe, J. A procedure for measuring triacylglyceride and cholesterol content using a small amount of tissue. **343**, 277–282 (2005).

58. Liang, W., Menke, A. L., Driessen, A., Koek, G. H. & Lindeman, J. H. Establishment of a General NAFLD Scoring System for Rodent Models and Comparison to Human Liver Pathology. 1–17 (2014) doi:10.1371/journal.pone.0115922.

59. Hildebrand, F., Tadeo, R., Voigt, A. Y., Bork, P. & Raes, J. LotuS: An efficient and user-friendly OTU processing pipeline. *Microbiome* **2**, (2014).

60. Özkurt, E. *et al.* LotuS2: An ultrafast and highly accurate tool for amplicon sequencing analysis. *bioRxiv* 474111 (2021) doi:10.1101/2021.12.24.474111.

61. Callahan, B. J. *et al.* DADA2: High-resolution sample inference from Illumina amplicon data. *Nat Methods* **13**, 581–583 (2016).

62. Bedarf, J. R. *et al.* Much ado about nothing? Off-target amplification can lead to false-positive bacterial brain microbiome detection in healthy and Parkinson's disease individuals. *Microbiome* **9**, (2021).

63. Yilmaz, P. *et al.* The SILVA and 'all-species Living Tree Project (LTP)' taxonomic frameworks. *Nucleic Acids Res* **42**, (2014).

64. Hildebrand, F. *et al.* Antibiotics-induced monodominance of a novel gut bacterial order. *Gut* **68**, 1781–1790 (2019).

65. Saary, P., Forslund, K., Bork, P. & Hildebrand, F. RTK: Efficient rarefaction analysis of large datasets. *Bioinformatics* **33**, 2594–2595 (2017).

66. Wu, Y., Feng, K., Wei, Z., Wang, Z. & Deng, Y. Ardep, a rapid degenerate primer design pipeline based on k-mers for amplicon microbiome studies. *Int J Environ Res Public Health* **17**, 1–12 (2020).

67. Puigarnau, S. *et al.* Metabolomics reveals that fittest trail runners show a better adaptation of bioenergetic pathways. *J Sci Med Sport* (2022) doi:10.1016/j.jsams.2021.12.006.

68. Liang, S.-H. *3-Minute, Comprehensive, Direct LC-MS/MS Analysis of Amino Acids in Plasma 13-Minute, Comprehensive, Direct LC-MS/ MS Analysis of Amino Acids in Plasma*. www.restek.com.

69. Yang, J. *et al.* Effects of Long-Term DHA Supplementation and Physical Aged Female Mice. (2021).

70. Ballak, D. B. *et al.* IL-37 protects against obesity-induced inflammation and insulin resistance. *Nat Commun* **5**, (2014).

71. Antraco, V. J. *et al.* Omega-3 polyunsaturated fatty acids prevent nonalcoholic steatohepatitis (Nash) and stimulate adipogenesis. *Nutrients* **13**, 1–20 (2021).

72. López-Yoldi, M. *et al.* Cardiotrophin-1 stimulates lipolysis through the regulation of main adipose tissue lipases. *J Lipid Res* **55**, 2634–2643 (2014).

73. Miranda, M. *et al.* Relation between human LPIN1, hypoxia and endoplasmic reticulum stress genes in subcutaneous and visceral adipose tissue. *Int J Obes (Lond)* **34**, 679–686 (2010).

74. Ritchie, M. E. *et al.* limma powers differential expression analyses for RNA-sequencing and microarray studies. *Nucleic Acids Res* **43**, e47–e47 (2015).

75. Ulgen, E., Ozisik, O. & Sezerman, O. U. pathfindR: An R Package for Comprehensive Identification of Enriched Pathways in Omics Data Through Active Subnetworks. *Front Genet* **10**, (2019).

76. Lin, H. & Peddada, S. das. Analysis of compositions of microbiomes with bias correction. *Nat Commun* **11**, 3514 (2020).

77. Carvajal-Rodríguez, A., de Uña-Alvarez, J. & Rolán-Alvarez, E. A new multitest correction (SGoF) that increases its statistical power when increasing the number of tests. *BMC Bioinformatics* **10**, 209 (2009).

Methods

Methods

Data and Code Availability

The data that support the findings of this study are available from the lead contact (jmfreal@idibgi.org) upon reasonable request. The raw metagenomic sequence data for the FLORINASH cohort (with human-associated reads removed) have been deposited under the study accession number PRJEB14215 (secondary accession number ERP015847).

EXPERIMENTAL MODEL AND SUBJECT DETAILS

Clinical Study

The discovery cohort included *n*=102 obese patients aged 22 to 63 years old recruited at the Endocrinology Service of the Hospital Universitari de Girona Dr. Josep Trueta (Girona, Spain) and Policlinico Tor Vergata University of Rome (Rome, Italy). The validation cohort 1 comprised *n*=313 obese patients aged 20 to 67 years old at the Endocrinology Service of the Hospital Universitari de Girona Dr Josep Trueta (*n* = 149) and at the Center for Atherosclerosis of Policlinico Tor Vergata University of Rome (Rome, Italy; n = 164). The validation cohort 2 comprised *n* = 283 obese patients aged 25 to 66 years old at the Endocrinology Service of the Hospital Universitari de Girona Dr Josep Trueta.

Inclusion criteria: Caucasian origin, stable body weight 3 months before the study, free of any infection 1 month preceding the study and absence of any systemic disease.

Exclusion criteria: Known history of diabetes or use of hypoglycemic agents, presence of liver disease (specifically hepatitis C virus infection and tumoral disease), thyroid dysfunction, > 20g/day of alcohol consumption, hepatitis B, or drug-induced liver injury.

Declarations Ethics approval and consent to participate Human study

All subjects gave written informed consent, validated, and approved by the ethical committee of the Hospital Universitari Dr Josep Trueta (Comitè d'Ètica d'Investigació Clínica, approval number 2009 046) and Policlinico Tor Vergata University of Rome (Comitato Etico Indipendente, approval number 28-05-2009).

Primary hepatocytes study

Cryopreserved primary human hepatocytes (HHs) were commercially sourced (Innoprot, Bizkaia, Spain) and cultured with hepatocytes medium (Innoprot) supplemented with 5% fetal bovine serum, 1% hepatocytes growth supplement (mixture of growth factors, hormones, and proteins necessary for the culture of primary hepatocytes) and 100 U/ml penicillin and streptomycin (P/S). HHs were grown on fibronectin pre-coated cell dishes at 37 °C and 5 % CO_2 atmosphere.

For histidine supplementation experiments in steatosis, histidine was dissolved in 0.5 M HCl and was used at 500 µM to treat HHs. After 48 h of histidine treatment, cells were treated with PA for 24 h. PA was prepared as follows: 27.84 mg of PA (Sigma-Aldrich, San Luis, MO) was dissolved in 1 mL sterile water to obtain a 100 mM stock solution. Five percent bovine serum albumin (BSA) was prepared in serum-free DMEM and then mixed with PA stock solution for at least 1 h at 40 °C to obtain a 5 mM solution. HHs were treated with PA at 200 µM or BSA as the vehicle. All experimental conditions were performed in 4 biological replicates. After treatments, cells were washed with PBS and collected with Qiazol for RNA purification or Protein extraction were performed.

For TAAR1 silencing experiments, 24 h after seeding, HHS were transfected with siRNA against TAAR1 or treated with histidine, for 72 h alone, or in combination with palmitic acid (PA) for 24 h following the siTAAR1/histidine treatment. Briefly, the siRNA (Sigma-Aldrich) against TAAR1 and Lipofectamine RNAiMAX (LifeTechnologies, Darmstadt, Germany) were diluted separately with Opti-MEM I Reduced Serum Medium (Life Technologies, Darmstadt, Germany) and mixed by pipetting afterward. The siRNA-RNAiMAX complexes were left to incubate for 20 min at room temperature and subsequently added on the top of the adherent cells drop-wise. The final concentrations of Lipofectamine RNAiMAX and siRNAs

were 1.6 mL/cm^2 and 75 nM, respectively, in 24-well cell culture plates, and the final amount of medium per well was 1 mL. Transfection efficiency was assessed by real-time PCR. The siRNAs (Sigma-Aldrich) used were human TAAR1 (SASI_HS01_00134799, with sequences 5'-CAGAAUAUAUCUUAUCGCU[dT][dT]-3' and 5'-AGCGAUAAGAUAUAUUCUG[dT][dT]-3').

Animal Studies

Animal model 1: Dietary induction of NAFLD in mice

Thirty-two C57BL/6J male mice (Envigo, Sant Feliu de Codines, Barcelona, Spain), 6 weeks old at the beginning of the experiment, were used. Animals were housed in groups (4 mice per cage) under controlled conditions of temperature (22 ± 2 °C) and humidity (55 ± 10%), and on a 12-hour light/dark cycle with free access to food and water. Mice were left undisturbed to acclimate to the animal facility for one week. NAFLD was induced as previously described [2,38,39]. Briefly, after the acclimatization period, animals were fed with HFHFr diet (HFHC: D12331, Research Diets) supplemented with 23.1 g/L fructose and 18.9 g/L sucrose in the drinking water. Mice were kept on these diets for a period of 20 weeks in ad libitum conditions.

For the last 4 weeks of the experiment (from the 16th to 20th week), NAFLD mice were randomly distributed into two groups: 16 mice were kept under the same fed conditions described before (NAFLD + vehicle), and 16 mice were exposed to histidine-related amino acids treatment (NAFLD + HAA). HAA is a mix of the following compounds: 210 mg/kg of L-histidine monohydrochloride monohydrate (Merck, GmbH Germany), 490 mg/kg L-cysteine hydrochloride (Merck), 210 mg/kg L-serine (Merck) and 210 mg/kg L-carnosine 98% (Acros Organics, Geel, Belgium). Histidine is an essential amino acid that cannot be synthesized de novo and therefore must be obtained from the diet. On the other hand, it is well-described that a natural inhibitor of histidine ammonia lyase (HAL), an enzyme that catabolizes histidine to urocanic acid, is cysteine [40]. Cysteine levels are regulated by its precursors, essentially serine, a non-essential amino acid. Finally, it has been suggested that supplementation with carnosine (dipeptide formed by histidine and β-alanine) may increase histidine levels from the degradation of carnosine through the enzyme Carnosine Dipeptidase 1 (CNDP1). HAA were diluted with drinking water with 23.1 g/L fructose and 18.9 g/L sucrose (vehicle). These specific doses were determined based on previous studies and a calculation of dose translation from human to animal dosage [41]. Fresh solutions were freshly prepared three times per week and prepared from stock powders and protected from light. Before being euthanized, 10 animals per group were randomly selected to perform an insulin challenge. They were intraperitoneally injected with 1 mU/g of insulin (n = 5 per group) or saline (n = 5 per group) and after 15 min, they were sacrificed.

Animal model 2: Fecal microbiota transplantation in mice.

We leveraged data from our previous fecal microbiota transplantation experiment [1]. Briefly, fecal samples from low- (*n* = 2) and high- (*n* = 2) histidine donors matched for age and BMI were suspended in sterile reduced PBS (N2 gas and thioglycolic acid, Sigma Aldrich, St. Louis, MO). Eight mice (8-week-old C57BL/6 male, Charles River) per patient were treated with an antibiotic mixture for 7 days (neomycin, ampicillin, metronidazole) and after a 4-day washout, mice were administered 20 mg/day of fecal matter for 4 consecutive days. Two weeks later, mice were sacrificed, and liver and plasma were collected and frozen. Experimental groups were randomly allocated.

METHOD DETAILS

Clinical and Laboratory Parameters

Stool and plasma samples from all subjects were obtained during the week before elective gastric bypass surgery, during which the liver biopsy was sampled. All samples were stored at − 80 °C. Liver samples were collected in RNAlater, fragmented, and immediately flash-frozen in liquid nitrogen before storage at − 80 °C.

Hepatic steatosis determination and liver histology in the clinical study

An ultrasound system with a 3.5 MHz convex transducer (Siemens Acuson S2000, Mochida Siemens Medical System, Tokyo, Japan) was used to scan the liver. Hepatic steatosis was defined as absent (grade 0: < 5% steatosis), mild (grade 1: 5–33% steatosis), moderate (grade 2: > 33–66% steatosis) or severe (grade 3: > 66% steatosis) using the scoring system for NAFLD [42]. Images were independently evaluated by two radiologists blinded to clinical and laboratory data [43]. Liver biopsies were previously obtained for n = 86 patients who underwent bariatric surgery [16]. The investigators were blind to group allocations. Liver biopsies were analyzed by a single pathologist expert in hepatic pathology. For each liver sample, hematoxylin and eosin, reticulin and Masson's trichrome staining were performed. Hepatic steatosis grade was determined according to the scoring system for NAFLD [42].

Transcriptome and metabolome data analysis in the clinical study

Transcriptomic analyses have been previously described [16]. Briefly, RNA from liver biopsy samples was extracted using standard extraction protocols (TRIzol) by Miltenyi Biotec as previously reported. RNA quality (gel images, RNA integrity number and electropherograms) was assessed using an Agilent 2100 Bioanalyzer platform (Agilent Technologies). An RNA integrity number > 6 was considered sufficient for gene expression experiments [44]. 100 ng of total RNA was used for linear T7-based amplification of RNA for each sample. cRNA was prepared by

amplification of the RNA and labeled with Cy3 using the Agilent Low Input Quick Amp Labeling Kit according to the manufacturer's instructions. The amounts of cRNA and dye that were incorporated were measured by an ND-1000 spectrophotometer (NanoDrop Technologies). Hybridization of the Agilent Whole Human Genome Oligo Microarrays 4 × 44K was done following the Agilent 60-mer oligo microarray processing protocol using the Agilent Gene Expression Hybridization Kit. The fluorescence signals of the hybridized Agilent microarrays were detected using Agilent's Microarray Scanner after washing with Agilent Gene Expression Wash Buffer twice and with acetonitrile once. Feature intensities were determined using Agilent Feature Extraction Software. Microarray data were processed and normalized using R and the BioConductor package LIMMA (Linear Models for Microarray Data) [45]. Raw data quality was assessed using pseudoMA and box plots. A background correction was applied and normalization of the green channel between arrays was done using 'cyclicloess' between pairs of arrays. Control and low-expressed probes were removed and only those probes brighter than the negative controls (≥ 10%) on at least one array were kept. Batch-corrected data was obtained using the remove batch effect based on 'Batch' [45]. Probes with no associated gene ID were removed. Finally, data were averaged based on an association with a particular gene. Raw data quality was assessed using pseudoMA and box plots. A background correction was applied and normalization of the green channel between arrays was done using 'cyclicloess' between pairs of arrays. Control and low-expressed probes were removed and only those probes brighter than the negative controls (≥ 10%) on at least one array were kept. Batch-corrected data was obtained using the remove batch effect based on 'Batch' [45], probes with no associated gene ID were removed. Finally, data were averaged based on an association to a particular gene.

Plasma histidine (metabolomics) in the clinical study

The plasma histidine levels were determined using ^{1}H-Nuclear Magnetic Spectroscopy (NMR). The analyses of the discovery and validation cohort 1 were performed on a Bruker DRX600 spectrometer equipped with either a 5-mm TXI probe operating at 600.13 MHz or a 5-mm BBI probe operating at 600.44 MHz. The 90º pulse length was determined prior to each run and field frequency was locked using D_2O as solvent. Plasma samples were thawed at room temperature and 350 µL aliquots were carefully placed in 5-mm NMR tubes. Then, 150 µL of saline solution (0.9 % NaCl prepared with 80:20 H_2O/D_2O and sodium azide) was added and the mixture was gently vortexed. Spectra were acquired using water suppressed Carr-Purcell-Meiboom-Gill (CPMG) using the Bruker program cpmgpr (recycle delay (RD) -90º-t1-180º-tm-acquire). An RD of 2 s was employed for net magnetization relaxation, during which noise irradiation was applied to suppress the large water proton signal. Several loops *n* = 100 and a spin-echo delay t = 400 µs were used to allow spectral editing through T2 relaxation and therefore

attenuation of broad signals. For each sample, 128 scans were recorded in 32K data points with a spectral of 20 ppm.

The analysis of the validation cohort 2 was performed on a Bruker AVANCE II 600 spectrometer fitted with an automatic sample changer and a multinuclear triple resonance (TBI) probe (Bruker Biospin, Germany) at 14.1 T (600.3 MHz). Plasma samples were thawed at room temperature and 400 µL aliquots were combined with 200 µL of saline buffer (9 % w/V NaCl, 100% D2O, 10mM TSP). Samples were mixed by vortex and spun for 10 min at 13,000 rpm prior to transferring 550 to a 5 mm NMR tube. Spectra were acquired using water suppressed Carr-Purcell-Meiboom-Gill (CPMG) using the Bruker program cpmgpr (RD-90ºt1-180º-tm - acquire free induction decay). The water signal was suppressed by irradiating the RD of 2s with a mixing time (tm) of 10 µs. The acquisition was set to 1.36s and the 90º pulse length of 10.43 µs. Several loops *n* = 40 and a spin-echo delay t = 400 µs were used to allow spectral editing through T2 relaxation and therefore attenuation of broad signals. For each sample, 256 scans were recorded in 32K data points with a spectral of 20 ppm.

Spectra were manually phased, corrected for baseline distortions and referenced to the center of the α-glucose anomeric doublet (δ 5.23). All spectra were imported to MATLAB and digitized into consecutive integrated spectral regions of equal width. The regions between δ 4.7–4.9 containing the residual water resonance were removed from all spectra to minimize the effect of baseline effects caused by imperfect water suppression. Each spectrum was then normalized using a probabilistic quotient normalization algorithm.

Extraction of Fecal Genomic DNA and Whole-Genome Shotgun Sequencing (metagenomics) in the clinical study

Fecal shotgun sequencing data was generated for *n* = 73 patients from the discovery cohort as previously described [16]. Briefly, total DNA was extracted from frozen human stools using the QIAamp DNA Stool Mini kit (Qiagen), with slight modifications by adding a bead-beating step. Quantification of DNA was performed with a Qubit 3.0 fluorometer (Thermo Fisher Scientific, USA), and 3 ng of extracted DNA for each sample was prepared using the Bioscientific PCR free library kit according to the manufacturer's instructions and sequenced on a Hiseq 2500 (Illumina) with 2x150 pair-end chemistry. The obtained input fastq files were decompressed, filtered and 3' ends-trimmed by quality, using prinseq-lite-0.20.4 program [46] and overlapping pairs were joined using FLASH-1.2.11 [47]. Fastq files were then converted into fast files, and human host reads were removed by mapping the reads against the reference human genome (GRCh38.p11, Dec 2013) using Bowtie 2 [48] with end-to-end and very sensitive options. Next, functional analyses were carried out by assembling the non-host reads into contigs by MEGAHIT v1.1.2 [49] and mapping those reads against the contigs with Bowtie 2.

Reads that did not assemble were appended to the contigs. Next, Prodigal v2.6.342 [50] was used for predicting codifying regions. Functional annotation was carried out with HMMER [51] against the Kyoto Encyclopedia of Genes and Genomes (KEGG) database, version 2016 [52] to obtain the functional subcategory, route and annotation of the genes. The filtering of the best annotations and the assignment of the orf annotation to every read were carried out using R 3.1.0 [53] which was also used to count the aligned reads and add the category and its coverage, and finally, build abundance matrices. Taxonomic annotation was implemented with Kaiju v1.6.2 [54] on the human-free reads using a greedy mode. The addition of lineage information, counting of taxa and generation of an abundance matrix for all samples were performed using the package R [55].

Preclinical and Laboratory Parameters in mice

Serum was obtained by centrifugation and stored at −80 °C for further analysis. Serum alanine aminotransferase (ALT) and aspartate aminotransferase (AST) were quantified by enzymatic colorimetric assays (QCA, Barcelona, Spain). Fasting insulinemia and glycemia were measured with the Mouse Insulin ELISA Kit (Mercodia, Uppsala, Sweden) and the Glucose Liquid Kit (QCA, Barcelona, Spain), respectively. Livers were rapidly collected, weighed, and divided into two sections—the lobus hepatis sinister medialis was kept in formalin, and the remaining tissue was frozen in liquid nitrogen and stored at −80 °C until further analysis.

Hepatic Fat Quantification in murine liver

Hepatic lipids were extracted and quantified following a method previously described [56]. Briefly, total lipids were extracted from 80–100 mg liver sections by adding 1 mL of hexane/isopropanol (3:2, v/v) and degassing with gas nitrogen. Then, they were left overnight under orbital agitation, at room temperature, and protected from light. After extracting 0.3 mL of Na_2SO_4 (0.47 M), the organic layer was separated and dried with gas nitrogen. Total lipids were quantified gravimetrically before emulsifying, as described previously [57]. Triglycerides and total cholesterol were measured using commercial enzymatic kits (QCA).

Histological Evaluation in murine liver

Liver portions fixed in buffered formalin (4% formaldehyde, 4 gr/L NaH_2PO_4, 6.5 gr/L Na_2HPO_4; pH 6.8) were cut at a thickness of 3.5 µm and stained with hematoxylin & eosin (H&E). Liver images (magnification 40X) were taken with a microscope (ECLIPSE Ti; Nikon, Tokyo, Japan) coupled to a digital sight camera (DS-Ri1, Nikon) and analysed using ImageJ NDPI software (National Institutes of Health, Bethesda, MD, USA; https://imagej.nih.gov/ij, version 1.52a). To avoid any bias in the analysis, the study had a double-blind design, preventing the reviewers from knowing any data from the mice during the histopathological analysis. A General NAFLD Scoring System was established to diagnose mice with

NAFLD/NASH. The key features of NAFLD and NASH were categorized as follows: steatosis was assessed by analyzing macrovesicular (0–3) and microvesicular steatosis (0–3) separately, followed by hepatocellular hypertrophy (0–3), which evaluates abnormal cellular enlargement, and finally giving a total score of 9 points of steatosis state. Inflammation was scored by counting cell aggregates (inflammatory foci). The score 0 to 3 depends on the grade of the feature. It is categorized as 0 (<5%), 1 (5–33%), 2 (34–66%) and 3 (>66%), and this scoring is used in each feature of steatosis and then added to the total steatosis score [58]. Ballooning was not included in the scoring system, because only quantitative measures were considered for the rodent NAFLD score. It is important to highlight that hypertrophy is not a sign of cellular injury and slightly refers to an anomalous enlargement of the cells without recognizing the source of this enlargement [58].

Bacterial genomic DNA isolation, 16S rRNA sequencing and analysis (metagenomics)

Bacterial genomic DNA was isolated from mice fecal samples using the MBP DNA Soil extraction kit. Genomic DNA was normalized to 5 ng/µL with EB (10 mM Tris-HCl) and libraries were performed. Briefly, following a first PCR and clean-up using KAPA Pure Beads (Roche Catalogue No. 07983298001) a second PCR master mix was made up using P7 and P5 of Nextera XT Index Kit v2 index primers (Illumina Catalogue No. FC-131-2001 to 2004). Following the PCR reaction, the libraries were quantified using the Quant-iT dsDNA Assay Kit, high sensitivity kit (Invitrogen Catalogue No. 10164582) and run on a FLUOstar Optima plate reader. Libraries were pooled and run on a High Sensitivity D1000 ScreenTape (Agilent Catalogue No. 5067-5579) using the Agilent Tapestation 4200 to calculate the final library pool molarity. The pool was run on an Illumina MiSeq instrument using MiSeq® Reagent Kit v3 (600 cycle) (Illumina Catalogue FC-102-3003) following the Illumina recommended denaturation and loading recommendations which included a 20% PhiX spike in (PhiX Control v3 Illumina Catalogue FC-110-3001). The raw data was analysed locally on the MiSeq using MiSeq reporter. For the 16S sequence analysis, The LotuS 1.36 used pipeline [59,60] in short amplicon mode with default quality filtering. Raw 16S rRNA gene reads were quality filtered to ensure a minimum length of 170 bp, not more than eight homonucleotides, no ambiguous bases, average quality >= 27 and an accumulated error below 0.5 and a dereplication filter set to “6:1,3:2”. Cleaned reads were clustered into amplicon sequencing variants (ASVs) using DADA2 [61], chimeric ASVs were removed using the DADA2 de novo chimera check. Remainder phiX reads were filtered by mapping ASVs against the phiX reference genome [62]. ASV taxonomy was assigned using the LotuS2 LCA algorithms against Silva 138.1 reference database [63]. We could assign on average 5500 ± 3108 reads to each sample that were of cyanobacterial origin. Further data analysis was conducted with R statistical language Version 3.00 (The R Foundation, https://www.r-project.org/) as

described in Hildebrand et al. [64], employing the rtk software [65] or all data normalizations. The 16S raw data can be found at:

https://1drv.ms/u/s!ApVezdktX3allZVJXYWok9s2qhgfvg?e=VDyr2c .

Primer Design for HutH and HutG microbiota functions

Several sequences from prokaryotes species were uploaded from databases to ARDEP program [66] in order to design degenerated primers that could amplify in conserved regions for HutH and HutG genes and cover all the species used for the primer design. Based on the k-mer algorithm, primer length is set as k, and all sequences are divided into k-mers. The analysis platform allows for sequence length statistics, length filtering, and redundancy removal to be performed on the sequence database using tools located in the "Sequence Processing" section. After performing sequence database quality control, we could run ARDEP for primer design in the "Primer Processing" section, and we obtained a list of different possibilities of primer sets. The "Covered Taxonomy Calculator "option was used to count the sequence number of taxonomy and functional group covered by primer sets. The basic primer properties were considered (Tm, GC%, primer length) choosing the best option.

Histidine quantification in mice serum samples (metabolomics)

For serum metabolite extraction, 10 µL of the sample was added to a 1.5-mL microcentrifuge tube containing 100 µL of water and 1 µg/mL of Phe-13C as internal standard. Then, samples were incubated in a sample mixer (Thermo Scientific, Barcelona, Spain) for 30 min at 1,200 rpm and 4°C. For protein precipitation, 300 µL of acetonitrile was added to the sample, and the resulting solution was vortexed and incubated in a sample mixer at 1,200 rpm for 30 min at 4°C. Afterward, samples were centrifuged at 13,000 rpm for 15 min at 4°C. The resulting supernatant was transferred into another 1.5-mL tube and incubated overnight at -20°C. The following day, samples were vortexed and centrifuged at 13,000 rpm for 15 min at 4°C. Finally, the supernatant was transferred to vials with glass inserts (Agilent Technologies, Barcelona, Spain) for further analysis after overnight incubation at -20°C. All reagents used were LC-MS grade.

For histidine detection, samples were injected based on the described method [67]. Briefly, 4 µL of the extracted sample was injected and chromatographic separation was achieved on a Cogent Diamond Hydride column (15P-2, VWR) equipped with a microfilter (502693, Supelco) with a column temperature of 40°C. The flow rate was 0.4 mL/min for 21 min. Solvent A was composed of water containing 0.1% formic acid (v/v) and solvent B was composed of acetonitrile containing 0.1% formic acid (v/v). The gradient started at 75% of solvent B and was held for 5 min. Then, solvent B was progressively reduced to 60% (in 1 min and held for 1 min), 50% (in 2 min and held for 1 min) and 40% (in 10 min). Finally, solvent B was

increased to 100% in 1 min. Post-time was established at 5 min. Electrospray ionization was performed in positive ion mode using N2 at a pressure of 15 psi for the nebulizer with a flow of 11 L/min and a temperature of 300°C, respectively. Data were collected using the MassHunter Data Analysis Software (Agilent Technologies, CA, USA). Samples were decoded and randomized before injection. Metabolite extraction quality controls (plasma samples with internal Phe-13C) were injected every 10 samples. Peak determination and peak area integration were carried out with MassHunter Quantitative Analyses (Agilent Technologies, CA, USA). Signal normalization was performed using internal standards. Quantification was performed by constructing standard curves. The analysis was performed through liquid chromatography coupled to a hybrid mass spectrometer with electrospray ionization and a triple quadrupole mass analyzer. The liquid chromatography system was an ultra-performance liquid chromatography model 1290 coupled to LC-ESI-QqQ-MS/MS model 6420 both from Agilent Technologies (Barcelona, Spain).

Histidine quantification in the liver of mice (metabolomics)

LC-MS-grade acetonitrile (ACN) was purchased from VWR International GmbH (Darmstadt, Germany). Analytical grade formic acid (97%) and hydrochloric acid (37%), LC-MS-grade ammonium formate and the certified reference material amino acids mix (TraceCERT®) used to prepare the standard curves were purchased from Merck KGaA (Darmstadt, Germany). The stable isotope-labelled amino acid mix MSK-CAA from Cambridge Isotope Laboratories, Inc., used as an internal standard, was obtained from CK Isotopes Limited (Leicestershire, UK). Sterile 0.45 µm PES filters were purchased from Fisher Scientific UK Ltd (Loughborough, UK).

A 12-point standard curve with concentrations ranging from 0.24 µM to 1 mM was freshly prepared using the commercially available amino acids mix TraceCERT®. Approximately 50 mg of liver tissue was homogenized by bead beating using a FastPrep-24 Tissue Homogenizer and 1 mL of 6 N HCl (3x30sec at 6.5 m/s cycles, with 5 min on ice in between). The homogenate was placed into a screw cap Pyrex tube and an extra 1 mL 6 N HCl was used to ensure all the sample was transferred, making the total volume for hydrolysis 2 mL. To prevent oxidation, the headspace was purged with nitrogen. Samples were then placed into a heat block at 110 °C and hydrolyzed overnight for 16h. Once cooled down, hydrolysates were dried at 55 °C using a Speedvac centrifugal concentrator, before being reconstituted using 2 mL of H_2O, filtered, and stored at −80°C until analysis. Right before being injected, samples were diluted 10X using the LC-MS solvent mix B (90% ACN, 10% H_2O, 0.5% FA and 20 mM ammonium formate). Each point of the standard curve and the diluted samples were spiked with the isotopically labelled internal standard mix MSK-CAA-1, to a final 50 µM concentration, before being transferred to LC-MS vials, ready to be analyzed.

Liquid chromatography coupled with mass spectrometry (LC-MS) analysis of amino acids was performed using a ACQUITY UPLC I-Class PLUS (Waters™, Wilmslow, UK) coupled to a Xevo TQ-S micro Triple Quadrupole mass spectrometer (Waters™), that was operated in positive electrospray ionization mode (ESI+). Separation was achieved using a Raptor HILIC-Si LC Column (100 × 2.1 mm, 2.7 µm particle size) with a Raptor Polar X EXP guard column cartridge (2.7 µm, 5 mm x 2.1 m), maintained at 35 °C (Thames Restek UK Limited, Saunderton, UK). The 13-minute gradient recommended by Restek to separate amino acids in human plasma was used [68], but with slight modifications in the mobile phases, injection volume and flow rate. Briefly, mobile phase A consisted of 0.5 % formic acid, and 20 mM ammonium formate in water and mobile phase B was 0.5 % formic acid, 20 mM ammonium formate, 10% H_2O and 90% acetonitrile. The injection volume was 3 µL and the flow rate was set to 400 µL/min. Triplicate injections for each sample were performed. Data was acquired and processed using the MassLynx V4.2 Data and TargetLynx software (Waters), integrating the area under the peak for each targeted analyte relative to the isotopically labelled internal standard. Processed data were exported to Excel and quantified against the analyzed calibration curves.

RNA Extraction and Quantitative Polymerase Chain Reaction

Homogenates from livers of Animal model 1 and Animal model 2, were used for total RNA extractions using TriPure reagent (Roche Diagnostic, Sant Cugat del Vallès, Barcelona, Spain) according to the manufacturer's instructions. RNA homogenates from human primary hepatocytes were extracted and purified using RNeasy Mini Kit (QIAGEN, Gaithersburg, MD). RNA concentration and purity were determined using a nanophotometer (Implen GmbH, München, Germany). RNA was converted to cDNA using the High-Capacity RNA-to-cDNA Kit (Applied Biosystems, Wilmington, DE, USA). The cDNAs were diluted 1:10 before incubation with commercial LightCycler 480 Sybr green I master on a Lightcycler ® 480 II (Roche Diagnostic) or TaqMan technology suitable for relative gene expression quantification. **Table S1** shows a list of used primers for this study. 36b4 was used as a housekeeping gene [69–71] in animal models and Peptidylprolyl isomerase A (PPIA) as a housekeeping gene in human primary hepatocytes.

Protein Extraction and Western Blot Analysis

Human primary hepatocytes were collected by scraping on ice with cell lysis buffer (Cell Signaling Technology). Cell lysates were kept in agitation for 30 min and were centrifuged at 12,000 x g for 10 min at 4°C to remove cell debris. Protein content was determined using the RC/DC Protein Assay (Bio-Rad Laboratories, Hercules, CA, USA). For western blotting, proteins extracts (15 µg) were separated using 4%-20% precast polyacrylamide gel (Bio-Rad) and transferred to polyvinylidene fluoride (PVDF) membranes. After blocking with 5 % BSA in TBS-Tween20 (Sigma-

Aldrich), membranes were exposed overnight at 4°C to primary antibodies against phospho Akt (pAkt [Ser473], rabbit monoclonal antibody [mAb] #9271) at 1/1,000 dilution (Cell Signaling, Danvers, MA, USA) diluted in 1X TBS containing 0,1 % Tween 20, following the recommendations of the manufacturer. After secondary antibody incubation (anti-rabbit HRP), signals were detected using enhanced chemiluminescence horseradish peroxidase substrate (Millipore, Burlington, MA, USA) and analyzed with a luminescent image and signals were quantified by Image J software (https://imagej.nih.gov/ij/). Anti-tubulin hFAB rhodamine at 1/1,000 (64225333, BioRad, Hercules, CA, USA) for 2 h exposure was used as control.

In Animal model 1, approximately 20 mg of the liver was homogenized with Tyssuelyser LT (Qiagen, Hilden, Germany) for 50 seconds in 300 µL lysis buffer (8 mmol/L NaH_2PO_4, 42 mmol/L Na_2HPO_4, 1% SDS, 0.1 mol/L NaCl, 0.1% NP40, 1 mmol/L NaF, 10 mmol/L sodium orthovanadate, 2 mmol/L PMSF, and 1% protease inhibitor cocktail 1 (Millipore)). The protein extracts were quantified by the standardized BCA method (Pierce BCA Protein assay kit (Thermo fisher scientific, Waltham, MA, USA). Protein extracts (20–25 µg) were electrophoretically separated on 10% SDS-PAGE and electroblotted to nitrocellulose membranes (LI-COR biosciences, NE, USA) [72]. Efficient protein transfer was monitored by the Ponceau-S stain. Next, membranes were blocked (5% BSA) at room temperature and probed with specific primary antibodies (diluted 1:1000) overnight at 4º C in 1% BSA: total Akt (4685) (Cell Signaling), phospho-Akt (Ser473) (4060) (Cell Signaling) and β-Actin (Santa Cruz Biotechnology, Inc; Dallas, TX, USA). Thereafter, infrared fluorescent secondary antibodies anti-rabbit 680, anti-rabbit 800 and anti-mouse 680 (LI-COR Biosciences; 926-68070, 926-32211, and 926-68071, respectively) were used for detection and quantified using ImageJ [73].

QUANTIFICATION AND STATISTICAL ANALYSIS

Statistical analyses for Animal models and human primary hepatocytes were performed using GraphPad Prism 9 software (Graph-Pad Software, La Jolla, CA, USA). Data are presented as mean ± SEM. Data distribution was analyzed by the Shapiro–Wilk normality test. Differences between the two groups were determined using an unpaired t-test (two-tailed, 95% confidence interval). A p-value below 0.05 was considered statistically significant.

Transcriptomic analysis

Differential expression gene analyses were performed using the “limma” R package [74]. A robust linear regression model adjusted for the age, BMI, sex, and country, was fitted using the “lmFit” function with the option method = “robust”, to limit the influence of outlying samples. Then, an empirical Bayes method was applied to borrow information between genes with the “eBayes” function. P-values were adjusted for multiple comparisons using the Benjamini-Hochberg procedure for False Discovery Rate (pFDR). A cut-off for the pFDR<0.1 was used

as a threshold for statistical significance. The functional roles of differentially expressed genes were characterized by integrating the information provided from differential expression analysis, gene-gene interaction networks, and pathway over-representation analysis using the R package "pathfinder" with default parameters [75]. Significant genes were initially mapped onto a STRING gene-gene interaction network. Then, active subnetworks of interconnected genes (including genes that are not significant themselves but connect significant genes) in this gene-gene interaction network were identified. Finally, separate pathway over-representation analyses based on the Reactome and KEGG databases were performed for each active subnetwork using the significant genes in each of the active subnetworks and genes in the PIN as the background genes. Pathway statistical significance was set at pFDR<0.05. Significantly enriched pathways were clustered via hierarchical clustering. Genes in each pathway were used to calculate the pairwise kappa statistics, a chance-corrected measure of co-occurrence between pathways. The distance matrix 1- kappa statistic was used for agglomerative hierarchical clustering and a threshold of 0.35 for the kappa statistics was used to define strong relations.

Metagenomic analysis

For metagenomics analyses, we excluded those microbial families, genera, or species having less than 10 counts in 10 % of the samples. Differential abundance analyses for taxa associated with the circulating histidine levels, hepatic steatosis or HAA treatment were performed using the analysis of compositions of microbiomes with bias correction (ANCOM-BC) methodology [76]. It considers the bias due to differential sampling fractions across samples by adding a sample-specific offset to a linear regression model, that is estimated from the observed data. The linear regression model in log scale is analogous to log-ratio transformation to consider the compositional nature of metagenomics datasets, while the offset term serves as the bias correction. We adjusted all models in humans for age, sex, BMI, and country. P-values were adjusted for multiple comparisons using a Sequential Goodness of Fit [77] as implemented in the "SGoF" R package. Unlike FDR methods, which decrease their statistical power as the number of tests increases, SGoF methods increase their power with an increasing number of tests. SGoF has proven to behave particularly better than FDR methods with a high number of tests and low sample size, which is the case of omics large datasets. Statistical significance was set at padj<0.1. To assess differences in the microbial Hut genes between patients with a degree of steatosis <33% and a degree of steatosis >33% we performed Mann-Whitney tests to the centered log-ratio transformed counts of the KEGG orthologs (KO) K01479, K01745, K01468, and K01712 corresponding to the hutG, hutH, hutI, and hutU, respectively.

Table S1. Sequences of the used RT-PCR oligonucleotides

	Forward	**Reverse**
hACSL1	5'-TGAGTGGGTGATTATTGAAC-3'	5'-GTTGACTATGTACGTGATGG-3'
hFASN	5'-CAATACAGATGGCTTCAAGG-3'	5'-GATGTATTCAAATGACTCAGGG-3'
hSCD1	5'-GCCCCTCTACTTGGAAGACGA-3'	5'-AAGTGATCCCATACAGGGCTC-3'
hTAAR1	5'-AAACAACTTCATACCCCAAC-3'	5'-AAAATACCAACAGTGCTCAG-3'
hPPIA	5'-ATGGTTCCCAGTTTTTCATC-3'	5'-CTCCACAATATTCATGCCTTC-3'
mAcc1	5’-GATGAACCATCTCCGTTGGC-3’	5’-CCCAATTATGAATCGGGAGTGC-3’
mCd11c	5’-ACGTCAGTACAAGGAGATGTTGGA-3’	5’-ATCCTATTGCAGAATGCTTCTTTACC-3’
mCd36	5’-GAACCACTGCTTTCAAAAACTGG-3’	5’-TGCTGTTCTTTGCCACGTCA-3’
mIl1a	5’-CCAGAAGAAAATGAGGTCGG-3’	5’-AGCGCTCAAGGAGAAGACC-3’
mIl10	5’-AAGGCAGTGGAGCAGGTGAA-3’	5’-CCAGCAGACTCAATACACAC-3’
mFabp4	5’-TGAAAGAAGTGGGAGTGGGC-3’	5’-CGAATTCCACGCCCAGTTTG-3’
mFasn	5’-GCTGCGGAAACTTCAGGAAAT-3’	5’-AGAGACGTGTCACTCCTGGACTT-3’
mF4/80	5’-CATAAGCTGGGCAAGTGGTA-3’	5’-GGATGTACAGATGGGGGATG-3’
mScd1	5’-AGATCTCCAGTTCTTACACGACCAC-3’	5’-GACGGATGTCTTCTTCCAGGTG-3’
mTaar1	5’-GGGTACTGGCGTTCATGACT-3’	5’-CGCCCACCATGATCCCTAAG-3’
mTnfa	5’-AGGGTCTGGGCCATAGAACT-3’	5’-CCACCACGCTCTTCTGTCTAC-3’
m36bB4	5’-AGTCCCTGCCCTTTGTACACA-3’	5’-CGATCCGAGGGCCTCACTA-3’
hutH_prok	5’- ATCAATAGCCTGGCGCGCGG -3’	5’- AAAGCCGGGCTGACGCCGA -3’
hutG_prok	5’-GCAGTGGCTCTGCTGGGTTA-3’	5’- AGAAACCGGCAGTGCTCAC-3’
16S	5’- GTGSTGCAYGGYYGTCGTCA -3’	5’- ACGTCRTCCMCNCCTTCCTC -3’
mPrkaa2	Mm01264789_m1	
mPgc1a	Mm01208835_m1	
mAcadsb	Mm00482171_m1	
mSlc2a2	Mm00446229_m1	
mInsr	Mm01211875_m1	
mActb	4352933E	

5. GENERAL DISCUSSION

5.1 Discussion

The increased number of obese and overweight subjects worldwide has highlighted NAFLD as one of the most common manifestations of metabolic syndrome. There is a strong positive association between obesity, intestinal microbiota and NAFLD. These associations are part of a set of risk factors including abdominal obesity, IR and dyslipidemia that promote metabolic syndrome [333,334]. Evidence from different studies demonstrated a vicious circle among them acting as key factors playing an important role in the development of these obesity-associated metabolic disorders [335,336]. High-caloric diets and sedentary lifestyles are hallmarks in the development of obesity and gut microbiota dysbiosis. As widely explained in the introductory section, the imbalance between food intake and energy expenditure causes obesity, which may lead to dysfunctional adipose tissue releasing FFAs to the circulatory system and ending up in an ectopic fat deposition, such as occurs in the liver, promoting hepatic steatosis [54]. On the other hand, gut dysbiosis caused by high-caloric diets can disrupt intestinal function and permeability triggering endotoxemia by the translocation of LPS or harmful bacterial metabolites into the portal vein, thereby activating a systemic inflammation leading to macrophage influx into the liver and promoting IR [334]. Therefore, both are recognized as key risk factors in the development of NAFLD by inducing its characteristic pathological features: hepatic steatosis, IR, and chronic inflammation.

In this context, some nutraceuticals have been widely studied as anti-inflammatory, antioxidant, and anti-lipogenic agents in several chronic inflammatory and metabolic diseases [254–256]. In line with these observations, Mardinoglu et al. performed a personal model-assisted identification of metabolic pathways affected in NAFLD to find metabolic cofactors that can modulate these affected or disrupted pathways [262]. Moreover, our group in collaboration with Dr. Fernández-Real's group has noticed an affection of histidine levels in NAFLD patients and in a preclinical model [298,299]. Thus, in the present work, it has been provided novel effects and mechanisms of action of both the specific combination of metabolic cofactors and histidine-related amino acids, which firsts are involved in the modulation of NAD^+ and GSH metabolism as targets against NAFLD and the modulation of histidine catabolism as a strategy to tackle

NAFLD respectively. In addition, as aforementioned, NAFLD is linked to different metabolic disorders that are key factors in the "multiple-hit" theory that promotes NAFLD development. Thus, the effect of the supplementation of both nutraceutical combinations has been also studied in obesity, intestinal dysfunction and dysbiosis.

5.1.1 MI supplementation, a novel multifactorial therapy against metabolic comorbidities

The first three studies were focused on the evaluation of the effects of administration of a specific combination of metabolic cofactors (MI, defined in **Chapter 1** to **3**) in NAFLD and metabolic disorders that participate in the development and progression of this hepatic manifestation. The MI supplementation was given in the three studies at two extrapolated human equivalent doses that can be considered acceptable and safe in a context of a nutraceuticals supplementation to tackle NAFLD. Considering an average mice's weight of 30 g, the doses of betaine, LC, NAC, and NR used were equivalent to the daily consumption of < 4 g of these metabolic activators for a 60 kg person [328].

According to **Chapter 1,** the principal objective was to evaluate whether this nutraceutical treatment could ameliorate the principal pathological features of NAFLD (*i.e.*, liver steatosis, hepatic inflammation, hepatic IR). As a first approach to the improvement of the hepatic state, the increased liver weight and circulant levels of hepatic transaminases as biomarkers of liver damage [337] were attenuated after MI supplementation. Regarding the improvement of serum metabolic biomarkers of the hepatic state concordant with a proof-of-concept clinical study [262], a significant amelioration of hepatic steatosis was also described after MI supplementation. The lipolytic and oxidative characteristics of the metabolic cofactors used in the MI treatment [292,338–340] are probably responsible for the reduction of the total hepatic lipid content, as well as the decreased triglycerides and cholesterol levels compared to NAFLD mice counterparts. Moreover, a notorious reduction of micro- and macro-vesicular steatosis and hypertrophy after MI supplementation was observed. This amelioration of hepatic steatosis was in accordance with

previous studies in which NAD^+ and GSH precursors were presented as probably useful for preventing and treating hepatic steatosis [262]. Hypothetically, the boost of NAD^+ and GSH metabolism suggested that MI supplementation could reduce the hepatic overload of FFAs by an increased mitochondrial FFAs' oxidative activity while protecting the liver against ROS-induced oxidative stress by GSH production [262]. However, after MI supplementation, it was not observed changes in FFAs oxidation-related genes nor hepatic lipogenic-related genes. Even though these results diverged from our hypothesis, gene expression data do not always match protein levels. Hence, further studies of protein quantification in the liver would be useful to support our hypothesis. It is worth mentioning that *G6pd* expression, which is a gene associated with the lipogenic activity and acts as a transcriptional factor and is positively correlated with NAFLD [341,342], was downregulated in MI-supplemented mice demonstrating an improvement in lipid homeostasis. Interestingly, hepatic fatty acid transporters *Cd36* and *Fabp4,* which are positively correlated with hepatic steatosis [343], were downregulated after MI treatment. Thus, one of the pathways that MI supplementation is modulating is the FFAs uptake into the hepatocytes, reducing fat accumulation within these cells.

Not only MI supplementation is a promising strategy to tackle NAFLD by reducing FFAs uptake, but also protects the liver against pro-inflammatory and fibrotic processes, which are characteristic features of NASH [344]. As aforementioned, ROS and the accumulation of harmful lipid species induce macrophage infiltration, which contributes to the chronic inflammatory state in the liver by releasing pro-inflammatory cytokines [345]. Thus, the release of pro-inflammatory cytokines has been linked to the loss of insulin sensitivity by degrading IRS-1, and the stimulation of profibrotic pathways [199,346]. Nevertheless, in this study MI supplementation showed anti-inflammatory and anti-fibrotic properties in the liver, observing a downregulated expressions of *F4/80* and *Tnfα*, as well as histopathology analysis and the downregulation of *Col1α1* confirmed a reduction of fibrosis [347], corroborating the reduction of hepatic fibrosis.

As aforementioned, IR is one of the principal hits in the development of NAFLD. There are some factors that have a critical role in the impairment of insulin sensitivity, such as oxidative stress, lipid peroxidation, mitochondrial dysfunction, and inflammation [199,348] , which contribute to the development of IR through the degradation of IRS-1, as explained extensively in the **Introduction** section and **Chapter 1**. In

contrast, MI supplementation partially induced an improvement in AKT activation compared to NAFLD mice, which was in conjunction with a reduction of circulating glucose and insulin and an upregulation of *Glut2* expression. Therefore, MI supplementation can exert an insulin-sensitizing action by improving the activation of the PI3K/Akt pathway and increasing the expression of *Glut2* in hepatocytes.

Although MI supplementation is acting directly in the hepatic hits that are implicated in the development of NAFLD, the treatment must be acting against NAFLD from other affected pathways that are key factors for the development of this liver disease. As explained above, the multiple hit theory also considers the ectopic lipid accumulation in the liver from adipose tissue dysfunction, and the intestinal dysbiosis that is part of the induction of a chronic inflammatory state in the liver from the worsening of intestinal permeability. For this reason, to explore whether MI supplementation also participates in the improvement of disrupted adipose tissue during obesity and ameliorates intestinal dysfunction and dysbiosis associated with NAFLD, **Chapters 2** and **3** studied MI supplementation's beneficial effects both in animal models.

According to **Chapter 2**, MC supplementation, also known as MI, repressed the characteristic increase of body weight in obese mice. Besides, LDL and total cholesterol are related to cardiometabolic disorders [19,20], and both were decreased in MC-treated mice compared to the placebo group suggesting an improvement in lipid metabolism after MC supplementation. Indeed, one of the main findings of this thesis is the identification of MC supplementation as an agent able to reduce visceral adipose tissue in obese animal models. The increase of VAT is linked to a raise of adipokines and cytokines triggering a pro-inflammatory state and the induction of IR that can end up in a disruption of the adipose tissue function releasing FFAs in the circulation [349]. In the present study, MC supplementation reduced VAT expansion, linked to an increase in lipid oxidation and reduction of respiratory quotient due to increased oxygen consumption. Therefore, these results suggest that MC treatment can modulate lipid homeostasis in VAT depots. Indeed, the reduction of VAT was confirmed in the histological analysis, in which adipocyte size was reduced in the MC-supplemented mice. Thus, this amelioration could be attributable to the increase in fat oxidation. To deepen into the molecular mechanisms related to the decrease in VAT, a study of gene expression related to lipid metabolism was performed. Lipolysis-related gene *Atgl*

expression in EWAT was upregulated in MC-treated mice indicating an increase in lipolysis in VAT that correlates with previous studies using two of the ingredients separately [350]. *Plin1* protects lipid droplets from lipolysis, but also its phosphorylation is necessary in the activation of ATGL. Hence, *Plin1*, which was upregulated after MC supplementation, may participate as compensatory response to the increased lipolytic activity [351], or can be connected to the need to increase PLIN1 levels to activate ATGL by PLIN1 phosphorylation [352]. Interestingly, FFAs oxidation-related gene *Acox1* was also upregulated after MC supplementation which corresponds with the results obtained in lipid oxidation and respiratory quotient.

There is strong evidence that BAT could develop a relevant physiological role in obesity as a glucose and triglycerides clearance organ [353,354]. Regarding the characterization of the potential involvement of MC supplementation in the promotion of BAT function, a reduction of BAT weight was observed in MC-treated mice. These results were tightly connected with a reduction in the number and size of lipid droplets. This data correlates with the idea that reversing BAT whitening may reduce obesity by amelioration of BAT dysfunction [355]. To elucidate the molecular mechanisms implicated in BAT improvement by MC supplementation, expression genes related to lipolysis (*Atgl, Mgl* and *Hsl*) and FFAs oxidation (*Acox1*) were upregulated after MC supplementation in BAT, similarly as occurs in VAT. However, not only was the increase in lipolysis and FFAs oxidation the reason for fat reduction in BAT but also MC supplementation upregulated thermogenic genes, which are responsible for the thermogenic BAT activation [36]. Moreover, the increase in thermogenic genes was consistent with the increase in BAT temperature. Therefore, MC supplementation improved adipose tissue dysfunction in obesity by reducing both VAT and BAT depots through the activation of lipolytic and oxidative pathways and promoting thermoregulation in BAT. Thus, this ameliorative effect in adipose tissue reduces ectopic fat accumulation, which is a key factor in NAFLD development. Moreover, MC is a promising treatment against obesity-related metabolic disorders that prevent IR in the affected tissues and, in consequence, improves basal glucose and insulin levels in the circulatory system. Further studies of adipokine, hepatokine, and cytokine levels may be helpful to discern the mechanisms in the improvement in adipocyte function, reduction of ectopic fat accumulation, and adipose-liver axis crosstalk.

With respect to **Chapter 3**, the MC supplementation effect on microbiota dysbiosis and gut barrier dysfunction associated with NAFLD was studied. Disruption in the gut barrier function when gut microbiota homeostasis is disturbed, can lead to the translocation of LPS and harmful bacteria metabolites into the portal vein promoting the production of pro-inflammatory mediators that are the principal contributors of the development of metabolic disorders by the gut-liver axis, such as NAFLD [356,357]. In the present study, it was analyzed the effect of MC supplementation on the gut morphology alterations. After MC supplementation, all these pathologic alterations were reverted improving intestinal barrier morphology, reducing intestinal permeability by upregulating tight-junctions' proteins, and increasing intestinal cell proliferation. Tight junctions are the principal responsible for the maintenance of barrier integrity [358]. In this sense, MC supplementation increased Occludin levels and the expression of *Zo-1*, *Occl* and *Cadh-1*, which improves barrier integrity and gut impermeability in NAFLD mice. Interestingly, the impairment of tight-junctions' proteins is strongly related to the increased presence of pro-inflammatory cytokines [358]. In contrast, MC treatment demonstrated downregulation of gut pro-inflammatory cytokines *Tnfα* and *Il-1β* and upregulated the expression of *Cbs*. Moreover, cell proliferation in villus, which is also associated with the loss of intestinal permeability, is negatively affected by obesogenic diets due to the promotion of oxidative stress and methyl donor deficiency [359]. In our study, we observed MC supplementation showed an amelioration in cell proliferation in the villus probably due to the recovery of a methyl donor by betaine supplementation and the antioxidant properties of NAC protecting against oxidative stress [360,361]. In addition, MC supplementation succeeded in increasing the number of goblet cells, which indicates a rise in goblet cell differentiation compared to NAFLD mice recovering mucus layer production and barrier impermeability [362]. Taking together, we concluded that MC supplementation has ameliorative effects on gut barrier integrity, including induction of cell proliferation, maintenance of the permeability and mucosa layer, and healthy gut morphology, which gives protection against NAFLD development and progression avoiding the translocation of pro-inflammatory metabolites produced by the gut microbiota that may impact the liver [363].

Regarding gut microbiota homeostasis, NAFLD and obesity are strongly related to gut microbiota dysbiosis as previously explained in the

Introduction section. In **Chapter 3**, a tendency to decrease bacterial diversity was observed in NAFLD mice, and this effect was linked to an increase in *Firmicutes* and *Proteobacteria*, consistent with previous studies [364,365]. Nonetheless, MC supplementation induced an increase in bacterial diversity and reduced *Firmicutes* and *Proteobacteria* levels, which was consistent with a clinical study with NAFLD patients in which bacterial diversity was recovered by combining NR, NAC, and LC [366]. Looking deeper into microbiota composition, NAFLD promoted an increase of bacterial genera, such as *Lachnospiraceae, Anaerotruncus, Lachnoclostridium, Eubacterium nodatum, Enterococcus* and *Escherichia/Shigella,* which were implicated in the impairment of the gut barrier and mucin layer and the induction of low-grade chronic inflammation state [367–373]. On the contrary, the supplementation of MC succeeded in reducing the level of these genera increased during NAFLD, restoring the gut bacterial homeostasis through the beneficial effects of the different ingredients of the treatment observed in previous studies [275,374]. One of the targets for the improvement of the intestinal mucosal barrier and the maintenance of the gut microbiota composition could be the inhibition of the TLR4/MyD88 signaling pathway, which is recognized by LPS and lead to the release of inflammatory mediators [275]. Finally, both *Butyricicoccus,* a butyrate genera producer, and *Peptococcus*, which were correlated with NAFLD amelioration [366,375], were increased after MC supplementation. Besides, it was studied fecal SCFAs, which are products of bacterial metabolism, considering their important impact on hepatic lipid accumulation and chronic inflammatory state during NAFLD development [376]. On the one hand, NAFLD mice showed increased propionate levels, which is described as a key precursor for gluconeogenesis and lipogenesis, inducing fat accumulation by inhibiting lipolysis [377], which corresponded with previous studies in NAFLD [376,377]. The rise in propionate levels correlated positively with elevated *Christensenella* and *Citrobacter* levels, which were previously found in NASH patients positively associated with fibrosis severity [378,379]. On the other hand, MC supplementation in NAFLD mice significantly reduced propionate levels, which could be related to the recovery of bacterial homeostasis observed above. Moreover, this reduction in propionate levels was correlated with the increase in *Ruminiclostridium* levels, confirming the negative correlation between propionate and *Ruminiclostridium* levels observed in a previous study [380]. The supply of LC from MC supplementation could be a route of action to

lower propionate levels by its transformation into propionyl-carnitine, which induces beneficial effects on the FFAs oxidation pathway [381].

Summarizing these three manuscripts, we concluded that MC supplementation is a promising therapeutic approach against NAFLD progression by improving metabolic parameters and acting on the multiple hits that promote NAFLD development (**Figure 27**). MC supplementation demonstrated beneficial effects on those mechanisms implicated in hepatic lipid accumulation, inflammation and fibrosis, and those extrahepatic mechanisms implicated in obesity-induced adipose tissue dysfunction responsible for ectopic fat accumulation, and gut barrier dysfunction and microbiota dysbiosis targeting the gut-liver crosstalk. Therefore, we propose this specific combination of metabolic cofactors as a multifactorial intervention against NAFLD and should be extensively explored in clinical studies.

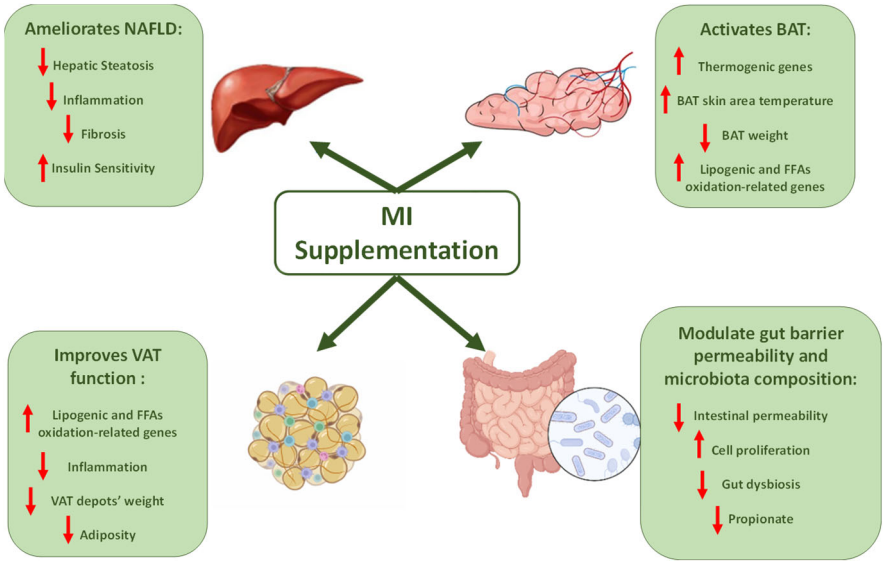

Figure 27. Summary of MI supplementation actions in the liver, white adipose tissue, brown adipose tissue, intestinal barrier, and microbiota.

5.1.2 HAA supplementation, a new player in the treatment of metabolic disorders.

As aforementioned, amino acids are common nutrients that act as cell-signaling molecules, which regulate gene expression and protein phosphorylation cascades [382]. There is evidence linking metabolic disorders with histidine levels pointing to this amino acid as a promising therapeutic target due to its protective role against metabolic syndrome and liver injury [383,384]. The last two studies were focused on the evaluation of the effects of administration of a specific combination of histidine-related amino acids (HAA) in NAFLD and obesity, which is the principal key factor in the development of metabolic comorbidities, such as the hepatic manifestation of metabolic syndrome.

As it has been described above in **Chapter 4**, the first approach to reveal the participation of histidine levels in the development of metabolic disorders was the study of histidine metabolism as a key player in the regulation of obesity and IR. Thus, it was unraveled the negative correlation between circulant histidine levels and obesity, and, interestingly, it was accompanied by the negative correlation between histidine levels and histamine metabolism-related genes. These results suggest that histamine-related enzymes and receptors are activated in obesity as a compensatory mechanism to prevent excess weight gain and the development of obesity, which was associated with the histaminergic system [385]. However, further studies with histamine-related gene KO models are needed to confirm their participation in the prevention of obesity or their participation as inducers of this metabolic disease. Moreover, the most important clusters negatively correlated with histidine levels were p53 regulation and NOTCH signaling, which were previously associated with IR in metabolic disorders. As explained above, high-caloric diets have been described to reduce circulatory histidine levels, but also promote oxidative stress that induces DNA damage, which triggers p53 activation [386,387]. Therefore, histidine may play an important role in regulating p53 expression to maintain insulin sensitivity in adipose tissue. Interestingly, prior studies described a functional interplay between the NOTCH signaling pathway and p53 in senescence [388]. Overall,

it could be determined that histidine might be used as a biomarker of obesity and adipose tissue disruption.

As the data for histidine supplementation are limited, we first considered the dose of histidine-related amino acids combination as a supplementation in an obese mice model. HAA supplementation was given at two extrapolated human equivalent doses that can be considered acceptable and safe in the context of amino acids supplementation to tackle metabolic diseases. The supplementation of HAA in obese mice induced changes associated with the improvement of lipid metabolism, activation of thermogenesis and amelioration of IR, which are therapeutic targets against obesity, as explained in the chapter. Indeed, both lipolysis and FFAs oxidation were upregulated in WAT and BAT by HAA supplementation, which confirms the ameliorative effect of histidine in lipid metabolism reducing adiposity in adipose tissue depots and body weight. In addition, further studies are needed to elucidate the implication of histaminergic pathways and p53 regulation mechanisms in the modulation of lipid metabolism in WAT. *Hal* is not expressed in white adipose tissue (data not shown), indicating that histidine degradation must exerted exclusively via *Hdc* in this tissue. In addition, more interesting effects are observed in BAT, since neither *Hal* nor *Hdc* are expressed in this tissue, which should be translated into higher histidine levels, and consequently, increased effects of HAA supplementation in this tissue. With respect to thermogenesis, one of the therapeutic targets in obesity is the increase of energy expenditure by the activation of BAT. In fact, HAA supplementation upregulates thermogenic genes in obese mice, increasing BAT temperature by its activation. Therefore, these results suggest that histidine activates thermogenic processes in response to pathophysiological conditions probably via histaminergic pathways [389], ameliorating disrupted adipose functions. In fact, the activation of histamine receptors (H1r, H2r, and H4r) was positively correlated with the increased thermogenic activity in BAT [390–392], concordant with the results observed in HAA-supplemented mice.

Regarding IR, the increase in adiponectin expression in WAT and BAT after HAA treatment could be explained by the anti-inflammatory and anti-oxidative stress effects of histidine. Since TNFα inhibits the transcription of adiponectin in adipocytes [393], histidine may increase adiponectin secretion in adipocytes by inhibiting inflammation and oxidative stress. Moreover, adiponectin plays a crucial role in protecting

against IR as an important physiological regulator of insulin action, glucose, and lipid metabolism [394]. Furthermore, cysteine also helps in the rise of adiponectin secretion in adipocytes by inhibiting ROS and cytokines action [395]. In addition, PPARγ seems to be implicated in the adiponectin release, being important in the improvement of hepatic insulin sensitivity, which is mediated via an adiponectin-dependent mechanism that involves the activation of AMPK [396]. Therefore, HAA supplementation could offer anti-inflammatory properties through the increase of adiponectin levels and stimulating the activation of PPARγ, which is also associated with the regulation of adipocyte differentiation and the modulation of many adipocyte genes as the principal transcriptional factor in adipose tissue [397]. Besides, reduced circulant insulin and glucose levels were observed in obese mice supplemented with HAA, which was associated with the amelioration of IR in WAT and BAT by upregulating *Glut4*, confirming the insulin-sensitizing effect of histidine in obesity. These results are coherent with a clinical study of obese women with metabolic syndrome that demonstrated histidine supplementation improved IR [383].

As aforementioned, circulant histidine levels were associated with p53 regulation and proteasomal pathways in obesity. To validate these negative associations and assess whether both pathways can be restored after a treatment based on histidine-related amino acids, further studies are needed to reinforce the results because the mRNA expression analysis of genes that participate in both pathways was performed in eWAT, iWAT and BAT in this study but there are differences depending on the tissue and more analysis are necessary to elucidate the mechanisms.

Overall, these results indicate that HAA supplementation exerts lipid-lowering effects in WAT and BAT and improves insulin sensitivity, ceasing FFAs release to the circulatory system and blocking ectopic fat deposition, which can end up in NAFLD development. However, we required to study the effects of HAA treatment on NAFLD at the hepatic and intestinal levels, to evaluate if the supplementation works as a multifactorial treatment being implicated in all the multiple hits that influence NAFLD progression extendedly explained in the introduction.

For this reason, in **Chapter 5** was focused in the potential diagnostic implications of histidine levels in NAFLD, demonstrating that the gut microbiota is altered in NAFLD associated with histidine level reduction. To characterize the role of histidine levels in NAFLD, we used

an integrative systems medicine approach in large, well-characterized human cohorts combining omics analysis explained in this chapter widely. Human liver transcriptome analysis revealed 93 gene transcripts related to circulating histidine levels, and the most significant clusters obtained positively correlated with histidine levels were G_{α} signaling events and the olfactory signaling pathways. This first cluster is related to cAMP, which is related to lipid metabolism, inflammation, cell differentiation and injury in the liver [398]. Moreover, other significant clusters were linked to circulatory histidine levels, such as IGF, the activation of FGFR and the PI3K-AKT pathway, and the fatty acyl-CoA biosynthesis. IGFs are mainly produced in the liver, and it was evidenced that levels of IGFs and the phosphorylation of AKT are lowered in NAFLD related to hepatic IR [399,400]. For instance, *TAAR1*, which was described to participate in the glucose levels regulation, was observed to be significantly involved in G_{α} signaling and circulatory histidine levels [401], which defines TAAR1 as a promising target to tackle NAFLD.

Serum histidine levels were negatively correlated to hepatic steatosis and with several bacterial families increased in patients with NAFLD. In this study, the *Proteobacteria* phylum has the strongest negative association with serum histidine levels and showed the strongest positive association with hepatic steatosis, which is consistent with the connection of the *Proteobacteria* phylum with NASH in patients [402]. Considering families from the *Proteobacteria* phylum that were positively correlated with hepatic steatosis, we identified *Desulfovibrionaceae, Xanthomonadaceae*, *Rickettsiaceae,* and *Alteromonadales,* consistent with the connection of the proteobacteria phylum and NASH [358,402–404], which correlates with our results. At the genus level, *Bilophila, Shigella* and *Campylobacter* were increased in NAFLD [404–406], which agrees with our study, in which these genera were correlated with low histidine levels found in NAFLD patients. At the same time, these hepatic steatosis-related families from the *Proteobacteria* phylum were associated with bacterial functions involved in histidine catabolism, which are *hutH, hutU, hutI, hutG* [407]. In our study, patients with higher steatosis degrees showed an increased expression of *hutH, hutU* and *hutI*; which could explain the lower plasma histidine levels found in these patients. Consistent with these findings, two recent studies have identified imidazole propionate, as a novel microbial-derived histidine catabolite, which impairs glucose metabolism and insulin signaling and is increased in T2DM [305,408]. In

addition, *hutH* abundance was increased in diabetes [408]. Interestingly, HAA supplementation reduced *hutH* and *hutG* functions in NAFLD mice, increasing gut histidine bioavailability. In fact, hepatic histidine levels were increased after HAA supplementation, which could explain the association of microbiota-induced low histidine levels with NAFLD development.

The upregulation of lipid transporter genes (*FABP4, FABP5, …*) and downregulation of *de novo* lipogenesis-related genes (*DGAT, FASN, SCD1*) in primary hepatocytes suggest that FFAs are transported into mitochondria to be oxidized, decreasing lipid deposition. This theory links a short-term AMPK activation to increased fatty acid oxidation and fatty acid transporters expression in hepatocytes [409]. Moreover, human fecal xenotransplantation from low histidine levels donors to mice resulted in higher hepatic triglycerides accumulation. Thus, one of the main causes of this hepatic lipid accumulation could be a consequence of the reduced histidine availability [264]. The increased lipid accumulation was associated with the upregulation of genes strongly connected with fatty acid metabolism, which is coherent with the upregulation of *Fabp4* observed in FMT mice from patients with liver steatosis [299].

Histidine, serine, carnosine, and cysteine were selected as HAA supplementation, rather than just histidine due to partial amelioration observed in different animal studies with histidine supplementation alone [410,411]. Hence, by using different amino acids connected with histidine level homeostasis, we may obtain stronger results in the amelioration of NAFLD. In addition, gene expression involved in lipid metabolism and inflammation (which are key features in NAFLD progression [358]) was improved. Upregulation of *Acc1* and the downregulation of hepatic inflammatory-related genes *F4/80* and *Tnfα* were observed after HAA supplementation. These results may be coherent with the NAFLD study with *Hdc* KO mice, observing a reduction of the macrophage infiltration marker *F4/80* [412], which could be linked to higher histidine bioavailability in the liver. A reduced expression of *Tnfα* could induce a reduction of inflammation, which is consistent with the results observed in a clinical study in obese women supplemented with histidine and with a preclinical study with a liver-damage mice model [326]. Regarding insulin resistance, increased hepatic insulin sensitivity was observed after HAA supplementation in mice.

Moreover, we performed the identification of several bacterial species and metagenome functions involved in histidine levels and NAFLD in mice after HAA supplementation. At the genus level, *Roseburia*, which was associated with NAFLD development in obese individuals [413], was decreased in NAFLD mice after histidine treatment, and at the family level, *Akkermansiaceae* and *Marinifilaceae* were importantly increased in histidine-supplemented mice, which is consistent with results observed in clinical studies in which *Akkermansiaceae* administration improved several metabolic parameters in obese patients [414] and *Marinifilaceae* was negatively correlated with liver fibrosis [415].

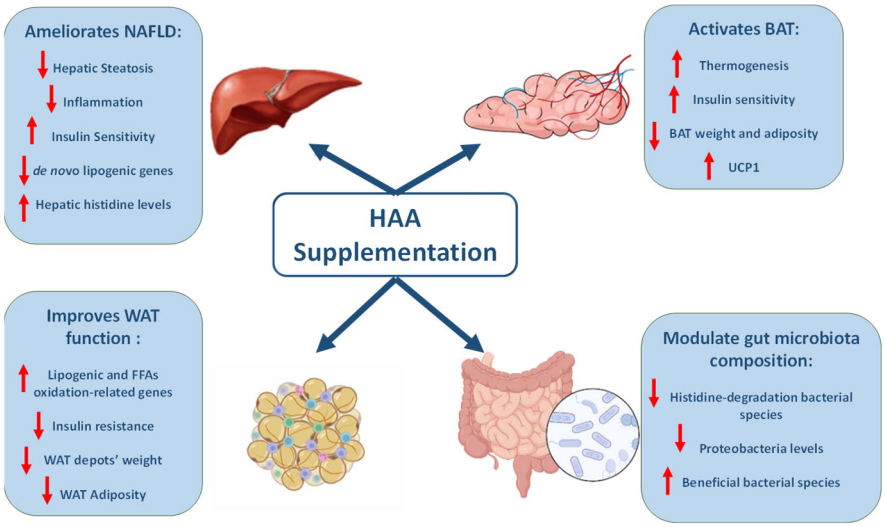

Figure 28. Summary of HAA supplementation actions in the liver, white adipose tissue, brown adipose tissue, and intestinal microbiota.

Therefore, based on the findings from **Chapter 4** and **5**, we demonstrated important crosstalk among histidine and metabolic disorders, considering the participation of the intestinal microbiota in the regulation of histidine levels (**Figure 28**). Above all, we revealed metabolomic and transcriptomic signatures linked to histidine and obesity or hepatic steatosis and uncovered the potential role of the microbiome as a regulator of histidine levels by increased abundances of histidine-degradation bacterial species. Concordant with these results, the supplementation of histidine-related amino acids has an ameliorative

effect on adipose tissue dysfunction and gut microbiota composition, both key participants in the development of hepatic steatosis, inflammation, and insulin resistance in the liver, which suggests that this supplementation is a promising therapeutic strategy against NAFLD development.

Overall, all the results of this thesis have led to the application for a patent titled "*Pharmaceutical and nutraceutical compositions with a combination of amino acids and its use in diseases characterized by lipid accumulation in tissues*" Ref. P6061EP00. EU patent EP22382390.7. The request for grant of a European patent is annexed at the end of the document.

5.2 Limitations

It should be mentioned that there are some limitations of the current studies. In addition to those explained in the different chapters, the fact that in the mice studies only male was included, limits the conclusion to this gender. Therefore, for future studies female mice should be included to confirm if the results obtained in male mice are replicated. A more precise overview of the mechanisms affected by the effects of NAFLD, obesity, or intestinal dysfunction could be obtained with the analysis of protein and activity levels, although mRNA expression and protein levels are usually well correlated [416]. Some strictly anaerobic bacterial species might have a role in NAFLD development but are lost during sample collection, storage, and manipulation. Histamine levels in NAFLD and obesity, and KO mice models of histamine-related genes should be studied to elucidate the implication of the histaminergic pathways and histidine levels in the modulation of the correct function of the tissues affected in these metabolic disorders. Notch signaling pathway has not been evaluated in the mouse model but is being finalized. In **Chapters 1, 2 and 3,** the beneficial effects observed in these preclinical studies should be corroborated in randomized clinical trials.

Regarding clinical studies, in **Chapter 4** and in **Chapter 5,** although the sample size of the different cohorts seems appropriate, population-based studies including subjects with different classes of obesity and ethnic groups would be more representative of this condition. In addition,

although our conclusions are based on the findings of cross-sectional and one-year longitudinal studies, longer term follow-up would be necessary to better understand the strength of our conclusions. The cohorts were formed according to BMI as main inclusion criterion, making it difficult to establish associations between circulating histidine levels, obesity and the different age stages and sex. In **Chapter 4,** to broaden the information about the correlation between circulant histidine levels and human obesity, further RNAseq analyses should be done in other fat depots like VAT or BAT, which differ physiologically from scWAT and could reveal the association of circulant histidine levels with adipose tissue depot-specific functions, and connect the results obtained in the obese mice model with the clinical study.

In addition, in the study with human primary hepatocytes in **Chapter 5,** we did not measure protein levels of those genes that were analysed their mRNA expression, which could be a good complemented in order to assess the effect of the histidine supplementation on the mechanisms that involve hepatic steatosis and de novo lipogenesis. Moreover, genes and proteins related to FFAs oxidation and transport, inflammation, and oxidative stress, which are involved in NAFLD [358], could also be analysed in order to elucidate more in detail the effect of histidine supplementation in the mechanisms implicated in NAFLD development.

In summary, all the data obtained in this project is a promising approach in the evaluation of new treatments against obese-related metabolic disorders based on metabolic cofactors, which modulate the affected pathways in these diseases, and histidine-related amino acids, which are used with the aim to recover histidine levels.

5.3 Futures perspectives

Taking together all the results, this thesis project has unravelled new nutraceutical treatments that ameliorate the metabolism and function of liver, white and brown adipose tissues, and intestine during the development of NAFLD and obesity-related comorbidities displaying their anti-lipogenic, anti-steatosis, anti-inflammatory and anti-oxidative properties. Therefore, we propose that further investigations should be

pursued in the evaluation of these nutraceutical interventions in the context of NAFLD: design clinical studies to evaluate the effect of the treatments in human subjects, *in vitro* mechanistic studies in cultured primary human cells to decipher the exact role of each ingredient used in both treatments respecting the improved pathways, include more protein expression analyses of hepatic, intestinal and adipose tissue key regulators, together with additional mechanistic studies, which would allow defining the specific actions of the treatments, further RNAseq analyses should be done in liver, adipose tissue and intestine, in order to broaden the information about the used mouse models, indirect calorimetry study would provide more information about the influence of the treatments on whole body energy homeostasis. Histidine, histamine GSH and ROS levels analysis in circulation and in the affected tissues would disclose mechanisms that participate in the amelioration of these metabolic comorbidities by the presented nutraceuticals in this project.

Besides, since metabolic disorders are multifactorial, the combination of different natural products with beneficial effects on metabolic pathways has been studied as a promising alternative of pharmacological treatments [417]. Hence, a promising strategy to prevent and treat metabolic comorbidities associated with NAFLD and / or obesity could be the combination of these metabolic activators and amino acids. We have seen during this project that these different nutraceutical compounds have an impact in different affected metabolic pathways that participate in the development and progression of metabolic comorbidities. Indeed, these metabolic cofactors could act on the NAD+ and GSH related pathways that are disrupted in NAFLD and obesity-related disorders, whereas histidine-related amino acids could participate in the modulation of histaminergic pathways affected during the development of these diseases at the same time, boosting the antisteatotic, antilipogenic, anti-inflammatory and antioxidant properties of these supplementations that we elucidated during this project. In this line, the combination of MI or HAA supplementations with other safe and promising bioactive compounds with beneficial effects on metabolic disorders, such as natural polyphenols that are extensively studied and used to reduce the risk of development of metabolic comorbidities [418,419], could be a novel strategy to treat these metabolic comorbidities. Metabolic cofactors and histidine-related amino acids have demonstrated to have antilipemic, anti-inflammatory, antifibrotic and antioxidant

properties in NAFLD, obesity-induced disrupted adipose tissue and intestinal dysfunction. However, to boost these potential characteristics to fight these metabolic comorbidities, polyphenols are an interesting option due to their detailed ameliorative properties against metabolic disorders observed in different studies [420–423]. Previous studies showed that combinatorial strategies using polyphenols can be an effective strategy against different diseases by synergistically or additively enhancing the efficacy of its beneficial properties [424–427], and multidisciplinary efforts are necessary to determine the most favorable combinatorial strategies. Therefore, the objective would be to find synergistic or additive effects between the metabolic cofactors or amino acids used in this project and polyphenols to fight against the progression and development of metabolic complications. Synergic effects are strongly dependent on bioaccessibility and bioavailability of the substances, which are susceptible to be changed by many different factors including food processing, chemical properties of the bioactive compounds and modifications that occurs during digestion [428,429]. However, the use of polyphenols has an advantage because they are the largest group of nutraceuticals that are studied for their chemo-preventive effects tested in several studies [429].

The combination of NAC and betaine with antioxidant polyphenols like green tea extracts, anthocyanins, carotenoids, and flavonoids may improve the antioxidant capacity of these compounds, indicating potential synergy [429,430]. A combination using epigallocatechin gallate, genistein, and quercetin may induce a major suppression of p53 in iWAT [431], which could be accompanied with histidine-related amino acids due to the ameliorative effect on p53 expression seen in this study after their administration. Regarding resveratrol and quercetin, it was numerously used in combination showing restorative effect on disturbed energy metabolism, lipid accumulation, fatty acid oxidation and inflammatory responses both in adipocytes and in the liver, which presents both polyphenols as promising compounds to be combined with metabolic cofactors and HAA to improve the beneficial effects of the treatment on metabolic disorders [427,432]. Moreover, carotenoids were also correlated with anti-inflammatory properties in combination with other compounds [433]. Indeed, Mediterranean diet is a dietary pattern rich in bioactive compounds that inspire the formulation of multi-ingredient supplements based on the beneficial effects of this diet [339]. Therefore, strategies based

on the synergistic combination of bioactive compounds to fight the different factors that influence the onset and evolution of these pathologies is the main objective to find the perfect combination between polyphenols and the treatments used in this study.

Previous studies demonstrated an ameliorative effect on the selected metabolic cofactors and amino acids used in this study. NAC mixed with a combination of polyphenols was useful to modulate immune system function implicated in cellular carcinogen mechanisms [434]. Moreover, the combination of LC with polyphenols promoted a lipid-lowering effect in hepatocytes by increasing FFAs oxidation [435], and doses based on the combination of nicotinamide riboside and pterostilbene displayed increased circulant NAD^+ levels in humans [436]. On the other hand, a study showed that digestibility of amino acids from food was not affected by the consumption of grape pomace, a source of polyphenols, and an antioxidant effect was increased [437]. In addition, cysteine in combination of functional amino acids and polyphenols increased beneficial short-chain fatty acids and of metabolites derived from the mix, and reduced *Proteobacteria* content, improving gut health [438]. Therefore, the synergistic combination of polyphenols with the combination of these metabolic cofactors and amino acids may improve the beneficial effects of these treatments.

To sum up, the present preliminary data from the studies suggest that the additive or synergistic combination of polyphenols with metabolic cofactors or histidine-related amino acids could lead to an improved protection against multifactorial pathologies by consistent amelioration of lipid accumulation, oxidative stress, and inflammation. Moreover, all these proposed studies will help us to gain a novel insight into the development of new therapeutic options for metabolic disease prevention and treatment.

6. CONCLUSIONS

Based on the presented hypothesis and objectives, the presented results and after discussing the chapters, the main conclusions of this thesis are:

1. **The supplementation of the specific combination of metabolic cofactors ameliorates NAFLD in an HFHFr diet-induced mice model**

    - This specific combination of metabolic cofactors reduces hepatic steatosis by the downregulation of lipid-transporters-related genes and the reduction of the hepatic lipid content.
    - The metabolic cofactors treatment has anti-inflammatory, antioxidant and antifibrotic modulatory effects on the liver that result in the reduction of hepatic inflammation and fibrosis.
    - The administration of these metabolic cofactors shows insulin-sensitizing properties on the liver, improving hepatic insulin resistance.

2. **The oral treatment of the specific combination of metabolic cofactors improves obesity in an obese mice model obtained with the HFHFr diet.**

    - The administration of a mix of specific metabolic cofactors reduces visceral adipose tissue depots and adiposity by upregulating lipolytic and oxidative genes and increasing fat oxidation.
    - The combination of selected metabolic cofactors reduces basal glycemic profile and insulinemia by improving insulin sensitivity.
    - The metabolic cofactors treatment reduces fat accumulation in BAT by inducing thermogenesis, lipolysis and FFAs oxidation.

3. **The administration of the specific combination of metabolic cofactors modulates gut barrier permeability and gut microbiota homeostasis in a NAFLD mice model induced by HFHFr diet targeting the gut-liver axis crosstalk.**

    - The supplementation of this nutraceutical treatment has anti-inflammatory effects and protects the barrier function and integrity in the intestine that results in a global improvement of intestinal health by contributing to diminishing proinflammatory bacterial product leakage.

- The treatment based on a combination of metabolic cofactors has ameliorative effects on microbiota diversity by reducing the raise of harmful bacterial species and the propionate-producing microbiota and inducing the growth of beneficial bacteria.

4. **Histidine metabolism plays a key role in the prevention of obesity development and progression by regulating lipid metabolism and thermogenesis in adipose tissue participating in histamine catabolism pathway**

- Circulant histidine levels are negatively correlated with obesity and are associated with the histidine metabolism, p53 regulation and NOTCH signaling pathways.
- Supplementation with histidine and histidine-related amino acids reduced WAT adiposity by upregulation lipolysis and FFAs oxidation and improves insulin sensitivity.
- BAT thermogenesis is activated by HAA supplementation in obese mice by upregulating thermogenic-related genes and increasing UCP1 levels.
- HAA supplementation modulates histamine receptors expression in iWAT, eWAT and BAT, which are associated with the improvement of adipose tissue function.

5. **Microbial-related histidine catabolism has a critical role in the interplay among gut microbiota, histidine catabolism and liver steatosis**

- Circulant histidine levels are negatively correlated with NAFLD, which is directly linked to the rise of microbial-related histidine catabolism levels in these patients.
- The transcriptomics signature unraveled a novel player in NAFLD: the trace amine-associated receptor-1 (*TAAR1*) that is implicated in insulin response.
- Supplementation with histidine and histidine-related amino acids may be a novel therapeutic agent against hepatic fat accumulation and insulin resistance.

7. REFERENCES

References

1. Upadhyay, J., Farr, O., Perakakis, N., Ghaly, W. & Mantzoros, C. Obesity as a Disease. *Medical Clinics of North America* vol. 102 13–33 Preprint at https://doi.org/10.1016/j.mcna.2017.08.004 (2018).

2. WHO. Obesity and overweight. (2021).

3. Chooi, Y. C., Ding, C. & Magkos, F. The epidemiology of obesity. *Metabolism* **92**, 6–10 (2019).

4. Wright, S. M. & Aronne, L. J. Causes of obesity. *Abdom Imaging* **37**, 730–732 (2012).

5. Blüher, M. Obesity: global epidemiology and pathogenesis. *Nature Reviews Endocrinology* vol. 15 288–298 Preprint at https://doi.org/10.1038/s41574-019-0176-8 (2019).

6. Talukdar, D., Seenivasan, S., Cameron, A. J. & Sacks, G. The association between national income and adult obesity prevalence: Empirical insights into temporal patterns and moderators of the association using 40 years of data across 147 countries. *PLoS One* **15**, e0232236 (2020).

7. Mitchell, N. S., Catenacci, V. A., Wyatt, H. R. & Hill, J. O. Obesity: Overview of an epidemic. *Psychiatric Clinics of North America* vol. 34 717–732 Preprint at https://doi.org/10.1016/j.psc.2011.08.005 (2011).

8. Prospective Studies Collaboration *et al.* Body-mass index and cause-specifi c mortality in 900 000 adults: collaborative analyses of 57 prospective studies. *Lancet* **373**, 1083–96 (2009).

9. WHO. Body mass index - BMI. (2022).

10. Dávila-Batista, V. *et al.* Escala colorimétrica del porcentaje de grasa corporal según el estimador de adiposidad CUN-BAE. *Aten Primaria* **48**, 422–423 (2016).

11. Gómez-Ambrosi, J. *et al.* Body mass index classification misses subjects with increased cardiometabolic risk factors related to elevated adiposity. *Int J Obes* **36**, 286–294 (2012).

12. Ashwell, M., Gunn, P. & Gibson, S. Waist-to-height ratio is a better screening tool than waist circumference and BMI for adult cardiometabolic risk factors: Systematic review and meta-analysis. *Obesity Reviews* vol. 13 275–286 Preprint at https://doi.org/10.1111/j.1467-789X.2011.00952.x (2012).

13. Yoo, E. G. Waist-to-height ratio as a screening tool for obesity and cardiometabolic risk. *Korean Journal of Pediatrics* vol. 59 425–431 Preprint at https://doi.org/10.3345/kjp.2016.59.11.425 (2016).

14. Traissac, P. *et al.* Within-subject non-concordance of abdominal v. general high adiposity: Definition and analysis issues. *British Journal of Nutrition* vol. 116 567–568 Preprint at https://doi.org/10.1017/S0007114516002154 (2016).

15. Kowalkowska, J. *et al.* General and abdominal adiposity in a representative sample of Portuguese adults: Dependency of measures and socio-demographic factors' influence. *British Journal of Nutrition* **115**, 185–192 (2016).

16. Engin, A. The Definition and Prevalence of Obesity and Metabolic Syndrome. in *Obesity and Lipotoxicity* (eds. Engin, A. B. & Engin, A.) 1–17 (Springer International Publishing, 2017). doi:10.1007/978-3-319-48382-5_1.

17. Falagas, M. E. & Kompoti, M. *Obesity and infection*. http://infection.thelancet.comVol (2006).

18. Godoy-Matos, A. F., Silva Júnior, W. S. & Valerio, C. M. NAFLD as a continuum: From obesity to metabolic syndrome and diabetes. *Diabetology and Metabolic Syndrome* vol. 12 Preprint at https://doi.org/10.1186/s13098-020-00570-y (2020).

19. Vekic, J., Zeljkovic, A., Stefanovic, A., Jelic-Ivanovic, Z. & Spasojevic-Kalimanovska, V. Obesity and dyslipidemia. *Metabolism* **92**, 71–81 (2019).

20. Mouton, A. J., Li, X., Hall, M. E. & Hall, J. E. Obesity, hypertension, and cardiac dysfunction novel roles of immunometabolism in macrophage activation and inflammation. *Circulation Research* 789–806 Preprint at https://doi.org/10.1161/CIRCRESAHA.119.312321 (2020).

21. Piché, M.-E., Tchernof, A. & Després, J.-P. Obesity Phenotypes, Diabetes, and Cardiovascular Diseases. *Circ Res* **126**, 1477–1500 (2020).

22. Andersen, C. J., Murphy, K. E. & Fernandez, M. L. Impact of obesity and metabolic syndrome on immunity. *Advances in Nutrition* vol. 7 66–75 Preprint at https://doi.org/10.3945/an.115.010207 (2016).

23. Zafar, U., Khaliq, S., Ahmad, H. U., Manzoor, S. & Lone, K. P. Metabolic syndrome: an update on diagnostic criteria, pathogenesis, and genetic links. *Hormones* vol. 17 299–313 Preprint at https://doi.org/10.1007/s42000-018-0051-3 (2018).

24. Karczewski, J. *et al.* Obesity and inflammation. *Eur Cytokine Netw* **29**, 83–94 (2018).

25. Kern, L. *et al.* Obesity-induced TNFα and IL-6 signaling: The missing link between obesity and inflammation- driven liver and colorectal cancers. *Cancers* vol. 11 Preprint at https://doi.org/10.3390/cancers11010024 (2019).

26. Marseglia, L. *et al.* Oxidative stress in obesity: A critical component in human diseases. *International Journal of Molecular Sciences* vol. 16 378–400 Preprint at https://doi.org/10.3390/ijms16010378 (2015).

27. Sun, K., Kusminski, C. M. & Scherer, P. E. Adipose tissue remodeling and obesity. *Journal of Clinical Investigation* **121**, 2094–2101 (2011).

28. Reilly, S. M. & Saltiel, A. R. Adapting to obesity with adipose tissue inflammation. *Nat Rev Endocrinol* **13**, 633–643 (2017).

29. Booth, A., Magnuson, A., Fouts, J. & Foster, M. T. Adipose tissue: An endocrine organ playing a role in metabolic regulation. *Hormone Molecular Biology and Clinical Investigation* vol. 26 25–42 Preprint at https://doi.org/10.1515/hmbci-2015-0073 (2016).

30. Esteve Ràfols, M. Tejido adiposo: heterogeneidad celular y diversidad funcional. *Endocrinología y Nutrición* **61**, 100–112 (2014).

31. Romacho, T., Elsen, M., Röhrborn, D. & Eckel, J. Adipose tissue and its role in organ crosstalk. *Acta Physiologica* vol. 210 733–753 Preprint at https://doi.org/10.1111/apha.12246 (2014).

32. Richard, A. J., White, U., Elks, C. M. & Stephens, J. M. *Adipose Tissue: Physiology to Metabolic Dysfunction*. (2020).

33. Kwok, K. H. M., Lam, K. S. L. & Xu, A. Heterogeneity of white adipose tissue: Molecular basis and clinical implications. *Experimental and Molecular Medicine* vol. 48 Preprint at https://doi.org/10.1038/emm.2016.5 (2016).

34. Villarroya, F., Cereijo, R., Villarroya, J. & Giralt, M. Brown adipose tissue as a secretory organ. *Nature Reviews Endocrinology* vol. 13 26–35 Preprint at https://doi.org/10.1038/nrendo.2016.136 (2017).

35. Cheong, L. Y. & Xu, A. Intercellular and inter-organ crosstalk in browning of white adipose tissue: Molecular mechanism and therapeutic complications. *Journal of Molecular Cell Biology* vol. 13 466–479 Preprint at https://doi.org/10.1093/jmcb/mjab038 (2021).

36. Fenzl, A. & Kiefer, F. W. Brown adipose tissue and thermogenesis. *Horm Mol Biol Clin Investig* **19**, 25–37 (2014).

37. Frühbeck, G., Becerril, S., Sáinz, N., Garrastachu, P. & García-Velloso, M. J. BAT: a new target for human obesity? *Trends Pharmacol Sci* **30**, 387–396 (2009).

38. Marlatt, K. L. & Ravussin, E. Brown Adipose Tissue: an Update on Recent Findings. *Current obesity reports* vol. 6 389–396 Preprint at https://doi.org/10.1007/s13679-017-0283-6 (2017).

39. Lee, P. *et al.* Brown Adipose Tissue Exhibits a Glucose-Responsive Thermogenic Biorhythm in Humans. *Cell Metab* **23**, 602–609 (2016).

40. Trayhurn, P. Recruiting brown adipose tissue in human obesity. *Diabetes* vol. 65 1158–1160 Preprint at https://doi.org/10.2337/dbi16-0002 (2016).

41. Bartesaghi, S. *et al.* Thermogenic activity of UCP1 in human white fat-derived beige adipocytes. *Mol Endocrinol* **29**, 130–9 (2015).

42. Reyes-Farias, M., Fos-Domenech, J., Serra, D., Herrero, L. & Sánchez-Infantes, D. White adipose tissue dysfunction in obesity and aging. *Biochemical Pharmacology* vol. 192 Preprint at https://doi.org/10.1016/j.bcp.2021.114723 (2021).

43. Pereira, S. S. & Alvarez-Leite, J. I. Low-Grade Inflammation, Obesity, and Diabetes. *Curr Obes Rep* **3**, 422–431 (2014).

44. Kahn, C. R., Wang, G. & Lee, K. Y. Altered adipose tissue and adipocyte function in the pathogenesis of metabolic syndrome. *Journal of Clinical Investigation* vol. 129 3990–4000 Preprint at https://doi.org/10.1172/JCI129187 (2019).

45. Choe, S. S., Huh, J. Y., Hwang, I. J., Kim, J. I. & Kim, J. B. Adipose tissue remodeling: Its role in energy metabolism and metabolic disorders. *Frontiers in Endocrinology* vol. 7 Preprint at https://doi.org/10.3389/fendo.2016.00030 (2016).

46. Vishvanath, L. & Gupta, R. K. Contribution of adipogenesis to healthy adipose tissue expansion in obesity. *Journal of Clinical Investigation* vol. 129 4022–4031 Preprint at https://doi.org/10.1172/JCI129191 (2019).

47. Rytka, J. M., Wueest, S., Schoenle, E. J. & Konrad, D. The portal theory supported by venous drainage-selective fat transplantation. *Diabetes* **60**, 56–63 (2011).

48. Hwang, Y.-C. *et al.* Visceral abdominal fat accumulation predicts the conversion of metabolically healthy obese subjects to an unhealthy phenotype. *Int J Obes* **39**, 1365–1370 (2015).

49. Mau, T. & Yung, R. Adipose tissue inflammation in aging. *Experimental Gerontology* vol. 105 27–31 Preprint at https://doi.org/10.1016/j.exger.2017.10.014 (2018).

50. Torres, S., Fabersani, E., Marquez, A. & Gauffin-Cano, P. Adipose tissue inflammation and metabolic syndrome. The proactive role of probiotics. *European Journal of Nutrition* vol. 58 27–43 Preprint at https://doi.org/10.1007/s00394-018-1790-2 (2019).

51. McLaughlin, T. *et al.* Adipose cell size and regional fat deposition as predictors of metabolic response to overfeeding in insulin-resistant and insulin-sensitive humans. *Diabetes* **65**, 1245–1254 (2016).

52. Birsoy, K., Festuccia, W. T. & Laplante, M. A comparative perspective on lipid storage in animals. *J Cell Sci* **126**, 1541–1552 (2013).

53. Ghaben, A. L. & Scherer, P. E. Adipogenesis and metabolic health. *Nature Reviews Molecular Cell Biology* vol. 20 242–258 Preprint at https://doi.org/10.1038/s41580-018-0093-z (2019).

54. Longo, M. *et al.* Adipose tissue dysfunction as determinant of obesity-associated metabolic complications. *Int J Mol Sci* **20**, (2019).

55. Blüher, M. Metabolically healthy obesity. *Endocrine Reviews* vol. 41 405–420 Preprint at https://doi.org/10.1210/endrev/bnaa004 (2020).

56. Naukkarinen, J. *et al.* Characterising metabolically healthy obesity in weight-discordant monozygotic twins. *Diabetologia* **57**, 167–176 (2014).

57. Landecho, M. F. *et al.* Relevance of leptin and other adipokines in obesity-associated cardiovascular risk. *Nutrients* vol. 11 Preprint at https://doi.org/10.3390/nu11112664 (2019).

58. Chait, A. & den Hartigh, L. J. Adipose Tissue Distribution, Inflammation and Its Metabolic Consequences, Including Diabetes and Cardiovascular Disease. *Frontiers in Cardiovascular Medicine* vol. 7 Preprint at https://doi.org/10.3389/fcvm.2020.00022 (2020).

59. Pereira, S. S. & Alvarez-Leite, J. I. Low-Grade Inflammation, Obesity, and Diabetes. *Curr Obes Rep* **3**, 422–431 (2014).

60. Feingold, K. R. Obesity and Dyslipidemia. *Endotext* (2020).

61. Rutkowski, J. M., Stern, J. H. & Scherer, P. E. The cell biology of fat expansion. *Journal of Cell Biology* vol. 208 501–512 Preprint at https://doi.org/10.1083/jcb.201409063 (2015).

62. Luo, L. & Liu, M. Adipose tissue in control of metabolism. *Journal of Endocrinology* vol. 231 R77–R99 Preprint at https://doi.org/10.1530/JOE-16-0211 (2016).

63. Beylot, M. Metabolism of White Adipose Tissue. in *Adipose Tissue and Adipokines in Health and Disease* (eds. Fantuzzi, G. & Mazzone, T.) 21–33 (Humana Press, 2007). doi:10.1007/978-1-59745-370-7_2.

64. Lee, C. H., Lui, D. T. W. & Lam, K. S. L. Adipocyte Fatty Acid-Binding Protein, Cardiovascular Diseases and Mortality. *Frontiers in Immunology* vol. 12 Preprint at https://doi.org/10.3389/fimmu.2021.589206 (2021).

65. Aitman, T. J. *et al.* Identification of Cd36 (Fat) as an insulin-resistance gene causing defective fatty acid and glucose metabolism in hypertensive rats. *Nat Genet* **21**, 76–83 (1999).

66. Ceddia, R. B. The role of AMP-activated protein kinase in regulating white adipose tissue metabolism. *Mol Cell Endocrinol* **366**, 194–203 (2013).

67. Matsui, H. *et al.* Stearoyl-Coa desaturase-1 (SCD1) augments saturated fatty acid-induced lipid accumulation and inhibits apoptosis in cardiac myocytes. *PLoS One* **7**, (2012).

68. Zechner, R. *et al.* FAT SIGNALS - Lipases and lipolysis in lipid metabolism and signaling. *Cell Metabolism* vol. 15 279–291 Preprint at https://doi.org/10.1016/j.cmet.2011.12.018 (2012).

69. Badimon, L., Oñate, B. & Vilahur, G. Adipose-derived Mesenchymal Stem Cells and Their Reparative Potential in Ischemic Heart Disease. *Revista Española de Cardiología (English Edition)* **68**, 599–611 (2015).

70. Yang, A. & Mottillo, E. P. Adipocyte lipolysis: From molecular mechanisms of regulation to disease and therapeutics. *Biochemical Journal* vol. 477 985–1008 Preprint at https://doi.org/10.1042/BCJ20190468 (2020).

71. DiPilato, L. M. *et al.* The Role of PDE3B Phosphorylation in the Inhibition of Lipolysis by Insulin. *Mol Cell Biol* **35**, 2752–2760 (2015).

72. Fredholm, B. B., Johansson, S. & Wang, Y. Q. Adenosine and the Regulation of Metabolism and Body Temperature. in *Advances in Pharmacology* vol. 61 77–94 (Academic Press Inc., 2011).

73. Schulz, H. *Fatty Acid Oxidation*. (2013).

74. Houten, S. M. & Wanders, R. J. A. A general introduction to the biochemistry of mitochondrial fatty acid β-oxidation. *Journal of Inherited Metabolic Disease* vol. 33 469–477 Preprint at https://doi.org/10.1007/s10545-010-9061-2 (2010).

75. Lopaschuk, G. D., Ussher, J. R., Folmes, C. D. L., Jaswal, J. S. & Stanley, W. C. Myocardial Fatty Acid Metabolism in Health and Disease. (2010) doi:10.1152/physrev.00015.2009.-There.

76. Jang, H. S., Noh, M. R., Kim, J. & Padanilam, B. J. Defective Mitochondrial Fatty Acid Oxidation and Lipotoxicity in Kidney Diseases. *Frontiers in Medicine* vol. 7 Preprint at https://doi.org/10.3389/fmed.2020.00065 (2020).

77. Zhang, Y. *et al.* Positional cloning of the mouse obese gene and its human homologue. *Nature* **372**, 425–432 (1994).

78. Martínez-Sánchez, N. There and back again: Leptin actions in white adipose tissue. *International Journal of Molecular Sciences* vol. 21 1–26 Preprint at https://doi.org/10.3390/ijms21176039 (2020).

79. Villanueva, E. C. & Myers, M. G. Leptin receptor signaling and the regulation of mammalian physiology. *Int J Obes* **32**, S8–S12 (2008).

80. Clément, K. *et al.* A mutation in the human leptin receptor gene causes obesity and pituitary dysfunction. *Nature* **392**, 398–401 (1998).

81. Stepien, M. *et al.* Waist circumference, ghrelin and selected adipose tissue-derived adipokines as predictors of insulin resistance in obese patients: Preliminary results. *Medical Science Monitor* **17**, PR13–PR18 (2011).

82. Izquierdo, A. G., Crujeiras, A. B., Casanueva, F. F. & Carreira, M. C. Leptin, obesity, and leptin resistance: where are we 25 years later? *Nutrients* vol. 11 Preprint at https://doi.org/10.3390/nu11112704 (2019).

83. Francisco, V. *et al.* Obesity, fat mass and immune system: Role for leptin. *Frontiers in Physiology* vol. 9 Preprint at https://doi.org/10.3389/fphys.2018.00640 (2018).

84. Francisco, V. *et al.* Adipokines: Linking metabolic syndrome, the immune system, and arthritic diseases. *Biochem Pharmacol* **165**, 196–206 (2019).

85. Rodríguez, A., Becerril, S., Hernández-Pardos, A. W. & Frühbeck, G. Adipose tissue depot differences in adipokines and effects on skeletal and cardiac muscle. *Current Opinion in Pharmacology* vol. 52 1–8 Preprint at https://doi.org/10.1016/j.coph.2020.04.003 (2020).

86. Singh, P. *et al.* Differential effects of leptin on adiponectin expression with weight gain versus obesity. *Int J Obes* **40**, 266–274 (2016).

87. Luo, Y. & Liu, M. Adiponectin: a versatile player of innate immunity. *J Mol Cell Biol* **8**, 120–128 (2016).

88. Vegiopoulos, A., Rohm, M. & Herzig, S. Adipose tissue: between the extremes. *EMBO J* **36**, 1999–2017 (2017).

89. Verduci, E. *et al.* Brown adipose tissue: New challenges for prevention of childhood obesity. A narrative review. *Nutrients* vol. 13 Preprint at https://doi.org/10.3390/nu13051450 (2021).

90. Vadde, R., Gupta, M. K. & Purnachandra Nagaraju, G. Is Adipose Tissue an Immunological Organ? *Crit Rev Immunol.* (2019).

91. Stanford, K. I. *et al.* Brown adipose tissue regulates glucose homeostasis and insulin sensitivity. *Journal of Clinical Investigation* **123**, 215–223 (2013).

92. Carpentier, A. C. *et al.* Brown adipose tissue energy metabolism in humans. *Frontiers in Endocrinology* vol. 9 Preprint at https://doi.org/10.3389/fendo.2018.00447 (2018).

93. Peterson, C. M. *et al.* The thermogenic responses to overfeeding and cold are differentially regulated. *Obesity* **24**, 96–101 (2016).

94. Hanssen, M. J. W. *et al.* Short-term cold acclimation improves insulin sensitivity in patients with type 2 diabetes mellitus. *Nat Med* **21**, 863–865 (2015).

95. Yoneshiro, T. *et al.* Recruited brown adipose tissue as an antiobesity agent in humans. *J Clin Invest* **123**, 3404–3408 (2013).

96. Scheele, C. & Wolfrum, C. Brown Adipose Crosstalk in Tissue Plasticity and Human Metabolism. *Endocr Rev* **41**, 53–65 (2020).

97. Lynes, M. D. *et al.* The cold-induced lipokine 12,13-diHOME promotes fatty acid transport into brown adipose tissue. *Nat Med* **23**, 631–637 (2017).

98. Villarroya, J., Cereijo, R., Giralt, M. & Villarroya, F. Secretory proteome of brown adipocytes in response to cAMP-mediated thermogenic activation. *Front Physiol* **10**, (2019).

99. Vosselman, M. J., van Marken Lichtenbelt, W. D. & Schrauwen, P. Energy dissipation in brown adipose tissue: From mice to men. *Mol Cell Endocrinol* **379**, 43–50 (2013).

100. Zoico, E. *et al.* Brown and beige adipose tissue and aging. *Front Endocrinol (Lausanne)* **10**, (2019).

101. Becker, A. S., Nagel, H. W., Wolfrum, C. & Burger, I. A. Anatomical Grading for Metabolic Activity of Brown Adipose Tissue. *PLoS One* **11**, e0149458 (2016).

102. Liu, X. *et al.* Brown adipose tissue transplantation improves whole-body energy metabolism. *Cell Res* **23**, 851–854 (2013).

103. Ouellet, V. *et al.* Brown adipose tissue oxidative metabolism contributes to energy expenditure during acute cold exposure in humans. *Journal of Clinical Investigation* **122**, 545–552 (2012).

104. Nedergaard, J., Bengtsson, T. & Cannon, B. New Powers of Brown Fat: Fighting the Metabolic Syndrome. *Cell Metab* **13**, 238–240 (2011).

105. Zhang, Z. *et al.* Non-shivering thermogenesis signalling regulation and potential therapeutic applications of brown adipose tissue. *International Journal of Biological Sciences* vol. 17 2853–2870 Preprint at https://doi.org/10.7150/ijbs.60354 (2021).

106. Kajimura, S. *et al.* Regulation of the brown and white fat gene programs through a PRDM16/CtBP transcriptional complex. *Genes Dev* **22**, 1397–1409 (2008).

107. Lidell, M. E., Betz, M. J. & Enerbäck, S. Brown adipose tissue and its therapeutic potential. *Journal of Internal Medicine* vol. 276 364–377 Preprint at https://doi.org/10.1111/joim.12255 (2014).

108. Arrojo e Drigo, R., Fonseca, T. L., Werneck-de-Castro, J. P. S. & Bianco, A. C. Role of the type 2 iodothyronine deiodinase (D2) in the control of thyroid hormone signaling. *Biochimica et Biophysica Acta (BBA) - General Subjects* **1830**, 3956–3964 (2013).

109. Peres Valgas da Silva, C., Hernández-Saavedra, D., White, J. & Stanford, K. Cold and Exercise: Therapeutic Tools to Activate Brown Adipose Tissue and Combat Obesity. *Biology (Basel)* **8**, 9 (2019).

110. Alcalá, M., Calderon-Dominguez, M., Serra, D., Herrero, L. & Viana, M. Mechanisms of impaired brown adipose tissue recruitment in obesity. *Frontiers in Physiology* vol. 10 Preprint at https://doi.org/10.3389/fphys.2019.00094 (2019).

111. Cinti, S. The role of brown adipose tissue in human obesity. *Nutrition, Metabolism and Cardiovascular Diseases* vol. 16 569–574 Preprint at https://doi.org/10.1016/j.numecd.2006.07.009 (2006).

112. Kuryłowicz, A. & Puzianowska-Kuźnicka, M. Induction of adipose tissue browning as a strategy to combat obesity. *Int J Mol Sci* **21**, 1–28 (2020).

113. Nøhr, M., Bobba, N., Richelsen, B., Lund, S. & Pedersen, S. Inflammation Downregulates UCP1 Expression in Brown Adipocytes Potentially via SIRT1 and DBC1 Interaction. *Int J Mol Sci* **18**, 1006 (2017).

114. Villarroya, F., Cereijo, R., Gavaldà-Navarro, A., Villarroya, J. & Giralt, M. Inflammation of brown/beige adipose tissues in obesity and metabolic disease. *J Intern Med* **284**, 492–504 (2018).

115. Pirzgalska, R. M. *et al.* Sympathetic neuron-associated macrophages contribute to obesity by importing and metabolizing norepinephrine. *Nat Med* **23**, 1309–1318 (2017).

116. Wibmer, A. G. *et al.* Brown adipose tissue is associated with healthier body fat distribution and metabolic benefits independent of regional adiposity. *Cell Rep Med* **2**, (2021).

117. Wondmkun, Y. T. Obesity, insulin resistance, and type 2 diabetes: Associations and therapeutic implications. *Diabetes, Metabolic Syndrome and Obesity: Targets and Therapy* vol. 13 3611–3616 Preprint at https://doi.org/10.2147/DMSO.S275898 (2020).

118. Li, M. *et al.* Trends in insulin resistance: insights into mechanisms and therapeutic strategy. *Signal Transduction and Targeted Therapy* vol. 7 Preprint at https://doi.org/10.1038/s41392-022-01073-0 (2022).

119. Sergi, D. *et al.* Mitochondrial (dys)function and insulin resistance: From pathophysiological molecular mechanisms to the impact of diet. *Frontiers in Physiology* vol. 10 Preprint at https://doi.org/10.3389/fphys.2019.00532 (2019).

120. Leto, D. & Saltiel, A. R. Regulation of glucose transport by insulin: Traffic control of GLUT4. *Nature Reviews Molecular Cell Biology* vol. 13 383–396 Preprint at https://doi.org/10.1038/nrm3351 (2012).

121. Pragallapati, S. & Manyam, R. Glucose transporter 1 in health and disease. *Journal of Oral and Maxillofacial Pathology* vol. 23 443–449 Preprint at https://doi.org/10.4103/jomfp.JOMFP_22_18 (2019).

122. Mueckler, M. Insulin resistance and the disruption of glut4 trafficking in skeletal muscle. *Journal of Clinical Investigation* vol. 107 1211–1213 Preprint at https://doi.org/10.1172/JCI13020 (2001).

123. DeFronzo, R. A. Insulin resistance, lipotoxicity, type 2 diabetes and atherosclerosis: The missing links. The Claude Bernard Lecture 2009. *Diabetologia* vol. 53 1270–1287 Preprint at https://doi.org/10.1007/s00125-010-1684-1 (2010).

124. Barazzoni, R., Gortan Cappellari, G., Ragni, M. & Nisoli, E. Insulin resistance in obesity: an overview of fundamental alterations. *Eating and Weight Disorders* vol. 23 149–157 Preprint at https://doi.org/10.1007/s40519-018-0481-6 (2018).

125. Atilla, E. *Obesity and Lipotoxicity*. *Advances in Experimental Medicine and Biology* vol. 960 (2017).

126. Wu, H. & Ballantyne, C. M. Metabolic Inflammation and Insulin Resistance in Obesity. *Circ Res* **126**, 1549–1564 (2020).

127. Yazıcı, D. & Sezer, H. Insulin Resistance, Obesity and Lipotoxicity. in 277–304 (2017). doi:10.1007/978-3-319-48382-5_12.

128. Blachnio-Zabielska, A. U., Koutsari, C., Tchkonia, T. & Jensen, M. D. Sphingolipid Content of Human Adipose Tissue: Relationship to Adiponectin and Insulin Resistance. *Obesity* **20**, 2341–2347 (2012).

129. Grycel, S. *et al.* Metformin treatment affects adipocytokine secretion and lipid composition in adipose tissues of diet-induced insulin-resistant rats. *Nutrition* **63–64**, 126–133 (2019).

130. Kojta, I., Chacińska, M. & Błachnio-Zabielska, A. Obesity, bioactive lipids, and adipose tissue inflammation in insulin resistance. *Nutrients* vol. 12 Preprint at https://doi.org/10.3390/nu12051305 (2020).

131. Sokolowska, E. & Blachnio-Zabielska, A. The Role of Ceramides in Insulin Resistance. *Frontiers in Endocrinology* vol. 10 Preprint at https://doi.org/10.3389/fendo.2019.00577 (2019).

132. Holland, W. L. *et al.* Lipid-induced insulin resistance mediated by the proinflammatory receptor TLR4 requires saturated fatty acid-induced ceramide biosynthesis in mice. *Journal of Clinical Investigation* **121**, 1858–1870 (2011).

133. Haczeyni, F., Bell-Anderson, K. S. & Farrell, G. C. Causes and mechanisms of adipocyte enlargement and adipose expansion. *Obesity Reviews* **19**, 406–420 (2018).

134. Morigny, P., Houssier, M., Mouisel, E. & Langin, D. Adipocyte lipolysis and insulin resistance. *Biochimie* vol. 125 259–266 Preprint at https://doi.org/10.1016/j.biochi.2015.10.024 (2016).

135. Kehlenbrink, S. *et al.* Elevated NEFA levels impair glucose effectiveness by increasing net hepatic glycogenolysis. *Diabetologia* **55**, 3021–3028 (2012).

136. Dresner, A. *et al. Effects of free fatty acids on glucose transport and IRS-1-associated phosphatidylinositol 3-kinase activity*. *The Journal of Clinical Investigation* vol. 103 (1999).

137. Opazo-Ríos, L. *et al.* Lipotoxicity and diabetic nephropathy: Novel mechanistic insights and therapeutic opportunities. *International Journal of Molecular Sciences* vol. 21 Preprint at https://doi.org/10.3390/ijms21072632 (2020).

138. Engin, A. B. What Is Lipotoxicity? in *Obesity and Lipotoxicity* (eds. Engin, A. B. & Engin, A.) 197–220 (Springer International Publishing, 2017). doi:10.1007/978-3-319-48382-5_8.

139. Trauner, M., Arrese, M. & Wagner, M. Fatty liver and lipotoxicity. *Biochimica et Biophysica Acta - Molecular and Cell Biology of Lipids* vol. 1801 299–310 Preprint at https://doi.org/10.1016/j.bbalip.2009.10.007 (2010).

140. Loomba, R. & Sanyal, A. J. The global NAFLD epidemic. *Nature Reviews Gastroenterology and Hepatology* vol. 10 686–690 Preprint at https://doi.org/10.1038/nrgastro.2013.171 (2013).

141. Vernon, G., Baranova, A. & Younossi, Z. M. Systematic review: The epidemiology and natural history of non-alcoholic fatty liver disease and non-alcoholic steatohepatitis in adults. *Alimentary Pharmacology and Therapeutics* vol. 34 274–285 Preprint at https://doi.org/10.1111/j.1365-2036.2011.04724.x (2011).

142. Chhimwal, J., Patial, V. & Padwad, Y. Beverages and Non-alcoholic fatty liver disease (NAFLD): Think before you drink. *Clinical Nutrition* vol. 40 2508–2519 Preprint at https://doi.org/10.1016/j.clnu.2021.04.011 (2021).

143. Argo, C. K., Northup, P. G., Al-Osaimi, A. M. S. & Caldwell, S. H. Systematic review of risk factors for fibrosis progression in non-alcoholic steatohepatitis. *J Hepatol* **51**, 371–379 (2009).

144. Bertot, L. C. & Adams, L. A. The natural course of non-alcoholic fatty liver disease. *International Journal of Molecular Sciences* vol. 17 Preprint at https://doi.org/10.3390/ijms17050774 (2016).

145. Yoshioka, N. *et al.* Effect of weight change and lifestyle modifications on the development or remission of nonalcoholic fatty liver disease: sex-specific analysis. *Sci Rep* **10**, 481 (2020).

146. Chiang, J. Y. L. Targeting bile acids and lipotoxicity for NASH treatment. *Hepatol Commun* **1**, 1002–1004 (2017).

147. Bellentani, S., Scaglioni, F., Marino, M. & Bedogni, G. Epidemiology of Non-Alcoholic Fatty Liver Disease. *Digestive Diseases* **28**, 155–161 (2010).

148. Simon, J. *et al.* Sphingolipids in non-alcoholic fatty liver disease and hepatocellular carcinoma: Ceramide turnover. *International Journal of Molecular Sciences* vol. 21 Preprint at https://doi.org/10.3390/ijms21010040 (2020).

149. Bugianesi, E. EASL–EASD–EASO Clinical Practice Guidelines for the management of non-alcoholic fatty liver disease: disease mongering or call to action? *Diabetologia* **59**, 1145–1147 (2016).

150. Dibba, P. *et al.* Emerging Therapeutic Targets and Experimental Drugs for the Treatment of NAFLD. *Diseases* **6**, 83 (2018).

151. Cohen, J. C., Horton, J. D. & Hobbs, H. H. Human Fatty Liver Disease: Old Questions and New Insights. *Science (1979)* **332**, 1519–1523 (2011).

152. Paschos P & Paletas K. Non alcoholic fatty liver disease two-hit process: Multifactorial character of the second hit. *Hippokratia* **13**, 128 (2009).

153. Zarghamravanbakhsh, P., Frenkel, M. & Poretsky, L. Metabolic causes and consequences of nonalcoholic fatty liver disease (NAFLD). *Metabol Open* **12**, 100149 (2021).

154. Valenti, L., Ludovica Fracanzani, A. & Fargion, S. The immunopathogenesis of alcoholic and nonalcoholic steatohepatitis: two triggers for one disease? *Semin Immunopathol* **31**, 359–369 (2009).

155. Peverill, W., Powell, L. W. & Skoien, R. Evolving concepts in the pathogenesis of NASH: Beyond steatosis and inflammation. *International Journal of Molecular Sciences* vol. 15 8591–8638 Preprint at https://doi.org/10.3390/ijms15058591 (2014).

156. Fang, Y. L., Chen, H., Wang, C. L. & Liang, L. Pathogenesis of non-alcoholic fatty liver disease in children and adolescence: From 'two hit theory' to 'multiple hit model'. *World Journal of Gastroenterology* vol. 24 2974–2983 Preprint at https://doi.org/10.3748/wjg.v24.i27.2974 (2018).

157. Dowman, J. K., Tomlinson, J. W. & Newsome, P. N. Pathogenesis of non-alcoholic fatty liver disease. *QJM* vol. 103 71–83 Preprint at https://doi.org/10.1093/qjmed/hcp158 (2009).

158. Fu, J.-F. *et al.* A rabbit model of pediatric nonalcoholic steatohepatitis: The role of adiponectin. *World J Gastroenterol* **15**, 912 (2009).

159. Wang, C.-L. *et al.* Effect of lifestyle intervention on non-alcoholic fatty liver disease in Chinese obese children. *World J Gastroenterol* **14**, 1598 (2008).

160. Mato, J. M., Alonso, C., Noureddin, M. & Lu, S. C. Biomarkers and subtypes of deranged lipid metabolism in nonalcoholic fatty liver disease. *World Journal of Gastroenterology* vol. 25 3009–3020 Preprint at https://doi.org/10.3748/wjg.v25.i24.3009 (2019).

161. Hudgins, L. C. *et al.* Relationship between carbohydrate-induced hypertriglyceridemia and fatty acid synthesis in lean and obese subjects. *J Lipid Res* **41**, 595–604 (2000).

162. Parks E.J. Dietary carbohydrate's effects on lipogenesis and the relationship of lipogenesis to blood insulin and glucose concentrations. *British Journal of Nutrition* **87**, 247–253 (2002).

163. Donnelly, K. L. *et al.* Sources of fatty acids stored in liver and secreted via lipoproteins in patients with nonalcoholic fatty liver disease. *Journal of Clinical Investigation* **115**, 1343–1351 (2005).

164. Fabbrini, E., Sullivan, S. & Klein, S. Obesity and nonalcoholic fatty liver disease: Biochemical, metabolic, and clinical implications. *Hepatology* vol. 51 679–689 Preprint at https://doi.org/10.1002/hep.23280 (2010).

165. Westerbacka, J. *et al.* Genes Involved in Fatty Acid Partitioning and Binding, Lipolysis, Monocyte/Macrophage Recruitment, and Inflammation Are Overexpressed in the Human Fatty Liver of Insulin-Resistant Subjects. *Diabetes* **56**, 2759–2765 (2007).

166. Pardina, E. *et al.* Increased Expression and Activity of Hepatic Lipase in the Liver of Morbidly Obese Adult Patients in Relation to Lipid Content. *Obes Surg* **19**, 894–904 (2009).

167. Fabbrini, E. *et al.* Intrahepatic fat, not visceral fat, is linked with metabolic complications of obesity. *Proceedings of the National Academy of Sciences* **106**, 15430–15435 (2009).

168. Greco, D. *et al.* Gene expression in human NAFLD. *American Journal of Physiology-Gastrointestinal and Liver Physiology* **294**, G1281–G1287 (2008).

169. Musso, G., Gambino, R. & Cassader, M. Recent insights into hepatic lipid metabolism in non-alcoholic fatty liver disease (NAFLD). *Progress in Lipid Research* vol. 48 1–26 Preprint at https://doi.org/10.1016/j.plipres.2008.08.001 (2009).

170. Ortega-Prieto, P. & Postic, C. Carbohydrate sensing through the transcription factor ChREBP. *Front Genet* **10**, (2019).

171. Song, Z., Xiaoli, A. M. & Yang, F. Regulation and metabolic significance of De Novo lipogenesis in adipose tissues. *Nutrients* vol. 10 Preprint at https://doi.org/10.3390/nu10101383 (2018).

172. Viollet, B. AMPK: Lessons from transgenic and knockout animals. *Frontiers in Bioscience* **Volume**, 19 (2009).

173. Zhang, D. & Yin, L. Transcriptional Regulation of De Novo Lipogenesis in Liver. in *Hepatic De Novo Lipogenesis and Regulation of Metabolism* (ed. Ntambi, J. M.) 1–31 (Springer International Publishing, 2016). doi:10.1007/978-3-319-25065-6_1.

174. Lambert, J. E., Ramos-Roman, M. A., Browning, J. D. & Parks, E. J. Increased de novo lipogenesis is a distinct characteristic of individuals with nonalcoholic fatty liver disease. *Gastroenterology* **146**, 726–735 (2014).

175. Ipsen, D. H., Lykkesfeldt, J. & Tveden-Nyborg, P. Molecular mechanisms of hepatic lipid accumulation in non-alcoholic fatty liver disease. *Cellular and Molecular Life Sciences* vol. 75 3313–3327 Preprint at https://doi.org/10.1007/s00018-018-2860-6 (2018).

176. Shimomura, I., Bashmakov, Y. & Horton, J. D. Increased Levels of Nuclear SREBP-1c Associated with Fatty Livers in Two Mouse Models of Diabetes Mellitus. *Journal of Biological Chemistry* **274**, 30028–30032 (1999).

177. Dentin, R. *et al.* Liver-Specific Inhibition of ChREBP Improves Hepatic Steatosis and Insulin Resistance in *ob/ob* Mice. *Diabetes* **55**, 2159–2170 (2006).

178. Shimano, H. *et al.* Isoform 1c of sterol regulatory element binding protein is less active than isoform 1a in livers of transgenic mice and in cultured cells. *Journal of Clinical Investigation* **99**, 846–854 (1997).

179. Kohjima, M. *et al.* Re-evaluation of fatty acid metabolism-related gene expression in nonalcoholic fatty liver disease. *Int J Mol Med* (2007) doi:10.3892/ijmm.20.3.351.

180. Liang, G. *et al.* Diminished Hepatic Response to Fasting/Refeeding and Liver X Receptor Agonists in Mice with Selective Deficiency of Sterol Regulatory Element-binding Protein-1c. *Journal of Biological Chemistry* **277**, 9520–9528 (2002).

181. Benhamed, F. *et al.* The lipogenic transcription factor ChREBP dissociates hepatic steatosis from insulin resistance in mice and humans. *Journal of Clinical Investigation* **122**, 2176–2194 (2012).

182. Higuchi, N. *et al.* Liver X receptor in cooperation with SREBP-1c is a major lipid synthesis regulator in nonalcoholic fatty liver disease. *Hepatology Research* **38**, 1122–1129 (2008).

183. Liss, K. H. H. & Finck, B. N. PPARs and nonalcoholic fatty liver disease. *Biochimie* vol. 136 65–74 Preprint at https://doi.org/10.1016/j.biochi.2016.11.009 (2017).

184. Begriche, K., Massart, J., Robin, M. A., Bonnet, F. & Fromenty, B. Mitochondrial adaptations and dysfunctions in nonalcoholic fatty liver disease. *Hepatology* vol. 58 1497–1507 Preprint at https://doi.org/10.1002/hep.26226 (2013).

185. Dasarathy, S. *et al.* Elevated hepatic fatty acid oxidation, high plasma fibroblast growth factor 21, and fasting bile acids in nonalcoholic steatohepatitis. *Eur J Gastroenterol Hepatol* **23**, 382–388 (2011).

186. Matthew Morris, E. *et al.* Intrinsic aerobic capacity impacts susceptibility to acute high-fat diet-induced hepatic steatosis. *American Journal of Physiology-Endocrinology and Metabolism* **307**, E355–E364 (2014).

187. Croci, I. *et al.* Whole-body substrate metabolism is associated with disease severity in patients with non-alcoholic fatty liver disease. *Gut* **62**, 1625–1633 (2013).

188. Kotronen, A. *et al.* Liver fat and lipid oxidation in humans. *Liver International* **29**, 1439–1446 (2009).

189. Koek, G. H., Liedorp, P. R. & Bast, A. The role of oxidative stress in non-alcoholic steatohepatitis. *Clinica Chimica Acta* vol. 412 1297–1305 Preprint at https://doi.org/10.1016/j.cca.2011.04.013 (2011).

190. Francque, S. *et al.* PPARα gene expression correlates with severity and histological treatment response in patients with non-alcoholic steatohepatitis. *J Hepatol* **63**, 164–173 (2015).

191. Abdelmegeed, M. A. *et al.* PPARα Expression Protects Male Mice from High Fat–Induced Nonalcoholic Fatty Liver. *J Nutr* **141**, 603–610 (2011).

192. Stienstra, R. *et al.* Peroxisome Proliferator-Activated Receptor α Protects against Obesity-Induced Hepatic Inflammation. *Endocrinology* **148**, 2753–2763 (2007).

193. Shulman, G. I. Ectopic Fat in Insulin Resistance, Dyslipidemia, and Cardiometabolic Disease. *New England Journal of Medicine* **371**, 1131–1141 (2014).

194. Kawano, Y. & Cohen, D. E. Mechanisms of hepatic triglyceride accumulation in non-alcoholic fatty liver disease. *Journal of Gastroenterology* vol. 48 434–441 Preprint at https://doi.org/10.1007/s00535-013-0758-5 (2013).

195. Sanders, F. W. B. & Griffin, J. L. De novo lipogenesis in the liver in health and disease: more than just a shunting yard for glucose. *Biological Reviews* **91**, 452–468 (2016).

196. Jwa, H. *et al.* Piperine, an LXRα antagonist, protects against hepatic steatosis and improves insulin signaling in mice fed a high-fat diet. *Biochem Pharmacol* **84**, 1501–1510 (2012).

197. Raddatz, K. *et al.* Time-dependent effects of Prkce deletion on glucose homeostasis and hepatic lipid metabolism on dietary lipid oversupply in mice. *Diabetologia* **54**, 1447–1456 (2011).

198. Kumashiro, N. *et al.* Cellular mechanism of insulin resistance in nonalcoholic fatty liver disease. *Proceedings of the National Academy of Sciences* **108**, 16381–16385 (2011).

199. Kitade, H., Chen, G., Ni, Y. & Ota, T. Nonalcoholic fatty liver disease and insulin resistance: New insights and potential new treatments. *Nutrients* **9**, 1–13 (2017).

200. Bugianesi, E. *et al.* Plasma Adiponectin in Nonalcoholic Fatty Liver Is Related to Hepatic Insulin Resistance and Hepatic Fat Content, Not to Liver Disease Severity. *J Clin Endocrinol Metab* **90**, 3498–3504 (2005).

201. Pagano, C. *et al.* Plasma adiponectin is decreased in nonalcoholic fatty liver disease. *Eur J Endocrinol* **152**, 113–118 (2005).

202. Du, K., Herzig, S., Kulkarni, R. N. & Montminy, M. TRB3: A tribbles homolog that inhibits Akt/PKB activation by insulin in liver. *Science (1979)* **300**, 1574–1577 (2003).

203. Koo, S.-H. *et al.* PGC-1 promotes insulin resistance in liver through PPAR-α-dependent induction of TRB-3. *Nat Med* **10**, 530–534 (2004).

204. Li, S. *et al.* The role of oxidative stress and antioxidants in liver diseases. *International Journal of Molecular Sciences* vol. 16 26087–26124 Preprint at https://doi.org/10.3390/ijms161125942 (2015).

205. Ramos-Tovar, E. & Muriel, P. Molecular mechanisms that link oxidative stress, inflammation, and fibrosis in the liver. *Antioxidants* vol. 9 1–21 Preprint at https://doi.org/10.3390/antiox9121279 (2020).

206. Chen, Z., Tian, R., She, Z., Cai, J. & Li, H. Role of oxidative stress in the pathogenesis of nonalcoholic fatty liver disease. *Free Radical Biology and Medicine* vol. 152 116–141 Preprint at https://doi.org/10.1016/j.freeradbiomed.2020.02.025 (2020).

207. Nassir, F. & Ibdah, J. A. Role of mitochondria in nonalcoholic fatty liver disease. *International Journal of Molecular Sciences* vol. 15 8713–8742 Preprint at https://doi.org/10.3390/ijms15058713 (2014).

208. Pessayre, D., Mansouri, A. & Fromenty, B. Nonalcoholic Steatosis and Steatohepatitis V. Mitochondrial dysfunction in steatohepatitis. *Am J Physiol Gastrointest Liver Physiol.* **282**, 193–199 (2002).

209. Begriche, K., Igoudjil, A., Pessayre, D. & Fromenty, B. Mitochondrial dysfunction in NASH: Causes, consequences and possible means to prevent it. *Mitochondrion* vol. 6 1–28 Preprint at https://doi.org/10.1016/j.mito.2005.10.004 (2006).

210. Cano, A. *et al.* Methionine adenosyltransferase 1A gene deletion disrupts hepatic very low-density lipoprotein assembly in mice. *Hepatology* **54**, 1975–1986 (2011).

211. Mato, J. M., Luz Martínez-Chantar, M. & Lu, S. C. S-adenosylmethionine metabolism and liver disease. *Ann Hepatol.* **12**, 183–189 (2013).

212. Mato, J. M. & Lu, S. C. Role of S-adenosyl-L-methionine in liver health and injury. *Hepatology* **45**, 1306–1312 (2007).

213. Aissa, A. F. *et al.* Effect of methionine-deficient and methionine-supplemented diets on the hepatic one-carbon and lipid metabolism in mice. *Mol Nutr Food Res* **58**, 1502–1512 (2014).

214. Caballero, F. *et al.* Specific Contribution of Methionine and Choline in Nutritional Nonalcoholic Steatohepatitis. *Journal of Biological Chemistry* **285**, 18528–18536 (2010).

215. Tryndyak, V. *et al.* Interstrain differences in the severity of liver injury induced by a choline- and folate-deficient diet in mice are associated with dysregulation of genes involved in lipid metabolism. *The FASEB Journal* **26**, 4592–4602 (2012).

216. Christensen, K. E. *et al.* Steatosis in Mice Is Associated with Gender, Folate Intake, and Expression of Genes of One-Carbon Metabolism. *J Nutr* **140**, 1736–1741 (2010).

217. Dahlhoff, C. *et al.* Hepatic Methionine Homeostasis Is Conserved in C57BL/6N Mice on High-Fat Diet Despite Major Changes in Hepatic One-Carbon Metabolism. *PLoS One* **8**, e57387 (2013).

218. Bindu Paul, C. D., Solomon Snyder, T. H., Sbodio, J. I., Snyder, S. H. & Paul, B. D. Regulators of the transsulfuration pathway. *British Journal of Pharmacology* **176**, 583–593 (2018).

219. Bravo, E. *et al.* High fat diet-induced non alcoholic fatty liver disease in rats is associated with hyperhomocysteinemia caused by down regulation of the transsulphuration pathway. *Lipids Health Dis* **10**, 60 (2011).

220. Liu, M. *et al.* Specific downregulation of cystathionine *β* -synthase expression in the kidney during obesity. *Physiol Rep* **6**, e13630 (2018).

221. Hwang, S.-Y., Sarna, L. K., Siow, Y. L. & O, K. High-fat diet stimulates hepatic cystathionine β-synthase and cystathionine γ-lyase expression. *Can J Physiol Pharmacol* **91**, 913–919 (2013).

222. Werge, M. P. *et al.* The Role of the Transsulfuration Pathway in Non-Alcoholic Fatty Liver Disease. *J Clin Med* **10**, 1081 (2021).

223. Petrescu, M. *et al.* Chronic Inflammation—A Link between Nonalcoholic Fatty Liver Disease (NAFLD) and Dysfunctional Adipose Tissue. *Medicina (Lithuania)* vol. 58 Preprint at https://doi.org/10.3390/medicina58050641 (2022).

224. Zou, Y.-X. *et al.* Mulberry leaf phenolics ameliorate hyperglycemia-induced oxidative stress and stabilize mitochondrial membrane potential in HepG2 cells. *Int J Food Sci Nutr* **65**, 960–966 (2014).

225. Buzzetti, E., Pinzani, M. & Tsochatzis, E. A. The multiple-hit pathogenesis of non-alcoholic fatty liver disease (NAFLD). *Metabolism* **65**, 1038–1048 (2016).

226. Aharoni-Simon, M., Hann-Obercyger, M., Pen, S., Madar, Z. & Tirosh, O. Fatty liver is associated with impaired activity of PPARγ-coactivator 1α (PGC1α) and mitochondrial biogenesis in mice. *Laboratory Investigation* **91**, 1018–1028 (2011).

227. Koliaki, C. *et al.* Adaptation of Hepatic Mitochondrial Function in Humans with Non-Alcoholic Fatty Liver Is Lost in Steatohepatitis. *Cell Metab* **21**, 739–746 (2015).

228. Lee, K. *et al.* Hepatic mitochondrial defects in a nonalcoholic fatty liver disease mouse model are associated with increased degradation of oxidative phosphorylation subunits. *Molecular and Cellular Proteomics* **17**, 2371–2386 (2018).

229. Fujii, H. & Kawada, N. Inflammation and fibrogenesis in steatohepatitis. *Journal of Gastroenterology* vol. 47 215–225 Preprint at https://doi.org/10.1007/s00535-012-0527-x (2012).

230. Arrese, M., Cabrera, D., Kalergis, A. M. & Feldstein, A. E. Innate Immunity and Inflammation in NAFLD/NASH. *Digestive Diseases and Sciences* vol. 61 1294–1303 Preprint at https://doi.org/10.1007/s10620-016-4049-x (2016).

231. Dixon, L. J., Barnes, M., Tang, H., Pritchard, M. T. & Nagy, L. E. Kupffer Cells in the Liver. in *Comprehensive Physiology* 785–797 (Wiley, 2013). doi:10.1002/cphy.c120026.

232. Gadd, V. L. *et al.* The portal inflammatory infiltrate and ductular reaction in human nonalcoholic fatty liver disease. *Hepatology* **59**, 1393–1405 (2014).

233. Jager, J., Aparicio-Vergara, M. & Aouadi, M. Liver innate immune cells and insulin resistance: the multiple facets of Kupffer cells. *J Intern Med* **280**, 209–220 (2016).

234. Marra, F. & Tacke, F. Roles for chemokines in liver disease. *Gastroenterology* vol. 147 Preprint at https://doi.org/10.1053/j.gastro.2014.06.043 (2014).

235. Leroux, A. *et al.* Toxic lipids stored by Kupffer cells correlates with their pro-inflammatory phenotype at an early stage of steatohepatitis. *J Hepatol* **57**, 141–149 (2012).

236. Noureddin, M. & Sanyal, A. J. Pathogenesis of NASH: the Impact of Multiple Pathways. *Curr Hepatol Rep* **17**, 350–360 (2018).

237. Haukeland, J. W. *et al.* Systemic inflammation in nonalcoholic fatty liver disease is characterized by elevated levels of CCL2. *J Hepatol* **44**, 1167–1174 (2006).

238. Peiseler, M. & Tacke, F. Inflammatory mechanisms underlying nonalcoholic steatohepatitis and the transition to hepatocellular carcinoma. *Cancers* vol. 13 1–26 Preprint at https://doi.org/10.3390/cancers13040730 (2021).

239. W. Zimmermann, H. & Tacke, F. Modification of Chemokine Pathways and Immune Cell Infiltration as a Novel Therapeutic Approach in Liver Inflammation and Fibrosis. *Inflamm Allergy Drug Targets* **10**, 509–536 (2011).

240. Ganz, M. & Szabo, G. Immune and inflammatory pathways in NASH. *Hepatology International* vol. 7 S771–S781 Preprint at https://doi.org/10.1007/s12072-013-9468-6 (2013).

241. Voiculescu, M. *The role of cytokines in non-alcoholic steatohepatitis. A review*. https://www.researchgate.net/publication/6596277 (2007).

242. Betrapally, N. S., Gillevet, P. M. & Bajaj, J. S. Changes in the Intestinal Microbiome and Alcoholic and Nonalcoholic Liver Diseases: Causes or Effects? *Gastroenterology* **150**, 1745-1755.e3 (2016).

243. Miele, L. *et al.* Increased intestinal permeability and tight junction alterations in nonalcoholic fatty liver disease. *Hepatology* **49**, 1877–1887 (2009).

244. Vajro, P., Paolella, G. & Fasano, A. Microbiota and gut-liver axis: Their influences on obesity and obesity-related liver disease. *Journal of Pediatric Gastroenterology and Nutrition* vol. 56 461–468 Preprint at https://doi.org/10.1097/MPG.0b013e318284abb5 (2013).

245. Federico, A., Dallio, M., Godos, J., Loguercio, C. & Salomone, F. Targeting gut-liver axis for the treatment of nonalcoholic steatohepatitis: translational and clinical evidence. *Translational Research* **167**, 116–124 (2016).

246. Kirpich, I. A., Marsano, L. S. & McClain, C. J. Gut-liver axis, nutrition, and non-alcoholic fatty liver disease. *Clinical Biochemistry* vol. 48 923–930 Preprint at https://doi.org/10.1016/j.clinbiochem.2015.06.023 (2015).

247. Kim, C. H. & Yuonossi, Z. M. Nonalcoholic fatty liver disease: A manifestation of the metabolic syndrome. *Cleve Clin J Med* **75**, 721–728 (2008).

248. Perdomo, C. M., Frühbeck, G. & Escalada, J. Impact of nutritional changes on nonalcoholic fatty liver disease. *Nutrients* **11**, (2019).

249. European Association for the Study of the Liver (EASL), European Association for the Study of Diabetes (EASD) & European Association for the Study of Obesity (EASO). EASL–EASD–EASO Clinical Practice Guidelines for the management of non-alcoholic fatty liver disease. *J Hepatol* **64**, 1388–1402 (2016).

250. Wong, V. W.-S. & Singal, A. K. Emerging medical therapies for non-alcoholic fatty liver disease and for alcoholic hepatitis. *Transl Gastroenterol Hepatol* **4**, 53–53 (2019).

251. DeFelice, S. L. The nutraceutical revolution: its impact on food industry R&D. *Trends Food Sci Technol* **6**, 59–61 (1995).

252. Kalra, E. K. *Nutraceutical - Definition and Introduction*. *AAPS PharmSci* vol. 5 http://vm.cfsan.fda.gov/~dms/dietsupp.html. (2003).

253. Scicchitano, P. *et al.* Nutraceuticals and dyslipidaemia: Beyond the common therapeutics. *J Funct Foods* **6**, 11–32 (2014).

254. Bagherniya, M., Nobili, V., Blesso, C. N. & Sahebkar, A. Medicinal plants and bioactive natural compounds in the treatment of non-alcoholic fatty liver disease: A clinical review. *Pharmacological Research* vol. 130 213–240 Preprint at https://doi.org/10.1016/j.phrs.2017.12.020 (2018).

255. Yan, T. *et al.* Herbal drug discovery for the treatment of nonalcoholic fatty liver disease. *Acta Pharmaceutica Sinica B* vol. 10 3–18 Preprint at https://doi.org/10.1016/j.apsb.2019.11.017 (2020).

256. Xu, J.-Y., Zhang, L., Li, Z.-P. & Ji, G. Natural Products on Nonalcoholic Fatty Liver Disease. *Curr Drug Targets* **16**, 1347–1355 (2015).

257. Salvoza, N., Giraudi, P. J., Tiribelli, C. & Rosso, N. Natural Compounds for Counteracting Nonalcoholic Fatty Liver Disease (NAFLD): Advantages and Limitations of the Suggested Candidates. *International Journal of Molecular Sciences* vol. 23 Preprint at https://doi.org/10.3390/ijms23052764 (2022).

258. Mardinoglu, A., Uhlen, M. & Borén, J. Broad Views of Non-alcoholic Fatty Liver Disease. *Cell Syst* **6**, 7–9 (2018).

259. Mardinoglu, A., Boren, J., Smith, U., Uhlen, M. & Nielsen, J. Systems biology in hepatology: approaches and applications. *Nat Rev Gastroenterol Hepatol* **15**, 365–377 (2018).

260. Mardinoglu, A. & Uhlén, M. Phenotypic and genetic variance: a systems approach to the liver. *Nat Rev Gastroenterol Hepatol* **13**, 439–440 (2016).

261. Mardinoglu, A. & Nielsen, J. New paradigms for metabolic modeling of human cells. *Curr Opin Biotechnol* **34**, 91–97 (2015).

262. Mardinoglu, A. *et al.* Personal model-assisted identification of NAD + and glutathione metabolism as intervention target in NAFLD . *Mol Syst Biol* **13**, 916 (2017).

263. Mardinoglu, A. *et al.* The potential use of metabolic cofactors in treatment of NAFLD. *Nutrients* **11**, 1–17 (2019).

264. Lee, D.-Y. & Kim, E.-H. Therapeutic Effects of Amino Acids in Liver Diseases: Current Studies and Future Perspectives. *J Cancer Prev* **24**, 72–78 (2019).

265. Yang, H. *et al.* Combined metabolic activators decrease liver steatosis by activating mitochondrial metabolism in hamsters fed with a high-fat diet. *Biomedicines* **9**, (2021).

266. Zhang, C. *et al.* The acute effect of metabolic cofactor supplementation: a potential therapeutic strategy against non-alcoholic fatty liver disease. *Mol Syst Biol* **16**, 1–16 (2020).

267. Abdelmalek, M. F., Angulo, P., Jorgensen, R. A., Sylvestre, P. B. & Lindor, K. D. Betaine, a promising new agent for patients with nonalcoholic steatohepatitis: results of a pilot study. *Am J Gastroenterol* **96**, 2711–2717 (2001).

268. Mukherjee, S. Role of betaine in liver disease-worth revisiting or has the die been cast? *World J Gastroenterol* **26**, 5745–5748 (2020).

269. Wang, Z. *et al.* Betaine improved adipose tissue function in mice fed a high-fat diet: a mechanism for hepatoprotective effect of betaine in nonalcoholic fatty liver disease. *Am J Physiol Gastrointest Liver Physiol* **298**, G634–G642 (2010).

270. Arumugam, M. K. *et al.* Beneficial effects of betaine: A comprehensive review. *Biology* vol. 10 Preprint at https://doi.org/10.3390/biology10060456 (2021).

271. Du, J. *et al.* Betaine supplementation enhances lipid metabolism and improves insulin resistance in mice fed a high-fat diet. *Nutrients* **10**, (2018).

272. Deminice, R. *et al.* Betaine supplementation prevents fatty liver induced by a high-fat diet: effects on one-carbon metabolism. *Amino Acids* **47**, 839–846 (2015).

273. Wang, L. *et al.* Betaine supplement alleviates hepatic triglyceride accumulation of apolipoprotein e deficient mice via reducing methylation of peroxisomal proliferator-activated receptor alpha promoter. *Lipids Health Dis* **12**, (2013).

274. Vesković, M. *et al.* Effect of Betaine Supplementation on Liver Tissue and Ultrastructural Changes in Methionine–Choline-Deficient Diet-Induced NAFLD. *Microscopy and Microanalysis* **26**, 997–1006 (2020).

275. Chen, Q. *et al.* Betaine inhibits Toll-like receptor 4 responses and restores intestinal microbiota in acute liver failure mice. *Sci Rep* **10**, 21850 (2020).

276. Yang, R., Le, G., Li, A., Zheng, J. & Shi, Y. Effect of antioxidant capacity on blood lipid metabolism and lipoprotein lipase activity of rats fed a high-fat diet. *Nutrition* **22**, 1185–1191 (2006).

277. Ma, Y., Gao, M. & Liu, D. N-acetylcysteine Protects Mice from High Fat Diet-induced Metabolic Disorders. *Pharm Res* **33**, 2033–2042 (2016).

278. Lai, I. K. *et al.* N-acetylcysteine (NAC) diminishes the severity of PCB 126-induced fatty liver in male rodents. *Toxicology* **302**, 25–33 (2012).

279. Lin, C. & Yin, M. Effects of cysteine-containing compounds on biosynthesis of triacylglycerol and cholesterol and anti-oxidative protection in liver from mice consuming a high-fat diet. *British Journal of Nutrition* **99**, 37–43 (2008).

280. Assimakopoulos, S. F. *et al.* Effect of antioxidant treatments on the gut-liver axis oxidative status and function in bile duct-ligated rats. *World J Surg* **31**, 2023–2032 (2007).

281. Savic, D., Hodson, L., Neubauer, S. & Pavlides, M. The importance of the fatty acid transporter l-carnitine in non-alcoholic fatty liver disease (Nafld). *Nutrients* vol. 12 1–17 Preprint at https://doi.org/10.3390/nu12082178 (2020).

282. Longo, N., Frigeni, M. & Pasquali, M. Carnitine transport and fatty acid oxidation. *Biochimica et Biophysica Acta (BBA) - Molecular Cell Research* **1863**, 2422–2435 (2016).

283. Mohammadi, M., Hajhossein Talasaz, A. & Alidoosti, M. Preventive effect of l-carnitine and its derivatives on endothelial dysfunction and platelet aggregation. *Clin Nutr ESPEN* **15**, 1–10 (2016).

284. Dong, S. *et al.* Urinary metabolomics analysis identifies key biomarkers of different stages of nonalcoholic fatty liver disease. *World J Gastroenterol* **23**, 2771 (2017).

285. El-Sheikh, A. A. K. & Rifaai, R. A. Peroxisome Proliferator Activator Receptor (PPAR)- *γ* Ligand, but Not PPAR- *α* , Ameliorates Cyclophosphamide-Induced Oxidative Stress and Inflammation in Rat Liver. *PPAR Res* **2014**, 1–10 (2014).

286. Su, C.-C. *et al.* L-carnitine ameliorates dyslipidemic and hepatic disorders induced by a high-fat diet via regulating lipid metabolism, self-antioxidant capacity, and inflammatory response. *J Funct Foods* **15**, 497–508 (2015).

287. Molfino, A. *et al.* L-CARNITINE ADMINISTRATION IMPROVES INSULIN SENSITIVITY IN PATIENTS WITH IMPAIRED GLUCOSE METABOLISM. *Eur J Intern Med* **19**, S48 (2008).

288. Keller, J. *et al.* Effect of L-carnitine on the hepatic transcript profile in piglets as animal model. *Nutr Metab (Lond)* **8**, 76 (2011).

289. Uziel, G., Garavaglia, B. & di Donato, S. Carnitine stimulation of pyruvate dehydrogenase complex (PDHC) in isolated human skeletal muscle mitochondria. *Muscle Nerve* **11**, 720–724 (1988).

290. Grandi, M., Pederzoli, S. & Sacchetti, C. Effect of acute carnitine administration on glucose insulin metabolism in healthy subjects. *Int J Clin Pharmacol Res* **17**, 143–7 (1997).

291. Askarpour, M. *et al.* Beneficial effects of L-carnitine supplementation for weight management in overweight and obese adults: An updated systematic review and dose-response meta-analysis of randomized controlled trials. *Pharmacological Research* vol. 151 Preprint at https://doi.org/10.1016/j.phrs.2019.104554 (2020).

292. Cantó, C. *et al.* The NAD+ precursor nicotinamide riboside enhances oxidative metabolism and protects against high-fat diet-induced obesity. *Cell Metab* **15**, 838–847 (2012).

293. Shi, W. *et al.* Effects of a wide range of dietary nicotinamide riboside (NR) concentrations on metabolic flexibility and white adipose tissue (WAT) of mice fed a mildly obesogenic diet. *Mol Nutr Food Res* **61**, (2017).

294. Lozada-Fernández, V. v *et al. Nicotinamide Riboside-Conditioned Microbiota Deflects High-Fat Diet-Induced Weight Gain in Mice*. https://journals.asm.org/journal/msystems (2022).

295. Yu, X. *et al.* Effect of nicotinamide riboside on lipid metabolism and gut microflora-bile acid axis in alcohol-exposed mice. *Food Sci Nutr* **9**, 429–440 (2021).

296. Lieu, E. L., Nguyen, T., Rhyne, S. & Kim, J. Amino acids in cancer. *Experimental and Molecular Medicine* vol. 52 15–30 Preprint at https://doi.org/10.1038/s12276-020-0375-3 (2020).

297. Gaggini, M. *et al.* Altered amino acid concentrations in NAFLD: Impact of obesity and insulin resistance. *Hepatology* **67**, 145–158 (2018).

298. Maria del Bas, J. *et al.* Hepatic accumulation of S-adenosylmethionine in hamsters with non-alcoholic fatty liver disease associated with metabolic syndrome under selenium and vitamin E deficiency. *Clin Sci* **133**, 409–423 (2019).

299. Hoyles, L. *et al.* Molecular phenomics and metagenomics of hepatic steatosis in non-diabetic obese women. *Nat Med* **24**, 1070–1080 (2018).

300. Simonson, M., Boirie, Y. & Guillet, C. Protein, amino acids and obesity treatment. *Reviews in Endocrine and Metabolic Disorders* vol. 21 341–353 Preprint at https://doi.org/10.1007/s11154-020-09574-5 (2020).

301. Wu, G. Intestinal Mucosal Amino Acid Catabolism. *J Nutr* **128**, 1249–1252 (1998).

302. Dai, Z., Wu, Z., Hang, S., Zhu, W. & Wu, G. Amino acid metabolism in intestinal bacteria and its potential implications for mammalian reproduction. *Mol Hum Reprod* **21**, 389–409 (2015).

303. Moro, J., Tomé, D., Schmidely, P., Demersay, T. C. & Azzout-Marniche, D. Histidine: A systematic review on metabolism and physiological effects in human and different animal species. *Nutrients* vol. 12 Preprint at https://doi.org/10.3390/nu12051414 (2020).

304. Liu, Y., Wang, X. & Hu, C. A. A. Therapeutic potential of amino acids in inflammatory bowel disease. *Nutrients* vol. 9 Preprint at https://doi.org/10.3390/nu9090920 (2017).

305. Vera-Aviles, M., Vantana, E., Kardinasari, E., Koh, N. & Latunde-Dada, G. Protective Role of Histidine Supplementation Against Oxidative Stress Damage in the Management of Anemia of Chronic Kidney Disease. *Pharmaceuticals* **11**, 111 (2018).

306. Thalacker-Mercer, A. E. & Gheller, M. E. Benefits and adverse effects of histidine supplementation. *Journal of Nutrition* **150**, 2588S-2592S (2020).

307. Endo, M. *et al.* Suppressed fat accumulation in rats fed a histidine-enriched diet. *Journal of Food Science and Nutrition* **15**, 1–6 (2010).

308. Sun, X. *et al.* Histidine supplementation alleviates inflammation in the adipose tissue of high-fat diet-induced obese rats via the NF-κB-and PPARγ-involved pathways. *British Journal of Nutrition* **112**, 477–485 (2014).

309. Feng, R. N. *et al.* Histidine supplementation improves insulin resistance through suppressed inflammation in obese women with the metabolic syndrome: a randomised controlled trial. *Diabetologia* **56**, 985–994 (2013).

310. Yasuda, T. *et al.* l-Histidine stimulates sympathetic nerve activity to brown adipose tissue in rats. *Neurosci Lett* **362**, 71–74 (2004).

311. Pugin, B. *et al.* A wide diversity of bacteria from the human gut produces and degrades biogenic amines. *Microb Ecol Health Dis* **28**, 1353881 (2017).

312. Gong, J. *et al.* Gut Microbiota Characteristics of People with Obesity by Meta-Analysis of Existing Datasets. *Nutrients* **14**, (2022).

313. Amelio, I., Cutruzzolá, F., Antonov, A., Agostini, M. & Melino, G. Serine and glycine metabolism in cancer. *Trends in Biochemical Sciences* vol. 39 191–198 Preprint at https://doi.org/10.1016/j.tibs.2014.02.004 (2014).

314. Zhou, X. *et al.* Serine prevented high-fat diet-induced oxidative stress by activating AMPK and epigenetically modulating the expression of glutathione synthesis-related genes. *Biochim Biophys Acta Mol Basis Dis* **1864**, 488–498 (2018).

315. Sim, W. C. *et al.* L-serine supplementation attenuates alcoholic fatty liver by enhancing homocysteine metabolism in mice and rats. *Journal of Nutrition* **145**, 260–267 (2015).

316. Holm, L. J. *et al.* L-serine supplementation lowers diabetes incidence and improves blood glucose homeostasis in NOD mice. *PLoS One* **13**, (2018).

317. Weber, K. & Rétey, J. *On the Nature of the Irreversible Inhibition of Histidine Ammonia Lyase by Cysteine and Dioxygen*. *Bioorganic & Medicinal Chemistry* vol. 4 (1996).

318. Mcgavigan, A. K. *et al.* L-cysteine suppresses ghrelin and reduces appetite in rodents and humans. *Int J Obes* **39**, 447–455 (2015).

319. Lin, C. C. & Yin, M. C. Effects of cysteine-containing compounds on biosynthesis of triacylglycerol and cholesterol and anti-oxidative protection in liver from mice consuming a high-fat diet. *British Journal of Nutrition* **99**, 37–43 (2008).

320. Jain, S. K., Kanikarla-Marie, P., Warden, C. & Micinski, D. L-cysteine supplementation upregulates glutathione (GSH) and vitamin D binding protein (VDBP) in hepatocytes cultured in high glucose and in vivo in liver, and increases blood levels of GSH, VDBP, and 25-hydroxy-vitamin D in Zucker diabetic fatty rats. *Mol Nutr Food Res* **60**, 1090–1098 (2016).

321. Holeček, M. Histidine in health and disease: Metabolism, physiological importance, and use as a supplement. *Nutrients* vol. 12 Preprint at https://doi.org/10.3390/nu12030848 (2020).

322. Baye, E. *et al.* Physiological and therapeutic effects of carnosine on cardiometabolic risk and disease. *Amino Acids* vol. 48 1131–1149 Preprint at https://doi.org/10.1007/s00726-016-2208-1 (2016).

323. Baye, E. *et al.* Carnosine supplementation improves serum resistin concentrations in overweight or obese otherwise healthy adults: A pilot randomized trial. *Nutrients* **10**, (2018).

324. de Courten, B. *et al.* Effects of carnosine supplementation on glucose metabolism: Pilot clinical trial. *Obesity* **24**, 1027–1034 (2016).

325. Mong, M. C., Chao, C. Y. & Yin, M. C. Histidine and carnosine alleviated hepatic steatosis in mice consumed high saturated fat diet. *Eur J Pharmacol* **653**, 82–88 (2011).

326. Yan, S. L., Wu, S. T., Yin, M. C., Chen, H. T. & Chen, H. C. Protective effects from carnosine and histidine on acetaminophen-induced liver injury. *J Food Sci* **74**, (2009).

327. Liu, W. hu, Liu, T. chung & Yin, M. chin. Beneficial effects of histidine and carnosine on ethanol-induced chronic liver injury. *Food and Chemical Toxicology* **46**, 1503–1509 (2008).

328. Reagan-Shaw, S., Nihal, M. & Ahmad, N. Dose translation from animal to human studies revisited. *The FASEB Journal* **22**, 659–661 (2008).

329. Loomba, R. *et al.* Gut Microbiome-Based Metagenomic Signature for Non-invasive Detection of Advanced Fibrosis in Human Nonalcoholic Fatty Liver Disease. *Cell Metab* **25**, 1054-1062.e5 (2017).

330. Boursier, J. *et al.* The Severity of Nonalcoholic Fatty Liver Disease Is Associated With Gut Dysbiosis and Shift in the Metabolic Function of the Gut Microbiota. *Hepatology* **63**, 764–775 (2016).

331. Cotillard, A. *et al.* Dietary intervention impact on gut microbial gene richness. *Nature* **500**, 585–588 (2013).

332. Quesada-Vázquez, S. *et al.* Supplementation with a Specific Combination of Metabolic Cofactors Ameliorates Non-Alcoholic Fatty Liver Disease and, Hepatic Fibrosis, and Insulin Resistance in Mice. *Nutrients* **13**, 3532 (2021).

333. Belei, O., Olariu, L., Dobrescu, A., Marcovici, T. & Marginean, O. The relationship between non-alcoholic fatty liver disease and small intestinal bacterial overgrowth among overweight and obese children and adolescents. *Journal of Pediatric Endocrinology and Metabolism* **30**, 1161–1168 (2017).

334. Machado, M. V. & Cortez-Pinto, H. Diet, microbiota, obesity, and NAFLD: A dangerous quartet. *International Journal of Molecular Sciences* vol. 17 1–20 Preprint at https://doi.org/10.3390/ijms17040481 (2016).

335. Moreno-Indias, I., Cardona, F., Tinahones, F. J. & Queipo-Ortuño, M. I. Impact of the gut microbiota on the development of obesity and type 2 diabetes mellitus. *Frontiers in Microbiology* vol. 5 Preprint at https://doi.org/10.3389/fmicb.2014.00190 (2014).

336. Leung, C., Rivera, L., Furness, J. B. & Angus, P. W. The role of the gut microbiota in NAFLD. *Nature Reviews Gastroenterology and Hepatology* vol. 13 412–425 Preprint at https://doi.org/10.1038/nrgastro.2016.85 (2016).

337. Hadizadeh, F., Faghihimani, E. & Adibi, P. Nonalcoholic fatty liver disease: Diagnostic biomarkers. *World J Gastrointest Pathophysiol* **8**, 11 (2017).

338. Xia, Y. *et al.* L-carnitine ameliorated fatty liver in high-calorie diet/STZ-induced type 2 diabetic mice by improving mitochondrial function. *Diabetol Metab Syndr* **3**, (2011).

339. Suárez, M. *et al.* Mediterranean Diet and Multi-Ingredient-Based Interventions for the Management of Non-Alcoholic Fatty Liver Disease. *Nutrients* **9**, 1052 (2017).

340. Khodayar, M. J., Kalantari, H., Khorsandi, L., Rashno, M. & Zeidooni, L. Betaine protects mice against acetaminophen hepatotoxicity possibly via mitochondrial complex II and glutathione availability. *Biomedicine and Pharmacotherapy* **103**, 1436–1445 (2018).

341. Hu, X. Q. *et al.* Dietary saponins of sea cucumber alleviate orotic acid-induced fatty liver in rats via PPAR and SREBP-1c signaling. *Lipids Health Dis* **9**, 1–9 (2010).

342. Ge, T. *et al.* The Role of the Pentose Phosphate Pathway in Diabetes and Cancer. **11**, 1–11 (2020).

343. Steneberg, P. *et al.* Hyperinsulinemia enhances hepatic expression of the fatty acid transporter Cd36 and provokes hepatosteatosis and hepatic insulin resistance. *Journal of Biological Chemistry* **290**, 19034–19043 (2015).

344. Savic, D., Hodson, L., Neubauer, S. & Pavlides, M. The importance of the fatty acid transporter l-carnitine in non-alcoholic fatty liver disease (Nafld). *Nutrients* **12**, 1–17 (2020).

345. Miura, K., Yang, L., van Rooijen, N., Ohnishi, H. & Seki, E. Hepatic recruitment of macrophages promotes nonalcoholic steatohepatitis through CCR2. *Am J Physiol Gastrointest Liver Physiol* **302**, G1310–G1321 (2012).

346. Lee, U. E. & Friedman, S. L. Mechanisms of Hepatic Fibrogenesis. *Best Pract Res Clin Gastroenterol* **25**, 195–206 (2011).

347. Wang, M. E. *et al.* Curcumin protects against thioacetamide-induced hepatic fibrosis by attenuating the inflammatory response and inducing apoptosis of damaged hepatocytes. *Journal of Nutritional Biochemistry* **23**, 1352–1366 (2012).

348. Alam, S., Mustafa, G., Alam, M. & Ahmad, N. Insulin resistance in development and progression of nonalcoholic fatty liver disease. *World J Gastrointest Pathophysiol* **7**, 211 (2016).

349. Donohoe, C. L., Doyle, S. L. & Reynolds, J. v. Visceral adiposity, insulin resistance and cancer risk. *Diabetology and Metabolic Syndrome* vol. 3 Preprint at https://doi.org/10.1186/1758-5996-3-12 (2011).

350. Xiang Gao, Guang Sun, Edward Randell, Yuan Tian & Haicheng Zhou. Systematic investigation of the relationships between Trimethylamine N-oxide and L-carnitine with obesity in both human and rodents. *Food Funct* **11**, 7707–7716 (2020).

351. Ju, L. *et al.* Obesity-associated inflammation triggers an autophagy–lysosomal response in adipocytes and causes degradation of perilipin 1. *Cell Death Dis* **10**, (2019).

352. Nielsen, T. S., Jessen, N., Jørgensen, J. O. L., Møller, N. & Lund, S. Dissecting adipose tissue lipolysis: Molecular regulation and implications for metabolic disease. *Journal of Molecular Endocrinology* vol. 52 Preprint at https://doi.org/10.1530/JME-13-0277 (2014).

353. Townsend, K. L. & Tseng, Y.-H. Brown fat fuel utilization and thermogenesis. *Trends in Endocrinology & Metabolism* **25**, 168–177 (2014).

354. Bartelt, A. *et al.* Brown adipose tissue activity controls triglyceride clearance. *Nat Med* **17**, 200–205 (2011).

355. Shimizu, I. & Walsh, K. The Whitening of Brown Fat and Its Implications for Weight Management in Obesity. *Current obesity reports* vol. 4 224–229 Preprint at https://doi.org/10.1007/s13679-015-0157-8 (2015).

356. Jiang, W. *et al.* Dysbiosis gut microbiota associated with inflammation and impaired mucosal immune function in intestine of humans with non-alcoholic fatty liver disease. *Sci Rep* **5**, (2015).

357. Lanthier, N. & Delzenne, N. Targeting the Gut Microbiome to Treat Metabolic Dysfunction-Associated Fatty Liver Disease: Ready for Prime Time? *Cells* **11**, 2718 (2022).

358. Quesada-Vázquez, S., Aragonès, G., del Bas, J. M. & Escoté, X. Diet, Gut Microbiota and Non-Alcoholic Fatty Liver Disease: Three Parts of the Same Axis. *Cells* **9**, 1–17 (2020).

359. Rohr, M. W., Narasimhulu, C. A., Rudeski-Rohr, T. A. & Parthasarathy, S. Negative Effects of a High-Fat Diet on Intestinal Permeability: A Review. *Advances in Nutrition* vol. 11 77–91 Preprint at https://doi.org/10.1093/advances/nmz061 (2020).

360. Bressenot, A. *et al.* Methyl donor deficiency affects small-intestinal differentiation and barrier function in rats. *British Journal of Nutrition* **109**, 667–677 (2013).

361. Lee, S. I. & Kang, K. S. N-acetylcysteine modulates lipopolysaccharide-induced intestinal dysfunction. *Sci Rep* **9**, (2019).

362. Katano, T., Bialkowska, A. B. & Yang, V. W. KLF4 Regulates Goblet Cell Differentiation in BMI1+ Reserve Intestinal Stem Cell Lineage during Homeostasis. *Int J Stem Cells* **13**, 424–431 (2020).

363. Safari, Z. & Gérard, P. The links between the gut microbiome and non-alcoholic fatty liver disease (NAFLD). *Cellular and Molecular Life Sciences* vol. 76 1541–1558 Preprint at https://doi.org/10.1007/s00018-019-03011-w (2019).

364. Wu, S. *et al.* Modulation of gut microbiota by lonicera caerulea l. Berry polyphenols in a mouse model of fatty liver induced by high fat diet. *Molecules* **23**, (2018).

365. Koliada, A. *et al.* Association between body mass index and Firmicutes/Bacteroidetes ratio in an adult Ukrainian population. *BMC Microbiol* **17**, (2017).

366. Zeybel, M. *et al.* Combined metabolic activators therapy ameliorates liver fat in nonalcoholic fatty liver disease patients. *Mol Syst Biol* **17**, (2021).

367. Raman, M. *et al.* Fecal microbiome and volatile organic compound metabolome in obese humans with nonalcoholic fatty liver disease. *Clinical Gastroenterology and Hepatology* **11**, 868-875.e3 (2013).

368. Raimondi, S., Musmeci, E., Candeliere, F., Amaretti, A. & Rossi, M. Identification of mucin degraders of the human gut microbiota. *Sci Rep* **11**, (2021).

369. Cui, H. *et al.* Da-Chai-Hu Decoction Ameliorates High Fat Diet-Induced Nonalcoholic Fatty Liver Disease Through Remodeling the Gut Microbiota and Modulating the Serum Metabolism. *Front Pharmacol* **11**, (2020).

370. Zhang, X. *et al.* Dietary cholesterol drives fatty liver-associated liver cancer by modulating gut microbiota and metabolites. *Gut* **70**, 761–774 (2021).

371. Kudo, C. *et al.* Relationship between non-alcoholic fatty liver disease and periodontal disease: a review and study protocol on the effect of periodontal treatment on non-alcoholic fatty liver disease. *J Transl Sci* **2**, (2016).

372. Yin, X. *et al.* Structural changes of gut microbiota in a rat non-alcoholic fatty liver disease model treated with a Chinese herbal formula. *Syst Appl Microbiol* **36**, 188–196 (2013).

373. John, U. v. & Carvalho, J. Enterococcus: Review of its physiology, pathogenesis, diseases and the challenges it poses for clinical microbiology. *Frontiers in Biology* vol. 6 357–366 Preprint at https://doi.org/10.1007/s11515-011-1167-x (2011).

374. Zheng, J. *et al.* N-Acetylcysteine alleviates gut dysbiosis and glucose metabolic disorder in high-fat diet-fed mice. *J Diabetes* **11**, 32–45 (2019).

375. Mu, H. *et al.* Naringin Attenuates High Fat Diet Induced Non-alcoholic Fatty Liver Disease and Gut Bacterial Dysbiosis in Mice. *Front Microbiol* **11**, (2020).

376. Rau, M. *et al.* Fecal SCFAs and SCFA-producing bacteria in gut microbiome of human NAFLD as a putative link to systemic T-cell activation and advanced disease. *United European Gastroenterol J* **6**, 1496–1507 (2018).

377. Schwiertz, A. *et al.* Microbiota and SCFA in lean and overweight healthy subjects. *Obesity* **18**, 190–195 (2010).

378. Portincasa, P. *et al.* Intestinal Barrier and Permeability in Health, Obesity and NAFLD. *Biomedicines* vol. 10 Preprint at https://doi.org/10.3390/biomedicines10010083 (2022).

379. Lee, G. *et al.* Distinct signatures of gut microbiome and metabolites associated with significant fibrosis in non-obese NAFLD. *Nat Commun* **11**, (2020).

380. Feng, Y., Huang, Y., Wang, Y., Wang, P. & Wang, F. Severe burn injury alters intestinal microbiota composition and impairs intestinal barrier in mice. *Burns Trauma* **7**, (2019).

381. Killingsworth, J., Sawmiller, D. & Shytle, R. D. Propionate and Alzheimer's Disease. *Frontiers in Aging Neuroscience* vol. 12 Preprint at https://doi.org/10.3389/fnagi.2020.580001 (2021).

382. Wu, G. Amino acids: metabolism, functions, and nutrition. *Amino Acids* **37**, 1–17 (2009).

383. Feng, R. N. *et al.* Histidine supplementation improves insulin resistance through suppressed inflammation in obese women with the metabolic syndrome: A randomised controlled trial. *Diabetologia* **56**, 985–994 (2013).

384. Dinicolantonio, J. J., McCarty, M. F. & Okeefe, J. H. Role of dietary histidine in the prevention of obesity and metabolic syndrome. *Open Heart* vol. 5 Preprint at https://doi.org/10.1136/openhrt-2017-000676 (2018).

385. Jørgensen, E. A. *et al.* Increased susceptibility to diet-induced obesity in histamine-deficient mice. *Neuroendocrinology* **83**, 289–294 (2006).

386. Shay, J. W. & Wright, W. E. Senescence and immortalization: role of telomeres and telomerase. *Carcinogenesis* **26**, 867–874 (2005).

387. Campisi, J. Senescent Cells, Tumor Suppression, and Organismal Aging: Good Citizens, Bad Neighbors. *Cell* **120**, 513–522 (2005).

388. Hoare, M. & Narita, M. Notch and Senescence. in 299–318 (2018). doi:10.1007/978-3-319-89512-3_15.

389. Morrison, S. F. & Madden, C. J. Central nervous system regulation of brown adipose tissue. *Compr Physiol* **4**, 1677–1713 (2014).

390. Masaki, T., Yoshimatsu, H., Chiba, S., Watanabe, T. & Sakata, T. *Central Infusion of Histamine Reduces Fat Accumulation and Upregulates UCP Family in Leptin-Resistant*

Obese Mice. *DIABETES* vol. 50 http://diabetesjournals.org/diabetes/article-pdf/50/2/376/646639/0500376.pdf (2001).

391. Desautels, M. *et al. Role of mast cell histamine in brown adipose tissue thermogenic response to VMH stimulation*. www.physiology.org/journal/ajpregu (1994).

392. Salazar-Tortosa, D. F., Enard, D., Itan, Y. & Ruiz, J. R. Novel brown adipose tissue candidate genes predicted by the human gene connectome. *Sci Rep* **12**, (2022).

393. Tilg, H. & Moschen, A. R. Role of adiponectin and PBEF/visfatin as regulators of inflammation: involvement in obesity-associated diseases. *Clin Sci* **114**, 275–288 (2008).

394. Achari, A. E. & Jain, S. K. Adiponectin, a therapeutic target for obesity, diabetes, and endothelial dysfunction. *International Journal of Molecular Sciences* vol. 18 Preprint at https://doi.org/10.3390/ijms18061321 (2017).

395. Achari, A. E. & Jain, S. K. l-Cysteine supplementation increases adiponectin synthesis and secretion, and GLUT4 and glucose utilization by upregulating disulfide bond A-like protein expression mediated by MCP-1 inhibition in 3T3-L1 adipocytes exposed to high glucose. *Mol Cell Biochem* **414**, 105–113 (2016).

396. Sharma, A. M. & Staels, B. Review: Peroxisome proliferator-activated receptor γ and adipose tissue - Understanding obesity-related changes in regulation of lipid and glucose metabolism. *Journal of Clinical Endocrinology and Metabolism* vol. 92 386–395 Preprint at https://doi.org/10.1210/jc.2006-1268 (2007).

397. Monsalve, F. A., Pyarasani, R. D., Delgado-Lopez, F. & Moore-Carrasco, R. Peroxisome proliferator-activated receptor targets for the treatment of metabolic diseases. *Mediators of Inflammation* vol. 2013 Preprint at https://doi.org/10.1155/2013/549627 (2013).

398. Wahlang, B., McClain, C., Barve, S. & Gobejishvili, L. Role of cAMP and phosphodiesterase signaling in liver health and disease. *Cell Signal* **49**, 105–115 (2018).

399. Arturi, F. *et al.* Nonalcoholic fatty liver disease is associated with low circulating levels of insulin-like growth factor-I. *Journal of Clinical Endocrinology and Metabolism* **96**, (2011).

400. Matsuda, S., Kobayashi, M. & Kitagishi, Y. Roles for PI3K/AKT/PTEN Pathway in Cell Signaling of Nonalcoholic Fatty Liver Disease. *ISRN Endocrinol* **2013**, 1–7 (2013).

401. Berry, M. D., Gainetdinov, R. R., Hoener, M. C. & Shahid, M. Pharmacology of human trace amine-associated receptors: Therapeutic opportunities and challenges. *Pharmacology and Therapeutics* vol. 180 161–180 Preprint at https://doi.org/10.1016/j.pharmthera.2017.07.002 (2017).

402. Vallianou, N. *et al.* Understanding the Role of the Gut Microbiome and Microbial Metabolites in Non-Alcoholic Fatty Liver Disease: Current Evidence and Perspectives. *Biomolecules* **12**, 56 (2021).

403. Sookoian, S. *et al.* Intrahepatic bacterial metataxonomic signature in non-alcoholic fatty liver disease. *Gut* **69**, 1483–1491 (2020).

404. Jian, C., Luukkonen, P., Sädevirta, S., Yki-Järvinen, H. & Salonen, A. Impact of short-term overfeeding of saturated or unsaturated fat or sugars on the gut microbiota in relation to liver fat in obese and overweight adults. *Clinical Nutrition* **40**, 207–216 (2021).

405. Mu, H. N. *et al.* Caffeic acid prevents non-alcoholic fatty liver disease induced by a high-fat diet through gut microbiota modulation in mice. *Food Research International* **143**, (2021).

406. Lanthier, N. *et al.* Microbiota analysis and transient elastography reveal new extra-hepatic components of liver steatosis and fibrosis in obese patients. *Sci Rep* **11**, (2021).

407. Leyn, S. A. *et al.* Comparative genomics and evolution of transcriptional regulons in Proteobacteria. *Microb Genom* **2**, (2016).

408. Molinaro, A. *et al.* Imidazole propionate is increased in diabetes and associated with dietary patterns and altered microbial ecology. *Nat Commun* **11**, (2020).

409. Foretz, M., Even, P. C. & Viollet, B. AMPK activation reduces hepatic lipid content by increasing fat oxidation in vivo. *Int J Mol Sci* **19**, (2018).

410. Mong, M., Chao, C. & Yin, M. Histidine and carnosine alleviated hepatic steatosis in mice consumed high saturated fat diet. *Eur J Pharmacol* **653**, 82–88 (2011).

411. Lee, Y. T., Hsu, C. C., Lin, M. H., Liu, K. sen & Yin, M. C. Histidine and carnosine delay diabetic deterioration in mice and protect human low density lipoprotein against oxidation and glycation. *Eur J Pharmacol* **513**, 145–150 (2005).

412. Kennedy, L. *et al.* Knockout of l-Histidine Decarboxylase Prevents Cholangiocyte Damage and Hepatic Fibrosis in Mice Subjected to High-Fat Diet Feeding via Disrupted Histamine/Leptin Signaling. *American Journal of Pathology* **188**, 600–615 (2018).

413. Mokhtari, Z., Gibson, D. L. & Hekmatdoost, A. Nonalcoholic fatty liver disease, the gut microbiome, and diet. *Advances in Nutrition* vol. 8 240–252 Preprint at https://doi.org/10.3945/an.116.013151 (2017).

414. Depommier, C. *et al.* Supplementation with Akkermansia muciniphila in overweight and obese human volunteers: a proof-of-concept exploratory study. *Nat Med* **25**, 1096–1103 (2019).

415. Kwan, S. Y. *et al.* Gut microbiome features associated with liver fibrosis in Hispanics, a population at high risk for fatty liver disease. *Hepatology* **75**, 955–967 (2022).

416. Maier, T., Güell, M. & Serrano, L. Correlation of mRNA and protein in complex biological samples. *FEBS Letters* vol. 583 3966–3973 Preprint at https://doi.org/10.1016/j.febslet.2009.10.036 (2009).

417. Tabatabaei-Malazy, O., Larijani, B. & Abdollahi, M. Targeting metabolic disorders by natural products. *Journal of Diabetes and Metabolic Disorders* vol. 14 Preprint at https://doi.org/10.1186/s40200-015-0184-8 (2015).

418. Carpéné, C., Gomez-Zorita, S., Deleruyelle, S. & Carpéné, M. A. *Novel Strategies for Preventing Diabetes and Obesity Complications with Natural Polyphenols*. *Current Medicinal Chemistry* vol. 22 http://www.phenol-explorer.eu. (2015).

419. Rodriguez-Ramiro, I., Vauzour, D. & Minihane, A. M. Polyphenols and non-alcoholic fatty liver disease: Impact and mechanisms. in *Proceedings of the Nutrition Society* vol. 75 47–60 (Cambridge University Press, 2016).

420. Procházková, D., Boušová, I. & Wilhelmová, N. Antioxidant and prooxidant properties of flavonoids. *Fitoterapia* **82**, 513–523 (2011).

421. Saeidnia, S. & Abdollahi, M. Toxicological and pharmacological concerns on oxidative stress and related diseases. *Toxicol Appl Pharmacol* **273**, 442–455 (2013).

422. Amiot, M. J., Riva, C. & Vinet, A. Effects of dietary polyphenols on metabolic syndrome features in humans: A systematic review. *Obesity Reviews* **17**, 573–586 (2016).

423. Llaha, F. & Zamora-Ros, R. The effects of polyphenol supplementation in addition to calorie restricted diets and/or physical activity on body composition parameters: A systematic review of randomized trials. *Frontiers in Nutrition* vol. 7 Preprint at https://doi.org/10.3389/fnut.2020.00084 (2020).

424. Massaro, M., Scoditti, E., Carluccio, M. A. & de Caterina, R. Nutraceuticals and Prevention of Atherosclerosis: Focus on ω-3 Polyunsaturated Fatty Acids and Mediterranean Diet Polyphenols. *Cardiovasc Ther* **28**, e13–e19 (2010).

425. SAKURAI, T. *et al.* Antioxidative Effects of a New Lychee Fruit-Derived Polyphenol Mixture, Oligonol, Converted into a Low-Molecular Form in Adipocytes. *Biosci Biotechnol Biochem* **72**, 463–476 (2008).

426. Park, H. J. *et al.* Combined Effects of Genistein, Quercetin, and Resveratrol in Human and 3T3-L1 Adipocytes. *J Med Food* **11**, 773–783 (2008).

427. Singh, C. K., George, J. & Ahmad, N. Resveratrol-based combinatorial strategies for cancer management. *Ann N Y Acad Sci* **1290**, 113–121 (2013).

428. Phan, M. A. T., Paterson, J., Bucknall, M. & Arcot, J. Interactions between phytochemicals from fruits and vegetables: Effects on bioactivities and bioavailability. *Crit Rev Food Sci Nutr* **58**, 1310–1329 (2018).

429. van Breda, S. G. J. & de Kok, T. M. C. M. Smart Combinations of Bioactive Compounds in Fruits and Vegetables May Guide New Strategies for Personalized Prevention of Chronic Diseases. *Molecular Nutrition and Food Research* vol. 62 Preprint at https://doi.org/10.1002/mnfr.201700597 (2018).

430. Moudache, M., Colon, M., Nerín, C. & Zaidi, F. Phenolic content and antioxidant activity of olive by-products and antioxidant film containing olive leaf extract. *Food Chem* **212**, 521–527 (2016).

431. Hsieh, T.-C. & Wu, J. M. Targeting CWR22Rv1 Prostate Cancer Cell Proliferation and Gene Expression by Combinations of the Phytochemicals EGCG, Genistein and Quercetin. *Anticancer Res* **29**, 4025–4032 (2009).

432. Zhou, M. *et al.* Transcriptomic and Metabonomic Profiling Reveal Synergistic Effects of Quercetin and Resveratrol Supplementation in High Fat Diet Fed Mice. *J Proteome Res* **11**, 4961–4971 (2012).

433. Hadad, N. & Levy, R. The synergistic anti-inflammatory effects of lycopene, lutein, β-carotene, and carnosic acid combinations via redox-based inhibition of NF-κB signaling. *Free Radic Biol Med* **53**, 1381–1391 (2012).

434. Niedzwiecki, A., Roomi, M. W., Kalinovsky, T. & Rath, M. Anticancer efficacy of polyphenols and their combinations. *Nutrients* vol. 8 Preprint at https://doi.org/10.3390/nu8090552 (2016).

435. Radler, U. *et al.* A Combination of (ω–3) Polyunsaturated Fatty Acids, Polyphenols and L-Carnitine Reduces the Plasma Lipid Levels and Increases the Expression of Genes Involved in Fatty Acid Oxidation in Human Peripheral Blood Mononuclear Cells and HepG2 Cells. *Ann Nutr Metab* **58**, 133–140 (2011).

436. Dellinger, R. W. *et al.* Repeat dose NRPT (nicotinamide riboside and pterostilbene) increases NAD+ levels in humans safely and sustainably: a randomized, double-blind, placebo-controlled study. *NPJ Aging Mech Dis* **3**, (2017).

437. Goñi, I. *et al.* Effect of Dietary Grape Pomace and Vitamin E on Growth Performance, Nutrient Digestibility, and Susceptibility to Meat Lipid Oxidation in Chickens. *Poultry Science Association Inc.* **86**, 508–516 (2006).

438. Beaumont, M. *et al.* A mix of functional amino acids and grape polyphenols promotes the growth of piglets, modulates the gut microbiota in vivo and regulates epithelial homeostasis in intestinal organoids. *Amino Acids* **54**, 1357–1369 (2022).

8. SCIENTIFIC PRODUCTION

Papers included in this thesis

Submitted or in preparation papers

Quesada-Vázquez S., Chomiciute G., Colom-Pellicer M., Aragonès G., Herrero L., Del Bas J.M., Caimari A., Escoté X., Fernández-Real J.M., Mayneris-Perxachs J. (2022). Histidine metabolism is a promising therapeutic target against obesity and insulin resistance. Manuscript in preparation.

Quesada-Vázquez S., Latorre J., Oliveras-Cañellas N., Tejera N., Tobajas Y., Hildebrand F., Beraza N., Burcelin R., Dumas M.E., Federici M., Hoyles L., Del Bas J.M., Escoté X., Fernández-Real J.M., Mayneris-Perxachs J. (2022). Potential therapeutic implications of Histidine catabolism by the gut microbiota in NAFLD. Under review in *Cell Reports Medicine*.

Published papers

Quesada-Vázquez S., Antolín A., Colom-Pellicer M., Aragonès G., Herrero L., Del Bas J.M., Caimari A., Escoté X. (2022). Reduction of Obesity and Insulin Resistance through Dual Targeting of VAT and BAT by a Novel Combination of Metabolic Cofactors*. International Journal of Molecular Sciences*, 23(23), 14923.

Quesada-Vázquez, S., Bone, C., Saha, S., Triguero, I., Colom-Pellicer, M., Aragonès, G., Hildebrand, F., Del Bas, J. M., Caimari, A., Beraza, N., & Escoté, X. (2022). Microbiota Dysbiosis and Gut Barrier Dysfunction Associated with Non-Alcoholic Fatty Liver Disease Are Modulated by a Specific Metabolic Cofactors' Combination. *International Journal of Molecular Sciences*, 23(22), 13675.

Quesada-Vázquez, S., Colom-Pellicer, M., Navarro-Masip, È., Aragonès, G., Del Bas, J. M., Caimari, A., & Escoté, X. (2021). Supplementation with a

Specific Combination of Metabolic Cofactors Ameliorates Non-Alcoholic Fatty Liver Disease, Hepatic Fibrosis, and Insulin Resistance in Mice. *Nutrients*, 13(10), 3532.

Quesada-Vázquez, S., Aragonès, G., Del Bas, J. M., & Escoté, X. (2020). Diet, Gut Microbiota and Non-Alcoholic Fatty Liver Disease: Three Parts of the Same Axis. *Cells*, 9(1), 176.

Contributions to other scientific papers

Submitted or in preparation papers

Kazakova, P., Cereto-Massagué, A., Palacios, H., Martinez de Cripan, S., Egea, C., **Quesada-Vázquez, S**., Boqué, N., Caimari, A., Escoté, X., Canela, N., Torrell, N. (2022). Multiomic approach for intestinal holobiont description in celiac disease in a rat model and in human patients. In preparation.

Escoté, X., Laiglesia, L.M., Sáinz, N., Felix-Soriano, E., Santamaría, E., Collantes, M., Fernández-Galilea, M., Colón-Mesa, I., Martínez-Fernández, L., Quesada-López, T., **Quesada-Vázquez, S**., Rodríguez-Ortigosa, C., Arbones-Mainar, J.M., Valverde, A.M., Martínez, J.A., Dalli, J., Herrero, L., Lorente-Cebrián, S., Villarroya, F., Moreno-Aliaga, M.J. (2022). Maresin 1 activates brown adipose tissue and promotes browning of white adipose tissue in mice. Under revisión in *Molecular Metabolism.*

Quesada-Vázquez, S., De Almagro, M.C., Del Bas, J.M., Caimari, A., Puiggrós, F., Escoté. X., Moreno-Muñoz, J.A. (2022). A combination of ORD0998 and CECT7210 postbiotics reduces LPS-induced preterm birth and reduces systemic inflammation in pregnant mice. In preparation.

Published papers

León, I. C.*, **Quesada-Vázquez, S.***, Sáinz, N., Guruceaga, E., Escoté, X., & Moreno-Aliaga, M. J. (2020). Effects of Maresin 1 (MaR1) on Colonic Inflammation and Gut Dysbiosis in Diet-Induced Obese Mice. Microorganisms, 8(8), 1156. *Equal contribution.

Hernandez-Baixauli, J*., **Quesada-Vázquez, S*.**, Mariné-Casadó, R., Gil Cardoso, K., Caimari, A., Del Bas, J. M., Escoté, X., & Baselga-Escudero, L. (2020). Detection of Early Disease Risk Factors Associated with Metabolic Syndrome: A New Era with the NMR Metabolomics Assessment. *Nutrients*, 12(3), 806. *Equal contribution.

Rodríguez, R.M., Monteiro de Assis, L.V., Colom-Pellicer, M., **Quesada-Vázquez, S.**, Cruz-Carrión, A., Escoté, X., Oster, H., Aragonès, G., Mulero, M. (2022). Grape-seed proanthocyanidin extract (GSPE) modulates diurnal oscillations of key hepatic metabolic genes and metabolites alleviating hepatic lipid deposition in cafeteria-fed obese rats in a time-of-day-dependent manner. *BioRxiv* 2022.07.20.500817.

Colom-Pellicer, M., Rodríguez, R. M., Soliz-Rueda, J. R., de Assis, L. V. M., Navarro-Masip, È., **Quesada-Vázquez, S.**, Escoté, X., Oster, H., Mulero, M., & Aragonès, G. (2022). Proanthocyanidins Restore the Metabolic Diurnal Rhythm of Subcutaneous White Adipose Tissue According to Time-Of-Day Consumption. *Nutrients*, 14(11), 2246.

Book Chapter

Quesada-Vázquez, S., Hernandez-Baixauli, J., Navarro-Masip, E., Escoté, X. (2022). NMR Metabolomics for Marker Discovery of Metabolic Syndrome. In: Patel, V.B., Preedy, V.R. (eds) Biomarkers in Nutrition. Biomarkers in Disease: Methods, Discoveries and Applications. Springer, Cham.

Congress contributions

Quesada-Vázquez S., Antolín A., Colom-Pellicer M., Aragonès G., Herrero L., Del Bas J.M., Caimari A., Escoté X. (2022). Reduction of Obesity and Insulin Resistance through Dual Targeting of VAT and BAT by a Novel Combination of Metabolic Cofactors in diet-induced obese mice. Presented at 19th meeting of the consortium for transpyrenean investigations in obesity &diabetes (CTPIOD), Jaca, Spain.

Quesada-Vázquez S., del Bas J.M., Fernández-Real J.M., Mayneris-Perxachs J., Escoté X. (2022). Gut microbiota histidine catabolism is a key player in the NAFLD disease. Presented at 18th NuGO week Congress, Tarragona, Spain.

Baudin-Luque J., Mercado-Valls N., Hernandez-Baixauli J., **Quesada-Vázquez S.**, Puiggròs F., Arola LL., Caimari A. (2022). Combined supplementation with hesperidin, phytosterols and curcumin improves body composition and decreases adiposity and LDL-cholesterol in ovariectomized rats. Presented at 18th NuGO week Congress, Tarragona, Spain.

Grants and Projects awards

“Spanish Universities for EU projects" project, co-financed by the Erasmus+ KA103 program of the European Union. (2021).

Modulation of histidine metabolism for the regulation of visceral adiposity and NAFLD (FATHIS). (2022). AGAUR Modality B. Producte grants for the obtaining of prototypes and the valorization and transfer of the results of the research created by research teams in Catalonia. Participated as a Scientific Entrepreneur.

Patents presented

Pharmaceutical and nutraceutical compositions with a combination of amino acids and its use in diseases characterized by lipid accumulation in tissues. EU patent EP22382390.7

---

9. ANNEX

Annex

Europäisches Patentamt
European Patent Office
Office européen des brevets

Request for grant of a European patent

For official use only		
1 Application number:	MKEY	
2 Date of receipt (Rule 35(2) EPC):	DREC	
3 Date of receipt at EPO (Rule 35(4) EPC):	RENA	
4 Date of filing:		

5 Grant of European patent, and examination of the application under Article 94, are hereby requested. ☒

Request for examination in an admissible non-EPO language: Se solicita el examen de la solicitud según el artículo 94.

5.1 The applicant waives his right to be asked whether he wishes to proceed further with the application (Rule 70(2)) ☐

Procedural language: en

Filing Language: en

6 Applicant's or representative's reference: P6061EP00

Filing Office: ES

Applicant 1

7-1 Name: FUNDACIÓ EURECAT

8-1 Address: Parc Tecnològic del Vallès
Av. Universitat Autònoma, núm. 23
08290 CERDANYOLA DEL VALLÈS
Spain

10-1 State of residence or of principal place of business: Spain

Applicant 2

7-2 Name: FUNDACIÓ INSTITUT D'INVESTIGACIÓ BIOMÈDICA DE GIRONA DR. JOSEP TRUETA

8-2 Address: C. Dr. Castany s/n
Edifici de la Mancomunitat 2 - Parc Hospitalari Martí i Julià
17190 SALT
Spain

10-1	State of residence or of principal place of business:	Spain

Applicant 3

7-3	Name:	CONSORCIO CENTRO DE INVESTIGACIÓN BIOMÉDICA EN RED
8-3	Address:	C. Monforte de Lemos 3-5. Pabellón 11 28029 MADRID Spain
10-1	State of residence or of principal place of business:	Spain

14.1 The/Each applicant hereby declares that he is an entity or a natural person under Rule 6(4) EPC. ☒

Representative 1

15-1	Name:	ZBM Patents - Zea, Barlocci & Markvardsen
	Association No.:	371
16-1	Address of place of business:	Rambla de Catalunya, 123 08008 Barcelona Spain
17-1	Telephone:	+34.93.3426472
17-1	Fax:	+34.93.3427970
17-1	E-mail:	formalities@zbm-patents.eu

Inventor(s)

23 Designation of inventor attached ☒

24 Title of invention

Title of invention:	PHARMACEUTICAL AND NUTRACEUTICAL COMPOSITIONS WITH A COMBINATION OF AMINO ACIDS AND ITS USE IN DISEASES CHARACTERIZED BY LIPID ACCUMULATION IN TISSUES

25 Declaration of priority (Rule 52) and search results under Rule 141(1)

A declaration of priority is hereby made for the following applications

25.2 Re-establishment of rights

Re-establishment of rights under Article 122 EPC in respect of the priority period is herewith requested for the following priority/priorities

25.3 The EPO is requested to retrieve a certified copy of the following previous application(s) (priority document(s)) via the WIPO Digital Access Service (DAS) using the indicated access code(s):

Request	Application number:	Access Code

25.4 This application is a complete translation of the previous application ☐

25.5 It is not intended to file a (further) declaration of priority ☒

26 Reference to a previously filed application

27 Divisional application ☐

28 Article 61(1)(b) application ☐

29 Claims

Number of claims: 14

29.1 ☒ as attached

29.2 ☐ as in the previously filed application (see Section 26.2)

29.3 ☐ The claims will be filed later

30 Figures

It is proposed that the abstract be published together with figure No.

31 Designation of contracting states

All the contracting states party to the EPC at the time of filing of the European patent application are deemed to be designated (see Article 79(1)).

32 Different applicants for different contracting states

33 Extension/Validation

This application is deemed to be a request to extend the effects of the European patent application and the European patent granted in respect of it to all non-contracting states to the EPC with which extension or validation agreements are in force on the date on which the application is filed. However, the request is deemed withdrawn if the extension fee or the validation fee, whichever is applicable, is not paid within the prescribed time limit.

33.1 It is intended to pay the extension fee(s) for the following state(s):

33.2 It is intended to pay the validation fee(s) for the following state(s):

34 Biological material

38 Nucleotide and amino acid sequences

38.1 The description contains a sequence listing. ☒

38.2a The sequence listing is attached in computer-readable format in accordance with WIPO Standard ST.25 (Rule 30(1)). ☒

38.2b The sequence listing is attached in PDF format ☐

Further indications

39 Additional copies of the documents cited in the European search report are requested

Number of additional sets of copies:

40 Refund of the search fee under Article 9(2) of the Rules relating to Fees is requested ☐

Application number or publication number of earlier search report:

42 **Payment**

Method of payment: Debit from deposit account

The European Patent Office is hereby authorised, to debit from the deposit account with the EPO any fees and costs indicated on the fees section below.

Currency: EUR

Deposit account number: 28120033

Account holder: Anna Barlocci

43 **Refunds**

Any refunds should be made to EPO deposit account: 28120033

Account holder: Anna Barlocci

Fees	Factor applied	Fee schedule	Amount to be paid
001 Filing fee - EP direct - online	1	130.00	130.00
002 Fee for a European search - Applications filed on/after 01.07.2005	1	1 390.00	1 390.00
015 Claims fee - For the 16th to the 50th claim	0	250.00	0.00
015e Claims fee - For the 51st and each subsequent claim	0	630.00	0.00
501 Additional filing fee for the 36th and each subsequent page	5	16.00	80.00
Total:		EUR	1 600.00

44-A Forms	Details:	System file name:
A-1 Request		as ep-request.pdf
A-2 1. Designation of inventor	1. Inventor	as f1002-1.pdf

44-B Technical documents		Original file name:	System file name:
B-1	Specification	P6061EP00_filing_text_25042022.pdf Description; 14 claims; 7 figure(s); abstract	SPECEPO-1.pdf
B-3	Sequence listings, ASCII	P6061EP00_SEQ LIST_ST25.txt	SEQLTXT.txt
B-4	Pre-conversion archive	P6061EP00_filing_pre.zip	OLF-ARCHIVE.zip
B-5	Translation of description, claims, abstract and drawings in Spanish	P6061EP00_filing_abstr OEPM.pdf	SPECTRANONEP.pdf

44-C Other documents	Original file name:	System file name:

45	General authorisation:	

46 Signature(s)

Place:	**Barcelona**
Date:	**25 April 2022**
Signed by:	**Carlos Maíllo Carbajo 75849**
Association:	**ZBM Patents - Zea, Barlocci & Markvardsen**
Representative name:	**Carlos Maíllo**
Capacity:	**(Representative)**

UNIVERSITAT ROVIRA I VIRGILI
EFFECTS OF NUTRACEUTICAL TREATMENTS BASED ON METABOLIC COFACTORS AND HISTIDINE AMINO ACIDS METABOLISM ON NAFLD AND OBESITY RESOLVING GUT-LIVER-ADIPOSE CROSSTALK
Sergio Quesada Vázquez

UNIVERSITAT
ROVIRA i VIRGILI

eurecat